Title
Total Synthesis of (–)-Chromodorolide B and Origins of Diastereoselectivity for Conjugate Additions of Trisubstituted Acetonide Radicals

Author
Tao, Daniel James

Publication Date
2016

Peer reviewed|Thesis/dissertation

UNIVERSITY OF CALIFORNIA,
IRVINE

Total Synthesis of (–)-Chromodorolide B

and

Origins of Diastereoselectivity for Conjugate Additions of Trisubstituted Acetonide Radicals

DISSERTATION

submitted in partial satisfaction of the requirements
for the degree of

DOCTOR OF PHILOSOPHY

in Chemistry

by

Daniel James Tao

Dissertation Committee:
Prof. Larry E. Overman, Chair
Prof. Jennifer A. Prescher
Prof. A. Richard Chamberlin

2016

Dedication

To Mom and Dad for raising me to give my utmost,

And to Jessica for loving me unconditionally.

Table of Contents

List of Figures

List of Schemes

List of Tables

List of Equations

Acknowledgements

In reflecting on my five years at UC Irvine, it's impossible to thank everyone who has impacted my growth as a chemist, as a writer, and as a person. I've been blessed to work among such caring individuals who have given hours and days to discuss ideas, read poorly-written drafts, and expand my knowledge of the chemical world. To everyone that follows (and those I forgot), know that this page doesn't begin to convey the gratitude I have for the investment placed into me at UC Irvine.

I must first acknowledge my Savior and my God, Who has been an ever constant in my five years as a graduate student. Nothing that I have achieved or will ever achieve has come by my skills or intellect alone, and graduate school has been a powerful time to see His work in my life. 2 Corinthians 12:9 says "My grace is sufficient for you, for My power is made perfect in weakness." I am reminded daily of my failures and deficiencies as a Christian, a chemist, and a person; and yet, God has been faithful to provide even in the most difficult moments of my life.

Professor Larry Overman has been an incredible mentor in every possible facet. He has driven me to approach problems with deep thought and criticism, providing a perfect balance of independence and input as a mentor. I have gained tremendous respect for Larry's integrity in scientific research, a quality that I hope to emulate. I sincerely desire for people see Larry's fingerprint on my professional career years from now, as he has been instrumental in shaping it.

Many professors have also gone above and beyond for me, from answering questions outside of class to writing letters of recommendation. Specifically, I had the pleasure of interacting with Professors Chris Vanderwal and Jennifer Prescher on a number

of occasions over the years. Their willingness to give their time and advice was truly appreciated. I would also like to thank Professor Richard Chamberlin for his willingness to be on my thesis committee with short notice. I would also like to thank Professor Steven Hanessian for giving me an opportunity to coauthor a review article with his group.

During my time in the Overman group, I have interacted with outstanding postdoctoral colleagues who have trained me during my first years in the laboratory. The earliest group included Dr. Martin Schnermann, Dr. Michael Shaghafi, Dr. John DeLorbe, Prof. Marcus Baumann, Dr. James Manning, Dr. Jonah Chang, and Dr. Philipp Kohler. They have my gratitude for setting a tone of excellence that reverberates in my mind to this day. I also must thank later postdoctoral colleagues including Dr. Bradley Loertscher, Dr. Christopher Jamison, Dr. Kyle Quasdorf, and Dr. Daniel Müller, who were excellent labmates and offered helpful advice.

Within Lab 4031, I have been closely mentored by several fantastic postdoctoral scientists. These include Dr. Nathan Genung, Dr. Tricia May-Dracka, and Dr. Michelle Garnsey. Thank you for putting up with my synthetic ignorance early on and for instilling the best of scientific qualities into me. A special thanks goes to Dr. André Dieskau, my German deskmate for nearly two years. I could not imagine a better scientist to be mentored by, as Dr. Dieskau was a constant source of advice and humor. A second thanks goes to Dr. Gerald Pratsch, another brilliant German chemist. I had the honor of befriending Dr. Pratsch over his two years in the Overman group, and he was a pleasure to interact with daily.

I have also had the privilege of working with fantastic Overman graduate students. Dr. Nicholas Untiedt and Dr. Salman Jabri were the senior graduate students in the

laboratory for two years. They invested more time and effort into me than I ever deserved. Dr. Untiedt was a constant encouragement when graduate school became stressful, and Dr. Jabri was a constant motivation to achieve my full potential. I am indebted for their mentorship and thankful for comradery that we shared in those years. Dr. Gregory Lackner has been my classmate and fellow Overman group member for these five years. It's been a pleasure to experience graduate school with Greg (misery *needs* company sometimes), and I have benefitted from his synthetic advice on many occasions. Lastly, I must also thank Yuriy Slutskyy, the youngest (and possibly last) graduate student in the Overman group. Despite his perpetual infidelity of 11:30 AM lunch time, it has been a pleasure to work together on the chromodorolides research with him, and I am excited to see amazing things from him in the coming years.

I would like to thank the friends I have made during my time at UC Irvine: Dr. Udara Premachandra, Janine Tom, Mariam Iftikar, Gregory Suryn, Stan Hiew, Dr. Du Nguyen, and Bao Ho. They have made my five years here special, and I will miss their company. I also must thank my Rooted group from Mariner's Church: Phillip and Priscilla Davey; Ron and Leah Silva; Renzo and Katrina Samame. I never imagined enjoying a small group so much, and it has been a blessing to experience life's highs and lows together.

I would not be in a position to write these acknowledgements if not for the tremendous family support I have received for 27 years of my life. Mom (Dianne) and Dad (Alvin) have been incredible parents, and I thank them for everything they have poured into me- from spending their evenings with me as a 1st grader reading books to financially supporting my college tuition in later years. I love them both so very much. I would also like to acknowledge my siblings: Matthew, Shannon, and Elizabeth. They offer love and

laughter when needed most. My Aunt Michela and Uncle David are the best extended family I could ever ask for. My in-laws, Steven and Corinne Frasso, have become wonderful additions to my family over the last two years, and I look forward to growing with them in the years to come. I must also acknowledge Dane Boersma, Andrew Johnson, and Casey Herman who have remained my close friends for nearly ten years. They remain invaluable support despite college years being long gone.

Lastly, I must acknowledge my wife and the love of my life, Jessica Marie Frasso (now Tao). She is the most wonderful and incredible woman I have ever known, and her support over my five years of graduate school has been instrumental to my success. Jessica has given all of her support and love to me inside and outside of the chemistry laboratory. I would not be the man I am today without her by my side, and I cannot wait for where God takes us in the coming years.

Curriculum Vitae

Daniel James Tao
Department of Chemistry
University of California, Irvine
Irvine, CA 92627-2025

Education

University of California, Irvine, Ph.D. Organic Chemistry 2016
Advisor: Prof. Larry Overman
Thesis: Total Synthesis of (–)-Chromodorolide B

Calvin College, B.S. Chemistry 2006-2010
Advisor: Prof. Larry Louters

Professional and Academic Experience

Lecture Teaching Assistant 2015
Organic Chemistry with Prof. James Nowick at UC-Irvine

Laboratory Teaching Assistant 2012-2014
Organic Chemistry with Prof. Renee Link at UC-Irvine

Lecture Teaching Assistant 2011-2012
General Chemistry with Prof. Don Blake at UC-Irvine

High School Chemistry Instructor 2010-2011
International School-Tegucigalpa, Tegucigalpa, Honduras

National Science Foundation Internship in Organometallic Chemistry 2009
University of Michigan, Ann Arbor, MI under Prof. John Montgomery

National Science Foundation Internship in Medicinal Chemistry 2008
Georgia Institute of Technology, Atlanta, GA under Prof. Stefan France

Head Supplemental Instructor for Chemistry 2009-2010
Calvin College Nursing Department

Laboratory Teaching Assistant 2007-2009
Calvin College Chemistry Department

Awards and Scholarships

Knollcrest Grant
Presidential Scholarship
John A. Bolt Memorial Scholarship
Pfizer Scholarship
National Science Foundation Summer Scholarship (2008 and 2009)
UC-Irvine Dissertation Fellowship Award

Publications

Tao, D. J.; Muuronen, M. J. Slutskyy, Y.; Le, A.; Furche, F.; Overman, L. E. Diastereoselective Coupling of Chiral Acetonide Trisubstituted Radicals with Alkenes. *Chem. Eur. J.* **2016**, *22*, 1–6.

Tao, D. J. Slutskyy, Y.; Overman, L. E. Total Synthesis of (–)-Chromodorolide B. *J. Am. Chem. Soc.* **2016**, *138*, 2186–2189.

Büschleb, M.; Dorich, S.; Hanessian, S.; Tao, D. J.; Schenthal, K. B.; Overman, L. E. Synthetic Strategies toward Natural Products Containing Contiguous Stereogenic Quaternary Carbon Atoms. *Angew. Chem. Int. Ed.* **2016**, *55*, 4156–4186.

Oral Presentations

"Progress Toward the Total Synthesis of Chromodorolides A, B, C, D, and E." Tao, D.; Overman, L. E. 246th ACS National Meeting and Exposition in Indianapolis, IN. September 9, 2013.

"Exploiting Photoredox Catalysis in Efforts Toward the Chromodorolide Natural Products." Tao, D.; Overman, L. E. Graduate Symposium at University of California, Irvine in Irvine, CA. June 4, 2015.

Poster Presentations

"Progress Toward the Total Synthesis of Chromodorolides A, B, C, D, and E." Tao, D.; Overman, L. E. The Overman Symposium at Eli Lilly in Indianapolis, IN. September 10, 2013

"Exploiting Photoredox Catalysis in Complex Molecule Synthesis: Total Synthesis of Chromodorolide B." Tao, D.; Overman, L. E. 44th National Organic Chemistry Symposium in College Park, MD. July 2, 2015.

Abstract of the Dissertation

Total Synthesis of (–)-Chromodorolide B

and

Origins of Diastereoselectivity for Conjugate Additions of Trisubstituted Acetonide Radicals

By

Daniel James Tao

Doctor of Philosophy in Chemistry

University of California, Irvine, 2016

Professor Larry E. Overman, Chair

In Chapter 1, the rearranged spongian diterpene class of natural products is discussed. The biological effects of the natural product family on the Golgi apparatus are highlighted along with previous completed total syntheses of members in the family. Early efforts by the Overman group towards the chromodorolide natural products are also discussed, as these model system studies revealed several key insights in developing a second-generation approach.

In Chapter 2, the synthetic routes to (3a*S*,7a*S*)-4,4,7a-trimethyloctahydro-1H-inden-1-one are reported. This chiral fragment is embedded within the hydrophobic subunit of the chromodorolides and is surprisingly difficult to access enantioenriched on multi-gram scale using previously reported routes. Chapter 2 discusses the multiple approaches

that have been developed by other research groups and ours to access this compound. In particular, a novel route using reductive transposition proved nearly thrice as high yielding relative to previously reported methods in preparing to (3a*S*,7a*S*)-4,4,7a-trimethyloctahydro-1H-inden-1-one.

In Chapter 3, the total synthesis of (–)-chromodorolide B is described. The first section discusses an unsuccessful approach to the chromodorolides using a formal [3+2] radical cycloaddition as a novel method to couple highly oxygenated nucleophiles. The second section discusses a revised synthetic strategy using a radical addition/cyclization/fragmentation (ACF) cascade to form two C–C bond and four stereocenters in a single step. Using this key transformation, (–)-chromodorolide B was completed in 21 steps by the longest linear sequence.

In Chapter 4, the diastereoselectivities observed in the ACF cascade are examined. As the cyclization step disfavored the desired C8 stereochemistry, strategies to synthesize α-substituted butenolides are reported. The stereoselection of the coupling reactions with trisubstituted acetonide radicals is also discussed as the couplings typically occurred with diastereoselectivity from the contrasteric face. Detailed experimental and computational studies are reported which reveal several parameters that govern the facial selectivity for the conjugate addition of trisubstituted acetonide radicals.

Chapter 1: Rearranged Spongian Diterpenes and Early Synthetic Efforts to the Chromodorolides

1.1 Rearranged Spongian Diterpenes and Their Biosynthesis

Rearranged spongian diterpenes (RSDs) are a family of natural products[1] with unique terpenoid structural motifs. Each member contains a hydrophobic fragment and an oxygen-rich, hydrophilic fragment often connected by a single C–C bond (Figure 1.1).[2] The oxygenated fragment varies dramatically in structure, from monocyclic (**1.7**) to complex bicyclic (**1.3**, **1.4**, **1.10**) and tricyclic (**1.1**, **1.5**, **1.6**, **1.12**, **1.14**) frameworks. These marine natural products exhibit a variety of biological activities, including antimicrobial,[2h,2k–m,3] anti-inflammatory,[4] antileukemic,[2m,5] and antinematocidal activity.[2m] RSDs are isolated from both marine sponges and their nudibranch predators. It is believed that nudibranches acquire these natural products from the marine sponges as a chemical defense mechanism.[6]

These natural products arise biosynthetically from a common spongian diterpenoid skeleton **1.17** (Scheme 1.1).[1b,7] The biosynthetic pathways for RSDs have not been elucidated to date, but certain insights have been made based on the structures of isolated family members. RSD biosynthesis is hypothesized to commence with oxidative cleavage of the C9/C11 bond of **1.17**,[8] which activates the C9 position for a Wagner-Meerwein shift. Subsequent alkyl shift from C8 or C10 to C9 of decalin **1.18** forms a variety of the observed bicyclic diterpene frameworks. These rearranged skeletons are then proposed to undergo oxidation of the tetrahydrofuran fragment and ring closure to afford the RSD natural products (e.g. **1.8**, **1.11**, **1.12**, **1.15**).

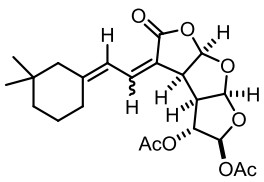

gracilin B, **1.1**: *E* isomer
gracilin C, **1.2**: *Z* isomer

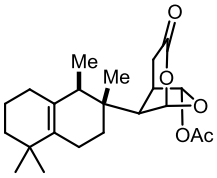

shahamin F, **1.3**

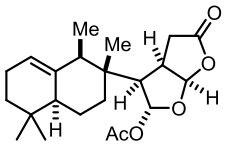

macfarlandin C, **1.4**

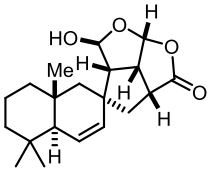

omriolide A, **1.5**

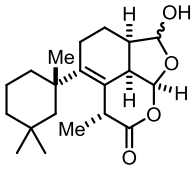

cadlinolide B, **1.6**

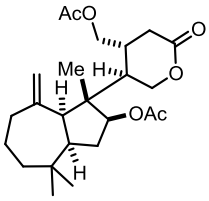

shahamin K, **1.7**

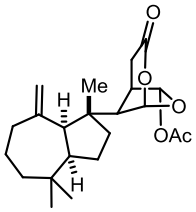

aplyviolene, **1.8**

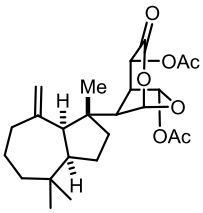

macfarlandin E, **1.9**

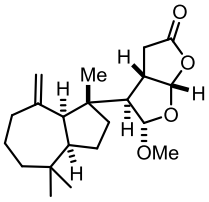

cheloviolene B, **1.10**

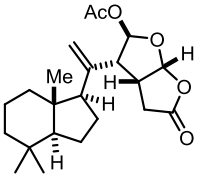

norrisolide, **1.11**

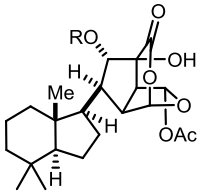

chromodorolide A, **1.12**: R = Ac
chromodorolide D, **1.13**: R = H

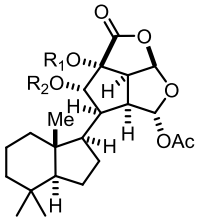

chromodorolide B, **1.14**: R_1, R_2 = Ac
chromodorolide C, **1.15**: R_1 = H, R_2 = Ac
chromodorolide E, **1.16**: R_1, R_2 = H

Figure 1.1. Representative Examples of Rearranged Spongian Diterpenes.

Scheme 1.1. Hypothesized Biosynthesis of Several RSDs.

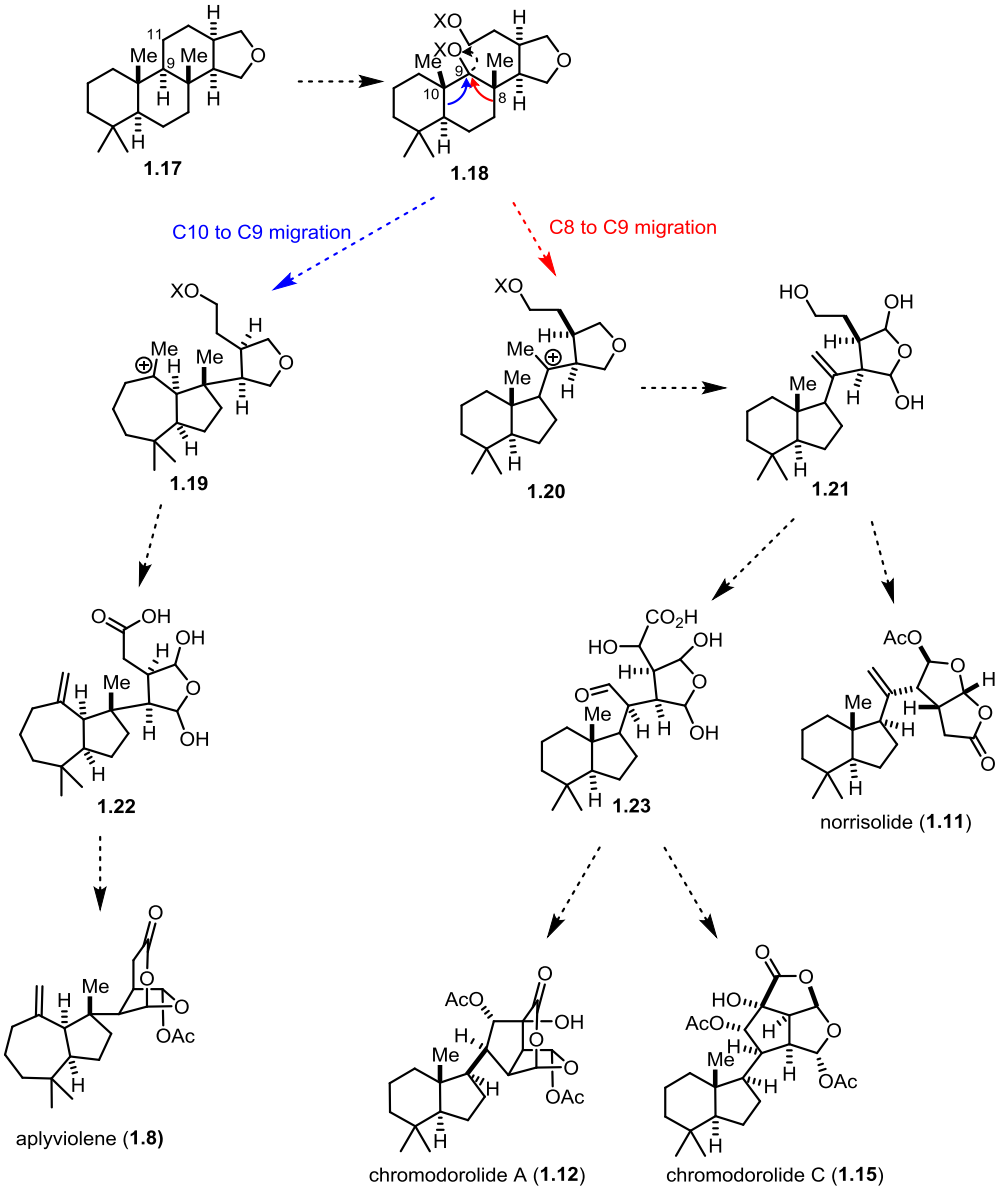

1.2 Previous Total Syntheses of Rearranged Spongian Diterpenes

Because of the structural complexity, the RSD natural product family has received little attention from the synthetic community. To date, total syntheses of only six members in the natural product family have been reported.[9,10] These total syntheses, with the exception of those of gracilin B and C,[9a] targeted RSDs which have the hydrophobic and

hydrophilic fragments joined by a single C–C bond. As this bond provides a convergent disconnection to two equally sized subunits, the total syntheses of these RSDs will be briefly highlighted with emphasis on construction of the central C–C bond.

1.2.1 The Total Synthesis of (+)-Shahamin K

The Overman group's first total synthesis of a RSD was reported in 2001, completing (+)-shahamin K in 18 steps and 4.2% overall yield (Scheme 1.2).[9b] The *cis*-perhydroazulene fragment was constructed from cyclohexanone **1.24** using a previously developed Prins-pinacol reaction[11] initiated by dimethyl(methylthio)sulfonium tetrafluoroborate (DMTSF).[12] Thioether **1.25** was then functionalized to ketone **1.26**, the nucleophilic precursor for fragment coupling. Treatment of ketone **1.26** with strong base under equilibrating conditions generated the thermodynamic enolate, which underwent an intermolecular Michael addition to activated cyclopentenone acceptor **1.27** to forge the central C–C bond in good yield as a single stereoisomer (**1.28**). The high diastereoselectivity of this coupling originates from enolate attack from the convex face of the *cis*-bicyclo[5.2.0]decanone *anti* to the substituted γ-methylene sidechain of acceptor **1.27**. With all requisite carbon bonds constructed, dione **1.28** was carried forward to complete (+)-shahamin K.

Scheme 1.2. Total Synthesis of (+)-Shahamin K.

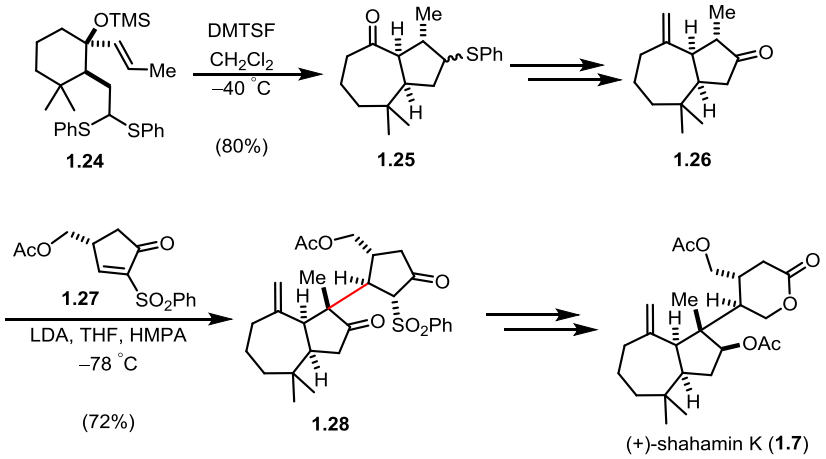

1.2.2 The Total Syntheses of Norrisolide

1.2.2.1 The Theodorakis Route

Theodorakis reported the first total synthesis of (+)-norrisolide in 2004 (Scheme 1.3).[9c] Synthesis of the oxygenated fragment commenced with a Diels-Alder reaction between 1,3-butadiene and butenolide **1.30**. Following carbonyl reduction and ring-opening oxidative cleavage, *cis*-dioxabicyclo[3.3.0]octane aldehyde **1.32** was transformed over several steps to electrophilic coupling precursor **1.33**. The hydrophobic fragment, vinyl iodide **1.34**,[13] underwent lithium-halogen exchange with *tert*-butyllithium. The corresponding vinyl lithium species then underwent 1,2-addition to aldehyde **1.32**, constructing the central C–C bond in 71% yield after oxidation to enone **1.35**. Following several manipulations, Theodorakis completed the synthesis of (+)-norrisolide in 24 steps and 1.3% overall yield.

Scheme 1.3. The Theodorakis Total Synthesis of (+)-Norrisolide.

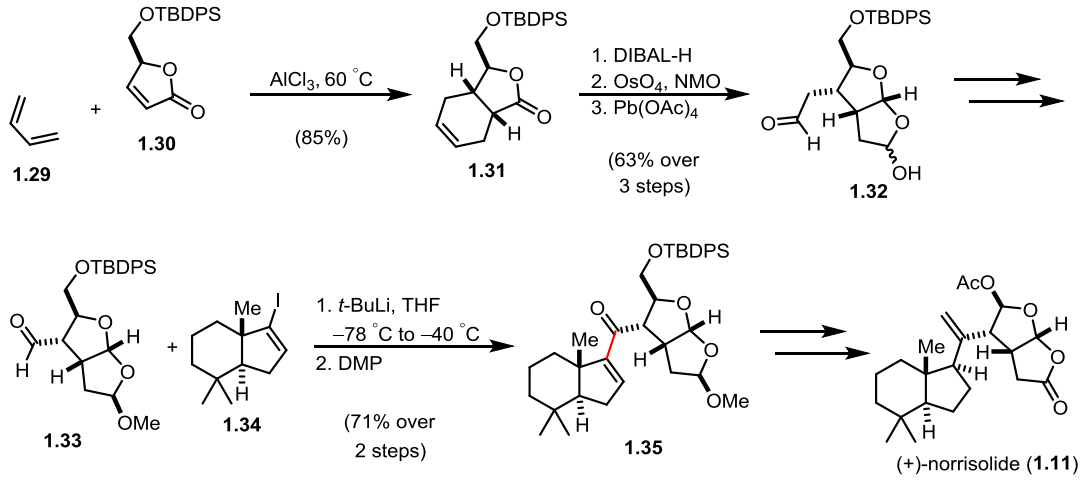

1.2.2.2 The Snapper Route

Snapper reported an alternate route to (+)-norrisolide in 2012 (Scheme 1.4),[9d] beginning with rhodium-catalyzed asymmetric cyclopropanation of furanone **1.36**.[14] Ring expansion of cyclopropane **1.38** and further functionalization afforded amide **1.39**. Hydrazone **1.40** was treated with *n*-butyllithium to mediate Shapiro-like decomposition to a vinyllithium intermediate which coupled to amide **1.39**, forming the central C–C bond of **1.41** in 92% yield. Following several redox manipulations, (+)-norrisolide was completed in 14 steps and 1.7% overall yield.

Scheme 1.4. The Snapper Total Synthesis of (+)-Norrisolide.

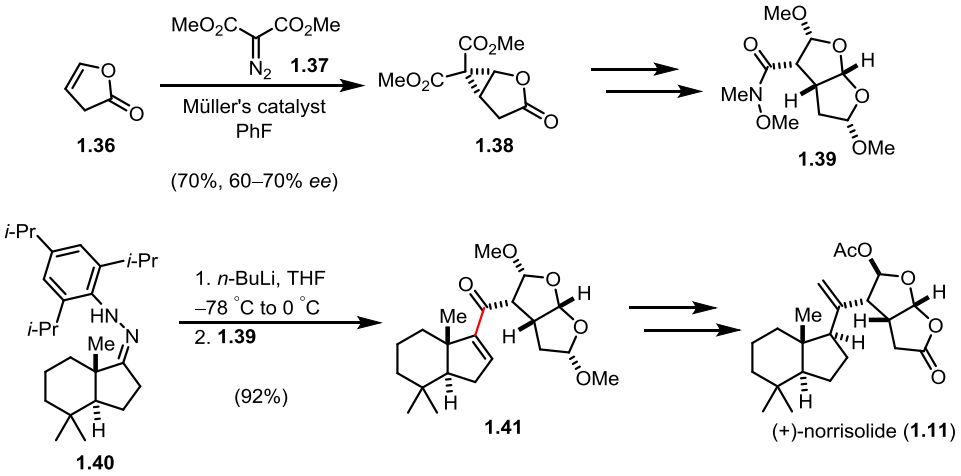

1.2.3 The Total Syntheses of Aplyviolene

1.2.3.1 The Overman First-Generation Route

The first total synthesis of (–)-aplyviolene was reported in 2011 by the Overman group,[9e] in which the hydrophobic and hydrophilic fragments were coupled using a Michael addition strategy similar to the approach utilized in the total synthesis of (+)-shahamin K. Shown in Scheme 1.5, ketone **1.26**[9b] underwent thermodynamic enolate formation and 1,4-addition to bromocyclopentenone **1.42** in 81% yield giving **1.43** as a single stereoisomer.[9b] Completion of (–)-aplyviolene required three steps to remove the extraneous C7 carbonyl after fragment coupling. Following deoxygenation and construction of the dioxabicyclo[3.2.1]octa-3-one ring system, the natural product was completed in 14 steps and 5.6% overall yield from **1.26**.

Scheme 1.5. The Overman First-Generation Total Synthesis of (–)-Aplyviolene.

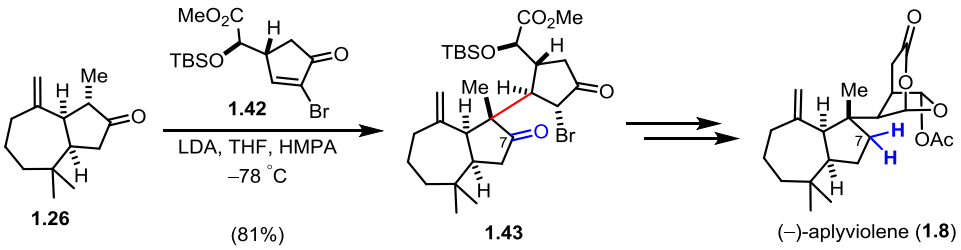

1.2.3.2 The Overman Second-Generation Route

The second-generation synthesis of (–)-aplyviolene[9f] circumvented the three-step sequence to remove the C7 ketone in the first-generation synthesis by employing a radical coupling strategy. The *cis*-perhydroazulene coupling partner, (*N*-acyloxy)phthalimide **1.44**, was synthesized in 15 steps from (+)-fenchone (Scheme 1.6). The (*N*-acyloxy)phthalimide functionality would serve as the radical precursor. Okada previously reported reductive photoredox conditions[15] that induced decarboxylation of (*N*-

acyloxy)phthalimides to generate carbon-centered radicals. The resulting nucleophilic radicals could be reduced by hydrogen atom abstraction or trapped by 1,4-addition to electron-deficient alkenes. Exposure of (*N*-acyloxy)phthalimide **1.44** to a modification of Okada's photoredox conditions generated tertiary radical **1.45**, which underwent 1,4-addition to chlorocyclopentenone **1.46**. Coupled product **1.47** was isolated in 61% yield as a single diastereomer with the desired configuration to be carried forward to (–)-aplyviolene using methods developed in the first-generation route. This key radical coupling reduced the step count of the overall synthesis, completing the natural product in 20 steps.

Scheme 1.6. The Overman Second-Generation Total Synthesis of (–)-Aplyviolene.

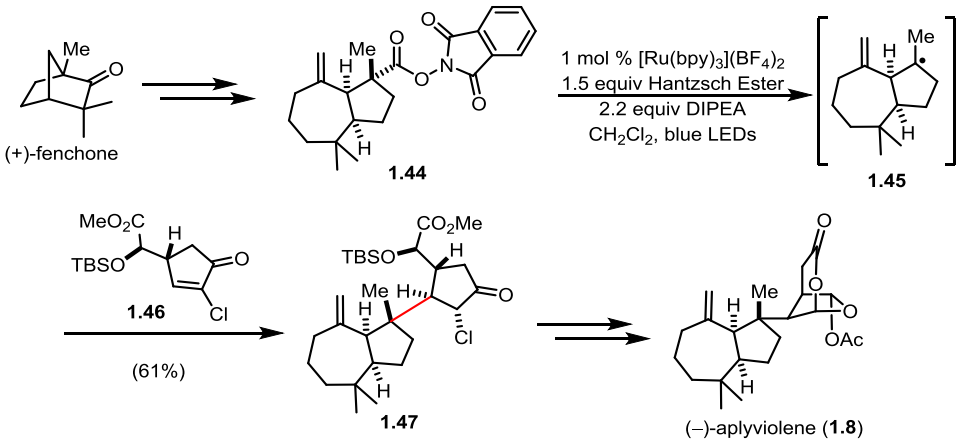

1.3 RSDs and Biological Effects on the Golgi Apparatus

The Overman group has been interested in RSDs for their structural complexity and more recently for their intriguing Golgi-modifying properties. The Golgi apparatus is an organelle in eukaryotic cells responsible for post-translational modifications and packaging of proteins into vesicles for transportation to various cellular destinations.[16] This organelle has garnered attention by the biological community as its function or dysfunction has been associated with a variety of ailments, including cancer[17] and neurodegenerative diseases.[18]

Previous research groups have elucidated key features of the Golgi's function in protein transport and regulation of membrane dynamics using small molecule Golgi disruptors (Figure 1.2: brefeldin A, **1.48**;[19] ilimaquinone, **1.49**;[20] norrisolide, **1.11**[21]). Upon exposure to rat kidney cells, these small molecules induced fragmentation of the Golgi wherein the resulting Golgi fragments dispersed throughout the cytosol (Figure 1.3B). Macfarlandin E (**1.9**), a RSD, exhibited a unique biological phenotype on the Golgi structure of rat kidney cells.[22] Upon exposure to rat kidney cells, **1.9** induced irreversible fragmentation of the Golgi apparatus, but the Golgi fragments remained localized around the endoplasmic reticulum (Figure 1.3D). A truncated macfarlandin E analog, *tert*-butyl MacE (**1.50**), was synthesized by the Overman group and found to exhibit the same phenotype as the natural product in rat kidney cells.[22] This study demonstrated that the oxygenated 2,7-dioxabicyclo[3.2.1]octan-3-one subunit was responsible for this unusual biological activity on Golgi morphology. Incorporation of oxidation at C6 of **1.9** and **1.50** was essential to induce this unique Golgi phenotype, as aplyviolene (**1.8**) and related analogues did not exhibit the same phenotype.[22,23] Shown in Scheme 1.7, the novel Golgi phenotype is hypothesized to arise from ring-opening to dialdehyde species **1.52** under physiological conditions in the cell. It is believed that a lysine residue then condenses with the dialdehyde portion to form pyrrole **1.53**. Gramine fragmentation of pyrrole **1.53** then generates an electrophile (**1.54**) for reaction with a separate nucleophile. Access to other RSDs or their truncated analogues embedding these structural features could provide novel biological probes for further insight into the Golgi's function.

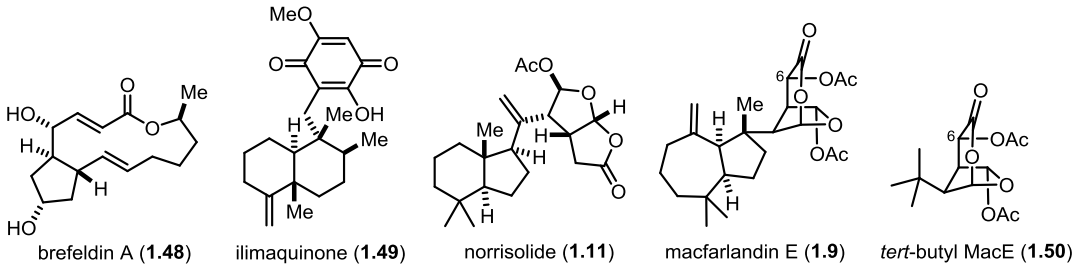

Figure 1.2. Known Golgi-Modifying Agents.

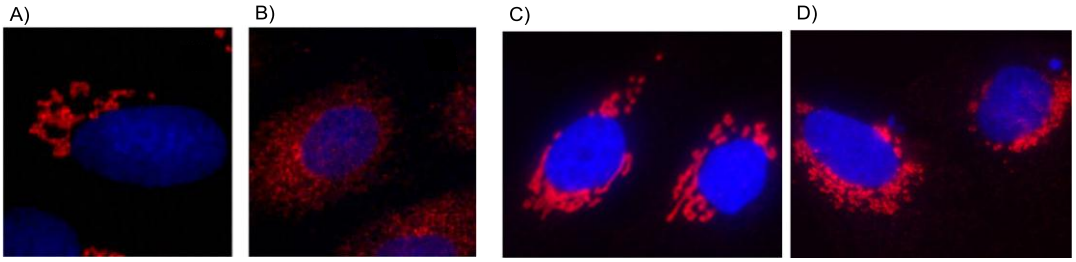

Effect of norrisolide (**1.11**) exposure on Golgi in rat kidney cells at t = 0 min (left, A) and t = 60 min (right, B). The Golgi fragments (red) were analyzed against the nucleus (blue).

Effect of macfarlandin E (**1.9**) exposure on Golgi in rat kidney cells at t = 0 min (left, C) and t = 60 min (right, D). The Golgi fragments (red) were analyzed against the nucleus (blue).

Figure 1.3. Fragmentation Phenotypes of Golgi Disruptors.

Scheme 1.7. Proposed Mechanism for Unique Golgi Phenotype of 6-Acetoxy-2,7-dioxabicyclo[3.2.1]octa-3-ones.

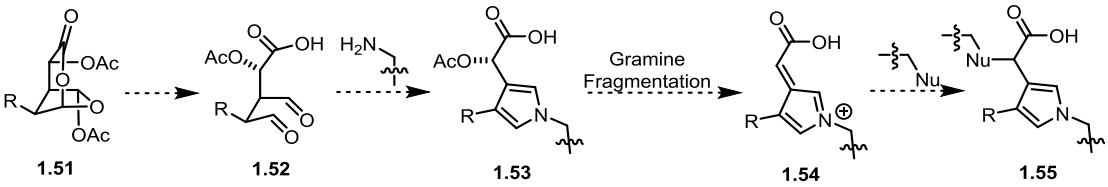

The 7-dioxabicyclo[3.2.1]octan-3-one subunit (highlighted in red, Figure 1.4) is also found in the RSDs chromodorolides A[2k] and D.[2n] These natural products feature an additional 5-membered ring fused to the biologically relevant 7-dioxabicyclo[3.2.1]octan-3-one moiety. Chromodorolides B, C, and E (**1.14**–**1.16**) also contain similar oxygenation patterns (highlighted in blue); but the lactones in these natural products are incorporated into a fused tricyclic motif. The impact of these bridged and fused tricyclic ring systems

on the Golgi apparatus has not been explored. At the start of my dissertation research, no synthetic efforts for any of the chromodorolides[24] or their highly functionalized, oxygen-rich tricyclic frameworks had been reported. The unprecedented ring systems and the potential Golgi-modifying properties of the chromodorolides prompted the Overman group to develop a synthetic strategy to access these natural products.

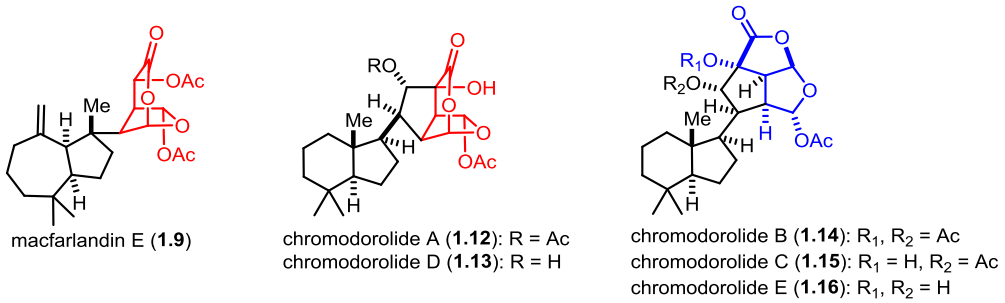

Figure 1.4. The 7-Dioxabicyclo[3.2.1]octan-3-one in Bridged Chromodorolides and Related Framework in Fused Chromodorolides.

1.4 Approach to Both Chromodorolide Scaffolds

Structural examination of representative bridged and fused chromodorolides A (**1.12**) and C (**1.15**), respectively, revealed similar carbon skeletons with variation of the lactone and acetyl group at C15 and C16. Retrosynthetically, disconnection of the lactone-acetal bond in **1.12** and **1.15** would arrive at acid intermediate **1.56** as a common precursor (Scheme 1.8). We envisioned that both fused and bridged tricyclic frameworks would be accessible from acid **1.56** by site-selective oxocarbenium ion formation followed by intramolecular carboxylic acid trapping. To generate fused chromodorolide **1.15**, we hypothesized that closure to the 5-membered lactone would be thermodynamically favorable if oxocarbenium ion formation occurred at both C15 and C16. In contrast, to construct the bridged system of **1.12**, oxocarbenium ion formation must occur

regioselectively at C15 to permit 6-membered ring closure. This result could potentially be accomplished by installation of a more activated leaving group on C15 relative to the acetal group on C16.

Scheme 1.8. Access to Bridged and Fused Chromodorolides from Acid 1.56.

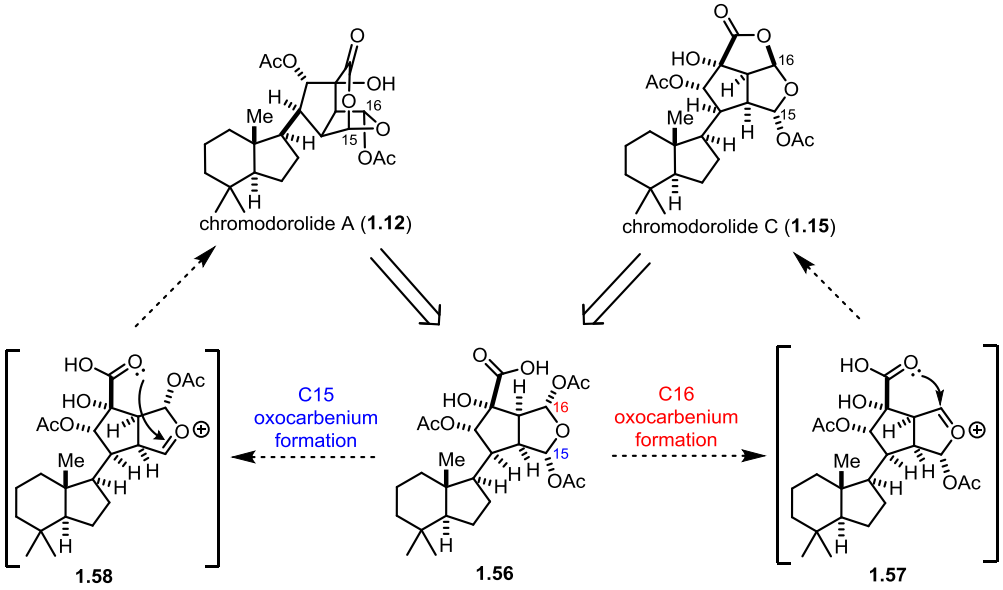

1.5 Preliminary Studies Toward the Chromodorolides

1.5.1 Model System Retrosynthetic Analysis

To assess the site-selective oxocarbenium ion formation/trapping strategy in accessing both the bridged and fused chromodorolides, truncated versions of the RSDs replacing the hydrophobic fragment for an isopropyl group were targeted (**1.59** and **1.60**, Scheme 1.9). These compounds would arise from site-selective oxocarbenium ion formation/carboxylic trapping at C15 or C16 from carboxylic acid **1.61**, in which C15 would harbor a more activated acetoxy group than C16's methoxy group. The vicinal *cis*-diols of acid **1.61** would be installed by dihydroxylation of an α,β-unsaturated ester from the convex face of the *cis*-oxabicyclo[3.3.0]octenone. The C15 acetoxy group would arise

from reduction and acylation of lactone **1.62**, which would arise from a phosphine-promoted [3+2] dipolar cycloaddition between allene **1.63** and butenolide **1.64**.[25]

Scheme 1.9. Retrosynthesis of Truncated Chromodorolide Analogues.

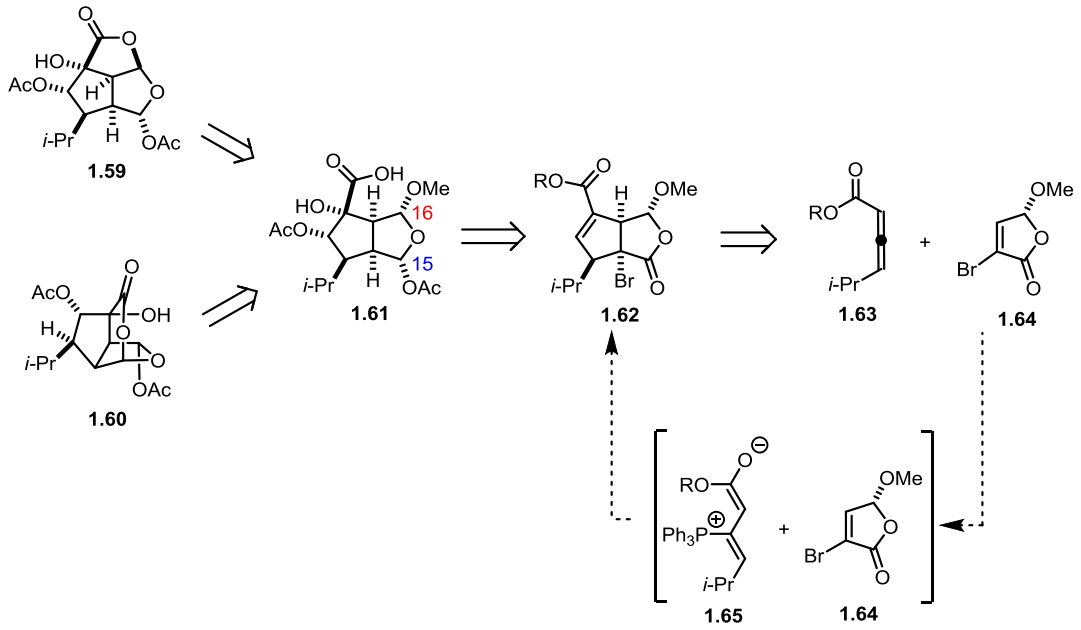

1.5.2 Synthesis of *Cis*-Oxabicyclo[3.3.0]octenone and Unexpected Dihydroxylation Diastereoselectivity

The synthesis commenced with preparation of the [3+2] dipolar cycloaddition precursors (Scheme 1.10), which was developed exclusively by Dr. Philipp Kohler.[26] The 1,3-dipole precursor was accessed by a three-step sequence from methyl bromoacetate **1.66**. Halogen displacement by triphenylphosphine followed by deprotonation afforded ylide **1.67**. Exposure of ylide **1.67** to acyl chloride **1.68** with triethylamine induced ketene Wittig olefination to give allene **1.63**. Dipolarophile **1.64** was accessed from (±)-3-hydroxybutenolide (**1.69**) by its conversion to methoxybutenolide **1.70** followed by one-pot dibromination and elimination.

Scheme 1.10. Synthesis of Dipolar Cycloaddition Precursors.

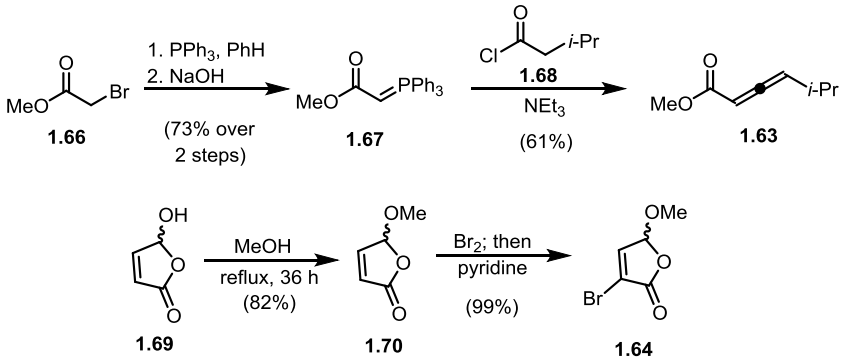

With both cycloaddition precursors in hand, the key [3+2] dipolar cycloaddition was then explored. Using slight modifications to reported conditions,[27] allene **1.63** and bromobutenolide **1.64** underwent a phosphine-promoted [3+2] dipolar cycloaddition in 36% yield as a single diastereomer (**1.71**, Scheme 1.11). The α-bromide of cycloadduct **1.71** was then reduced with zinc,[28] and dihydroxylation of enoate **1.72** was examined. Unexpectedly, dihydroxylation using NMO and catalytic OsO_4 took place with high selectivity from the undesired concave face of the *cis*-oxabicyclo[3.3.0]octenone (product **1.74**). A collaboration with the Houk group[29] revealed the contrasteric selectivity for dihydroxylation arose from torsional steering effects. The computed transition state structures for osmium-mediated dihydroxylation from the convex face (Figure 1.5, right) revealed larger destabilizing eclipsing interactions than from the concave face (Figure 1.5, left). As Dr. Kohler was unable to find conditions favoring dihydroxylation or epoxidation from the desired convex face (requisite for the chromodorolides),[26] I sought an alternative route to investigate the site-selective oxocarbenium formation/trapping strategy.

Scheme 1.11. [3+2] Dipolar Cycloaddition and Dihydroxylation of Resulting Cycloadduct.

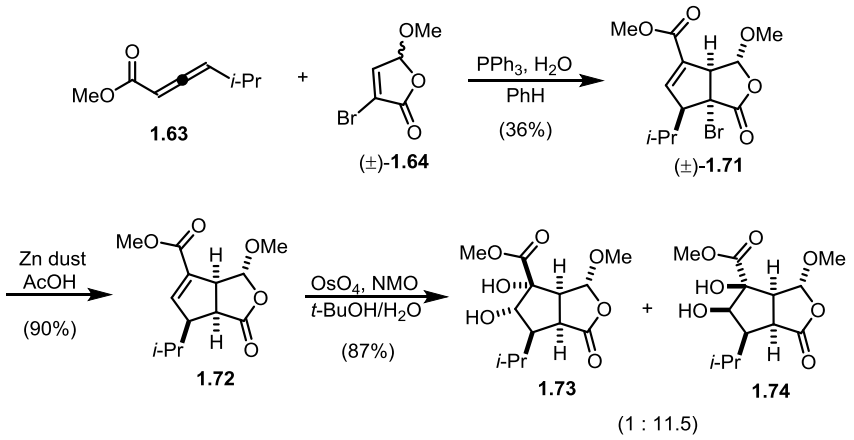

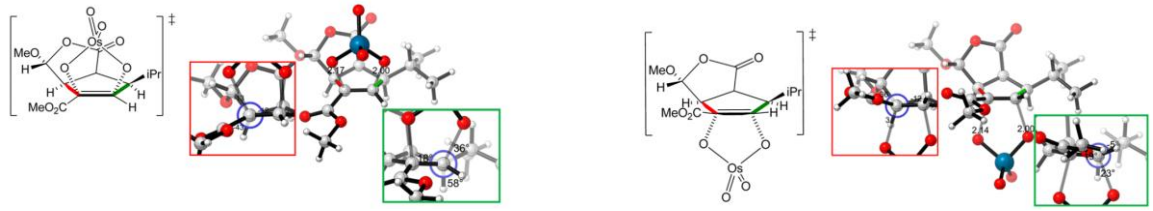

Figure 1.5. Torsional Steering Effects in Osmium-Mediated Dihydroxylation of *Cis*-oxabicyclo[3.3.0]octenone.

1.5.3 Hydrogenation and Cyclization to Fused Tricyclic Framework

As the vicinal diol functionality was not essential for probing site-selective oxocarbenium ion trapping, I investigated these issues in a model system lacking the natural products' oxygenation. Cycloadduct **1.75**[30] underwent chemoselective lactone reduction and *in situ* acetylation to give diacetal **1.76** in low yield (Scheme 1.12). A variety of reduction conditions were attempted, but selective reduction of the lactone proved difficult in the presence of the enoate.[31] Small quantities of diacetal **1.76** were obtained as an anomeric mixture, which underwent palladium-catalyzed benzyl ester deprotection and alkene hydrogenation to give a mixture of carboxylic acid diastereomers **1.77**. I believed

these diastereomers were inconsequential as the carboxylic acid's α-stereocenter could epimerize under oxocarbenium ion formation reaction conditions. Treatment with BF_3•Et_2O at 23 ºC afforded fused tricyclic product **1.78** as a mixture of anomers in 80% yield. The exclusive formation of the fused tricyclic product **1.78** under strongly Lewis acidic conditions provided experimental support for our hypothesis that the fused tricyclic framework was thermodynamically favorable compared to the analogous bridged framework.

These preliminary studies were successful in constructing the tricyclic carbon skeleton embedded within fused chromodorolides B, C, and E. However, the model system also revealed that the proposed synthetic route would not install the vicinal diol functionality with the desired stereochemistry. Therefore, I required an alternative strategy to incorporate this challenging oxygenation and access the chromodorolides.

Scheme 1.12. Construction of the Truncated Fused Chromodorolide Framework.

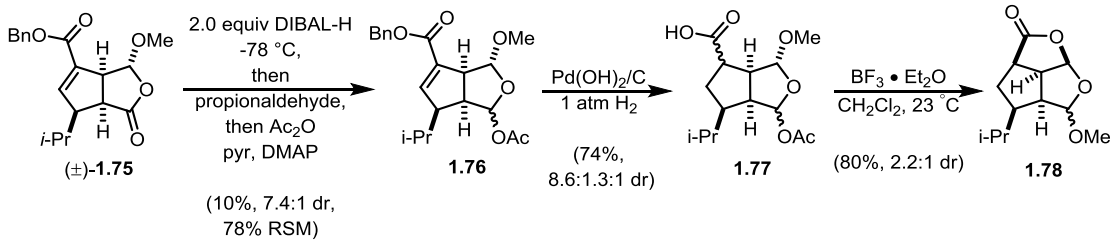

1.6 Experimental Section

1.6.1 General Experimental Details

Unless stated otherwise, reactions were conducted in oven-dried glassware under an atmosphere of nitrogen or argon. Tetrahydrofuran (THF), diethylether, toluene, dichloromethane, methanol (MeOH), pyridine, and triethylamine were dried by passage through activated alumina. All commercial reagents were used as received unless otherwise

noted. Reaction temperatures were controlled using an IKAmag temperature modulator. Thin-layer chromatography (TLC) was conducted with E. Merck silica gel 60 F254 pre-coated plates (0.25 mm), and visualized by exposure to UV light (254 nm) or stained with anisaldehyde, ceric ammonium molybdate, and potassium permanganate. Flash column chromatography was performed using normal phase silica gel (60 Å, 230─240 mesh, Merck KGA). ^{1}H NMR spectra were recorded on Bruker spectrometers (at 500 or 600 MHz) and are reported relative to $CHCl_3$ signals. Data for ^{1}H NMR spectra are reported as follows: chemical shift (δ ppm), multiplicity, coupling constant (Hz) and integration. ^{13}C NMR spectra were recorded on Bruker Spectrometers (at 125 MHz). Data for ^{13}C NMR spectra are reported in terms of chemical shift (δ ppm). IR spectra were recorded on a Varian 640-IR spectrometer and are reported in terms of frequency of absorption (cm^{-1}). High resolution mass spectra were obtained from the UC Irvine Mass Spectrometry Facility with a Micromass LCT spectrometer. See JOC Standard Abbreviations and Acronyms for abbreviations (available at http://pubs.acs.org/userimages/ContentEditor/1218717864819/joceah_abbreviations.pdf).

1.6.2 Experimental Procedures

(Triphenyl-λ^5-phosphanylidene)benzyl acetate (S1.1): The procedure for the preparation of **S1.1** was followed from the literature procedure.[32] To a solution of triphenylphosphine (44.9 g, 171 mmol) in benzene (100 mL) at 0 °C was added benzyl bromoacetate (40.0 g, 175 mmol) dropwise over 15 min to maintain the temperature below 30 °C. The solution was stirred at 23 °C for

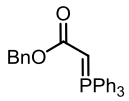

S1.1: $C_{27}H_{23}O_2P$
Molecular Weight: 410.4528

3 h, at which point the resulting suspension was filtered, retaining the solid formed from the reaction. This solid was washed with benzene (1 x 100 mL) and pentanes (1 x 100 mL). The solid was air dried and dissolved in CH_2Cl_2 (180 mL). Solid NaOH pellets (6.85 g, 171 mmol) dissolved in water (60 mL) was added dropwise over 20 min at 23 °C, and the mixture stirred for 40 min. The solution was filtered, dried over Na_2SO_4, and concentrated *in vacuo*. The resulting solid was recrystallized from EtOAc. Upon concentration *in vacuo*, **S1.1** was obtained as a colorless powder (52.4 g, 127 mmol, 73%). Spectral data were consistent with previously reported data.[32]

***rac*-5-Methylhexa-2,3-dienoic acid benzyl ester (S1.2):** The procedure for the preparation of **S1.2** was followed from the literature procedure.[29] To a solution of NEt_3 (1.97 g, 19.5 mmol) in CH_2Cl_2 (48 mL) was added **S1.1** (8.00 g, 19.5 mmol) and, the solution was maintained for 10 min at 0 °C. Isovaleryl chloride (2.35 g, 19.5 mmol) in CH_2Cl_2 (16 mL) was then added slowly over 20 min and then allowed to warm to 23 °C over 1 h. The solution was concentrated *in vacuo*, and hexanes (100 mL) was added. After sitting for 30 min, the solution was filtered and concentrated *in vacuo*. The resulting yellow filtrate was then purified by flash column chromatography (100% CH_2Cl_2) to yield **S1.2** as a clear oil (2.58 g, 11.9 mmol, 61% yield). Spectral data were consistent with previously reported data.[33]

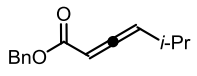

S1.2: $C_{14}H_{16}O_2$
Molecular Weight: 216.2800

***rac*-(3*R*,3a*S*,6*S*,6a*R*)-Benzyl 6a-bromo-6-isopropyl-3-methoxy-1-oxo-3,3a,6,6a-tetrahydro-1*H*-cyclopenta[*c*]furan-4-carboxylate (S1.3):** The procedure for the preparation of **S1.3** was followed from the literature procedure.[29] Butenolide **1.64** (1.16 g, 6.01 mmol) and allene **S1.2** (1.95 g, 9.02 mmol) were charged in a flask in benzene (6 mL). Triphenylphosphine (3.15 g, 12.0 mmol) in benzene (6 mL) was degassed by bubbling nitrogen gas through the solution for 10 min, which was added to the flask followed by H_2O (0.210 g, 12.0 mmol). The solution stirred at 23 °C for 50 min at which point silica gel (~ 3 g) was added, and the solution was concentrated *in vacuo*. Upon purification with flash column chromatography (5% EtOAc in hexanes), cycloadduct **S1.3** (0.619 g, 1.92 mmol, 32% yield) was isolated as a yellow oil. ^{1}H NMR (500 MHz, $CDCl_3$) δ 7.43–7.32 (m, 5H), 6.88 (app t, *J* = 2.0 Hz, 1H), 5.42 (d, *J* = 1.0 Hz, 1H), 5.33 (d, *J*= 12.0 Hz, 1H), 5.16 (d, *J*= 12.0 Hz, 1H), 4.05 (m, 1H), 3.51 (s, 3H), 3.38 (dt, *J* = 6.6 Hz, 2.0 Hz, 1H), 2.35 (app sext, *J* = 6.6 Hz, 1H), 1.27 (d, *J* = 6.6 Hz, 3H), 0.89 (d, *J* = 6.6 Hz, 3H); ^{13}C NMR (125 MHz, $CDCl_3$) δ 172.1, 162.1, 146.2, 135.2, 131.5, 128.8, 128.7, 128.4, 105.2, 67.0, 66.8, 64.1, 57.5, 53.6, 27.4, 23.5, 20.6; IR (thin film) 2960, 2927, 1784, 1714, 1349 cm^{-1}; HRMS (ESI) calculated for $C_{19}H_{21}{}^{79}BrO_5Na$ (M+Na) 431.0470, observed 431.0453.

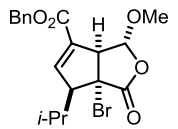

S1.3: $C_{19}H_{21}BrO_5$
Molecular Weight: 409.2760

***rac*-(3*R*,3a*S*,6*S*,6a*S*)-Benzyl-6-isopropyl-3-methoxy-1-oxo-3,3a,6,6a-tetrahydrohydro-1*H*-cyclopenta[*c*]furan-4-carboxylate (1.75):** The procedure for the preparation of **1.75** was followed from the literature procedure.[29] To a solution of cycloadduct **S1.3** (0.568 g, 1.39 mmol) in AcOH (10 mL), Zn dust (1.42 g, 21.7 mmol) was added. The mixture stirred at 23 °C for 3 h before the solution was filtered through Celite with EtOAc (30 mL), washed with aqueous $NaHCO_3$ (3 x 25 mL), and washed with brine (1 x 25 mL). The combined organic layers were dried over Na_2SO_4, filtered, and concentrated *in vacuo* to afford lactone **1.75** (0.411 g, 1.25 mmol, 90% yield) as a colorless solid. ^{1}H NMR (500 MHz, $CDCl_3$) δ 7.43–7.31 (m, 5H), 6.96 (s, 1H), 5.423(s, 1H), 5.29 (d, *J*= 9.0 Hz, 1H), 5.15 (d, *J*= 9.0 Hz, 1H), 3.66 (d, *J* = 7.2 Hz, 1H), 3.46 (s, 3H), 3.39 (app t, *J* = 8.3 Hz, 1H), 2.82 (app t, *J* = 8.8 Hz, 1H), 2.19 (sept, *J* = 6.6 Hz, 1H), 1.17 (d, *J* = 6.6 Hz, 3H), 0.89 (d, *J* = 6.6 Hz, 3H); ^{13}C NMR (125 MHz, $CDCl_3$) δ 175.5, 163.4, 148.3, 135.4, 132.4, 128.5, 128.3, 128.2, 104.7, 66.4, 56.5, 55.9, 53.2, 42.7, 26.9, 22.9, 21.1; IR (thin film) 2960, 1778, 1713, 1270 cm^{-1}; HRMS (ESI) calculated for $C_{19}H_{22}O_5Na$ (M+Na) 353.1365, observed 353.1374.

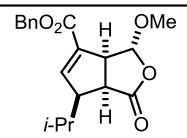

1.75: $C_{19}H_{22}O_5$
Molecular Weight: 330.3800

***rac*-(3*R*,3a*S*,6*S*,6a*S*)-Benzyl 1-acetoxy-6-isopropyl-3-methoxy-3,3a,6,6a-tetrahydro-1H-cyclopenta[*c*]furan-4-carboxylate (1.76):** Lactone **1.75** (0.286 g, 0.866 mmol) was issolved in toluene (5 mL) and THF (2 mL). The solution was then cooled to –78 °C, and DIBAL-H (0.15 g, 1.0 mmol, 0.19 mL) dissolved in toluene (0.7 mL) was added to the reaction flask slowly over 10 min. The solution then stirred at –78 °C for 2 h, at

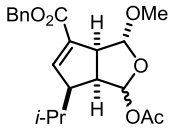

1.76: $C_{21}H_{26}O_6$
Molecular Weight: 374.4330

which point propionaldehyde (0.181 g, 3.12 mmol) was added to quench remaining DIBAL-H. The solution was maintained at –78 °C for 30 min before the addition of DMAP (0.212 g, 1.73 mmol) and pyridine (0.21 g, 2.6 mmol) were added, followed by slow addition of Ac_2O (0.53 g, 5.2 mmol) over 15 min. After 1 h, saturated aqueous NH_4Cl soln (2.5 mL) and saturated aqueous Rochelle's salt soln (2.5 mL) were added. The reaction mixture was then warmed to 23 °C. The aqueous layer was extracted with EtOAc (3 x 10 mL), followed by washes with aqueous $NaHCO_3$ soln (3 x 15 mL) and brine (15 mL). The organic layers were then dried with Na_2SO_4, filtered, and concentrated *in vacuo*. The crude residue was purified by flash column chromatography (10% EtOAc in hexanes) to provide recovered starting material **1.75** (0.225 g, 0.681 mmol, 79%) and **1.76** (32 mg, 0.085 mmol, 10% yield) as a clear oil in a 7.4:1 ratio of inseparable diastereomers. Data for major anomeric isomer of **1.76**: ^{1}H NMR (500 MHz, $CDCl_3$) δ 6.88 (t, *J* = 2.1 Hz, 1H), 6.36 (d, *J* = 2.7 Hz, 1H), 5.27 (s, 1H), 5.25 (d, *J* = 12.4 Hz, 1H), 5.14 (d, *J* = 12.4 Hz, 1H), 3.64 (app dt, *J* = 7.4, 2.4 Hz, 1H), 3.34 (s, 3H), 3.20 (app td, *J* = 7.7, 2.6 Hz, 1H), 2.66 (ddd, *J* = 7.8, 2.2, 2.1 Hz, 1H), 2.09 (s, 3H), 1.82 (sept, *J* = 6.5 Hz, 1H), 1.06 (d, *J* = 6.5 Hz, 3H) 0.94 (d, *J* = 6.5 Hz, 3H); ^{13}C NMR (125 MHz, $CDCl_3$) δ 170.6, 164.2, 148.0, 135.9, 133.7, 128.8, 128.5, 128.4, 108.8, 99.8, 66.5, 56.9, 55.8, 55.1, 48.7, 28.6, 22.1, 21.8, 21.4; IR (thin film) 2962, 2873, 1734, 1368, 1235 cm^{-1}; HRMS (ESI) calculated for $C_{21}H_{26}O_6Na$ (M+Na) 397.1627, observed 397.1620.

***rac*-(3*R*,3a*S*,6*R*,6a*S*)-1-Acetoxy-6-isopropyl-3-methoxyhexahydro-1H-cyclopenta[*c*]furan-4-carboxylic acid (1.77):** Diacetal **1.76** (24 mg, 0.064 mmol) was dissolved in EtOAc (3 mL) and AcOH (4 mg, 0.06 mmol). Pearlman's catalyst (13 mg, 0.019 mmol) was then added to the solution. The flask was placed under vacuum and backfilled with hydrogen gas before being maintained at 23 °C for 12 h. The mixture was filtered through Celite with EtOAc (5 mL) and concentrated *in vacuo*. The resulting yellow oil was washed in the flask with hexanes (2 x 1 mL), and the hexane layer was removed. The resulting product was then concentrated *in vacuo* to provide **1.77** as a yellow oil (14 mg, 0.047 mmol, 74% yield) as a 8.6:1.3:1 mixture of diastereomers. Data for major diastereomer of **1.77**: ^{1}H NMR (500 MHz, $CDCl_3$) δ 6.32 (s, 1H), 4.98 (s, 1H), 3.31 (s, 3H), 3.12 (app t, *J* = 8.7 Hz, 1H), 2.99 (app t, *J* = 7.5 Hz, 1H), 2.96–2.92 (m, 1H), 2.09 (s, 3H), 1.99 (app dt, *J* = 11.2, 5.6 Hz, 1H), 1.73–1.66 (m, 1H), 1.63–1.56 (m, 1H), 1.45 (app q, *J* = 12.6 Hz, 1H), 0.97 (d, *J* = 6.5 Hz, 3H), 0.93 (d, *J* = 6.5 Hz, 3H); ^{13}C NMR (125 MHz, $CDCl_3$) δ 170.6, 109.3, 99.6, 55.0, 51.3, 50.4, 49.8, 32.0, 29.6, 22.5, 21.8, 21.4; IR (thin film) 3527, 2962, 2873, 1738, 1235 cm^{-1}; HRMS (ESI) calculated for $C_{14}H_{21}O_6$ (M–H) 285.1138, observed 285.1142.

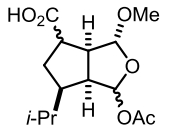

1.77: $C_{14}H_{22}O_6$
Molecular Weight: 286.3240

***rac*-(2a*S*,2a[1]*S*,3*R*, 4a*R*, 6a*R*)- 3-Isopropyl-2-methoxyhexahydro-1,6-dioxa-cyclopenta[*cd*]pentalen-5(2H)-one (1.78):** Carboxylic acid **1.77** (13 mg, 0.045 mmol) was dissolved in CH_2Cl_2 (1 mL), and BF_3•OEt_2 (17 mg, 0.14 mmol) was added slowly over 15 min. The solution stirred at 23 °C for 3 h, and saturated aqueous $NaHCO_3$ solution (1.5 mL) was added. The aqueous layer was diluted with water (1.5 mL), and the aqueous layer was extracted with CH_2Cl_2 (3 x 2 mL) and EtOAc (2 mL). The combined organic layers were dried over Na_2SO_4 and concentrated *in vacuo*. The crude residue was then purified by flash column chromatography (30% EtOAc in hexanes) to provide **1.78** as a yellow oil (8 mg, 0.04 mmol, 80% yield) as a 2.2:1 ratio of acetal diastereomers. Data for major anomeric isomer of **1.78**: ^{1}H NMR (500 MHz, $CDCl_3$) δ 6.02 (d, *J* = 6.0 Hz, 1H), 5.06 (d, *J* = 3.6 Hz, 1H), 3.57–3.51 (m, 1H), 3.44 (s, 3H), 3.02 (app q, *J* = 9.8 Hz, 1H), 2.79–2.73 (m, 1H), 2.39 (ddd, *J* = 12.9, 9.4, 6.7 Hz), 1.85 (ddd, *J* = 17.1, 13.3, 6.8 Hz), 1.64 (ddd, *J* = 17.1, 13.0, 6.5 Hz), 1.52 (app dt, *J* = 13.0, 10.1 Hz, 1H), 0.98 (d, *J* = 6.5 Hz, 3H), 0.95 (d, *J* = 6.5 Hz, 3H); ^{13}C NMR (125 MHz, $CDCl_3$) δ 107.2, 105.7, 56.5, 53.7, 52.4, 50.0, 43.6, 34.8, 30.1, 22.6, 21.7; IR (thin film) 2958, 2929, 2871, 1779, 1364 cm^{-1}; HRMS (ESI) calculated for $C_{12}H_{18}O_4Na$ (M+Na) 249.1103, observed 249.1106.

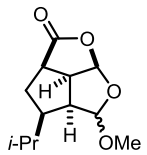

1.78: $C_{12}H_{18}O_4$
Molecular Weight: 226.2720

1.7 References and Notes

[1] For reviews, see: a) Faulkner, D. J. *Nat. Prod. Rep.* **2001**, *18*, 1–49. b) Keyzers, R. A.; Northcote, P. T.; Davies-Coleman, M. T. *Nat. Prod. Rep.* **2006**, *23*, 321–334. c) González, M. *Curr. Bioact. Compd.* **2007**, *3*, 1–36.

[2] Isolation of representative RSDs: a) Gracilins B and C: Mayol, L. *J. Nat. Prod.* **1986**, *49*, 823–828. b) Shahamin F: Dilip de Silva, E.; Morris, S. A.; Miao, S.; Dumdei, E.; Andersen, R. J. *J. Nat. Prod.* **1991**, *54*, 993–997. c) Macfarlandin C: Cun-heng, H.; Van Duyne, G. D.; Clardy, J. *J. Org. Chem.* **1986**, *51*, 4564–4567. d) Omriolide A: Rudi, A.; Erez, Y.; Benayau, Y.; Kashman, Y. *Tetrahedron Lett.* **2005**, *46*, 8613–8616. e) Cadlinolide B: Tischler, M.; Andersen, R. J. *J. Org. Chem.* **1991**, *56*, 42–47. f) Shahamin K: Dilip de Silva, E.; Morris, S. A.; Miao, S.; Dumdei, E.; Andersen, R. J. *J. Nat. Prod*. **1991**, *54*, 993–997. g) Aplyviolene: Hambley, T. W.; Poiner, A.; Taylor, W. C. *Tetrahedron Lett*. **1986**, *27*, 3281–3282. h) Macfarlandin E: Molinski, T. F.; Faulkner, D. J.; He, C. H.; Van Duyne, G. D.; Clardy, J. *J. Org. Chem*. **1986**, *51*, 4564–4567. i) Cheloviolene B: Bergquist, P. R.; Bowden, B. F.; Cambie, R. C.; Craw, P. A.; Karuso, P.; Poiner, A.; Taylor, W. C. *Aust. J. Chem.* **1993**, *46*, 623–632. j) Norrisolide: Hochlowski, J. E.; Faulkner, D. J. *J. Org. Chem.* **1984**, *49*, 3204–3206. k) Chromodorolide A: Dumdei, E. J.; De Silva, E. D.; Andersen, R. J.; Choudhary, M. I.; Clardy, J. *J. Am. Chem. Soc.* **1989**, *111*, 2712–2713. l) Chromodorolide B: Morris, S. A.; Dilip de Silva, E.; Andersen, R. J. *Can. J. Chem.* **1991**, *69*, 768–771. m) Chromodorolide C: Rungprom, W.; Chavasiri, W.; Kokpol, U.; Kotze, A.; Garson, M. J. *Mar. Drugs* **2004**, *2*, 101–107. n) Chromodorolide D: Uddin, M. H.; Hossain, M. K.; Nigar, M.; Roy, M. C.; Tanaka, J. *Chem. Nat. Compd.* **2012**, *48*, 412–415. o) Chromodorolide E: Katavic, P. L.; Jumaryatno, P.; Hooper, J. N. A.; Blanchfield, J. T.; Garson, M. J. *Aust. J. Chem.* **2012**, *65*, 531–538.

[3] Bobzin, S. C.; Faulkner, D. J. *J. Nat. Prod.* **1991**, *54*, 225–232.

[4] Keyzers, R. A.; Northcote, P. T.; Zubkov, O. A. *Eur. J. Org. Chem.* **2004**, 419–425.

[5] Schmitz, F. J.; Chang, J. S.; Hossain, M. B.; Van der Helm, D. *J. Org. Chem.* **1985**, *50*, 2862–2865.

[6] Gavagnin, M.; Fontana, A. *Curr. Org. Chem.* **2000**, *4*, 1201–1248.

[7] White, A. M.; Pierens, G. K.; Forster, L. C.; Winters, A. E.; Cheney, K. L.; Garson, M. J. *J. Nat. Prod.* **2016**, *79*, 477–483.

[8] For certain RSDs (e.g. **1.1**, **1.2**, **1.6**), oxidative cleavage is proposed to occur at the C5/C6 bond rather than the C9/C11 bond.

[9] a) Gracilins B and C: Corey, E. J.; Letavic, M. A. *J. Am. Chem. Soc.* **1995**, *117*, 9616–9617. b) Shahamin K: Lebsack, A. D.; Overman, L. E.; Valentekovich, R. J. *J. Am. Chem. Soc.* **2001**, *123*, 4851–4852. c) Norrisolide: Brady, T. P.; Kim, S. H.; Wen, K.; Theodorakis, E. A. *Angew. Chem. Int. Ed.* **2004**, *116*, 757–760. d) Norrisolide: Granger, K.; Snapper, M. L. *Eur. J. Org. Chem.* **2012**, *12*, 2308–2311. e) Aplyviolene: Schnermann,

M. J.; Overman, L. E. *J. Am. Chem. Soc.* **2011**, *133*, 16425–16427. f) Aplyviolene: Schnermann, M. J.; Overman, L. E. *Angew. Chem. Int. Ed.* **2012**, *51*, 9576–9580. g) Chromodorolide B: Tao, D. J.; Slutskyy, Y.; Overman, L. E. *J. Am. Chem. Soc.* **2016**, *138*, 2186–2189.

[10] The total synthesis of (–)-cheloviolene was completed by Dr. Michelle Garnsey in 2014 but has not been published as of April 2016.

[11] a) Hirst, G. C.; Howard, P. N.; Overman. L. E. *J. Am. Chem. Soc.* **1989**, *111*, 1514–1515. b) Johnson, T. O., Jr.; Overman. L. E. *Tetrahedron Lett.* **1991**, *32*, 7361–7365. (c) Ando, S.; Minor, K. P.; Overman, L. E. *J. Org. Chem*. **1997**, *62*, 6379–6387. (d) Hirst, G. C.; Johnson, T. O., Jr.; Overman, L. E. *J. Am. Chem. Soc.* **1993**, *115*, 2992–2993. (e) Minor, K. P.; Overman, L. E. *Tetrahedron* **1997**, *53*, 8927–8940. (f) Overman, L. E.; Pennington, L. P. *Can. J. Chem.* **2000**, *78*, 732–738.

[12] Kim, J. K.; Pau, J. K.; Caserio, M. C. *J. Org. Chem.* **1979**, *44*, 1544–1550.

[13] Syntheses concerning the *trans* hydrindanone will be discussed in detail in Chapter 2.

[14] Müller, P.; Allenbach, Y.; Robert, E. *Tetrahedron: Asymmetry* **2003**, *14*, 779–785.

[15] Okada, K.; Okamoto, K.; Morita, N.; Okubo, K.; Oda, J. *J. Am. Chem. Soc.* **1991**, *113*, 9401–9402.

[16] For a review, see Shorter, J.; Warren, G. *Ann. Rev. Cell Dev. Biol.* **2002**, *18*, 379–420.

[17] Wlodkowic, D.; Skommer, J.; McGuinness, D.; Hillier, C.; Darzynkiewicz, Z. *Leuk. Res.* **2009**, *33*, 1440–1447.

[18] Fan, J.; Hu, Z.; Zeng, L.; Lu, W.; Tang, X.; Zhang, J.; Li, T. *Neuroscience* **2008**, *26*, 523–534.

[19] a) Klausner, R. D.; Donaldson, J. G.; Lippincott-Schwartz, J. *J. Cell Bio.* **1992**, *116*, 1071–1080. b) Donaldson, J. G.; Finazzi, D.; Klausner, R. D. *Nature* **1992**, *360*, 350–352. c) Renault, L.; Guibert, B.; Cherfils, J. *Nature* **2003**, *426*, 525–530.

[20] a) Takizawa, P. A., Yucel, J. K.; Veit, B.; Faulkner, D. J.; Deerinck, T.; Soto, G.; Ellisman, M.; Malhotra, V. *Cell* **1993**, *73*, 1079–1090. b) Radeke, H. S.; Digits, C. A.; Casaubon, R. L.; Snapper, M. L. *Chem. Biol.* **1999**, *6*, 639–647.

[21] a) Brady, T. P.; Wallace, E. K.; Kim, S. H.; Guizzunti, G.; Malhotra, V.; Theodorakis, E. A. *Bioorg. Med. Chem. Let.* **2004**, *14*, 5035–5039. b) Brady, T. P.; Kim, S. H.; Wen, K.; Theodorakis, E. A. *Angew. Chem., Int. Ed*. **2004**, *43*, 739−742. c) Guizzunti, G.; Brady, T. P.; Malhotra, V.; Theodorakis, E. A. *J. Am. Chem. Soc.* **2006**, *128*, 4190–4191. d) Guizzunti, G.; Brady, T. P.; Malhotra, V.; Theodorakis, E. A. *Bioorg. Med. Chem. Lett.* **2007**, *17*, 320–325.

[22] Schnermann, M. J.; Beaudry, C. M.; Egorova, A. V.; Polishchuk, R. S.; Sütterlin, C.; Overman, L. E. *Proc. Nat. Acad. Sci. USA* **2010**, *107*, 6158–6163.

[23] Schnermann, M.; Beaudry, C. M.; Genung, N. E.; Canham, S. M.; Untiedt, N. L.; Karanikolas, B. D. W.; Sütterlin, C.; Overman, L. E. *J. Am. Chem. Soc.* **2011**, *133*, 17494–17503.

[24] As of April 2016, the Overman group is the only group having reported synthetic efforts towards the chromodorolides.[9g]

[25] This model system was proposed as a racemic route.

[26] Detailed commentary on the initial route and dihydroxylation studies can be found in Dr. Kohler's reports.

[27] Ruano, J. L. G.; Núñez, A. J.; Martín, M. R.; Fraile, A. *J. Org. Chem.* **2008**, *73*, 9366–9371.

[28] The bromide is required for high diastereoselectivity in the [3+2] dipolar cycloaddition.[27]

[29] Wang, H.; Kohler, P.; Overman, L. E.; Houk, K. N. *J. Am. Chem. Soc.* **2012**, *134*, 16054–16058.

[30] Benzyl ester cycloadduct **1.75** was synthesized using an identical route as methyl ester cycloadduct **1.72** starting from benzyl bromoacetate.

[31] The literature contains numerous examples of chemoselective lactone reductions in the presence of enoates, and it isn't apparent why this particular substrate was an exception.

[32] Tran, Y. S.; Kwon, O. *Org. Lett*. **2005**, *7*, 4289–4291.

[33] Lambert, T.; MacMillan, D. W. C. *J. Am. Chem. Soc.* **2002**, *123*, 13646–13647.

Chapter 2: Synthesis of (3a*S*,7a*S*)-4,4,7a-Trimethyloctahydro-1H-inden-1-one

2.1 Previous Syntheses of (+)-Hydrindanone 2.1

Central to completing the total synthesis of the chromodorolides was accessing multi-gram quantities of (+)-hydrindanone **2.1**. Despite a seemingly simple scaffold, this molecule presents two major synthetic challenges (Figure 2.1): 1) two quaternary carbons, C4 and C9, with C9 being stereogenic; and 2) a kinetically[1] and thermodynamically[2] disfavored *trans*-bicyclo[4.3.0]nonane (shown in red). In choosing how to access (+)-hydrindanone **2.1**, I first considered the three reported syntheses of (+)-hydrindanone **2.1**; and a brief discussion of each strategy is highlighted below.

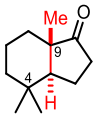

2.1

Figure 2.1. Hydrindanone 2.1 and its Synthetic Challenges.

2.1.1 The Theodorakis Route

The first synthesis of (+)-hydrindanone **2.1** was reported in 2004 by Theodorakis.[3] The synthesis was completed in 11 steps and 20% overall yield from Hajos-Parrish ketone **2.2** (Scheme 2.1). (+)-Dione **2.2** was a choice starting material because of accessibility on large scale in high enantiomeric purity with a preformed quaternary C9 stereocenter.[4] Theodorakis found construction of the *trans*-bicyclo[4.3.0]nonane particularly challenging, ultimately performing hydroboration on alkene **2.3** with modest selectivity

(~2.3:1) for the *trans*-bicyclic framework. Considering its long sequence with stereoselectivity challenges, I decided against this route to (+)-**2.1**.

Scheme 2.1. Theodorakis Route to (+)-Hydrindanone 2.1.

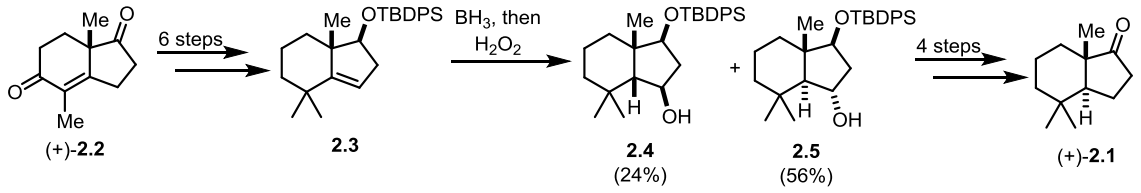

2.1.2 The Alvarez-Manzaneda Route

The second synthesis of (+)-hydrindanone **2.1** was reported in 2007 by Alvarez-Manzaneda from (–)-sclareol (**Error! Reference source not found.**).[5] A ring-contracting pinacol rearrangement of **2.6** transformed sclareol's *trans*-bicyclo[4.4.0]decane to the desired *trans*-bicyclo[4.3.0]nonane (**2.7**). Unfortunately, (+)-hydrindanone **2.1** was obtained in 2% overall yield as a result of inefficient removal of the hydroxyacetyl group of hydrindane **2.7** to install the ketone functionality. This ring contraction was an innovative method to obtain the desired *trans* ring system, but the low overall yield would not permit access sufficient quantities of (+)-**2.1**.

Scheme 2.2. Alvarez-Manzaneda Route to (+)-Hydrindanone 2.1.

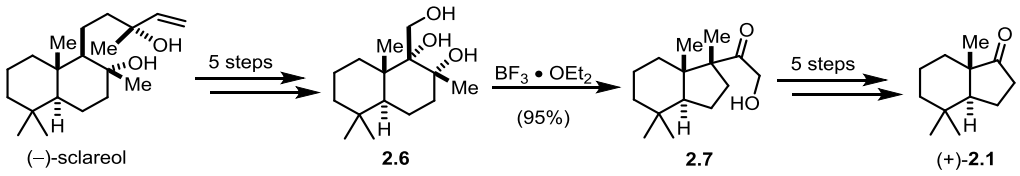

2.1.3 The Snapper Route

The Snapper group reported a third route to (+)-hydrindanone **2.1** in 2012,[6] requiring five steps and providing (+)-**2.1** in 15% overall yield and 98% *ee* (Scheme 2.3).

The quaternary centers were constructed in the first two steps to give diene **2.10**, and subsequent ring-closing metathesis constructed the *trans*-hydrindene framework. Hydrogenation followed by kinetic resolution provided (+)-hydrindanone **2.1** with high enantiomeric enrichment (98%). Despite a modest 15% overall yield, I believed this route to be the preferred method for accessing multi-gram quantities of (+)-**2.1**.

Scheme 2.3. Snapper Route to (+)-Hydrindanone 2.1.

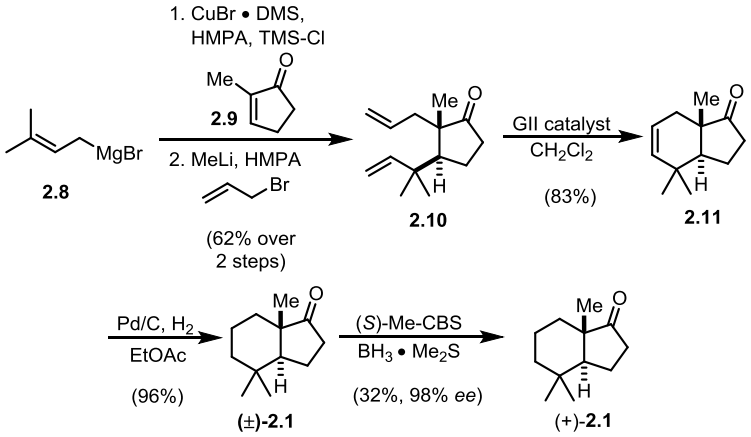

2.2 Modified Snapper Route to (+)-Hydrindanone 2.1

I began exploring the Snapper route with copper-mediated conjugate addition of prenyl magnesium bromide (**2.8**)[7] to 2-methylcyclopenten-2-one (**2.9**) in the presence of HMPA, followed by trapping of the resulting enolate with TMS-Cl (Equation 2.1). An important limitation for this initial conjugate addition was the dilute concentrations. Prenyl magnesium bromide solution was generated in 0.15–0.25 M concentrations,[8] which rendered a large scale reaction difficult. The resulting enoxysilane underwent activation with methyllithium and alkylation with allyl bromide to give an unexpected mixture of ketones **2.10** and **2.12** resulting from γ- and α-prenylation, respectively.

Equation 2.1

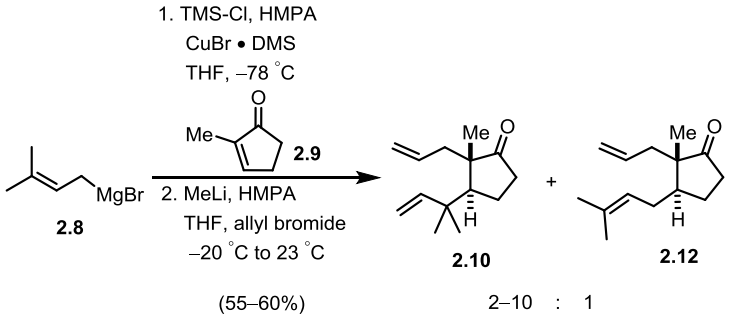

Surprisingly, ketone **2.12** was not mentioned as a byproduct by the Snapper group. Lipshutz previously observed α-prenylation as a minor byproduct (<5%) in the copper-mediated conjugate addition of prenyl magnesium bromide to 2-methylcyclopenten-2-one.[7] Using the reported conditions by Snapper, ketones **2.10** and **2.12** were obtained in variable ratios, from 2:1 to 10:1, respectively. The inconsistent regioselectivity of prenylation led me to examine the conditions reported by Lipschutz, in which LiCl was employed as an additive. By adding LiCl prior to addition of HMPA[9] and TMS-Cl, the conjugate addition and alkylation sequence afforded ketones **2.10** and **2.12** in a consistent 10:1 ratio favoring **2.10** and 52–61% combined yield (Equation 2.2). As these ketones were inseparable, the next challenge was to remove undesired ketone **2.12**.

Equation 2.2

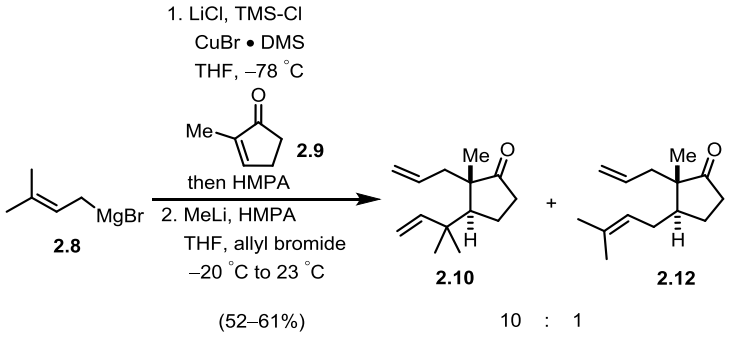

Attempts to separate undesired ketone **2.12** by distillation or column chromatography were unsuccessful. Separation of these isomers at a later stage in the

synthesis of (+)-hydrindanone **2.1** failed as well. Fortunately, the undesired ketone **2.12** was chemically distinguishable from ketone **2.10**. Taking advantage of **2.12**'s trisubstituted alkene, exposure of the ketone mixture to 11 mol % *m*-CPBA selectively oxidized ketone **2.12** to epoxide **2.13**. Epoxide **2.13** was then separable by column chromatography, and desired ketone **2.10** was recovered in pure form (Scheme 2.4). Subsequent RCM and hydrogenation afforded (±)-hydrindanone **2.1** in high yield over two steps, leaving kinetic resolution as the final step in the sequence.

Scheme 2.4. Modified Snapper Route to (+)-Hydrindanone 2.1.

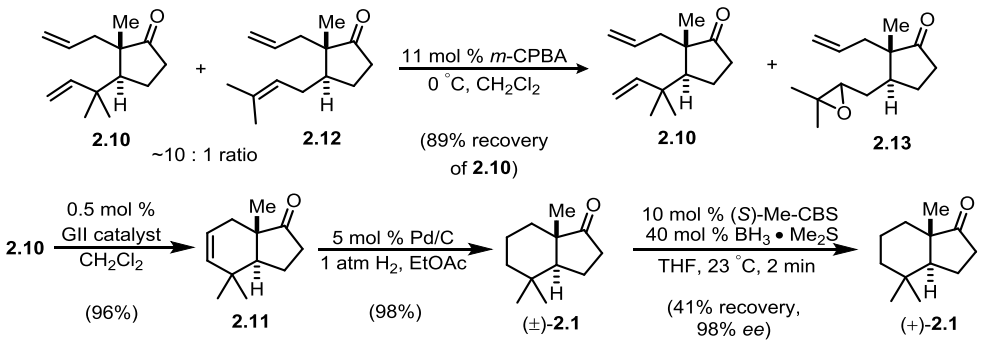

Employing Snapper's reported conditions for the CBS-mediated kinetic resolution afforded (+)-**2.1** with low enantioenrichment (50–60% *ee*). By examining a number of reaction parameters to improve enantioenrichment, I found temperature to be a critical factor. By running the reaction at 23 ºC rather than the reported 0 ºC, ketone **2.1** was consistently recovered in 41% yield and 98% *ee* on gram scale. With access to sufficient quantities of (+)-**2.1**, this material was carried forward to complete the synthesis of (–)-chromodorolide B (Chapter 3). However, this route's modest overall yield (20%) coupled with scalability issues and a late-stage kinetic resolution left an opportunity to develop an improved route to (+)-hydrindanone **2.1**.

2.3 First-Generation Approach: Biomimetic Polyene Cyclization

In light of the previous approaches to (+)-hydrindanone **2.1**, I considered a biomimetic approach to constructing *trans*-hydrindanes. In steroid synthesis, enzymatically-controlled polyene cyclizations are remarkable transformations which form *trans*-hydrindanes in a single step with high stereochemical fidelity (Equation 2.3).[10] Nature, as well as the synthetic chemist, typically initiates cationic polyene reactions by Lewis acid activation of epoxides, ketones, or ketals,[11] but these activating groups are not always required.

Equation 2.3

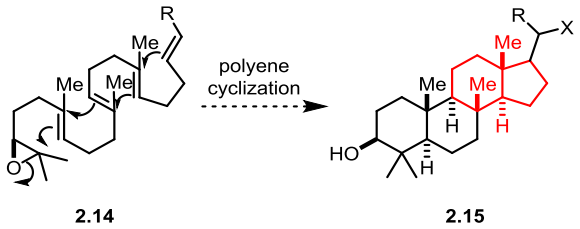

2.3.1 Retrosynthetic Approach and Literature Precedent

Retrosynthetically, I proposed ketone **2.1** could arise from oxidative cleavage of allene **2.16**, the product of a proton-initiated polyene cyclization (Scheme 2.5). Dieneyne **2.17** would be protonated at the terminal alkene, generating tertiary carbocation **2.18**. Two bond-forming events would then construct the *trans*-bicyclic system harboring both quaternary centers by a polyene cyclization in a chair-like conformation. The resulting linear vinyl carbocation **2.19** could be quenched by elimination to give allene **2.16**. Dieneyne **2.17** is not only readily accessible but prochiral, presenting the opportunity for an enantioselective polyene cyclization.

Scheme 2.5. Retrosynthesis using a Proton-Initiated Polyene Cyclization.

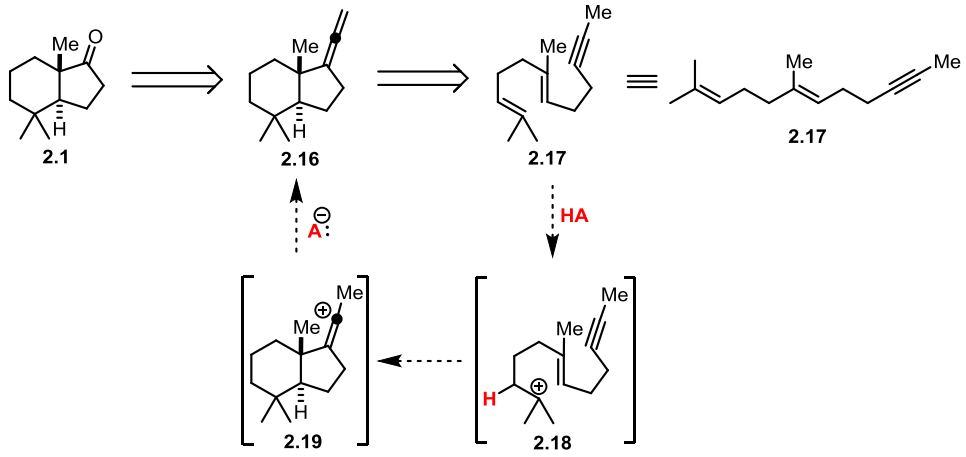

Enantioselective proton-initiated polyene cyclizations (EPIPCs) are biomimetic transformations that utilize a chiral cation-anion complex to facilitate stereoselective formation of the carbon skeleton upon protonation of an alkene. The first report of an EPIPC by Yamamoto[12] in 1999 (Equation 2.4) found BINOL derivative **2.21** in the presence of a strong Lewis acid capable of facilitating EPIPCs to give cyclized products (e.g. **2.22**) in high yields (56–95%) with varying enantioselectivity (42–87% *ee*). The acid promoting this EPIPC was proposed to be complex **2.23** in which BINOL coordination to the Lewis acid dramatically increases phenol acidity. Yamamoto's EPIPC precursors (e.g. **2.20**) were always functionalized with an alcohol,[12,13] phenol,[14] or arene[15] to terminate the cationic cascade.

Equation 2.4

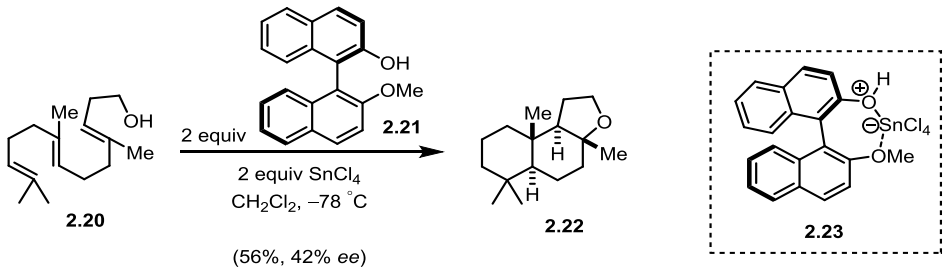

Since Yamamoto's seminal contributions to EPIPCs, few advancements in this area have been reported.[16] Recent methodology developed by Corey[17] (Equation 2.5) used the same ligand class as Yamamoto. Specifically, *o-o'*-dichloro-BINOL **2.25** with $SbCl_5$ accomplished EPIPCs of arylated polyene substrates (e.g. **2.24**) in high yields and high *ee*'s. While Yamamoto's and Corey's work were encouraging for the proposed cyclization with dieneyne **2.17**, this substrate's cyclization had two key differences: 1) termination of the polyene sequence with an alkyne rather than precedented alcohol or arene nucleophiles; and 2) cyclization to a *trans*-bicyclo[4.3.0]nonane instead of a *trans*-bicyclo[4.4.0]decane.

Equation 2.5

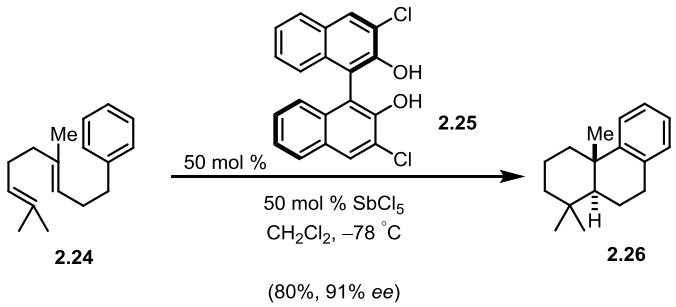

In considering these important differences, pioneering work by Johnson in the 1970's shed light on both of these issues. Johnson previously examined formation of *trans*-bicyclo[4.3.0]nonanes using allylic alcohols for cationic initiation in polyene cyclizations with tethered alkynes as the cascade terminators.[18] Seen in Equation 2.6, allylic alcohol **2.27** was exposed to $SnCl_4$ at low temperatures to generate an allylic carbocation which underwent polyene cyclization to afford three identified products.[19] The major product was *trans*-hydrindane **2.28**, with a small amount of *cis*-hydrindane **2.29** also formed (9.3:1 dr). The other identified product, *trans*-decaline **2.30**, arose via either *6-endo* cyclization by the alkyne or 1,2-alkyl shift of intermediate vinyl carbocation **2.31** prior to chloride trapping.

Equation 2.6

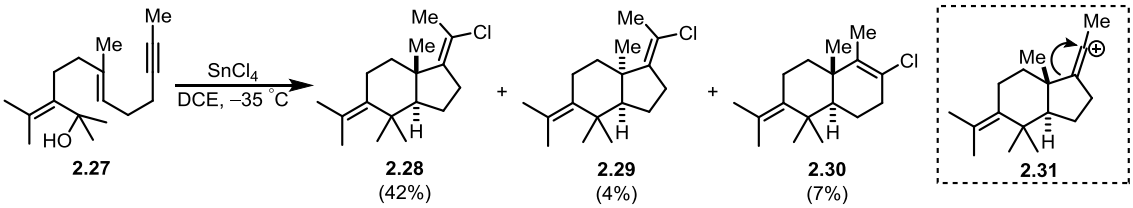

Johnson also examined the effects of alkyne substitution (Scheme 2.6), observing that terminal or silylated alkynes (**2.32**)[20] favored formation of 6-*endo* products (**2.33**) while internal alkyl alkynes (**2.34**) favored formation of 5-*exo* products (**2.35**). Therefore, proposed EPIPC precursor **2.17** would require alkyl substitution on the alkyne to favor formation of the required 5-*exo* product.

Scheme 2.6. Alkyne Substitution Effects on 5-*exo* versus 6-*endo* Products.

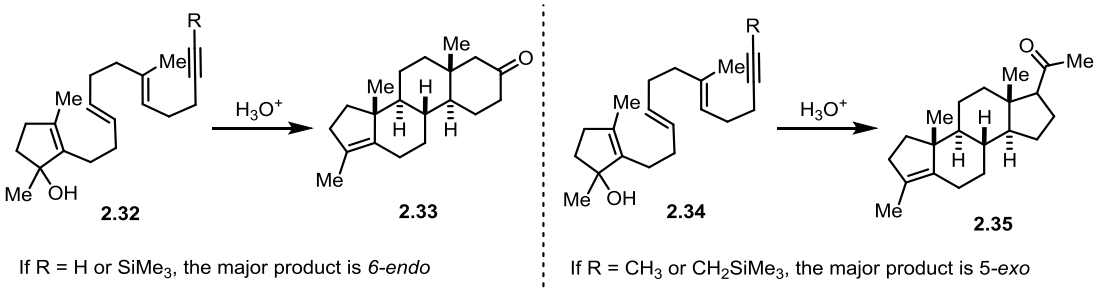

2.3.2 Optimization of the Proton-Initiated Polyene Cyclization

With precedent for the proposed EPIPC to construct the *trans*-bicyclo[4.3.0]nonane, I synthesized the requisite cascade precursor, dieneyne **2.17** (Scheme 2.7). Starting from 1-trimethylsilyl-propyne **2.36**, propargylic deprotonation with *n*-BuLi followed by exposure to geranyl chloride **2.37** gave the alkylated product.[21] Upon *in situ* desilylation with TBAF, terminal alkyne **2.38** was obtained in 73% yield. Subsequent alkylation with methyl iodide[22] afforded desired polyene cyclization precursor

2.17 in only two steps and 62% overall yield from commercially available 1-trimethylsilyl-propyne.

Scheme 2.7. Synthesis of EPIPC Precursor 2.17.

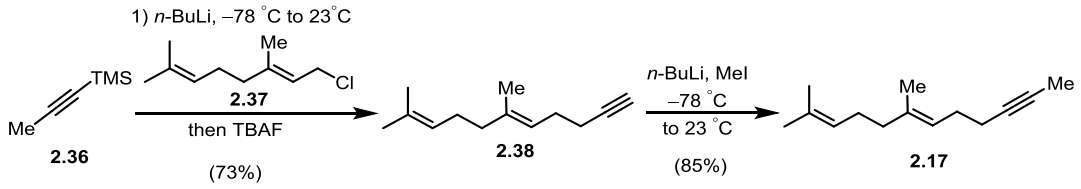

Having accessed multiple grams of dieneyne **2.17**, the EPIPC was investigated using conditions reported by Corey[17] (Scheme 2.8). Employing 50 mol % of *o,o'*-dichloro-(*R*)-BINOL **2.25** and $SbCl_5$ at –78 ºC in CH_2Cl_2, a mixture of two bicyclic products was isolated in 35% yield. The major product, vinyl chloride **2.39**, contained the desired *trans*-bicyclo[4.3.0]nonane while minor product **2.40** contained the *trans*-bicyclo[4.4.0]decane. Ozone-mediated oxidative cleavage of vinyl chloride **2.39** verified the structure via conversion to known ketone **2.1** in modest yield. Unfortunately, HPLC analysis of a hydrazone derivative[6] of **2.1** revealed the ketone to be racemic, indicating no enantioinduction occurred in the polyene cyclization.

Scheme 2.8. EPIPC and Ozonolysis to Hydrindanone 2.1.

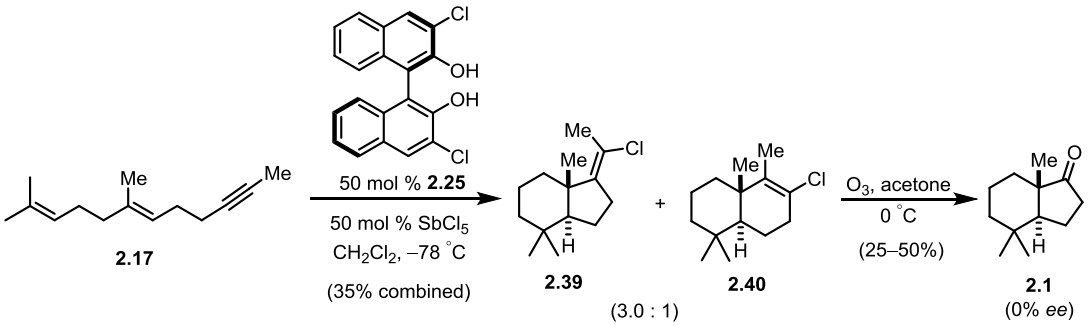

Shown in Table 2.1, a number of conditions were screened to improve both yield and enantioinduction of the EPIPC. The reported conditions by Corey afforded a low

combined yield favoring vinyl chloride **2.39** with no enantioenrichment (entry 1). Several other Lewis acids were screened (entries 2–3), in which $SnCl_4$ (entry 3) was found superior in yield (55%) and enantioinduction (–18% *ee*). However, the ratio of products **2.39**:**2.40** decreased to 1.5:1. Lower temperatures using $SnCl_4$ were also explored. At –90 ºC (entry 4), formation of desired vinyl chloride **2.39** was further disfavored relative to vinyl chloride **2.40** (1.1:1). At –50 ºC (entry 5), a complex product mixture was observed with a low yield of desired **2.39**.[23] Lastly, unsubstituted BINOL was examined as a ligand, which provided similar results to the chlorinated variant (entry 6). As the bicyclo[4.4.0]decane **2.40** was generally the major byproduct, I aimed to attenuate this unproductive reaction pathway and increase the yield of vinyl chloride **2.39**.

Table 2.1. Screening of Conditions for the EPIPC of Dieneyne 2.17.

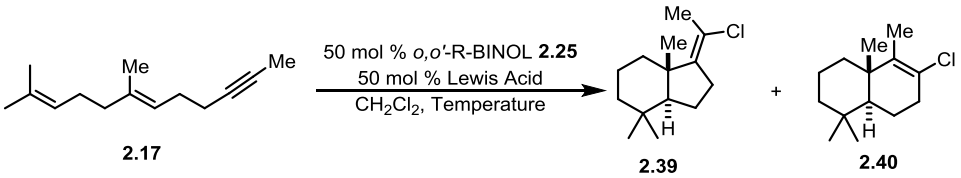

Entry	Lewis Acid	R	Temperature	Yield[a]	Ratio of 2.39:2.40[b]	ee[c]
1	$SbCl_5$	Cl	–78 °C	35%	3.0 : 1	0%
2	**$TiCl_4$**	Cl	–78 °C	<5%[d]	-	-
3	**$SnCl_4$**	Cl	–78 °C	55%	1.5 : 1	–18%
4	$SnCl_4$	Cl	**–90 °C**	53%	1.1 : 1	–20%
5	$SnCl_4$	Cl	**–50 °C**	12%[d]	1 : 0	-
6	$SnCl_4$	**H**	–78 °C	53%	1 : 1.1	–13%

[a]The isolated yield of the combined vinyl chlorides.[b] Determined by ^{1}H NMR. [c] *ee* determined from the corresponding trisyl hydrazone of ketone **2.1** following ozonolysis. [d] Multiple uncharacterized byproducts were observed in the reaction.

2.3.3 Attempts to Trap Linear Vinyl Carbocation

In one mechanistic scenario to undesired vinyl chloride **2.40** (Scheme 2.9), competitive rates between chloride attack on carbocation **2.19** and 1,2-alkyl shift would determine the distribution of products **2.39** and **2.40**, respectively. If this mechanistic pathway was operative, increasing the concentration of the reaction mixture may favor

trapping to give vinyl chloride **2.39** over undesired alkyl shift to **2.41**. Shown in Table 2.2, reaction concentration (relative to **2.17**) had no effect on the product ratio of **2.39**:**2.40**, indicating that the chloride anion was not involved in the product-determining step between **2.39** and **2.40**.

Scheme 2.9. Possible Mechanism to Vinyl Chlorides 2.39 and 2.40.

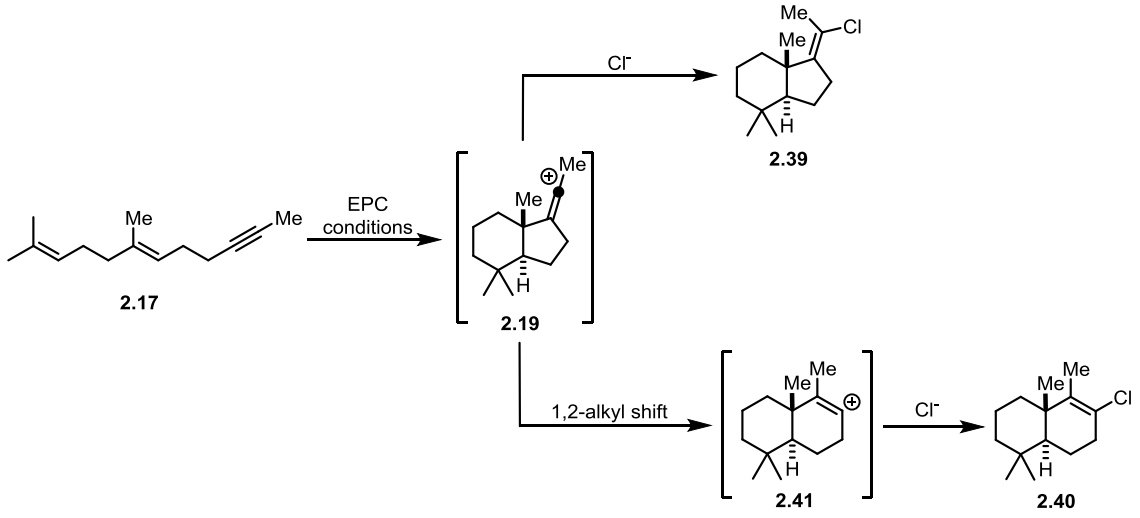

Table 2.2. Concentration Effects on EPIPC Product Distribution.

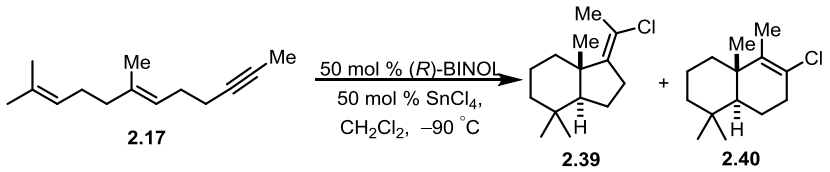

[2.17]	Combined Yield	Ratio 2.39:2.40 (by ^{1}H NMR)
0.2 M	34%	1 : 1.3
0.4 M	37%	1 : 1.4
0.6 M	37%	1 : 1.4

An alternative method to prevent formation of **2.40** would be intramolecular trapping of the vinyl carbocation. Propargylic silanes were previously employed by Johnson in polyene cyclizations in which the silyl substituent stabilized the final vinyl

carbocation intermediate in the cascade. Upon loss of the trimethylsilyl group, allene products would be obtained.[20,24] To examine this strategy, propargylic silane **2.42** was synthesized from terminal alkyne **2.38** (Scheme 2.10). Exposure to EPIPC conditions with $SnCl_4$ unfortunately afforded low yields of desired allene **2.43**. Analysis by ^{1}H NMR of the crude reaction mixtures showed multiple polyene byproducts, which may result from undesired protonation of the propargylic silane rather than the terminal alkene. In light of the modest yields and poor enantioinduction, the EPIPC route was ultimately abandoned.[25]

Scheme 2.10. Synthesis of Propargylic Silane 2.42 and EPIPC.

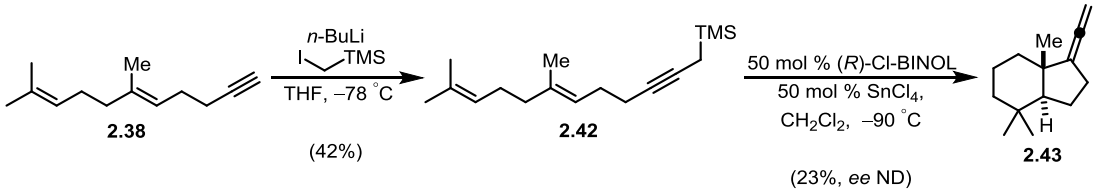

2.4 Second-Generation Approach: Reductive Transposition

2.4.1 Synthetic Considerations and Retrosynthesis

Dissatisfied with the available routes to synthesize (+)-hydrindanone **2.1**, the molecule was again reexamined for a more efficient approach. Hajos-Parrish ketone **2.2** seemed a logical starting material because of its accessibility in high enantioenrichment. Only two formal transformations of Hajos-Parrish ketone **2.2** would be required to arrive at hydrindanone **2.1** (Figure 2.2): 1) full reduction of the enone carbonyl (in red); and 2) stereoselective hydromethylation to give the *trans*-hydrindane (in blue). This synthetic approach would require a stereospecific transformation to set the *trans*-bicyclo[4.3.0]nonane and avoid formation of the thermodynamically and kinetically favored *cis* ring fusion.

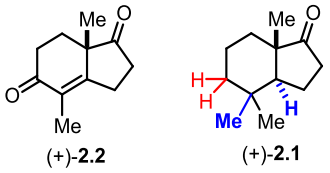

Figure 2.2. Structural Comparison Between Ketones 2.2 and 2.1.

In this second-generation retrosynthesis of (+)-hydrindanone **2.1** (Scheme 2.11), the desired product would arise from formal hydromethylation of trisubstituted alkene **2.44** via two-step cyclopropanation/C–C bond hydrogenolysis. The *trans* ring fusion of **2.44** would then be constructed from a stereospecific reductive transposition of allylic alcohol **2.46**, transferring the stereochemistry of the β-alcohol to the bridgehead methine stereocenter with inversion. Reductive transpositions of allylic alcohols[26] and their derivatives[27] have relayed stereochemical information in related systems with high fidelity (Scheme 2.12). Allylic alcohol **2.46** would then arise from selective 1,2-reduction of Hajos-Parrish ketone **2.2**.

Scheme 2.11. Second-Generation Retrosynthesis of Hydrindanone 2.1

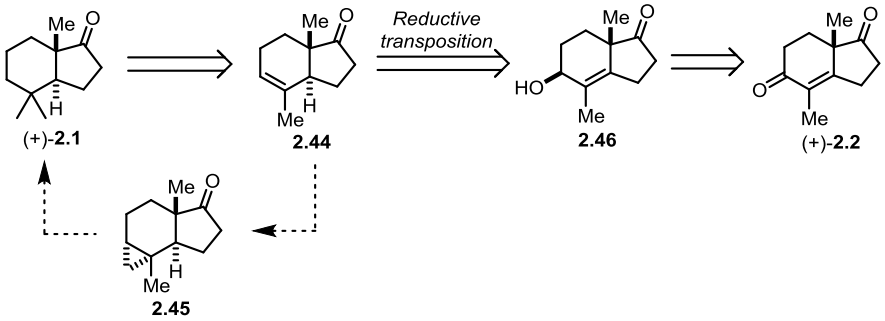

Scheme 2.12. Examples of Stereospecific Reductive Transpositions

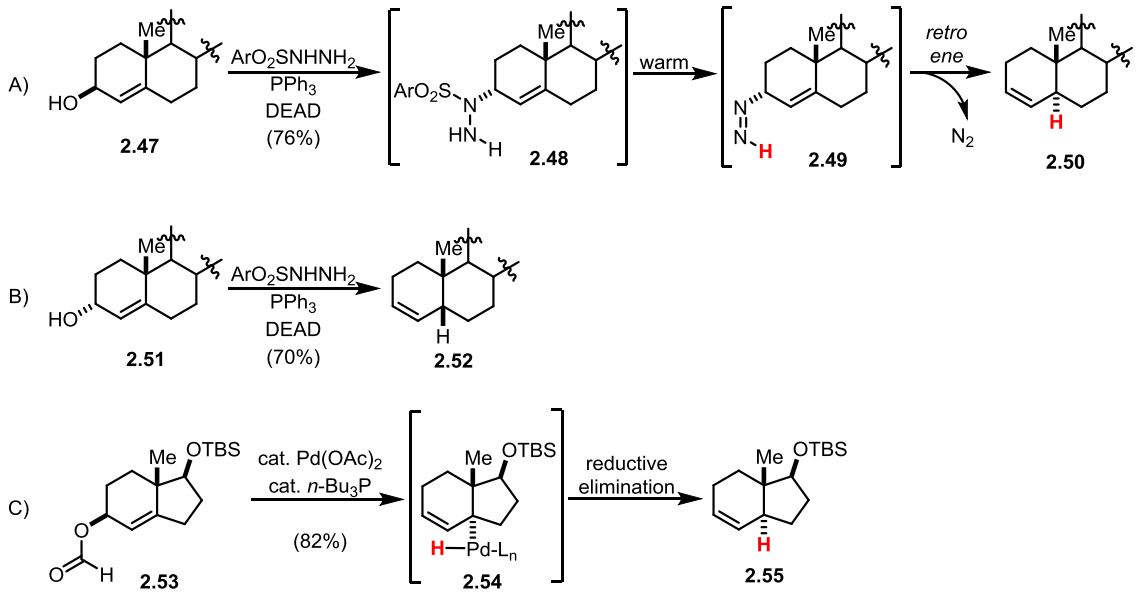

2.4.2 Forward Synthesis of Hydrindanone 2.1

As Yuriy Slutskyy experimentally developed this second-generation route, a brief summary of the optimized sequence is provided below.[28] Starting from (+)-enone **2.2** which is commercially available or synthesized in two steps and 98% *ee*,[4] ketalization of the unsaturated ketone followed by stereoselective 1,2-reduction of the enone afforded β-allylic alcohol **2.56** as a single diastereomer. **2.56** was initially examined in the Myers reductive transposition,[26] but low yields and undesired byproducts rendered this approach inefficient. Rather, acylation of **2.56** with methyl chloroformate gave allylic carbonate **2.57**, which could undergo Tsuji-Trost reductive transposition.[29]

Scheme 2.13. Synthesis of Allylic Carbonate 2.57.

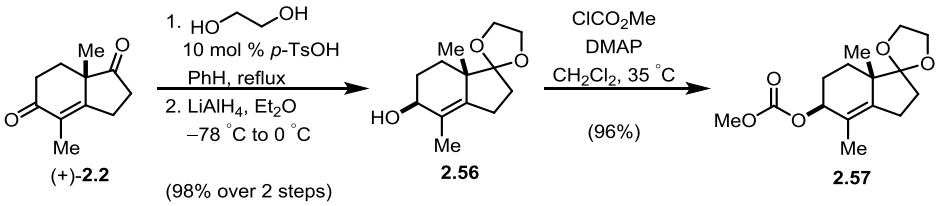

Exposure of allylic carbonate **2.57** to Tsuji's reported conditions[27] with $Pd(acac)_2$ precatalyst and $(n\text{-Bu})_3P$ gratifyingly resulted in the stereospecific transposition. S_N2-like displacement of the allylic carbonate and palladium-hydride reductive elimination provided desired *trans* hydrindene **2.58** in 77% yield without formation of *cis*-hydrindane (Scheme 2.14).[30] Miyano-modified Simmons-Smith cyclopropanation with chloroiodomethane[31] and *in situ* acid-mediated deketalization afforded cyclopropyl ketone **2.45** in high yield as a single diastereomer. Subsequent platinum-catalyzed hydrogenolysis afforded alcohol **2.59** containing the necessary geminal dimethyl functionality. At this stage, removal of a minor impurity by recrystallization[32] gave alcohol **2.59** in high purity; and upon oxidation, (+)-hydrindanone **2.1** was obtained in 59% overall yield and 7 steps from Hajos-Parrish ketone **2.2**.

Scheme 2.14. Transformation of Allylic Carbonate 2.57 to Hydrindanone 2.1.

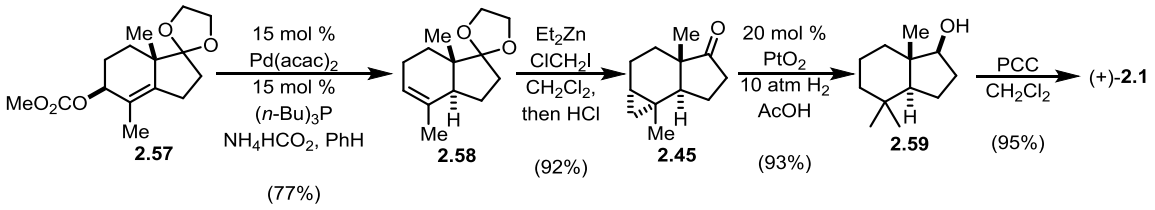

Highlighted in Table 1 are the unique approaches that have been developed synthesize (+)-hydrindanone **2.1**. Upon completion of this second generation approach, I believe this route to be the best currently available method to access multi-gram quantities of (+)-hydrindanone **2.1**. Its scalability and high overall yield should assist future research groups in need of enantioenriched hydrindanone **2.1**.

Table 2.3. Known Routes to (+)-Hydrindanone 2.1.

Synthetic Route	Group (Year)	Step Count (from commercially available material)	Overall Yield (*ee*)
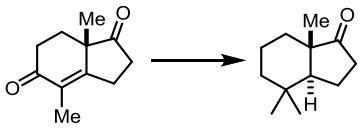	Theodorakis (2004)	11 steps	20% (98% *ee*)
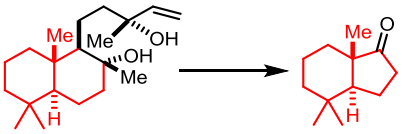 (−)-sclareol	Alvarez-Manzaneda (2011)	11 steps	2% (99% *ee*)
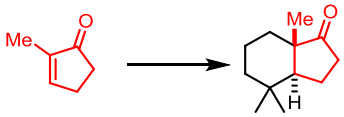	Revised Snapper (2012)	6 steps	20% (98% *ee*)
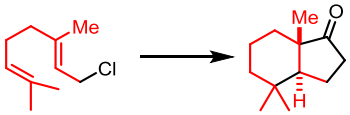	Overman (2013)	4 steps	17% (18% *ee*)
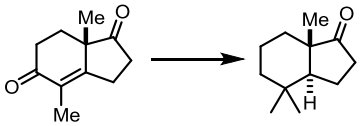	Overman (2015)	7 steps	59% (98% *ee*)

2.5 Experimental Section

2.5.1 General Experimental Details

Unless stated otherwise, reactions were conducted in oven-dried glassware under an atmosphere of nitrogen or argon. Tetrahydrofuran (THF), deithylether, toluene, dichloromethane, methanol (MeOH), pyridine, and triethylamine were dried by passage through activated alumina. TMSCl was distilled directly before use from CaH. All commercial reagents were used as received unless otherwise noted. Reaction temperatures were controlled using an IKAmag temperature modulator. Thin-layer chromatography (TLC) was conducted with E. Merck silica gel 60 F254 pre-coated plates (0.25 mm), and visualized by exposure to UV light (254 nm) or stained with anisaldehyde, ceric

ammonium molybdate, and potassium permanganate. Flash column chromatography was performed using normal phase silica gel (60 Å, 230─240 mesh, Merck KGA). ^{1}H NMR spectra were recorded on Bruker spectrometers (at 500 or 600 MHz) and are reported relative to $CHCl_3$ signals. Data for ^{1}H NMR spectra are reported as follows: chemical shift (δ ppm), multiplicity, coupling constant (Hz) and integration. ^{13}C NMR spectra were recorded on Bruker Spectrometers (at 125 MHz). Data for ^{13}C NMR spectra are reported in terms of chemical shift (δ ppm). IR spectra were recorded on a Varian 640-IR spectrometer and are reported in terms of frequency of absorption (cm^{-1}). High resolution mass spectra were obtained from the UC Irvine Mass Spectrometry Facility with a Micromass LCT spectrometer. See JOC Standard Abbreviations and Acronyms for abbreviations (available at http://pubs.acs.org/userimages/ContentEditor/1218717864819/joceah_abbreviations.pdf).

2.5.2 Experimental Procedures

***rac*-(2*S*,3*S*)-2-allyl-2-methyl-3-(2-methylbut-3-en-2-yl)cyclopentan-1-one (2.10)**: The procedure for preparation of **2.10** was a modification from the literature.[6] CuBr•DMS (14.38 g, 75.51 mmol) and anhydrous LiCl (4.26 g, 101 mmol) were charged into a flask with THF (130 mL). After maintaining the solution at 23 °C for 15 min, the flask was cooled to –78 °C. Prenyl magnesium bromide solution[7] (62.9 mmol, 286 mL, 0.22 M in THF) was added slowly over 15 min. After maintaining the reaction at –78 °C for 15 min, TMS-Cl (12.7 mL, 101 mmol) was added followed immediately by 2-methyl-cyclopent-2-enone (4.84 g, 50.3 mmol) in THF (5 mL). The reaction was maintained at –78 °C for 1 h, and then HMPA

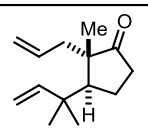

2.10: $C_{14}H_{22}O$
Molecular Weight: 206.3290

(17.5 mL, 101 mmol) was added. After 1 h, NEt_3 (15.4 mL, 111 mmol) was added, and the reaction was then warmed to 0 °C over 1 h. The reaction was diluted with Et_2O (200 mL), and 10% aq. NH_4Cl solution precooled to 0 ºC (200 mL) was added. Upon separation of the heterogeneous mixture, the organic layer was washed with 10% aq. NH_4Cl solution precooled to 0 ºC (3 x 100 mL). The organic layer was then dried over $MgSO_4$, filtered, and concentrated *in vacuo* to give the crude enoxysilane as a yellow oil which was carried forward immediately.

The crude enoxysilane was dissolved in THF (150 mL) and cooled to –20 °C. MeLi (33.5 mL, 50.3 mmol, 1.50 M in hexanes) was added at a rate which kept the reaction temperature below –10 °C. The reaction was then allowed to warm to 23 °C over 1 h. The reaction was then cooled to –78 °C. HMPA (35.0 mL, 201 mmol) was added, and the reaction was maintained at –78 °C for 15 min. Freshly distilled allyl bromide (21.8 mL, 252 mmol) was added to the reaction flask, which was allowed to warm to 23 °C over 6 h. The reaction was quenched with sat. aq. NH_4Cl (200 mL), and the resulting aqueous layer was extracted with Et_2O (3 x 100 mL). The combined organic layers were washed with brine (150 mL), dried over $MgSO_4$, filtered, and concentrated *in vacuo*. Purification of the resulting residue by column chromatography (0% Et_2O in hexanes to 3% Et_2O in hexanes) provided a mixture of ketones **2.10** and **2.12** as a clear oil (5.38 g, 26.1 mmol, ~10:1 ratio, 52%).

Ketones **2.10** and **2.12** (14.9 g, 72.1 mmol, ~10:1 ratio) were dissolved in CH_2Cl_2 (150 mL) and cooled to 0 °C. *m*-CPBA (1.83 g, 7.93 mmol) was then added, and the reaction was maintained at 0 °C for 1 h. The reaction was concentrated *in vacuo* and directly purified by column chromatography (6% Et_2O in hexanes) to afford ketone **2.10**

(13.3 g, 64.6 mmol, 89% recovery) as a clear oil. Spectral data was consistent with reported values.[6]

***rac*-(3a*S*,7a*S*)-4,4,7a-trimethyl-2,3,3a,4,7,7a-hexahydro-1H-inden-1-one (2.11)**: The procedure for preparation of **2.11** was a slight modification from the literature.[6] Ketone **2.10** (3.26 g, 15.8 mmol) was dissolved in CH_2Cl_2 (80 mL), and Grubb's GII catalyst (67 mg, 0.079 mmol) was added to the flask. The reaction was maintained for 16 h, at which point silica (~3 g) was added. Upon stirring for 30 min, the suspension was concentrated *in vacuo* and filtered over Celite with Et_2O (20 mL). Concentration *in vacuo* and distillation (195 °C, 10 torr) provided ketone **2.11** (2.68 g, 15.0 mmol, 95%) as a colorless oil. Spectral data was consistent with reported values.[6]

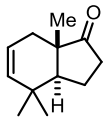

2.11: $C_{12}H_{18}O$
Molecular Weight: 178.2750

***rac*-(3a*S*,7a*S*)-4,4,7a-trimethyloctahydro-1H-inden-1-one (2.1)**: The procedure for preparation of (±)-**2.1** was a slight modification from the literature.[6] 10% Pd/C (1.59 g, 1.50 mmol) was added to a solution of ketone **2.11** (2.68 g, 15.0 mmol) in EtOAc (60 mL). The reaction vessel was evacuated and filled with 1 atm H_2 (repeated 3x). The reaction was maintained at 23 ºC for 20 h before purging the vessel of H_2. The resulting black suspension was filtered through Celite with EtOAc (30 mL). Upon concentration, (±)-ketone **2.1** (2.65 g, 14.7 mmol, 98%) was isolated as a colorless, amorphous solid. Spectral data was consistent with reported values.[6]

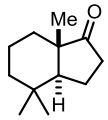

(±)-**2.1**: $C_{12}H_{20}O$
Molecular Weight: 180.2910

(+)-(3a*S*,7a*S*)-4,4,7a-trimethyloctahydro-1H-inden-1-one (2.1): The procedure for preparation of (+)-**2.1** was a slight modification from the literature.[6] BH_3•Me_2S (0.326 mL, 3.44 mmol) was added to a flask of (*S*)-1-methyl-3,3-diphenyl-tetrahydro-pyrrolo[1,2*c*][1,3,2]oxazaborole (0.86 mL, 0.86 mmol, 1.0 M in toluene) dissolved in THF (40 mL) at 23 °C. The solution was maintained at 23 °C for 15 min, at which point (+)-**2.1** (1.55 g, 8.60 mmol) in THF (40 mL) was added rapidly as a single potion. After 2 min, MeOH (40 mL) and aq. HCl (40 mL of 1 M soln) were added to quench the reaction. Et_2O (100 mL) and H_2O (50 mL) were added. The aqueous layer was extracted with Et_2O (3 x 30 mL), and the combined organic layers were dried over $MgSO_4$, filtered, and concentrated *in vacuo*. Purification by flash column chromatography (5% Et_2O in hexanes to 15% Et_2O in hexanes) provided (+)-ketone **2.1** (0.652 g, 3.62 mmol, 98% *ee*, 42% recovery) as a colorless, amorphous solid. Spectral data was consistent with reported values.[6] *Ee* was determined by chiral HPLC of corresponding hydrazone **S1** (*vide infra*).

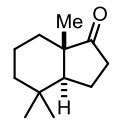

(+)-**2.1**: $C_{12}H_{20}O$
Molecular Weight: 180.2910

(3a*S*,7a*S*)-4,4,7a-trimethyloctahydro-1H-inden-1-one (S2.1): The procedure of hydrazone **S2.1** was repeated from literature.[6] (+)-Ketone **2.1** (0.105 g, 0.582 mmol) was dissolved in MeCN (3 mL), and 2,4,6-triisopropylbenzenesulfonylhydrazide (0.182 g, 0.611 mmol) was added. The suspension was vigorously stirred for 15 min before one drop of HBF_4 was added to the suspension (which immediately became a homogeneous solution). The reaction was left 14 h before adding Et_2O (2 mL). The crude product was dried over SiO_2 (~2 g) and purified by flash column

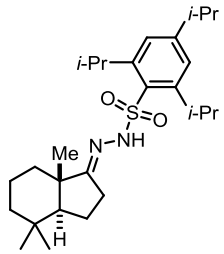

S2.1: $C_{27}H_{44}N_2O_2S$
Molecular Weight: 460.7210

chromatography (10% Et_2O in hexanes to 20% Et_2O in hexanes) to provide hydrazone **S2.1** as a colorless solid (0.110 g, 0.238 mmol, 41%). Spectral data was consistent with reported values.[6] HLPC analysis was used to determine enantiomeric ratios to be 99:1 (Chiracel OD-H column; flow: 1.0 mL/min, 1% isopropanol:*n*-hexane; λ = 254 nm; minor enantiomer t_R = 13.65 min, major enantiomer t_R = 21.34 min).

(*E*)-6,10-dimethyl-5,9-undecadien-1-yne (2.38): The procedure for preparation of **2.38** was a modification from the literature.[33] 1-Trimethylsilyl-propyne (2.96 g, 26.4 mmol) was dissolved in THF (100 mL) and cooled to –78 °C. *n*-BuLi (30.8 mmol, 11.8 mL, 2.5 M in hexanes) was added slowly, and the reaction was then warmed to 0 °C over 1 h. The reaction was cooled to –78 °C, and geranyl chloride (3.80 g, 22.0 mmol) was added. The reaction was allowed to warm to 23 °C over 16 h. The reaction vessel was then cooled to –78 °C, and TBAF (28.6 mmol, 28.6 mL, 1.0 M in THF) was then added. The reaction was allowed to warm to 23 °C before diluting with H_2O (50 mL). The aqueous layer was extracted with hexanes (3 x 50 mL); and the combined organic layers were washed with brine (50 mL), dried over magnesium sulfate, filtered, and concentrated *in vacuo*. The resulting oil was then purified by flash column chromatography (100% hexanes) to provide dieneyne **2.38** as a clear oil (2.85 g, 16.1 mmol, 73%). Spectral data was consistent with reported values.[33]

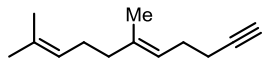

2.38: $C_{13}H_{20}$
Molecular Weight: 176.3030

(*E*)-7,11-dimethyl-6,10-dodecadien-2-yne (2.17): Dieneyne **2.38** (2.17 g, 12.3 mmol) was dissolved in THF (120 mL) and cooled to –78 °C. *n*-BuLi (18.5 mmol, 7.10 mL, 2.5 M in hexanes) was added slowly to the reaction, which was then warmed to 0 °C. After 10 min, the reaction was cooled to –78 °C, and methyl iodide (8.73 g, 61.5 mmol) was added. The reaction was then allowed to warm to 23 °C over 2 h. The reaction was quenched with saturated aq. NH_4Cl (50 mL). The aqueous layer was extracted with hexanes (3 x 50 mL), and the combined organic layers were washed with brine (50 mL), dried over magnesium sulfate, filtered, and concentrated *in vacuo*. The resulting residue was purified by flash column chromatography (100% hexanes) to provide dieneyne **2.17** as a clear oil (1.99 g, 10.5 mmol, 85%). ^{1}H NMR (500 MHz, $CDCl_3$) δ 5.16 (dt, *J* = 6.6, 1.2 Hz, 1H), 5.09 (tt, *J* = 6.9, 1.3 Hz,1H), 2.20–2.10 (m, 4H), 2.09–2.02 (m, 2H), 2.01–1.94 (m, 2H), 1.78 (t, *J* = 2.5 Hz, 3H), 1.68 (s, 3H), 1.61 (app s, 3H), 1.60 (app s, 3H); ^{13}C NMR (125 MHz, $CDCl_3$) δ 136.41, 131.48, 124.40, 123.09, 79.36, 75.51, 39.80, 27.91, 26.79, 25.82, 19.35, 17.81, 16.20, 3.62; IR (thin film) 2966, 2918, 2855, 1443, 1377 cm^{-1}; HRMS (ESI) calculated for $C_{14}H_{22}NH_4$ (M+NH_4) 208.2065, observed 208.2067.

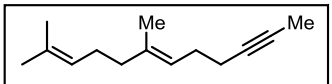

2.17: $C_{14}H_{22}$
Molecular Weight: 190.3300

***rac*-(3a*S*,7a*S*,*E*)-1-(1-chloroethylidene)-4,4,7a-trimethyloctahydro-1H-indene (2.39)** and ***rac*-(4a*S*,8a*S*)-7-chloro-4,4,8,8a-tetramethyl-1,2,3,4,4a,5,6,8a-octahydronaphthalene (2.40)**: (Procedure for entry 3 from Table 2.1) To a solution of

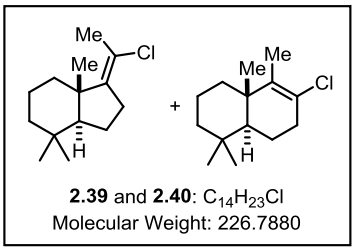

o,o'-dichloro-(*R*)-BINOL **2.25**[34] (0.357 g, 1.25 mmol) in CH_2Cl_2 (6.5 mL) at –78 °C was added $SnCl_4$ (1.25 mmol, 1.25 mL, 1.0 M in CH_2Cl_2) dropwise. After 15 min, a solution of dieneyne **2.17** (0.475 g, 2.49 mmol) in CH_2Cl_2 (6.5 mL) cooled to –78 °C was added via cannula to the reaction. Upon full consumption of dieneyne **2.17** (monitored by TLC), saturated aq. NH_4Cl (5 mL) was added, and the reaction warmed to 23 °C. The aqueous layer was extracted with Et_2O (3 x 10 mL), and the combined organic layers were dried over magnesium sulfate, filtered, and concentrated *in vacuo*. The resulting residue was concentrated over SiO_2 (~1 g) and then purified by flash column chromatography (100% hexanes) to provide an inseparable mixture of vinyl chlorides **2.39** and **2.40** as a clear oil (0.310 g, 1.37 mmol, 55%) in a 1.5:1 ratio by ^{1}H NMR. Diagnostic peaks for 5-*exo* product **2.39** on ^{1}H NMR (500 MHz, $CDCl_3$) δ 2.13 (app t, J = 2.0 Hz, 3H), 0.99 (s, 3H); diagnostic peaks for 5-*exo* product **2.39** on ^{13}C NMR (125 MHz, $CDCl_3$) δ 147.41, 120.84. Diagnostic peaks for 6-*endo* product **2.40** on ^{1}H NMR (500 MHz, $CDCl_3$) δ 1.72 (app t, J = 2.1 Hz, 3H), 1.01 (s, 3H); diagnostic peaks for 6-*endo* product **2.40** on ^{13}C NMR (125 MHz, $CDCl_3$) δ 139.28, 127.12; IR (thin film) 2949, 2866, 1665, 1458, 1378 cm^{-1}; HRMS (ESI) calculated for $C_{14}H_{23}Cl$ (M^+) 226.1488, observed 226.1497.

(3a*S*,7a*S*)-4,4,7a-trimethyloctahydro-1H-inden-1-one (2.1): A mixture of vinyl chlorides **2.39** and **2.40** (0.303 g, 1.42 mmol) were dissolved in acetone (10 mL) and H_2O (0.5 mL) and cooled to 0 °C. Ozone was passed through the solution until TLC analysis confirmed complete consumption of starting material. The solution was sparged with O_2 and then concentrated over SiO_2 (~1 g) *in vacuo*. Purification by flash column chromatography (5% Et_2O in hexanes to 15% Et_2O in hexanes) to provide ketone **2.1** as a clear oil (91 mg, 0.50 mmol, 38%). Spectral data was consistent with reported values.[6] *Ee* was determined to be –18% by chiral HPLC of corresponding hydrazone **S2.1**.[6]

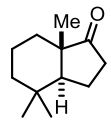

2.1: $C_{12}H_{20}O$
Molecular Weight: 180.2910

2.6 References and Notes

[1] For examples of alkene reductions to *cis*-hydrindanes, see: a) Paquette, L. A.; Wang, T.-Z.; Savik, M. R. *J. Am. Chem. Soc.* **1994**, *116*, 11323–11334. b) Sharpe, R. J.; Johnson, J. S. *J. Org. Chem.* **2015**, *80*, 9740–9766.

[2] A *trans* hydrindane with a methyl at the ring juncture is ~2 kcal/mol higher in energy. For more details, see Gordon, H. L.; Freeman, S.; Hudlicky, T. *Synlett* **2005**, *19*, 2911–2914.

[3] Brady, T. P.; Kim, S. H.; Wen, K.; Theodorakis, E. A. *Angew. Chem. Int. Ed*. **2004**, *43*, 739−742.

[4] Shigehisa, H.; Mizutani, T.; Tosaki, S.-Y.; Ohshima, T.; Shibasaki, M. *Tetrahedron* **2005**, *61*, 5057–5065.

[5] Alvarez-Manzaneda, E.; Chahboun, R.; Barranco, I.; Cabrera, E.; Alvarez, E.; Lara, A.; Alvarez-Manzaneda, R.; Hmamouchi, M.; Es-Samti, H. *Tetrahedron* **2007**, *63*, 11943–11951.

[6] Granger, K.; Snapper, M. L. *Eur. J. Org. Chem.* **2012**, *12*, 2308–2311.

[7] Lipshutz, B. H.; Hackmann, C. *J. Org. Chem.* **1994**, *59*, 7437–7444.

[8] Attempts to form prenyl magnesium bromide at higher concentrations were unsuccessful, as increasing the concentration of prenyl bromide and Mg^0 had a deleterious effect on the yield of the allylic magnesium bromide formation.

[9] HMPA was still required to trap the enolate with TMS-Cl. See SI for details on order of addition.

[10] For a reviews, see: Giner, J. L. *Chem. Rev.* **1993**, *93*, 1735–1752.

[11] For a review, see: Yoder, R. A.; Johnston, J. N. *Chem. Rev.* **2005**, *105*, 4730–4756.

[12] Ishihara, K.; Nakamura, S.; Yamamoto, H. *J. Am. Chem. Soc.* **1999**, *121*, 4906–4907.

[13] a) Uyanik, M.; Ishibashi, H.; Ishihara, K.; Yamamoto, H. *Org. Lett.* **2005**, *7*, 1601–1604. b) Ishihara, K.; Ishibashi, H.; Yamamoto, H. *J. Am. Chem. Soc.* **2002**, *124*, 3647–3655.

[14] Ishibashi, H.; Ishihara, K.; Yamamoto, H. *J. Am. Chem. Soc.* **2004**, *126*, 11122–11123.

[15] Ishihara, K.; Ishibashi, H.; Yamamoto, H. *J. Am. Chem. Soc.* **2001**, *123*, 1505–1506.

[16] Beside Yamamoto's and Corey's work, the only example I could find in the literature is Sakakura, A.; Sakuma, M.; Ishihara, K. *Org. Lett.* **2011**, *13*, 3130–3133.

[17] a) Surendra, K.; Corey, E. J. *J. Am. Chem. Soc.* **2012**, *134*, 11992–11994. b) Surendra, K.; Rajendar, G.; Corey, E. J. *J. Am. Chem. Soc.* **2014**, *136*, 642–645.

[18] First reported example by Johnson: Gravestock, M. B.; Johnson, W. S.; Myers, R. F.; Bryson, T. A.; Miles, D. H.; Ratcliffe, B. E. *J. Am. Chem. Soc.* **1978**, *100*, 4268–4273.

[19] Johnson, W. S.; Ward, C. E.; Boots, S. G.; Gravestock, M. B.; Markezich, R. L.; McCarry, B. E.; Okorie, D. A.; Parry, R. J. *J. Am. Chem. Soc.* **1981**, *103*, 88–98.

[20] Johnson, W. S.; Gravestock, M. B.; McCarry, B. E. *J. Am. Chem. Soc.* **1971**, *93*, 4332–4334.

[21] Bergman, J. A.; Hahne, K.; Song, J.; Hrycyna, C. A.; Gibbs, R. A. *ACS Med. Chem. Lett.* **2012**, *3*, 15–19.

[22] Attempts to deprotect the trimethylsilyl group *in situ* and trap with methyl iodide were unsuccessful.

[23] At –50 ºC, it appeared that the other byproducts arose from an interrupted cascade via premature chloride quenching, but none of these products were ever verified.

[24] Guay, D.; Johnson, W. S.; Schubert, U. *J. Org. Chem.* **1989**, *54*, 4731–4732.

[25] If this route was to be reinvestigated, I would suggest examining a number of factors: 1) Lewis acids with different halogens such as $SnBr_4$; 2) BINOL ligands that are mono-protected as in the examples from Yamamoto's work; 3) a detailed solvent screen besides CH_2Cl_2; and 4) further temperature screening between –78 ºC and –50 ºC.

[26] Myers, A. G.; Zheng, B. *Tetrahedron Lett.* **1996**, *37*, 4841–4844.

[27] Mandai, T.; Matsumoto, T.; Kawada, M.; Tsuji, J. *J. Org. Chem.* **1992**, *57*, 1326–1327.

[28] For a detailed report of this route's challenges, see Yuriy Slutskyy's reports. As well, for procedures and spectra, see: Tao, D. J.; Slutskyy, Y.; Overman, L. E. *J. Am. Chem. Soc.* **2016**, *138*, 2186–2189.

[29] The allylic formate[27] derivative reported by Tsuji was not a competent leaving group for the Pd-catalyzed reductive transposition.

[30] The reductive transposition is the sequence's limiting step for scaling. Upon scaling the reaction above 3 g of allylic carbonate **2.57**, undesired byproducts including *cis*-hydrindane variants began to form and diminished the yield of desired alkene **2.58**. However, at 3 g scale or below, the reaction is reliable.

[31] a) Miyano, S.; Hashimoto, H. *Bull. Chem. Soc. Jpn.* **1973**, *46*, 892–897. b) Denmark, S. E.; Edwards, J. P. *J. Org. Chem.* **1991**, *56*, 6974–6981.

[32] The yield of the reaction before recrystallization is 93% and 75% afterwards. The ~5% impurity was never identified, but it was hypothesized to arise from the previous step via unregioselective hydrogenolysis of the cyclopropane. This impurity was separable after the NHK reaction in the chromodorolide B route, but the recrystallization is crucial at this point if high purity (+)-hydrindanone **2.1** is required.

[33] Clausen, D. J.; Wan, S.; Floreancig, P. E. *Angew. Chem. Int. Ed.* **2011**, *50*, 5178–5181.

[34] Turner, H, M.; Patel, J.; Niljianskul, N.; Chong, J. M. *Org. Lett.* **2011**, *13*, 5796-5799.

Chapter 3: Total Synthesis of (–)-Chromodorolide B

3.1 Radical-Mediated Formal [3+2] Cycloaddition Approach

The initial synthetic approach to the chromodorolides was complicated by the diastereoselectivity of alkene dihydroxylation of the *cis*-oxabicyclo[3.3.0]octenone model system (Section 1.5). The phosphine-promoted [3+2] dipolar cycloaddition efficiently assembled the carbon skeleton requisite for the chromodorolides, but subsequent dihydroxylation revealed that torsional steering effects would likely direct oxidation to occur from the undesired concave face of the *cis*-oxabicyclo[3.3.0]octenone. Attempts to perform a dipolar cycloaddition reaction with analogous substrates possessing this oxygenation (**3.1**) would likely result in elimination of the β-alkoxy group to generate enoate **3.4** (Scheme 3.1). As installation of the vicinal diols would not be feasible before or after the dipolar cycloaddition, access to the chromodorolides required an alternative approach that would tolerate the additional oxygenation.

Scheme 3.1. Consideration of Complex [3+2] Dipolar Cycloaddition.

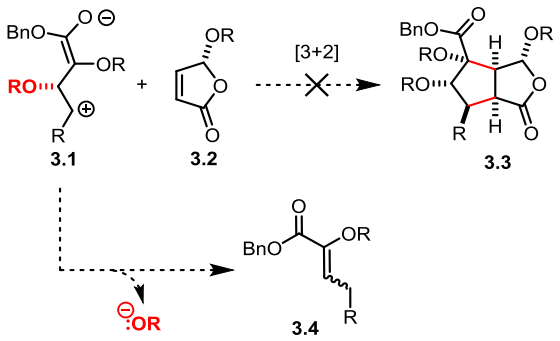

3.1.1 Retrosynthesis using a Formal [3+2] Radical Cycloaddition

Prior to efforts developing a revised approach toward the chromodorolides, the Overman group demonstrated that visible-light photoredox catalysis could facilitate

construction of sterically congested C–C bonds. Dr. Martin Schnermann devised a strategy wherein conjugate addition of a tertiary radical, generated by photoredox-mediated fragmentation of an (*N*-acyloxy)phthalimide,[1] to a complex cyclopentenone was critical in forging vicinal quaternary and tertiary stereocenters towards completion of (–)-aplyviolene (Section 1.2.3.2).[2] Separate methods using tertiary alcohols in a related fragmentation of oxalate esters/acids as radical precursors were subsequently developed by our group and others.[3]

Applying related methodology in a biological context, Dr. Michelle Garnsey focused on utilizing (*N*-acyloxy)phthalimides in radical conjugate additions to butenolide acceptor **3.7** to synthesize truncated analogues of rearranged spongian diterpenes.[4] Her synthetic work was part of a collaborative effort[5] to study the Golgi-modifying properties of molecules of this type (Section 1.3). Of particular note, a photoredox reaction by Dr. Garnsey between (*N*-acyloxy)phthalimide **3.5** and butenolide **3.7** produced *cis*-oxabicyclo[3.3.0]octenone **3.9** in 55% yield (Scheme 3.2). The intermediate α-acyl radical **3.8**, formed from addition of tertiary radical **3.6** to butenolide **3.7**, underwent 5-*exo* cyclization on the tethered alkyne prior to hydrogen atom abstraction. This radical cascade constructed the two analogous bonds that the [3+2] dipolar cycloaddition formed in the original strategy toward the chromodorolides. Because of the thermodynamic preference for a carbon-centered radical over an oxygen-centered radical (Figure 3.1), I speculated that a similar radical cascade with a highly oxygenated substrate could be developed to circumvent the issues encountered in the previous strategy and allow access to the chromodorolides.

Scheme 3.2. Formal [3+2] Radical Cycloaddition.

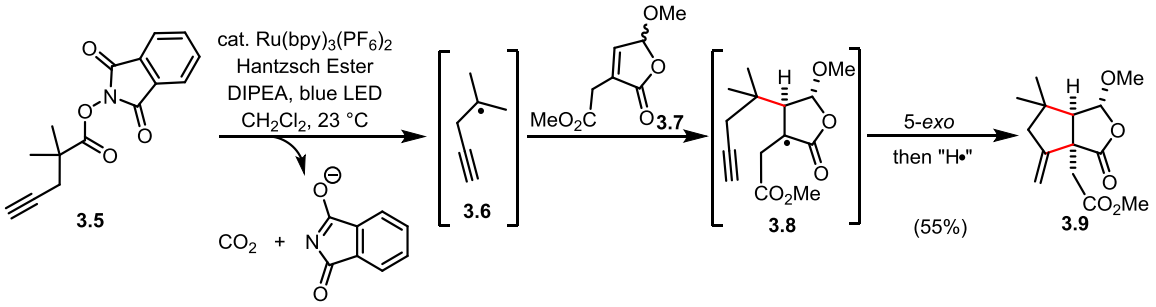

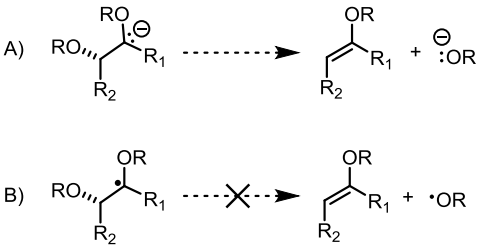

Figure 3.1. Differences between α-Oxy Radicals and Anions.

In light of Dr. Garnsey's discovery, I was interested in applying this bimolecular radical addition/cyclization cascade, or formal [3+2] radical cycloaddition, to the synthesis of the chromodorolides. In a retrosynthetic sense (Scheme 3.3), both bridged and fused chromodorolides would arise from site-selective oxocarbenium ion formation and trapping of common precursor **3.10** (Section 1.4). This acid would be formed by a series of redox manipulations of *tert*-butyldimethylsilyl ether **3.11**,[6] the product of late-stage coupling between hydrindanone **3.12** (Chapter 2) and highly oxidized fragment **3.13**. The *cis*-oxabicyclo[3.3.0]octenone of **3.13** would be formed from a formal [3+2] radical cycloaddition between (*N*-acyloxy)phthalimide **3.16** and chiral, nonracemic butenolide **3.2**. Under visible-light photoredox conditions, **3.16** would undergo reductive decomposition to trisubstituted acetonide radical **3.15**.[1] This radical would then undergo conjugate

addition to butenolide **3.2** to yield α-acyl radical intermediate **3.14**. Cyclization of **3.14** with the tethered alkyne followed by hydrogen atom abstraction would give alkene **3.13**, constructing three contiguous stereocenters and two C–C bonds in the radical cascade.

Scheme 3.3. Retrosynthetic Analysis from the Chromodorolides Using Formal [3+2] Radical Cycloaddition.

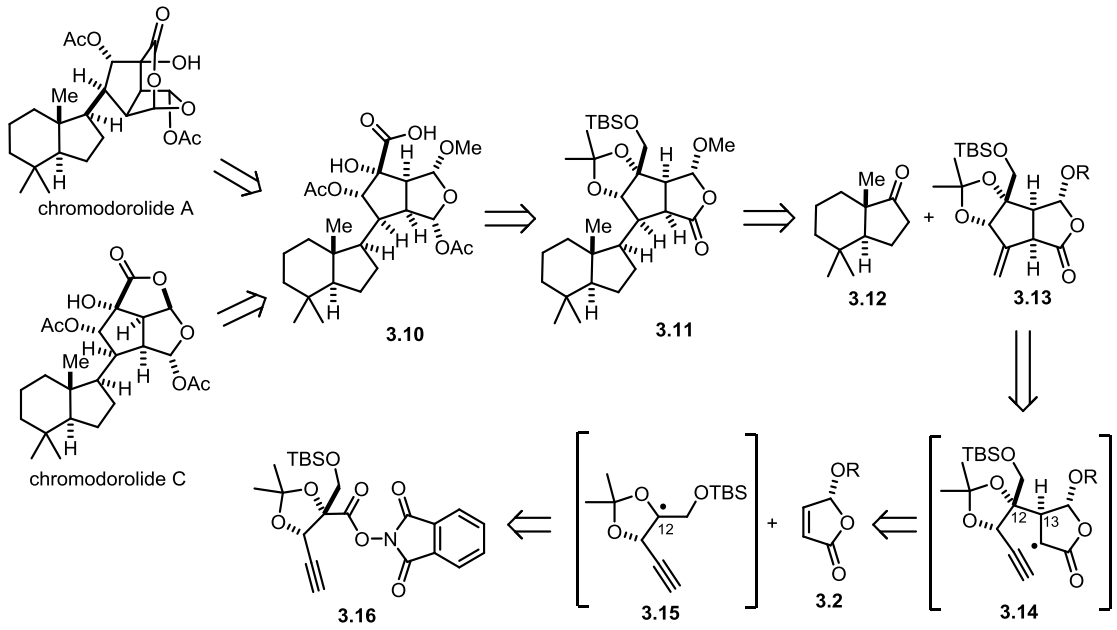

Critical to the success of this approach would be the diastereoselectivity obtained during the formal [3+2] radical cycloaddition. Intermediate **3.14** would be formed by conjugate addition generating vicinal stereocenters, the fully substituted carbon (C12) and the tertiary stereocenter at C13 (β-position of butenolide **3.2**). The C13 stereocenter was expected to form stereoselectively by addition of the trisubstituted radical *anti* to the γ-substituent of the butenolide.[3] However, it was unclear at the outset whether addition of radical **3.15** to butenolide **3.2** would occur from the requisite face *syn* to the tethered alkyne to set the desired C12 stereochemistry. Approach from the same face of the alkyne would be sterically disfavored; but to my knowledge,[7] diastereoselective couplings of trisubstituted acetonide radicals were without precedent. Thus, I believed this ambitious

approach to be an opportunity to investigate a radical addition/cyclization strategy and showcase photoredox catalysis in a complex setting.

3.1.2 Synthesis of Radical Precursor 3.16

Radical precursor **3.16** proved more challenging to synthesize than anticipated. Initial efforts toward radical precursor **3.16** by alkylation of desymmetrized tartrate derivative **3.17** were unsuccessful (Scheme 3.4A). Instead, an alternate approach was taken using known alcohol **3.23**,[8] which can be prepared in a reported five-step sequence from *L*-arabinose (Scheme 3.4B). In this route, *L*-arabinose underwent selective acetonide formation followed by oxidative cleavage and hydrolysis to give bicyclic lactol **3.19** as an anomeric mixture. Base-promoted aldol reaction of lactol **3.19** with paraformaldehyde (via aldehyde **3.20**) provided primary alcohol **3.21** as a mixture of anomers. Selective silyl protection of the primary alcohol and ring-opening Wittig olefination afforded known alcohol **3.23**[8] in 20% overall yield from *L*-arabinose. Oxidation of **3.23** to the corresponding aldehyde occurred smoothly, but purification of the aldehyde proved challenging.[9] Instead, exposure the crude aldehyde directly to K_2CO_3 and dimethyl (1-diazo-2-oxopropyl)phosphonate[10] (**3.24**) in MeOH provided eneyne **3.25** in 71% yield over the two steps.[11] Eneyne **3.25** then underwent chemoselective ozonolytic cleavage of the alkene, which was directly oxidized under Pinnick-Lindgren conditions to acid **3.26**. Coupling *N*-hydroxyphthalimide to acid **3.26** using Steglich conditions[12] then provided radical cascade precursor (*N*-acyloxy)phthalimide **3.16** in ten steps from *L*-arabinose.

Scheme 3.4. Synthetic Approaches to (*N*-acyloxy)phthalimide 3.16.

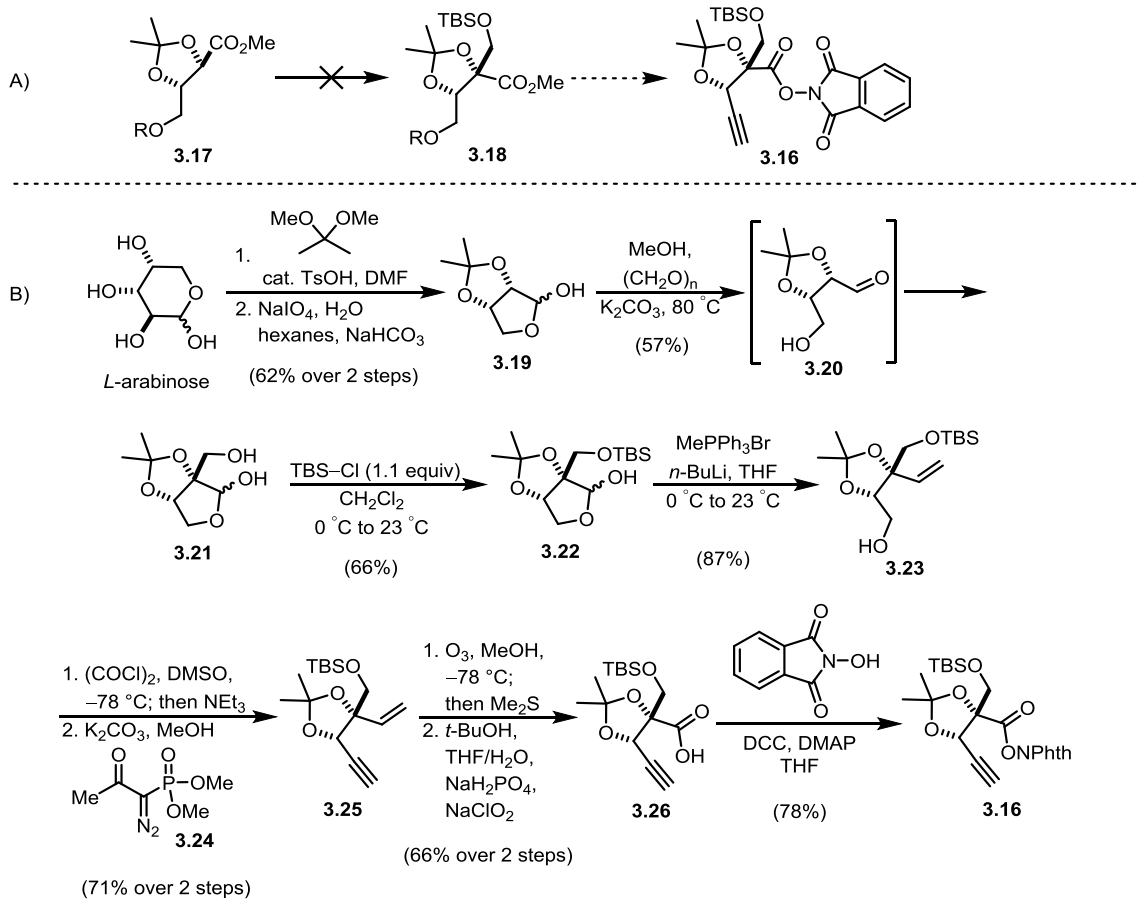

3.1.3 Formal [3+2] Radical Cycloaddition

With sufficient quantities of radical precursor **3.16** in hand, the photoredox-catalyzed formal [3+2] radical cycloaddition was then examined. Detailed mechanistic studies of the photoredox-catalyzed decarboxylation mechanism will not be discussed here as they were thoroughly investigated by Dr. Gerald Pratsch and Greg Lackner in previous studies.[13] Under standard photoredox conditions,[1,13] (*N*-acyloxy)phthalimide **3.16** underwent decarboxylative radical coupling and cyclization with enantiopure butenolide **3.27**[14] to provide tricyclic lactone **3.28** in 43% yield.[15] The only other isolated product was

alkyne **3.29** in 11% yield, with NOE data supporting orientation of the lactone fragment *anti* to the alkyne on the acetonide.

Equation 3.1

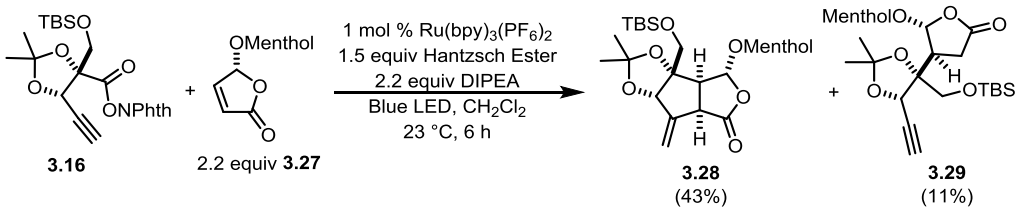

Shown in Scheme 3.5, the proposed mechanism begins with reductive fragmentation of radical precursor **3.16** to trisubstituted acetonide radical **3.15**. Conjugate addition of **3.15** to butenolide **3.27** from the acetonide face *syn* to the alkyne (blue arrows) forms the fully substituted C12 stereocenter as desired. Resulting α-acyl radical **3.30** then undergoes 5-*exo* cyclization onto the pendant alkyne. The resulting vinyl radical **3.31** abstracts a hydrogen atom to yield desired product **3.28**. Byproduct **3.29** arises from addition of radical **3.15** to **3.27** from the acetonide face *anti* to the alkyne (red arrows), affording the undesired configuration at C12 in **3.32**. Resulting α-acyl radical **3.32** is not positioned to cyclize onto the tethered alkyne. Instead, the radical is quenched either by hydrogen atom abstraction or SET reduction/protonation to give minor product **3.29**. The origin for the observed C12 diastereoselectivity favoring *syn* addition of the trisubstituted radical (~4:1 dr) was unclear;[16] but at the time, effort was directed towards optimization of the formal [3+2] radical cycloaddition.

Scheme 3.5. Proposed Mechanism to Formal [3+2] Radical Cycloaddition Products.

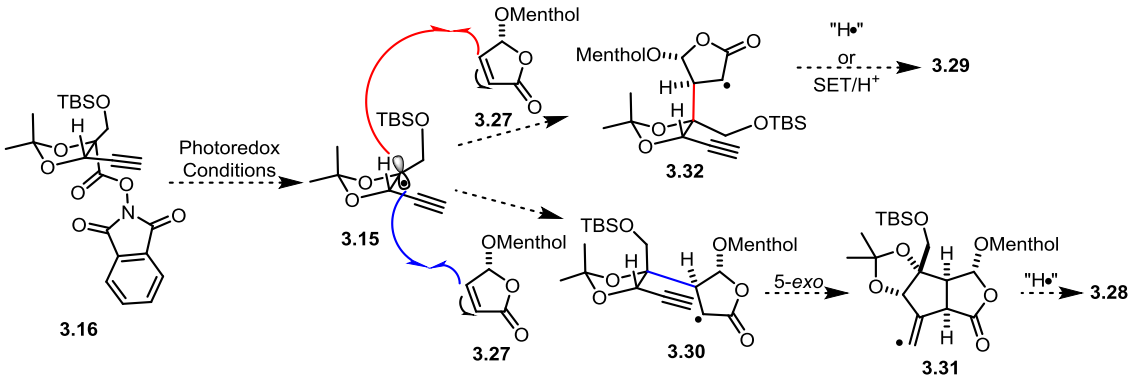

Having now verified the success of this key step, I aimed to increase the yield of radical cycloadduct **3.28**. Shown in Table 3.1, different equivalents of the coupling partners were examined (entries 1–3). Employing an excess butenolide **3.27** was preferred (entry 1) to an excess of (*N*-acyloxy)phthalimide **3.16** (entry 2), as the radical precursor was the more valuable starting material. Adding greater than 1.5 equiv of acceptor **3.27** was detrimental to product formation (entries 4 and 5). Changing the additives such as $(i\text{-Pr})_2NEt{\bullet}HBF_4$ (entry 6) or solvents (entries 7–9) did not increase the yield of desired product **3.28**. On a larger scale (entry 10), **3.28** was consistently isolated in 38% yield. Despite accounting for only 50% of the mass balance, access to sufficient quantities of **3.28** allowed for investigation of its late-stage coupling to the hydrindane fragment.

Table 3.1. Formal [3+2] Radical Cycloaddition Optimization.

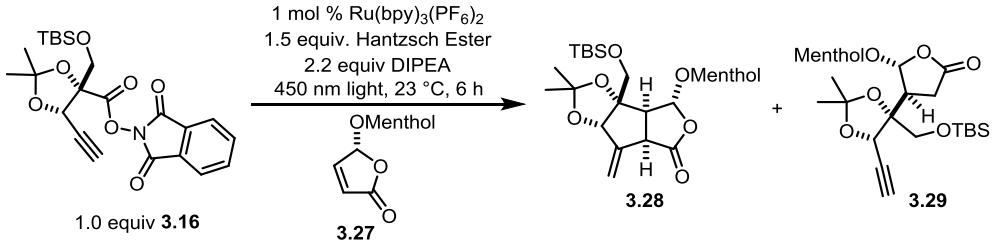

Entry	Scale	Solvent	Equiv 3.27	Other Variations	Yield of 3.28 (NMR)[1]	Yield of 3.29 (NMR)
1	50 mg	CH_2Cl_2	1.5	-	43%	-
2	50 mg	CH_2Cl_2	0.66	-	48%[2]	-
3	30 mg	CH_2Cl_2	1.0	-	30% (36%)	(11%)
4	30 mg	CH_2Cl_2	2.0	14 h LED exposure	39%	-
5	30 mg	CH_2Cl_2	3.0	14 h LED exposure	27%	-
6	30 mg	CH_2Cl_2	1.5	HBF_4 salt of DIPEA	(31%)	(13%)
7	30 mg	MeCN	1.5	-	(29%)	(12%)
8	30 mg	THF/CH_2Cl_2 (1:1)	1.5	-	(32%)	(14%)
9	30 mg	THF/H_2O (4:1)	1.5	$Ru(bpy)_3Cl_2$ cat.; BNAH[3]	(22%)	(13%)
10	100 mg	CH_2Cl_2	1.5	-	38%	9%

[1] NMR yields in parentheses were taken with an internal standard of ethylene glycol. [2] Yield based on butenolide **3.27** as limiting reagent.[3] 1-Benzyl-1,4-dihydronicotinamide.

3.1.4 Attempted Coupling of Hydrophobic and Hydrophilic Fragments

To connect the hydrophobic fragment to the radical cycloadduct **3.28**, hydrindanone **3.12**[17] was transformed into several potential coupling precursors (Scheme 3.6). These coupling precursors were previously employed for uniting the hydrindane subunit to oxygenated fragments in the total syntheses of (+)-norrisolide[18] (Scheme 3.7). Hydrindanone **3.12** was converted to vinyl iodide **3.32** in a two-step sequence in 78% yield by hydrazone formation and iodination in the presence of 1,1,3,3-tetramethylguanidine (TMG).[19] Vinyl iodide **3.32** could then act as a cross-coupling partner by oxidative addition or as a nucleophile after lithium-halogen exchange. Alternative coupling precursor, such

as vinyl triflate **3.33** and 2,4,6-triisopropylbenzenesulfonyl (trisyl) hydrazone **3.34**, were also prepared from ketone **3.12**.

Scheme 3.6. Synthesis of Hydrindane Coupling Precursors.

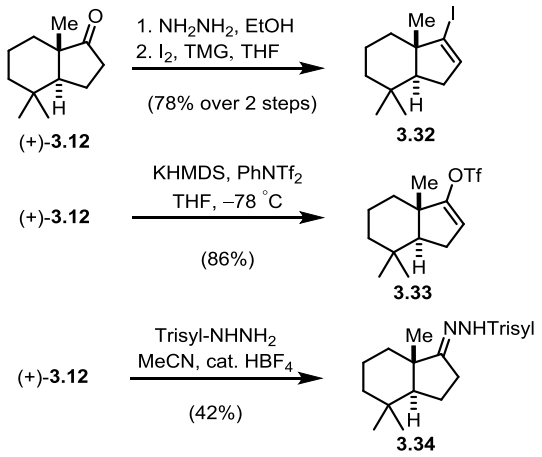

Scheme 3.7. Previous Examples of Coupling Derivatives 3.32, 3.33, and 3.34.

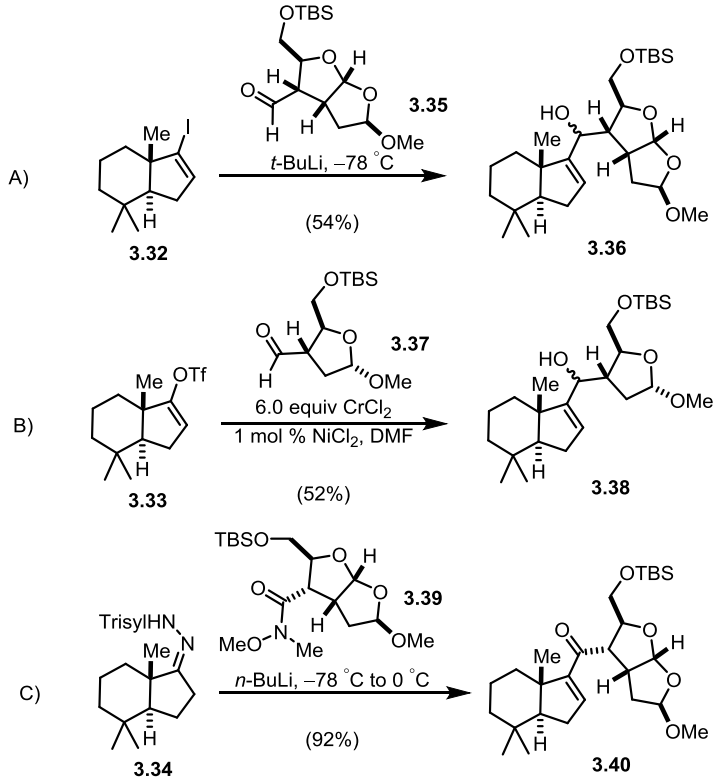

Union of the two fragments also required elaboration of radical cascade product **3.28** (Scheme 3.8). The *exo* methylene group of **3.28** was excised by ozonolysis, which

gave β-ketolactone **3.41** in 74% yield. Attempts to form the vinyl triflate **3.42** from **3.41** using a variety of bases (e.g., NaH, LHMDS or KHMDS) and triflating reagents (*N*-phenyl-bis(trifluoromethanesulfonimide) or *N*-(5-chloro-2-pyridyl)bis(trifluoromethanesulfonimide)[20]) were unsuccessful. It was unclear whether deprotonation of the β-ketoester or *O*-triflation was inefficient as vinyl triflate **3.42** was never observed. Starting material **3.41** was the only readily characterized compound in the reaction mixtures. Deprotonation of this *cis*-bicyclo[3.3.0]octanone to form bridgehead enolates may be particularly difficult despite adjacent carbonyl groups for two reasons: 1) poor orbital overlap of the α-C-H σ-bond and carbonyl π-bonds would render the α-proton relatively non-acidic; and 2) deprotonation to the enolate would generate an additional sp^2 carbon in the highly functionalized and considerably strained central cyclopentane. Of note, deprotonation and *O*-alkylation of a similar system was previously reported.[21]

Scheme 3.8. Formation of β-Ketolactone 3.41 and Failed Triflation.

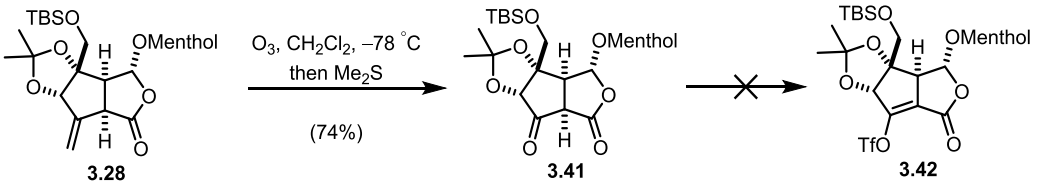

Unable to functionalize β-ketolactone **3.41**, I then investigated its potential as an electrophile for 1,2-alkylation. Both pronucleophiles **3.32** and **3.34** would generate the same vinyl lithium intermediate (**3.43**) when treated with *n*-butyllithium. Subsequent 1,2-addition of this organolithium intermediate to β-ketolactone **3.41** would give tertiary alcohol **3.44** (Scheme 3.9). Under no conditions, including the use of additives such as $CeCl_3$,[22] was a coupled product observed using either pronucleophiles **3.32** or **3.34**. Analysis of crude reaction mixtures provided little insight,[23] as β-ketolactone **3.41** was the sole identifiable compound. Other synthetic manipulations of **3.41** were considered, but

this route was ultimately abandoned in favor of one that would bypass this challenging coupling between two sterically congested fragments (**3.43** bears a vicinal quaternary carbon and ketone **3.41** is embedded within a complex tricyclic framework).

Scheme 3.9. Failed 1,2-Alkylation with Vinyl Iodide 3.32 and Trisyl Hydrazone 3.34.

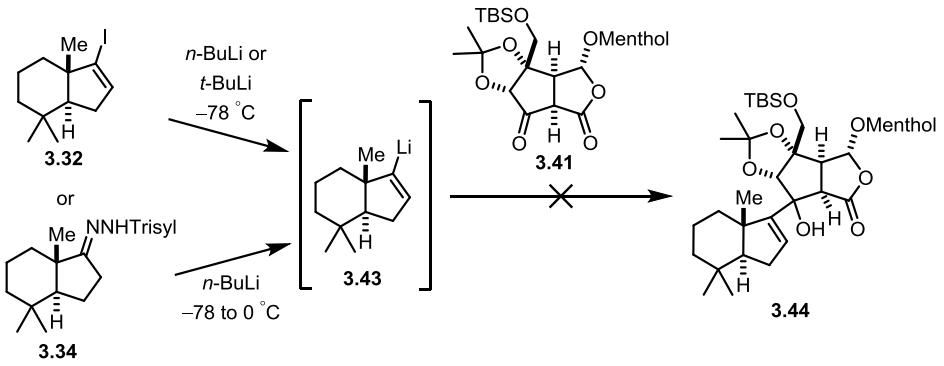

3.2 Radical Addition/Cyclization/Fragmentation Cascade

Formation of radical cycloaddition product **3.28** was an encouraging step toward completion of the chromodorolides. However, the ten-step synthesis of (*N*-acyloxy)phthalimide **3.16** was inefficient, requiring alkyne homologation and later oxidative removal of that carbon unit to access β-ketolactone **3.41** (Scheme 3.10). This inefficiency, along with the inability to couple β-ketolactone **3.41**, led me to propose the following route to the chromodorolides.

Scheme 3.10. Summary of the Formal [3+2] Radical Cycloaddition Route.

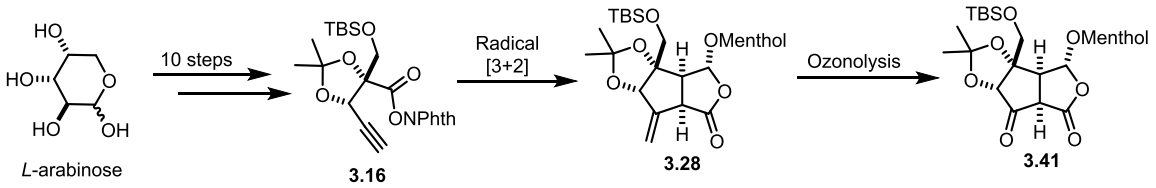

3.2.1 Revised Retrosynthesis of the Chromodorolides

Centered on developing a more efficient route, a revised retrosynthesis was proposed from the fused and bridged chromodorolides, which would arise from site-

selective oxocarbenium ion formation and trapping of common precursor **3.10** (Scheme 3.11). Acid **3.10** would be formed from several redox and protecting group manipulations of lactone **3.45**. The oxygenated framework of lactone **3.45** would then be constructed from a related radical addition/cyclization cascade with butenolide acceptor **3.2**, wherein α-acyl radical intermediate **3.46** would undergo a 5-*exo* cyclization onto a tethered alkylidene hydrindane subunit. The desired C8 stereochemistry was hypothesized to be favored in the 5-*exo* cyclization via a conformation **3.46'** which minimizes destabilizing allylic $A^{1,3}$ interactions. The C12 and C13 stereocenters would be set in analogous fashion to the previous alkyne radical **3.15** in that addition of the trisubstituted acetonide radical to butenolide **3.2** would occur *syn* to the hydrindane fragment and *anti* to the butenolide's γ-methoxy substituent (Section 3.1.3). The initial trisubstituted acetonide radical for the cascade would be generated from (*N*-acyloxy)phthalimide **3.47**, which would be assembled from hydrindanone **3.12** and tartrate derivative **3.48**.

Scheme 3.11. Revised Retrosynthesis of the Chromodorolides.

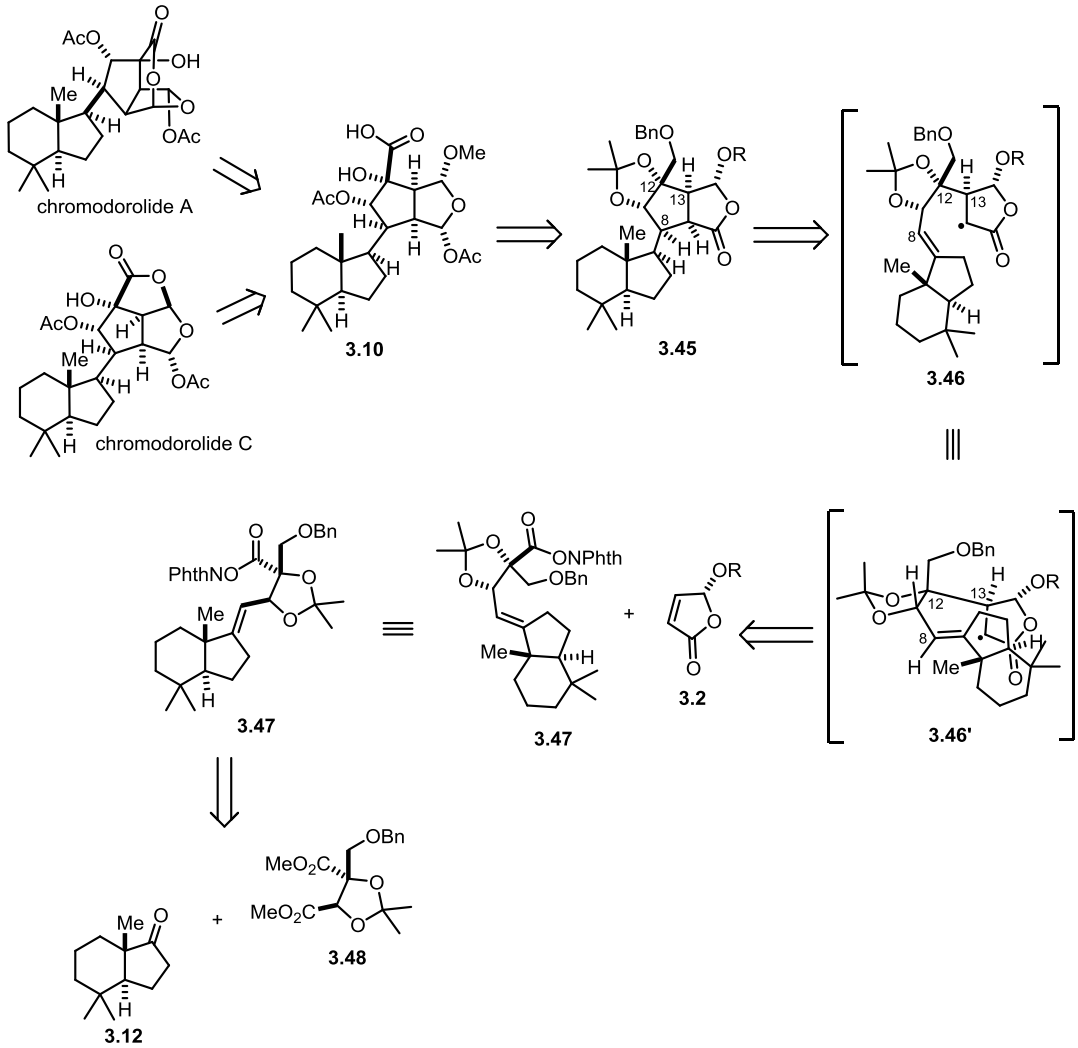

3.2.2 Synthesis of Tartrate-Derived Aldehyde 3.55

I aimed to access diester **3.48** from inexpensive and enantiopure *L*-dimethyl tartrate. This route required a desymmetrizing alkylation of dimethyl 2,3-*O*-isopropylidene-*L*-tartrate (**3.49**). Desymmetrizing alkylations and aldol reactions with tartrate-based nucleophiles were previously examined by Seebach[24] and Evans.[25] Both groups reported these derivatives to be competent in enolate-mediated transformations (Scheme 3.12A and B). Crich later applied Seebach's methodology for alkylation of tartrate derivative **3.52**

with benzyloxymethyl chloride (BOM-Cl),[26] a useful electrophile for my synthetic efforts (Scheme 3.12C).

Scheme 3.12. Previous Examples of Tartrate Derivative Desymmetrizing Alkylations/Aldol Reactions.

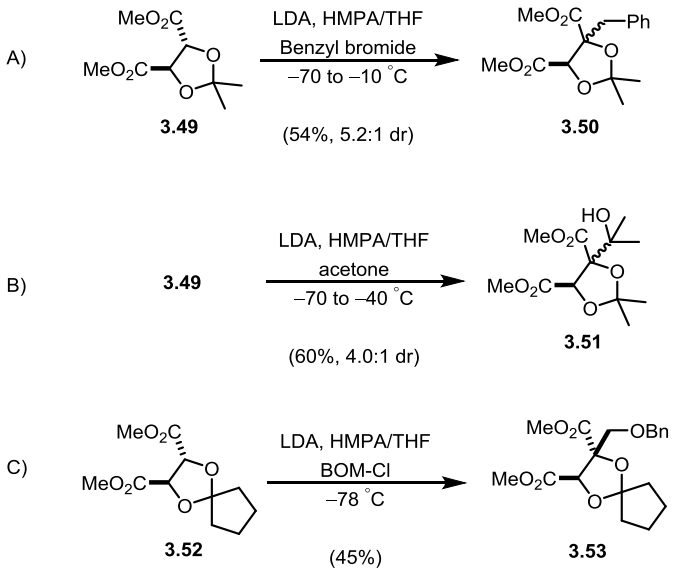

Applying Crich's procedure to the tartrate-based acetonide **3.49**, LDA-mediated alkylation with BOM-Cl afforded benzyl ether **3.48** in 46% yield (Scheme 3.13). The modest yield for this step was mitigated by the value of formally alkylating and benzylating a formaldehyde equivalent in one step as a single diastereomer and enantiomer. Subsequent reduction of the less hindered ester of **3.48** using Crich's procedure[19] afforded alcohol **3.54** in modest yield.[27] Oxidation of **3.54** to aldehyde **3.55** was achieved by a number of methods, but purification of this aldehyde proved challenging. However, use of Dess-Martin periodinane (DMP) and filtration with hexanes[28] afforded aldehyde **3.55** with trace impurities (<5%). Notably, decomposition was observed within 24 h regardless of storage conditions,[29] and the compound was carried forward immediately to minimize degradation.[30] This route proved to be a concise and scalable route to aldehyde **3.55**, which allowed examination of the coupling between **3.55** and hydrindanone **3.12**.

Scheme 3.13. Synthesis of Aldehyde 3.55.

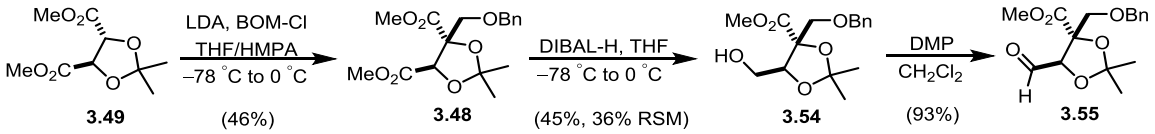

3.2.3 Coupling of Hydrindane Fragment to Aldehyde 3.55

With access to several hydrindane-based nucleophilic precursors (Section 3.1.4), early screening revealed that vinyl anions generated from vinyl iodide **3.32** or trisyl hydrazone **3.34** were too reactive for coupling to sensitive aldehyde **3.55**.[31] Desiring a milder method to couple the two fragments, Nozaki-Hiyama-Kishi (NHK) protocols were examined, which Theodorakis previously employed to couple vinyl iodide **3.32** to monocyclic aldehyde **3.56** in 71% yield (Scheme 3.14A).[32] Theodorakis found that analogous attempts to couple **3.32** to a more hindered bicyclic aldehyde (**3.58**) resulted in low conversion to the desired coupling product **3.59** (Scheme 3.14B).[18b] Employing similar NHK coupling conditions between vinyl iodide **3.32** with aldehyde **3.55** proved inefficient (Scheme 3.14C),[33] likely because of fragments' steric congestion and the instability of aldehyde **3.55**. A survey of the literature reaffirmed that NHK couplings between hindered aldehydes and/or hindered nucleophiles are challenging because of the attenuated nucleophilicity of organochromium compounds.[34]

Scheme 3.14. NHK Couplings of Vinyl Iodide 3.32.

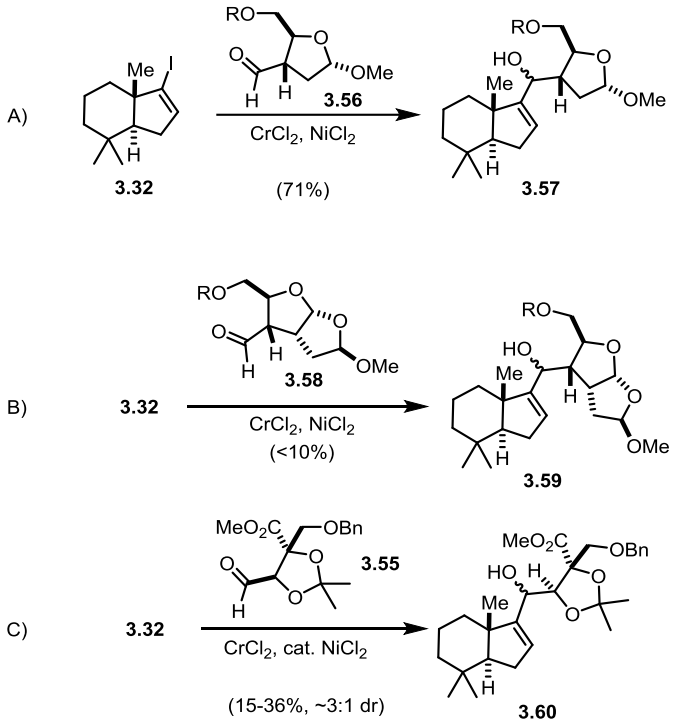

To counteract the low reactivity of organochromium reagents, ligands for chromium have been developed over the last two decades to enhance reactivity and induce asymmetry in NHK couplings to aldehydes (Figure 3.2).[35] Specifically, oxazoline ligand (*R*)-**3.62** was employed to accelerate an NHK coupling on process scale by Eisai Co. in the synthesis of eribulin.[36] Employing ligand (*R*)-**3.62** in an NHK coupling between vinyl iodide **3.32** (1.6 equiv) and aldehyde **3.55** (1.0 equiv) afforded allylic alcohol (*R*)-**3.64** as a single alcohol diastereomer in 28% yield (Scheme 3.15A).[37] Identical reaction conditions with enantiomer (*S*)-ligand **3.62** inverted diastereoselectivity favoring epimeric (*S*)-alcohol **3.65** (4:1 dr, Scheme 3.15B).

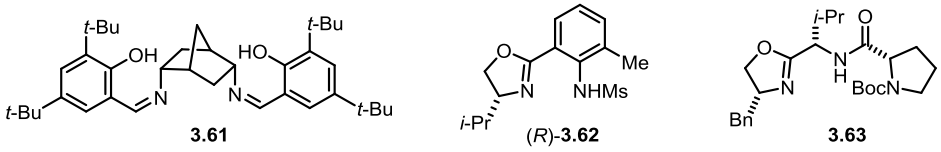

Figure 3.2. Representative Ligands Developed for Asymmetric NHK Couplings.

Scheme 3.15. Ligand-Accelerated NHK Coupling of Vinyl Iodide 3.32 and Aldehyde 3.55.

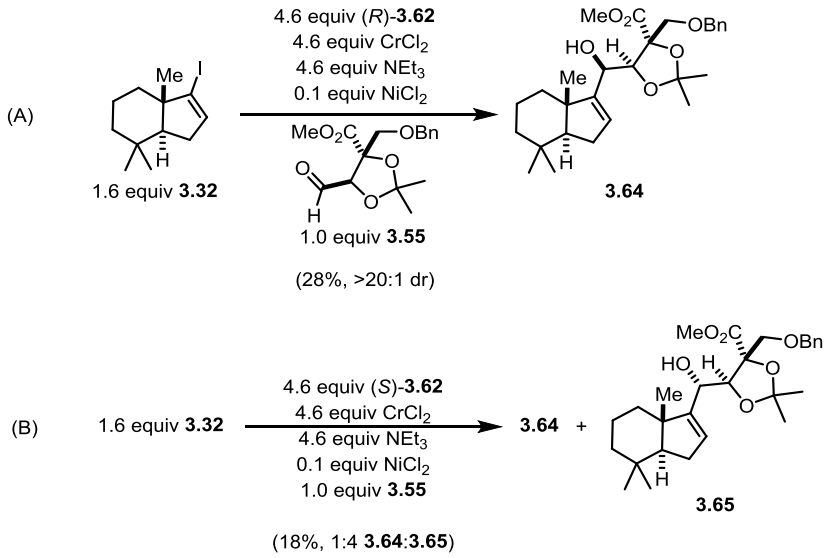

With high diastereoselectivity observed with oxazoline (*R*)-**3.62**, I then optimized the ligand-accelerated NHK coupling. Because of the aldehyde's proclivity to decompose, an excess of aldehyde **3.55** (1.6 equiv)[38] was used relative to vinyl iodide **3.32**, which afforded allylic alcohol **3.64** in 43% yield (Scheme 3.16, entry 1). As the reaction scale increased from 0.35 mmol to 2.74 mmol (entry 4), the yield of allylic alcohol **3.64** steadily increased. A minor byproduct was observed in large scale reactions, which was later identified as lactone **3.66**.[39] This compound arose from epimerization of aldehyde **3.55** to **3.67** followed by NHK coupling and lactonization. This was a surprising result as organochromium reagents are typically considered nonbasic nucleophiles.[34] As lactone **3.66** was easily separated, no significant efforts were taken to prevent *in situ* epimerization;[40] and allylic alcohol **3.64** was carried forward.

Scheme 3.16. Optimized Ligand-Accelerated NHK Coupling of Vinyl Iodide 3.32 and Aldehyde 3.55.

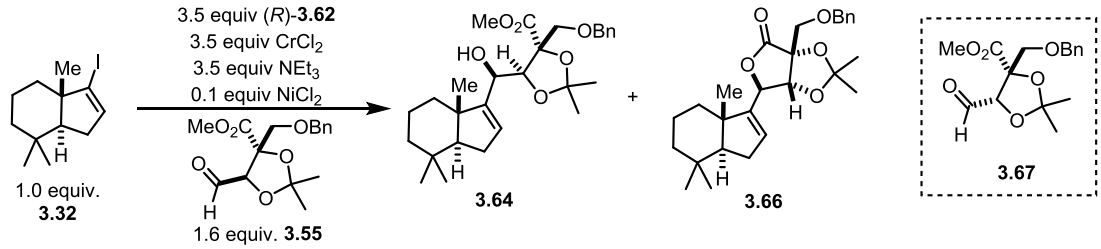

Entry	Scale	Yield of 3.64	Yield of 3.66
1	0.35 mmol	43%	Not observed
2	0.86 mmol	52%	Not observed
3	1.94 mmol	62%	4%
4	2.74 mmol	66%	10%

3.2.4 Alkene Transposition/Functionalization to Radical Precursor

Having forged all C–C bonds required for the radical cascade precursor, the next challenge was transposition of the alkene (Equation 3.2) to the requisite position (**3.68**) for the 5-*exo* cyclization event in the addition/cyclization cascade. To accomplish this transformation, palladium-catalyzed carbonate reductions[41] and reductive retro ene reactions using *o*-nitrobenzenesulfonylhydrazine (NBSH)[42] were the most precedented methods. The latter with NBSH was preferable as it facilitates a stereospecific reductive transposition.[43] Unfortunately, efforts to induce reductive transposition of allylic alcohol **3.64** with this reagent proved ineffective, only affording recovered starting material.[44]

Equation 3.2

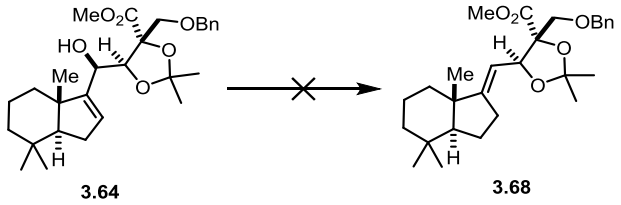

I turned my attention to a [3,3]-sigmatropic rearrangement, as a similar transformation with hydrindene **3.69** to allylic thiocarbonate **3.72** had been reported (Scheme 3.17). In light of the difficulties attempting the Mitsunobu/retro ene sequence with NBSH, I hoped that acylation of **3.64** would overcome the secondary alcohol's hindered nature. To facilitate thioacylation and rearrangement with chlorothionoformate **3.70**, a variety of conditions were screened with alcohol **3.64**. Typical bases for this transformation (pyridine, imidazole) did not facilitate thioacylation of the hindered allylic alcohol, even at refluxing temperatures. Stronger bases such as LiHMDS and NaHMDS were also unsuccessful in thioacylation with chlorothionoformate **3.70**. However, treatment of alcohol **3.64** with KHMDS at –78 ºC followed by addition of **3.70** resulted in thioacylation and spontaneous [3,3]-sigmatropic rearrangement upon warming to 23 ºC to give allylic thiocarbonate **3.73** as a single stereoisomer with *E* configuration (Scheme 3.18).[45]

Scheme 3.17. Previous Sigmatropic Rearrangement to Allylic Thiocarbonate 3.72.

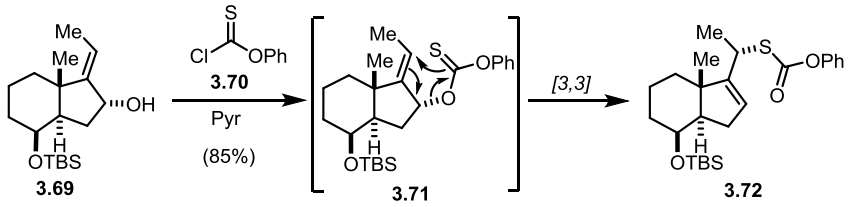

Scheme 3.18. Rearrangement of Allylic Alcohol 3.64 and Attempted Saponification to Acid 3.74.

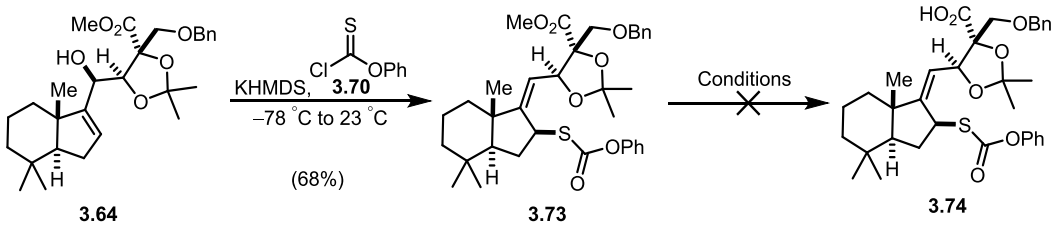

With the alkene transposed, installation of the (*N*-acyloxy)phthalimide functionality was attempted via two-step saponification and DCC coupling. I presumed selective hydrolysis of the methyl ester in the presence of a thiocarbonate would be feasible because of the greater electrophilicity of the ester. Unfortunately, the methyl ester of thiocarbonate **3.73** could not be selectively cleaved to acid **3.74** under a variety of conditions. Classical hydroxide conditions resulted in complex mixtures, while S_N2 methods[46] resulted in uncontrolled allylic displacement of the thiocarbonate of **3.73**. Other nonbasic methods[47] also failed to provide acid **3.74**.

In an effort to circumvent this selectivity issue, the order of alkene transposition and ester hydrolysis was reversed. Hydrolysis of allylic alcohol **3.64** and amide coupling yielded (*N*-acyloxy)phthalimide **3.75**, which proved sensitive to column chromatography (Scheme 3.19).[48] Subsequent treatment of **3.75** with KHMDS in the presence of phenyl chlorothionoformate **3.70** at –78 ºC resulted in immediate decomposition of the (*N*-acyloxy)phthalimide functionality.[49] Switching to LHMDS or NaHMDS did not decompose (*N*-acyloxy)phthalimide **3.75**, but no thioacylation or rearrangement was observed.[50] The ineffectiveness of these bases presumably arose from the less ionic nature of the sodium and lithium counterions. Screening other potassium bases (KO*t*-Bu, KDA, trityl potassium, $TMSCH_2K$,[51] potassium 1,1,3,3-tetramethyl-1,3-diphenyldisilazane[52]) uniformly led to decomposition of the (*N*-acyloxy)phthalimide functionality. Unable to selectively activate the hindered alcohol of **3.75** for acylation with chlorothionoformate **3.70**, a more reactive electrophile to facilitate alkene transposition was then pursued.

Scheme 3.19. Attempted Alternate Route to Access Radical Precursor 3.76.

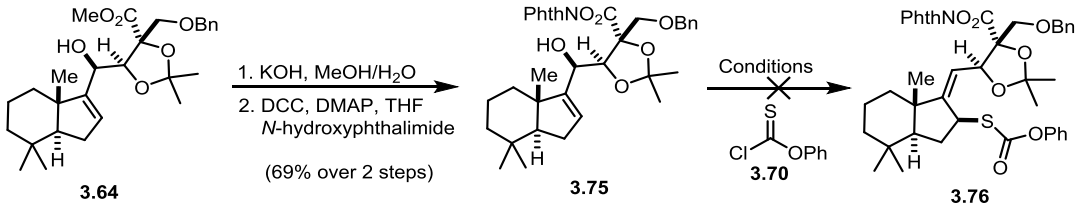

Among the most reactive reagents mediating allylic rearrangements are halogen-substituted thionyl compounds which transform allylic alcohols to allylic halides. While the mechanism of these rearrangements varies depending on substrate and reaction conditions,[53] other research groups successfully transposed allylic alcohols with thionyl bromide,[54] thionyl chloride,[55] and I_2/PPh_3.[56] A survey of conditions found Br_2/PPh_3 and PBr_3 to be suitably reactive with alcohol **3.75** to transpose the alkene and give allylic bromide **3.77**; however, low conversion and unidentified byproducts were observed (Scheme 3.20A). When thionyl bromide was employed at –40 ºC,[54] a suprafacial rearrangement occurred to deliver the desired allylic bromide **3.77** in 90% yield (Scheme 3.20B). The analogous reaction with thionyl chloride was attempted in the hope that an allylic chloride would be less photolabile in the photoredox cascade.[57] Rearrangement to allylic chloride **3.78** occurred smoothly in 62% yield (Scheme 3.20).[58,59] With radical precursor **3.78** in hand, the key radical cascade reaction was investigated.

Scheme 3.20. Transposition Reactions of Allylic Alcohol 3.75 to Allylic Halides.

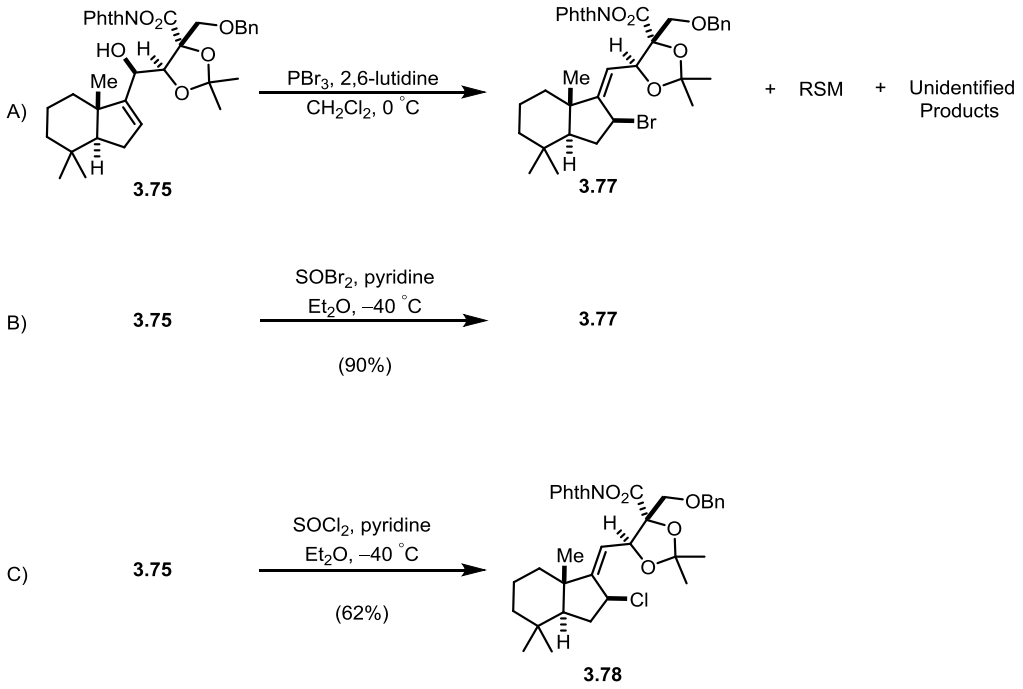

3.2.5 Radical Addition/Cyclization/Fragmentation Cascade

3.2.5.1 Proposed Mechanism of ACF Cascade

Radical precursor **3.78** differed from the proposed radical precursor **3.47** in the revised retrosynthesis (Scheme 3.11) with the addition of an allylic chloride. However, this halogen was anticipated to have a beneficial role in the radical cascade. Scheme 3.21 highlights the proposed reaction pathway of radical precursor **3.78** in the cascade sequence to yield the desired product **3.82**. Allylic chloride **3.78**, under reductive photoredox conditions, would undergo loss of phthalimide anion and CO_2 to generate trisubstituted acetonide radical **3.79**. Diastereoselective conjugate addition of radical **3.79** to chiral butenolide **3.2** from the face *syn* to the hydrindane fragment would construct the first C–C bond and two stereocenters (C12 and C13) to provide α-acyl radical **3.80**. Subsequent 5-*exo* cyclization of α-acyl radical **3.80** onto the trisubstituted alkene would forge the second

C–C bond and two additional stereocenters (C8 and C14). The resulting tertiary radical **3.81**, adjacent to the chloride, would undergo β-fragmentation of the homolytically weak C–Cl σ-bond[60] to form a double bond. Extrusion of the chloride radical would quench the cascade and pentacyclic product **3.82**. For the previously proposed radical precursor **3.47** lacking an allylic chloride, a bimolecular termination of the tertiary radical by hydrogen atom abstraction would be required to quench the cascade. Presence of the chloride atom was hoped to result in rapid intramolecular termination by β-fragmentation, preventing potential deleterious reaction pathways. This overall sequence can be described as an addition/cyclization/fragmentation (ACF) cascade.

Scheme 3.21. Proposed Mechanism for ACF Cascade with Allylic Chloride 3.78.

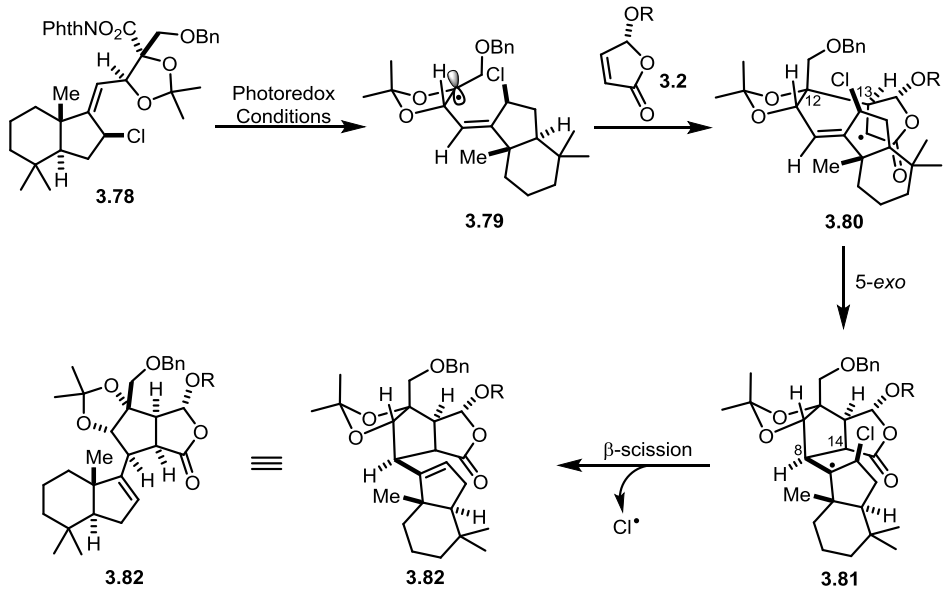

3.2.5.2 Initial ACF Cascade Results and Product Identification

Exposure of allylic chloride **3.78** to standard reductive photoredox conditions[13] with enantiopure butenolide **3.27** generated ACF product **3.83** as the major product along

with several unidentified minor products (Equation 3.3). Upon detailed NMR analysis, NOE data confirmed ACF product **3.83** to be the undesired C8 epimer.

Equation 3.3

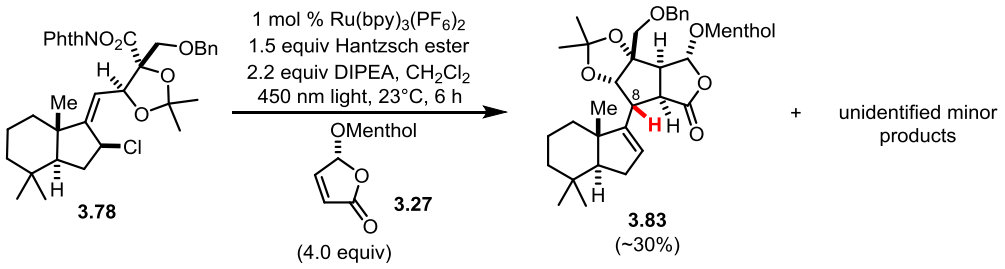

As identification of the minor products proved difficult with menthol butenolide **3.27**, the methoxy variant (**3.84**) was then employed in the reaction to simplify analysis and purification of the products. Upon exposure of (*R*)-methoxy butenolide **3.84**[61] to photoredox conditions with radical precursor **3.78**, ACF C8 epimer **3.85** was again the major product (35%) along with desired ACF product **3.86** (20%) and prematurely quenched product **3.87** (29%) as minor products (Equation 3.4). A fourth minor product, **3.88** (11%), was later assigned as the product of radical addition from the undesired face of the acetonide radical *anti* to the hydrindane fragment (**3.88**).[62]

Equation 3.4

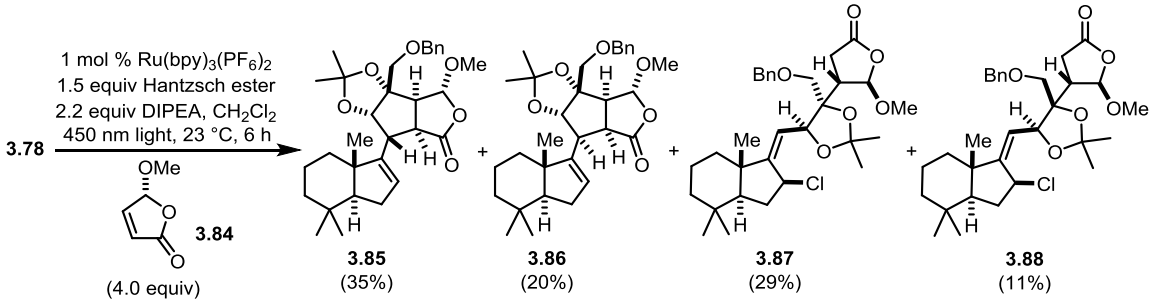

Scheme 3.22 highlights the complexity of the ACF cascade with reaction pathways to each of these observed products, which together typically account for >80% of the mass

balance. The product distribution from Equation 3.4 revealed that the initial conjugate addition of the trisubstituted acetonide radical (**3.79**) to the butenolide occurred with high diastereoselectivity (~7:1) favoring the desired but more hindered face *syn* to the hydrindane. The product distribution also indicated two key areas for optimization: 1) preventing premature quenching of α-acyl radical **3.89** to permit 5-*exo* cyclization; and 2) finding conditions/substrates to favor 5-*exo* cyclization giving the desired C8 stereochemistry.

Scheme 3.22. Reaction Pathways to Observed Products in ACF Cascade.

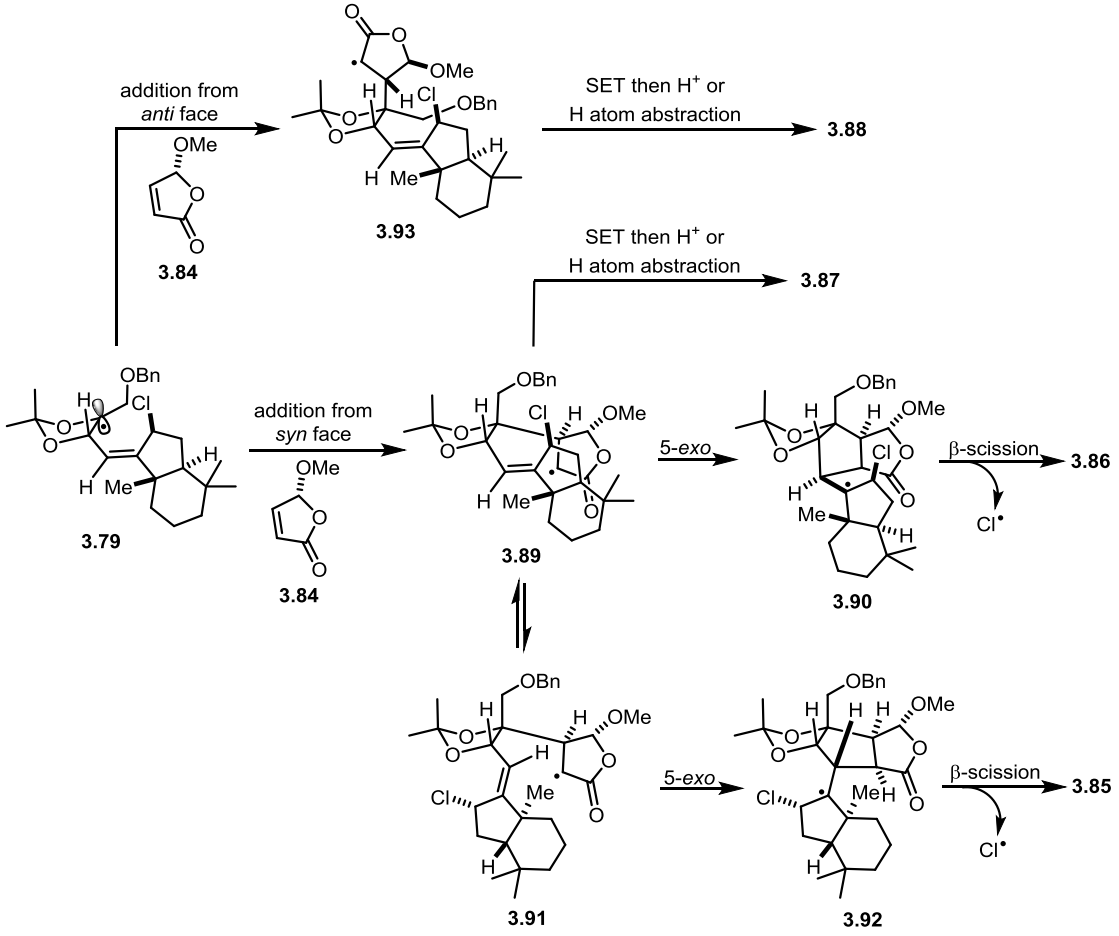

3.2.5.3 Optimization to Prolong Radical Lifetime

The 29% yield of prematurely quenched product **3.87** revealed that intramolecular 5-*exo* cyclization onto the tethered alkene was kinetically competitive with intermolecular radical quenching of the α-acyl radical. Prevention of premature radical quenching was challenging, as the α-acyl radical was quenched by both SET reduction/enolate protonation and direct hydrogen atom abstraction under the standard photoredox conditions (Scheme 3.23).[13] Therefore, prolonging the lifetime of α-acyl radical **3.89** in the ACF cascade would require addressing both of these pathways.

Scheme 3.23. Pathways to Quenching α-Acyl Radical Under Reductive Photoredox Conditions.

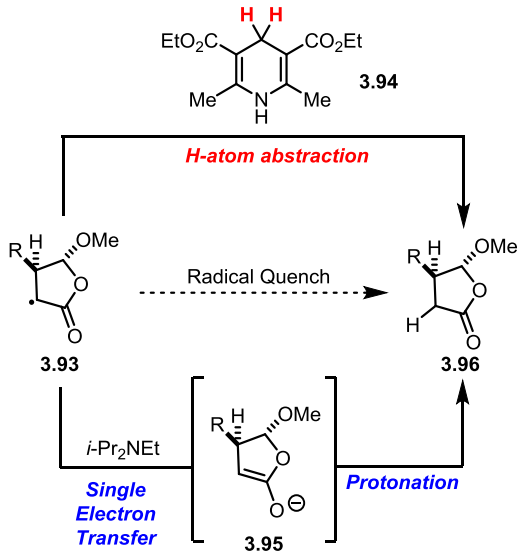

In considering attenuation of both pathways, the roles of diisopropylethylamine (DIPEA) and diethyl 1,4-dihydro-2,6-dimethyl-3,5-pyridinedicarboxylate (Hantzsch ester) were first considered in the photoredox mechanism. DIPEA promotes SET reduction of the α-acyl radical to the corresponding enolate, and Hantzsch ester is a stoichiometric reductant which turns over the catalytic cycle.[13] As the ACF cascade quenches the radical cascade by β-fragmentation to release chloride radical, DIPEA should not be mechanistically

required to obtain ACF products **3.85** or **3.86**. Shown in Table 3.2, standard conditions with DIPEA (entry 1) afforded a significant amount of prematurely quenched product **3.87** (29%). By removing DIPEA (entry 2), the amount of quenched product **3.87** diminished from 29% to 14% without an increase in the yields of ACF products **3.85** and **3.86** (52% combined). The remaining 14% of quenched product **3.87** presumably arose from hydrogen atom abstraction from Hantzsch ester. Because of its role in turning over the photocatalyst,[13] removal of Hantzsch ester was not possible under these conditions. Thus, dilution of the reaction mixture was investigated to slow intermolecular hydrogen atom abstraction (entry 3). The dilution lessened the amount of prematurely quenched product **3.87** (3%) at the expense of lower yields for ACF products **3.85** and **3.86** (45% combined). As dilution decreased the combined yield of the ACF products, I then attempted to slow hydrogen atom abstraction with deuterium incorporation into Hanzsch ester. I presumed that employing d_2-Hantzsch ester at the 4-position of the dihydropyridine would slow premature deuterium abstraction of the α-acyl radical but still allow turnover of the photocatalyst. Use of d_2-Hantzch ester without DIPEA (entry 4) increased the combined yield of ACF products **3.85** and **3.86** to 70% while affording minimal prematurely quenched product **3.87** (with deuterium incorporation at the α-position). Lowering the equivalents of d_2-Hantzch ester did not further improve the combined yield of the ACF products (entry 5).

Table 3.2. Optimization to Minimize Premature Radical Quenching.

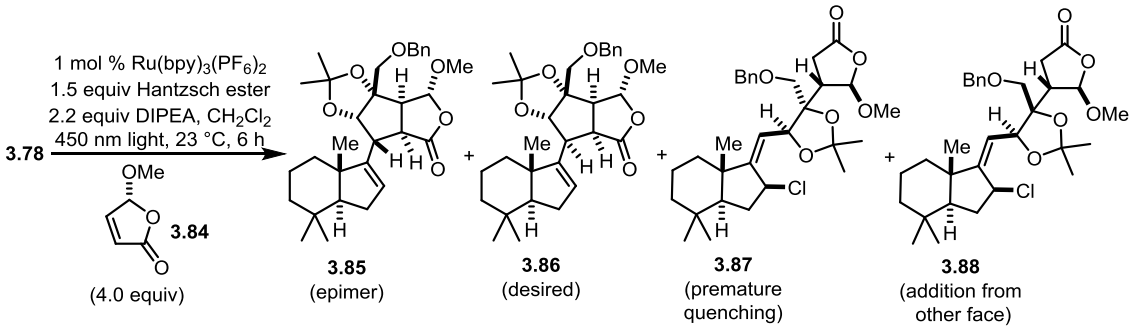

Entry	Changes	[M]	Respective Yields by ^{1}H NMR (with internal standard)
1	None	0.10 M	35% : 20% : 29% : 11%
2	No DIPEA	0.10 M	34% : 18% : 14% : 7%
3	No DIPEA	0.02 M	29% : 16% : 3% : 6%
4	No DIPEA, d_2-Hantzsch ester	0.10 M	45% : 25% : 6% : 10%
5	No DIPEA, 1.2 equiv. d_2-Hantzsch ester	0.10 M	32% : 23% : 6% : 10%

As these photoredox conditions used Hantzsch ester as a stoichoimetric reductant, I also examined redox-neutral processes with the hope of improving the overall yield. Photoredox methodology with carboxylic acids was recently reported by MacMillan[63] using an iridium photocatalyst which acted as both an oxidant to initiate decarboxylation and a reductant for the α-acyl radical following conjugate addition. Because of the dual roles of the iridium photocatalyst, the reaction did not contain a stoichiometric reductant such as Hantzsch ester, which would presumably minimize premature quenching of α-acyl radical **3.89**. Acid radical precursor **3.98** was synthesized by an alternative route from NHK alcohol **3.64**, in which thionyl chloride-mediated transposition followed by nonbasic hydrolysis[47b] afforded the desired acid radical precursor (Scheme 3.24). Exposure of acid **3.98** to butenolide **3.84** under MacMillan's reported photoredox conditions[63] resulted in minimal formation of prematurely quenched product **3.87** (8%) with ACF products **3.85** and **3.86** obtained in 51% combined yield. While this result was promising, I ultimately

settled on optimization of the ACF cascade with (*N*-acyloxy)phthalimide **3.78** over acid **3.95** for two reasons: 1) acid **3.98** was found more difficult to obtain in pure form than crystalline (*N*-acyloxy)phthalimide **3.78**; and 2) the MacMillan conditions permitted examination of fewer solvents because of the low solubility of K_2HPO_4.

Scheme 3.24. Synthesis of Acid Radical Precursor 3.98 and ACF Cascade.

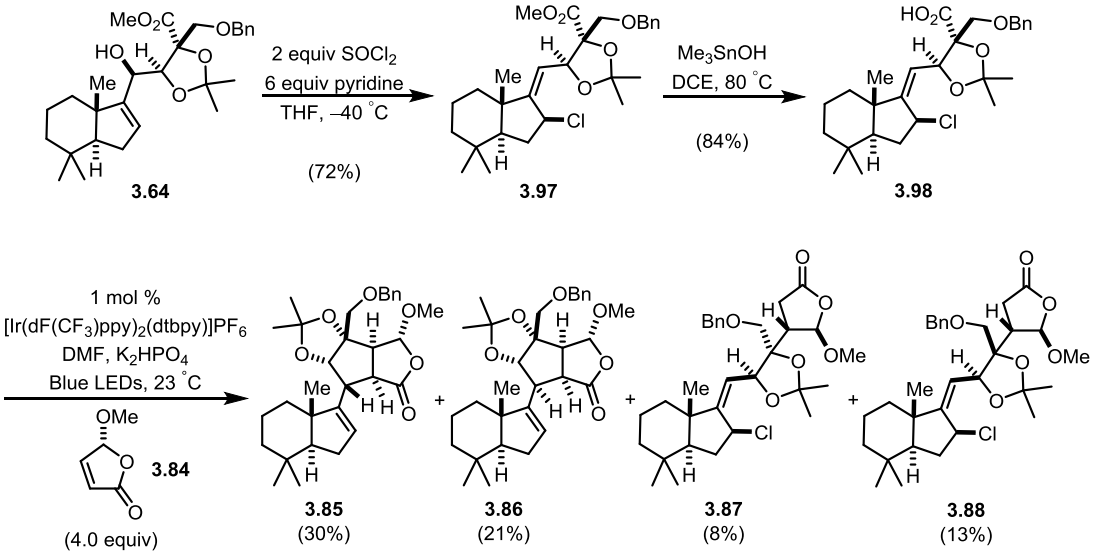

3.2.5.4 Attempts to Improve Diastereoselectivity of 5-*Exo* Cyclization

Having now attenuated premature radical quenching, I turned my attention to finding conditions to favor desired ACF product **3.86** over the undesired C8 epimer **3.85**. I sought to explore temperature, solvent, and structural modifications to improve diastereoselectivity for desired ACF product **3.86** (1.8:1 dr favoring epimeric ACF product **3.85** from Table 3.2, entry 4). Investigations with different enantioenriched butenolide acceptors revealed that decreasing steric bulk at the γ-position was beneficial for the desired C8 diastereoselectivity (Table 3.3, entries 1–3). In addition, studies of the reaction temperature showed a slight increase in diastereoselectivity at a lower temperature (entries 3–5). Operationally, the photoredox reactions were difficult to cool below room

temperature while still permitting adequate light penetration into the reaction vessel. Therefore, the reactions were run at 23 ºC because of ease in screening further conditions.

Table 3.3. Screening Butenolide γ-Substitution and Temperature.

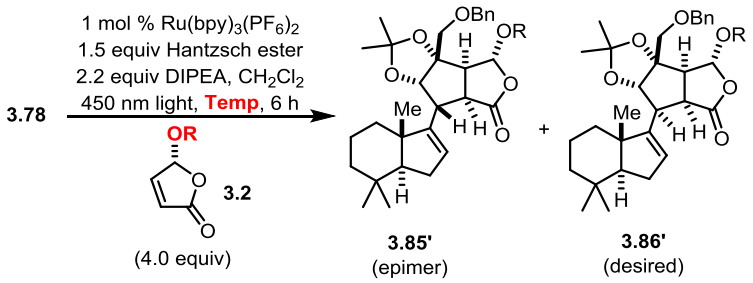

Entry	R	Rxn Temp.	Ratio 3.85':3.86'
1	Menthol	23 °C	3.1 : 1
2	Ac	23 °C	2.7 : 1
3	Me	23 °C	1.8 : 1
4	Me	38 °C	1.8 : 1
5	Me	0 °C	1.5 : 1

I then sought to further bias 5-*exo* cyclization diastereoselectivity by solvent effects. Having performed all previous reactions in CH_2Cl_2, I surveyed other solvents in hopes of improving the yield and diastereoselectivity (Table 3.4). An examination of five additional solvents did not reveal a meaningful trend in diastereoselectivity. Acetonitrile as the solvent (entry 4) provided the best combination of yield and diastereoselectivity (1.3:1 dr) in the ACF cascade, affording **3.86** as the minor diastereomer in 28% yield (27% isolated). To date, these conditions are the highest yielding for desired ACF product **3.86** and have been scaled to 0.2 mmol to access sufficient amounts of material to carry forward in the total synthesis of (–)-chromodorolide B (Section 3.2.6). As epimer **3.85** remained the major product, I investigated structural derivation of radical precursor **3.78** to potentially bias diastereoselectivity of the 5-*exo* cyclization.

Table 3.4. Solvent Screen for ACF Cascade.

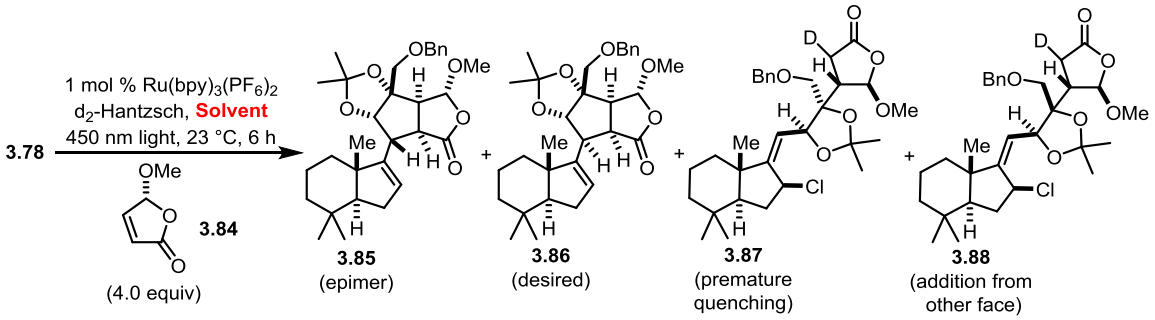

Entry	Solvent	Respective Yields by ^{1}H NMR (with internal standard)	dr 3.85:3.86
1	CH_2Cl_2	45% : 25% : 6% : 10%	1.8 : 1
2	DME	36% : 23% : 4% : 9%	1.6 : 1
3	THF	34% : 21% : 5% : 8%	1.6 : 1
4	MeCN	37% : 28% : 8% : 13%	1.3 : 1
5	MeOH	24% : 12% : 15% : 12%	2.0 : 1
6	DMSO	20% : 17% : 17% : 15%	1.2 : 1

Proposing impactful structural modifications of **3.78** to affect the diastereoselectivity of the 5-*exo* cyclization in the ACF cascade was challenging, as well as developing efficient syntheses for these derivatives. Previously synthesized radical precursor **3.77** containing an allylic bromide (Scheme 3.20) was examined in the ACF cascade, but the alternate halogen had no effect on diastereoselectivity of the 5-*exo* cyclization. With no working hypothesis for diastereoselectivity, readily accessible derivatives **3.100** and **3.101** were then targeted (Scheme 3.25). Thiophenol radical precursor **3.100**[64] containing an inverted allylic stereocenter had no effect on the 5-*exo* diastereoselectivity, whereas ethyl ketal radical precursor **3.101** increased selectivity for the undesired C8 epimer (**3.102**). With a limited supply of radical precursor **3.78** available and no predictive model, I prioritized completion of the total synthesis of the chromodorolides with the intent of returning to this challenge at a later juncture.

Scheme 3.25. Synthesis and Coupling of Structurally Modified Radical Precursors 3.100 and 3.101.

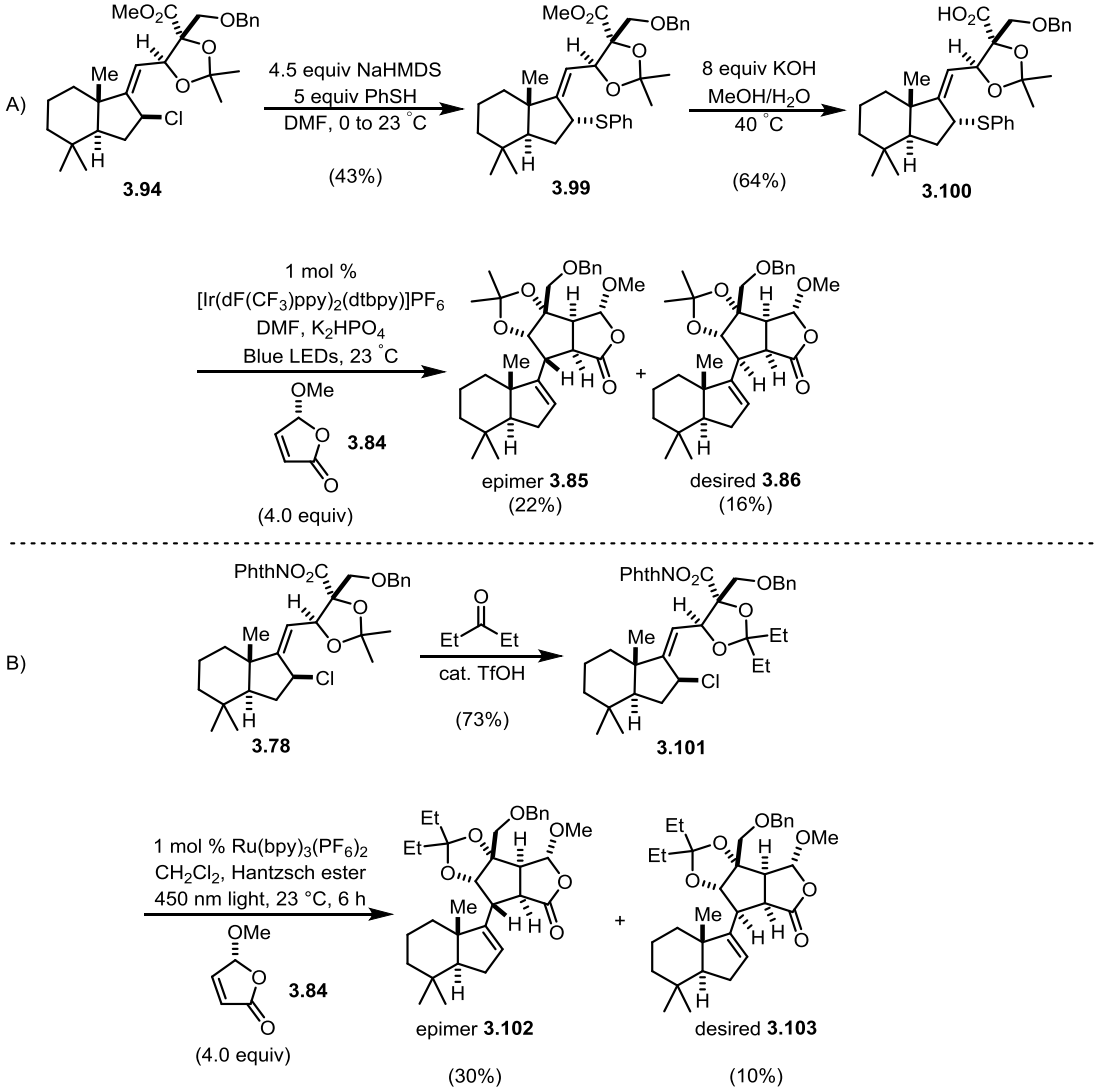

3.2.6 Completion of the Total Synthesis of (–)-Chromodorolide B

With access to small quantities of ACF product **3.86**, I targeted common acid precursor **3.10**, which required acetonide deprotection of ACF product **3.86** at this stage.[65] Numerous conditions[66,67] for acetonide deprotection were investigated with epimeric ACF product **3.85**, but enal formation from lactone opening (**3.105**, Equation 3.5) or decomposition were consistently observed. After significant effort exploring conditions for

selective acetonide deprotection, the most useful conditions were found to be a 1:1:1 mixture of MeOH/4 M HCl/dioxanes at 23 ºC which unreliably provided diol **3.104** in 30–40% yield. Because of low and irreproducible yields, acetonide deprotection was postponed to later in the sequence when formation of enal **3.105** would be disfavored.

Equation 3.5

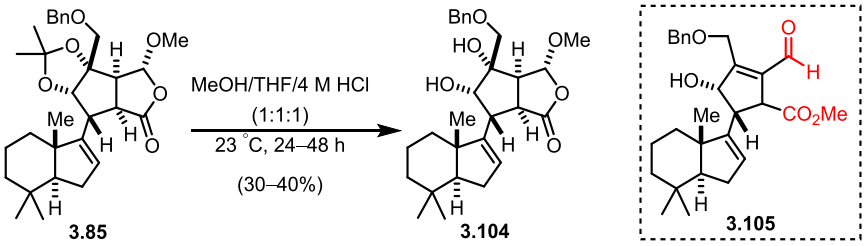

In delaying acetonide deprotection, ACF product **3.86** was instead exposed to DIBAL-H and trapped *in situ* with acetic anhydride to provide diacetal **3.106** in 82% yield (Scheme 3.26). This diacetal was isolated as a single diastereomer, with NOE correlations supporting hydride delivery from the concave face of the bicyclic motif. The contrasteric hydride delivery may have arisen from unanticipated directing effects by the benzyl ether.[68] I then attempted concurrent alkene hydrogenation and debenzylation of diacetal **3.106**, which were unsuccessful in providing reduced alcohol **3.107** in a single step.[69] Rather, a two-step process was required wherein debenzylation under transfer hydrogenation conditions,[68,70] followed by platinum-mediated hydrogenation, afforded saturated alcohol **3.107** in 83% yield over two steps. Alcohol **3.107** was then oxidized to acid **3.108** over two steps using DMP and a Pinnick-Lindgren oxidation.[71,72] At this stage, removal of the acetonide on **3.108** was attempted with the anticipation that the carboxylic acid would thermodynamically favor equilibration to lactol **3.109** over decomposition to the enal (e.g. **3.105**). Exposure to 4 M HCl/THF for 72 hours provided a 1.6:1 anomeric mixture of desired lactol **3.109**.[73,74] Treatment of this mixture with acetic anhydride and pyridine

converged the anomers to a single triacetylated product, (–)-chromorodolide B (**3.110**), which was isolated in 49% yield from alcohol **3.107**.[75] Spectroscopic data of the synthetic compound correlated closely with reported values of the natural product.[76] Additionally, recrystallization of **3.110** afforded single crystals which allowed for the first X-ray structure of a fused chromodorolide to be obtained (Figure 3.3).[77] This unambiguously verified the constitution and absolute configuration of the natural product.

Scheme 3.26. Late-Stage Sequence Transforming ACF Product 3.86 to (–)-Chromodorolide B.

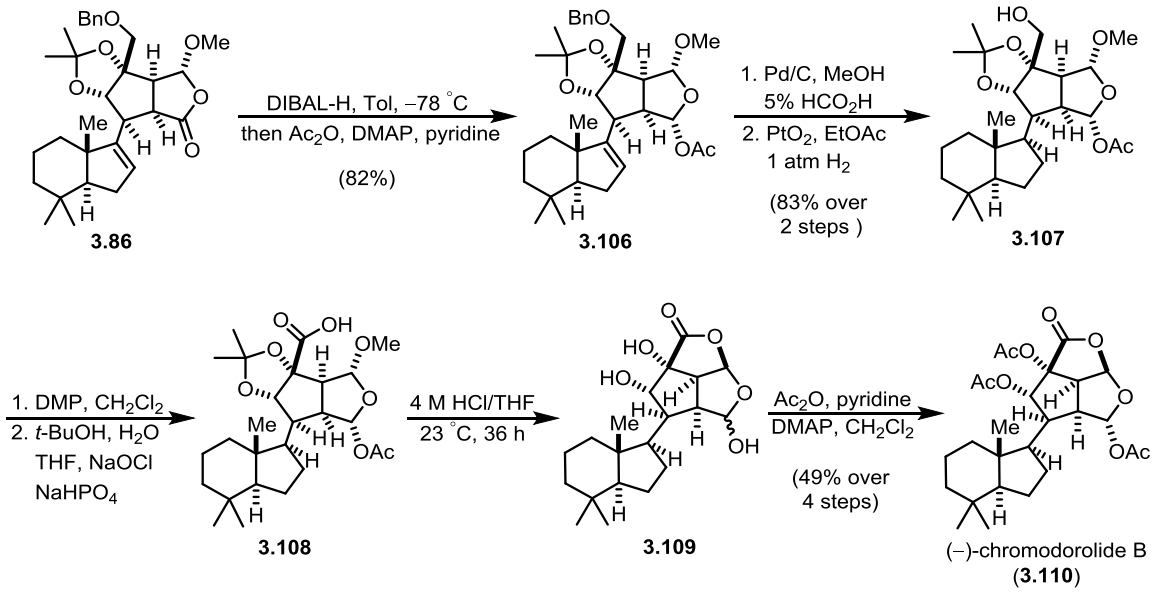

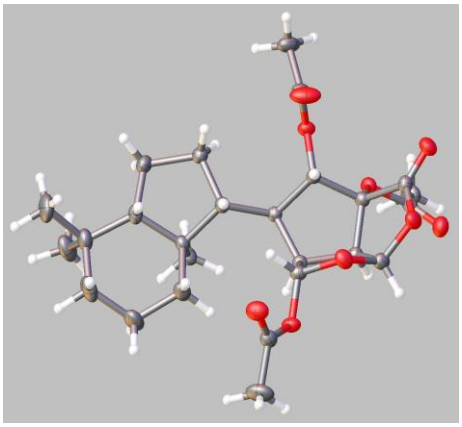

Figure 3.3. Single Crystal X-Ray Image of (–)-Chromodorolide B.

3.3 Experimental Section

3.3.1 General Experimental Details

Unless stated otherwise, reactions were conducted in oven-dried glassware under an atmosphere of nitrogen or argon. Tetrahydrofuran (THF), diethyl ether, toluene, benzene, dichloromethane, methanol (MeOH), pyridine, DIPEA, and triethylamine were dried by passage through activated alumina. Benzyloxymethyl chloride (BOM-Cl) distilled under Ar from CaH directly before use. 1,1,3,3-Tetramethylguanidine was distilled under Ar from barium oxide directly before use. Thionyl chloride was distilled from quinoline under Ar. All other commercial reagents were used as received unless otherwise noted. Hantzsch ester[78] and its 4-dideutero derivative[79] were prepared according to literature procedures. All other commercial reagents were used as received unless otherwise noted. Reaction temperatures were controlled using a temperature modulator, and unless stated otherwise, reactions were performed at 23 ºC (rt, approximately 23 °C). Thin-layer chromatography (TLC) was conducted with silica gel 60 F254 pre-coated plates, (0.25 mm) and visualized by exposure to UV light (254 nm) or by *p*-anisaldehyde, ceric ammonium molybdate, and

potassium permanganate staining. Silica gel 60 (particle size 0.040–0.063 mm) was used for flash column chromatography. pH 7 Silica gel was prepared according to previous literature procedure.[80] ^{1}H NMR spectra were recorded at 500 or 600 MHz and are reported relative to deuterated solvent signals. Data for ^{1}H NMR spectra are reported as follows: chemical shift (δ ppm), multiplicity, coupling constant (Hz), and integration. ^{13}C NMR spectra were recorded at 125 MHz and reported in terms of chemical shift. IR spectra were recorded on a FT-IR spectrometer and are reported in terms of frequency of absorption (cm^{-1}). High-resolution mass spectra were obtained with a LCT spectrometer. Optical rotations were measured with a Jasco P-1010 polarimeter. Kessil KSH150B LED Grow Light 150, Blue LEDs were purchased from http://www.amazon.com. The radical coupling reactions using these blue LEDs were maintained at approximately 23 ºC by passing a constant stream of air over the reaction vessels for the 18 h period. See JOC Standard Abbreviations and Acronyms for abbreviations (available at http://pubs.acs.org/userimages/ContentEditor/1218717864819/joceah_abbreviations.pdf).

3.3.2 Experimental Procedures

(+)-Tert-butyl(((4*S*,5*S*)-5-ethynyl-2,2-dimethyl-4-vinyl-1,3-dioxolan-4-yl)methoxy)dimethylsilane (3.25): To a suspension of known alcohol **3.23**[8] (0.732 g, 2.42 mmol) and solid $NaHCO_3$ (1.01 g, 12.1 mmol) in CH_2Cl_2 (4 mL) was added Dess-Martin periodinane (1.23 g, 2.90 mmol). The reaction was vigorously stirred for 2 h, at which point the suspension was filtered through Celite and concentrated *in vacuo*. The residue was then washed with pentanes (4 x 8 mL), and the combined organic washes were filtered through Celite and concentrated *in vacuo* to afford the crude aldehyde as a yellow oil which was carried forward immediately.

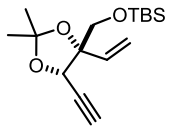

3.25: $C_{16}H_{28}O_3Si$
Molecular Weight: 296.4820

The crude aldehyde and dimethyl (1-azoacetonyl)phosphonate **3.24**[10] (0.558 g, 2.90 mmol) were dissolved in MeOH (9 mL). Solid K_2CO_3 (0.669 g, 4.84 mmol) was then added, and the suspension was vigorously stirred for 2 h. Celite (~5 g) was added to the reaction vessel, and the reaction was concentrated *in vacuo.* Purification by flash column chromatography (5% EtOAc in hexanes to 7% EtOAc in hexanes) afforded alkyne **3.25** (0.550 g, 1.86 mmol, 77% yield) as a colorless solid. R_f 0.90 (20% EtOAc in hexanes; visualized with $KMnO_4$). ^{1}H NMR (500 MHz, $CDCl_3$) δ 6.12 (dd, *J* = 17.2, 10.9 Hz, 1H), 5.53 (dd, *J* = 17.5, 1.6 Hz, 1H), 5.30 (dd, *J* = 10.9, 1.6 Hz, 1H), 4.99 (d, *J* = 2.1 Hz, 1H), 3.58 (d, *J* = 10.6 Hz, 1H), 3.55 (d, *J* = 10.7 Hz, 1H), 2.60 (d, *J* = 2.2 Hz, 1H), 1.54 (s, 3H), 1.43 (s, 3H), 0.89 (s, 9H), 0.07 (s, 6H); ^{13}C NMR (125 MHz, $CDCl_3$) δ 136.46, 116.73, 110.27, 85.75, 79.25, 77.10, 69.70, 65.41, 27.87, 27.01, 26.00, 18.44, –5.23, –5.49; IR (thin film) 3312, 2988, 2955, 2858, 1741, 1378, 1253 cm^{-1}; $[\alpha]^{25}_D$: +0.79 (c = 2.5, CH_2Cl_2);

HRMS (ESI) calculated for $C_{16}H_{29}O_3Si$ (M+H) 297.1887, observed 297.1890; mp 39–41 ºC.

(–)-(**4*S*,5*S*)-4-(((Tert-butyldimethylsilyl)oxy)methyl)-5-ethynyl-2,2-dimethyl-1,3-dioxolane-4-carboxylic acid (3.26):** A solution of alkyne **3.25** (0.553 g, 1.87 mmol) in methanol (8 mL) was cooled to –78 °C. Ozone from an ozone generator was bubbled through the solution until a pale blue color was observed (~5 min). The solution was then sparged with oxygen until the pale blue color disappeared. Dimethyl sulfide (0.31 mL, 4.3 mmol) was added to the solution, which was maintained at –78 °C for 1 h. The reaction vessel was allowed to warm to 23 °C and concentrated *in vacuo* to afford the crude aldehyde which was carried forward without further purification.

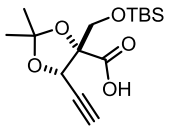

3.26: $C_{15}H_{26}O_5Si$
Molecular Weight: 314.4530

The crude aldehyde was dissolved in a 3:1 solution of *t*-BuOH/H_2O (8 mL). A solution of 2-methyl-2-butene (2.0 mL, 19 mmol) was added to the mixture, followed by NaH_2PO_4 (1.80 g, 15.0 mmol) and $NaClO_2$ (0.845 g, 9.35 mmol). The reaction was maintained at 23 °C for 2 h, at which point H_2O (4 mL) was added. This mixture was washed with EtOAc (3 x 10 mL), and the combined organic layers were washed with aq. NaOH (5 mL of 0.5 M soln). The aqueous layer was then acidified with aq. HCl (7 mL of 0.5 M soln). The aqueous layer was then washed with EtOAc (3 x 10 mL), and the combined organic layers were washed with brine (1 x 10 mL), dried over Na_2SO_4, filtered, and concentrated *in vacuo* to provide acid **3.26** as a colorless oil (0.450 g, 1.43 mmol, 76% yield). ^{1}H NMR (500 MHz, $CDCl_3$) δ 4.97 (d, *J* = 2.3 Hz, 1H), 3.94 (d, *J* = 11.0 Hz, 1H), 3.92 (d, *J* = 11.0 Hz, 1H), 2.63 (d, *J* = 2.2 Hz, 1H), 1.67 (s, 3H), 1.47 (s, 3H), 0.90 (s, 9H),

0.09 (s, 3H), 0.08 (s, 3H); ^{13}C NMR (500 MHz, $CDCl_3$) δ 173.25, 113.33, 88.23, 77.69, 69.04, 63.64, 26.99, 26.97, 25.95, 18.48, 14.32, –5.26, –5.48; IR (thin film) 3505, 3277, 2990, 2931, 2858, 1731, 1379 cm^{-1}; $[\alpha]^{25}_{D}$: –30.0 (c = 2.1, CH_2Cl_2); HRMS (ESI) calculated for $C_{15}H_{25}O_5Si$ (M–H) 313.1471, observed 313.1467.

(+)-1,3-Dioxoisoindolin-2-yl(4*S*,5*S*)-4-(((tert-butyldimethylsilyl)oxy)methyl)-5-ethynyl-2,2-dimethyl-1,3-dioxolane-4-carboxylate (3.16): Acid **3.26** (0.453 g, 1.44 mmol) was charged into a flask with THF (8 mL). *N*-hydroxyphthalimide (0.399 g, 2.45 mmol), *N*,*N*'-dicycylohexylcarbodiimide (0.446 g, 2.16 mmol), and DMAP (9 mg, 0.07 mmol) were added to the reaction vessel, which was maintained at 23 °C for 20 h. Hexanes (5 mL) was added to the reaction, and the resulting suspension was filtered through Celite. The yellow filtrate was concentrated *in vacuo* and then purified by flash column chromatography (10% EtOAc in hexanes to 15% EtOAc in hexanes) to provide (*N*-acyloxy)phthalimide **3.16** (0.539 g, 1.18 mmol, 82% yield) as a colorless, crystalline solid. R_f 0.25 (20% EtOAc in hexanes; visualized with ceric ammonium molybdate). ^{1}H NMR (500 MHz, $CDCl_3$) δ 7.88 (m, 2H), 7.78 (m, 2H), 5.14 (d, *J* = 2.2 Hz, 1H), 4.10 (d, *J* = 11.5 Hz, 1H), 4.07 (d, *J* = 11.3 Hz, 1H), 2.78 (d, *J* = 2.2 Hz, 1H), 1.71 (s, 3H), 1.50 (s, 3H), 0.93 (s, 9H), 0.13 (s, 3H), 0.12 (s, 3H); ^{13}C NMR (500 MHz, $CDCl_3$) δ 166.77, 161.37, 134.87, 129.09, 124.07, 113.53, 88.06, 78.80, 76.25, 68.81, 62.80, 26.7, 26.64, 26.00, 18.54, –5.18, –5.49; IR (thin film) 3283, 2930, 2855, 2360, 2340, 2118, 1789, 1748 cm^{-1}; $[\alpha]^{25}_{D}$: +38.3 (c = 2.0, CH_2Cl_2); HRMS (ESI) calculated for $C_{23}H_{29}NO_7SiNa$(M+Na) 482.1611, observed 482.1612; mp 105–109 ºC.

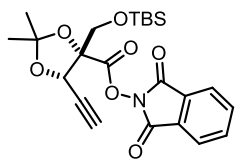

3.16: $C_{23}H_{29}NO_7Si$
Molecular Weight: 459.5700

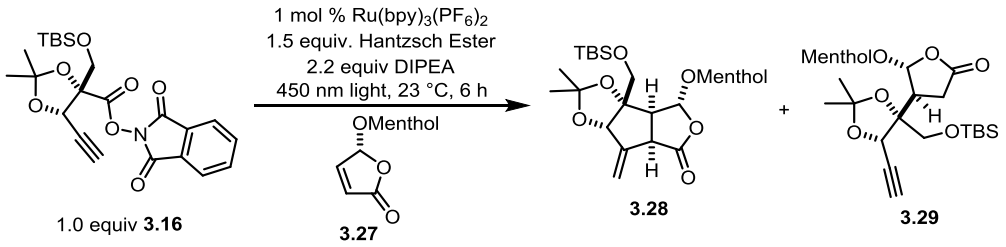

(–)-(3a*S*,3b*S*,4*R*,6a*R*,7a*S*)-3a-(((Tert-butyldimethylsilyl)oxy)methyl)-4-(((1*R*,2*S*,5*R*)-2-isopropyl-5-methylcyclohexyl)oxy)-2,2-dimethyl-7-methylenehexahydro-6H-furo[3',4':3,4]cyclopenta[1,2-d][1,3]dioxol-6-one (3.28) and **(–)-(4*S*,5*R*)-4-((4*R*,5*S*)-4-(((tert-butyldimethylsilyl)oxy)methyl)-5-ethynyl-2,2-dimethyl-1,3-dioxolan-4-yl)-5-(((1*R*,2*S*,5*R*)-2-isopropyl-5-methylcyclohexyl)oxy)dihydrofuran-2(3H)-one (3.29):** To a vial charged with (*N*-acyloxy)phthalimide **3.16** (100 mg, 0.218 mmol) was added CH_2Cl_2 (2 mL) that had been separately sparged with argon for 5 min. Butenolide **3.27**[14] (78 mg, 0.32 mmol), Hantzsch ester (82 mg, 0.32 mmol), $Ru(bpy)_3(PF_6)_2$ (2 mg, 0.002 mmol), and Hünig's base (80 µL, 0.48 mmol) were then added to the reaction. The vial was then vigorously stirred while being irradiated by a single strip of blue LED lights (450 nm) at 23 ºC. After 6 h, the reaction mixture was diluted with hexanes (2 mL) and filtered through Celite. The resulting solution was then concentrated *in vacuo* and separated by flash column chromatography (3% EtOAc in hexanes to 5% EtOAc in hexanes) to provide lactone **3.28** (42 mg, 0.083 mmol, 38% yield) as a colorless, crystalline solid and addition product **3.29** (7.5 mg, 0.015 mmol, 7% yield) as an oil. A single crystal X-ray structure of lactone **3.28** was obtained after recrystallization in MeOH/hexanes. R_f for **3.28**: 0.65 (10% EtOAc in hexanes; visualized with ceric ammonium molybdate). R_f for **3.29**: 0.60 (10% EtOAc in hexanes; visualized with ceric ammonium molybdate).

Characterization data for **3.28**: for ^{1}H NMR (500 MHz, $CDCl_3$) δ 5.90 (d, *J* = 2.6 Hz, 1H), 5.62 (dd, *J* = 2.3, 1.0 Hz, 1H), 5.50 (dd, *J* = 2.7, 0.8 Hz, 1H), 4.73 (app s, 1H), 3.96–3.92 (m, 1H), 3.86 (d, *J* = 10.7 Hz, 1H), 3.77 (d, *J* = 10.8 Hz, 1H), 3.51 (dt, *J* = 10.6, 4.3 Hz, 1H), 3.07 (dd, *J* = 10.3, 2.3 Hz, 1H), 2.14–2.03 (m, 2H), 1.69–1.60 (m, 2H), 1.47 (s, 3H), 1.40–1.32 (m, 4H), 1.27–1.16 (m, 2H), 1.04–0.93 (m, 1H), 0.92 (d, *J* = 6.5 Hz, 3H), 0.90–0.80 (m, 13H), 0.77 (d, *J* = 6.9 Hz, 3H), 0.09 (s, 3H), 0.08 (s, 3H); ^{13}C NMR (125 MHz, $CDCl_3$) δ 175.05, 143.32, 116.61, 112.69, 99.71, 90.76, 86.88, 77.22, 64.36, 57.42, 48.22, 47.87, 40.01, 34.42, 31.51, 28.37, 27.04, 25.93, 25.51, 23.20, 22.39, 21.03, 18.41, 15.81, –5.45, –5.50; IR (thin film) 2953, 2929, 2858, 1779, 1461 cm^{-1}; $[\alpha]^{25}_{D}$: –133 (c = 1.9, CH_2Cl_2); HRMS (ESI) calculated for $C_{28}H_{48}O_6SiNa$ (M+Na) 531.3118, observed 531.3126; mp 136–142 ºC.

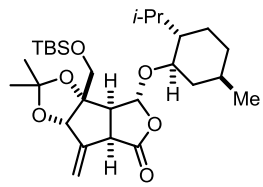

3.28: $C_{28}H_{48}O_6Si$
Molecular Weight: 508.7710

Characterization data for **3.29**: ^{1}H NMR (500 MHz, $CDCl_3$) δ 5.82 (d, *J* = 2.2 Hz, 1H), 4.59 (d, *J* = 2.2 Hz, 1H), 3.98 (d, *J* = 10.7 Hz, 1H), 3.75 (d, *J* = 10.7 Hz, 1H), 3.52 (dt, *J* = 10.9, 4.4 Hz, 1H), 2.82–2.65 (m, 3H), 2.58 (d, *J* = 2.3 Hz, 1H), 2.17–2.04 (m, 2H), 1.69–1.59 (m, 2H), 1.50 (s, 3H), 1.38 (s, 3H), 1.37–1.32 (m, 1H), 1.27–1.17 (m, 2H), 0.99 (app qd, *J* = 12.5, 3.3 Hz, 1H), 0.91 (d, *J* = 6.9 Hz, 3H), 0.90 (s, 9H), 0.87 (d, *J* = 7.0 Hz, 3H), 0.86–0.81 (m, 1H), 0.77 (d, *J* = 7.0 Hz, 3H), 0.09 (s, 6H); ^{13}C NMR (125 MHz, $CDCl_3$) δ 175.88, 110.04, 100.76, 83.81, 78.81, 77.21, 76.74, 71.62, 64.38, 47.88, 46.89, 39.88, 34.46, 31.50, 29.82, 28.24, 27.07, 26.04, 25.56, 23.22, 22.42, 21.02, 18.36, 15.80, –5.44, –5.46; IR (thin film) 3311,

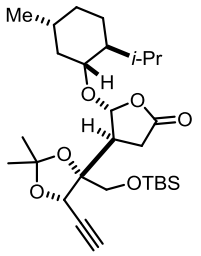

3.29: $C_{28}H_{48}O_6Si$
Molecular Weight: 508.7710

3262, 2955, 2929, 2858, 1791, 1462, 1374, 1252 cm^{-1}; $[\alpha]^{25}_{D}$: –93.7 (c = 1.2, CH_2Cl_2); HRMS (ESI) calculated for $C_{28}H_{48}O_6SiNa$ (M+Na) 531.3118, observed 531.3131.

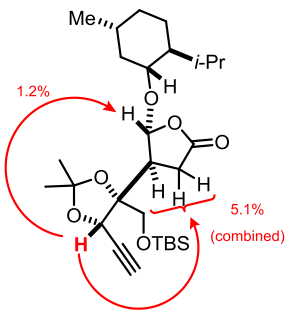

NOE Correlations

(3a*S*,3b*S*,4*R*,6a*R*,7a*R*)-3a-(((tert-butyldimethylsilyl)oxy)methyl)-4-(((1*R*,2*S*,5*R*)-2-isopropyl-5-methylcyclohexyl)oxy)-2,2-dimethyltetrahydro-4Hfuro[3',4':3,4]cyclopenta[1,2-d][1,3]dioxole-6,7-dione (3.41): Lactone **3.28** (20 mg, 0.039 mmol) was charged into a flask with CH_2Cl_2 (0.5 mL) and cooled to –78 °C. Ozone from an ozone generator was passed through the solution until a pale blue color was observed. The solution was then sparged with oxygen until the pale color disappeared. Dimethyl sulfide (20 µL, 0.20 mmol) was added to the solution which was maintained at –78 °C for 1 h. The reaction was then warmed to 23 °C, concentrated, and separated by column chromatography (10% EtOAc in hexanes to 20% EtOAc in hexanes) to provide β-ketolactone **3.41** (15 mg, 0.029 mmol, 74% yield) as a colorless oil. ^{1}H NMR (500 MHz, $CDCl_3$) δ 6.08 (s, 1H), 4.37 (s, 1H), 4.00 (d, *J* = 10.6 Hz, 1H), 3.89 (d, *J* = 10.2 Hz, 1H), 3.79 (d, *J* = 10.7 Hz, 1H), 3.54 (td, *J* = 10.7, 4.4 Hz, 1H), 3.29 (d, *J* = 10.2 Hz, 1H), 2.13 (d, *J* = 11.6, 1H), 2.06–1.98 (m, 1H), 1.71–1.62 (m, 3H), 1.42 (s, 3H), 1.39 (s, 3H), 1.24–1.18 (m, 2H), 1.04–0.92 (m, 5H), 0.89 (s, 9H), 0.87

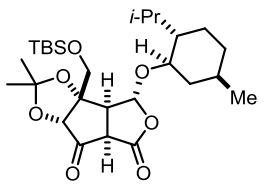

3.41: $C_{27}H_{46}O_7Si$
Molecular Weight: 510.7430

(d, J = 6.9 Hz, 3H), 0.75 (d, J = 6.9 Hz, 3H), 0.11 (s, 3H), 0.10 (s, 3H); ^{13}C NMR (125 MHz, $CDCl_3$) δ 202.0, 168.2, 114.4, 100.0, 87.1, 83.1, 64.7, 54.0, 53.6, 47.8, 40.0, 34.4, 31.5, 29.9, 28.5, 27.7, 25.9, 25.6, 23.2, 22.4, 21.0, 18.4, 15.8, –5.41, –5.54; IR (thin film) 2953, 2928, 2857, 1797, 1751, 1461 cm–1; HRMS (ESI) calculated for $C_{27}H_{46}O_7SiNa$ (M+Na) 533.2911, observed 533.2903.

(–)-(3a*S*,7a*S*)-3-iodo-3a,7,7-trimethyl-3a,4,5,6,7,7a-hexahydro-1H-indene (3.32):

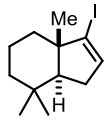

3.32: $C_{12}H_{19}I$
Molecular Weight: 290.1885

Hydrazine hydrate (20 mL) and NEt_3 (16.3 mL, 118 mmol) were added to a solution of (+)-ketone **3.12** (1.06 g, 5.88 mmol) in EtOH (45 mL). The reaction was heated to reflux for 20 h; upon cooling to 23 °C, CH_2Cl_2 (100 mL) and H_2O (150 mL) were added. The aqueous layer was washed with CH_2Cl_2 (3 x 100 mL), and the combined organic layers were dried over Mg_2SO_4, filtered, and concentrated *in vacuo*. The remaining white solid (excess hydrazine) was removed by filtration using hexanes. Concentration *in vacuo* provided the crude hydrazone as a yellow oil, which was carried forward without further purification.

A solution of 1,1,3,3-tetramethylguanidine (5.15 mL, 41.2 mmol) in THF (30 mL) was added dropwise over 10 min to a solution of I_2 (3.28 g, 12.9 mmol) in THF (30 mL). The hydrazone (5.88 mmol) in THF (6 mL) was then added dropwise over 10 min, and the reaction was maintained for 30 min. The dark red solution was then concentrated *in vacuo*, and the resulting red oil was heated neat at 90 °C for 5 h with a reflux condenser attached. The reaction was then cooled to 23 °C, diluted with Et_2O (60 mL), and concentrated *in vacuo* over SiO_2 (~10 g). Purification by flash column chromatography (100% hexanes)

provided light-sensitive vinyl iodide **3.32** (1.33 g, 4.58 mmol, 78%) as a colorless, crystalline solid. Spectral data were consistent with reported values.[18c]

(–)-Dimethyl (4*R*,5*R*)-4-((benzyloxy)methyl)-2,2-dimethyl-1,3-dioxolane-4,5-dicarboxylate (3.48): The procedure for the preparation of diester **3.48** was a slight modification from the literature procedure.[26] Dimethyl 2,3,-*O*-isopropylidene-*L*-tartrate (3.83 g, 17.6 mmol) was dissolved in THF (67 mL) and cooled to –78 °C. HMPA (13 mL) was added, followed by BOM-Cl (5.6 mL, 40 mmol). Freshly prepared LDA (17.7 mmol) in THF (50 mL) was then added to the reaction flask via cannula over ~30 min. The reaction was maintained for 5 h at –78 °C, before warming to 0 °C. After 3 h, the reaction was quenched with sat. aq. NH_4Cl solution (50 mL). The organic layer was washed with H_2O (3 x 40 mL) and brine (1 x 40 mL), dried over $MgSO_4$, and concentrated *in vacuo.* Unreacted dimethyl 2,3,-*O*-isopropylidene-*L*-tartrate was distilled from the crude product (120 °C, 0.3 torr). The remaining oil was purified by flash column chromatography (8% EtOAc in hexanes to 15% EtOAc in hexanes) to provide diester **3.48** (2.75 g, 8.14 mmol, 46%) as a light yellow oil. This reaction could be run on larger scale (~6x) with similar yields (41–43%). R_f 0.80 (40% EtOAc in hexanes; visualized with ceric ammonium molybdate). ^{1}H NMR (500 MHz, $CDCl_3$) δ 7.34–7.23 (m, 5H), 5.12 (s, 1H), 4.52 (d, *J* = 12.2 Hz, 1H), 4.47 (d, *J* = 12.2 Hz, 1H), 3.82 (s, 3H), 3.73 (d, *J* = 9.8 Hz, 1H), 3.70 (d, *J* = 9.8 Hz, 1H), 3.63 (s, 3H), 1.59 (s, 3H), 1.42 (s, 3H); ^{13}C NMR (125 MHz, $CDCl_3$) δ 170.80, 168.80, 137.60, 128.43, 127.77, 127.53, 112.71, 85.27, 77.56, 73.71, 70.11, 53.17, 52.40, 27.44, 25.95; IR (thin

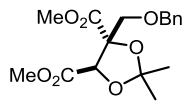

3.48: $C_{17}H_{22}O_7$
Molecular Weight: 338.3560

film) 2989, 2950, 1743, 1442, 1436, 1391, 1382, 1256, 1211 cm^{-1}; $[\alpha]^{25}_{D}$: –33.8 (c = 1.7, CH_2Cl_2); HRMS (ESI) calculated for $C_{17}H_{22}O_7Na$ (M+Na) 361.1263, observed 361.1271.

(–)-Methyl (4*R*,5*S*)-4-((benzyloxy)methyl)-5-(hydroxymethyl)-2,2-dimethyl-1,3-dioxolane-4-carboxylate (3.54): The procedure for the preparation of alcohol **3.54** was a slight modification from the literature procedure.[26] Diester **3.48** (17.7 g, 52.3 mmol) was dissolved in THF (450 mL) and cooled to –78 °C. DIBAL-H (14 mL, 79 mmol) was added dropwise to the reaction. After 5 min, the reaction was warmed to 0 °C. After 1 h, a saturated solution of Rochelle's salt (250 mL) and EtOAc (100 mL) were added. The reaction was allowed to warm to 23 °C, and the heterogeneous mixture was extracted with EtOAc (4 x 150 mL). The combined organic layers were dried over $MgSO_4$, filtered, and concentrated *in vacuo*. The crude residue was then purified by flash column chromatography (20% EtOAc in hexanes to 50% EtOAc in hexanes) to provide recovered diester **3.48** (6.34 g, 18.6 mmol, 36%) as a light yellow oil and alcohol **3.54** (7.44 g, 23.9 mmol, 46%) as a clear oil. R_f 0.35 (40% EtOAc in hexanes; visualized with ceric ammonium molybdate). ^{1}H NMR (500 MHz, $CDCl_3$) δ 7.36–7.25 (m, 5H), 4.56–4.51 (m 3H), 3.91 (dd, *J* = 12.1, 5.3 Hz, 1H), 3.85 (dd, *J* = 12.2, 5.5 Hz, 1H), 3.80 (s, 3H), 3.72 (d, *J* = 9.4 Hz, 1H), 3.65 (d, *J* = 9.4 Hz, 1H), 2.37 (bs, 1H), 1.47 (s, 3H), 1.40 (s, 3H); ^{13}C NMR (125 MHz, $CDCl_3$) δ 171.80, 137.24, 128.70, 128.07, 127.89, 110.16, 83.83, 73.94, 70.51, 60.65, 52.91, 27.75, 25.34; IR (thin film) 3500, 2989, 2937, 2871, 1743, 1454, 1380 cm^{-1}; $[\alpha]^{25}_{D}$: –2.17 (c = 1.2); HRMS (ESI) calculated for $C_{16}H_{22}O_6NH_4$ (M+NH_4) 328.1760, observed 328.1754.

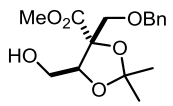

3.54: $C_{16}H_{22}O_6$
Molecular Weight: 310.3460

(–)-Methyl (4*R*,5*R*)-4-((benzyloxy)methyl)-5-formyl-2,2-dimethyl-1,3-dioxolane-4-carboxylate (3.55): To a stirring suspension of alcohol **3.54** (4.80 g, 15.5 mmol) and

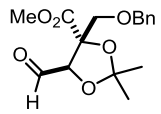

3.55: $C_{16}H_{20}O_6$
Molecular Weight: 308.3300

$NaHCO_3$ (6.50 g, 77.4 mmol) in CH_2Cl_2 (40 mL) was added Dess-Martin periodinane (7.87 g, 18.6 mmol) in two portions over 5 min. After 2 h, the reaction mixture was diluted with Et_2O (40 mL) and filtered through a cotton plug to remove solid $NaHCO_3$. The filtrate was concentrated *in vacuo*, resulting in a white solid. The solid was then washed with hexanes (6 x 30 mL), and the combined hexane washes were filtered through Celite. Upon concentration, aldehyde **3.55** (4.33 g, 14.0 mmol, 91%) was obtained as a colorless oil. Notes: 1) Aldehyde **3.55** was found to decompose within 14 h upon its formation (at room temperature or in the freezer), possibly from self-aldol polymerization. Therefore, it was always carried forward *immediately* into the next reaction. 2) Aldehyde **3.55** did not appear unstable to column chromatography, but it could not be purified in that manner. 3) Aqueous washes diminished the yields, possibly from hydrate formation. ^{1}H NMR (500 MHz, $CDCl_3$) δ 9.69 (s, 1H); 7.36–7.24 (m, 5H), 4.89 (s, 1H), 4.47 (d, *J* = 12.1 Hz, 1H), 4.44 (d, *J* = 12.1 Hz, 1H), 3.82 (s, 3H), 3.66 (d, *J* = 10.0 Hz, 1H), 3.63 (d, *J* = 10.0 Hz, 1H), 1.59 (s, 3H), 1.42 (s, 3H); ^{13}C NMR (125 MHz, $CDCl_3$) δ 197.23, 170.67, 137.15, 128.54, 127.84, 127.68, 112.75, 86.30, 82.95, 73.47, 69.28, 53.27, 27.30, 25.77; IR (thin film) 2991, 2937, 2868, 1740, 1454, 1374 cm^{-1}; $[\alpha]^{25}_D$: –2.37 (c = 2.5, CH_2Cl_2); HRMS (ESI) calculated for $[C_{16}H_{20}O_6NH_4]^+$ (M+NH_4) 326.1604, observed 326.1612.

(–)-Methyl (4*R*,5*S*)-4-((benzyloxy)methyl)-5-((*R*)-hydroxy((3a*S*,7a*S*)-3a,7,7-trimethyl-3a,4,5,6,7,7a-hexahydro-1H-inden-3-yl)methyl)-2,2-dimethyl-1,3-dioxolane-4-carboxylate (3.64): (*R*)-Oxazoline **3.62**[35a] (2.86 g, 9.65 mmol) and $CrCl_2$ (1.19 g, 9.65 mmol) were dissolved in THF (20 mL) in the glove box, and NEt_3 (1.34 mL, 9.65 mmol) was then added. The suspension was vigorously stirred for 6 h, and then $NiCl_2$ (36 mg, 0.28 mmol) was added, followed by a solution of vinyl iodide **3.32** (0.80 g, 2.8 mmol) and aldehyde **3.55** (1.30 g, 4.21 mmol) in THF (10 mL). Vigorous stirring was maintained for 20 h before removing the flask from the glovebox and cooling the solution to 0 ºC. Ethylene diamine (2 mL) was added to quench the reaction. After stirring for 30 min, H_2O (40 mL) and Et_2O (40 mL) were added. The aqueous layer was extracted with EtOAc (4 x 20 mL), and the combined organic layers were washed with sat. aq. $NaHCO_3$ solution (40 mL) and brine (1 x 40 mL), dried over $MgSO_4$, filtered, and concentrated *in vacuo*. Purification by flash column chromatography (5% EtOAc in hexanes to 11% EtOAc in hexanes) provided a single diastereomer, alcohol **3.64** (0.860 g, 1.82 mmol, 66%) as a clear oil. (*R*)-Oxazoline **3.62** was recovered during flash column chromatography (60–80% recovery) and recrystallized from Et_2O/hexanes for reuse. R_f 0.50 for **3.64** (20% EtOAc in hexanes; visualized with ceric ammonium molybdate). ^{1}H NMR (500 MHz, $CDCl_3$) δ 7.36–7.24 (m, 5H), 5.78–5.74 (m, 1H), 4.61 (d, *J* = 12.6 Hz, 1H), 4.55 (d, *J* = 12.6 Hz, 1H), 4.44 (d, *J* = 9.0 Hz, 1H), 4.37 (s, 1H), 3.97 (d, *J* = 9.8 Hz, 1H), 3.80 (d, *J* = 9.8 Hz, 1H), 3.77 (s, 3H), 2.58 (d, *J* = 9.0 Hz, 1H), 2.12–1.99 (m, 2H), 1.74–1.70 (m, 2H), 1.58–1.56 (m, 1H), 1.54 (s, 3H), 1.5–1.43 (m, 2H), 1.42 (s, 3H), 1.25–1.19 (m, 1H), 1.11–1.01 (m, 1H), 0.98 (s, 3H), 0.95 (s, 3H), 0.88 (s, 3H); ^{13}C

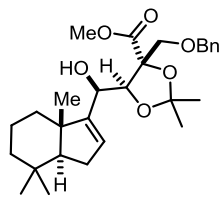

3.64: $C_{28}H_{40}O_6$
Molecular Weight: 472.6220

NMR (125 MHz, $CDCl_3$) δ 172.59, 155.05, 137.89, 128.42, 127.76, 127.72, 126.03, 110.24, 80.41, 73.71, 71.94, 65.50, 59.97, 52.69, 41.51, 35.53, 33.29, 32.93, 28.76, 27.61, 25.46, 21.45, 20.15, 18.15; IR (thin film) 3527, 2989, 2926, 2848, 1741, 1454, 1380 cm^{-1}; $[\alpha]^{25}_{D}$: –4.85 (c = 1.5, CH_2Cl_2); HRMS (ESI) calculated for $C_{28}H_{40}O_6NH_4$ ($M+NH_4$) 490.3169, observed 490.3165.

(–)-1,3-Dioxoisoindolin-2-yl (4*S*,5*R*)-4-((benzyloxy)methyl)-5-((*R*)-hydroxy((3a*S*,7a*S*)-3a,7,7-trimethyl-3a,4,5,6,7,7a-hexahydro-1H-inden-3-yl)methyl)-2,2-dimethyl-1,3-dioxolane-4-carboxylate (3.75): Alcohol **3.64** (0.850 g, 1.80 mmol) was dissolved in a mixture of MeOH (10 mL) and H_2O (10 mL). KOH pellets (0.807 g, 14.4 mmol) were then added, and the reaction was warmed to 50 ºC. After 3 h, TLC analysis confirmed starting material was consumed; and the reaction was cooled to 23 ºC. Aqueous HCl (18 mL of 1 M soln) was added to the flask, and the heterogeneous mixture was extracted with EtOAc (5 x 15 mL). The combined organic layers were washed with brine (1 x 20 mL), dried over $MgSO_4$, filtered, and concentrated *in vacuo* to provide the crude acid as a clear oil which was carried forward without further purification.

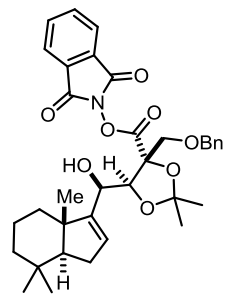

3.75: $C_{35}H_{41}NO_8$
Molecular Weight: 603.7120

The crude acid was dissolved in THF (20 mL) to which *N*-hydroxyphthalimide (0.881 g, 5.40 mmol), DCC (0.483 g, 2.34 mmol), and DMAP (11 mg, 0.090 mmol) were added. The reaction was maintained for 3 h at 23 ºC, at which point Celite (~2 g) was added. The reaction mixture was concentrated *in vacuo*, and the resulting residue was purified by flash column chromatography using pH 7 silica gel (10% EtOAc in hexanes to

20% EtOAc in hexanes) to provide (*N*-acyloxy)phthalimide **3.75** as a colorless solid. Recrystallization from acetone/hexanes afforded (*N*-acyloxy)phthalimide **3.75** (0.750 g, 1.24 mmol, 69%) as colorless needles. R_f 0.25 (20% EtOAc in hexanes; visualized with ceric ammonium molybdate). ^{1}H NMR (600 MHz, $CDCl_3$) δ 7.91–7.88 (2H, m), 7.81–7.78 (2H, m), 7.42–7.26 (m, 5H), 5.80 (s, 1H), 4.75 (d, *J* = 12.4 Hz, 1H), 4.71 (d, *J* = 12.4 Hz, 1H), 4.69 (s, 1H), 4.49 (d, *J* = 9.7 Hz, 1H), 4.14 (d, *J* = 9.9 Hz, 1H), 3.97 (d, *J* = 10.1 Hz, 1H), 2.47 (d, *J* = 9.6 Hz, 1H), 2.11–2.00 (m, 2H), 1.74–1.64 (m, 2H), 1.59 (s, 3H), 1.56-1.51 (m, 2H), 1.54 (s, 3H), 1.43 (app d, *J* = 13.3 Hz, 1H), 1.27 (app td, *J* = 12.5, 3.7 Hz, 1H), 1.13 (app td, *J* = 13.5, 4.3 Hz, 1H), 0.98 (s, 3H), 0.95 (s, 3H), 0.88 (s, 3H); ^{13}C NMR (125 MHz, $CDCl_3$) δ 169.29, 161.58, 154.82, 137.69, 134.94, 129.11, 128.46, 128.03, 127.75, 126.32, 124.17, 111.30, 85.13, 80.61, 74.20, 71.82, 65.56, 59.87, 47.34, 41.49, 35.42, 33.28, 32.93, 28.79, 27.39, 25.05, 21.48, 20.13, 18.18; IR (thin film) 3524, 2989, 2928, 2862, 1813, 1788, 1747, 1454, 1373 cm^{-1}; $[\alpha]^{25}_D$: –7.60 (c = 1.6, CH_2Cl_2); HRMS (ESI) calculated for $C_{35}H_{41}NO_8Na$ (M+Na) 626.2730, observed 626.2712; mp 139–141 ºC.

(+)-1,3-Dioxoisoindolin-2-yl (4*R*,5*S*)-4-((benzyloxy)methyl)-5-(((2*S*,3a*S*,7a*S*,*Z*)-2-chloro-4,4,7a-trimethyloctahydro-1H-inden-1-ylidene)methyl)-2,2-dimethyl-1,3-dioxolane-4-carboxylate (3.78): (*N*-acyloxy)phthalimide **3.75** (0.223 g, 0.369 mmol) was dissolved in a 10:1 mixture of Et_2O/pyridine (3.5 mL) and cooled to –45 ºC. A solution of $SOCl_2$ (54 µL, 0.74 mmol) in a 10:1 mixture of Et_2O/pyridine (0.5 mL) was then added dropwise to the reaction over 5 min. The reaction was maintained at –45 ºC until full conversion of starting material was observed by TLC analysis (~45 min). Saturated aq. $NaHCO_3$ solution (2 mL) was added, and the reaction was allowed to warm to 23 ºC. The mixture was then diluted with H_2O (2 mL) and washed with EtOAc (3 x 3 mL). The combined organic layers were washed with brine (1 x 2 mL), dried over $MgSO_4$, filtered, and concentrated *in vacuo* onto Celite (~1 g). Purification by flash column chromatography using pH 7 silica gel (5% EtOAc in hexanes to 11% EtOAc in hexanes) provided allylic chloride **3.78** as a colorless solid. Recrystallization from acetone/hexanes afforded allylic chloride **3.78** (0.143 g, 0.229 mmol, 62%) as colorless needles. R_f 0.40 (20% EtOAc in hexanes; visualized with ceric ammonium molybdate). ^{1}H NMR (500 MHz, $CDCl_3$) δ 7.95-7.88 (m, 2H), 7.83-7.78 (m, 2H), 7.40–7.26 (m, 5H), 5.59 (d, *J* = 9.6 Hz, 1H), 5.18 (d, *J* = 9.6 Hz, 1H), 4.96 (app t, *J* = 7.6 Hz, 1H), 4.70 (d, *J* = 12.3 Hz, 1H), 4.64 (d, *J* = 12.3 Hz, 1H), 3.78 (d, *J* = 10.0 Hz, 1H), 3.71 (d, *J* = 10.0 Hz, 1H), 2.32 (app quint, *J* = 6.4 Hz, 1H), 1.84 (td, *J* = 13.7 Hz, 7.5 Hz, 1H), 1.74 (app d, *J* = 12.6 H, 1H), 1.67–1.59 (m, 1H), 1.59 (s, 6H), 1.55–1.48 (m, 1H), 1.41 (app d, *J* = 13.6 Hz, 1H), 1.13 (s, 3H), 0.99–0.84 (m, 3H), 0.87 (s, 3H), 0.77 (s, 3H); ^{13}C NMR (125 MHz, $CDCl_3$) δ 169.07, 161.68, 161.30, 137.64, 134.99, 129.09, 128.45,

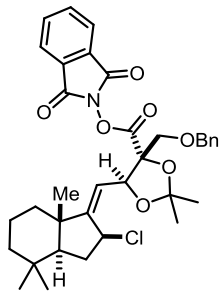

3.78: $C_{35}H_{40}ClNO_7$
Molecular Weight: 622.1550

127.95, 127.80, 124.25, 114.32, 111.61, 84.96, 76.44, 74.04, 71.07, 54.60, 54.10, 45.10, 41.19, 37.03, 34.08, 32.24, 32.81, 27.55, 24.78, 21.25, 21.11, 19.49; IR (thin film) 2986, 2928, 2866, 2350, 2336, 1813, 1787, 1747, 1459 cm^{-1}; $[\alpha]^{25}_{D}$: +83.2 (c = 1.8, CH_2Cl_2); HRMS (ESI) calculated for $C_{35}H_{40}ClNO_7Na$ (M+Na) 644.2391, observed 644.2383; mp 154–158 ºC.

(–)-(*R*)-5-Acetoxyfuran-2(5H)-one (S3.1): The procedure for preparation of acetoxy butenolide **S3.1** was a slight modification from the literature procedure.[81] 5-Hydroxyfuran-2(5H)-one[14] (2.90 g, 28.9 mmol) was dissolved in vinyl acetate (30 mL). Amano lipase AK (2.00 g) was then added, and the suspension was stirred for 8 days at 23 ºC. The suspension was then filtered through Celite, and the filtrate was concentrated *in vacuo*. Purification of the residue by flash column chromatography (40% EtOAc in hexanes) provided (*R*)-5-acetoxyfuran-2(5H)-one **S3.1** (3.58 g, 25.3 mmol, 87% yield) as a yellow oil. R_f 0.35 (40% EtOAc in hexanes; visualized with $KMnO_4$). Spectral data were consistent with reported values.[81] The enantiomeric excess was determined to be 92% by known methods.[81]

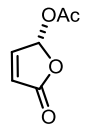

S3.1: $C_6H_6O_4$
Molecular Weight: 142.1100

(–)-(*R*)-5-Methoxyfuran-2(5H)-one (3.84): Acetoxy butenolide **S3.1** (1.23 g, 8.65 mmol) was dissolved in MeOH (35 mL), and $Pd(PPh_3)_4$ (0.500 g, 0.433 mmol) was added to the solution. The solution, which turned a deep red, was maintained at 23 ºC for 50 min. Upon TLC analysis confirming consumption of starting material (TLC, 10% acetone

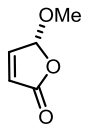

3.84: $C_5H_6O_3$
Molecular Weight: 114.1000

in hexanes and running the TLC plate 3x), the reaction solution was directly filtered through a silica gel plug (250 mL of 40% acetone in hexanes). The eluent was concentrated *in vacuo*, and the residue was distilled (0.8 torr, 110 ºC) to provide methoxy butenolide **3.84** and a trace amount of AcOH. Removal of AcOH upon further concentration *in vacuo* afforded methoxy butenolide **3.84** (0.705 g, 6.18 mmol, 71% yield) as a clear oil. Spectral data were consistent with reported values.[82] HLPC analysis was used to determine the enantiomeric ratio to be 92:8 (Chiracel AS column; flow: 2.0 mL/min, 10% isopropanol:*n*-hexane; λ = 210 nm; major enantiomer t_R = 8.70 min, minor enantiomer t_R = 11.60 min); $[\alpha]^{25}_D$: –124 (c = 1.2, CH_2Cl_2).

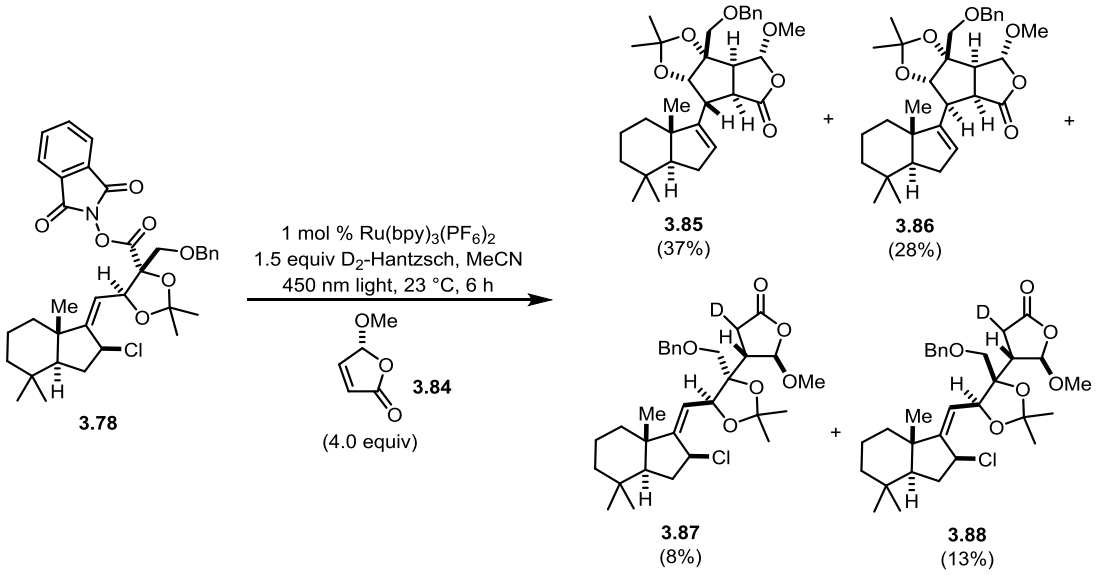

Radical ACF Cascade Reaction (Table 3.4, entry 4): Allylic chloride **3.78** (70 mg, 0.11 mmol), methoxy butenolide **3.84** (51 mg, 0.45 mmol), D_2-Hantzsch ester (43 mg, 0.17 mmol), and $[Ru(bpy)_3](PF_6)_2$ (1 mg, 0.001 mmol) were charged into a vial. Acetonitrile

(1.1 mL) was added, and the solution was sparged with argon for 5 min. The vial was then vigorously stirred while being irradiated by a single strip of blue LED lights (450 nm) at 23 ºC. After 6 h, the reaction mixture was concentrated *in vacuo*. The resulting residue was dissolved in EtOAc (1 mL) and washed with aq. HCl (4 x 2 mL of 4 M soln) followed by brine (2 x 2 mL). The organic layer was dried over $MgSO_4$, filtered, and concentrated *in vacuo*. ^{1}H NMR analysis of the crude residue using an internal standard (dimethoxybenzene) showed 37% yield of **3.85**, 28% yield of **3.86**, 8% yield of **3.87**, and 13% yield of **3.88**. Purification of the crude residue by flash column chromatography (0% acetone in hexanes to 5% acetone in hexanes) provided desired ACF product **3.86** (15 mg, 0.030 mmol, 27%) as a clear oil. R_f for **3.86**: 0.55 (20% acetone in hexanes; visualized with ceric ammonium molybdate). Flash column chromatography under separate conditions of the remaining mixed fractions from the first purification (4% EtOAc in hexanes to 10% EtOAc in hexanes) provided epimeric ACF product **3.85** (20 mg, 0.039 mmol, 35%) as a clear oil. R_f for **3.85**: 0.45 (20% acetone in hexanes; visualized with ceric ammonium molybdate).

(–)-(3a*S*,3b*S*,4*R*,6a*S*,7a*S*)-3a-((Benzyloxy)methyl)-4-methoxy-2,2-dimethyl-7-((3a*S*,7a*S*)-3a,7,7-trimethyl-3a,4,5,6,7,7a-hexahydro-1H-inden-3-yl)hexahydro-6H-furo[3',4':3,4]cyclopenta[1,2-d][1,3]dioxol-6-one (3.86): ^{1}H NMR (500 MHz, $CDCl_3$) δ

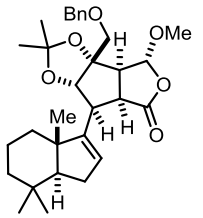

3.86: $C_{31}H_{42}O_6$
Molecular Weight: 510.6710

7.38–7.28 (m, 5H), 5.48 (app s, 1H), 5.38 (app s, 1H), 4.62 (d, *J* = 12.0 Hz, 1H), 4.59 (d, *J* = 12.1 Hz, 1H), 4.41 (d, *J* = 7.5 Hz, 1H), 3.64 (d, *J* = 10.5 Hz, 1H), 3.50 (d, *J* = 10.3 Hz, 1H), 3.43 (app t, *J* = 8.7 Hz, 1H), 3.38 (s, 3H), 3.07 (app d, *J* = 8.7 Hz, 1H), 3.00 (app t, *J* = 8.2 Hz, 1H), 2.10 (ddd, *J* = 14.9, 6.3, 3.0 Hz, 1H), 2.02 (app

t, J = 13.3 Hz, 1H), 1.76 (dd, J = 11.7, 6.3 Hz, 1H), 1.60–1.50 (m, 2H), 1.58 (s, 3H), 1.50 (s, 3H), 1.45–1.39 (m, 1H), 1.19 (td, J = 13.2, 3.4 Hz, 1H), 0.95 (s, 3H), 0.92–0.82 (m, 2H), 0.89 (s, 3H), 0.87 (s, 3H); ^{13}C NMR (125 MHz, $CDCl_3$) δ 174.65, 150.69, 137.18, 128.71, 128.38, 128.30, 124.70, 113.17, 103.64, 89.95, 86.77, 73.97, 70.81, 58.24, 56.76, 55.12, 47.84, 45.94, 43.72, 41.46, 34.73, 33.05, 32.90, 20.22, 29.38, 29.16, 21.45, 20.18, 17.70; $[\alpha]^{25}_{D}$: –84.9 (c = 1.0, CH_2Cl_2); IR (thin film) 2993, 2934, 2862, 1785, 1636, 1455, 1371, 1234, 1215 cm^{-1}; HRMS (ESI) calculated for $C_{31}H_{42}O_6NH_4$ (M+NH_4) 528.3325, observed 528.3331.

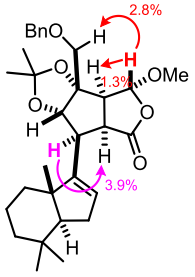

(–)-(3a*S*,3b*S*,4*R*,6a*S*,7*R*,7a*S*)-3a-((Benzyloxy)methyl)-4-methoxy-2,2-dimethyl-7-((3a*S*,7a*S*)-3a,7,7-trimethyl-3a,4,5,6,7,7a-hexahydro-1H-inden-3-yl)hexahydro-6H-furo[3',4':3,4]cyclopenta[1,2-d][1,3]dioxol-6-one (3.85): ^{1}H NMR (500 MHz, $CDCl_3$) δ

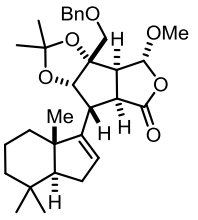

3.85: $C_{31}H_{42}O_6$
Molecular Weight: 510.6710

7.39–7.29 (m, 5H), 5.75 (app s, 1H), 5.53 (d, J = 4.8 Hz, 1H), 4.57 (d, J = 12.3 Hz, 1H), 4.55 (d, J = 12.3 Hz, 1H), 4.47 (d, J = 3.7 Hz, 1H), 3.82 (d, J = 9.6 Hz, 1H), 3.61 (d, J = 9.7 Hz, 1H), 3.50 (app t, J = 10.8 Hz, 1H) , 3.41 (s, 3H), 2.88 (dd, J = 9.7, 4.8 Hz, 1H), 2.72 (app d, J = 11.3 Hz, 1H), 2.13–2.06 (m, 2H), 1.76–1.65 (m, 1H), 1.61–1.52 (m, 2H), 1.43 (s, 3H), 1.36–1.27 (m, 1H), 1.28 (s, 3H), 1.15 (td, J = 13.6, 4.1 Hz, 1H), 0.96 (s, 3H), 0.92–0.81 (m, 2H), 0.89 (s, 3H), 0.83 (s, 3H); ^{13}C NMR (125

MHz, $CDCl_3$) δ 175.80, 148.52, 137.12, 128.69, 128.26, 128.05, 127.25, 111.58, 105.02, 89.60, 87.36, 73.83, 72.05, 59.28, 58.09, 57.57, 47.71, 47.54, 45.77, 41.61, 35.68, 33.09, 32.97, 29.17, 27.80, 26.00, 21.47, 20.22, 17.36; $[\alpha]^{25}_{D}$: –88.2 (c = 2.0, CH_2Cl_2); IR (thin film) 2988, 2929, 2861, 1775, 1454, 1373, 1246 cm^{-1}; HRMS (ESI) calculated for $C_{31}H_{42}O_6Na$ (M+Na) 533.2879, observed 533.2897.

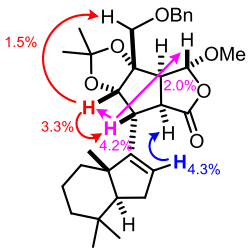

(+)-(4*S*,5*R*)-4-((4*S*,5*S*)-4-((Benzyloxy)methyl)-5-(((2*S*,3a*S*,7a*S*,*Z*)-2-chloro-4,4,7a-trimethyloctahydro-1H-inden-1-ylidene)methyl)-2,2-dimethyl-1,3-dioxolan-4-yl)-5-methoxydihydrofuran-2(3H)-one-3-*d* (3.87): An analytical sample of clean **3.87** was obtained from flash column chromatography (0% acetone in hexanes to 4% acetone in hexanes). R_f: 0.60 (20% acetone in hexanes; visualized with ceric ammonium molybdate). ^{1}H NMR (600 MHz, $CDCl_3$) δ 7.36–7.27 (m, 5H), 5.61 (s, 1H), 5.18 (d, *J* = 9.6, 1H), 5.09 (dd, *J* = 9.6, 1.6 Hz, 1H), 4.57 (td, *J* = 8.0 Hz, 1.6 Hz, 1H), 4.46 (d, *J* = 10.4 Hz, 1H), 4.41 (d. *J* = 10.4 Hz, 1H), 3.63 (d, *J* = 9.6 Hz, 1H), 3.53 (d, *J* = 9.6 Hz, 1H), 3.51 (s, 3H), 2.68 (d, *J* = 2.1 Hz, 1H), 2.50 (d, *J* = 2.1 Hz, 1H), 1.93–1.86 (m, 1H), 1.76–1.51 (m, 4H), 1.48 (s, 3H), 1.42 (s, 3H), 1.09 (s, 3H), 1.04–0.95 (m, 2H), 0.91–0.83 (m, 1H), 0.85 (s, 3H), 0.74 (s, 3H), 0.60 (dd, *J* = 14.4, 6.0 Hz, 1H); ^{13}C NMR (125 MHz, $CDCl_3$) δ 176.81, 159.67, 137.02, 128.73, 128.34, 128.26, 115.56, 109.03, 106.81, 82.60, 78.24, 74.46, 74.39, 56.90, 54.57, 54.53, 45.17, 44.93, 41.17, 36.72,

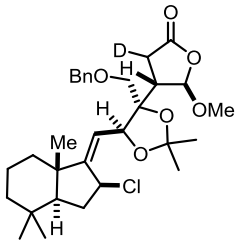

3.87: $C_{31}H_{42}DClO_6$
Molecular Weight: 548.1351

33.93, 33.15, 32.96, 29.85, 27.58, 26.19, 21.49, 21.15, 19.49; $[\alpha]^{25}_{D}$: +109.1 (c = 0.57, CH_2Cl_2); IR (thin film) 2986, 2931, 2864, 2359, 2342, 1787, 1455, 1370, 1252 cm^{-1}; HRMS (ESI) calculated for $C_{31}H_{42}DClO_6Na$ (M+Na) 570.2709, observed 570.2702.

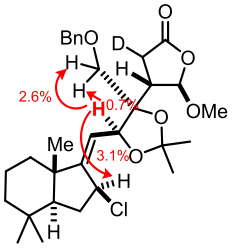

(4*S*,5*R*)-4-((4*R*,5*S*)-4-((Benzyloxy)methyl)-5-(((2*S*,3a*S*,7a*S*,*Z*)-2-chloro-4,4,7a-trimethyloctahydro-1H-inden-1-ylidene)methyl)-2,2-dimethyl-1,3-dioxolan-4-yl)-5-methoxydihydrofuran-2(3H)-one-3-*d* (3.88): Addition product **3.88** could never be isolated in pure form. Diagnostic peaks of addition product **3.88** for ^{1}H NMR (500 MHz, $CDCl_3$) δ 5.43 (d, *J* = 2.9 Hz, 1H), 5.21 (d, *J* = 9.6, 1.7 Hz, 1H), 4.75 (d, *J* = 9.6 Hz, 1H), 4.59 (app t, *J* = 7.0 Hz, 1H).

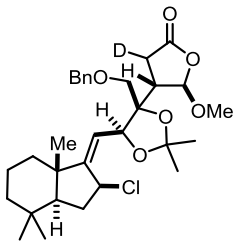

3.88: $C_{31}H_{42}DClO_6$
Molecular Weight: 548.1351

(–)-(3a*S*,3b*S*,4*R*,6*R*,6a*S*,7*S*,7a*S*)-3a-((Benzyloxy)methyl)-4-methoxy-2,2-dimethyl-7-((3a*S*,7a*S*)-3a,7,7-trimethyl-3a,4,5,6,7,7a-hexahydro-1H-inden-3-yl)hexahydro-4H-furo[3',4':3,4]cyclopenta[1,2-d][1,3]dioxol-6-yl acetate (3.106): Desired ACF product

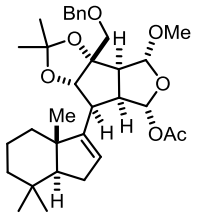

3.106: $C_{33}H_{46}O_7$
Molecular Weight: 554.7240

3.86 (40 mg, 0.078 mmol) was charged into a flask with toluene (1.4 mL) and then cooled to –78 ºC. A solution of DIBAL-H (18 µL, 0.10 mmol) in toluene (0.2 mL) was added dropwise to the reaction vessel, keeping the temperature near –78 ºC. After 45 min, TLC analysis showed some remaining starting material, and an additional solution of DIBAL-H (5 µL, 0.03 mmol) in toluene (0.05 mL) was added. After 45 min, a solution of DMAP (19 mg, 0.16 mmol), pyridine (20 µL, 0.23 mmol), and CH_2Cl_2 (0.2 mL) was added, followed by Ac_2O (44 µL, 0.47 mmol). The reaction was maintained at –78 ºC for 12 h, at which point it was allowed to warm to 23 ºC. An aqueous solution saturated with Rochelle's salt (3 mL) was added, and the aqueous layer was extracted with EtOAc (3 x 2 mL). The combined organic layers were washed with brine (1 x 5 mL), dried over $MgSO_4$, filtered, and concentrated *in vacuo*. Purification of the residue by flash column chromatography (6% EtOAc in hexanes to 10% EtOAc in hexanes) provided a single diastereomer, diacetal **3.106** (36 mg, 0.065 mmol, 83%), as a colorless oil. R_f 0.35 (20% EtOAc in hexanes; visualized with ceric ammonium molybdate). ^{1}H NMR (500 MHz, $CDCl_3$) δ 7.38–7.27 (m, 5H), 5.92 (d, *J* = 4.1 Hz, 1H), 5.60 (app s, 1H), 5.17 (s, 1H), 4.61 (d, *J* = 12.3 Hz, 1H), 4.58 (d, *J* = 12.3 Hz, 1H), 4.30 (d, *J* = 8.8 Hz, 1H), 3.60 (d, *J* = 10.4 Hz, 1H), 3.54 (d, *J* = 10.5 Hz, 1H), 3.27 (s, 3H), 3.20 (app td, *J* = 7.8, 4.0 Hz, 1H), 3.03 (d, *J* = 8.0 Hz, 1H), 2.92 (app t, *J* = 8.1 Hz, 1H), 2.05 (s, 3H), 2.06–2.00 (m, 2H), 1.72–1.51 (m, 2H), 1.51 (s, 3H), 1.46 (app d, *J* = 13.6 Hz, 1H), 1.35 (s, 3H), 1.28–

1.24 (m, 1H), 1.20 (td, J = 12.7, 3.9 Hz, 1H), 0.98 (td, J = 13.7, 4.4 Hz, 1H), 0.93 (s, 3H), 0.90–0.85 (m, 1H), 0.84 (s, 6H); ^{13}C NMR (125 MHz, $CDCl_3$) δ 170.46, 151.77, 137.54, 128.61, 128.36, 128.13, 125.03, 113.25, 107.80, 99.65, 90.22, 85.91, 73.84, 70.54, 50.88, 47.64, 43.33, 42.11, 36.75, 35.58, 33.29, 32.95, 31.72, 30.64, 29.72, 29.01, 24.81, 22.79, 21.25, 21.17, 20.09, 17.24, 14.27; $[\alpha]^{25}_{D}$: –46.3 (c = 2.1, CH_2Cl_2); IR (thin film) 2991, 2930, 2861, 1748, 1455, 1367 cm^{-1}; HRMS (ESI) calculated for $C_{33}H_{46}O_7Na$ (M+Na) 577.3141, observed 577.3127.

(–)-(3a*S*,3b*S*,4*R*,6*R*,6a*S*,7*R*,7a*S*)-3a-(Hydroxymethyl)-4-methoxy-2,2-dimethyl-7-((1*R*,3a*S*,7a*R*)-4,4,7a-trimethyloctahydro-1H-inden-1-yl)hexahydro-4H-furo[3',4':3,4]cyclopenta[1,2-d][1,3]dioxol-6-yl acetate (3.107): Diacetal **3.106** (28 mg, 0.050 mmol) and 10% Pd/C (28 mg) were charged into a flask with MeOH (1.0 mL). The reaction vessel was then evacuated and refilled with Ar (3x). Formic acid (50 µL) was then added dropwise to the vigorously stirring suspension. After 2 h, TLC analysis showed full consumption of starting material. The reaction mixture was diluted with MeOH (1 mL), filtered through Celite, and concentrated *in vacuo* to provide the crude alcohol, which was carried forward to the subsequent step.

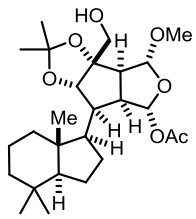

3.107: $C_{26}H_{42}O_7$
Molecular Weight: 466.6150

To a flask containing the crude alcohol (0.050 mmol) was added PtO_2 (12 mg, 0.050 mmol) and EtOAc (1.0 mL). The reaction vessel was then evacuated and refilled with H_2 (3x, 1 atm H_2). The reaction was maintained under 1 atm of H_2 for 12 h at 23 ºC, at which point the reaction vessel was refilled first with Ar and then air. Filtration of the suspension through Celite, concentration of the filtrate *in vacuo*, and purification of the residue by

flash column chromatography (30% EtOAc in hexanes) provided alcohol **3.107** (20 mg, 0.043 mmol, 86%) as a colorless oil. R_f 0.25 (30% EtOAc in hexanes; visualized with ceric ammonium molybdate). ^{1}H NMR (500 MHz, $CDCl_3$) δ 6.13 (d, *J* = 3.5 Hz, 1H), 5.31 (s, 1H), 3.86 (d, *J* = 9.6 Hz, 1H), 3.65 (bs, 2H), 3.31 (s, 3H), 3.19 (app td, *J* = 7.4, 3.6 Hz, 1H), 2.87 (app d, *J* = 7.6 Hz, 1H), 2.30 (app dt, *J* = 10.1, 7.3 Hz, 1H), 2.16 (bs, 1H), 2.05 (s, 3H), 1.80–1.66 (m, 2H), 1.63–1.56 (m, 2H), 1.53 (s, 3H), 1.43 (s, 6H), 1.36–1.28 (m, 1H), 1.11–0.93 (m, 2H), 0.90–0.86 (m, 1H), 0.85 (s, 3H), 0.83 (s, 3H), 0.76 (s, 3H), 0.76–0.69 (m, 1H); ^{13}C NMR (125 MHz, $CDCl_3$) δ 170.84, 112.73, 106.84, 97.67, 90.98, 88.07, 63.62, 57.74, 56.04, 54.85, 52.29, 50.68, 44.98, 42.90, 41.39, 40.00, 33.60, 33.26, 30.71, 30.49, 29.84, 25.75, 21.20, 20.99, 20.94, 20.22, 13.86; $[\alpha]^{25}_D$: –17.6 (c = 1.7, CH_2Cl_2); IR (thin film) 3490, 2951, 2931, 2873, 1745, 1459, 1368 cm^{-1}; HRMS (ESI) calculated for $C_{26}H_{42}O_7Na$ (M+Na) 489.2828, observed 489.2813.

(–)-Chromodorolide B (3.110): Alcohol **3.107** (9.0 mg, 0.019 mmol) and Dess-Martin periodinane (12 mg, 0.029 mmol) were charged into a flask with CH_2Cl_2 (0.3 mL). The reaction mixture was maintained at 23 ºC for 5 h, at which point it was diluted with hexanes (0.5 mL), filtered through Celite, and concentrated *in vacuo*. The residue was dissolved in hexanes (1 mL) and filtered through Celite. The filtrate was then concentrated *in vacuo* to afford the crude aldehyde which was carried forward into the next step.

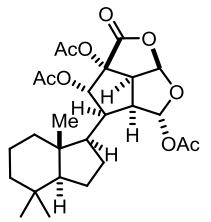

chromodorolide B (**3.110**): $C_{26}H_{36}O_9$
Molecular Weight: 492.5650

To a solution of crude aldehyde in THF (0.1 mL) was added *t*-BuOH (0.1 mL), H_2O (0.1 mL), 2-methyl-2-butene (50 µL), NaH_2PO_4 (25 mg, 0.21 mmol), and $NaClO_2$ (14 mg, 0.15 mmol). The reaction was maintained at 23ºC for 12 h and then diluted with H_2O (1

mL). The solution was washed with EtOAc (3 x 1 mL); and the combined organic layers were dried over Na_2SO_4, filtered, and concentrated *in vacuo* to provide crude carboxylic acid **3.108**.

Crude acid **3.108** was then dissolved in a solution of THF (0.3 mL) and aq. HCl (0.3 mL of 4 M soln), which was maintained at 23 ºC for 72 h. The reaction was then diluted with H_2O (1 mL), and the solution was washed with EtOAc (3 x 1 mL). The combined organic layers were washed with brine (1 mL), dried over Na_2SO_4, filtered, and concentrated *in vacuo* to afford crude lactol anomers **3.109**.

Crude lactol **3.109** was then dissolved in CH_2Cl_2 (0.3 mL). Next, DMAP (2 mg, 0.019 mmol) and pyridine (31 µL, 0.38 mmol) were added, followed by Ac_2O (28 µL, 0.29 mmol). The reaction was maintained at 23 ºC for 24 h, at which point it was diluted with H_2O (2 mL), and the heterogeneous solution was washed with EtOAc (3 x 2 mL). The combined organic layers were washed with brine (3 mL), dried over Na_2SO_4, filtered, and concentrated *in vacuo*. Purification by flash column chromatography (20% EtOAc in hexanes to 30% EtOAc in hexanes) provided **3.110** (4.7 mg, 0.010 mmol, 49% from **3.107**) as a colorless solid. Recrystallization of the solid from acetone/hexanes afforded colorless needles. The NMR data correlated closely to the isolation data.[76] $[\alpha]^{25}_{D}$: –66.8 (c = 0.12, CH_2Cl_2) compared to isolation sample $[\alpha]^{25}_{D}$: –95 (c = 0.10, CH_2Cl_2)[12]; IR (thin film) 2948, 2876, 1813, 1752, 1370, 1214, 1093, 1000, 964 cm^{-1}; HRMS (ESI) calculated for $C_{26}H_{36}O_9Na$ (M+Na) 515.2257, observed 515.2260; mp 236–238 ºC (decomp).

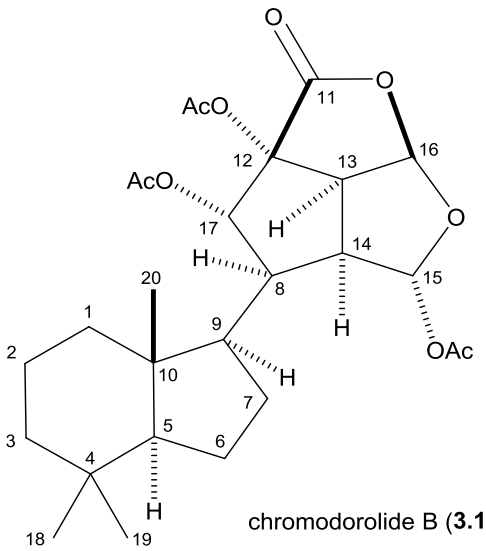

chromodorolide B (**3.110**)

	Literature (400 MHz,$CDCl_3$)		**Synthetic (500 MHz, $CDCl_3$)**	
Pos	δH (multiplicity, *J* / Hz)	δC	δH (multiplicity, *J* / Hz)	δC
1	1.03 (dt, *J* = 12.3, 3.6)	40.9	1.03 (dt, *J* = 12.3, 3.6)	41.06
1a	1.38 (m)		1.39 (m)	
2	1.55 (m, 2H)	21.1	1.56 (m, 2H)	21.27
3	0.95 (m)	39.1	0.95 (dt, *J* = 12.6, 3.6)	39.26
3a	1.51 (m)		1.52 (m)	
4		33.1		33.31
5	1.09 (dd, *J* = 13.1, 6.6)	57.0	1.10 (dd, *J* = 13.7, 3.7)	57.10
6	1.40 (m)	19.9	1.42 (m)	20.08
6a	1.56 (m)		1.57 (m)	
7	1.48 (m)	25.2	1.50 (m)	25.36
7a	1.58 (m)		1.61 (m)	
8	2.57 (ddd, *J* = 12.1, 11.6, 7.9)	48.0	2.58 (ddd, *J* = 12.2, 11.1, 7.6)	48.13
9	1.69 (bdd, *J* = 12.0, 9.9)	50.3	1.71 (q, *J* = 10.0)	50.43
10		43.9		44.00
11		169.1		169.24
12		81.4		81.48
13	3.79 (dd, *J* = 8.9, 6.1)	50.4	3.80 (dd, *J* = 9.0, 6.0)	50.56
14	2.93 (bt, *J* = 8.2)	45.6	2.94 (bt, *J* = 8.2)	45.74
15	6.50 (bs)	97.8	6.51 (bs)	97.88
16	6.08 (d, *J* = 6.1)	103.4	6.09 (d, *J* = 6.0)	103.51
17	5.30 (d, *J* = 11.6)	73.9	5.31 (d, *J* = 12.4)	74.06
18	0.79 (s, 3H)	33.4	0.79 (s, 3H)	33.55
19	0.83 (s, 3H)	21.0	0.84 (s, 3H)	21.11
20	0.84 (s, 3H)	13.7	0.85 (s, 3H)	13.82
OAc	2.04 (s, 3H)	20.8	2.05 (s, 3H)	20.96
		169.2		169.32
OAc	2.11 (s, 3H)	20.8	2.12 (s, 3H)	20.98
		170.0		170.13
OAc	2.19 (s, 3H)	20.9	2.21 (s, 3H)	21.05
		170.2		170.38

3.4 References and Notes

[1] Okada, K.; Okamoto, K.; Morita, N.; Okubo, K.; Oda, J. *J. Am. Chem. Soc.* **1991**, *113*, 9401–9402.

[2] Schnermann, M. J.; Overman, L. E. *Angew. Chem. Int. Ed.* **2012**, *51*, 9576–9580.

[3] a) Lackner, G. L.; Quasdorf, K. W.; Overman, L. E. *J. Am. Chem. Soc.* **2013**, *135*, 15342–15345. b) Nawrat, C. C.; Jamison, C. R.; Slutskyy, Y.; MacMillan, D. W. C.; Overman, L. E. *J. Am. Chem. Soc.* **2015**, *137*, 11270–11273.

[4] For more details, see Dr. Garnsey's previous reports and presentations.

[5] a) Schnermann, M. J.; Beaudry, C. M.; Egorova, A. V.; Polishchuk, R. S.; Sütterlin, C.; Overman, L. E. *Proc. Nat. Acad. Sci. USA* **2010**, *107*, 6158–6163. b) Schnermann, M.; Beaudry, C. M.; Genung, N. E.; Canham, S. M.; Untiedt, N. L.; Karanikolas, B. D. W.; Sütterlin, C.; Overman, L. E. *J. Am. Chem. Soc.* **2011**, *133*, 17494–17503.

[6] While an ester (instead of a *tert*-butyldimethylsilyl ether) would have the desired oxidation state of the natural product for the radical [3+2] cycloaddition, the generated α-acyl radical would be too stabilized to undergo intermolecular addition to the butenolide.

[7] Two related examples of trisubstituted acetonide radicals were later found in the literature. These are discussed further in Section 4.2.

[8] a) Thompson, D. K.; Hubert, C. N.; Wightman, R. H. *Tetrahedron* **1993**, *49*, 3827–3840. b) Kim, H.-J.; Ricardo, A.; Illangkoon, H. I.; Kim, M. J.; Carrigan, M. A.; Frye, F.; Benner, S. A. *J. Am. Chem. Soc.* **2011**, *133*, 9457–9468.

[9] These glyceraldehyde derivatives were particularly challenging to purify, as flash column chromatography was ineffective.

[10] Ohira, S. *Synth. Commun.* **1989**, *19*, 561–564.

[11] The Ohira-Bestmann conditions were invaluable for this transformation as other methods (e.g. Corey-Fuchs or Seyferth-Gilbert conditions) facilitated aldehyde epimerization under the strongly basic conditions.

[12] Neises, B.; Steglich, W. *Angew. Chem. Int. Ed.* **1978**, *17*, 522–524.

[13] Pratsch, G.; Lackner, G. L.; Overman, L. E. *J. Org. Chem.* **2015**, *80*, 6025–6036.

[14] Moradei, O. M.; Paquette, L. A. *Org. Syn.* **2003**, *80*, 66.

[15] Structural assignment of **3.28** was verified by single crystal X-ray analysis: CCDC 1447146.

[16] See Chapter 4 for more details.

[17] See Chapter 2 for more details.

[18] a) Scheme 3.7A: Brady, T. P.; Kim, S. H.; Wen, K.; Theodorakis, E. A. *Angew. Chem. Int. Ed.* **2004**, *43*, 739–742. b) Scheme 3.7B: Brady, T. P.; Kim, S. H.; Wen, K.; Kim, C.; Theodorakis, E. A. *Chem. Eur. Joc.* **2005**, *11*, 7175–7190. c) Scheme 3.7C: Granger, K.; Snapper, M. L. *Eur. J. Org. Chem.* **2012**, 2308–2311.

[19] Surprisingly, literature examples typically used NEt_3 as the base in hydrazone iodination transformations. However, Barton previously demonstrated that TMG was superior to NEt_3 in this reaction. See: Barton, D. H. R.; Bashiardes, G.; Pourrey, J.-L. *Tetrahedron Lett.* **1983**, *24*, 1605–1608.

[20] Comins, D. L.; Dehghani, A. *Tetrahedron Lett.* **1992**, *33*, 6299–6302.

[21] He, W.; Huang, J.; Sun, X.; Frontier, A. J. *J. Am. Chem. Soc.* **2008**, *130*, 300–308.

[22] Dunn, T. B.; Ellis, J. M.; Kofink, C. C.; Manning, J. R.; Overman, L. E. *Org. Lett.* **2009**, *11*, 5658–5661.

[23] While this 1,2-alkylation is demanding between two sterically congested fragments, the high oxygen content of the acceptor or the β-ketolactone's α-proton may also be responsible for failure to couple.

[24] Naef, R.; Seebach, D. *Angew. Chem. Int. Ed.* **1981**, *20***,** 1030–1031.

[25] a) Evans, D. A.; Barrow, J. C.; Leighton, J. L.; Robichaud, A. J. *J. Am. Chem. Soc.* **1994**, *116*, 12111–12112. b) Evans, D. A.; Trotter, W.; Barrow, J. C. *Tetrahedron* **1997**, *53*, 8779–8794.

[26] Crich, D.; Hao, X. *J. Org. Chem.* **1999**, *64*, 4016–4024.

[27] Other reductants (borohydrides, aluminum hydrides, Red-Al®), temperatures, and solvents were screened in unsuccessful attempts to improve the reduction's efficiency. The main challenge was preventing partial reduction of diester **3.48** which gave variable amounts of aldehyde **3.55** which I could not cleanly separate from alcohol **3.54**.

[28] See experimental procedure for details.

[29] Storage of the reaction under vacuum or in –20 ºC freezer resulted in decomposition by the next day. Storage of aldehyde **3.55** in a frozen benzene matrix was never attempted.

[30] Though never proven, ^{1}H NMR of decomposed material showed similar peaks to starting material, suggesting polymerization or self-Aldol reactions as the aldehyde **3.55** may be prone to enolization.

[31] Attempts to couple via vinyl lithium intermediate **3.43** resulted in low yields (15–25%) with no diastereoselectivity in the resulting allylic alcohol (**3.60**).

[32] Brady, T. P.; Wallace, E. K.; Kim, S. H.; Guizzunti, G.; Malhotra, V.; Theodorakis, E. A. *Bioorg. Med. Chem. Let.* **2004**, *14*, 5035–5039.

[33] Vinyl triflate **3.33** is also an NHK coupling precursor, but preliminary screens found it to be less reactive in Ni-mediated oxidative insertion. Vinyl iodide **3.32** underwent full conversion at 23 ºC while vinyl triflate **3.33** required heating (40–50 ºC). As aldehyde **3.55** was prone to decomposition, I did not optimize the NHK coupling with vinyl triflate **3.33** to avoid heating.

[34] For reviews, see: (a) Fürstner, A. *Chem. Rev*. **1999**, *99*, 991–1046. (b) Wessjohann, L. A.; Scheid, G. *Synthesis* **1999**, 1–36.

[35] Representative examples: (a) Wan, Z.-K.; Choi, H.W.; Kang, F.A.; Nakajima, K.; Demeke, D.; Kishi, Y. *Org. Lett.* **2002**, *4*, 4431–4434. (b) Berkessel, A.; Menche, D.; Sklorz, C. A.; Schröder, M.; Paterson, I. *Angew. Chem. Int. Ed.* **2003**, *42*, 1032–1035. (c) Lee, J.-Y.; Miller, J. J.; Hamilton, S. S.; Sigman, M. S. *Org. Lett.* **2005**, *7*, 1837–1839.

[36] (a) Yu, M. J.; Zheng, W.; Seletsky, B. M. *Nat. Prod. Rep.* **2013**, *30*, 1158–1164. (b) Austad, B. C. *et al*. *Synlett* **2013**, *24*, 327–332. (c) Austad, B. C. *et al*. *Synlett* **2013**, *24*, 333–337.

[37] The stereochemistry of the alcohol was confirmed by X-ray crystallography when derivatized to (*N*-acyloxy)phthalimide **3.75 (**CCDC 1446028).

[38] Using more than 1.6 equiv of aldehyde **3.55** did not increase (or decrease) the yield of the reaction.

[39] This X-ray crystal structure was never submitted to the CCDC. Within the Overman group, the X-ray crystal file is LEO-284.

[40] I examined variable amounts of NEt_3 which is used in superstoichometric amounts. However, the amount of excess NEt_3 did not seem to alter the amount of the epimerization product obtained.

[41] Lautens, M.; Paquin, J.-F. *Org. Lett.* **2003**, *5*, 3391–3394.

[42] Myers, A. G.; Zheng, B. *Tetrahedron Lett.* **1996**, *37*, 4841–4844.

[43] Palladium-catalyzed transfer hydrogenation was not preferred because of potential alkene scrambling by a non-selective palladium π-allyl intermediate. For more details into these methods, see Section 2.4.1.

[44] This failed reaction was the first sign to the hindered steric environment surrounding the secondary alcohol of **3.64**.

[45] Though thiocarbonate **3.73** was not crystalline, the allylic stereochemical assignment is consistent with a suprafacial rearrangement to afford the *E* olefin. The allylic methine proton has similar shifts and splitting to that of allylic chloride **3.78** which was confirmed by X-ray crystallography.

[46] Müller, P.; Siegfried, B. *Helv. Chim. Acta* **1974**, *57*, 987–994.

[47] a) Ishiwata, A.; Ito, Y.; *Synlett* **2003**, *9*, 1339–1343. b) Nicolaou, K. C.; Estrada, A. A.; Zak, M.; Lee, S. H.; Safina, B. S. *Angew. Chem. Int. Ed.* **2005**, *44*, 1378–1382.

[48] Typically, (*N*-acyloxy)phthalimides are chromatographically stable crystalline solids. (*N*-Acyloxy)phthalimides **3.75** and **3.78** are two atypical examples which required chromatography with pH 7 silica (though small amounts of decomposition were always observed).

[49] Addition of KHMDS to a colorless solution of **3.75** at –78 ºC immediately changed the solution to red, indicating the presence of phthalimide anion.

[50] Addition of crown ethers with lithium or sodium bases did not facilitate acylation either.

[51] Clegg, W.; Conway, B.; Graham, D. V.; Hevia, E.; Kennedy, A. R.; Mulvey, R. E.; Russo, L.; Wright, D. S. *Chem. Eur. J.* **2009**, *15*, 7074–7082.

[52] Masamune, S.; Ellingboe, J. W.; Choy, W. J. *J. Am. Chem. Soc.* **1982**, *104*, 5526–5528.

[53] a) Caserio, F. F.; Dennis, G. E.; DeWolfe, R. H.; Young, W. G. *J. Am. Chem. Soc.* **1955**, *77*, 4182–4183. b) Young, W. G.; Caserio, F. F., Jr.; Brandon, D. D., Jr. *J. Am. Chem. Soc.* **1960**, *82*, 6163–6168.

[54] Wender, P. A.; Buschmann, N.; Cardin, N.; Jones, L. R.; Kan, C.; Kee, J.-M.; Kowalski, J. A.; Longcore, K. E. *Nature Chem.* **2011**, *3*, 615–619.

[55] Magnus, P.; Westwood, N.; Spyvee, M.; Frost, C.; Linnane, P.; Tavares, F.; Lynch, V. *Tetrahedron* **1999**, *55*, 6435–6452.

[56] Smith, A. B.; Basu, K.; Bosanac, T. *J. Am. Chem. Soc.* **2007**, *129*, 14872–14874.

[57] Examples of bromide reductions in photoredox catalysis: a) Narayanam, J. M. R.; Tucker, J. W.; Stephenson, C. R. J. *J. Am. Chem. Soc.* **2009**, *131*, 8756–8757. b) Pratsch, G.; Overman, L. E. *J. Org. Chem.* **2015**, *80*, 11388–11397.

[58] Attempts to purify/crystallize allylic chloride **3.78** without column chromatography were unsuccessful. Likewise, other chromatography mediums (Florisil®, alumina, etc.) also induced partial decomposition of **3.78**.

[59] Assignments of alkene and chloride stereochemistry were confirmed by X-ray crystallography: CCID 1446026.

[60] Heinrich, M. R.; Blank, O.; Ullrich, D.; Kirschstein, M. *J. Org. Chem.* **2007**, *72*, 9609–9616.

[61] van der Deen, H.; van Oeveren, A.; Kellogg, R. M.; Feringa, B. L. *Tetrahedron Lett.* **1999**, *40*, 1755−1758.

[62] I was never able to isolate **3.88** in pure form for characterization.

[63] Chu, L.; Ohta, C.; Zuo, Z.; MacMillan, D. W. C. *J. Am. Chem. Soc.* **2014**, *136*, 10886–10889.

[64] Thiophenolic acid **3.100** was used as the radical precursor using the MacMillan conditions[63] with Ir photocatalysis.

[65] Acetonide deprotection at this stage was essential as the primary alcohol was protected as a benzyl ether. Acetonide deprotection will induce oxocarbenium ion formation at C16, and an unprotected alcohol will cyclize to generate the fused tricyclic motif. Once this ring system is formed, access to the bridged framework in chromodorolides A and D will be impossible.

[66] Wuts, P. G. M.; Greene, T. W. *Greene's Protective Groups in Organic Synthesis*, 4th Edition; A. John Wiley & Sons, Inc., Hoboken, New Jersey, 2007.

[67] Lewis acid-mediated deprotection conditions only afforded recovered starting material, and hindered/internal acetonides typically require strong Brønsted acids at elevated temperatures.

[68] Jung, M. E.; Usui, Y.; Vu, C. T. *Tetrahedron Lett.* **1987**, *28*, 5977–5980.

[69] Activated palladium sources as well as other transition metals (rhodium, platinum, iridium) were unable to cleanly accomplish both olefin reduction and benzyl hydrogenolysis. Traditional palladium-mediated hydrogenation conditions (1–10 atm H_2, variety of solvents) resulted in partial alkene reduction but no observed debenzylation.

[70] Several transfer hydrogenation reagents (1,4-cyclohexadiene, ammonium formate) were screened, but formic acid was the only transfer hydrogenation reagents which facilitated benzyl deprotection at room temperature.

[71] One-step oxidations were not examined because of the limited amount of **3.107** available.

[72] Acid **3.108** was unable to be purified by column chromatography, which required its to be carried forward crude into the acetonide deprotection.

[73] Use of MeOH/4 M HCl/THF facilitates acetonide deprotection to the methoxy acetal variant of **3.109**, which can be cleaved to **3.109** with 4 M HCl/THF.

[74] ^{1}H and NOE NMR analysis of this mixture suggested that the major anomer of **3.109** placed the lactol on the concave face of the tricyclic framework, opposite the C15 stereochemistry in chromodorolides B, C, and E.

[75] Tao, D. J.; Slutskyy, Y.; Overman, L. E. *J. Am. Chem. Soc.* **2016**, *138*, 2186–2189.

[76] MorGris, S. A.; Dilip de Silva, E.; Andersen, R. J. *Can. J. Chem.* **1991**, *69*, 768–771.

[77] CCDC 1446027.

[78] Eey, S. T. C; Lear, M. J. *Org. Lett.* **2010**, *12*, 5510–5513.

[79] Larraufie, M.-H.; Pellet, R.; Fensterbank, L.; Goddard, G.-P.; Lacote, E.; Malacria, M.; Ollivier, C. *Angew. Chem., Int. Ed.* **2001**, *50*, 4463–4466.

[80] D. S. Coffey, L. E. Overman, F. Stappenbeck, *J. Am. Chem. Soc.* **2000**, *122*, 4904–4914.

[81] Morita, Y.; Tokuyama, H.; Fukuyama, T. *Org. Lett.* **2005**, *7*, 4337–4340.

[82] Feringa, B. L.; De Lange, B. *Tetrahedron* **1988**, *44*, 7213–7222.

Chapter 4: Origins of Radical Diastereoselectivity in ACF Cascade

4.1 Investigations of Selectivity in ACF Cascade's 5-*Exo* Cyclization

Upon completion of the total synthesis of (–)-chromodorolide B, a thorough investigation of the diastereoselectivities observed in the ACF cascade was conducted. This study focused on the origins of stereoselection in the initial addition of the trisubstituted acetonide radical to the butenolide and the subsequent 5-*exo* cyclization onto the appended alkene (Section 3.2.5). Concerning the latter, I never observed conditions in which 5-*exo* cyclization onto the pendant alkene favored the desired C8 stereoisomer (Section 3.2.5.4). I aimed to probe the diastereoselectivity of the 5-*exo* cyclization by subjecting α-substituted butenolides to the ACF cascade. I hypothesized that substitution at this position would increase the destabilizing steric interactions in undesired conformation **4.1**, favoring cyclization from conformation **4.2** to give the desired C8 stereochemistry (Figure 4.1).

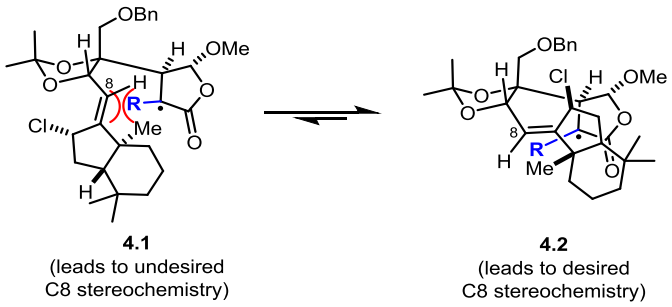

Figure 4.1. Potential Effects of α-Substituted Butenolides in ACF Cascade.

To access enantioenriched α-substituted butenolides, I chose to start from (*R*)-methoxybutenolide **4.3** (Equation 4.1) as it was accessible in 84% *ee* on gram scale. This butenolide's sole stereocenter is sensitive to a variety of reaction conditions, leaving few synthetic options to accomplish α-functionalization without racemization. Previously reported bromination conditions[1] successfully provided enantioenriched bromobutenolide

4.2,[2] which was then subjected to the optimized ACF reaction conditions (Table 3.4, entry 4) with (*N*-acyloxy)phthalimide **4.5**. Analysis by ^{1}H NMR of the crude reaction revealed a more complex product mixture than previous ACF reactions with butenolide **4.3**, but three coupled products (**4.6**, **4.7**, and **4.8**) were identified (Equation 4.2). For ACF products **4.6** and **4.7**, it was unclear whether the α-acyl bromides were retained under the reaction conditions or reduced *in situ* to the deuterated products. Desired ACF product **4.7** was favored over its C8 epimer in ~2:1 ratio, indicating α-substitution on the butenolide did bias the diastereoselectivity of the 5-*exo* cyclization. The major product, **4.8**, resulted from premature quenching of α-acyl radical, which revealed that the bromide stabilized the intermediate α-acyl radical and likely slowed 5-*exo* cyclization more than its reduction.

Equation 4.1

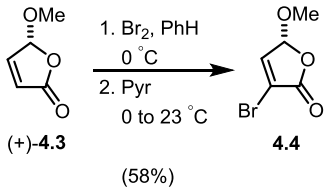

Equation 4.2

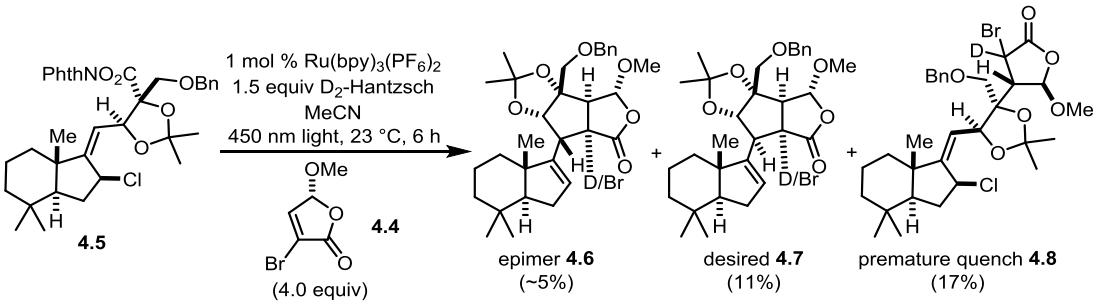

I then pursued the analogous α-chlorobutenolide which would have similar steric implications to a bromide but might not inhibit 5-*exo* cyclization relative to reductive quenching. (±)-Chlorobutenolide **4.9** is both commercially available[3] and accessible by a

known sequence,[4] but I required enantioenriched chlorobutenolide **4.9** as the trisubstituted acetonide radical in the ACF was enantiopure.[5] I first attempted to synthesize chlorobutenolide **4.9** by direct chlorination of enantioenriched butenolide **4.3** using tetraethyl ammonium trichloride (Mioskoski's reagent)[6] or chlorine gas (Equation 4.3), but no chlorination was ever observed.[7]

Equation 4.3

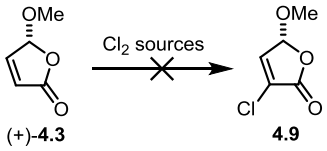

I then examined Baylis-Hillman type transformations for chloride installation, which were previously reported with butenolides using organoselenides (Scheme 4.1).[8] These literature examples only employed aldehyde electrophiles, but I hypothesized the enolate intermediate would react with an electrophilic chlorine source. Exposure of phenylselenyl magnesium bromide to butenolide **4.3**, followed by addition of a variety of electrophilic chlorine reagents (*N*-chlorosuccinimide, Mioskowski's reagent, 2-chloro-2-fluoro-2-phenylacetonitrile[9]), resulted in decomposition or recovered starting material. I also attempted this transformation in a stepwise fashion by isolating the 1,4-addition product, selenolactone **4.17** (Scheme 4.2B). I then exposed **4.17** to strong bases (LHMDS, KHMDS) with electrophilic chlorine sources. These reactions also failed to provide either chlorinated products **4.9** or **4.16**. Having exhausted ideas to access enantioenriched chlorobutenolide **4.9**, I abandoned these efforts and turned my attention to studying the diastereoselectivity of the reaction of the trisubstituted acetonide radical with butenolide **4.3** in the ACF cascade.

Scheme 4.1. Previous Seleno Baylis-Hillman Examples with Butenolides.

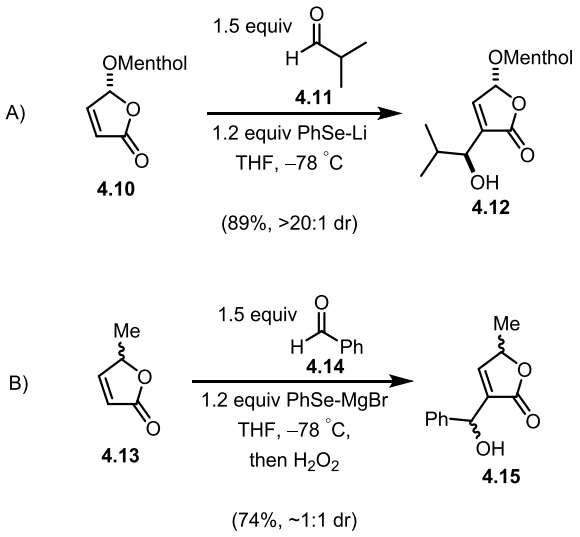

Scheme 4.2. Failed Seleno Baylis-Hillman Route to Chlorobutenolide 4.9.

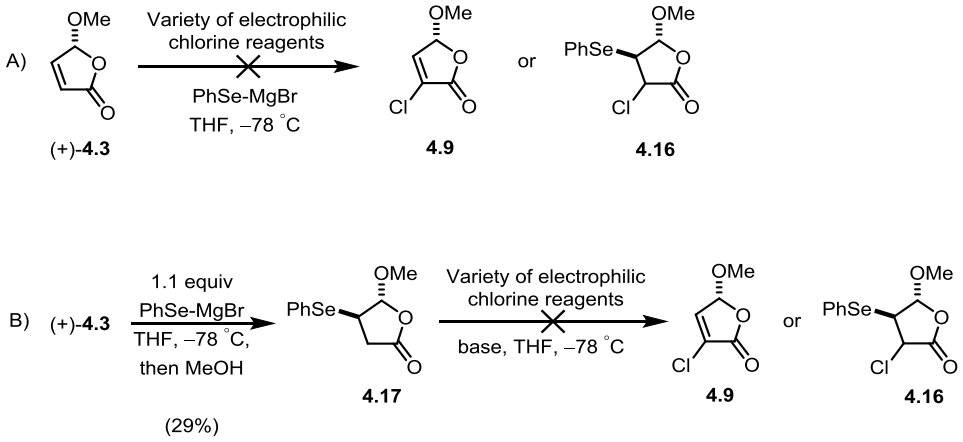

4.2 Diastereoselective Additions of Trisubstituted Acetonide Radicals

4.2.1 Initial Considerations and Previous Examples in the Literature

The contrasteric diastereoselectivity of addition of trisubstituted acetonide radicals was first observed with alkyne radical **4.18** (Section 3.1.3) which favored addition to butenolide **4.10** from the face *syn* to the alkyne (~1:4 dr, Figure 4.2). Trisubstituted

acetonide radical **4.19** from the ACF cascade (Section 3.2.5.2) preferentially added to butenolide **4.3** *syn* to the hydrindane fragment (~1:7 *anit*:*syn*[10]).

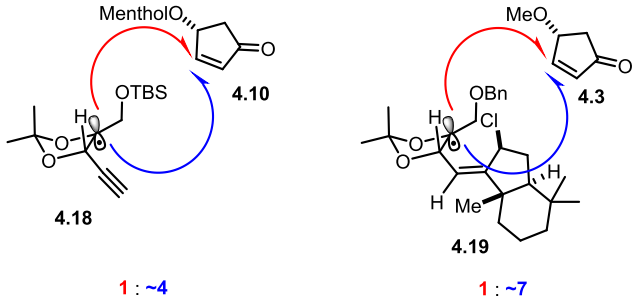

Figure 4.2. Observed Diastereoselectivity of Trisubstituted Acetonide Radicals to Butenolides.

To rationalize this observed diastereoselectivity, I searched the literature for reactions with related acetonide radicals. Only three references in the literature of similar acetonide radicals coupling to electron deficient alkenes were found.[11] Shown in Scheme 4.3A, Barton unambiguously demonstrated that disubstituted acetonide radical **4.20** underwent conjugate addition to methacrylate **4.21** with high *anti* facial selectivity (25:1 dr),[12] coinciding with steric predictions. Renaud examined trisubstituted acetonide radicals and found that the diastereoselectivity was dependent on the adjacent alkyl substituent.[13] In the case of benzyl radical precursor **4.23** (Scheme 4.3B), radical generation and addition to phenyl vinyl sulfone (**4.25**) occurred with low *anti* selectivity (2.4:1 dr favoring **4.26**). However, when the benzyl group was exchanged for a *tert*-butyl group (Scheme 4.3C), radical precursor **4.28** coupled to **4.25** favoring the contrasteric *syn* addition product **4.31** in a 1:6.3 ratio. These results indicated that factors beyond the trisubstituted acetonide radical's facial accessibility influenced the diastereoselectivity of additions. Therefore, I investigated this diastereoselectivity on an experimental level to identify the origins of *anti*/*syn* addition for acetonide radicals.

Scheme 4.3. Previous Examples of Acetonide Radicals Coupling with Acceptors.

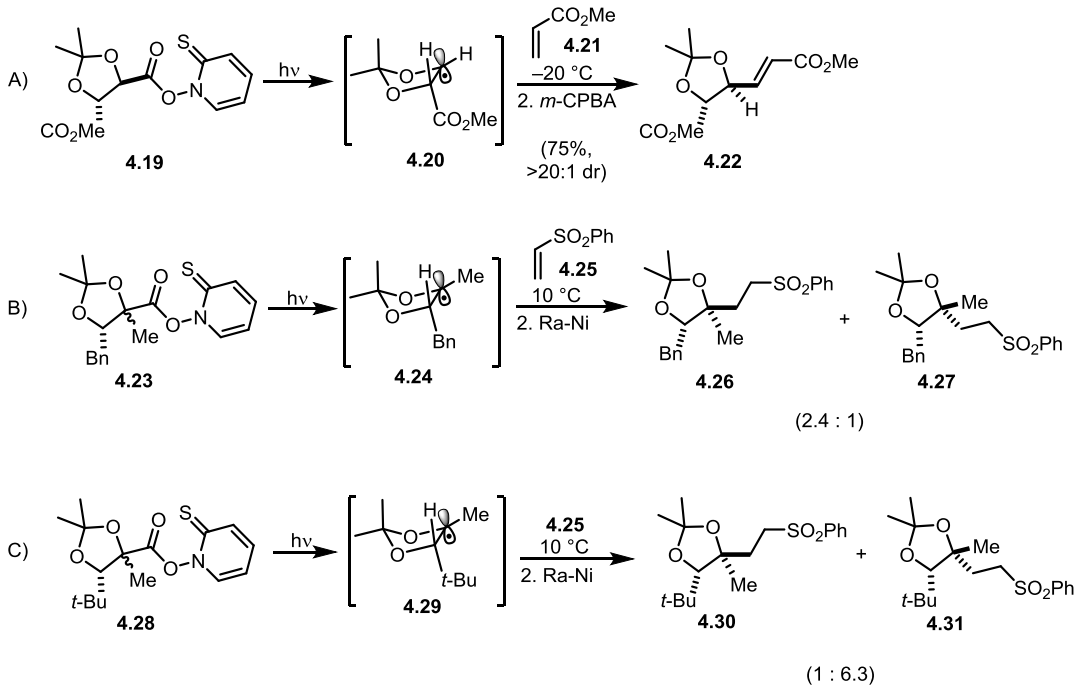

4.2.2 Experimental Results with Simplified System

I initially proposed a hypothesis similar to Renaud's,[13,14] in that increasing the steric bulk of the acetonide radical's substituents (R^1 and R^2 in Figure 4.3) would increase selectivity for *syn* addition because of destabilizing eclipsing interactions between R^1 and R^2 in the *anti* addition transition state (**4.32**). I conducted studies using simplified (*N*-acyloxy)phthalimides **4.34a**–**4.34c** with increasing steric bulk on oxygen. However, upon coupling to butenolide **4.3**, all radical substrates underwent addition with low stereoselectivity *syn* to the β-substituent with minimal influence from the oxygen substituent.[15]

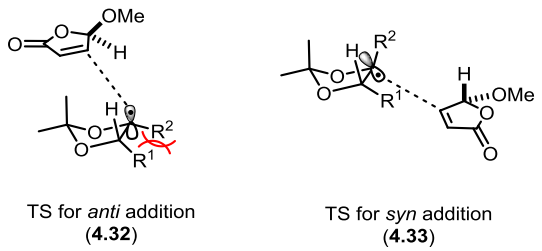

Figure 4.3. Destabilizing Interactions Influencing Radical Diastereoselectivity.

Table 4.1. Probing *O*-Substitution on Radical Diastereoselectivity.

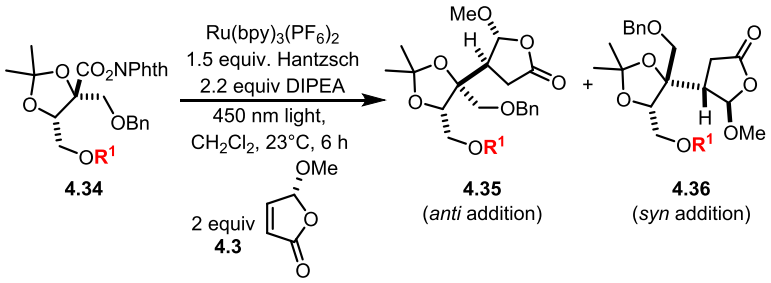

Entry	Radical Precursor	R^1	*anti* : *syn* (by ^{1}H NMR)	Combined Yield
1	**4.34a**	Me	1:2.2	46%
2	**4.34b**	TBS	1:2.5	63%
3	**4.34c**	TIPS	1:2.9	62%

Stereochemical assignments for *syn* addition products were determined by diagnostic NOE correlations between the acetonide methine and the methylene hydrogens of the acetonide alkoxymethyl substituent (Figure 4.4). Likewise, *anti* addition products were assigned by NOE correlations between the acetonide methine and the methylene hydrogens of the lactone.[16] These stereochemical assignments were further validated by chemical derivation of *syn* addition product **4.36b** to **4.39** (Scheme 4.4B) and a single crystal X-ray structure of *syn* addition product **4.42f**.[17]

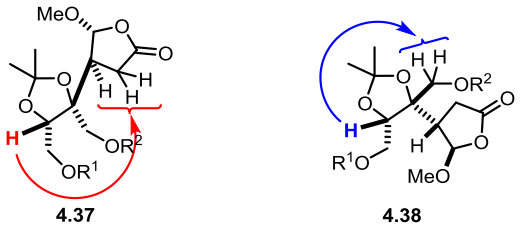

Figure 4.4. Diagnostic NOEs for *Syn*- and *Anti* Addition Products.

Scheme 4.4. Chemical Derivation of Addition Products.

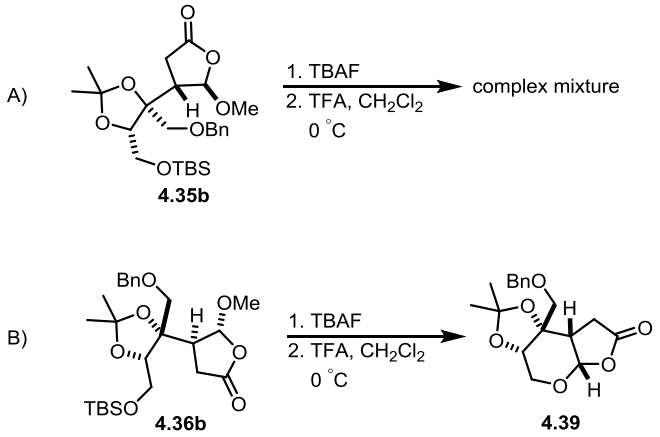

At this point in exploring these photoredox couplings, I switched to the MacMillan methodology using carboxylic acids[18] as radical precursors. The carboxylic acids required one less synthetic step than corresponding (*N*-acyloxy)phthalimides; and the coupling reactions were typically easier to analyze and purify. Shown in Table 4.2, I first examined the coupling of the disubstituted acetonide radical generated from acid **4.40a** with butenolide **4.3**, which occurred in 3.5:1 dr favoring *anti* addition (entry 1). This lower diastereoselectivity is not a reflection of a chirality mismatch between the (*R*)-butenolide **4.3** and the chiral radical of acid **4.40a**. The coupling of the (*S*)-butenolide **4.3** with the radical of **4.40a** gave a similar 4.0:1 dr favoring *anti* addition (Equation 4.4).[19]

Table 4.2. Photoredox-Catalyzed Radical Couplings of Simplified Acids.

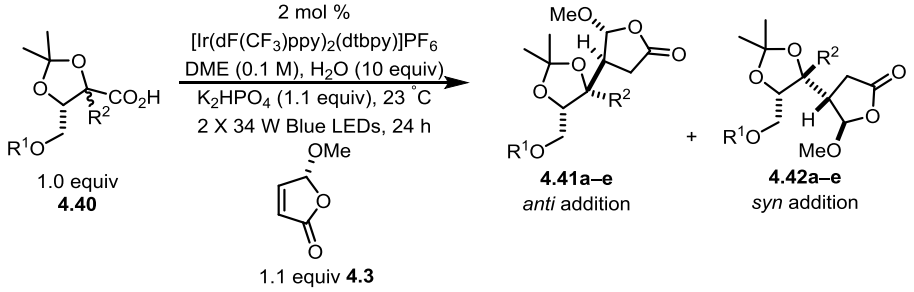

Entry	Radical Precursor	*anti* : *syn* (by ^{1}H NMR)	Yield	Entry	Radical Precursor	*anti* : *syn* (by ^{1}H NMR)	Yield
1	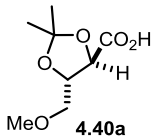 **4.40a**	3.5:1	37%	4	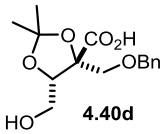 **4.40d**	1:2.6	66%
2	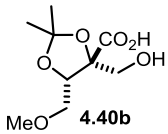 **4.40b**	1:3.3	54%	5	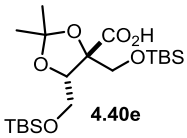 **4.40e**	1:2.2	67%
3	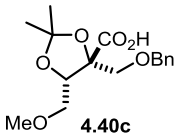 **4.40c**	1:2.8	64%	6	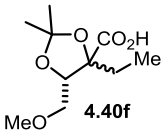 **4.40f**	1:9.3	53%

Equation 4.4

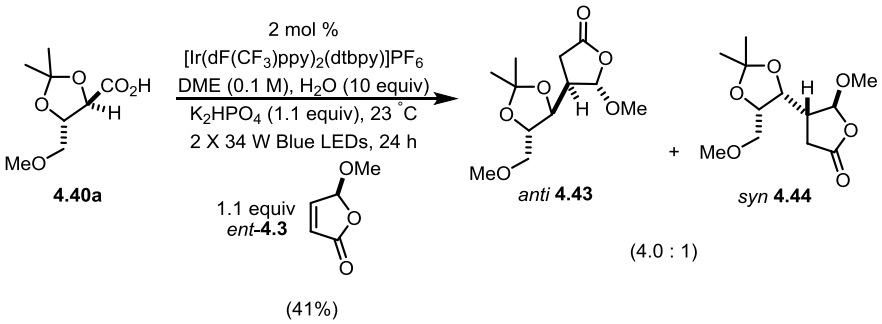

I then turned my attention to precursors which would yield trisubstituted radical intermediates. In entries 2–5 of Table 4.2, the radical center bore a hydroxymethyl or protected-hydroxymethyl substituent, and addition occurred with low stereoselectivity *syn* to the β-substituent. The only outlier was ethyl variant **4.40e** (entry 6), which gave high

selectivity for the *syn* addition product (1:9.3 dr). This increase in *syn* selectivity presumably arose from increased steric interactions between the larger ethyl group and the methyloxymethylene substituent in the transition state, supporting our hypothesis from Figure 4.3. Concerning the minimal changes in diastereoselectivity with varying *O*-functionalization (Table 4.2, entries 2–5), the oxygen substituents' ability to freely rotate away from each other likely rendered their steric bulk insignificant. With a working hypothesis to explain the observed diastereoselectivity, I then assessed radical precursors relevant to the synthetic efforts towards the chromodorolides in analogous couplings.

4.2.3 Coupling with Hydrindane-Based Radical Precursors

I synthesized radical precursors embedding the requisite hydrindane fragment embedded in the chromodorolides. Reduction of the double bond on allylic alcohol **4.45** (Section 3.2.3) was performed to prevent potential side reactions with the alkene in the radical coupling. Selective alkene reduction proved challenging,[20] but hydrogen atom transfer conditions[21] afforded saturated product **4.46** in 65% yield. Hydrolysis of methyl ester **4.46** gave carboxylic acid radical precursor **4.47**, which was subjected to photoredox coupling conditions with butenolide **4.3**.

I anticipated higher *syn* diastereoselectivity than that observed with analogous simplified radical precursor **4.40d** (1:2.6 *anti*:*syn*, Table 4.2), but acid **4.47** underwent coupling to butenolide **4.3** favoring *anti* addition in a 1.2:1 ratio. While the energetic difference between these two diastereoselectivities is small,[22] the result stood in contrast to our hypothesis (Figure 4.3). Addition of the bulky hydrindane fragment would increase destabilizing interactions between the vicinal substituents in the *anti* addition transition

state, which should translate to higher *syn* selectivity under the eclipsing interaction-based hypothesis.

Scheme 4.5. Synthesis and Coupling of Acid Radical Precursor 4.47.

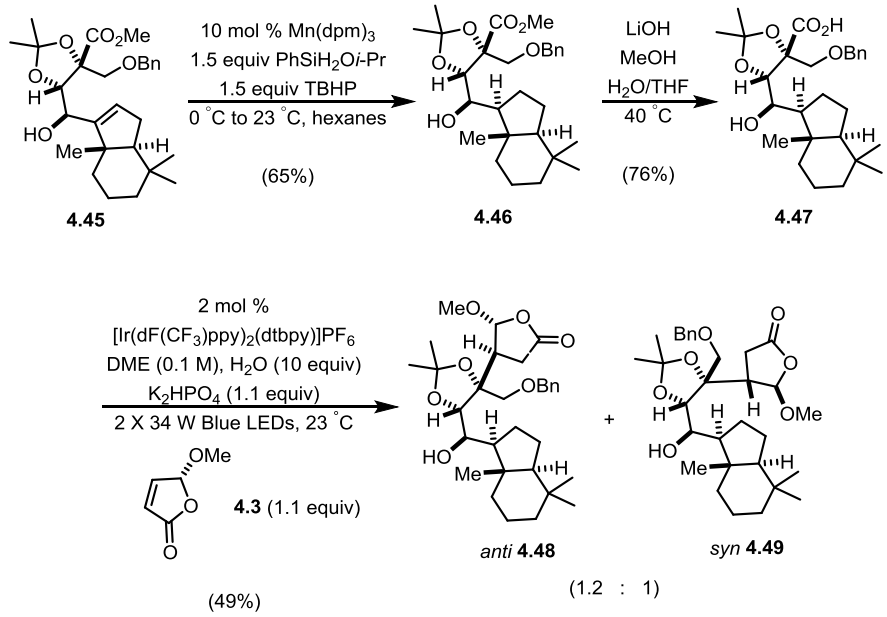

Perplexed by this experimental result, I synthesized a second hydrindane-containing radical precursor with two unprotected hydroxyl groups. Exposure of allylic alcohol **4.45** to Pd/C under 1 atm H_2 cleanly afforded diol ester **4.50**. Saponification of ester **4.50** with LiOH afforded diol carboxylic acid radical precursor **4.51**. Exposure of this acid to photoredox conditions with butenolide **4.3** yielded coupling product **4.52** and **4.53** with high *anti* preference (9.8:1 dr) in 45% yield.[23] The high *anti* diastereoselectivity was unexpected, as Table 4.2 indicated that *O*-functionalization had minimal effect on the radical addition's diastereoselectivity.

Scheme 4.6. Synthesis and Coupling of Acid Radical Precursor 4.51.

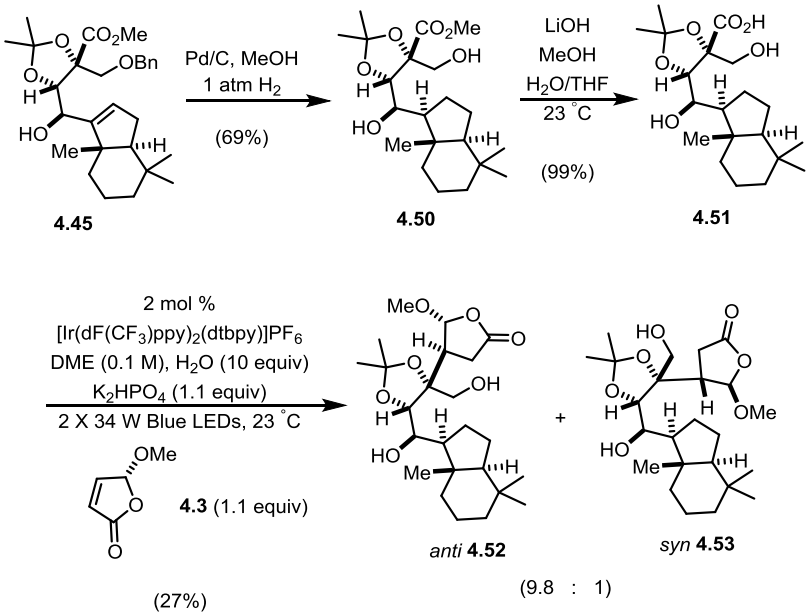

At this point, I initiated a computational collaboration with Dr. Mikko Muuronen and Prof. Filipp Furche to understand the intricate factors controlling radical diastereoselectivity. We systematically examined the roles of protected and unprotected alcohols on the radical substrates experimentally and computationally.

Experimentally, I synthesized several additional radical precursors from allylic alcohol **4.45**. First, *tert*-butyldimethylsilyl protection of **4.45** followed by debenzylation and hydrogenation gave ester **4.55**.[24] To prevent silyl migration, ester hydrolysis under nonbasic conditions with Me_3SnOH[25] yielded radical precursor **4.56** with a free primary alcohol. To access the free secondary alcohol radical precursor, diol ester **4.50** was exposed to TBS-Cl for selective silylation of the primary alcohol. Nonbasic saponification afforded the desired free secondary alcohol radical precursor **4.58**. The third radical precursor, bis(*tert*-butyldimethylsilyl) acid **4.60**, was accessed from exposure of diol ester **4.50** to TBS-OTf followed by nonbasic saponification. With these three radical precursors in hand, I examined their diastereoselectivities in radical coupling to butenolide **4.3**.

Scheme 4.7. Synthesis of Acid Radical Precursors 4.56, 4.58, 4.60.

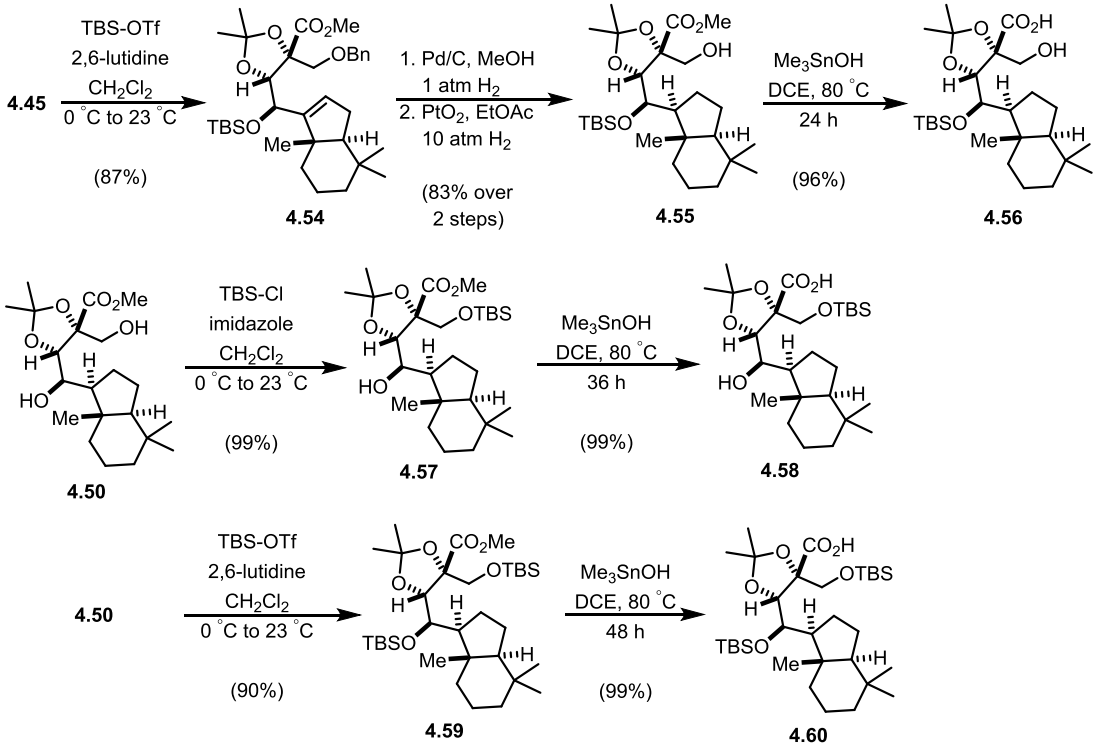

Shown in Table 4.3, coupling of the hydrindane-containing acids under photoredox conditions revealed a trend in the diastereoselectivity. For reference, benzyl ether acid **4.47** coupled to butenolide **4.3** with 1.2:1 dr favoring *anti* addition (entry 1), while diol acid **4.51** coupled with 9.8:1 dr favoring the *anti* product (entry 2). Switching from a primary benzyl ether to a primary *tert*-butyldimethylsilyl ether (**4.58**, entry 3) had virtually no effect on the diastereoselectivity (1.3:1 dr favoring *anti* addition). Silyl protection of both alcohols (**4.60**, entry 4) inverted diastereoselectivity to give 1:8.2 ratio favoring the *syn* addition product. Acid **4.56** with a free primary alcohol (entry 5) coupled also with high *syn* addition preference in 1:7.0 ratio, further confirming the secondary alcohol's role in diastereoselectivity.[26] Having experimentally observed the reversal in diastereoselectivity between acids **4.51** and **4.60** (entries 2 and 4), I then turned to computational modeling of

the *syn* and *anti* transition states of these radicals coupling to butenolide **4.3** to rationalize the origins of this diastereoselectivity.

Table 4.3. Photoredox-Catalyzed Radical Couplings of Hydrindane-Substituted Acids.

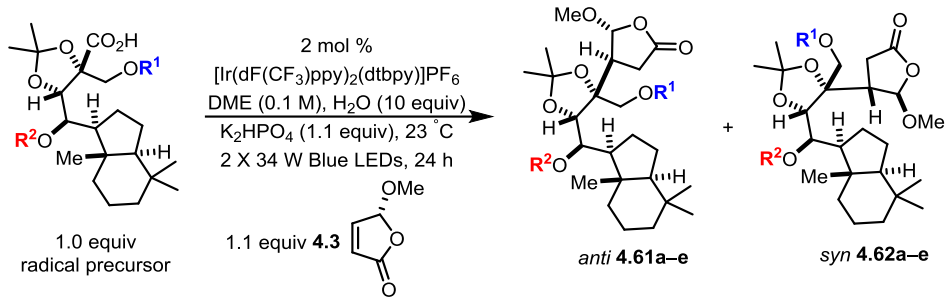

Entry	Radical Precursor	R^1	R^2	*anti* : *syn* (by ^{1}H NMR)	Isolated Yield
1 (a)	**4.47**	Bn	H	1.2:1	49%
2 (b)	**4.51**	H	H	9.8:1	27%
3 (c)	**4.58**	TBS	H	1.3:1	71%
4 (d)	**4.60**	TBS	TBS	1:8.2	37%
5 (e)	**4.56**	H	TBS	1:7.0	22%

4.2.4 Computational Methods and Parameters Guiding Selectivity

After combining the Furche group's computational work with my experimental results,[27] I can provide three parameters which govern the diastereoselectivity for addition of trisubstituted acetonide radicals to electron-deficient alkenes.

4.2.4.1 Destabilizing Steric Interactions

The first parameter that affects the diastereoselectivity of trisubstituted acetonide radical additions is destabilizing eclipsing interactions between the acetonide substituents. My and Renaud's initial hypothesis concerning destabilizing eclipsing interactions

between the substituents (Figure 4.3) was correct in that increasing the size of the alkyl substituents will increase selectivity for *syn* addition, presuming all other parameters (*vide infra*) are not affected. This principle is exemplified in Renaud's work[13] (Figure 4.5A) and by comparison of radicals **4.63** and **4.64** (Figure 4.5B). This diastereoselectivity is counterintuitive as bulky substituents typically direct reactivity to occur from the opposite, sterically-accessible face. However, for trisubstituted acetonide radicals, the eclipsing interactions between these substituents along with an early radical transition state (the forming bond is calculated to be 2.40 Å) overcome the sterically-disfavored approach of the electrophile. To visual the destabilizing effects of the vicinal substituents, a three dimensional image of the computationally optimized transition state structure[28] for *syn* addition of bis(trimethylsilyl) radical **4.65** shows the acetonide substituents oriented away from each other during addition to butenolide **4.3** (Figure 4.6). However, destabilizing eclipsing interactions between acetonide substituents alone cannot rationalize the observed diastereoselectivities from other radical precursors in Table 4.3.

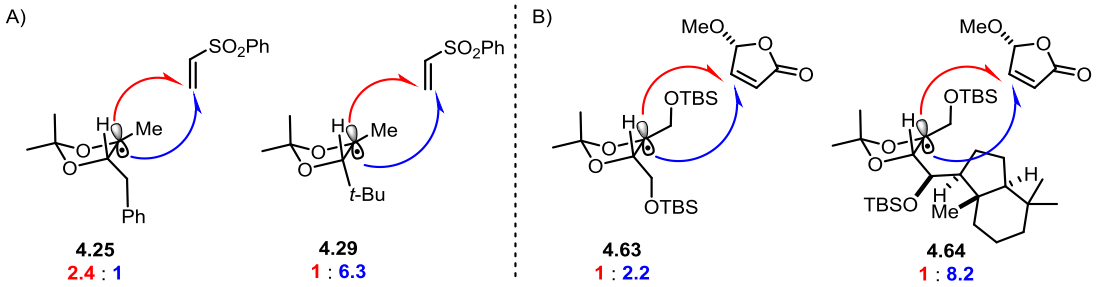

Figure 4.5. Destabilizing Interactions Affecting Radical Diastereoselectivity.

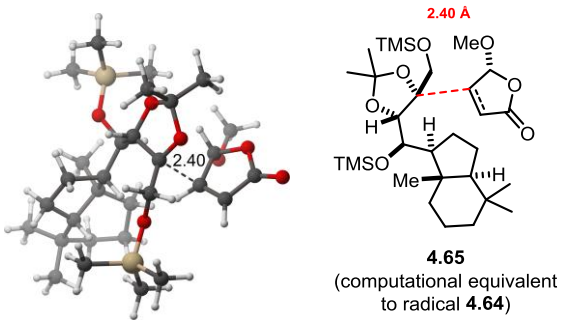

Figure 4.6. Computational Transition State for *Syn* Addition of Bis-trimethylsilyl Radical 4.65 to Butenolide 4.3.

4.2.4.2 Stabilizing Noncovalent Interactions

The second parameter that guides diastereoselectivity is stabilizing noncovalent interactions between the vicinal substituents on the acetonide radical. In the case of unprotected alcohols, diol radical **4.66** displayed high *anti* selectivity (Figure 4.7); and stepwise protection of the alcohols increased selectivity for *syn* addition (Table 4.3). Shown in Figure 4.8, optimized transition state structures of radicals **4.66**, **4.69**, and **4.70** undergoing *anti* addition to butenolide **4.3** revealed a hydrogen bond between the two oxygens on the side chains.[29] The length of the computed hydrogen bond correlated to the *syn*:*anti* selectivity, which I rationalized as stronger/shorter hydrogen bonds increasing stability for the transition state leading to *anti* addition. Impeding this hydrogen bonding by alcohol protection minimized these stabilizing interactions in the *anti* transition state and thus decreases selectivity for *anti* addition products.

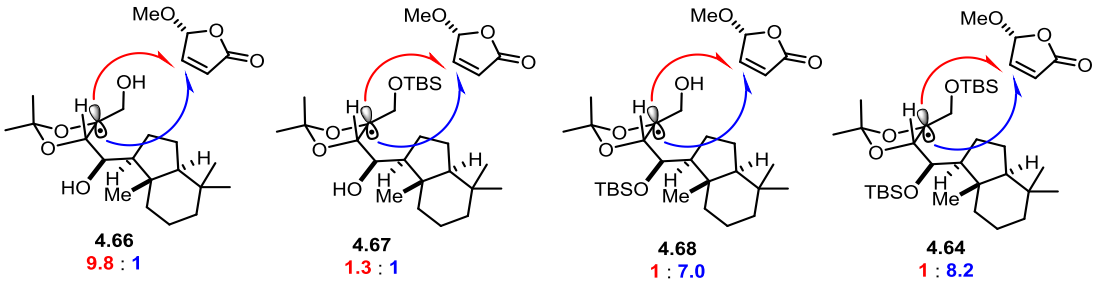

Figure 4.7 Noncovalent Stabilizing Interactions Affecting Radical Diastereoselectivity.

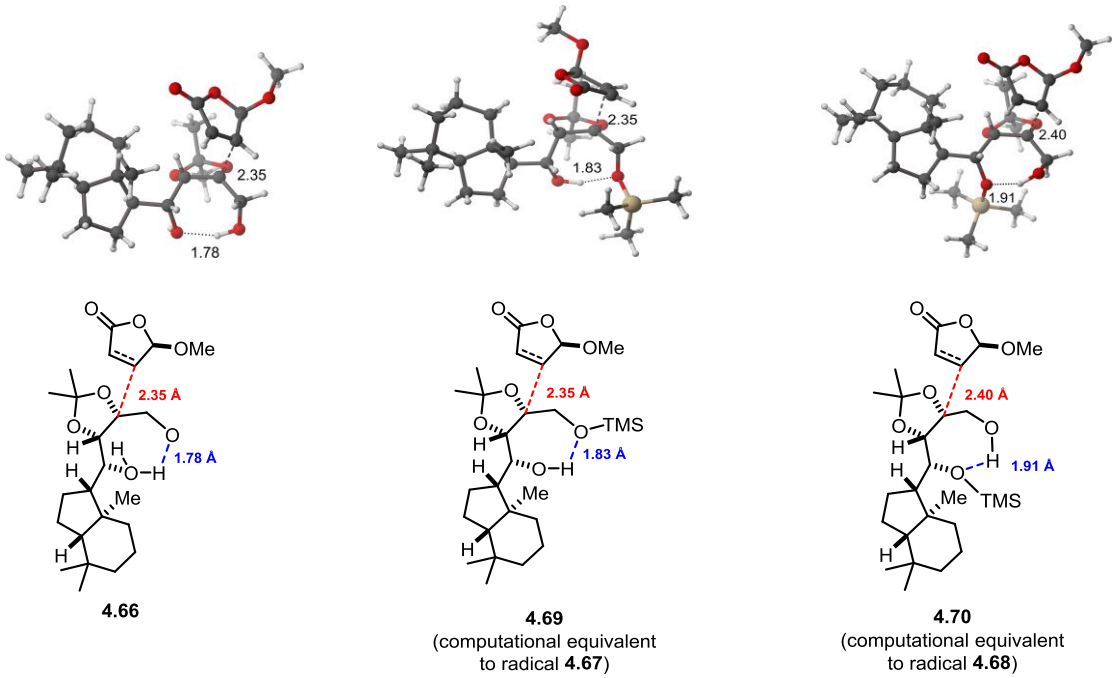

Figure 4.8. Computational Transition States for *Anti* Addition with Hydrogen Bonding.

4.2.4.3 Radical/Acceptor Interactions

The last parameter guiding diastereoselectivity is interaction between the radical intermediate and the acceptor. Subtle interactions between the nucleophilic radical and the acceptor can alter diastereoselectivity, but these interactions may not be readily apparent. For example, coupling of bis(*tert*-butyldimethylsilyl) radical **4.64** to methacrylate **4.21**

resulted in lower selectivity for the *syn* addition (1:2.2 dr, Figure 4.9) than to butenolide **4.3** (1:8.2).[30] Deprotection of the secondary silyl ether on the trisubstituted acetonide radical (**4.67**) predictably led to increased selectivity for *anti* addition to methacrylate **4.21** (5.8:1 dr), and deprotection of both silyl groups (**4.66**) shifted addition to **4.21** further favoring *anti* addition (>10:1 dr). In comparing acceptors **4.21** (Figure 4.9) and butenolide **4.3** (Figure 4.7), the observed diastereoselectivities were quantitatively different with identical trisubstituted radicals, but the trends of stereoselection remained consistent. It is not obvious whether this differing stereoselection arose from steric or electronic differences between acceptors, which makes predicting the radical/accepter interactions challenging.

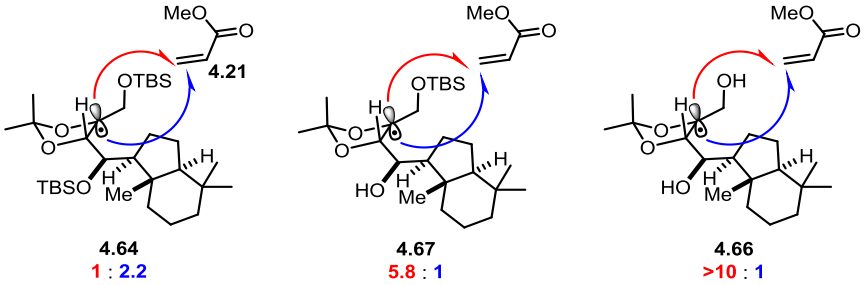

Figure 4.9. Radical/Acceptor Interactions Affecting Radical Diastereoselectivity.

4.2.4.4 Reliability of Computational Predictions

Structural modifications to radical precursors inevitably alter more than one parameter governing the radical addition's diastereoselectivity. The complexity in changing multiple parameters between radical precursors highlights the utility of advanced computational methods to account for the combination of these subtle interactions in radical couplings. Shown in Figure 4.10, correlations between computationally predicted diastereoselectivity and experimentally observed diastereoselectivity for the trisubstituted

radical substrates mentioned in this chapter are consistent,[31] and the computational analysis developed by the Furche group provides accuracy within 1 kcal/mol (±0.5 kcal/mol). While these results are an exciting showcase for their methods, many organic transformations determining diastereoselectivity and enantioselectivity require computational accuracy below 1 kcal/mol for quantitative predictions on stereochemical outcomes. As these and other computational methods continue to improve in accuracy, experimental organic chemists will find a plethora of applications to exploit computational prediction.

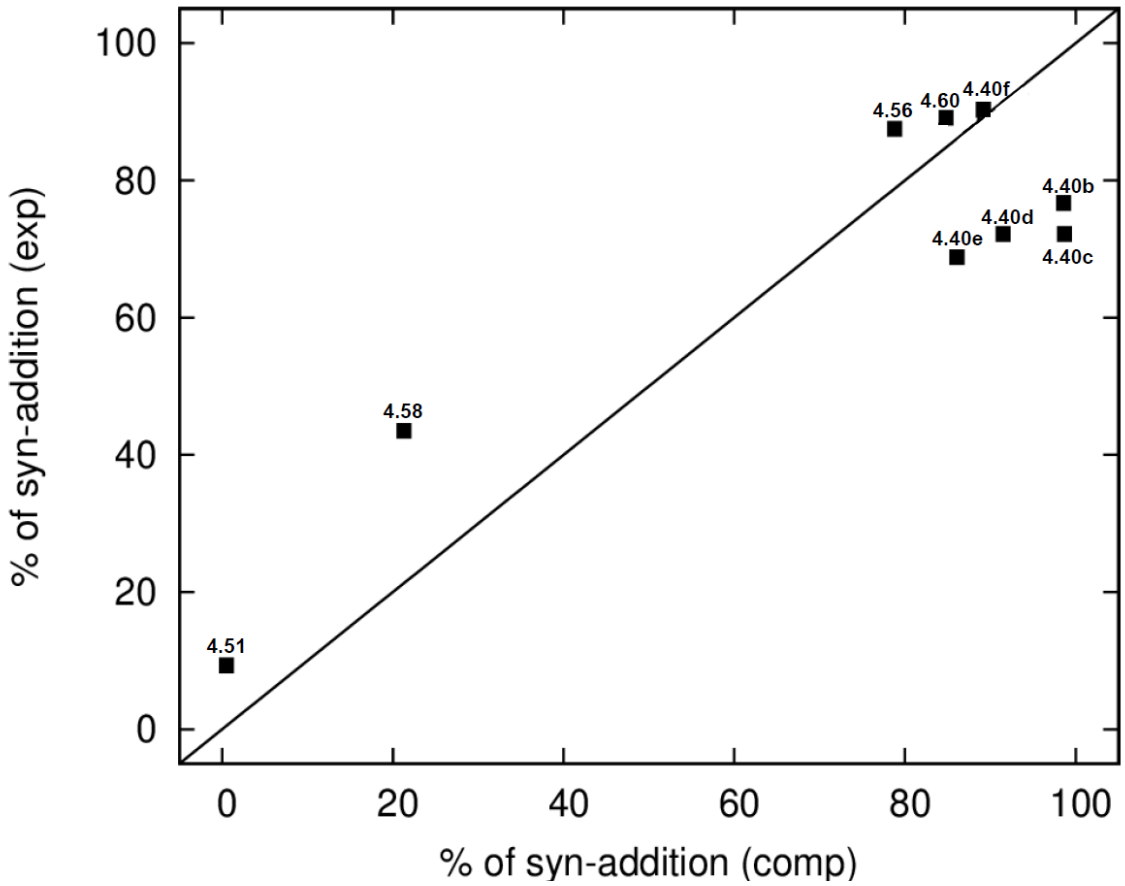

Figure 4.10. Computational and Experimental Correlations for Trisubstituted Acetonide Radical Additions to Butenolide 4.3.

4.3 Experimental Section

4.3.1 General Experimental Details

Unless stated otherwise, reactions were conducted in oven-dried glassware under an atmosphere of nitrogen or argon. Tetrahydrofuran (THF), diethyl ether, toluene, benzene, dichloromethane, methanol (MeOH), pyridine, DIPEA, and triethylamine were dried by passage through activated alumina. TBS-OTf was distilled prior to use and stored in a Schlenk tube. 2,6-lutidine was distilled prior to use and stored in a Schlenk tube. Butenolide **4** was prepared according to literature procedures.[32] All other commercial reagents were used as received unless otherwise noted. Reaction temperatures were controlled using a temperature modulator, and unless stated otherwise, reactions were performed at 23 ºC (rt, approximately 23 °C). Thin-layer chromatography (TLC) was conducted with silica gel 60 F254 pre-coated plates, (0.25 mm) and visualized by exposure to UV light (254 nm) or by *p*-anisaldehyde, ceric ammonium molybdate, and potassium permanganate staining. Silica gel 60 (particle size 0.040–0.063 mm) was used for flash column chromatography. pH 7 Silica gel was prepared according to previous literature procedure.[33] ^{1}H NMR spectra were recorded at 500 or 600 MHz and are reported relative to deuterated solvent signals. Data for ^{1}H NMR spectra are reported as follows: chemical shift (δ ppm), multiplicity, coupling constant (Hz), and integration. ^{13}C NMR spectra were recorded at 125 MHz. Data for ^{13}C NMR spectra are reported in terms of chemical shift. IR spectra were recorded on a FT-IR spectrometer and are reported in terms of frequency of absorption (cm^{-1}). High-resolution mass spectra were obtained with a LCT spectrometer. Optical rotations were measured with a Jasco P-1010 polarimeter. Kessil KSH150B LED Grow Light 150, Blue LEDs were purchased from http://www.amazon.com. The radical coupling reactions using these blue

LEDs were maintained at approximately 23 ºC by passing a constant stream of air over the reaction vessels for the 18 h period. See JOC Standard Abbreviations and Acronyms for abbreviations (available at http://pubs.acs.org/userimages/ContentEditor/1218717864819/joceah_abbreviations.pdf).

4.3.2 Experimental Procedures

(–)-Methyl (4*R*,5*S*)-5-(hydroxymethyl)-2,2-dimethyl-1,3-dioxolane-4-carboxylate (S4.1): A solution of methyl (4*R*,5*S*)-5-(hydroxymethyl)-2,2-dimethyl-1,3-dioxolane-4-carboxylate[34] (1.06 g, 5.57 mmol) in DMF (40 mL) was cooled to 0 ºC, and methyl iodide (1.7 mL, 28 mmol) was added. NaH (60% dispersion in mineral oil, 0.234 g, 5.85 mmol) was then added at 0 ºC, and the reaction vessel was allowed to slowly warm to 23 ºC over 4 h. Sat. aq. NH_4Cl soln (50 mL) and EtOAc (50 mL) were then added, and the resulting layers were separated. The aqueous phase was extracted with EtOAc (3 x 50 mL), and the combined organic layers were washed with brine (1 x 100 mL). The organic phase was dried over Na_2SO_4 and concentrated *in vacuo.* The crude residue was purified by flash column chromatography (20% EtOAc in hexanes to 25% EtOAc in hexanes) to yield ester **S4.1** as a colorless oil (0.671 g, 3.29 mmol, 59% yield). R_f 0.30 (40% EtOAc in hexanes; visualized with ceric ammonium molybdate). ^{1}H NMR (500 MHz, $CDCl_3$) δ 4.32–4.26 (m, 2H), 3.77 (s, 3H), 3.66 (dd, *J* = 10.6, 2.7 Hz, 1H), 3.54 (dd, *J* = 10.6, 5.4 Hz, 1H), 3.40 (s, 3H), 1.46 (s, 3H), 1.41 (s, 3H); ^{13}C NMR (125 MHz, $CDCl_3$) δ 171.11, 111.74, 78.18,

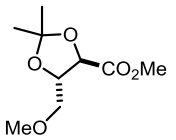

S4.1: $C_9H_{16}O_5$
Molecular Weight: 204.2220

75.53, 72.57, 59.62, 52.55, 26.95, 25.71; IR (thin film) 2990, 2938, 2892, 1762, 1439, 1383 cm^{-1}; $[\alpha]^{25}_{D}$: –15.5 (c = 2.5, CH_2Cl_2); HRMS (ESI) calculated for $C_9H_{16}O_5Na$ (M+Na) 227.0895, observed 227.0900.

(–)-(4*R*,5*S*)-5-(Methoxymethyl)-2,2-dimethyl-1,3-dioxolane-4-carboxylic acid (4.40a): Ester **S4.1** (0.104 g, 0.509 mmol) was dissolved in 1:1:1 THF:H_2O:MeOH (1.5 mL), and KOH pellets (43 mg, 0.76 mmol) were added. The resulting homogeneous solution was maintained at 23 ºC for 3 h before Et_2O (2 mL) and H_2O (2 mL) were added. The resulting organic layer was discarded, and the remaining aqueous layer was acidified with HCl (0.5 mL of 4 M soln) and then washed with EtOAc (3 x 2 mL). The combined organic layers were then washed with brine (3 mL) and dried over Na_2SO_4. Concentration *in vacuo* afforded acid **4.40a** (69 mg, 0.36 mmol, 71% yield) as a colorless oil. ^{1}H NMR (500 MHz, $CDCl_3$) δ 4.39 (app d, *J* = 7.9 Hz, 1H), 4.37–4.31 (m, 1H), 3.73 (dd, *J* = 10.6, 3.3 Hz, 1H), 3.64 (dd, *J* = 10.6, 5.5 Hz, 1H), 3.46 (s, 3H), 1.51 (s, 3H), 1.46 (s, 3H); ^{13}C NMR (125 MHz, $CDCl_3$) δ 173.96, 112.24, 77.94, 75.34, 72.43, 59.77, 26.96, 25.73; IR (thin film) 3504, 2991, 2938, 1737, 1384, 1215 cm^{-1}; $[\alpha]^{25}_{D}$: –1.2 (c = 4.2, CH_2Cl_2); HRMS (ESI) calculated for $C_8H_{14}O_5Na$ (M+Na) 213.0739, observed 213.0741.

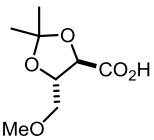

4.40a: $C_8H_{14}O_5$
Molecular Weight: 190.1950

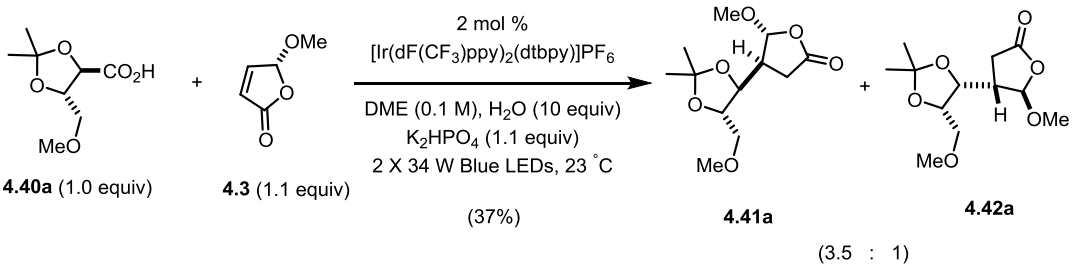

(–)-(4*R*,5*S*)-5-Methoxy-4-((5*S*)-5-(methoxymethyl)-2,2-dimethyl-1,3-dioxolan-4-yl)dihydrofuran-2(3H)-one (4.41a/4.42a): A 4 mL scintillation vial equipped with a Teflon septum and magnetic stir bar was charged with carboxylic acid **4.40a** (18 mg, 0.094 mmol), K_2HPO_4 (18 mg, 0.10 mmol), and $Ir[dF(CF_3)ppy)]_2(dtbbpy)PF_6$ (2 mg, 0.002 mmol). Next, DME (0.9 mL, 0.1 M) was added, followed by water (17 µL, 0.94 mmol), and butenolide **4.3** (12 mg, 0.10 mmol). The reaction mixture was degassed by sparging with argon for 15 min and the vial was sealed and irradiated (2 x 34 W blue LED lamps) for 24 h at 23 ºC. The reaction mixture was filtered through $MgSO_4$, and evaporated under reduced pressure. ^{1}H NMR analysis of the crude residue displayed a 3.5:1 ratio of **4.41a**:**4.42a**. The crude residue was purified by flash column chromatography (10% EtOAc in hexanes to 25% EtOAc in hexanes) to yield an inseparable mixture of lactones **6a** and **7a** as a yellow oil (9 mg, 0.03 mmol, 37% yield). R_f 0.35 (30% EtOAc in hexanes; visualized with ceric ammonium molybdate). ^{1}H NMR for major diastereomer **4.41a** (500 MHz, $CDCl_3$) 5.31 (d, *J* = 2.7 Hz, 1H), 4.02 (dd, *J* = 8.2, 2.8 Hz, 1H), 3.79–3.74 (m, 1H), 3.55 (dd, *J* = 9.8, 4.7 Hz, 1H), 3.51 (s, 3H), 3,46 (dd, *J* = 9.7, 5.4 Hz, 1H), 3.38 (s, 3H), 2.67 (dd, *J* = 18.5, 10.3 Hz, 1H), 2.59–2.51 (m, 2H), 1.39 (app s, 6H); ^{13}C NMR for major diastereomer **4.41a** (125 MHz, $CDCl_3$) δ 175.19, 109.94, 107.49, 77.59, 77.56, 72.99, 59.71, 57.28, 43.38, 28.64, 27.07, 27.01; IR (thin film) 2987, 2936, 1789, 1585, 1451, 1381

cm^{-1}; $[\alpha]^{25}_{D}$: –96.7 (c = 0.8, CH_2Cl_2); HRMS (ESI) calculated for $C_{12}H_{20}O_6Na$ (M+Na) 283.1158, observed 283.1160.

^{1}H NMR NOE studies were unsuccessful to assign diastereomers **4.41a** and **4.42a**. The distinctive vicinal coupling constant of the methine hydrogens noted below was 3.2 Hz for the major product and 9.7 Hz for the minor product. Conformer populations of **4.41a** and **4.42a** were generated by molecular mechanics, and low energy conformations were optimized by DFT calculations at the B3LYP/631-G* level. Calculations and predictions of Boltzmann-weighted vicinal coupling constants for low-energy conformers were done using Spartan 14 (Wavefunction, Inc.).

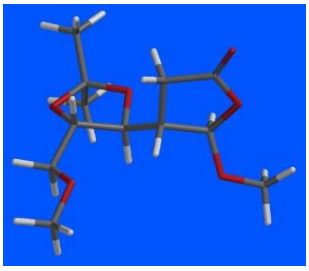

Image of conformer **4.41a** representing 61% of the Boltzmann distribution

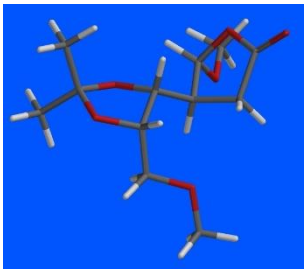

Image of conformer **4.42a** representing 76% of the Boltzmann distribution

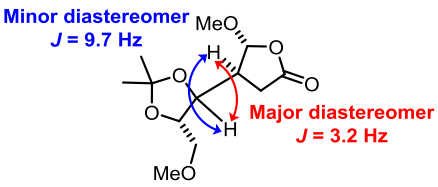

Observed Coupling Constants on 600 MHz ^{1}H NMR ($CDCl_3$)

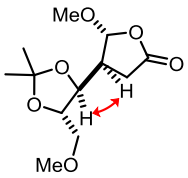

4.41a

Computational Prediction: *J* = 2.4 Hz

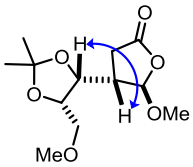

4.42a

Computational Prediction: *J* = 10.0 Hz

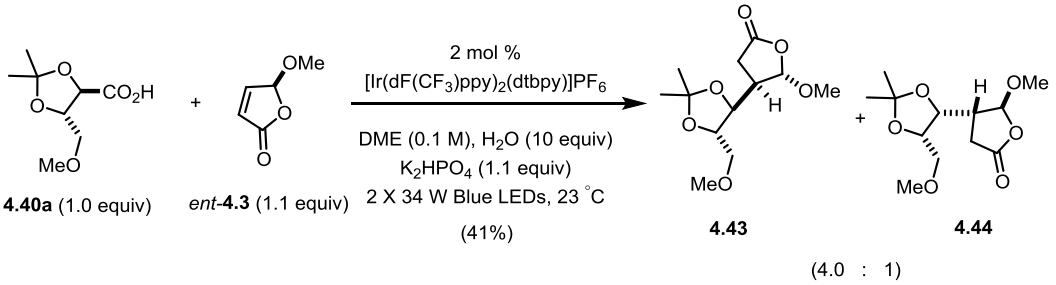

(+)-(4*R*,5*S*)-5-Methoxy-4-((5*S*)-5-(methoxymethyl)-2,2-dimethyl-1,3-dioxolan-4-yl)dihydrofuran-2(3H)-one (4.43/4.44): A 4 mL scintillation vial equipped with a Teflon septum and magnetic stir bar was charged with carboxylic acid **4.40a** (18 mg, 0.094 mmol), K_2HPO_4 (18 mg, 0.10 mmol), and $Ir[dF(CF_3)ppy)]_2(dtbbpy)PF_6$ (2 mg, 0.002 mmol). Next, DME (0.9 mL, 0.1 M) was added, followed by water (17 µL, 0.94 mmol), and *ent*-butenolide **4.3** (12 mg, 0.10 mmol). The reaction mixture was degassed by sparging with argon for 15 min and the vial was sealed and irradiated (2 x 34 W blue LED lamps) for 24 h at 23 ºC. The reaction mixture was filtered through $MgSO_4$, and evaporated under reduced pressure. ^{1}H NMR analysis of the crude residue displayed a 4.0:1 ratio of **4.43**:**4.44**. The crude residue was purified by flash column chromatography (0% acetone in hexanes to 12% acetone in hexanes) to yield lactone **4.43** as a colorless oil (10 mg, 0.038 mmol, 41% yield). R_f 0.20 (20% EtOAc in hexanes; visualized with ceric ammonium molybdate). ^{1}H NMR for major diastereomer **4.43** (500 MHz, C_6D_6) δ 5.33 (d, *J* = 1.9 Hz, 1H), 3.67 (ddd, *J* = 7.3, 6.3, 4.3 Hz, 1H), 3.61 (app t, *J* = 6.3 Hz, 1H), 3.19 (dd, *J* = 9.9, 4.3 Hz, 1H), 3.10–3.07 (m, 1H), 3.08 (s, 3H), 2.95 (s, 3H), 2.36–2.21 (m, 3H), 1.27 (s, 3H), 1.25 (s, 3H); ^{13}C NMR for major diastereomer **4.43** (125 MHz, C_6D_6) δ 174.24, 109.34, 105.99, 78.86, 78.20, 73.29, 58.98, 56.31, 44.58, 30.32, 27.31, 27.10; IR (thin film) 2986, 2922, 2851, 1787, 1454, 1371, 1240 cm^{-1}; $[\alpha]^{25}_D$: +51.0 (c = 1.0, CH_2Cl_2); HRMS (ESI) calculated for $C_{12}H_{20}O_6Na$ (M+Na) 283.1158, observed 283.1150.

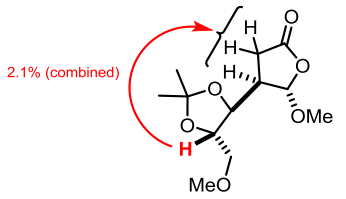

NOE for **4.43**
(NOE in d^6-benzene)

(–)-Methyl (4*R*,5*S*)-4-((benzyloxy)methyl)-5-(methoxymethyl)-2,2-dimethyl-1,3-dioxolane-4-carboxylate (S4.2): A 25 mL round-bottom flask was charged with methyl (4*R*,5*S*)-4-((benzyloxy)methyl)-5-(hydroxymethyl)-2,2-dimethyl-1,3-dioxolane-4-carboxylate[32] (500 mg, 1.61 mmol), followed by the addition of DMF (11 mL, 0.15 M). The resulting mixture was cooled down to 0 ºC. Next, the solution was treated with NaH (60% dispersion in mineral oil, 77 mg, 1.9 mmol). After 15 min at 0 ºC, MeI (0.5 mL, 8 mmol) was added dropwise. After 1 h at 0 ºC, the heterogeneous reaction mixture was allowed to warm to 23 ºC over 2 h. Upon complete consumption of the starting material, as indicated by TLC analysis (30% EtOAc in hexanes; visualized ceric ammonium molybdate), the reaction was quenched via dropwise addition of sat. aq. NH_4Cl soln. (10 mL). The mixture was transferred to a separatory funnel and extracted with Et_2O (3 x 30 mL). The combined organic layers were washed with brine (1 x 100 mL), dried over $MgSO_4$, and evaporated under reduced pressure to yield a yellow oil. The crude residue was purified by flash column chromatography (10% EtOAc in hexanes to 15% EtOAc in hexanes) to yield acid **S4.2** as a colorless oil (468 mg, 1.41 mmol, 88% yield). R_f 0.20 (20% EtOAc in hexanes; visualized with ceric ammonium molybdate). ^{1}H NMR (500 MHz, $CDCl_3$) δ 7.35–7.27 (m, 5H), 4.57–4.50 (m, 3H), 3.79 (s, 3H), 3.76 (dd, *J* = 10.5, 3.0 Hz, 1H), 3.65 (d, *J* = 9.5 Hz,

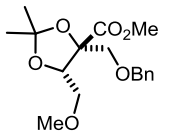

S4.2: $C_{17}H_{24}O_6$
Molecular Weight: 324.3730

1H), 3.56–3.52 (m, 2H), 3.40 (s, 3H), 1.50 (s, 3H), 1.42 (s, 3H); ^{13}C NMR (125 MHz, $CDCl_3$) δ 171.69, 137.78, 128.56, 127.93, 127.81, 110.77, 83.90, 78.66, 73.79, 70.83, 70.60, 59.57, 52.89, 27.94, 25.43; IR (thin film) 2988, 2874, 1742, 1454, 1103 cm^{-1}; $[\alpha]^{23}_D$: –3.65 (c = 6.7, CH_2Cl_2); HRMS (ESI) calculated for $C_{17}H_{24}O_6Na$ (M+Na) 347.1471, observed 347.1464.

(–)-Methyl (4*R*,5*S*)-4-(hydroxymethyl)-5-(methoxymethyl)-2,2-dimethyl-1,3-dioxolane-4-carboxylate (S4.3): A 4 mL scintillation vial was charged with ester **S4.2** (200 mg, 0.616 mmol), followed by the addition of MeOH (1.8 mL, 0.14 M). Next, 10% Pd/C (200 mg) was added. The reaction vessel was then evacuated and refilled with Ar (3x). The heterogenous mixture was then treated with formic acid (90 µL) and stirred vigorously for 18 h at 23 ºC. The reaction mixture was filtered through Celite, and evaporated under reduced pressure to provide ester **S4.3** (143 mg, 0.610 mmol, 99% yield) as a colorless oil. ^{1}H NMR (600 MHz, $CDCl_3$) δ 4.50 (dd, *J* = 6.6, 4.2 Hz, 1H), 3.82 (s, 3H), 3.79–3.76 (m, 3H), 3.71 (dd, *J* = 10.2, 6.0 Hz, 1H), 3.45 (s, 3H), 2.62 (br s, 1H), 1.53 (s, 3H), 1.44 (s, 3H); ^{13}C NMR (125 MHz, $CDCl_3$) δ 172.14, 110.69, 84.72, 78.46, 70.33, 63.73, 59.80, 53.09, 27.87, 25.35; IR (thin film) 3472, 2938, 1741, 1383, 1098 cm^{-1}; $[\alpha]^{21}_D$: –4.44 (c = 3.4, CH_2Cl_2); HRMS (ESI) calculated for $C_{10}H_{18}O_6Na$ (M+Na) 257.1001, observed 257.0997.

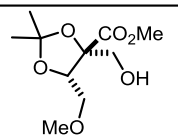

S4.3: $C_{10}H_{18}O_6$
Molecular Weight: 234.2480

(+)-(4*R*,5*S*)-4-(Hydroxymethyl)-5-(methoxymethyl)-2,2-dimethyl-1,3-dioxolane-4-carboxylic acid (4.40b): A 4 mL scintillation vial was charged with ester **S4.3** (80 mg, 0.34 mmol), followed by the addition of 1:1 dioxane:H_2O (2 mL, 0.17 M). Next, KOH (76 mg, 1.4 mmol) was added. The resulting biphasic mixture was stirred vigorously at 40 ºC for 18 h. Upon allowing reaction mixture to cool down to 23 ºC, aq. HCl (1 mL of 1 N soln) and EtOAc (1 mL) were added. The resulting biphasic mixture was extracted with EtOAc (3 x 2 mL). The combined organic layers were washed with brine (1 x 10 mL), dried over $MgSO_4$, and evaporated under reduced pressure to yield acid **4.40b** (56 mg, 0.25 mmol, 75% yield) as a colorless oil. ^{1}H NMR (600 MHz, $CDCl_3$) δ 4.46 (dd, *J* = 6.0, 3.6 Hz, 1H), 3.84–3.77 (m, 3H), 3.72–3.66 (m, 2H), 3.45 (s, 3H), 1.53 (s, 3H), 1.45 (s, 3H); ^{13}C NMR (125 MHz, $CDCl_3$) δ 173.27, 109.96, 77.23, 68.93, 66.13, 62.50, 58.69, 26.70, 24.23; IR (thin film) 3509, 2984, 1740, 1377, 1091 cm^{-1}; $[\alpha]^{21}_D$: +3.69 (c = 1.9, CH_2Cl_2); HRMS (ESI) calculated for $C_9H_{16}O_6Na$ (M+Na) 243.0845, observed 243.0845.

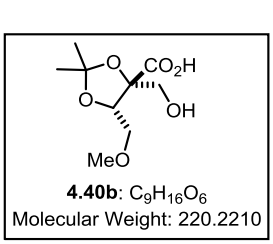

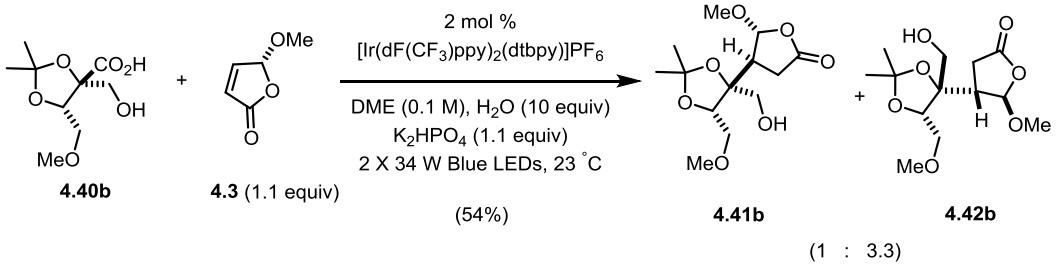

(–)-(4*S*,5*R*)-4-((5*S*)-4-(Hydroxymethyl)-5-(methoxymethyl)-2,2-dimethyl-1,3-dioxolan-4-yl)-5-methoxydihydrofuran-2(3H)-one (4.41b/4.42b): A 4 mL scintillation vial equipped with a Teflon septum and magnetic stir bar was charged with carboxylic acid **4.40b** (16 mg, 0.070 mmol), K_2HPO_4 (13 mg, 0.77 mmol), and

$Ir[dF(CF_3)ppy)]_2(dtbbpy)PF_6$ (1.6 mg, 0.0014 mmol). Next, DME (0.7 mL, 0.1 M) was added, followed by water (13 µL, 0.70 mmol), and butenolide **4.3** (9 mg, 0.08 mmol). The reaction mixture was degassed by sparging with argon for 15 min and the vial was sealed and irradiated (2 x 34 W blue LED lamps) for 24 h at 23 ºC. The reaction mixture was filtered through $MgSO_4$, and evaporated under reduced pressure to yield a yellow oil. ^{1}H NMR analysis of the crude residue displayed a 1:3.3 ratio of **4.41b**:**4.42b**. The crude residue was purified by flash column chromatography (20% EtOAc in hexanes to 35% EtOAc in hexanes) to yield an inseparable mixture of lactones **4.41b** and **4.42b** as a colorless oil (11 mg, 0.38 mmol, 54% yield). R_f 0.2 (40% EtOAc in hexanes; visualized with ceric ammonium molybdate). ^{1}H NMR for major diastereomer **4.42b** (500 MHz, $CDCl_3$) δ 5.61 (s, 1H), 4.31 (dd, *J* = 7.5, 5.5 Hz, 1H), 3.69 (dd, *J* = 9.5, 5.5 Hz, 1H), 3.62–3.60 (m, 2H), 3.58–3.52 (m, 1H), 3.49 (s, 3H), 3.42 (s, 3H), 2.75–2.67 (m, 2H), 2.54 (d, *J* = 15.0 Hz, 1H), 2.36 (br s, 1H), 1.45 (s, 3H), 1.39 (s, 3H); ^{13}C NMR for major diastereomer **4.42b** (125 MHz, $CDCl_3$) δ 176.42, 109.33, 106.45, 83.86, 78.92, 69.39, 65.01, 59.73, 56.97, 43.64, 29.25, 27.12, 26.31; IR (thin film) 2986, 2925, 1785, 1375, 1108 cm^{-1}; $[\alpha]^{22}_D$: –10.5 (c = 1.3, CH_2Cl_2); HRMS (ESI) calculated for $C_{13}H_{22}O_7Na$ (M+Na) 313.1263, observed 313.1262.

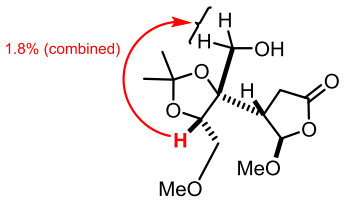

NOE for **4.42b**

(+)-(4*R*,5*S*)-4-((Benzyloxy)methyl)-5-(methoxymethyl)-2,2-dimethyl-1,3-dioxolane-4-carboxylic acid (4.40c): A 4 mL scintillation vial was charged with ester **S4.2** (100 mg, 0.308 mmol), followed by the addition of 1:1 THF:H_2O (1.8 mL, 0.17 M). Next, LiOH•H_2O (26 mg, 0.62 mmol) was added. The resulting biphasic mixture was stirred vigorously at 23 ºC for 18 h. The reaction was then treated with aq. HCl (1 mL of 1 N soln) and EtOAc (1 mL). The resulting biphasic mixture was extracted with EtOAc (3 x 2 mL). The combined organic layers were washed with brine (1 x 10 mL), dried over $MgSO_4$, and evaporated under reduced pressure to yield acid **4.40c** (84 mg, 0.27 mmol, 88% yield) as a colorless oil. ^{1}H NMR (500 MHz, $CDCl_3$) δ 9.14 (br s, 1 H), 7.32–7.28 (m, 5H), 4.57 (app s, 2 H), 4.46 (dd, *J* = 8.0, 3.0 Hz, 1H), 3.75–3.71 (m, 2H), 3.60–3.54 (m, 2H), 3.38 (s, 3H), 1.50, (s, 3H), 1.44 (s, 3H); ^{13}C NMR (125 MHz, $CDCl_3$) δ 173.29, 136.20, 127.34, 126.77, 126.61, 109.98, 82.89, 77.23, 72.71, 69.19, 69.13, 58.29, 26.60, 24.14; IR (thin film) 2989, 2934, 1738, 1375, 1099 cm^{-1}; $[\alpha]^{23}_D$: +10.4 (c = 3.0, CH_2Cl_2); HRMS (ESI) calculated for $C_{16}H_{22}O_6Na$ (M+Na) 333.1314, observed 333.1303.

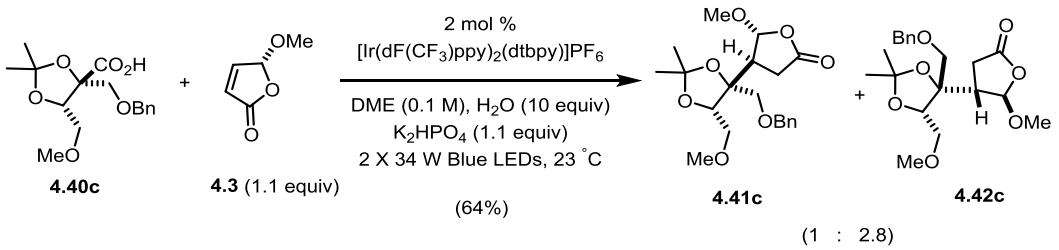

(–)-(4*S*,5*R*)-4-((5*S*)-4-((benzyloxy)methyl)-5-(methoxymethyl)-2,2-dimethyl-1,3-dioxolan-4-yl)-5-methoxydihydrofuran-2(3H)-one (4.41c/4.42c): A 4 mL scintillation vial equipped with a Teflon septum and magnetic stir bar was charged with carboxylic acid

4.40c (22 mg, 0.070 mmol), K_2HPO_4 (13 mg, 0.77 mmol), and $Ir[dF(CF_3)ppy)]_2(dtbbpy)PF_6$ (1.6 mg, 0.0014 mmol). Next, DME (0.7 mL, 0.1 M) was added, followed by water (13 µL, 0.70 mmol), and butenolide **4.3** (9 mg, 0.08 mmol). The reaction mixture was degassed by sparging with argon for 15 min and the vial was sealed and irradiated (2 x 34 W blue LED lamps) for 24 h at 23 ºC. The reaction mixture was filtered through $MgSO_4$, and evaporated under reduced pressure to yield a yellow oil. ^{1}H NMR analysis of the crude residue displayed a 1:2.8 ratio of **4.41c**:**4.42c**. The crude residue was purified by flash column chromatography (10% EtOAc in hexanes to 17.5% EtOAc in hexanes) to yield **4.42c** as a colorless oil (13 mg, 0.33 mmol, 47% yield) and **4.41c** as a colorless oil (4 mg, 0.1 mmol, 17% yield). R_f of **4.42c**: 0.33 (20% EtOAc in hexanes; visualized with ceric ammonium molybdate); R_f of **4.41c**: 0.27 (20% EtOAc in hexanes; visualized with ceric ammonium molybdate).

^{1}H NMR for major diastereomer **4.42c** (500 MHz, $CDCl_3$) δ 7.37–7.28 (m, 5H), 5.64 (s, 1H), 4.51 (d, *J* = 12.0 Hz, 1H), 4.47 (d, *J* = 12.0 Hz, 1H), 4.53 (t, *J* = 4.0 Hz, 1H), 3.67–3.56 (m, 2H), 3.49–3.48 (m, 5H), 3.38 (s, 3H), 2.60–2.58 (m, 2H), 2.45–2.41 (m, 1H), 1.46 (s, 3H), 1.36 (s, 3H); ^{13}C NMR for major diastereomer **4.42c** (125 MHz, $CDCl_3$) δ 176.44, 137.33, 128.71, 128.20, 128.03, 109.52, 106.89, 82.36, 80.41, 74.03, 73.52, 70.64, 59.64, 57.01, 44.42, 29.68, 27.24, 26.31; IR (thin film) 2986, 2927, 1785, 1598, 1106 cm^{-1}; $[\alpha]^{23}_D$: –20.1 (c = 1.2, CH_2Cl_2); HRMS (ESI) calculated for $C_{20}H_{28}O_7Na$ (M+Na) 403.1733, observed 403.1727.

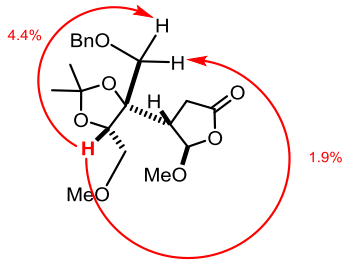

NOE for **4.42c**

^{1}H NMR for minor diastereomer **4.41c** (500 MHz, $CDCl_3$) δ 7.38–7.28 (m, 5H), 5.41 (d, *J* = 2.5 Hz, 1H), 4.51 (d, *J* = 12.0 Hz, 1H), 4.43 (d, *J* = 12.0 Hz, 1H), 3.92 (dd *J* = 7.5, 3.5 Hz, 1 H), 3.61 (dd, *J* = 10.5, 3.5 Hz, 1H), 3.58–3.55 (m, 1H), 3.52–3.50 (m, 1H), 3.46 (s, 3H), 3.35 (s, 3H), 3.30 (d, *J* = 9.5 Hz, 1H), 2.86–2.83 (m, 1H), 2.73–2.68 (m, 1H), 2.62–2.57 (m, 1H), 1.40 (s, 3H), 1.37 (s, 3H); ^{13}C NMR for minor diastereomer **4.41c** (125 MHz, $CDCl_3$) δ 175.17, 137.59, 128.72, 128.22, 128.08, 109.22, 106.43, 81.38, 79.84, 73.75, 70.60, 69.58, 59.58, 57.22, 44.23, 29.76, 28.75, 26.67; IR (thin film) 2985, 2923, 1787, 1598, 1107 cm^{-1}; $[\alpha]^{23}_{D}$: –19.4 (c = 0.4, CH_2Cl_2); HRMS (ESI) calculated for $C_{20}H_{28}O_7Na$ (M+Na) 403.1733, observed 403.1740.

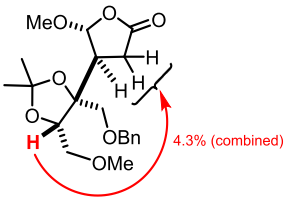

NOE for **4.41c**

(+)-(4*R*,5*S*)-4-((Benzyloxy)methyl)-5-(hydroxymethyl)-2,2-dimethyl-1,3-dioxolane-4-carboxylic acid (4.40d): A 4 mL scintillation vial was charged with a (4*R*,5*S*)-5-(hydroxymethyl)-2,2-dimethyl-1,3-dioxolane-4-carboxylate[32] (200 mg, 0.644 mmol), followed by the addition of 1:1:1 THF:MeOH:H_2O (2.0 mL, 0.32 M). Next, KOH (72 mg, 1.3 mmol) was added. The resulting biphasic mixture was stirred vigorously at 23 ºC for 18 h. The reaction was then treated with aq. HCl (1 mL of 1 N soln) and EtOAc (1 mL). The resulting biphasic mixture was extracted with EtOAc (3 x 2 mL). The combined organic layers were washed with brine (1 x 10 mL), dried over $MgSO_4$, and evaporated under reduced pressure to yield acid **4.40d** (188 mg, 0.634 mmol, 99% yield) as a colorless oil. ^{1}H NMR (600 MHz, $CDCl_3$) δ 7.35–7.30 (m, 5H), 4.59 (app s, 2H), 4.43 (t, *J* = 3.2 Hz, 1H), 3.92 (dd, *J* = 12.0, 4.8 Hz, 1H), 3.85 (dd, *J* = 12.0, 5.4 Hz, 1H), 3.79 (d, *J* = 9.6 Hz, 1H), 3.69 (d, *J* = 9.0 Hz, 1 H), 1.51 (s, 3H), 1.46 (s, 3H); ^{13}C NMR (125 MHz, $CDCl_3$) δ 173.92, 137.15, 128.70, 128.19, 127.95, 111.01, 84.37, 79.36, 74.15, 70.56, 60.35, 27.79, 25.48; IR (thin film) 3457, 2989, 2937, 1738, 1382, 1100 cm^{-1}; $[\alpha]^{22}_D$: +9.53 (c = 4.3, CH_2Cl_2); HRMS (ESI) calculated for $C_{15}H_{20}O_6Na$ (M+Na) 319.1158, observed 319.1157.

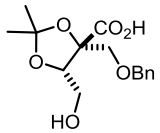

4.40d: $C_{15}H_{20}O_6$
Molecular Weight: 296.3190

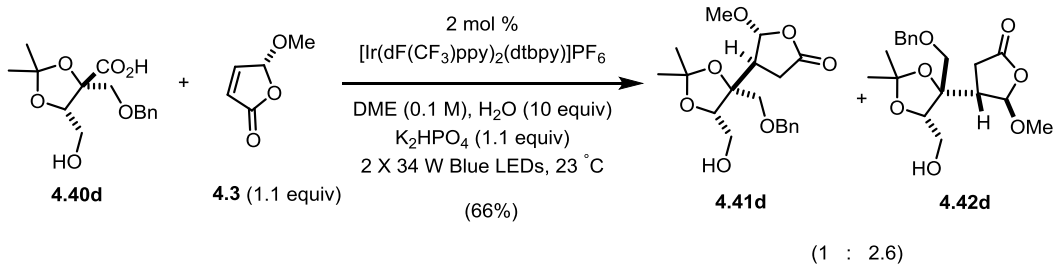

(–)-(4*S*,5*R*)-4-((5*S*)-4-((Benzyloxy)methyl)-5-(hydroxymethyl)-2,2-dimethyl-1,3-dioxolan-4-yl)-5-methoxydihydrofuran-2(3H)-one (4.41d/4.42d): A 4 mL scintillation vial equipped with a Teflon septum and magnetic stir bar was charged with carboxylic acid **4.40d** (21 mg, 0.070 mmol), K_2HPO_4 (13 mg, 0.77 mmol), and $Ir[dF(CF_3)ppy)]_2(dtbbpy)PF_6$ (1.6 mg, 0.0014 mmol). Next, DME (0.7 mL, 0.1 M) was added, followed by water (13 µL, 0.70 mmol), and butenolide **4.3** (9 mg, 0.08 mmol). The reaction mixture was degassed by sparging with argon for 15 min and the vial was sealed and irradiated (2 x 34 W blue LED lamps) for 24 h at 23 ºC. The reaction mixture was filtered through $MgSO_4$, and evaporated under reduced pressure to yield a yellow oil. ^{1}H NMR analysis of the crude residue displayed a 1:2.6 ratio of **4.41d**:**4.42d**.The crude residue was purified by flash column chromatography (20% EtOAc in hexanes to 32% EtOAc in hexanes) to yield an inseparable mixture of lactones **4.41d** and **4.42d** as a colorless oil (17 mg, 0.46 mmol, 66% yield). R_f 0.25 (40% EtOAc in hexanes; visualized with ceric ammonium molybdate). ^{1}H NMR for major diastereomer **4.42d** (600 MHz, $CDCl_3$) δ 7.39–7.27 (m, 5H), 5.57 (s, 1H), 4.48–4.46 (m, 2H), 4.21 (t, *J* = 4.0 Hz, 1H), 3.88–3.82 (m, 2H), 3.54 (d, *J* = 9.0 Hz, 1H), 3.40 (s, 3H), 3.31 (d, *J* = 9.6 Hz, 1H), 2.67–2.60 (m, 2H), 2.43 (dd, *J* = 17.4, 2.4 Hz, 1 H), 2.28 (m, 1H), 1.53 (s, 3H), 1.46 (s, 3H); ^{13}C NMR for major diastereomer **4.42d** (125 MHz, $CDCl_3$) δ 176.43, 136.75, 128.92, 128.49, 128.33, 109.39, 106.51, 83.03, 81.98, 74.20, 73.54, 60.47, 56.95, 44.32, 29.74, 27.16, 26.25; IR (thin film)

3468, 2986, 2935, 1784, 1373 cm^{-1}; $[\alpha]^{22}_{D}$: –21.7 (c = 1.7, CH_2Cl_2); HRMS (ESI) calculated for $C_{19}H_{26}O_7Na$ (M+Na) 389.1576, observed 389.1576.

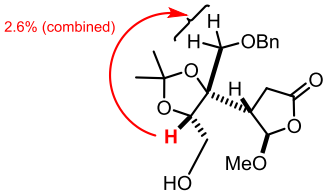

NOE for
4.42d

(+)-Methyl (4*R*,5*S*)-4,5-bis(hydroxymethyl)-2,2-dimethyl-1,3-dioxolane-4-carboxylate (S4.4): A reaction vessel was charged with methyl (4*R*,5*S*)-4-((benzyloxy)methyl)-5-(hydroxymethyl)-2,2-dimethyl-1,3-dioxolane-4-carboxylate[32] (0.250 g, 0.806 mmol) and 10% Pd/C (0.200 g). The vessel was then evacuated and refilled with Ar (3x) before MeOH (4 mL) was added followed by formic acid (0.2 mL). The suspension was then vigorously stirred for 4 h at 23 ºC before filtering through Celite. Upon concentration *in vacuo*, ester **S4.4** was isolated (0.172 g, 0.781 mmol, 97% yield) as a colorless solid. R_f 0.25 (60% EtOAc in hexanes; visualized with ceric ammonium molybdate). ^{1}H NMR (500 MHz, $CDCl_3$) δ 4.42 (t, *J* = 5.1 Hz, 1H), 3.98 (dd, *J* = 12.3, 5.1 Hz, 1H), 3.94 (dd, *J* = 12.3, 5.1 Hz, 1H), 3.84–3.77 (m, 2H), 3.81 (s, 3H), 2.97 (bs, 1H), 2.82 (bs, 1H), 1.50 (s, 3H), 1.42 (s, 3H); ^{13}C NMR (125 MHz, $CDCl_3$) δ 172.37, 110.37, 84.48, 79.44, 63.50, 60.23, 53.06, 27.75, 25.29; IR (thin film) 3426, 2990, 2954, 2886, 1742, 1457, 1438, 1384 cm^{-1}; $[\alpha]^{25}_{D}$: +6.1 (c = 2.6, CH_2Cl_2); HRMS (ESI) calculated for $C_9H_{16}O_6Na$ (M+Na) 243.0845, 243.0842.

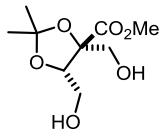

S4.4: $C_9H_{16}O_6$
Molecular Weight: 220.2210

(–)-Methyl (4*R*,5*S*)-4,5-bis(((*tert*-butyldimethylsilyl)oxy)methyl)-2,2-dimethyl-1,3-dioxolane-4-carboxylate (S4.5): To a solution of ester **S4.4** (0.108 g, 0.490 mmol) in CH_2Cl_2 (2.5 mL) at 23 ºC was added imidazole (0.167 g, 2.45 mmol) followed by DMAP (3 mg, 0.03 mmol) and then TBS-Cl (0.222 g, 1.47 mmol). The reaction was maintained for 2 h before quenching with H_2O (2 mL), and the heterogeneous solution was concentrated *in vacuo* over Celite (~2 g). The resulting solid was purified by flash column chromatography (8% EtOAc in hexanes) to yield ester **S4.5** as a colorless oil (0.185 g, 0.412 mmol, 84% yield). R_f 0.80 (10% EtOAc in hexanes; visualized with ceric ammonium molybdate). ^{1}H NMR (500 MHz, $CDCl_3$) δ 4.43 (dd, *J* = 7.5, 3.0 Hz, 1H), 4.11 (dd, *J* = 12.0, 3.0 Hz, 1H), 3.85–3.80 (m, 2H), 3.76 (s, 3H), 3.71 (d, *J* = 9.5 Hz, 1 H), 1.47 (s, 3H), 1.38 (s, 3H), 0.91 (s, 9H), 0.85 (s, 9H), 0.09 (s, 6H), 0.03 (s, 3H), 0.02 (s, 3H); ^{13}C NMR (125 MHz, $CDCl_3$) δ 171.87, 109.96, 84.46, 80.68, 64.26, 62.21, 52.52, 28.06, 26.17, 25.90, 25.55, 18.67, 18.30, –4.98, –5.0, –5.42, –5.57; IR (thin film) 2930, 2857, 1747, 1472, 1381 cm^{-1}; $[\alpha]^{22}_D$: –7.84 (c = 4.0, CH_2Cl_2); HRMS (ESI) calculated for $C_{21}H_{44}O_6Si_2Na$ (M+Na) 471.2574, observed 471.2574.

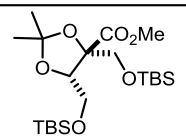

S4.5: $C_{21}H_{44}O_6Si_2$
Molecular Weight: 448.7470

(+)-(4*R*,5*S*)-4,5-Bis(((*tert*-butyldimethylsilyl)oxy)methyl)-2,2-dimethyl-1,3-dioxolane-4-carboxylic acid (4.40e): The procedure for the preparation of **4.40e** was a slight modification from the literature procedure.[25] A 4 mL scintillation vial was charged with ester **S4.5** (80 mg, 0.18 mmol), followed by the addition of DCE (1.1 mL, 0.16 M). Next, Me_3SnOH (225 mg, 1.25 mmol) was added. The resulting

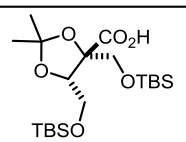

4.40e: $C_{20}H_{42}O_6Si_2$
Molecular Weight: 434.7200

heterogeneous mixture was stirred vigorously at 80 ºC for 48 h. Upon allowing reaction mixture to cool down to 23 ºC, the solution was treated with aq. HCl (1 mL of 1 N soln) and CH_2Cl_2 (1 mL). The resulting biphasic mixture was extracted with aq. HCl (5 x 1 mL of 1 N soln). The organic layer was washed with brine (1 x 5 mL), dried over $MgSO_4$, and evaporated under reduced pressure to yield a colorless oil. The crude residue was purified by flash column chromatography (20% acetone in hexanes) to yield **4.40e** as a colorless oil (72 mg, 0.17 mmol, 94% yield). R_f 0.5 (20% acetone in hexanes; visualized with ceric ammonium molybdate). ^{1}H NMR (600 MHz, $CDCl_3$) δ 4.30 (t, *J* = 9.6 Hz, 1H), 4.02 (dd, *J* = 11.4, 4.2 Hz, 1H), 3.94 (d, *J* = 10.2 Hz, 1H), 3.87 (dd, *J* = 11.4, 5.4 Hz, 1H), 3.80 (d, *J* = 10.8 Hz, 1H), 1.51 (s, 3H), 1.44 (s, 3H), 0.91 (s, 9H), 0.88 (s, 9H), 0.09 (s, 6H), 0.06 (s, 3H), 0.05 (s, 3H); ^{13}C NMR (125 MHz, $CDCl_3$) δ 173.73, 110.81, 85.95, 80.04, 64.96, 61.56, 28.22, 26.29, 26.22, 25.83, 18.76, 18.69, –4.87, –4.96, –5.09; IR (thin film) 2954, 2858, 1726, 1472, 1382 cm^{-1}; $[\alpha]^{22}_D$: +2.70 (c = 1.3, CH_2Cl_2); HRMS (ESI) calculated for $C_{20}H_{42}O_6Si_2Na$ (M+Na) 457.2418, observed 457.2430.

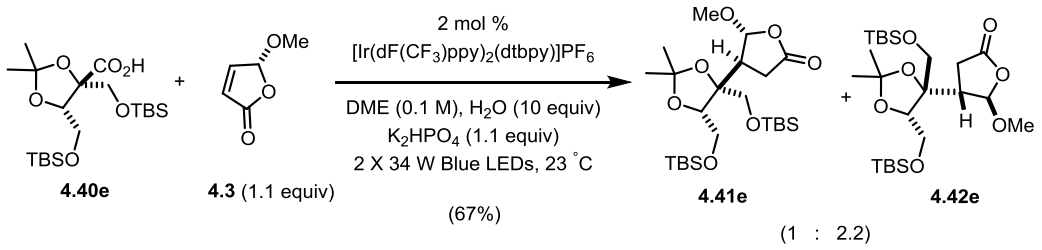

(–)-(4*S*,5*R*)-4-((5*S*)-4,5-Bis(((tert-butyldimethylsilyl)oxy)methyl)-2,2-dimethyl-1,3-dioxolan-4-yl)-5-methoxydihydrofuran-2(3H)-one (4.41e/4.42e): A 4 mL scintillation vial equipped with a Teflon septum and magnetic stir bar was charged with carboxylic acid **4.40e** (30 mg, 0.070 mmol), K_2HPO_4 (13 mg, 0.77 mmol), and $Ir[dF(CF_3)ppy)]_2(dtbbpy)PF_6$ (1.6 mg, 0.0014 mmol). Next, DME (0.7 mL, 0.1 M) was

added, followed by water (13 µL, 0.70 mmol), and butenolide **4.3** (9 mg, 0.077 mmol). The reaction mixture was degassed by sparging with argon for 15 min and the vial was sealed and irradiated (2 x 34 W blue LED lamps) for 24 h at 23 ºC. The reaction mixture was filtered through $MgSO_4$, and evaporated under reduced pressure to yield a yellow oil. ^{1}H NMR analysis of the crude residue displayed a 1:2.2 ratio of **4.41e**:**4.42e**.The crude residue was purified by flash column chromatography (0% EtOAc in hexanes to 4% EtOAc in hexanes) to yield **4.42e** as a colorless oil (16 mg, 0.32 mmol, 45% yield) and **4.41e** as a colorless oil (8 mg, 0.2 mmol, 22% yield). R_f of **4.42e**: 0.18 (5% EtOAc in hexanes; visualized with ceric ammonium molybdate); R_f of **4.41e**: 0.13 (5% EtOAc in hexanes; visualized with ceric ammonium molybdate).

^{1}H NMR for major diastereomer **4.42e** (600 MHz, $CDCl_3$) δ 5.65 (s, 1H), 4.07 (t, *J* = 6.0 Hz, 1H), 3.85 (dd, *J* = 10.8, 6.6 Hz, 1H), 3.75–3.60 (m, 2H), 3.59 (d, *J* = 10.2 Hz, 1H), 3.48 (s, 3H), 2.63 (dd, *J* = 18.6, 11.4 Hz, 1H), 2.58–2.55 (m, 2H), 1.43 (s, 3H), 1.36 (s, 3H), 0.90–0.89 (m, 18H), 0.08–0.06 (m, 12H); ^{13}C NMR for major diastereomer **4.42e** (125 MHz, $CDCl_3$) δ 176.61, 108.91, 107.21, 83.83, 80.51, 66.89, 61.26, 56.96, 44.07, 30.01, 27.40, 26.56, 26.09, 18.57, 18.48, –5.14, –5.22, –5.41, –5.51; IR (thin film) 2954, 2930, 1790, 1254, 1104 cm^{-1}; $[\alpha]^{22}_D$: –18.0 (c = 1.4, CH_2Cl_2); HRMS (ESI) calculated for $C_{24}H_{48}O_7Si_2Na$ (M+Na) 527.2836, observed 527.2828.

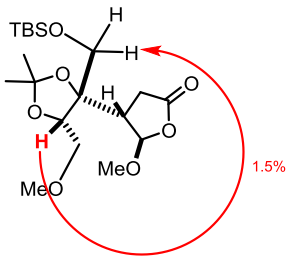

NOE for **4.42e**

^{1}H NMR for minor diastereomer **4.41e** (600 MHz, $CDCl_3$) δ 5.43 (d, *J* = 3.0 Hz, 1H), 3.92 (d, *J* = 2.4 Hz, 1H), 3.80–3.75 (m, 2H), 3.73 (d, *J* = 10.2 Hz, 1H), 3.46 (s, 3H), 3.41 (d, *J* = 10.2, 1H), 2.83 (t, *J* = 2.0 Hz, 1H), 2.69 (dd, *J* = 17.4, 9.0 Hz, 1H), 2.58 (dd, *J* = 17.4, 6.0 Hz, 1H), 1.38 (s, 3H), 1.35 (s, 3H), 0.91–0.88 (m, 18H), 0.08–0.05 (m, 12H); ^{13}C NMR for minor diastereomer **4.41e** (125 MHz, $CDCl_3$) δ 175.63, 108.68, 106.44, 82.21, 82.12, 62.60, 62.03, 56.97, 43.43, 29.68, 28.95, 26.64, 26.25, 25.91, 18.65, 18.23, –4.92, –5.04, –5.64, –5.71; IR (thin film) 2954, 2930, 1795, 1253, 1098 cm^{-1}; $[\alpha]^{23}_{D}$: –19.7 (c = 0.7, CH_2Cl_2); HRMS (ESI) calculated for $C_{24}H_{48}O_7Si_2Na$ (M+Na) 527.2836, observed 527.2825.

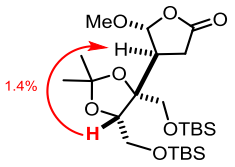

NOE for **4.41e**

(+)-(5*S*)-4-Ethyl-5-(methoxymethyl)-2,2-dimethyl-1,3-dioxolane-4-carboxylic acid (S4.6): Ester **S4.1** (0.151 g, 0.739 mmol) was dissolved in a mixture of THF (3 mL) and HMPA (0.6 mL). The solution was then cooled to –78 ºC, and ethyl iodide (0.24 mL, 3.0 mmol) was added followed by LHMDS (0.8 mL of 1.0 M soln in THF, 0.8 mmol). The reaction was maintained for 1 h at –78 ºC before sat. aq. NH_4Cl soln (2 mL) was added. The vessel was then allowed to warm to 23 ºC, and Et_2O (2 mL) was added. The resulting aqueous layer was extracted with Et_2O (3 x 3 mL), and the combined organic layers were washed with brine (1 x 5 mL). The organic phases were dried over $MgSO_4$ and concentrated *in vacuo*. The crude residue was purified by flash column chromatography

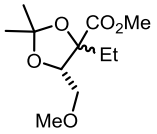

S4.6: $C_{11}H_{20}O_5$
Molecular Weight: 232.2760

(0% EtOAc in hexanes to 8% EtOAc in hexanes) to afford ester **S4.6** as a colorless oil in a 9:1 mixture of diastereomers (0.108 g, 0.465 mmol, 63% yield). R_f 0.25 (10% EtOAc in hexanes; visualized with ceric ammonium molybdate). ^{1}H NMR for **S4.6**'s major diastereomer (500 MHz, $CDCl_3$) δ 4.27 (dd, *J* = 8.5, 2.5 Hz, 1H), 3.75 (s, 3H), 3.66 (dd, *J* = 10.1, 2.5 Hz, 1H), 3.54 (dd, *J* = 10.1, 8.6 Hz, 1H), 3.39 (s, 3H), 1.75–1.66 (m, 1H), 1.62–1.55 (m, 1H), 1.47 (s, 3H), 1.40 (s, 3H), 0.87 (t, *J* = 7.5 Hz, 3H); ^{13}C NMR for **S4.6**'s major diastereomer (125 MHz, $CDCl_3$) δ 172.84, 110.23, 85.18, 79.32, 71.20, 59.45, 52.57, 27.99, 26.21, 25.40, 8.11; IR (thin film) 2987, 2938, 2883, 1759, 1731, 1458, 1381 cm^{-1}; $[\alpha]^{25}_D$: +10.1 (c = 1.7, CH_2Cl_2); HRMS (ESI) calculated for $C_{11}H_{20}O_5Na$ (M+Na) 255.1208, observed 255.1218.

(+)-(5*S*)-4-Ethyl-5-(methoxymethyl)-2,2-dimethyl-1,3-dioxolane-4-carboxylic acid (4.40f): Ester **S4.6** (59 mg, 0.25 mmol) was dissolved in 1:1:1 MeOH:THF:H_2O (0.9 mL), and KOH pellets (29 mg, 0.51 mmol) were added to the solution. The reaction was maintained at 23 ºC for 14 h, at which point the reaction was diluted with H_2O (1 mL) and Et_2O (1 mL). The aqueous layer was washed with Et_2O (3 x 1 mL), and the combined organic layers were discarded. The aqueous layer was then acidified with aq. HCl (0.5 mL of 4 M soln) and then extracted with EtOAc (3 x 1 mL). The combined organic phases were washed with brine (1 x 3 mL), dried over $MgSO_4$, and concentrated *in vacuo* to provide acid **4.40f** as a colorless solid in a 9:1 mixture of diastereomers (50 mg, 0.23 mmol, 90% yield). ^{1}H NMR for **4.40f**'s major diastereomer (500 MHz, $CDCl_3$) δ 4.32 (dd, *J* = 8.3, 2.0 Hz, 1H), 3.72 (dd, *J* = 10.1, 2.0 Hz, 1H), 3.63 (app t, *J* = 8.9 Hz, 1H), 3.43 (s, 3H), 1.83–1.75 (m, 1H), 1.70–1.62 (m, 1H), 1.52 (s, 3H), 1.48 (s, 3H), 0.94 (t, *J* = 7.2 Hz, 3H);

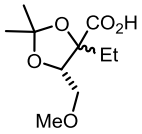

4.40f: $C_{10}H_{18}O_5$
Molecular Weight: 218.2490

^{13}C NMR for **4.40f**'s major diastereomer (125 MHz, $CDCl_3$) δ 174.55, 110.83, 85.31, 78.92, 70.76, 59.58, 27.26, 25.61, 25.56, 7.92; IR (thin film) 3472, 3180, 2988, 2939, 2884, 1731, 1459, 1381, 1247 cm^{-1}; $[\alpha]^{25}_{D}$: +37.8 (c = 1.1, CH_2Cl_2); HRMS (ESI) calculated for $C_{10}H_{18}O_5Na$ (M+Na) 241.1052, observed 241.1054.

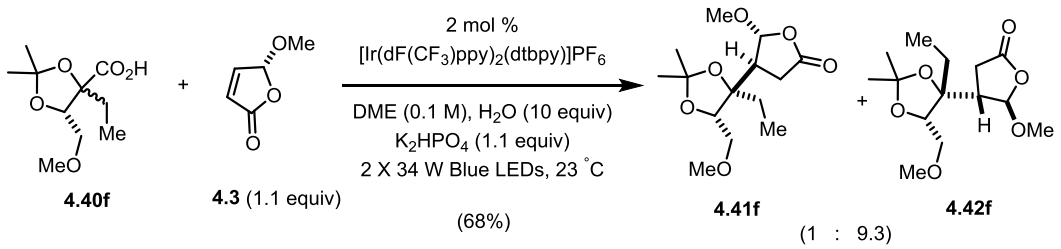

(–)-(4*S*,5*R*)-4-((5*S*)-4-ethyl-5-(methoxymethyl)-2,2-dimethyl-1,3-dioxolan-4-yl)-5-methoxydihydrofuran-2(3H)-one (4.41f/4.42f): A 4 mL scintillation vial equipped with a Teflon septum and magnetic stir bar was charged with carboxylic acid **4.40f** (20 mg, 0.092 mmol), K_2HPO_4 (18 mg, 0.10 mmol), and Ir[dF(CF_3)ppy)]$_2$(dtbbpy)PF_6 (2 mg, 0.002 mmol). Next, DME (0.9 mL, 0.1 M) was added, followed by water (17 µL, 0.94 mmol), and butenolide **4.3** (12 mg, 0.10 mmol). The reaction mixture was degassed by sparging with argon for 15 min and the vial was sealed and irradiated (2 x 34 W blue LED lamps) for 24 h at 23 ºC. The reaction mixture was filtered through $MgSO_4$, and evaporated under reduced pressure.^{1}H NMR analysis of the crude residue displayed a 1:9.3 ratio of **4.41f**:**4.42f**. The crude residue was purified by flash column chromatography (20% EtOAc in hexanes) to afford an inseparable mixture of lactones **4.41f** and **4.42f** as a yellow solid (18 mg, 0.062 mmol, 68% yield). R_f 0.20 (20% EtOAc in hexanes; visualized with ceric ammonium molybdate). Recrystallization from acetone and hexanes afforded yellow crystals suitable for single crystal X-ray diffraction of **4.42f**.[17] ^{1}H NMR for **4.42f** (500 MHz, $CDCl_3$) δ 5.53 (d, *J* = 1.1 Hz, 1H), 4.19 (app t, *J* = 6.2 Hz, 1H), 3.56 (dd, *J* = 10.0,

6.5 Hz, 1H), 3.48 (s, 3H), 3.41 (dd, J = 10.0, 5.8 Hz, 1H), 3.38 (s, 3H), 2.68 (dd, J = 18.0, 10.3 Hz, 1H), 2.61–2.57 (m, 1H), 2.44 (dd, J = 18.1, 2.7 Hz, 1H), 1.68–1.59 (m, 1H), 1.58–1.50 (m, 1H), 1.44 (s, 3H), 1.37 (s, 3H), 0.94 (t, J = 7.5 Hz, 3H); ^{13}C NMR for **4.42f** (125 MHz, $CDCl_3$) δ 176.65, 108.24, 106.94, 83.81, 78.47, 70.35, 59.57, 56.89, 45.48, 29.39, 27.56, 26.44, 25.82, 7.89; IR (thin film) 2975, 2937, 2900, 2812, 1780, 1459, 1382 cm^{-1}; $[\alpha]^{25}_{D}$: –17.7 (c = 1.0, CH_2Cl_2); HRMS (ESI) calculated for $C_{14}H_{24}O_6Na$ (M+Na) 311.1471, observed 311.1474; mp 105–113 ºC; X-ray: CCDC 146074.

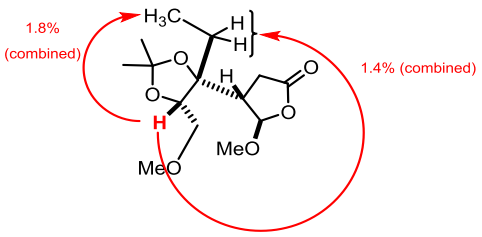

NOE for **4.42f**

(+)-Methyl (4*R*,5*S*)-4-((benzyloxy)methyl)-5-((*R*)-hydroxy((1*S*,3a*S*,7a*S*)-4,4,7a-trimethyloctahydro-1*H*-inden-1-yl)methyl)-2,2-dimethyl-1,3-dioxolane-4-carboxylate (4.46): A 4 mL scintillation vial was charged with alcohol **4.45**[32] (130 mg, 0.275 mmol), followed by the addition of *n*-hexanes (0.55 mL, 0.5 M). To this stirring solution, $PhSiH_2OiPr$ (69 mg, 0.41 mmol), and a solution of TBHP in hexanes (75 µL mL of 5.5 M soln, 0.41 mmol) were added and the resulting mixture was degassed by sparging with argon for 10 min. Next, $Mn(dpm)_3$ (17 mg, 0.028 mmol) was added in one portion and the reaction was then further degassed for an additional 30 seconds. The resulting mixture was allowed to stir at 23 ºC for 1 h. Upon complete consumption of the starting material, as indicated by TLC analysis (10% EtOAc in hexanes; visualized with

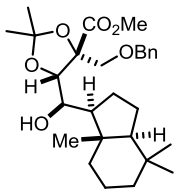

4.46: $C_{28}H_{42}O_6$
Molecular Weight: 474.6380

ceric ammonium molybdate), the reaction was transferred directly onto a silica gel column and purified by flash column chromatography (5% EtOAc in hexanes to 8% EtOAc in hexanes), yielding ester **4.46** as a colorless oil (83 mg, 0.18 mmol, 63% yield). R_f 0.40 (20% EtOAc in hexanes; visualized with ceric ammonium molybdate). ^{1}H NMR (500 MHz, $CDCl_3$) δ 7.32–7.23 (m, 5H), 4.58 (d, *J* = 12.5 Hz, 1H), 4.52 (d, *J* = 12.5 Hz, 1H), 4.31 (s, 1H), 3.94 (d, *J* = 9.5 Hz, 1H), 3.85 (t, *J* = 8.5 Hz, 1H), 3.78–3.76 (m, 4H), 2.20 (d, *J* = 9.5 Hz, 1H), 1.88–1.82 (m, 1H), 1.70–1.68 (m, 1H), 1.62–1.50 (m, 4H), 1.48 (s, 3H), 1.47–1.43 (m, 2H), 1.42–1.35 (m, 4H), 1.12–1.02 (m, 3H), 0.85 (s, 3H), 0.84 (s, 3H), 0.78 (s, 3H); ^{13}C NMR (125 MHz, $CDCl_3$) δ 172.78, 138.02, 128.47, 127.81, 127.76, 109.91, 85.32, 80.22, 73.71, 72.28, 69.97, 58.54, 55.63, 52.71, 42.26, 41.47, 39.67, 33.70, 33.27, 27.67, 25.34, 25.19, 20.94, 20.68, 19.20, 13.81; IR (thin film) 2923, 1765, 1727, 1598, 1382 cm^{-1}; $[\alpha]^{23}_D$: +19.1 (c = 0.4, CH_2Cl_2); HRMS (ESI) calculated for $C_{28}H_{42}O_6Na$ (M+Na) 497.2879, observed 497.2855.

(+)-(4*R*,5*S*)-4-((Benzyloxy)methyl)-5-((*R*)-hydroxy((1*S*,3a*S*,7a*S*)-4,4,7a-trimethyloctahydro-1*H*-inden-1-yl)methyl)-2,2-dimethyl-1,3-dioxolane-4-carboxylic acid (4.47): A 20 mL scintillation vial was charged with ester **4.46** (76 mg, 0.16 mmol), followed by the addition of 1:1:1 MeOH:THF:H_2O (4.9 mL, 0.033 M). Next, LiOH•H_2O (42 mg, 1.0 mmol) was added. The resulting heterogeneous mixture was stirred vigorously at 40 ºC for 72 h. Upon allowing reaction mixture to cool down to 23 ºC, the solution was treated with aq. HCl (1 mL of 1 N soln) and EtOAc (1 mL). The resulting biphasic mixture was extracted with EtOAc (3 x 2 mL).

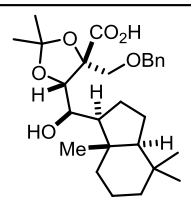

4.47: $C_{27}H_{40}O_6$
Molecular Weight: 460.6110

Combined organic layers washed with brine (1 x 10 mL), dried over $MgSO_4$, and evaporated under reduced pressure to yield acid **4.47** as a colorless oil (55 mg, 0.12 mmol, 76% yield). ^{1}H NMR (500 MHz, $CDCl_3$) δ 7.34–7.26 (m, 5H), 4.58 (s, 2H), 4.27 (s, 1H), 3.94 (d, *J* = 10.5 Hz, 1H), 3.87–3.83 (m, 2H), 1.85–1.83 (m, 1H), 1.68–1.66 (m, 1H), 1.68–1.53 (m, 4H), 1.45 (s, 3H), 1.43–1.40 (m, 7H), 1.11–0.99 (m, 3H), 0.85 (s, 3H), 0.83 (s, 3H), 0.79 (s, 3H); ^{13}C NMR (125 MHz, $CDCl_3$) δ 172.82, 137.68, 128.59, 127.92, 127.81, 110.64, 85.84, 80.40, 73.97, 72.19, 70.18, 58.56, 55.60, 42.34, 41.46, 39.61, 33.69, 33.27, 27.76, 25.56, 25.04, 20.95, 20.68, 19.92, 13.89; IR (thin film) 1943, 2924, 1737, 1383, 1217 cm^{-1}; $[\alpha]^{23}_D$: +27.8 (c = 2.7, CH_2Cl_2); HRMS (ESI) calculated for $C_{27}H_{40}O_6Na$ (M+Na) 483.2722, observed 483.2706.

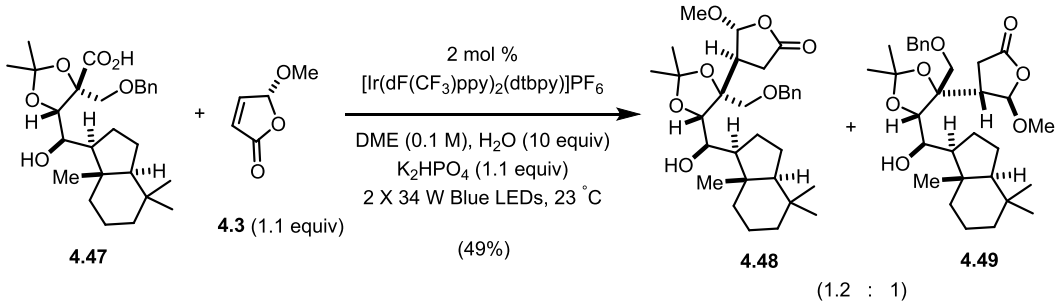

(+)-(4*S*,5*R*)-4-((4*R*,5*S*)-4-((Benzyloxy)methyl)-5-((*R*)-hydroxy((1*S*,3a*S*,7a*S*)-4,4,7a-trimethyloctahydro-1*H*-inden-1-yl)methyl)-2,2-dimethyl-1,3-dioxolan-4-yl)-5-methoxydihydrofuran-2(3*H*)-one (4.48): A 4 mL scintillation vial equipped with a Teflon septum and magnetic stir bar was charged with carboxylic acid **4.47** (32 mg, 0.070 mmol), K_2HPO_4 (13 mg, 0.77 mmol), and Ir[dF(CF_3)ppy)]$_2$(dtbbpy)PF_6 (1.6 mg, 0.0014 mmol). Next, DME (0.7 mL, 0.1 M) was added, followed by water (13 µL, 0.70 mmol), and butenolide **4.3** (9 mg, 0.08 mmol). The reaction mixture was degassed by sparging with argon for 15 min and the vial was sealed and irradiated (2 x 34 W blue LED lamps)

for 24 h at 23 ºC. The reaction mixture was filtered through $MgSO_4$, and evaporated under reduced pressure to yield a yellow oil. ^{1}H NMR analysis of the crude residue displayed a 1.2:1 ratio of **4.48**:**4.49**.The crude residue was purified by flash column chromatography (4% EtOAc in hexanes to 8% EtOAc in hexanes) to yield **4.48** as a colorless oil (18 mg, 0.34 mmol, 49% yield). Minor diastereomer **4.49** could not be isolated in pure form by column chromatography. R_f 0.26 (10% EtOAc in hexanes; visualized with ceric ammonium molybdate). ^{1}H NMR for **4.48** (500 MHz, $CDCl_3$) δ 7.37–7.26 (m, 5H), 5.42 (d, *J* = 4.0, 1H), 4.56 (d, *J* = 11.5 Hz, 1H), 4.44 (d, *J* = 11.5 Hz, 1H), 3.86 (d, *J* = 10.0 Hz, 1H), 3.81 (br s, 1H), 3.65 (s, 1H), 3.47 (s, 3H), 3.30 (d, *J* = 10.0 Hz, 1H), 2.88–2.81 (m, 2H), 2.65–2.62 (m, 2H), 1.80–1.75 (m, 1H), 1.66–1.57 (m, 5H), 1.43–1.38 (m, 5H), 1.35–1.28 (m, 4H), 1.10–0.96 (m, 3H), 0.84 (s, 3H), 0.83 (s, 3H), 0.73 (s, 3H); ^{13}C NMR for **4.48** (125 MHz, $CDCl_3$) δ 175.01, 137.45, 129.00, 128.57, 128.53, 108.43, 106.83, 81.72, 81.70, 74.27, 69.88, 68.34, 58.62, 57.63, 54.99, 44.99, 42.63, 41.68, 40.07, 33.91, 33.47, 30.38, 28.97, 27.13, 24.38, 21.19, 20.95, 20.18, 14.81; IR (thin film) 2924, 2873, 1789, 1454, 1382 cm^{-1}; $[\alpha]^{23}_D$: +12.17 (c = 1.2, CH_2Cl_2); HRMS (ESI) calculated for $C_{31}H_{46}O_7Na$ (M+Na) 553.3141, observed 553.3146.

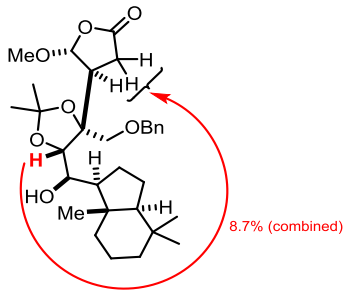

NOE for **4.48**

(+)-Methyl (4*R*,5*S*)-5-((*R*)-hydroxy((1*S*,3a*S*,7a*S*)-4,4,7a-trimethyloctahydro-1H-inden-1-yl)methyl)-4-(hydroxymethyl)-2,2-dimethyl-1,3-dioxolane-4-carboxylate (4.50): To a suspension of 10% Pd/C (0.207 g, 0.195 mmol) in MeOH (4 mL) was added alcohol **4.45**[32] (0.230 g, 0.487 mmol) in a solution of MeOH (0.5 mL). The reaction vessel was then evacuated and refilled with H_2 (3x). The reaction was then vigorously stirred at 23 ºC for 18 h, at which point the reaction vessel was purged with Ar to remove remaining H_2. The suspension was then filtered through Celite and concentrated *in vacuo*. The crude residue was purified by flash column chromatography (20% EtOAc in hexanes to 40% EtOAc in hexanes) to yield diol ester **4.50** as a colorless solid (0.127 g, 0.330 mmol, 69% yield). R_f 0.40 (50% EtOAc in hexanes; visualized with ceric ammonium molybdate). ^{1}H NMR (500 MHz, $CDCl_3$) δ 4.34 (s, 1H), 3.98 (d, *J* = 8.8 Hz, 1H), 3.86 (s, 2H), 3.82 (s, 3H), 2.82–1.98 (bs, 2H), 1.94–1.85 (m, 1H), 1.76–1.56 (m, 5H), 1.54–1.34 (m, 3H), 1.52 (s, 3H), 1.42 (s, 3H), 1.19–1.11 (m, 2H), 1.04 (td, *J* = 13.4, 4.0 Hz, 1H), 0.87 (s, 3H), 0.85 (s, 3H), 0.83 (s, 3H); ^{13}C NMR (125 MHz, $CDCl_3$) δ 172.21, 109.67, 84.93, 79.61, 70.20, 63.99, 58.49, 55.50, 52.84, 42.33, 41.36, 39.59, 33.63, 33.22, 27.76, 25.60, 25.26, 20.87, 20.60, 19.88, 13.69; IR (thin film) 3415, 2985, 2963, 2875, 1739, 1457 cm^{-1}; $[\alpha]^{25}_D$: +40.1 (c = 1.3, CH_2Cl_2); HRMS (ESI) calculated for $C_{21}H_{36}O_6Na$ (M+Na) 407.2410, observed 407.2393.

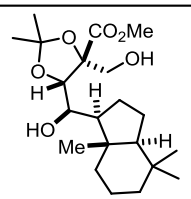

4.50: $C_{21}H_{36}O_6$
Molecular Weight: 384.5130

(+)-(4*R*,5*S*)-5-((*R*)-Hydroxy((1*S*,3a*S*,7a*S*)-4,4,7a-trimethyloctahydro-1*H*-inden-1-yl)methyl)-4-(hydroxymethyl)-2,2-dimethyl-1,3-dioxolane-4-carboxylic acid (4.51): A 20 mL scintillation vial was charged with ester **4.50** (82 mg, 0.21 mmol), followed by the addition of 1:1:1 MeOH:THF:H_2O (3.6 mL, 0.06 M). Next, LiOH•H_2O (18 mg, 0.42 mmol) was added. The resulting heterogeneous mixture was stirred vigorously at 23 ºC for 18 h. Next, the solution was treated with aq. HCl (1 mL of 1 N soln) and EtOAc (1 mL). The resulting biphasic mixture was extracted with EtOAc (3 x 2 mL). Combined organic layers washed with brine (1 x 10 mL), dried over $MgSO_4$, and evaporated under reduced pressure to yield acid **4.51** as a colorless solid (77 mg, 0.21 mmol, 100% yield). ^{1}H NMR (500 MHz, $CDCl_3$) δ 5.62–4.43 (br s, 2H), 4.31 (s, 1H), 3.98–3.88 (m, 3H), 1.92–1.85 (m, 1H), 1.73–1.54 (m, 8H), 1.48–1.35 (m, 6H), 1.14–1.00 (m, 3H), 0.84 (s, 3H), 0.80 (s, 3H), 0.72 (s, 3H); ^{13}C NMR (125 MHz, $CDCl_3$) δ 174.05, 110.29, 84.97, 79.86, 70.35, 63.83, 58.56, 55.47, 42.40, 41.40, 39.60, 33.68, 33.28, 27.61, 25.60, 25.33, 20.93, 20.64, 19.92, 13.83; IR (thin film) 3418, 2932, 1733, 1373, 763 cm^{-1}; $[\alpha]^{23}_D$: +22.6 (c = 1.7, CH_2Cl_2); HRMS (ESI) calculated for $C_{20}H_{34}O_6Na$ (M+Na) 393.2253, observed 393.2256.

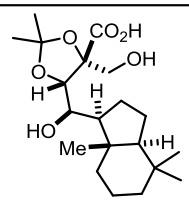

4.51: $C_{20}H_{34}O_6$
Molecular Weight: 370.4860

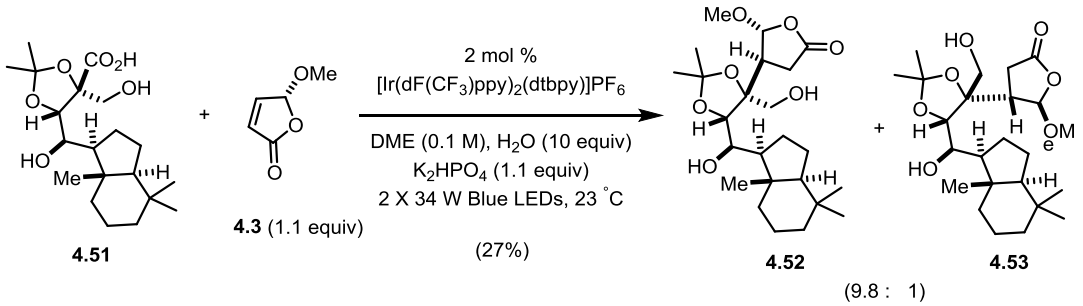

(+)-(4*S*,5*R*)-4-((4*R*,5*S*)-5-((*R*)-Hydroxy((1*S*,3a*S*,7a*S*)-4,4,7a-trimethyloctahydro-1H-inden-1-yl)methyl)-4-(hydroxymethyl)-2,2-dimethyl-1,3-dioxolan-4-yl)-5-methoxydihydrofuran-2(3H)-one (4.52/4.53): A 4 mL scintillation vial equipped with a Teflon septum and magnetic stir bar was charged with carboxylic acid **4.51** (25 mg, 0.067 mmol), K_2HPO_4 (13 mg, 0.77 mmol), and Ir[dF(CF_3)ppy)]$_2$(dtbbpy)PF_6 (1.6 mg, 0.0014 mmol). Next, DME (0.7 mL, 0.1 M) was added, followed by water (13 µL, 0.67 mmol), and butenolide **4.3** (9 mg, 0.08 mmol). The reaction mixture was degassed by sparging with argon for 15 min and the vial was sealed and irradiated (2 x 34 W blue LED lamps) for 24 h at 23 ºC. The reaction mixture was filtered through $MgSO_4$, and evaporated under reduced pressure. ^{1}H NMR analysis of the crude residue displayed a 9.8:1 ratio of **9c**:**10c**. The crude residue was purified by flash column chromatography using pH 7 buffered silica gel (15% EtOAc in hexanes to 23% EtOAc in hexanes) to yield lactone **4.52** as a clear oil (8 mg, 0.02 mmol, 27% yield). Minor diastereomer **4.53** could not be isolated in pure form by column chromatography. R_f 0.25 (40% EtOAc in hexanes; visualized with ceric ammonium molybdate). ^{1}H NMR (500 MHz, $CDCl_3$) δ 5.51 (d, *J* = 5.3 Hz, 1H), 3.92 (d, *J* = 12.5 Hz, 1H), 3.79 (d, *J* = 8.9 Hz, 1H), 3.62–3.58 (m, 1H), 3.59 (s, 3H), 3.33 (d, *J* = 12.5 Hz, 1H), 2.85 (td, *J* = 9.4, 5.4 Hz, 1H), 2.71 (dd, *J* = 16.9, 9.1 Hz, 1H), 2.62 (dd, *J* = 16.9, 9.3 Hz, 1H), 1.95–1.85 (m, 1H), 1.75–1.49 (m, 7H), 1.49 (s, 3H), 1.34 (s, 3H), 1.20–1.11 (m, 2H), 1.08–1.00 (m, 1H), 0.91–0.83 (m, 1H), 0.86 (s, 3H), 0.85 (s, 3H), 0.74 (s, 3H);

^{13}C NMR (125 MHz, $CDCl_3$) δ 173.87, 108.25, 106.39, 81.73, 80.31, 68.96, 61.66, 58.46, 57.94, 55.01, 43.60, 42.26, 41.24, 39.86, 33.57, 33.20, 30.14, 28.68, 26.85, 25.29, 20.86, 20.54, 19.89, 14.28; IR (thin film) 3453, 2927, 1790, 1460, 1382 cm^{-1}; $[\alpha]^{25}_{D}$: +37.0 (c = 0.7, CH_2Cl_2); HRMS (ESI) calculated for $C_{24}H_{40}O_7Na$ (M+Na) 463.2672, observed 463.2667.

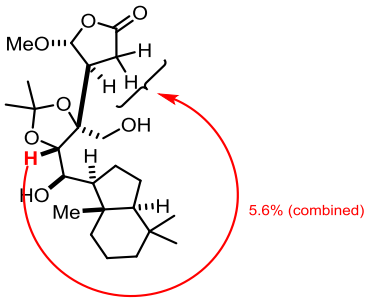

NOE for **4.52**

(+)-Methyl (4*R*,5*S*)-4-(((tert-butyldimethylsilyl)oxy)methyl)-5-((*R*)-hydroxy((1*S*,3a*S*,7a*S*)-4,4,7a-trimethyloctahydro-1H-inden-1-yl)methyl)-2,2-dimethyl-1,3-dioxolane-4-carboxylate (4.57): To a solution of **4.50** (80 mg, 0.21 mmol) in CH_2Cl_2 (2.5 mL) at 0 ºC was added imidazole (85 mg, 1.3 mmol) followed by TBS-Cl (94 mg, 0.62 mmol). The reaction was stirred at 0 ºC until starting material was consumed as monitored by TLC (about 45 min). H_2O (1 mL) was added to the solution, and the aqueous layer was extracted with CH_2Cl_2 (3 x 1 mL). The combined organic layers were then dried over Na_2SO_4 and concentrated *in vacuo*. The crude residue was purified by flash column chromatography (5% EtOAc in hexanes) to yield ester **4.57** as a light yellow oil (0.104 g, 0.209 mmol, 99% yield). R_f 0.50 (10% EtOAc in hexanes; visualized with ceric ammonium molybdate). ^{1}H NMR (500 MHz, $CDCl_3$) δ 4.47 (s, 1H), 4.14 (d, *J*

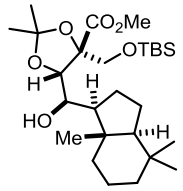

4.57: $C_{27}H_{50}O_6Si$
Molecular Weight: 498.7760

= 10.0 Hz, 1H), 3.98 (app t, *J* = 8.6 Hz, 1H), 3.81 (d, *J* = 10.0 Hz, 1H), 3.78 (s, 3H), 2.53 (d, *J* =8.7 Hz, 1H), 1.95–1.84 (m, 1H), 1.79 (dt, *J* = 12.2, 3.0 Hz, 1H), 1.67–1.58 (m, 3H), 1.49 (s, 3H), 1.45–1.38 (m, 1H), 1.36 (s, 3H), 1.32–1.23 (m, 3H), 1.18–1.10 (m, 1H), 1.09–1.08 (m, 1H), 0.96 (d, *J* = 6.8 Hz, 1H), 0.89–0.81 (m, 18H), 0.05 (s, 3H), 0.04 (s, 3H); ^{13}C NMR (125 MHz, $CDCl_3$) δ 172.60, 109.24, 85.12, 79.41, 69.39, 64.80, 58.51, 55.57, 52.44, 42.20, 41.48, 39.64, 33.67, 33.22, 27.67, 25.84, 25.45, 25.41, 20.90, 20.62, 19.95, 18.24, 13.72, –5.44, –5.59; IR (thin film) 3568, 2952, 2929, 2858, 1742, 1462 cm^{-1}; $[\alpha]^{25}_{D}$: +23.0 (c = 2.9, CH_2Cl_2); HRMS (ESI) calculated for $C_{27}H_{50}O_6SiNa$ (M+Na) 521.3275, observed 521.3280.

(+)-(4*R*,5*S*)-4-(((*Tert*-butyldimethylsilyl)oxy)methyl)-5-((*R*)-hydroxy((1*S*,3a*S*,7a*S*)-4,4,7a-trimethyloctahydro-1*H*-inden-1-yl)methyl)-2,2-dimethyl-1,3-dioxolane-4-carboxylic acid (4.58): The procedure for the preparation of **4.58** was a slight modification from the literature procedure.[25] A 4 mL scintillation vial was charged with ester **4.57** (94 mg, 0.19 mmol), followed by the addition of DCE (1.2 mL, 0.16 M). Next, Me_3SnOH (170 mg, 0.94 mmol) was added. The resulting heterogeneous mixture was stirred vigorously at 80 ºC for 36 h. Upon allowing reaction mixture to cool down to 23 ºC, the solution was treated with aq. HCl (1 mL of 1 N soln) and CH_2Cl_2 (1 mL). The resulting biphasic mixture was extracted with aq. HCl (5 x 1 mL of 1 N soln). Organic layer was washed with brine (1 x 5 mL), dried over $MgSO_4$, and evaporated under reduced pressure to yield acid **4.58** as a colorless oil (91 mg, 0.19 mmol, 99% yield). ^{1}H NMR (500 MHz, $CDCl_3$) δ 4.34 (s, 1H), 4.09 (d, *J* = 10.5 Hz, 1H), 3.92 (d, *J* = 10.5 Hz, 1H), 3.87 (d, *J* = 8.0

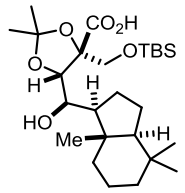

4.58: $C_{26}H_{48}O_6Si$
Molecular Weight: 484.7490

Hz, 1H), 1.92–1.84 (m, 1H), 1.75–1.69 (m, 1H), 1.64–1.55 (m, 4H), 1.53 (s, 3H), 1.49–1.22 (m, 7H), 1.14–0.94 (m, 3H), 0.87–0.84 (m, 15H), 0.80 (s, 3H), 0.05 (s, 6H); ^{13}C NMR (125 MHz, $CDCl_3$) δ 174.37, 110.05, 86.30, 79.82, 70.10, 65.66, 58.58, 55.66, 42.31, 41.48, 39.63, 33.71, 33.28, 27.77, 25.97, 25.48, 25.28, 20.95, 20.67, 19.95, 18.41, 13.84, –5.29, –5.31; IR (thin film) 3322, 2922, 2613, 1734, 1073 cm^{-1}; $[\alpha]^{23}_{D}$: +24.4 (c = 2.0, CH_2Cl_2); HRMS (ESI) calculated for $C_{26}H_{48}O_6SiNa$ (M+Na) 507.3118, observed 507.3131.

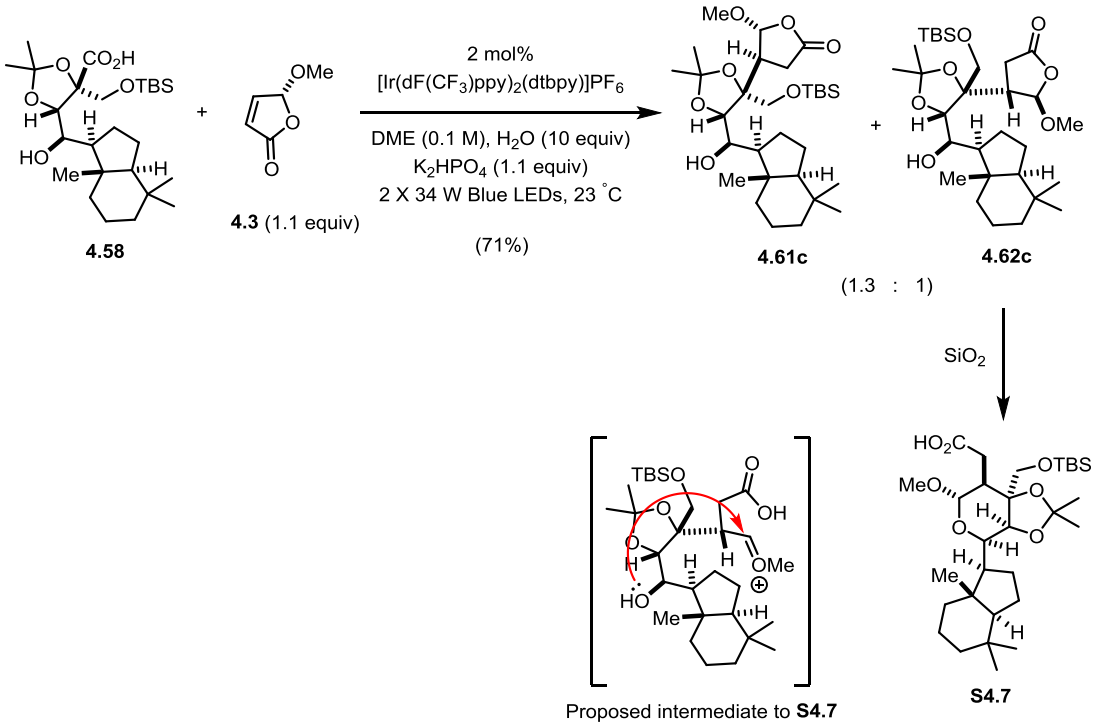

(–)-(4*S*,5*R*)-4-((5*S*)-4-(((Tert-butyldimethylsilyl)oxy)methyl)-5-((*R*)-hydroxy((1*S*,3a*S*,7a*S*)-4,4,7a-trimethyloctahydro-1H-inden-1-yl)methyl)-2,2-dimethyl-1,3-dioxolan-4-yl)-5-methoxydihydrofuran-2(3H)-one (4.61c/4.62c): A 4 mL scintillation vial equipped with a Teflon septum and magnetic stir bar was charged with carboxylic acid **4.58** (32 mg, 0.067 mmol), K_2HPO_4 (13 mg, 0.77 mmol), and

$Ir[dF(CF_3)ppy)]_2(dtbbpy)PF_6$ (1.6 mg, 0.0014 mmol). Next, DME (0.7 mL, 0.1 M) was added, followed by water (13 µL, 0.67 mmol), and butenolide **4.3** (9 mg, 0.08 mmol). The reaction mixture was degassed by sparging with argon for 15 min and the vial was sealed and irradiated (2 x 34 W blue LED lamps) for 24 h at 23 ºC. The reaction mixture was filtered through $MgSO_4$, and evaporated under reduced pressure. ^{1}H NMR analysis of the crude residue displayed a 1.3:1 ratio of **4.61c**:**4.62c**. The crude residue was purified by flash column chromatography (5% EtOAc in hexanes to 30% EtOAc in hexanes) to yield lactone **4.61c** as a yellow oil (15 mg, 0.027 mmol, 41% yield) and acid **S4.7** from SiO_2-mediated rearrangement of **4.62c** (11 mg, 0.020 mmol, 30% yield) as a yellow oil. R_f of **4.61c**: 0.40 (20% EtOAc in hexanes; visualized with ceric ammonium molybdate). R_f of **S4.7**: 0.20 (50% EtOAc in hexanes; visualized with ceric ammonium molybdate).

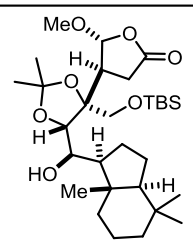

4.61c: $C_{30}H_{54}O_7Si$
Molecular Weight: 554.8400

^{1}H NMR for major diastereomer **4.61c** (500 MHz, $CDCl_3$) δ 5.48 (d, *J* = 3.1 Hz, 1H), 4.08 (d, *J* = 10.5 Hz, 1H), 3.82 (app t, *J* = 6.9 Hz, 1H), 3.68 (s, 1H), 3.49 (s, 3H), 3.43 (d, *J* = 10.5 Hz, 1H), 2.88 (app d, *J* = 7.1 Hz, 1H), 2.83–2.79 (m, 1H), 2.71 (dd, *J* = 17.3, 9.4 Hz, 1H), 2.57 (dd, *J* = 17.3, 6.0 Hz, 1H), 1.94–1.85 (m, 1H), 1.65–1.45 (m, 7H), 1.44–1.40 (m, 1H), 1.42 (s, 3H), 1.36–1.32 (m, 1H), 1.34 (s, 3H), 1.18–1.08 (m, 1H), 1.04 (app td, *J* = 13.1, 4.2 Hz, 1H), 0.91 (s, 9H), 0.85 (s, 3H), 0.84 (s, 3H), 0.75 (s, 3H), 0.10 (s, 6H); ^{13}C NMR for major diastereomer **4.61c** (125 MHz, $CDCl_3$) δ 175.28, 108.33, 106.27, 82.33, 81.30, 67.57, 62.26, 58.41, 56.96, 55.79, 44.42, 42.14, 41.37, 39.94, 33.60, 33.18, 30.00, 28.85, 26.98, 25.83, 24.94, 20.87, 20.55, 19.91, 18.17, 14.29, –5.59, –5.77; IR (thin film) 3568, 2953, 2929, 2858, 1794, 1463, 1382 cm^{-1}; $[\alpha]^{25}_D$

: –1.7 (c = 2.5, CH_2Cl_2); HRMS (ESI) calculated for $C_{30}H_{54}O_7SiNa$ (M+Na) 577.3536, observed 577.3520.

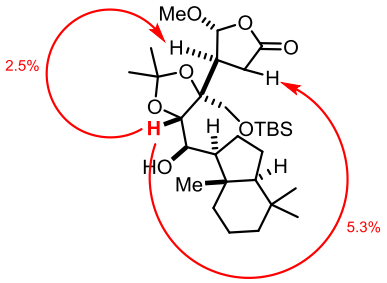

NOE for **4.61c**

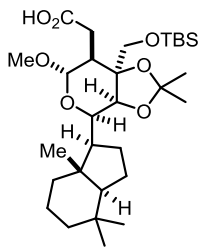

S4.7: $C_{60}H_{108}O_{14}Si_2$
Molecular Weight: 1109.6800

^{1}H NMR for minor diastereomer **S4.7** (500 MHz, $CDCl_3$) δ 4.54 (d, *J* = 7.3 Hz, 1H), 4.20 (app s, 1H), 3.66 (d, *J* = 10.2 Hz, 1H), 3.58 (app d, *J* = 8.7 Hz, 1H), 3.48 (d, *J* = 10.3 Hz, 1H), 3.36 (s, 3H), 2.66 (dd, *J* = 14.6, 4.1 Hz, 1H), 2.41 (app td, *J* = 8.1, 4.2 Hz, 1H), 2.33 (dd, *J* = 14.5, 8.7 Hz, 1H), 1.97–1.90 (m, 1H), 1.78–1.67 (m, 2H), 1.63–1.46 (m, 4H), 1.45–1.39 (m, 1H), 1.43 (s, 3H), 1.35 (s, 3H), 1.34–1.30 (m, 1H), 1.22–1.14 (m, 2H), 1.09–1.02 (m, 1H), 0.88 (s, 9H), 0.86 (s, 3H), 0.85 (s, 3H), 0.76 (s, 3H), 0.07 (s, 3H), 0.06 (s, 3H); ^{13}C NMR for minor diastereomer **S4.7** (125 MHz, $CDCl_3$) δ 177.52, 110.52, 102.00, 82.19, 79.43, 72.01, 65.56, 58.29, 55.32, 51.03, 41.96, 41.57, 39.50, 37.81, 33.71, 33.36, 33.21, 29.22, 27.38, 25.95, 25.40, 20.94, 20.79, 19.99, 18.26, 14.24, –5.43, –5.48; IR (thin film) 2928, 2858, 1712, 1463, 1366 cm^{-1}; $[\alpha]^{25}_D$: +45.1 (c = 1.2, CH_2Cl_2); HRMS (ESI) calculated for $C_{30}H_{54}O_7Na$ (M+Na) 577.3536, observed 577.3536.

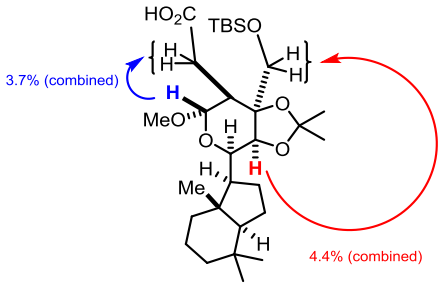

NOE for **S12**

(–)-Methyl (4*R*,5*S*)-4-((benzyloxy)methyl)-5-((*R*)-((tert-butyldimethylsilyl)oxy)((3a*S*,7a*S*)-3a,7,7-trimethyl-3a,4,5,6,7,7a-hexahydro-1H-inden-3-yl)methyl)-2,2-dimethyl-1,3-dioxolane-4-carboxylate (4.54): To a solution at 0 ºC of alcohol **4.45** (0.132 g, 0.279 mmol), in CH_2Cl_2 (2 mL) and 2,6-lutidine (0.10 mL, 1.1 mmol) was added TBSOTf (160 µL, 0.56 mmol). The reaction was maintained at 0 ºC for 15 min before allowing to warm to 23 ºC for 6 h, at which point H_2O (1 mL) was added to the reaction. The aqueous layer was extracted with CH_2Cl_2 (3 x 1 mL), and the combined organic layers were then dried over Na_2SO_4 and concentrated *in vacuo*. The crude residue was purified by flash column chromatography (0% EtOAc in hexanes to 8% EtOAc in hexanes) to afford ester **4.54** as a yellow oil (0.142 g, 0.242 mmol, 87% yield). R_f 0.70 (20% EtOAc in hexanes; visualized with ceric ammonium molybdate). ^{1}H NMR (500 MHz, $CDCl_3$) δ 7.34–7.23 (m, 5H), 5.68 (app s, 1H), 4.62 (d, *J* = 12.6 Hz, 1H), 4.54 (d, *J* = 12.6 Hz, 1H), 4.38 (app s, 1H), 4.25 (d, *J* = 2.4 Hz, 1H), 3.85 (d, *J* = 9.8 Hz, 1H), 3.78 (d, *J* = 9.8 Hz, 1H), 3.74 (s, 3H), 2.04 (ddd, *J* = 15.2, 6.4, 3.2 Hz, 1H), 1.94 (app t, *J* = 11.9 Hz, 1H), 1.69 (app qt, *J* = 12.9, 3.2 Hz, 1H), 1.60–1.43 (m, 2H), 1.55 (s, 3H), 1.41 (s, 3H), 1.32–1.14 (m, 2H), 1.10 (td, *J* = 13.4, 4.6 Hz, 1H), 1.03 (dd, *J* = 14.4, 7.6 Hz, 1H), 0.94 (s, 6H), 0.86 (s, 3H), 0.85 (s, 9H), –0.03 (s, 3H), –0.05 (s, 3H); ^{13}C NMR (125 MHz,

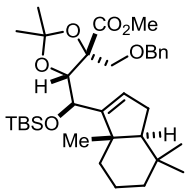

4.54: $C_{34}H_{54}O_6Si$
Molecular Weight: 586.8850

$CDCl_3$) δ 173.16, 153.08, 138.24, 128.39, 127.66, 127.64, 127.36, 110.37, 85.45, 82.22, 73.62, 71.84, 67.04, 59.66, 52.52, 47.30, 41.56, 35.62, 32.29, 32.89, 28.54, 27.69, 26.25, 25.87, 21.48, 20.15, 18.43, 18.14, –2.82, –4.37; IR (thin film) 2987, 2950, 2855, 1744, 1461, 1379 cm^{-1}; $[\alpha]^{25}_{D}$: –27.9 (c = 2.2, CH_2Cl_2); HRMS (ESI) calculated for $C_{34}H_{54}O_6SiNa$ (M+Na) 609.3588, observed 609.3602.

(+)-Methyl (4*R*,5*S*)-5-((*R*)-((tert-butyldimethylsilyl)oxy)((1*S*,3a*S*,7a*S*)-4,4,7a-trimethyloctahydro-1H-inden-1-yl)methyl)-4-(hydroxymethyl)-2,2-dimethyl-1,3-dioxolane-4-carboxylate (4.55): Ester **4.54** (32 mg, 0.055 mmol) and 10% Pd/C (12 mg, 0.011 mmol) were charged into a flask with MeOH (1.0 mL). The reaction vessel was then evacuated and refilled with H_2 (3x). The reaction was then vigorously stirred at 23 ºC for 12 h, at which point the reaction vessel was purged with Ar to remove remaining H_2. The reaction mixture was filtered through Celite, concentrated *in vacuo*, and then dissolved EtOAc (1 mL). To the solution was added PtO_2 (25 mg, 0.11 mmol) which was then placed in a Parr high pressure vessel and subsequently filled with H_2 (10 atm). The vessel was placed on top of an IKA magnetic plate and stirred for 3 h before being removed. The resulting suspension was filtered through Celite and concentrated *in vacuo*. The afforded residue was then purified by flash column chromatography (20% EtOAc in hexanes) provided alcohol **4.55** (23 mg, 0.046 mmol, 83%) as a colorless solid. R_f 0.30 (30% EtOAc in hexanes; visualized with ceric ammonium molybdate). ^1H NMR (500 MHz, $CDCl_3$) δ 4.17 (d, *J* = 9.2 Hz, 1H), 4.06 (d, *J* = 9.2 Hz, 1H), 4.01 (dd, *J* = 11.6, 8.1

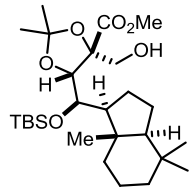

4.55: $C_{27}H_{50}O_6Si$
Molecular Weight: 498.7760

Hz, 1H), 3.81 (s, 3H), 3.63 (dd, J = 11.6, 5.8 Hz, 1H), 2.17 (dd, J = 7.9, 5.8 Hz, 1H), 2.06–1.98 (m, 1H), 1.71 (dt, J = 12.1, 3.2 Hz, 1H), 1.66–1.40 (m, 4H), 1.52 (s, 3H), 1.47 (s, 3H), 1.39–1.23 (m, 3H), 1.08–0.92 (m, 3H), 0.87 (s, 9H), 0.84 (s, 6H), 0.80 (s, 3H), 0.09 (s, 3H), 0.07 (s, 3H); ^{13}C NMR (125 MHz, $CDCl_3$) δ 172.18, 109.71, 84.30, 83.38, 68.54, 62.38, 58.27, 53.05, 52.55, 43.02, 41.81, 39.55, 33.68, 33.19, 28.07, 26.81, 24.98, 21.14, 20.99, 19.75, 19.48, 19.16, 16.07, –2.21, –3.19; IR (thin film) 3491, 2928, 2899, 2856, 1738, 1469, 1383 cm^{-1}; $[\alpha]^{25}_{D}$: +23.7 (c = 1.4, CH_2Cl_2); HRMS (ESI) calculated for $C_{27}H_{50}O_6SiNa$ (M+Na) 521.3275, observed 521.3281.

(+)-(4*R*,5*S*)-5-((*R*)-((Tert-butyldimethylsilyl)oxy)((1*S*,3a*S*,7a*S*)-4,4,7a-trimethyloctahydro-1H-inden-1-yl)methyl)-4-(hydroxymethyl)-2,2-dimethyl-1,3-dioxolane-4-carboxylic acid (4.56): The procedure for the preparation of **4.56** was a slight modification from the literature procedure.[25] To a solution of ester **4.55** (61 mg, 0.12 mmol) in DCE(0.5 mL) was added Me_3SnOH (0.110 g, 0.608 mmol). The heterogeneous mixture was then heated to 80 ºC for 24 h, at which point TLC analysis confirmed full consumption of starting material. The reaction was cooled to 23 ºC and diluted with CH_2Cl_2 (1 mL) and aq. HCl (1 mL of 1 M soln). The organic layer was washed with aq. HCl (5 x 1 mL of 4 M soln) and brine (1 x 2 mL) before being dried over Na_2SO_4. Upon concentration *in vacuo*, acid **4.56** was obtained (57 mg, 0.12 mmol, 96% yield) as a colorless solid. ^{1}H NMR (500 MHz, $CDCl_3$) δ 4.19 (d, J = 8.6 Hz, 1H), 4.06 (d, J = 8.6 Hz, 1H), 4.02 (d, J = 11.8 Hz, 1H), 3.68 (d, J = 11.7 Hz, 1H), 2.01 (app q, J = 11.0

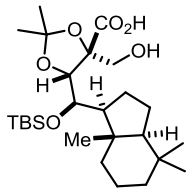

4.56: $C_{26}H_{48}O_6Si$
Molecular Weight: 484.7490

Hz, 1H), 1.69 (app d, J = 11.8 Hz, 1H), 1.63–1.22 (m, 6H), 1.54 (s, 3H), 1.47 (s, 3H), 1.10–0.91 (m, 4H), 0.88 (s, 9H), 0.84 (s, 6H), 0.80 (s, 3H), 0.09 (s, 3H), 0.07 (s, 3H); ^{13}C NMR (125 MHz, $CDCl_3$) δ 174.34, 109.87, 84.43, 82.63, 68.77, 62.49, 58.03, 52.28, 42.99, 41.73, 39.53, 33.62, 33.18, 27.99, 26.80, 24.95, 21.09, 21.00, 19.77, 19.58, 19.17, 16.07, –2.20, –3.11; IR (thin film) 3454, 2951, 2927, 2896, 1734, 1461 cm^{-1}; $[\alpha]^{25}_{D}$: +32.7 (c = 1.0, CH_2Cl_2); HRMS (ESI) calculated for $C_{26}H_{48}O_6SiNa$ (M+Na) 507.3118, observed 507.3113.

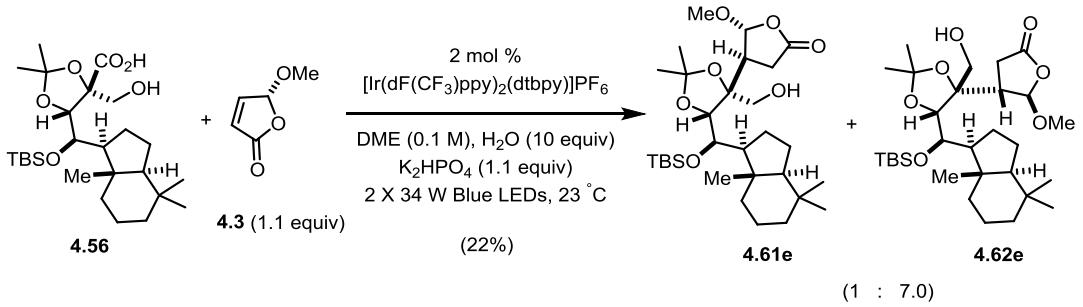

(+)-(4*S*,5*R*)-4-((5*S*)-5-((*R*)-((Tert-butyldimethylsilyl)oxy)((1*S*,3a*S*,7a*S*)-4,4,7a-trimethyloctahydro-1H-inden-1-yl)methyl)-4-(hydroxymethyl)-2,2-dimethyl-1,3-dioxolan-4-yl)-5-methoxydihydrofuran-2(3H)-one (4.61e/S4.62e): A 4 mL scintillation vial equipped with a Teflon septum and magnetic stir bar was charged with carboxylic acid **4.56** (32 mg, 0.067 mmol), K_2HPO_4 (13 mg, 0.77 mmol), and Ir[dF(CF_3)ppy)]$_2$(dtbbpy)PF_6 (1.6 mg, 0.0014 mmol). Next, DME (0.7 mL, 0.1 M) was added, followed by water (13 µL, 0.70 mmol), and butenolide **4.3** (9 mg, 0.08 mmol). The reaction mixture was degassed by sparging with argon for 15 min and the vial was sealed and irradiated (2 x 34 W blue LED lamps) for 24 h at 23 ºC. The reaction mixture was filtered through $MgSO_4$, and evaporated under reduced pressure. ^{1}H NMR analysis of the crude residue displayed a 1:7.0 ratio of **4.61e**:**4.62e**. The crude residue was purified by flash column chromatography (10%

EtOAc in hexanes to 20% EtOAc in hexanes) to yield lactone **4.62e** as a colorless oil (8 mg, 0.01 mmol, 22% yield). Minor diastereomer **4.62e** could not be isolated in pure form by column chromatography. R_f 0.20 (20% EtOAc in hexanes; visualized with ceric ammonium molybdate). ^{1}H NMR for major diastereomer **4.62e** (500 MHz, $CDCl_3$) δ 5.90 (s, 1H), 4.19 (d, *J* = 9.8 Hz, 1H), 4.17 (d, *J* = 9.9 Hz, 1H), 3.63 (dd, *J* = 12.2, 4.0 Hz, 1H), 3.51 (s, 3H), 3.47 (dd, *J* = 12.2, 8.4 Hz, 1H), 2.70 (dd, *J* = 18.2, 10.0 Hz, 1H), 2.60 (dd, *J* = 18.1, 3.0 Hz, 1H), 2.43 (dd, *J* = 9.9, 3.0 Hz, 1H), 2.17–2.10 (m, 1H), 1.87 (app dd, *J* = 8.3, 4.2 Hz, 1H), 1.78 (dt, *J* = 12.5, 3.3 Hz, 1H), 1.65–1.58 (m, 2H), 1.53–1.44 (m, 3H), 1.47 (s, 3H), 1.37 (s, 3H), 1.30–1.22 (m, 2H), 1.06–0.91 (m, 2H), 0.90 (s, 9H), 0.86 (s, 6H), 0.85 (s, 3H), 0.81–0.77 (m, 1H), 0.12 (s, 3H), 0.11 (s, 3H); ^{13}C NMR for major diastereomer **4.62e** (125 MHz, $CDCl_3$) δ 176.46, 107.41, 105.93, 83.34, 81.17, 68.47, 65.19, 58.51, 56.66, 53.15, 44.36, 43.14, 41.82, 40.00, 33.70, 33.21, 29.19, 26.82, 26.51, 25.86, 21.11, 20.97, 19.85, 19.18, 19.16, 16.48, –1.74, –2.83; IR (thin film) 3473, 2952, 2927, 2855, 1781, 1462, 1384 cm^{-1}; $[\alpha]^{25}_D$: +11.7 (c = 0.7, CH_2Cl_2); HRMS (ESI) calculated for $C_{30}H_{54}O_7SiNa$ (M+Na) 577.3536, observed 577.3541.

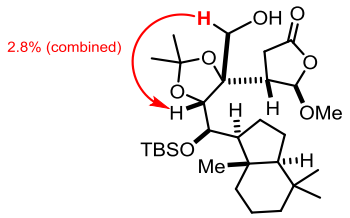

NOE for **4.62e**
(NOE in d^4-MeOH)

(+)-Methyl (4*R*,5*S*)-5-((*R*)-((tert-butyldimethylsilyl)oxy)((1*S*,3a*S*,7a*S*)-4,4,7a-trimethyloctahydro-1H-inden-1-yl)methyl)-4-(((tert-butyldimethylsilyl)oxy)methyl)-2,2-dimethyl-1,3-dioxolane-4-carboxylate (4.59): To a solution of **4.50** (0.117 g, 0.304 mmol) in CH_2Cl_2 (2 mL) at 0 ºC was added 2,6-lutidine (170 µL, 1.8 mmol) followed by TBSOTf (260 µL, 0.91 mmol). The reaction was then allowed to warm to 23 ºC over 12 h before H_2O (2 mL) was added. Celite (3 g) was then added to the heterogeneous mixture, and the suspension was concentrated *in vacuo*. The resulting crude residue suspending on Celite was then purified by flash column chromatography (0% EtOAc in hexanes to 4% EtOAc in hexanes) to yield ester **4.59** as a colorless oil (0.168 g, 0.274 mmol, 90% yield). R_f 0.60 (5% EtOAc in hexanes; visualized with ceric ammonium molybdate). ^{1}H NMR (500 MHz, $CDCl_3$) δ 4.27 (app d, *J* = 8.7 Hz, 1H), 4.16 (d, *J* = 8.7 Hz, 1H), 4.02 (d, *J* = 10.8 Hz, 1H), 3.87 (d, *J* = 10.8 Hz, 1H), 3.82 (s, 3H), 2.11–2.02 (m, 1H), 1.80 (dt, *J* = 12.1, 3.0 Hz, 1H), 1.71–1.47 (m, 4H), 1.58 (s, 3H), 1.49 (s, 3H), 1.45–1.30 (m, 3H), 1.16–1.01 (m, 3H), 0.96 (s, 9H), 0.94 (s, 9H), 0.91 (s, 6H), 0.87 (s, 3H), 0.16 (s, 3H), 0.14 (s, 3H), 0.13 (s, 3H), 0.12 (s, 3H); ^{13}C NMR (125 MHz, $CDCl_3$) δ 172.71, 109.12, 85.08, 82.62, 69.36, 63.92, 58.20, 52.65, 52.25, 42.94, 41.82, 39.70, 33.68, 33.22, 27.46, 26.88, 26.15, 24.92, 21.20, 21.04, 19.88, 19.79, 19.25, 18.62, 16.04, –1.96, –2.92, –5.08, –5.23; IR (thin film) 2953, 2928, 2857, 1736, 1462, 1379 cm^{-1}; $[\alpha]^{25}_D$: +24.4 (c = 1.2, CH_2Cl_2); HRMS (ESI) calculated for $C_{33}H_{64}O_6Si_2Na$ (M+Na) 635.4139, observed 635.4146.

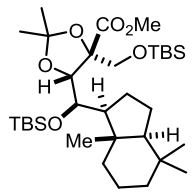

4.59: $C_{33}H_{64}O_6Si_2$
Molecular Weight: 613.0390

(+)-(4*R*,5*S*)-5-((*R*)-((Tert-butyldimethylsilyl)oxy)((1*S*,3a*S*,7a*S*)-4,4,7a-trimethyloctahydro-1H-inden-1-yl)methyl)-4-(((tert-butyldimethylsilyl)oxy)methyl)-2,2-dimethyl-1,3-dioxolane-4-carboxylic acid (4.60): The procedure for the preparation of **4.60** was a slight modification from the literature procedure.[25] To a solution of ester **4.59** (0.122 g, 0.199 mmol) in DCE (1.2 mL) was added Me_3SnOH (0.252 g, 1.39 mmol). The heterogeneous mixture was then heated to 80 ºC for 48 h, at which point TLC analysis confirmed full consumption of starting material. The reaction was cooled to 23 ºC and diluted with CH_2Cl_2 (2 mL) and aq. HCl (2 mL of 1 M soln). The organic layer was washed with aq. HCl (5 x 2 mL of 1 M soln) and brine (1 x 4 mL) before being dried over Na_2SO_4. Upon concentration *in vacuo*, acid **4.60** was obtained (0.109 g, 0.182 mmol, 91% yield) as a colorless foam. ^{1}H NMR (500 MHz, $CDCl_3$) δ 4.17 (d, *J* = 8.7 Hz, 1H), 4.05–3.99 (m, 2H), 3.72 (d, *J* = 10.6 Hz, 1H), 1.99 (app q, *J* = 10.7 Hz, 1H), 1.75 (t, *J* = 9.4 Hz, 1H), 1.70–1.56 (m, 3H), 1.53 (s, 3H), 1.52–1.45 (m, 2H), 1.43 (s, 3H), 1.38–1.28 (m, 1H), 1.10–0.94 (m, 4H), 0.89 (s, 9H), 0.87 (s, 9H), 0.84 (s, 6H), 0.80 (s, 3H), 0.09 (s, 6H), 0.08 (s, 6H); ^{13}C NMR (125 MHz, $CDCl_3$) δ 171.92, 109.19, 84.96, 81.27, 69.22, 64.08, 57.73, 51.90, 42.79, 41.65, 39.78, 33.47, 33.13, 27.72, 26.74, 25.85, 24.90, 21.03, 20.97, 19.77, 19.74, 19.16, 18.35, 15.95, –2.13, –2.98, –5.33, –5.36; IR (thin film) 2953, 2928, 2857, 1717, 1462, 1381 cm^{-1}; $[\alpha]^{25}_D$: +31.6 (c = 2.5, CH_2Cl_2); HRMS (ESI) calculated for $C_{32}H_{62}O_6Si_2Na$ (M+Na) 621.3983, observed 621.3972.

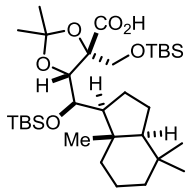

4.60: $C_{32}H_{62}O_6Si_2$
Molecular Weight: 599.0120

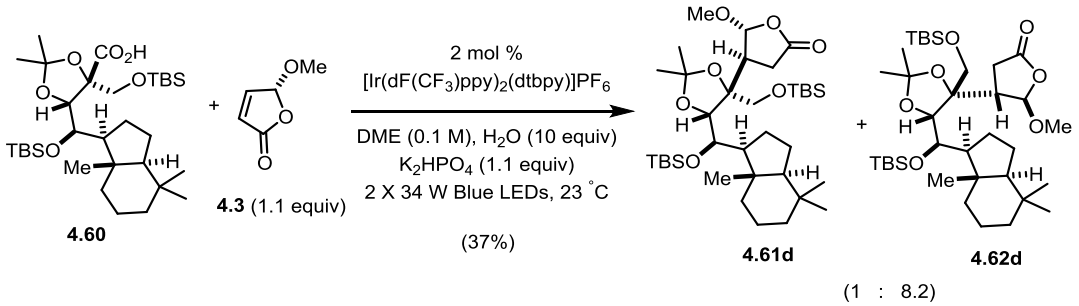

(+)-(4*S*,5*R*)-4-((5*S*)-5-((*R*)-((Tert-butyldimethylsilyl)oxy)((1*S*,3a*S*,7a*S*)-4,4,7a-trimethyloctahydro-1H-inden-1-yl)methyl)-4-(((tert-butyldimethylsilyl)oxy)methyl)-2,2-dimethyl-1,3-dioxolan-4-yl)-5-methoxydihydrofuran-2(3H)-one (4.61d/4.62d): A 4 mL scintillation vial equipped with a Teflon septum and magnetic stir bar was charged with carboxylic acid **4.60** (40 mg, 0.067 mmol), K_2HPO_4 (13 mg, 0.77 mmol), and $Ir[dF(CF_3)ppy)]_2(dtbbpy)PF_6$ (1.6 mg, 0.0014 mmol). Next, DME (0.7 mL, 0.1 M) was added, followed by water (13 µL, 0.67 mmol), and butenolide **4.3** (9 mg, 0.08 mmol). The reaction mixture was degassed by sparging with argon for 15 min and the vial was sealed and irradiated (2 x 34 W blue LED lamps) for 24 h at 23 ºC. The reaction mixture was filtered through $MgSO_4$, and evaporated under reduced pressure. ^{1}H NMR analysis of the crude residue displayed a 1:8.2 ratio of **4.61d**:**4.62d**. The crude residue was purified by flash column chromatography (0% EtOAc in hexanes to 5% EtOAc in hexanes) to yield an inseparable mixture of lactones **4.61d** and **4.62d** as a colorless oil (17 mg, 0.025 mmol, 37% yield). R_f 0.50 (10% EtOAc in hexanes; visualized with ceric ammonium molybdate). ^{1}H NMR for major diastereomer **4.62d** (500 MHz, $CDCl_3$) δ 5.84 (s, 1H), 4.12 (d, *J* = 9.8 Hz, 1H), 4.08 (d, *J* = 9.7 Hz, 1H), 3.64 (s, 2H), 3.51 (s, 3H), 2.70 (dd, *J* = 17.9, 9.9 Hz, 1H), 2.57 (dd, *J* = 10.1, 2.1 Hz, 1H), 2.43 (dd, *J* = 17.8, 2.4 Hz, 1H), 2.18–2.08 (m, 1H), 1.77 (dt, *J* = 12.4, 3.1 Hz, 1H), 1.65–1.43 (m, 4H), 1.42 (s, 3H), 1.41–1.23 (m, 2H), 1.29 (s, 3H), 1.07–0.94 (m, 4H), 0.91 (s, 9H), 0.89 (s, 9H), 0.85 (s, 3H), 0.84 (s, 3H), 0.83 (s,

3H), 0.11 (s, 3H), 0.10 (s, 3H), 0.08 (app s, 6H); ^{13}C NMR for major diastereomer **4.62d** (125 MHz, $CDCl_3$) δ 176.91, 106.72, 106.21, 84.12, 83.65, 68.60, 68.09, 57.98, 56.57, 51.80, 43.43, 42.96, 41.81, 39.62, 33.57, 33.22, 29.46, 26.84, 26.29, 26.23, 25.81, 21.05, 21.01, 19.86, 19.23, 19.04, 18.65, 16.61, –1.68, –2.79, –5.23, –5.43; IR (thin film) 2953, 2930, 2857, 1794, 1471, 1385, 1253 cm^{-1}; $[\alpha]^{25}_{D}$: +10.2 (c = 1.6, CH_2Cl_2); HRMS (ESI) calculated for $C_{36}H_{68}O_7Si_2Na$ (M+Na) 691.4401, observed 691.4407.

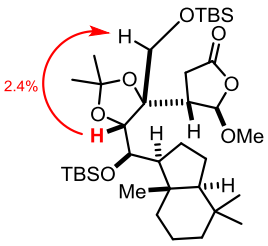

NOE for **4.62d**
(NOE in d^6-acetone)

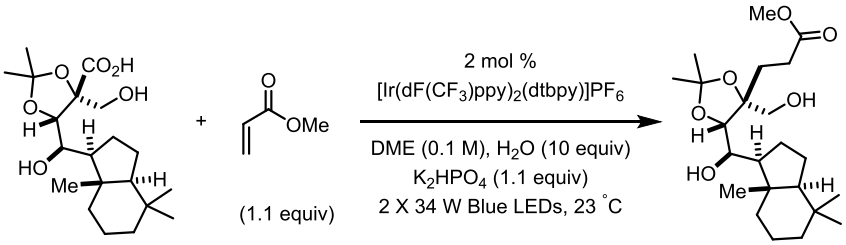

(+)-Methyl 3-((4*R*,5*S*)-5-((*R*)-hydroxy((1*S*,3a*S*,7a*S*)-4,4,7a-trimethyloctahydro-1*H*-inden-1-yl)methyl)-4-(hydroxymethyl)-2,2-dimethyl-1,3-dioxolan-4-yl)propanoate (S4.8): A 4 mL scintillation vial equipped with a Teflon septum and magnetic stir bar was charged with carboxylic acid **4.51** (26 mg, 0.070 mmol), K_2HPO_4 (13 mg, 0.77 mmol), and Ir[dF(CF_3)ppy)]$_2$(dtbbpy)PF_6 (1.6 mg, 0.0014 mmol). Next, DME (0.7 mL, 0.1 M) was added, followed by water (13 µL, 0.67 mmol), and methacrylate (6 mg, 0.08 mmol). The reaction mixture was degassed by sparging with argon for 15 min and the vial was sealed

and irradiated (2 x 34 W blue LED lamps) for 24 h at 23 ºC. The reaction mixture was filtered through $MgSO_4$, and evaporated under reduced pressure to yield a yellow oil. The crude residue was purified by flash column chromatography (20% EtOAc in hexanes to 30% EtOAc in hexanes) to yield ester **S4.8** as a colorless oil (22 mg, 0.053 mmol, 78% yield). R_f 0.23 (30% EtOAc in hexanes; visualized with ceric ammonium molybdate). ^{1}H NMR (500 MHz, CD_3OD) δ 3.82 (s, 1H), 3.75 (d, *J* = 8.5 Hz, 1H), 3.70–3.68 (m, 3H), 3.36–3.33 (m, 1H), 2.52–2.48 (m, 2H), 2.18–2.13 (m, 1H), 1.94–1.85 (m, 1H), 1.83–1.64 (m, 7H), 1.54–1.51 (m, 2H), 1.48–1.42 (m, 5H), 1.34–1.32 (m, 4H), 1.34–1.20 (m, 3H), 0.93 (s, 3H), 0.90 (s, 3H), 0.83 (s, 3H); ^{13}C NMR (125 MHz, CD_3OD) δ 176.60, 109.37, 84.81, 84.27, 70.90, 64.66, 60.62, 56.64, 53.05, 44.12, 43.38, 41.89, 34.92, 34.89, 31.19, 30.46, 29.46, 27.91, 27.03, 22.33, 22.07, 21.62, 15.25; IR (thin film) 3434, 2925, 1741, 1438, 1051 cm^{-1}; $[\alpha]^{23}_D$: +20.5 (c = 1.6, CH_2Cl_2); HRMS (ESI) calculated for $C_{23}H_{40}O_6Na$ (M+Na) 435.2722, observed 435.2729.

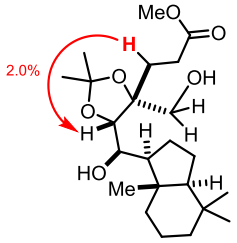

NOE for **S4.8**
(NOE in d^4-MeOH)

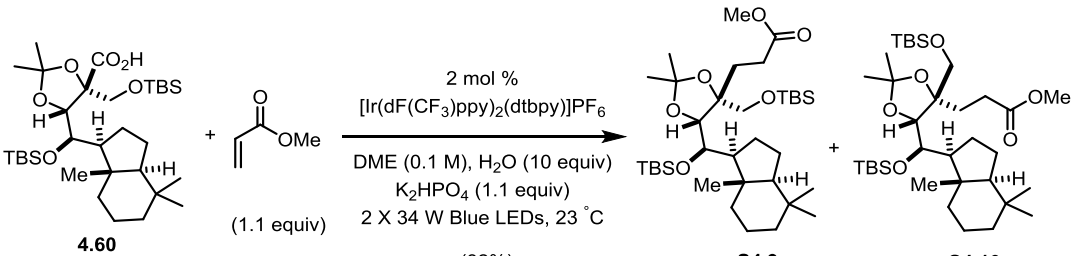

(+)-Methyl 3-((5*S*)-5-((*R*)-((Tert-butyldimethylsilyl)oxy)((1*S*,3a*S*,7a*S*)-4,4,7a-trimethyloctahydro-1H-inden-1-yl)methyl)-4-(((tert-butyldimethylsilyl)oxy)methyl)-2,2-dimethyl-1,3-dioxolan-4-yl)propanoate (S4.9/S4.10): A 4 mL scintillation vial equipped with a Teflon septum and magnetic stir bar was charged with carboxylic acid **4.60** (40 mg, 0.067 mmol), K_2HPO_4 (13 mg, 0.77 mmol), and Ir[dF(CF_3)ppy)]$_2$(dtbbpy)PF_6 (1.6 mg, 0.0014 mmol). Next, DME (0.7 mL, 0.1 M) was added, followed by water (13 µL, 0.67 mmol), and methacrylate (6 mg, 0.08 mmol). The reaction mixture was degassed by sparging with argon for 15 min and the vial was sealed and irradiated (2 x 34 W blue LED lamps) for 24 h at 23 ºC. The reaction mixture was filtered through $MgSO_4$, and concentrated under reduced pressure. ^{1}H NMR analysis of the crude residue displayed a 1:2.1 ratio of **S4.9**:**S4.10**. The crude residue was purified by flash column chromatography (2% EtOAc in hexanes to 4% EtOAc in hexanes) to yield an inseparable mixture of esters **S4.9** and **S4.10** as a colorless oil (35 mg, 0.055 mmol, 82% yield). R_f 0.5 (5% EtOAc in hexanes; visualized with ceric ammonium molybdate). ^{1}H NMR for major diastereomer **S4.10** (500 MHz, $CDCl_3$) δ 3.99 (d, *J* = 10.0 Hz, 1H), 3.97 (d, *J* = 10.0 Hz, 1H), 3.67–3.63 (m, 4H), 3.53 (d, *J* = 11.0 Hz, 1H), 2.57–2.47 (m, 1H), 2.35–2.27 (m, 1H), 2.15–2.05 (m, 1H), 1.92–1.82 (m, 1H), 1.76–1.67 (m, 2H), 1.65–1.41 (m, 5H), 1.40 (s, 3H), 1.39–1.21 (m, 2H), 1.29 (s, 3H), 1.09–0.94 (m, 3H), 0.91 (s, 9H), 0.88 (s, 9H), 0.87 (s, 3H), 0.84 (s, 3H), 0.82 (s, 3H), 0.09 (s, 3H), 0.08 (s, 3H), 0.07 (s, 6H); ^{13}C NMR for major diastereomer **4.10** (125 MHz, $CDCl_3$) δ 174.50, 105.73, 83.16, 81.24, 69.44, 66.31, 58.22, 52.06, 51.74, 42.82, 41.92, 39.53, 33.62, 33.20, 28.50, 28.20, 26.92, 26.33, 26.25, 26.13, 20.99, 20.94, 19.87, 19.27, 19.12, 18.58, 16.25, –1.91, –3.24, –5.34, –5.41; IR (thin film) 2953, 2857,

1744, 1463, 1379, 1252 cm^{-1}; $[\alpha]^{25}_{D}$: 30.8 (c = 2.5, CH_2Cl_2); HRMS (ESI) calculated for $C_{35}H_{68}O_6Si_2Na$ (M+Na) 663.4452, observed 663.4431.

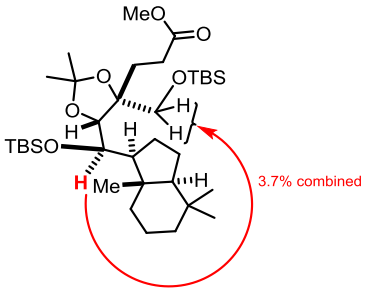

NOE for **S4.10**

4.3.3 Computational Details

To model the reactive radical species, the Furche group developed a multi-level computational approach[35] that included extensive sampling of conformational freedom, thermal corrections within the quasi rigid-rotor harmonic-oscillator approximation,[36] geometry optimization using the TPSS-D3 functional,[37] and single-point calculations at the random-phase approximation (RPA) level. RPA is comparable in computational cost to conventional second-order Møller-Plesset (MP2) theory but more reliable for weak interactions,[38] especially for the radical species considered in these diastereoselectivity studies.

All force-field computations were performed using Maestro 2015 with the OPLS-2005 force field.[39,40] The relaxed potential energy surfaces (PES) were optimized using Orca 3.0.3 with additional settings "Grid4" and "TightSCF".[41] Other computations were performed using Turbomole 7.0 with grid *m4*.[42] All structures were optimized using the TPSS[43] functional with def2-SVP or def2-TZVP basis sets[44] as described in the text in combination with the BJ-damped D3-dispersion correction, denoted -D3 in the following.[45] The resolution-of-the-identity approximation for Coulomb term (RI-J)[46] or multipole-accelerated RI-J (MARI-J)[47] were used with the corresponding auxiliary basis sets[48] in Orca and Turbomole, respectively. Solvation effects were taken into account using the COSMO solvation model with a dielectric constant of 8.9 (dichloromethane).[49] Pictures of the computed structures were generated using Cylview.[50]

The experimentally observed differences in the diastereoselectivities are raised by very small energy differences, e.g., 1 kcal/mol error in the computation is enough to change the selectivity from 2.3:1 to 1:2.3. Thus, we used TPSS-D3/def2-TZVP structures to further

compute single-point energies with TPSSh-D3[51] and resolution-of-identity random phase approximation (RI-RPA)[52] with corresponding auxiliary basis sets.[53] We also calculated single-point energies using the TPSS functional without dispersion corrections for comparison. For RPA, solvated PBE[54] orbitals were used, and the core orbitals were kept frozen for computation of correlation energy.

Harmonic vibrational frequencies were computed numerically for all studied transition states (TS) at the level of optimization (TPSS-D3/def2-TZVP/COSMO). The chemical potentials (c.p.), which are needed to study the Gibbs free energies (G = E(0) + c.p.), were then calculated using two variations: (i) the standard rigid-rotor harmonic-oscillator (RRHO) approximation and (ii) the quasi-RRHO approach proposed by Grimme.[55] In the quasi-RRHO approach the vibrational entropy is replaced by the free-rotor entropy for all modes with frequencies less than 100 cm^{-1}. Method (ii) is considered more reliable for systems with many vibrational modes below 100 cm^{-1}.[55]

We chose the TPSS functional for the optimizations because of its solid performance across the periodic table.[56] TPSS can be combined efficiently with RI-approximation, which significantly sped up the computations (approx. by factor of 10) and enabled the use of triple-ζ basis set for large set of transition states. The hybrid variant of TPSS, TPSSh, was used for single-point energies. TPSSh contains 10% of Hartree-Fock exchange, which reduces the self-interaction error (SIE), and therefore we consider it to be more accurate to describe interaction between the nucleophilic acetonide radical and electron deficient olefin. These functionals were further coupled with the atom-pairwise D3 dispersion correction. RPA was chosen because it captures the non-pairwise-additive nature of long-range interactions accurately[13] and from first principles. In our preliminary

study for radical **4.40d**, we also employed MP2/def2-QZVP to study the selectivity. The wave-functions were, however, spin-contaminated at Hartree-Fock level (the total spin expectation value was ~1 instead of 0.75) and the norm of the T_2 amplitudes was high (>1). This suggested that the reliability of MP2 for these systems is questionable, and therefore MP2 was not used further. The basis-set convergence of RPA was tested for radicals **4.40a** and **4.40c** by extrapolating the correlation energy to the complete basis-set (CBS) limit using a two-point extrapolation scheme[57] with Dunning's cc-pVXZ[58] basis-sets, where X=3,4 (Table 4.4).

Table 4.4. The RPA energy difference between TS-anti and TS-syn for different basis-sets in kcal/mol.

Basis set	ΔΔE(XX-anti – XXa-syn)	ΔΔE(XXc-anti – XXc-syn)
def2-TZVP	0.12	3.26
cc-pVTZ	-0.08	3.01
cc-pVQZ	0.13	3.24
CBS(3,4)	0.13	3.30

4.3.3.1 Protocol for Selectivities

To explain the experimentally observed selectivities, diastereoselectivities were computed to radicals **4.40a**-**4.40f**, **4.51**, **4.56**, **4.58**, and **4.60**. The OBn and OTBS-groups were simplified to OMe and OTMS, respectively.

We started by studying the reaction profile for the radical addition for radical **4.40d.** First, the lowest energy conformer of the addition products was located, and then the relaxed PES was optimized (Figure 4.11). The PES was studied for different values for

bond distance r with TPSS-D3 and TPSSh-D3 using def2-SVP basis sets and in the gas-phase.

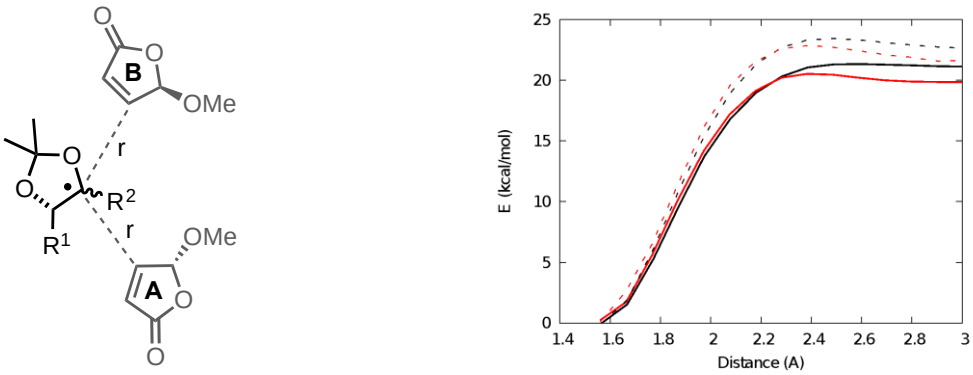

Figure 4.11. The PES using different r values to describe the C-C bond formation step for radical 4.40d.

(Solid lines = TPSS-D3/def2-SVP; dashed lines = TPSSh-D3/def2-SVP; black = syn; red = anti.)

The two functionals provided slightly different PESs: TPSS-D3 predicted lower activation energy barriers than TPSSh-D3, and the PES for *syn*-reaction was found to be barrierless, which might be an artifact due to SIE. However, both methods agreed that the interaction between radical and the olefin starts at approximately r = 2.5 Å; thus this distance was used in the conformational sampling of the transition states. The C–C bond formation step is very exothermic (by ~20-25 kcal/mol, Figure 4.11) and was thus not considered reversible.

The selectivity was then studied using a multi-level protocol. First, the preliminary TSs were formed for all studied radicals by freezing r at 2.5 Å and optimizing the syn and anti TSs with TPSS-D3/def2-SVP in the gas-phase. Then, the lowest energy conformers were determined at this distance. For conformers within 1 kcal/mol, the PES was studied

using TPSS-D3/def2-TZVP with COSMO for bond distances of r = 2.3–2.5 Å in 0.05 Å steps. These optimized structures were then used to compute the PES with TPSS, TPSS-D3, TPSSh-D3 and RPA. All methods employed COSMO and def2-TZVP basis sets. The PES scan was extended up to 2.7 Å if the PES was not converged at the RPA level.

The maximum of the PES was taken as the as the absolute energy of the TS and used to determine the selectivity. The PESs for different methods are shown in Figure 4.14. Thermal corrections were calculated for the transition states according to RPA, i.e., we chose the TPSS-D3/def2-TZVP optimized structure, which has the highest energy in the RPA PES.

4.3.3.2 Conformational Search

To perform a conformational search using molecular mechanics methods, the constrained TS structure was first optimized with TPSS-D3/def2-SVP to obtain the correct relative position for C^1 and C^2, which were set 2.5 Å apart. In Maestro, a long bond of 2.5 Å was inserted between the respected atoms and the electrophile was modified to be an enolate anion instead of a radical (Figure 4.12A) because we did not have access to force field, which is parameterized for sp^3 carbon radicals. The Cartesian coordinates of C^1 and C^2 were kept frozen during the conformational search. Systematic torsional sampling was employed using the OPLS-2005 force field with the following settings: Torsion sampling options “Intermediate”; maximum number of steps “2000”; steps per rotatable bond “4”; energy window for saving structures “6 kcal/mol”.

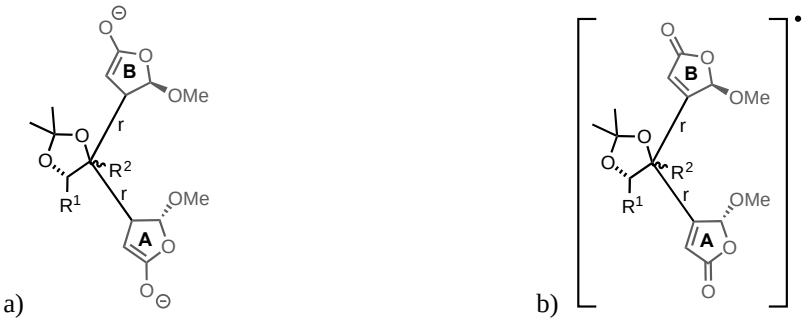

Figure 4.12. Maestro Computational Search.

a) In force field calculations, the system was modified to be an enolate anion; b) in quantum chemical computations, the system was treated as radical. In both cases, the bond distance r was fixed at 2.5 Å.

All structures within 6 kcal/mol were then re-optimized using TPSS-D3/def2-SVP in gas-phase. The bond length was kept fixed at 2.5 Å, but unlike in the force field optimization, the relative orientation of C^1 and C^2 was allowed to relax freely instead of fixing the Cartesian coordinates. The system was treated as a radical instead of enolate anion (Figure 4.12B), which was not possible in the force field computations as explained above. The conformers below 1 kcal/mol where then visually inspected and taken to PES study if the structures differed from each other. Optimization of all conformers of radical **4.40d** with COSMO and computing single-point energies with TPSSh-D3/def2-SVP leads to identical lowest energy conformer confirming the validity of our approach.

4.3.3.3 Correlation between Theory and Experiment

The computed energy difference between *syn*- and *anti*-TSs was used to calculate the diastereoselectivity using the Boltzmann distribution at 298 K. The correlation between experiment and theory was studied using three approaches:

(i) Selectivity was determined according to ΔE values (Figure 4.15)

(ii) Thermal corrections were added to the ΔE values using the RRHO-approximation (Figure 4.16)

(iii) Thermal corrections were added to the ΔE values using the quasi-RRHO approach (Figure 4.17)

Approach (iii) was found to be most realistic for the following reasons: First, the selectivities arise from very small energy differences and thus the thermal corrections are important. Second, small errors in low-lying frequencies cause significant error in the vibrational entropy; for example, the *syn*-selectivity of radical **4.60** is underestimated using approach (ii) with RPA (experiment 89%; theory 60%) whereas with approach (iii) the correlation is quantitative with the experiment (experiment 89%; theory 85%). Approaches (i) and (ii) are only shown for comparison.

With approach (iii), the correlation between the experiment and theory is semi-quantitative for most studied radicals when TPSS-D3, TPSSh-D3 or RPA is used, whereas the result is worse with non-dispersion corrected TPSS, which illustrates the importance of medium- and long-range non covalent interactions. The correlation is best for TPSSh-D3 and RPA. The *anti*-selectivity of radical **4.40a** was not reproduced but this originates from very small energy error (1-2 kcal/mol) and is within the error margin of the methods used here. All methods except RPA also produce the *anti*-selectivity qualitatively correctly at ΔE-level. The *syn*-selectivity is overestimated slightly for most radicals with prefix **4.40**, whereas the more complex radicals (**4.51**, **4.56**, **4.58**, **4.60**) are computed with quantitative accuracy using TPSSh-D3 and RPA.

The effect of entropy on the selectivity can be assessed by comparing approaches (i) and (iii) (Figure **4.15** and Figure **4.17**). In most cases, the correlation is still qualitative but not quantitative for approach (i). Thus, the effect of entropy on these results is significant. The standard RRHO-approximation predicts too high entropies especially for larger complexes (**4.51**, **4.56**, **4.58**, **4.60**) with more low-lying frequencies whereas the smaller complexes (**4.40**) are not affected much.

In summary, the selectivity of the radical addition can be computed with high accuracy if the following aspects are carefully taken into account: For large molecules, the conformational freedom causes much larger deviation to the energy than is needed to induce the selectivity. In addition, the computational method needs to accurately account for dispersive interactions between the different functional groups of the radical and between the radical and the approaching olefin. Especially for large complexes thermal effects should be computed with the quasi-RRHO-approximation.

4.3.3.4 Computational Tables and Transition State Figures

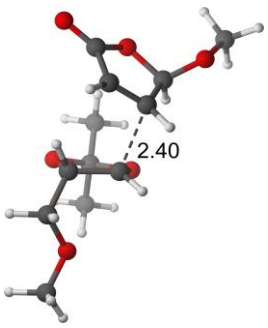	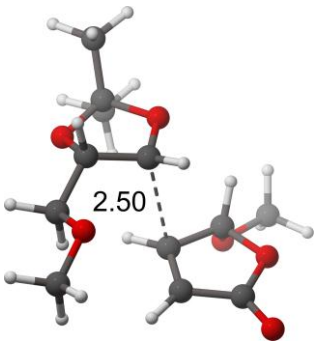
4.40a-anti	**4.40a-syn**

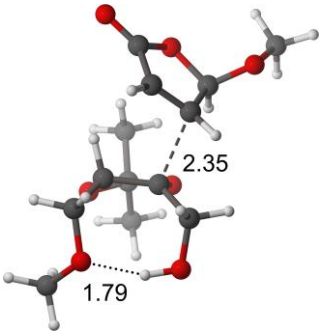	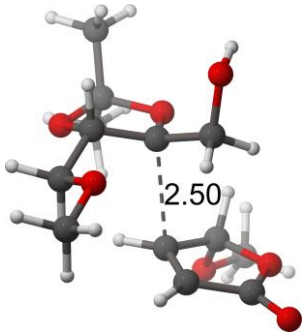
4.40b-anti	**4.40b-syn**
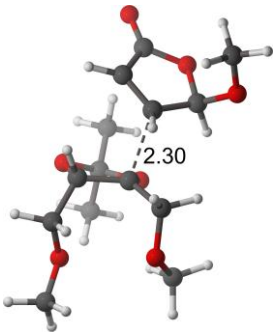	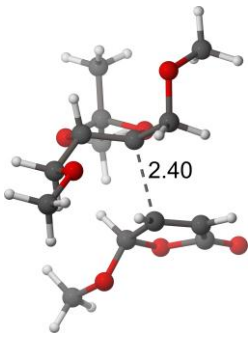
4.40c-anti	**4.40c-syn**
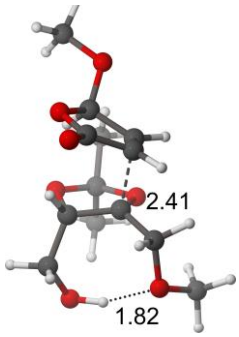	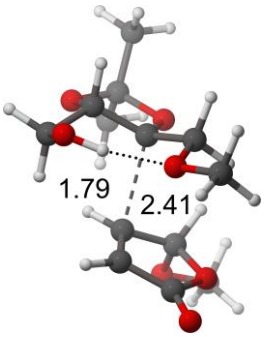
4.40d-anti	**4.40d-syn**
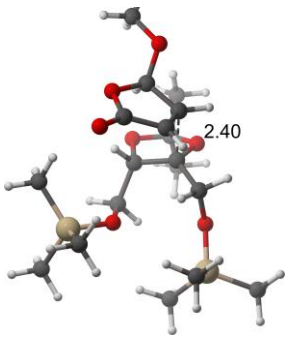	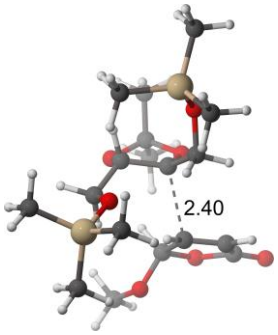
4.40e-anti	**4.40e-syn**

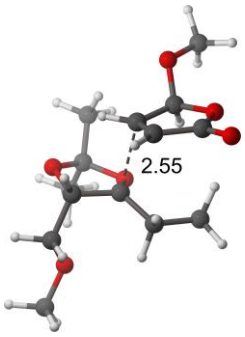	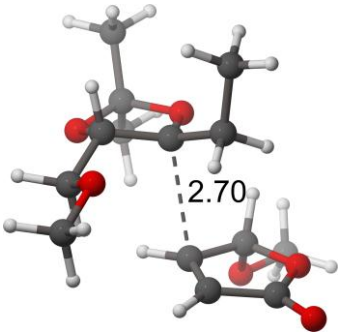
4.40f-anti	**4.40f-syn**
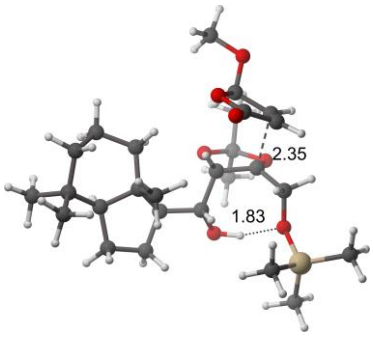	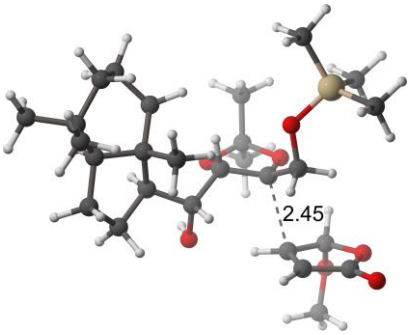
4.58-anti	**4.58-syn**
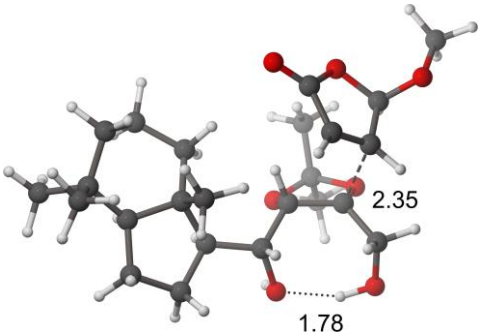	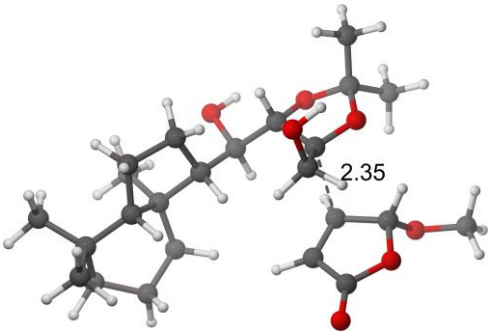
4.51-anti	**4.51-syn**
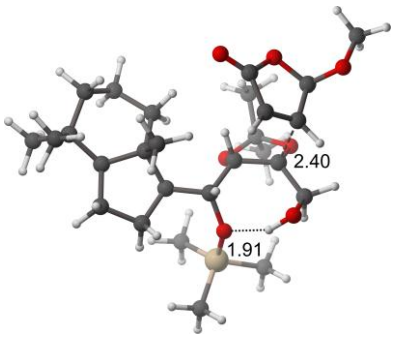	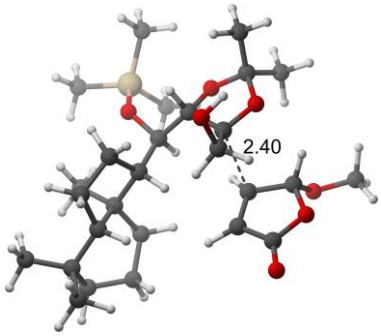
4.56-anti	**4.56-syn**

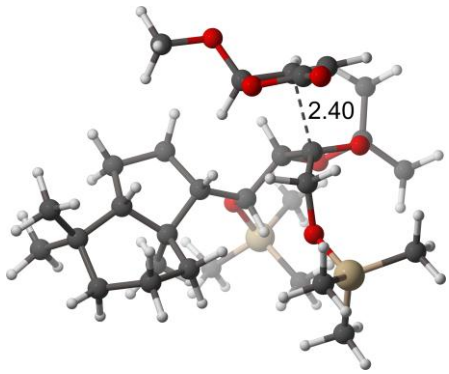	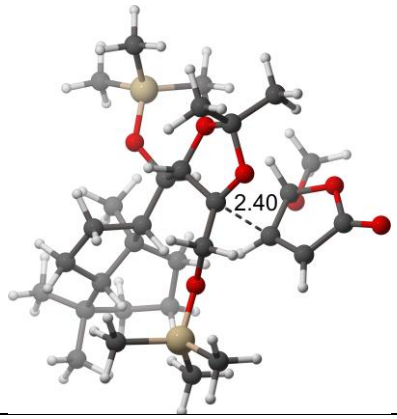
4.60-anti	**4.60-syn**

Figure 4.13. RPA/def2-TZVP/COSMO Transition State Structures Optimized Using TPSS-D3/def2-TZVP/COSMO.

4.40a

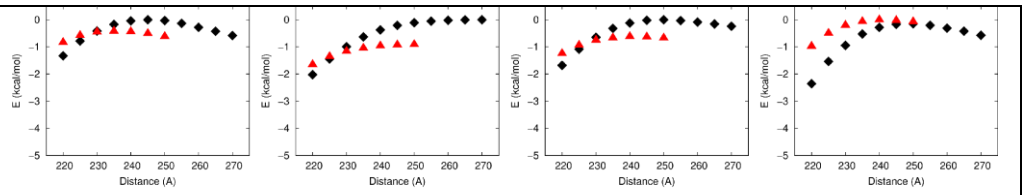

(a) TPSS (b) TPSS-D3 (c) TPSSh-D3 (d) RPA

4.40b

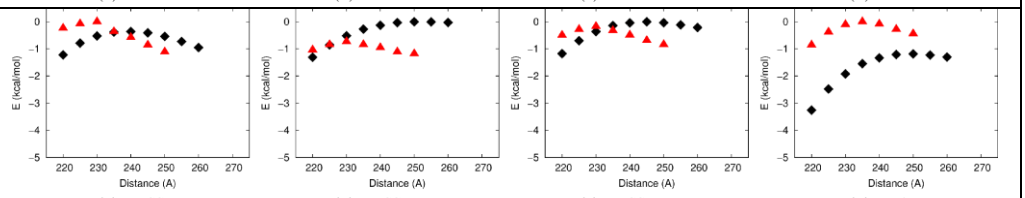

(a) TPSS (b) TPSS-D3 (c) TPSSh-D3 (d) RPA

4.40c

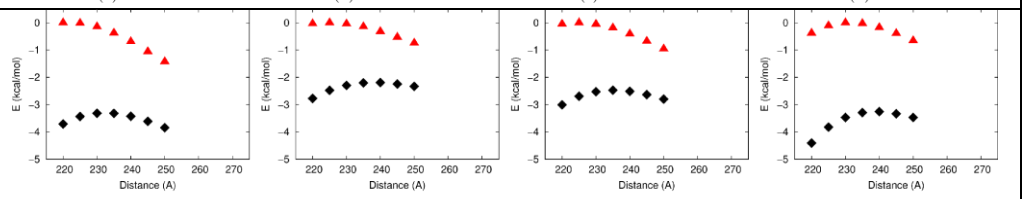

(a) TPSS (b) TPSS-D3 (c) TPSSh-D3 (d) RPA

4.40d

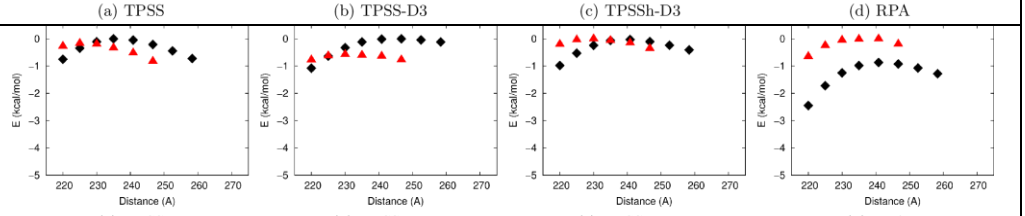

(a) TPSS (b) TPSS-D3 (c) TPSSh-D3 (d) RPA

4.40e

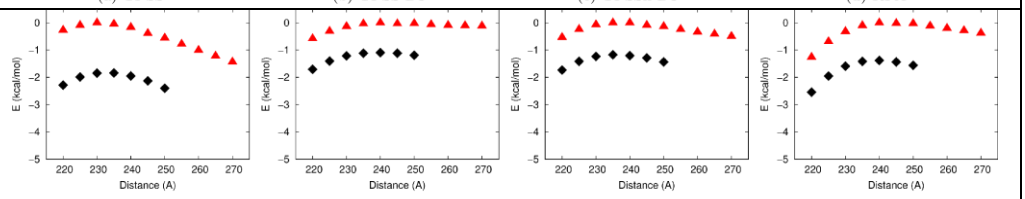

(a) TPSS (b) TPSS-D3 (c) TPSSh-D3 (d) RPA

4.40f

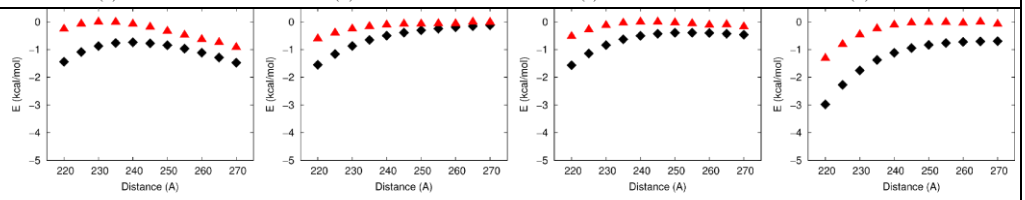

(a) TPSS (b) TPSS-D3 (c) TPSSh-D3 (d) RPA

4.58

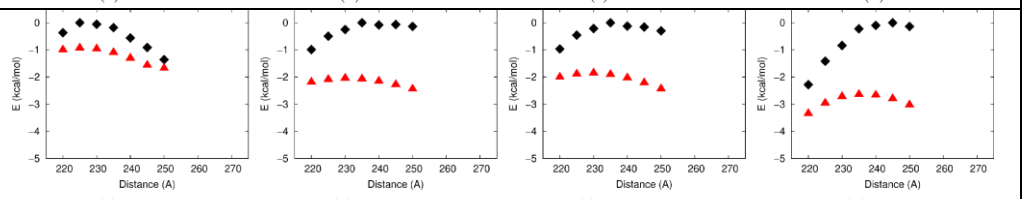

(a) TPSS (b) TPSS-D3 (c) TPSSh-D3 (d) RPA

4.51

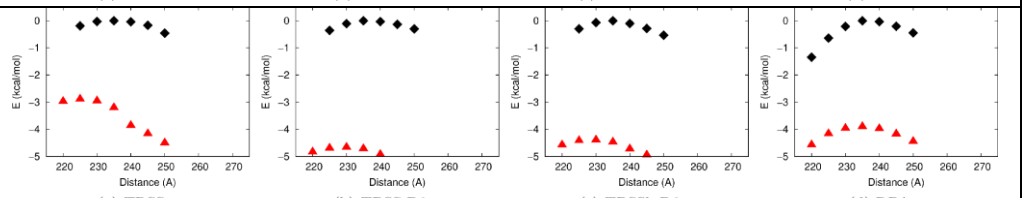

(a) TPSS (b) TPSS-D3 (c) TPSSh-D3 (d) RPA

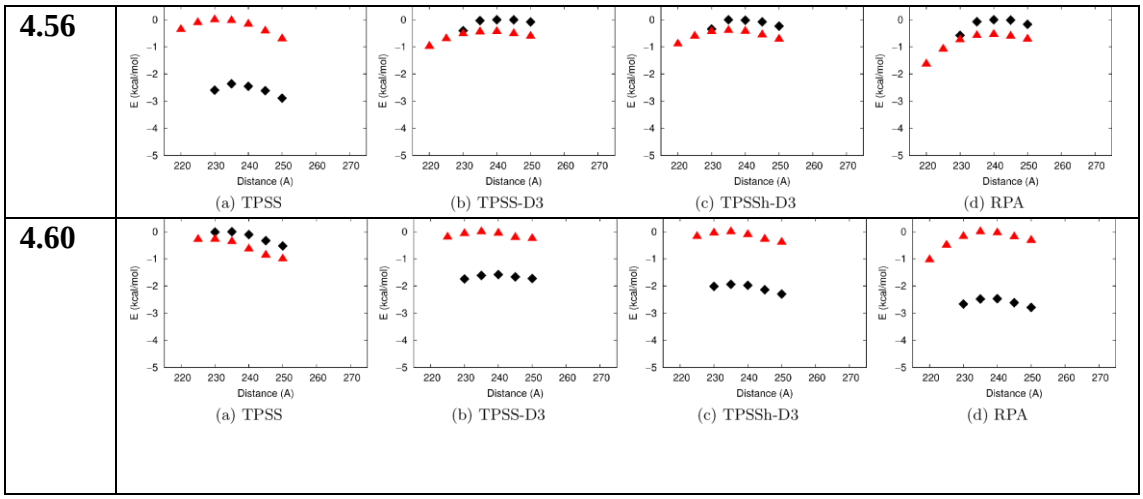

Figure 4.14. The PES's for the studied radicals computed using different methods.

The geometries were relaxed at TPSS-D3/def2-TZVP/COSMO level and different methods were used for single-point energies with def2-TZVP basis set and COSMO. The red-triangles represent the *anti*-pathway and black diamonds represent the *syn*-pathway.

	TPSS		TPSS-D3		TPSSh-D3		RPA		Exp
Radical	ΔE	%	ΔE	%	ΔE	%	ΔE	%	%
4.40a	-0.4	33	-0.9	18	-0.6	26	0.1	55	22
4.40b	0.4	65	-0.7	22	-0.2	43	1.2	88	77
4.40c	3.3	100	2.2	98	2.5	98	3.3	100	72
4.40d	-0.2	43	-0.6	28	0.0	51	0.9	81	72
4.40e	1.8	96	1.1	86	1.2	88	1.4	91	69
4.40f	0.7	77	0.1	55	0.4	66	0.7	76	90
4.58	-0.9	17	-2.0	3	-1.9	4	-2.6	1	43
4.51	-2.9	1	-4.7	0	-4.4	0	-3.9	0	9
4.56	2.4	98	-0.4	32	-0.4	34	-0.5	29	88
4.60	-0.3	39	1.6	93	1.9	96	2.5	98	89

Figure 4.15. The energy difference (ΔE) between TS-anti and TS-syn computed with several methods in kcal/mol.

The %-values represent the computed amount of *syn*-product which is calculated from the ΔE values using the Boltzmann distribution at 298 K.

	TPSS		TPSS-D3		TPSSh-D3		RPA		Exp
Radical	ΔG	%	ΔG	%	ΔG	%	ΔG	%	%
4.40a	0.5	70	0.0	50	0.3	62	1.0	85	22
4.40b	2.1	97	1.0	85	1.6	94	2.9	99	77
4.40c	2.7	99	1.5	93	1.8	96	2.6	99	72
4.40d	0.6	74	0.2	59	0.8	80	1.7	94	72
4.40e	1.5	93	0.8	78	0.8	80	1.0	85	69
4.40f	1.9	96	1.2	89	1.5	93	1.8	96	90
4.58	1.2	88	0.1	53	0.3	61	-0.5	29	43
4.51	-1.9	4	-3.7	0	-3.5	0	-3.0	1	9
4.56	3.9	100	1.1	87	1.2	88	1.0	85	88
4.60	-2.5	1	-0.6	25	-0.3	38	0.2	60	89

Figure 4.16. The energy difference (ΔG 298) between TS-anti and TS-syn computed with several methods in kcal/mol.

The %-values present the computed amount of *syn*-product, which is calculated from the ΔG values using the Boltzmann distribution at 298 K. Thermal corrections are accounted using standard RRHO-approximation.

	TPSS		TPSS-D3		TPSSh-D3		RPA		Exp
Radical	ΔG	%	ΔG	%	ΔG	%	ΔG	%	%
4.40a	0.3	62	-0.2	41	0.1	54	0.8	80	22
4.40b	1.7	95	0.6	74	1.2	88	2.5	99	77
4.40c	2.6	99	1.5	93	1.8	95	2.6	99	72
4.40d	0.4	65	0	49	0.6	72	1.4	91	72
4.40e	1.5	93	0.8	79	0.9	81	1.1	86	69
4.40f	1.3	90	0.7	76	1	83	1.3	89	90
4.58	0.9	83	-0.2	43	0	51	-0.8	21	43
4.51	-2.2	3	-3.9	0	-3.7	0	-3.2	0	9
4.56	3.7	100	0.9	82	0.9	83	0.8	79	88
4.60	-1.7	5	0.1	56	0.5	70	1	85	89

Figure 4.17. The energy difference (ΔG 298) between TS-anti and TS-syn computed with several methods in kcal/mol.

The %-values present the computed amount of *syn*-product, which is calculated from the ΔG values using the Boltzmann distribution at 298 K. Thermal corrections are accounted using quasi-RRHO approach.

Table 4.5. Absolute energies for transition states in *Hartrees*.

	TPSS	TPSS-D3	TPSSh-D3	RPA
4.40a-anti	-920.475563	-920.525971	-920.418546	-919.972228
4.40a-syn	-920.474888	-920.524515	-920.41756	-919.97242
4.40b-anti	-1035.07049	-1035.13179	-1035.01093	-1034.51537
4.40b-syn	-1035.07107	-1035.13062	-1035.01065	-1034.51726
4.40c-anti	-1074.3841	-1074.45138	-1074.32649	-1073.81699
4.40c-syn	-1074.38939	-1074.45488	-1074.33043	-1073.82218
4.40d-anti	-1035.07171	-1035.13381	-1035.01282	-1034.51728
4.40d-syn	-1035.07145	-1035.1329	-1035.01287	-1034.51866
4.40e-anti	-1813.36302	-1813.46534	-1813.31944	-1811.93735
4.40e-syn	-1813.36596	-1813.46708	-1813.32131	-1811.93955
4.40f-anti	-999.147161	-999.210532	-999.096534	-998.624269
4.40f-syn	-999.14832	-999.210717	-999.097153	-998.625353
4.58-anti	-1874.12141	-1874.2673	-1874.09605	-1872.97609
4.58-syn	-1874.11993	-1874.26405	-1874.0931	-1872.97188
4.51-anti	-1465.3137	-1465.43771	-1465.28123	-1464.61189
4.51-syn	-1465.3091	-1465.43028	-1465.27423	-1464.60567
4.56-anti	-1874.10962	-1874.26208	-1874.09122	-1872.97076
4.56-syn	-1874.11339	-1874.26139	-1874.09059	-1872.96991
4.60-anti	-2282.91775	-2283.09017	-2282.90445	-2281.33148
4.60-syn	-2282.91731	-2283.09269	-2282.90754	-2281.33541

Table 4.6. TPSS-D3/def2-TZVP/COSMO chemical potentials (c.p. in kJ/mol).

All transition states calculated using RRHO and quasi-RRHO approximations and imaginary-frequencies ν_{im} in cm^{-1}.

	c.p.(RRHO) kJ/mol	c.p.(quasi-RRHO) kJ/mol	ν_{im} (cm^{-1})
4.40a-anti	656.93	663.44	91.03
4.40a-syn	653.1	660.484	86.54
4.40b-anti	736.35	743.378	122.91
4.40b-syn	729	737.74	-
4.40c-anti	800.13	807.942	129.47
4.40c-syn	802.88	810.821	107.26
4.40d-anti	736.93	743.257	66.41
4.40d-syn	733.65	740.999	136.35
4.40e-anti	1141.97	1158.31	74.16
4.40e-syn	1143.42	1159.57	100.48
4.40f-anti	788.59	797.36	-
4.40f-syn	783.89	794.98	-
4.58-anti	1635.21	1652.98	94.68
4.58-syn	1626.38	1645.16	74.42
4.51-anti	1400.76	1412.39	121.61
4.51-syn	1396.82	1409.37	146.72
4.56-anti	1645.36	1659.31	92.47
4.56-syn	1638.8	1653.8	135.18
4.60-anti	1866.89	1891.22	73.36
4.60-syn	1876.19	1897.28	113.09

4.4 References and Notes

[1] Wang, H.; Kohler, P.; Overman, L. E.; Houk, K. N. *J. Am. Chem. Soc.* **2012**, *134*, 16054–16058.

[2] This reaction was done on a small scale, and *ee* was not determined of bromobutenolide **4.4**. The analogous reaction was performed with enantiopure menthol butenolide, which gave a single diastereomer, indicating these reaction conditions did not epimerize the γ-stereocenter. However, bromobutenolide **4.4** was never analyzed by HPLC analysis.

[3] Available for $1,080 per gram at Accel Pharmtech as of 3/25/16.

[4] Barhoumi-Slimi, T. M.; Ben Dhia, M. T.; Nsangou, M.; El Gaied, M. M.; Khaddar, M. R. *J. Struct. Chem.* **2010**, *2*, 251–257.

[5] Coupling to ACF radical precursor **4.5** with (±)-chlorobutenolide **4.9** would likely be impractical as each enantiomer of chlorobutenolide **4.9** could react with the trisubstituted acetonide radical to form twice the number of addition products.

[6] Schlama, T.; Gabriel, K.; Gouverneur, V.; Mioskowski, C. *Angew. Chem. Int. Ed.* **1997**, *36*, 2342–2344.

[7] Butenolide **4.3** was unreactive to any chlorine source, and starting material was always recovered. I did not heat these reactions due to potential racemization of the butenolide's labile stereocenter.

[8] a) Jauch, J. *J. Org. Chem.* **2001**, *66*, 609–611. b) Sousa, B. A.; Keppler, A. F.; Gariani, R. A.; Comasseto, J. V.; Dos Santos, A. A. *Tetrahedron* **2012**, *68*, 10406–10413.

[9] Pitta, B. R.; Fleming, F. F. *Org. Lett.* **2010**, *12*, 2810–2813.

[10] This diastereoselectivity is based on Table 3.4, entry 1; but the diastereoselectivity changed depending on solvent and conditions.

[11] The other known literature reference not discussed is Yamada, K.; Yamamoto, Y.; Maekawa, M.; Tomioka, K. *J. Org. Chem*. **2004**, *69*, 1531−1534.

[12] Barton, D. H. R.; Gateau-Olesker, A.; Géro, S. D.; Lacher, B.; Tachdjian, C.; Zard, S. Z. *Tetrahedron* **1993**, *49*, 4589−4602.

[13] Gerster, M.; Renaud, P. *Synthesis* **1997**, 1261–1267.

[14] Renaud proposed the diastereoselectivity could arise from either destabilizing eclipsing interactions of the intermediate radical itself or the transition state of the radical with the acceptor.

[15] The differences in diastereoselectivities (2.2–2.9:1) is energetically translated to less than 0.2 kcal/mol.

[16] See experimental details for NOE correlations of *syn* and *anti* addition products.

[17] CCID 146074.

[18] Chu, L.; Ohta, C.; Zuo, Z.; MacMillan, D. W. C. *J. Am. Chem. Soc.* **2014**, *136*, 10886–10889.

[19] The nature of the butenolide radical acceptor and the 40 °C difference in reaction temperature must be responsible for the lower stereoselectivity that I observe when compared to Barton's work (Scheme 4.3A).

[20] Palladium-mediated hydrogenation facilitated both alkene reduction and debenzylation, while platinum-mediated hydrogenation reduced the alkene and also the benzene ring to a cyclohexyl group.

[21] a) Iwasaki, K.; Wan, K. K.; Oppedisano, A.; Crossley, S. W. M.; Shenvi, R. A. *J. Am. Chem. Soc.* **2014**, *136*, 1300–1303. b) Obradors, C.; Martinez, R. M.; Shenvi, R. A. *J. Am. Chem. Soc.* **2016**, *138*, 4962–4971.

[22] The relative difference in diastereoselectivities is energetically translated to ~0.6 kcal/mol.

[23] 45% yield by ^{1}H NMR with an internal standard. The major *anti* addition diastereomer was isolated in 27% yield. This low yield is a result of two factors: 1) acid **4.51** has poor solubility in DME; and 2) the product partially decomposed on silica gel during column chromatography. I believe this yield could be readily optimized by running these reactions

in a more polar solvent (DMF or THF)/solvent mixture and more concentrated than 0.1 M. I kept identical reaction conditions for comparison of diastereoselectivities.

[24] With the allylic *tert*-butyldimethylsilyl silyl ether, the trisubstituted alkene did not undergo reduction under Pd-catalyzed hydrogenation, presumably from the steric environment.

[25] Nicolaou, K. C.; Estrada, A. A.; Zak, M.; Lee, S. H.; Safina, B. S. *Angew. Chem. Int. Ed.* **2005**, *44*, 1378–1382.

[26] The relative energetic difference based on observed diastereoselectivities between a free secondary alcohol (entry 2) and a *tert*-butyldimethylsilyl-protected secondary alcohol (entry 5) is estimated at 2.5 kcal/mol.

[27] See experimental Section 4.3.3 for computational method details.

[28] These transition state structures were optimized using TPSS-D3/def2-TZVP/COSMO.

[29] For computational simplicity, the *tert*-butyldimethylsilyl groups were substituted with trimethylsilyl groups while optimizing transition state geometries and energies.

[30] The relative energetic difference based on observed diastereoselectivities between the butenolide and methacrylate acceptors is estimated at 0.7 kcal/mol.

[31] Some of the radical precursors synthesized and tested in this chapter were not examined computationally (e.g. **4.47**).

[32] Tao, D. J., Slutskyy, Y.; Overman, L. E. *J. Am. Chem. Soc.* **2016**, *138*, 2186–2189.

[33] Coffey, D. S.; Overman, L. E.; Stappenbeck, F. *J. Am. Chem. Soc.* **2000**, *122*, 4904–4914.

[34] Ortuno, R. M.; Alonso, D.; J. Font. *Tetrahedron Lett.* **1986**, *27*, 1079–1080.

[35] Further details of the computational methodology and its validation are provided in the supporting information.

[36] Grimme, S. *Chem. Eur. J.* **2012**, *18*, 9955–9964.

[37] a) Grimme, S.; Antony, J.; Ehrlich, S.; Krieg, H. J. *Chem. Phys.* **2010**, *132*, 154104–154119. b) Grimme, S.; Ehrlich, S.; Goerigk, L. *J. Comp. Chem.* **2011**, *32*, 1456–1465. c) Tao, J.; Perdew, J. P.; Staroverov, V. N.; Scuseria, G. E. *Phys. Rev. Lett.* **2003**, *91*, 146401.

[38] Eshuis, H.; Furche, F. *J. Chem. Phys*. **2012**, *136*, 084105.

[39] Schrödinger Release 2015-1**:** Maestro, version 10.1, Schrödinger, LLC, New York, NY, **2015**.

[40] Banks, J. L.; Beard, H. S.; Cao, Y.; Cho, A. E.; Damm, W.; Farid, R.; Felts, A. K.; Halgren, T. A.; Mainz, D. T.; Maple, J. R.; Murphy, R.; Philipp, D. M.; Repasky, M. P.;

Zhang, L. Y.; Berne, B. J.; Friesner, R. A.; Gallichio, E.; Levy, R. M. *J. Comp. Chem.* **2005**, *26*, 1752.

[41] Neese, F. The ORCA program system, *Wiley Interdiscip. Rev.: Comput. Mol. Sci.* **2012**, *2*, 73–78.

[42] TURBOMOLE V7.0 2014, a development of University of Karlsruhe and Forschungszentrum Karlsruhe GmbH, 1989-2007, TURBOMOLE GmbH, since 2007; available from http://www.turbomole.com.

[43] Tao, J.; Perdew, J. P.; Staroverov, V. N.; Scuseria, G. E. *Phys. Rev. Lett.* **2003**, *91*, 146401.

[44] Weigend, F.; Ahlrichs, R. *Phys. Chem. Chem. Phys.* **2005**, *7*, 3297–3305.

[45] a) Grimme, S.; Atony, J.; Ehrlich, S.; Krieg, H. J. *Chem. Phys.* **2010**, *132*, 154104. b) Grimme, S.; Ehrlich, S.; Goerigk, L. *J. Comput. Chem*. **2011**, *32*, 1456–1465.

[46] Eichkorn, K., Treutler, O.; Öhm, H.; Häser, M.; Ahlrichs, R. *Chem. Phys. Lett.* **1995**, *240*, 283.

[47] Sierka, M.; Hogekamp, A.; Ahlrichs, R. *J. Chem. Phys.* **2003**, *118*, 9136–9148.

[48] Weigend, F. *Phys. Chem. Chem. Phys.* **2006**, *8*, 1057–1065.

[49] Schäfer, A.; Klamt, A.; Sattel, D.; Lohrenz, J. C. W.; Eckert, F. *Phys. Chem. Chem. Phys.* **2000**, *2*, 2187–2193.

[50] CYLview, 1.0b, C.Y., Legault. Université de Sherbrooke, 2009 (http://www.cylview.org)

[51] Staroverov, V.N.; Scuseria, G. E.; Tao, J.; Perdew, J. P. *Chem. Phys.* **2003**, *119*, 12129−12137.

[52] a) Eshuis, H.; Yarkony, J.; Furche, F. *J. Chem. Phys.* **2010**, *132*, 234114. b) Eshuis, H.; Bates, J. E.; Furche, F. *Theor. Chem. Acc*. **2012**, *131*, 1084.

[53] Weigend, F.; Häser, M.; Patzelt, H.; Ahlrichs, R. *Chem. Phys. Lett.* **1998**, *294*, 143–152.

[54] Perdew, J. P.; Burke, K.; Ernzerhof, M. *Phys. Rev. Lett.* **1996**, *77*, 3865–3868.

[55] Grimme, S. *Chem. Eur. J.* **2012**, *18*, 9955–9964.

[56] Goerigk, L.; Grimme, S. *Phys. Chem. Chem. Phys.* **2011**, *13*, 6670–6688.

[57] a) Eshuis, H.; Furche, F. *J. Chem. Phys.* **2012**, *136*, 084105; b) Halkier, A.; Helgaker, T.; Jørgensen, P.; Klopper, W.; Koch, H.; Olsen, J.; Wilson, A. K. *Chem. Phys. Lett.* **1998**,

286, 243. c) Schwartz, C. *Phys. Rev.* **1962**, *126*, 1015. d) Helgaker, T.; Klopper, W.; Koch, H.; Noga, J. *J. Chem. Phys.* **1997**, *106*, 9639.

[58] a) Dunning, T. H. *J. Chem. Phys.* **1989**, *90*, 1007; b) Weigend, F.; Köhn, A.; Hättig, C. *J. Chem. Phys.* **2002**, *116*, 3175.

Appendix A: Chapter 1 NMR Spectra

1H spectrum

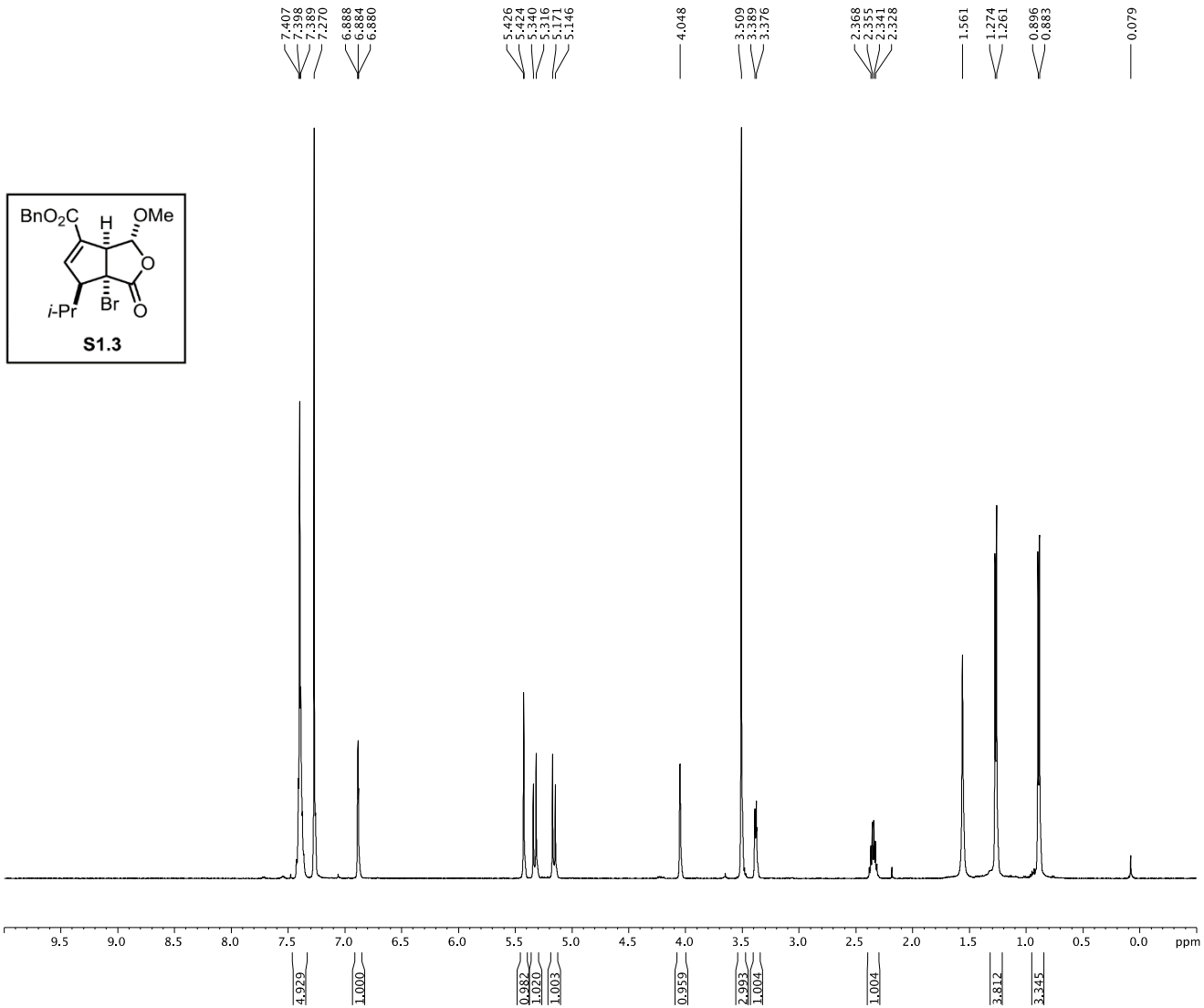

Current Data Parameters
NAME DJT-I-068
EXPNO 3
PROCNO 1

F2 - Acquisition Parameters
Date_ 20120926
Time 20.27
INSTRUM cryo500
PROBHD 5 mm CPTCI 1H-
PULPROG zg30
TD 81728
SOLVENT CDCl3
NS 18
DS 2
SWH 8012.820 Hz
FIDRES 0.098043 Hz
AQ 5.0998273 sec
RG 5.7
DW 62.400 usec
DE 6.00 usec
TE 298.0 K
D1 0.10000000 sec
MCREST 0 sec
MCWRK 0.01500000 sec

======== CHANNEL f1 =====
NUC1 1H
P1 7.50 usec
PL1 1.60 dB
SFO1 500.2235015 MHz

F2 - Processing parameters
SI 65536
SF 500.2200258 MHz
WDW EM
SSB 0
LB 0.30 Hz
GB 0
PC 4.00

Z-restored spin-echo 13C spectrum with 1H decoupling

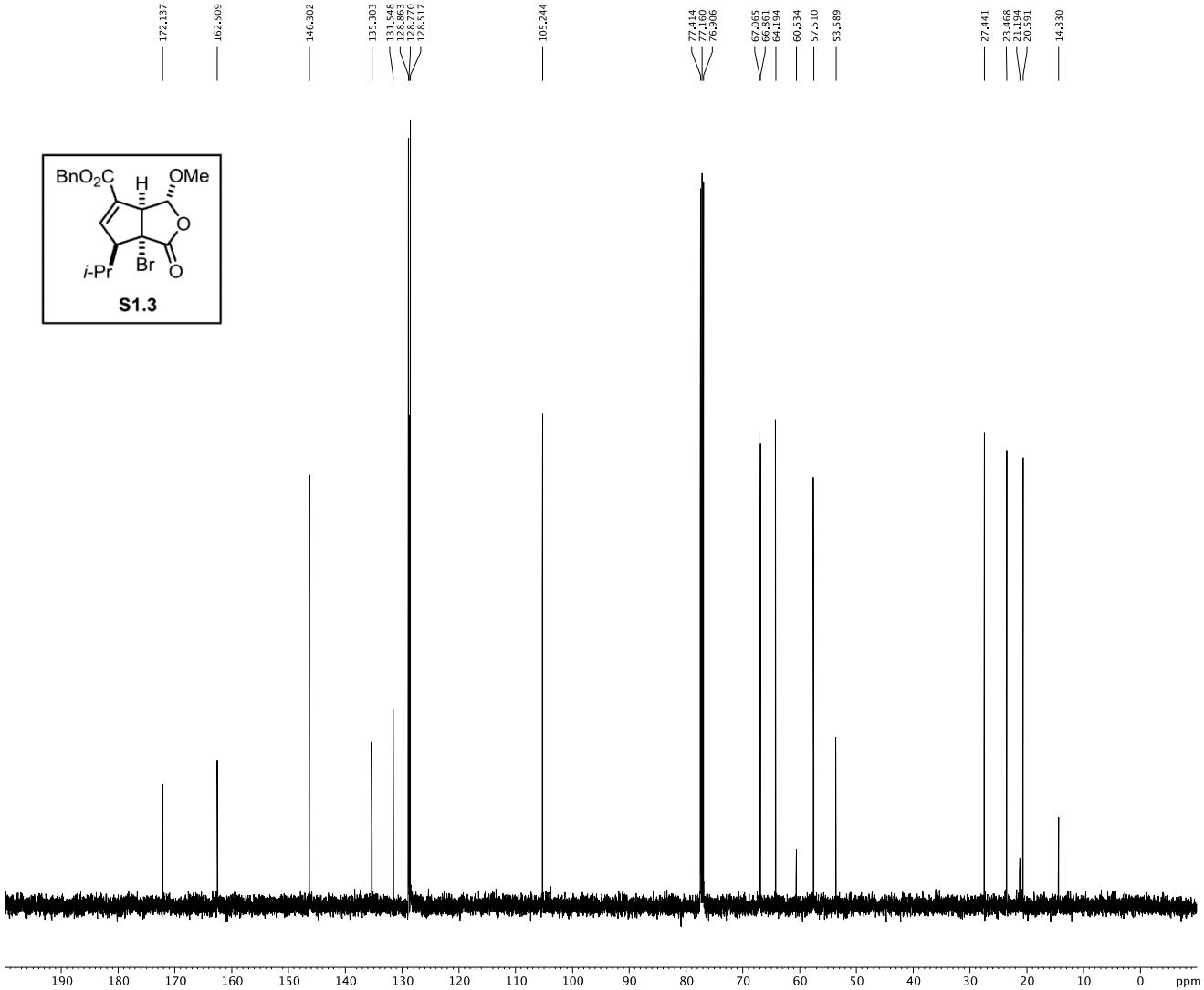

Current Data Parameters
NAME DJT-I-215
EXPNO 1
PROCNO 1

F2 - Acquisition Parameters
Date_ 20120914
Time 15.59
INSTRUM cryo500
PROBHD 5 mm CPTCI 1H-
PULPROG SpinEchopg30gp.prd
TD 65536
SOLVENT CDCl3
NS 100
DS 16
SWH 30303.031 Hz
FIDRES 0.462388 Hz
AQ 1.0813440 sec
RG 2048
DW 16.500 usec
DE 6.00 usec
TE 298.0 K
D1 0.25000000 sec
d11 0.03000000 sec
D16 0.00020000 sec
d17 0.00019600 sec
MCREST 0 sec
MCWRK 0.01500000 sec
P2 31.00 usec

======== CHANNEL f1 ========
NUC1 13C
P1 15.50 usec
P11 500.00 usec
P12 2000.00 usec
PL0 120.00 dB
PL1 -1.00 dB
SFO1 125.7942548 MHz
SP1 3.20 dB
SP2 3.20 dB
SPNAM[1] Crp60,0.5,20.1
SPNAM[2] Crp60comp.4
SPOFF1 0 Hz
SPOFF2 0 Hz

======== CHANNEL f2 ========
CPDPRG[2 waltz16
NUC2 1H
PCPD2 100.00 usec
PL2 1.60 dB
PL12 24.60 dB
SFO2 500.2225011 MHz

====== GRADIENT CHANNEL =====
GPNAM[1] SINE.100
GPNAM[2] SINE.100
GPX1 0 %
GPX2 0 %
GPY1 0 %
GPY2 0 %
GPZ1 30.00 %
GPZ2 50.00 %
p15 500.00 usec
p16 1000.00 usec

F2 - Processing parameters
SI 65536
SF 125.7804096 MHz
WDW EM
SSB 0
LB 1.00 Hz
GB 0
PC 2.00

1H spectrum

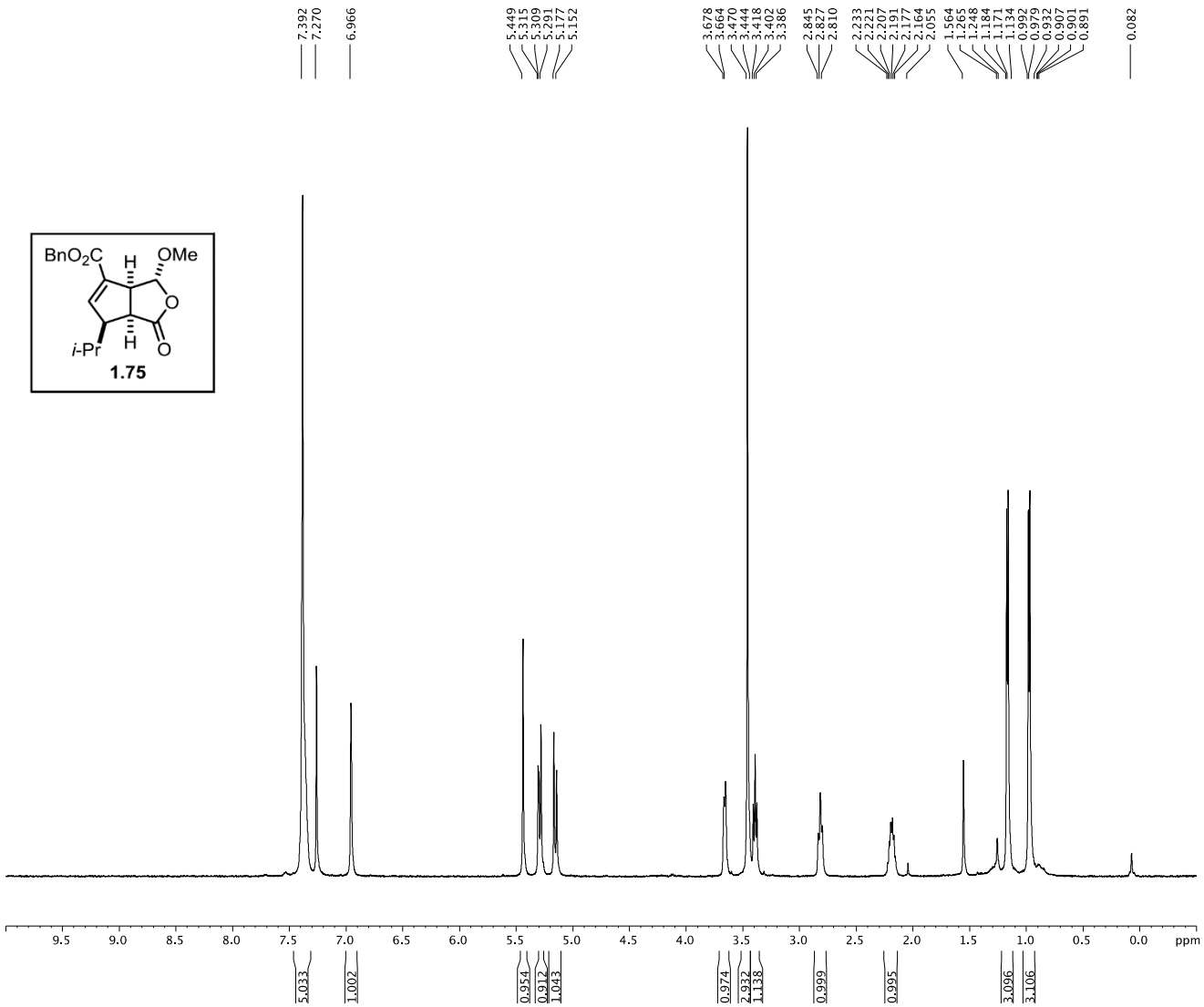


```
Current Data Parameters
NAME          DJT-I-152
EXPNO               2
PROCNO              1

F2 - Acquisition Parameters
Date_         20120707
Time             16.35
INSTRUM          qn500
PROBHD   5 mm broadband
PULPROG           zg30
TD               81728
SOLVENT          CDCl3
NS                   8
DS                   2
SWH           8012.820 Hz
FIDRES        0.098043 Hz
AQ            5.0998273 sec
RG                1024
DW              62.400 usec
DE               6.00 usec
TE             298.0 K
D1          0.10000000 sec
MCREST   0 sec
MCWRK       0.01500000 sec

======== CHANNEL f1 =====
NUC1               1H
P1             12.20 usec
PL1            -5.00 dB
SFO1       499.4034958 MHz

F2 - Processing parameters
SI              65536
SF        499.4000311 MHz
WDW               EM
SSB      0
LB             0.30 Hz
GB       0
PC             1.00
```

Z-restored spin-echo 13C spectrum with 1H decoupling

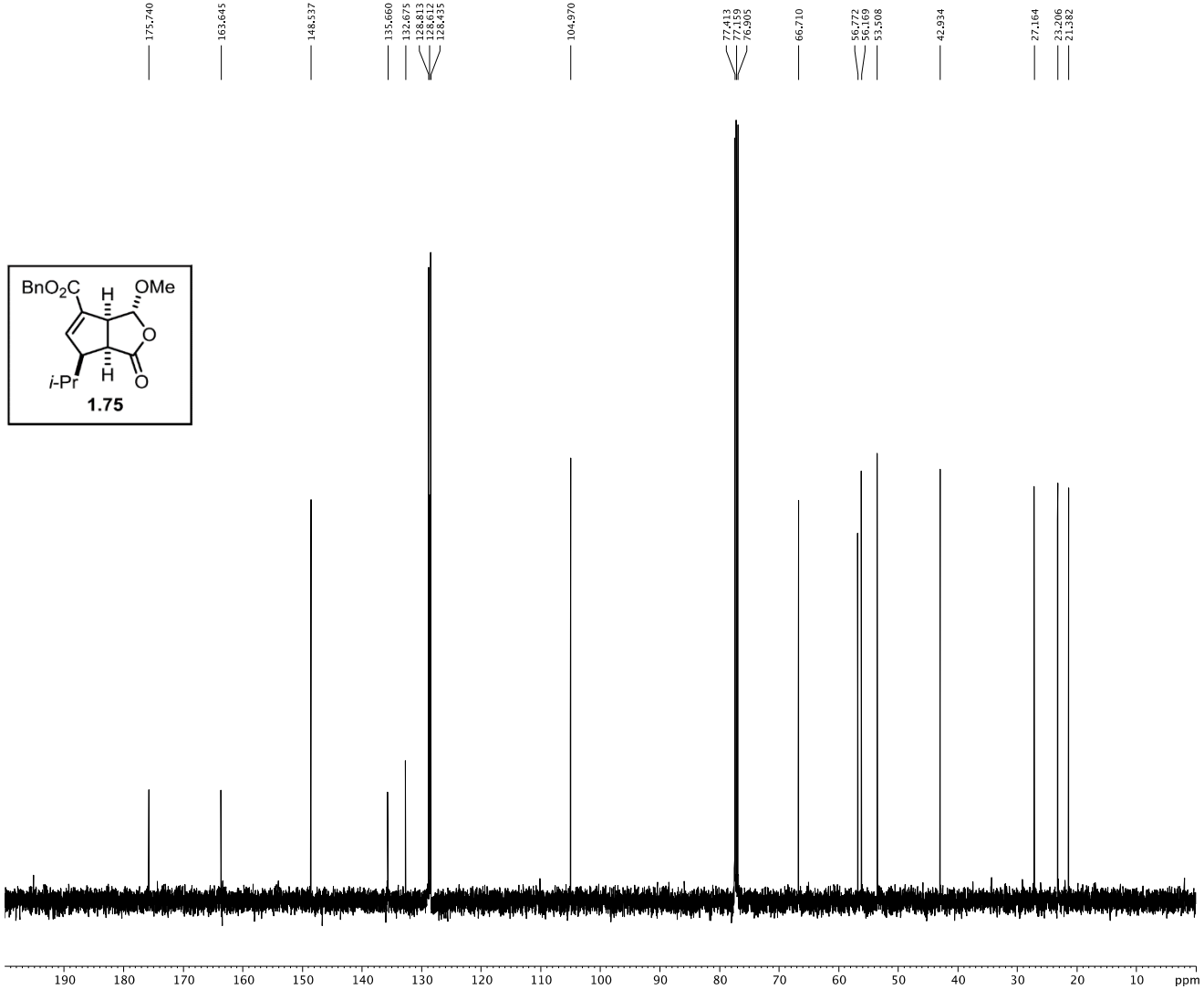


```
Current Data Parameters
NAME          DJT-I-144
EXPNO               4
PROCNO              1

F2 - Acquisition Parameters
Date_        20120828
Time            18.17
INSTRUM        cryo500
PROBHD  5 mm CPTCI 1H-
PULPROG  SpinEchopg30gp.prd
TD            65536
SOLVENT         CDCl3
NS              140
DS               16
SWH         30303.031 Hz
FIDRES       0.462388 Hz
AQ          1.0813440 sec
RG            7298.2
DW            16.500 usec
DE             6.00 usec
TE            298.0 K
D1          0.25000000 sec
d11         0.03000000 sec
D16         0.00020000 sec
d17         0.00019600 sec
MCREST   0 sec
MCWRK       0.01500000 sec
P2            31.00 usec

======== CHANNEL f1 ========
NUC1            13C
P1            15.50 usec
P11          500.00 usec
P12         2000.00 usec
PL0          120.00 dB
PL1           -1.00 dB
SFO1       125.7942548 MHz
SP1           3.20 dB
SP2           3.20 dB
SPNAM[1] Crp60,0.5,20.1
SPNAM[2]    Crp60comp.4
SPOFF1   0 Hz
SPOFF2   0 Hz

======== CHANNEL f2 ========
CPDPRG[2        waltz16
NUC2             1H
PCPD2          100.00 usec
PL2            1.60 dB
PL12          24.60 dB
SFO2       500.2225011 MHz

====== GRADIENT CHANNEL =====
GPNAM[1]       SINE.100
GPNAM[2]       SINE.100
GPX1     0 %
GPX2     0 %
GPY1     0 %
GPY2     0 %
GPZ1           30.00 %
GPZ2           50.00 %
p15           500.00 usec
p16          1000.00 usec

F2 - Processing parameters
SI            65536
SF       125.7804089 MHz
WDW              EM
SSB     0
LB            1.00 Hz
GB      0
PC            2.00
```

1H spectrum

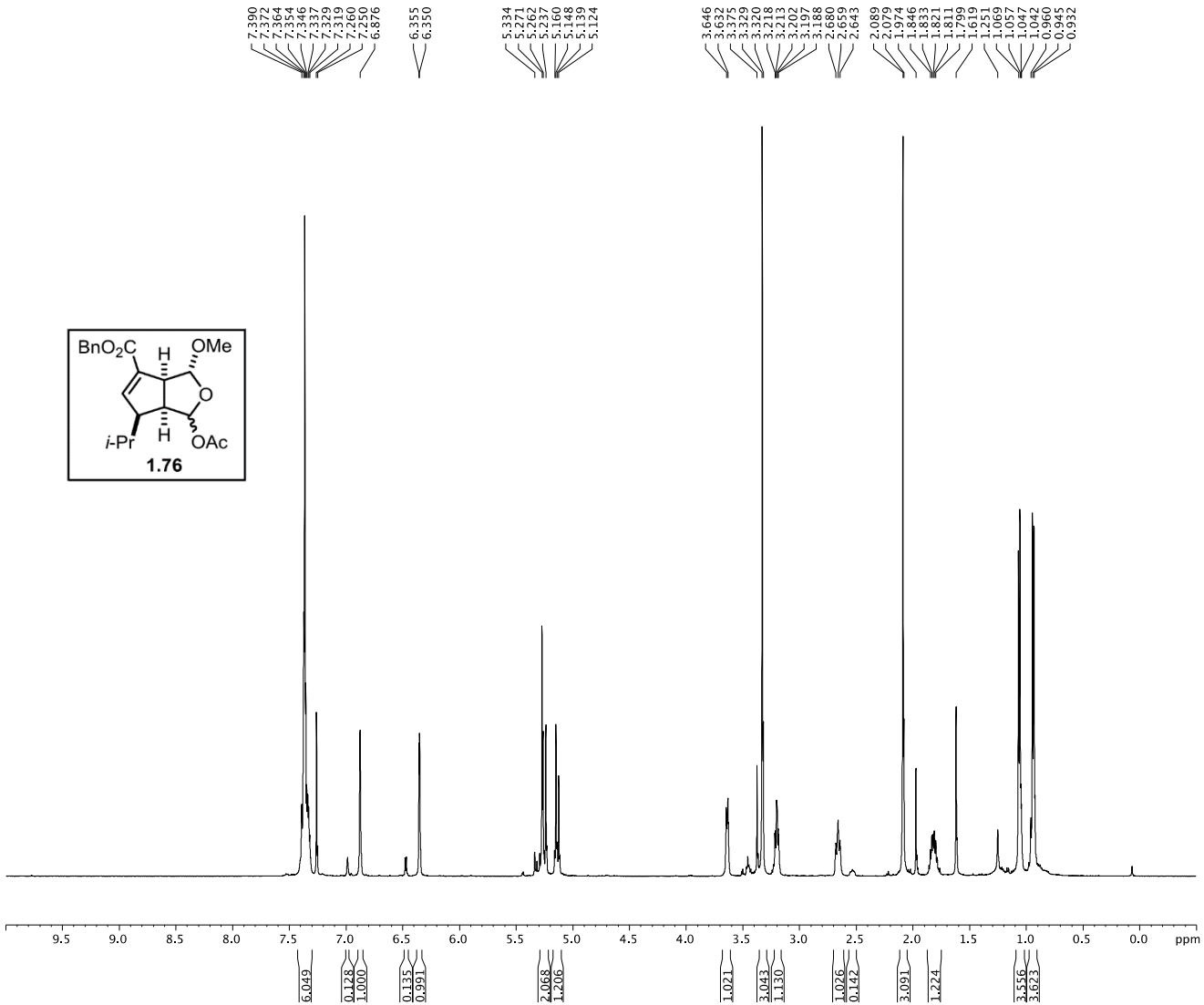

Current Data Parameters
NAME DJT-I-207
EXPNO 7
PROCNO 1

F2 - Acquisition Parameters
Date_ 20120830
Time 13.01
INSTRUM cryo500
PROBHD 5 mm CPTCI 1H-
PULPROG zg30
TD 81728
SOLVENT CDCl3
NS 8
DS 2
SWH 8012.820 Hz
FIDRES 0.098043 Hz
AQ 5.0998273 sec
RG 5.7
DW 62.400 usec
DE 6.00 usec
TE 298.0 K
D1 0.10000000 sec
MCREST 0 sec
MCWRK 0.01500000 sec

======== CHANNEL f1 =====
NUC1 1H
P1 7.50 usec
PL1 1.60 dB
SFO1 500.2235015 MHz

F2 - Processing parameters
SI 65536
SF 500.2200313 MHz
WDW EM
SSB 0
LB 0.30 Hz
GB 0
PC 4.00

Z-restored spin-echo 13C spectrum with 1H decoupling

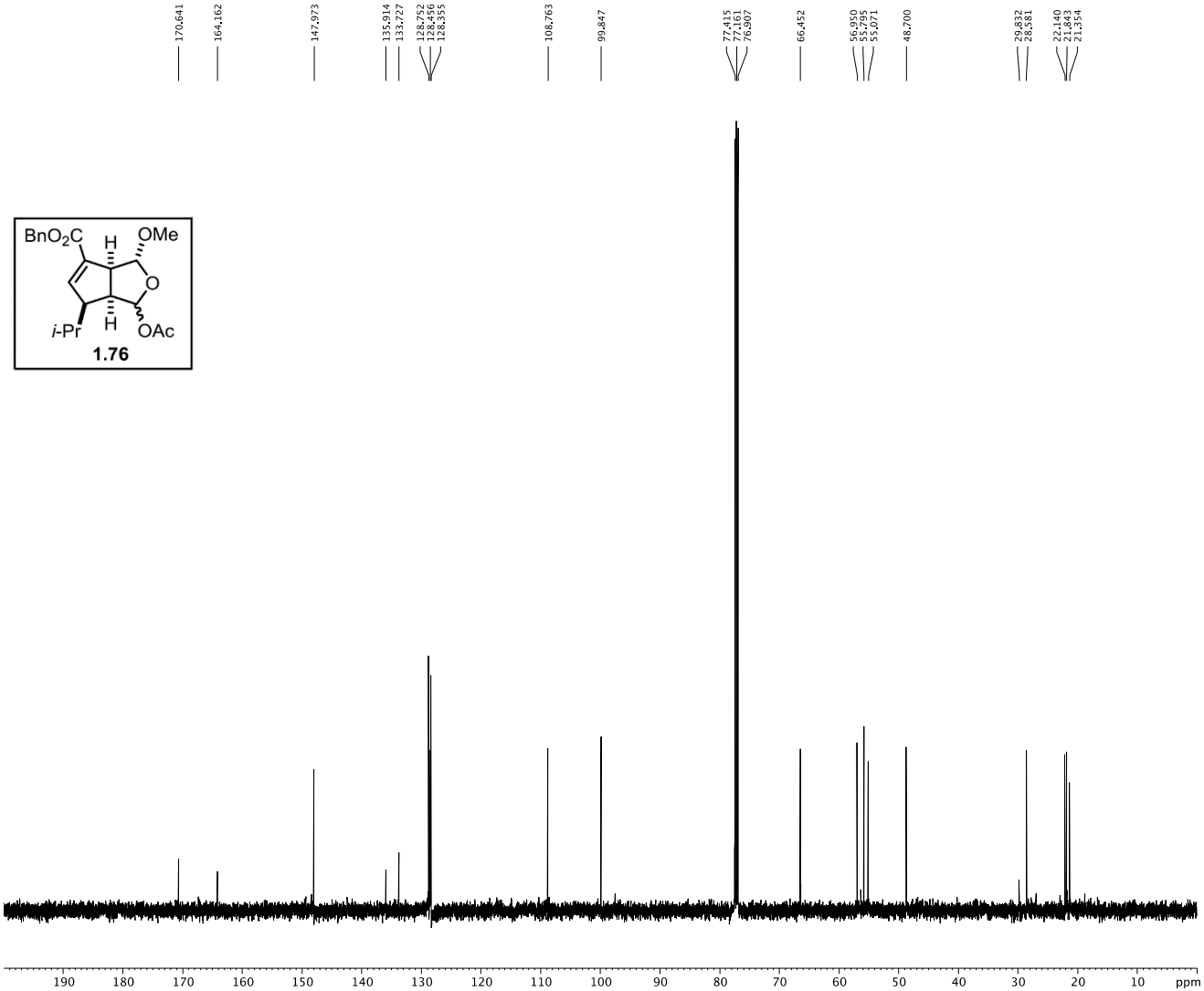


```
Current Data Parameters
NAME        DJT-I-218
EXPNO             2
PROCNO            1

F2 - Acquisition Parameters
Date_       20120914
Time           15.49
INSTRUM       cryo500
PROBHD   5 mm CPTC1 1H-
PULPROG  SpinEchopg30gp.prd
TD          65536
SOLVENT       CDCl3
NS              326
DS               16
SWH        30303.031 Hz
FIDRES      0.462388 Hz
AQ         1.0813440 sec
RG             3251
DW           16.500 usec
DE            6.00 usec
TE          298.0 K
D1         0.25000000 sec
d11        0.03000000 sec
D16        0.00020000 sec
d17        0.00019600 sec
MCREST   0 sec
MCWRK      0.01500000 sec
P2           31.00 usec

======== CHANNEL f1 ========
NUC1            13C
P1            15.50 usec
P11          500.00 usec
P12         2000.00 usec
PL0          120.00 dB
PL1           -1.00 dB
SFO1      125.7942548 MHz
SP1           3.20 dB
SP2           3.20 dB
SPNAM[1] Crp60,0.5,20.1
SPNAM[2]   Crp60comp.4
SPOFF1   0 Hz
SPOFF2   0 Hz

======== CHANNEL f2 ========
CPDPRG[2       waltz16
NUC2             1H
PCPD2         100.00 usec
PL2            1.60 dB
PL12          24.60 dB
SFO2      500.2225011 MHz

====== GRADIENT CHANNEL =====
GPNAM[1]      SINE.100
GPNAM[2]      SINE.100
GPX1     0 %
GPX2     0 %
GPY1     0 %
GPY2     0 %
GPZ1          30.00 %
GPZ2          50.00 %
p15          500.00 usec
p16         1000.00 usec

F2 - Processing parameters
SI          65536
SF      125.7804076 MHz
WDW            EM
SSB     0
LB           1.00 Hz
GB      0
PC           2.00
```

1H spectrum

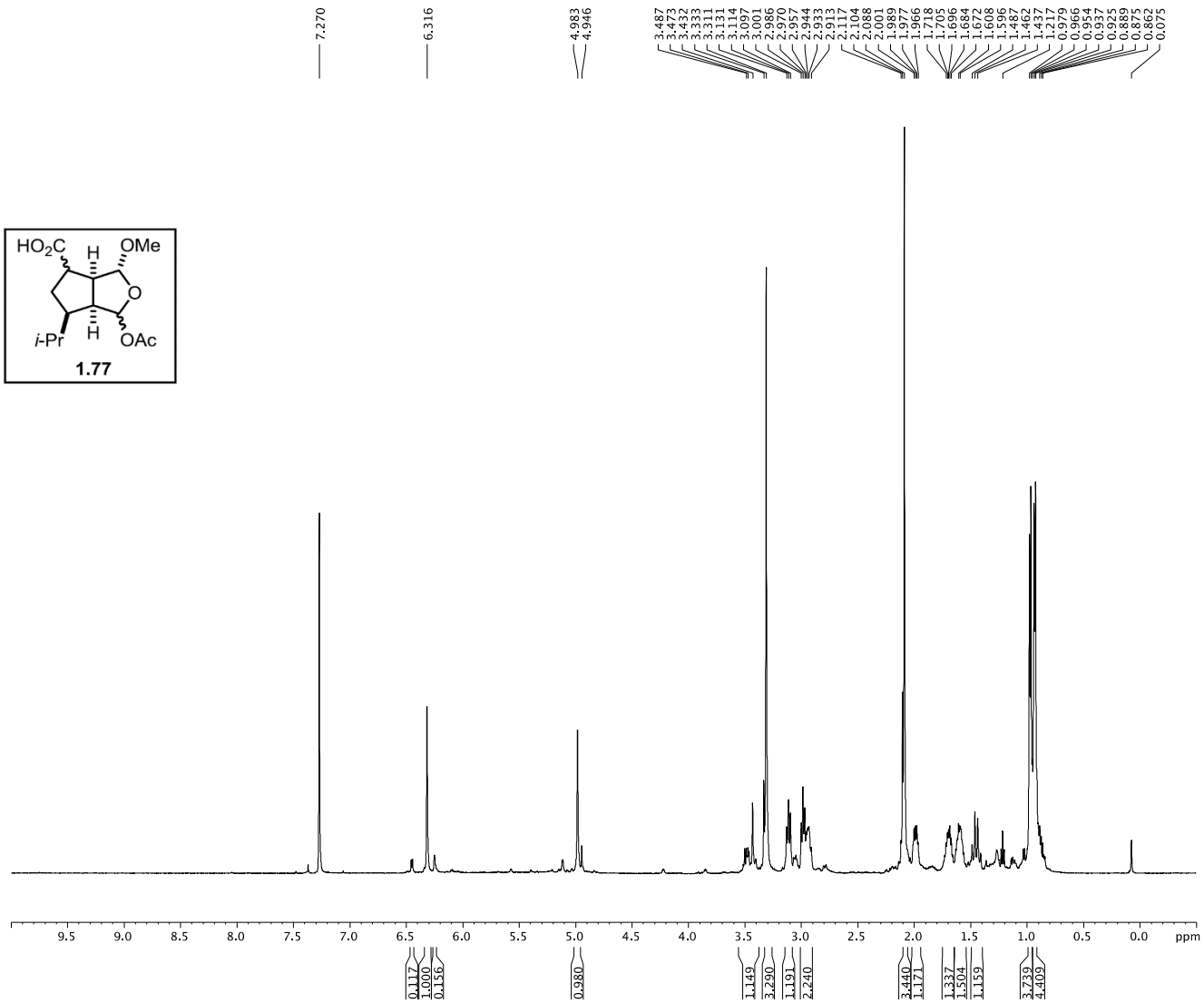

Current Data Parameters
NAME DJT-I-210
EXPNO 1
PROCNO 1

F2 - Acquisition Parameters
Date_ 20120831
Time 15.17
INSTRUM cryo500
PROBHD 5 mm CPTCI 1H-
PULPROG zg30
TD 81728
SOLVENT CDCl3
NS 16
DS 2
SWH 8012.820 Hz
FIDRES 0.098043 Hz
AQ 5.0998273 sec
RG 6.3
DW 62.400 usec
DE 6.00 usec
TE 298.0 K
D1 0.10000000 sec
MCREST 0 sec
MCWRK 0.01500000 sec

======== CHANNEL f1 =====
NUC1 1H
P1 7.50 usec
PL1 1.60 dB
SFO1 500.2235015 MHz

F2 - Processing parameters
SI 65536
SF 500.2200256 MHz
WDW EM
SSB 0
LB 0.30 Hz
GB 0
PC 4.00

Z-restored spin-echo 13C spectrum with 1H decoupling

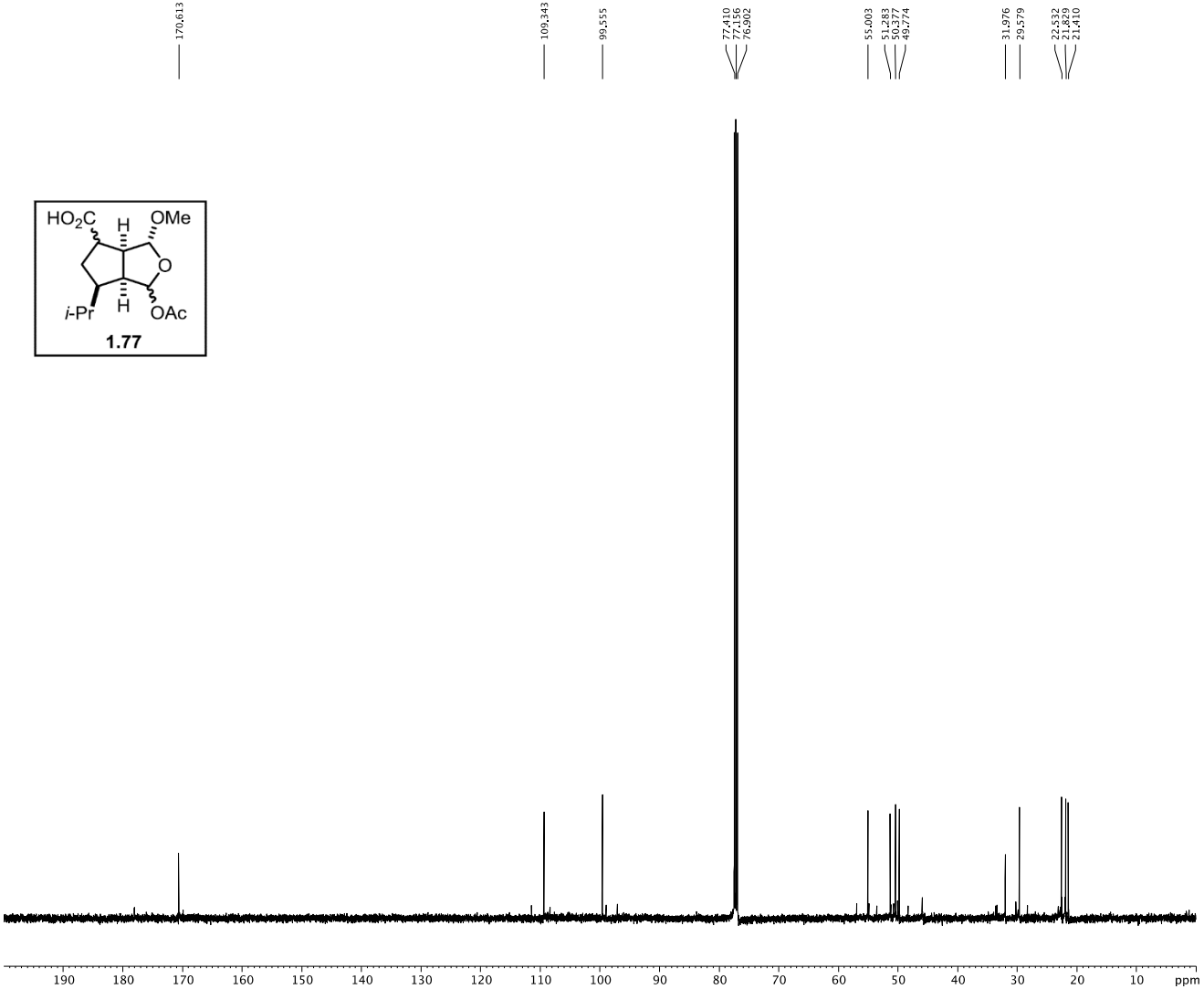

Current Data Parameters
NAME DJT-I-210
EXPNO 2
PROCNO 1

F2 - Acquisition Parameters
Date_ 20120831
Time 18.35
INSTRUM cryo500
PROBHD 5 mm CPTCI 1H-
PULPROG SpinEchopg30gp.prd
TD 65536
SOLVENT CDCl3
NS 332
DS 16
SWH 30303.031 Hz
FIDRES 0.462388 Hz
AQ 1.0813440 sec
RG 2896.3
DW 16.500 usec
DE 6.00 usec
TE 298.0 K
D1 1.50000000 sec
d11 0.03000000 sec
D16 0.00020000 sec
d17 0.00019600 sec
MCREST 0 sec
MCWRK 0.01500000 sec
P2 31.00 usec

======== CHANNEL f1 ========
NUC1 13C
P1 15.50 usec
P11 500.00 usec
P12 2000.00 usec
PL0 120.00 dB
PL1 -1.00 dB
SFO1 125.7942548 MHz
SP1 3.20 dB
SP2 3.20 dB
SPNAM[1] Crp60.0.5.20.1
SPNAM[2] Crp60comp.4
SPOFF1 0 Hz
SPOFF2 0 Hz

======== CHANNEL f2 ========
CPDPRG[2 waltz16
NUC2 1H
PCPD2 100.00 usec
PL2 1.60 dB
PL12 24.60 dB
SFO2 500.2225011 MHz

====== GRADIENT CHANNEL =====
GPNAM[1] SINE.100
GPNAM[2] SINE.100
GPX1 0 %
GPX2 0 %
GPY1 0 %
GPY2 0 %
GPZ1 30.00 %
GPZ2 50.00 %
p15 500.00 usec
p16 1000.00 usec

F2 - Processing parameters
SI 65536
SF 125.7804085 MHz
WDW EM
SSB 0
LB 1.00 Hz
GB 0
PC 2.00

1H spectrum

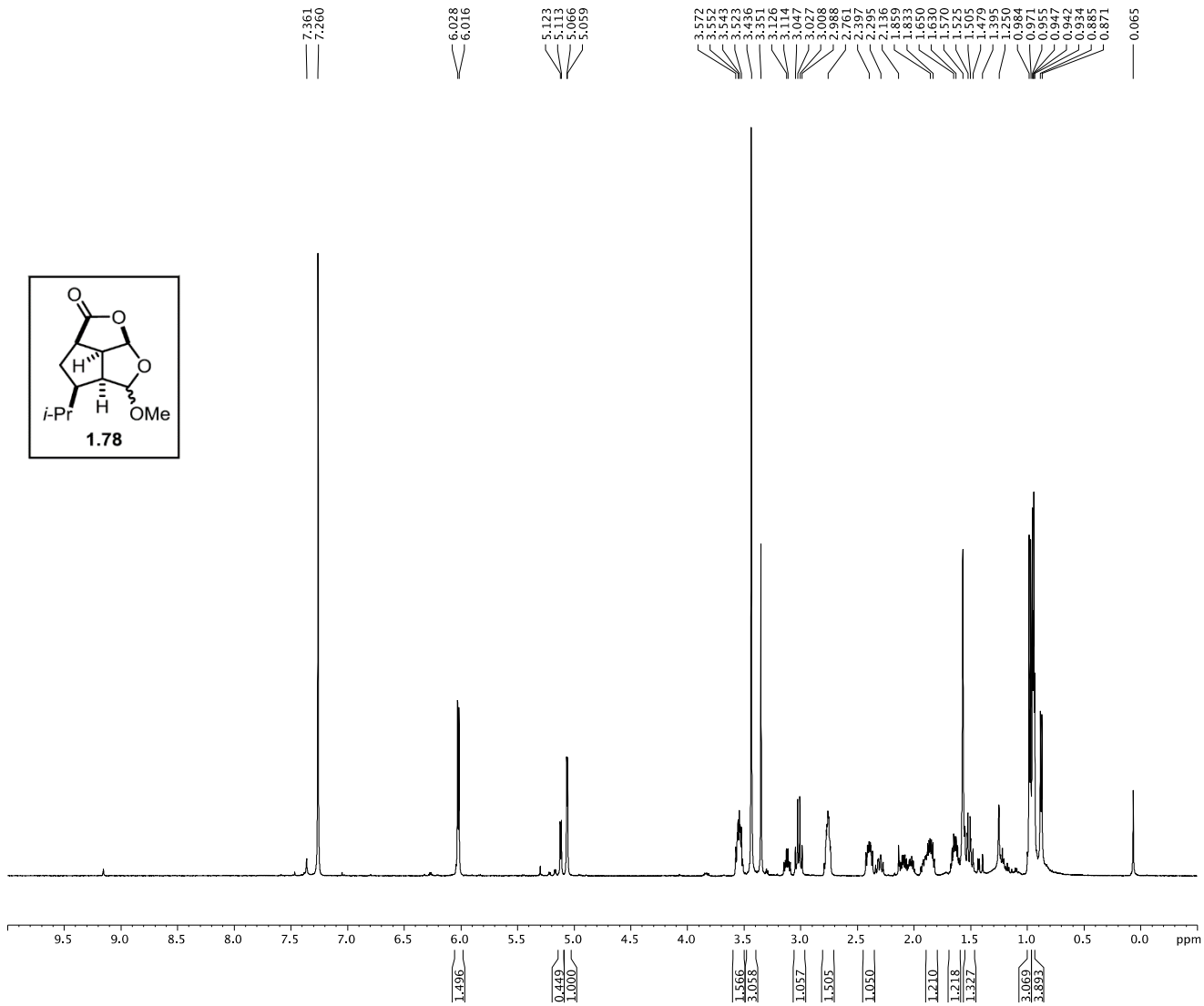

1.78

Current Data Parameters
NAME DJT-I-211
EXPNO 2
PROCNO 1

F2 - Acquisition Parameters
Date_ 20120903
Time 17.55
INSTRUM cryo500
PROBHD 5 mm CPTCI 1H-
PULPROG zg30
TD 81728
SOLVENT CDCl3
NS 16
DS 2
SWH 8012.820 Hz
FIDRES 0.098043 Hz
AQ 5.0998273 sec
RG 8
DW 62.400 usec
DE 6.00 usec
TE 298.0 K
D1 0.10000000 sec
MCREST 0 sec
MCWRK 0.01500000 sec

======== CHANNEL f1 =====
NUC1 1H
P1 7.50 usec
PL1 1.60 dB
SFO1 500.2235015 MHz

F2 - Processing parameters
SI 65536
SF 500.2200308 MHz
WDW EM
SSB 0
LB 0.30 Hz
GB 0
PC 4.00

Z-restored spin-echo 13C spectrum with 1H decoupling

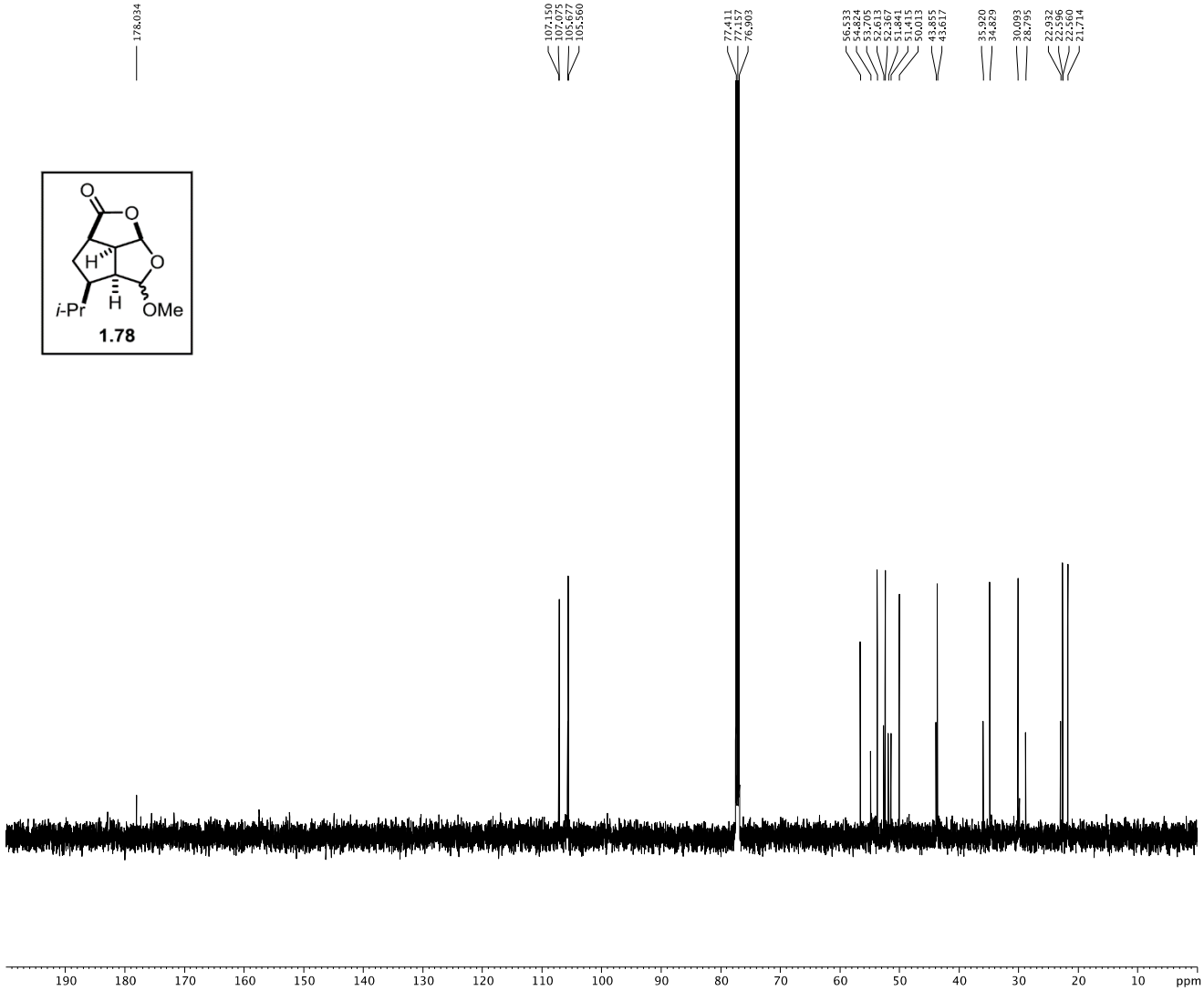


```
Current Data Parameters
NAME          DJT-I-211
EXPNO               3
PROCNO              1

F2 - Acquisition Parameters
Date_         20120903
Time            18.02
INSTRUM         cryo500
PROBHD   5 mm CPTCI 1H-
PULPROG  SpinEchopg30gp.prd
TD              65536
SOLVENT          CDCl3
NS                551
DS                 16
SWH           30303.031 Hz
FIDRES        0.462388 Hz
AQ            1.0813440 sec
RG                6502
DW              16.500 usec
DE               6.00 usec
TE              298.0 K
D1            0.25000000 sec
d11           0.03000000 sec
D16           0.00020000 sec
d17           0.00019600 sec
MCREST   0 sec
MCWRK         0.01500000 sec
P2              31.00 usec

======== CHANNEL f1 ========
NUC1              13C
P1              15.50 usec
P11            500.00 usec
P12           2000.00 usec
PL0            120.00 dB
PL1             -1.00 dB
SFO1         125.7942548 MHz
SP1              3.20 dB
SP2              3.20 dB
SPNAM[1] Crp60,0.5,20.1
SPNAM[2]    Crp60comp.4
SPOFF1   0 Hz
SPOFF2   0 Hz

======== CHANNEL f2 ========
CPDPRG[2         waltz16
NUC2              1H
PCPD2           100.00 usec
PL2              1.60 dB
PL12            24.60 dB
SFO2         500.2225011 MHz

====== GRADIENT CHANNEL =====
GPNAM[1]       SINE.100
GPNAM[2]       SINE.100
GPX1     0 %
GPX2     0 %
GPY1     0 %
GPY2     0 %
GPZ1            30.00 %
GPZ2            50.00 %
p15            500.00 usec
p16           1000.00 usec

F2 - Processing parameters
SI              65536
SF         125.7804080 MHz
WDW                EM
SSB      0
LB              1.00 Hz
GB       0
PC               2.00
```

Appendix B: Chapter 2 NMR Spectra

1H spectrum

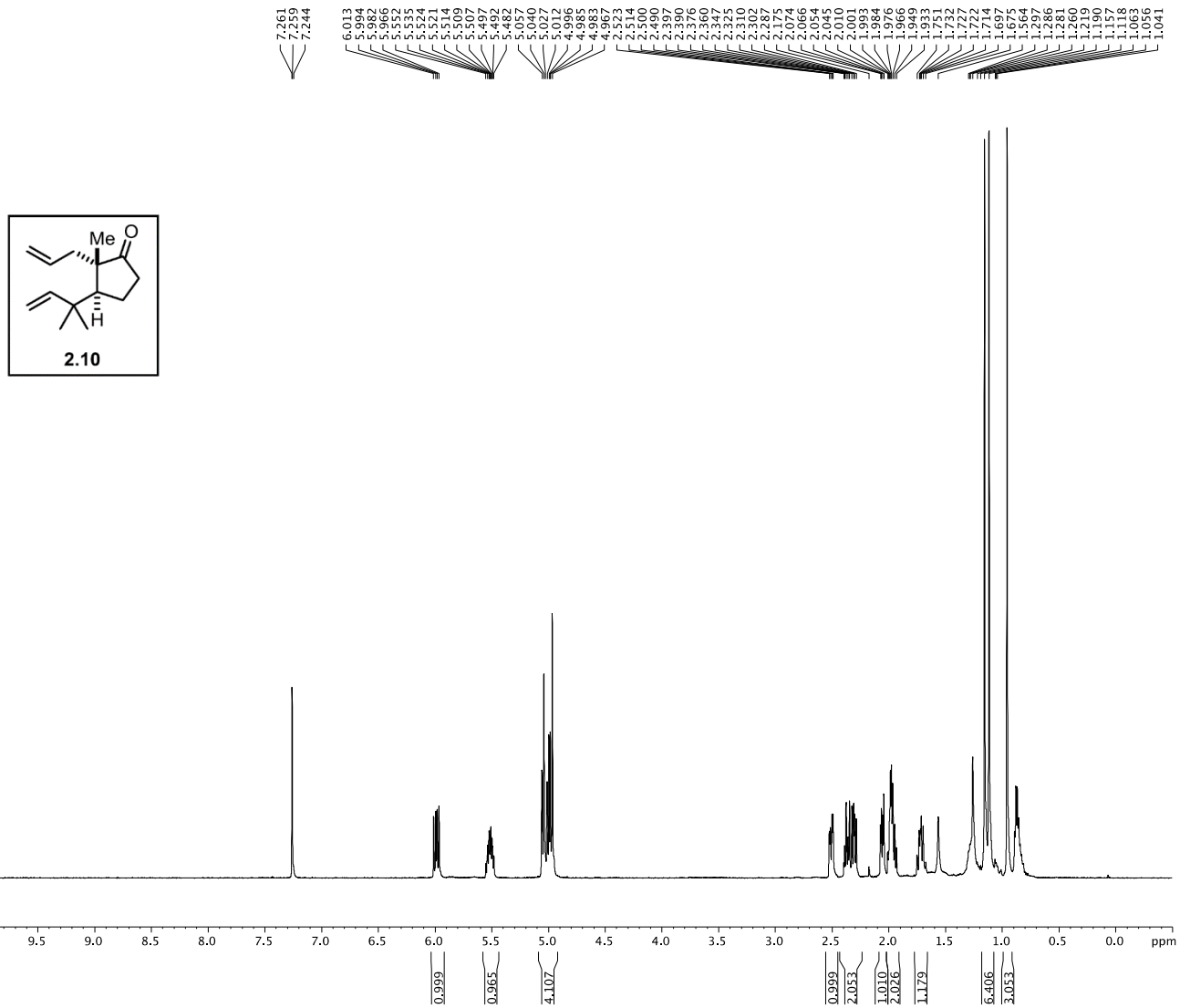

Current Data Parameters
NAME DJT-III-297
EXPNO 1
PROCNO 1

F2 - Acquisition Parameters
Date_ 20140520
Time 15.02
INSTRUM av600
PROBHD 5 mm TBI 1H/13
PULPROG zg30
TD 98074
SOLVENT CDCl3
NS 20
DS 0
SWH 9615.385 Hz
FIDRES 0.098042 Hz
AQ 5.0998478 sec
RG 406
DW 52.000 usec
DE 14.54 usec
TE 298.1 K
D1 0.10000000 sec
TD0 1

======== CHANNEL f1 =====
SFO1 600.1342009 MHz
NUC1 1H
P1 8.00 usec
PLW1 23.01441956 W

F2 - Processing parameters
SI 65536
SF 600.1300345 MHz
WDW EM
SSB 0
LB 0.30 Hz
GB 0
PC 1.00

Z-restored spin-echo 13C spectrum with 1H decoupling

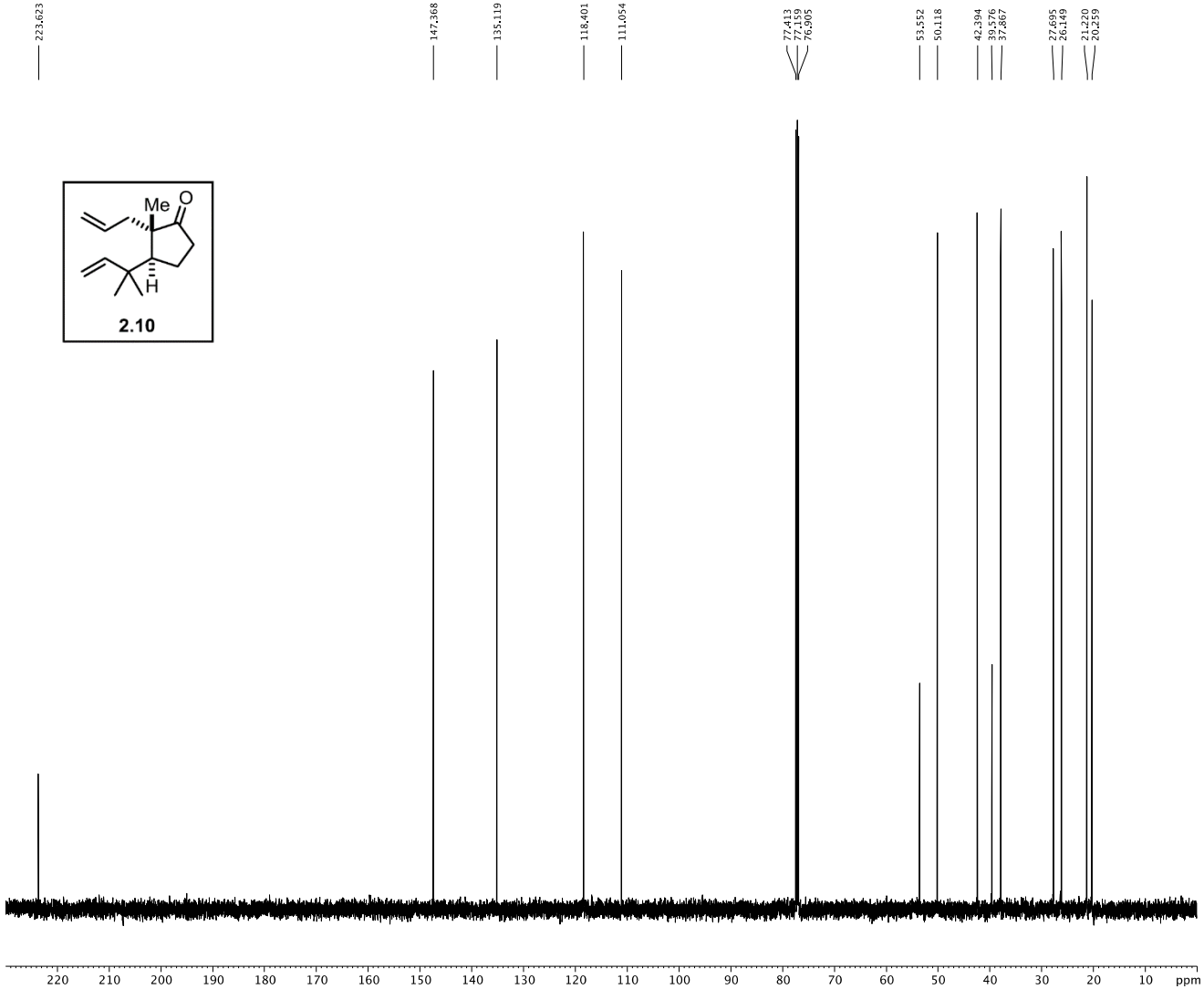


```
Current Data Parameters
NAME        DJT-IV-293
EXPNO              3
PROCNO             1

F2 - Acquisition Parameters
Date_        20150108
Time            8.02
INSTRUM        cryo500
PROBHD   5 mm CPTCI 1H-
PULPROG  SpinEchopg30gp.prd
TD             65536
SOLVENT         CDCl3
NS               142
DS                16
SWH          30303.031 Hz
FIDRES        0.462388 Hz
AQ          1.0813440 sec
RG           10321.3
DW             16.500 usec
DE              6.00 usec
TE             298.0 K
D1          0.25000000 sec
d11         0.03000000 sec
D16         0.00020000 sec
d17         0.00019600 sec
MCREST    0 sec
MCWRK       0.01500000 sec
P2             33.10 usec

======== CHANNEL f1 ========
NUC1             13C
P1             16.55 usec
P11            500.00 usec
P12           2000.00 usec
PL0            120.00 dB
PL1            -1.00 dB
SFO1       125.7942548 MHz
SP1             2.70 dB
SP2             2.70 dB
SPNAM[1] Crp60,0.5,20.1
SPNAM[2]   Crp60comp.4
SPOFF1   0 Hz
SPOFF2   0 Hz

======== CHANNEL f2 ========
CPDPRG[2       waltz16
NUC2             1H
PCPD2          100.00 usec
PL2             1.60 dB
PL12           24.50 dB
SFO2       500.2225011 MHz

====== GRADIENT CHANNEL =====
GPNAM[1]       SINE.100
GPNAM[2]       SINE.100
GPX1     0 %
GPX2     0 %
GPY1     0 %
GPY2     0 %
GPZ1           30.00 %
GPZ2           50.00 %
p15           500.00 usec
p16          1000.00 usec

F2 - Processing parameters
SI             65536
SF        125.7804090 MHz
WDW               EM
SSB     0
LB             1.00 Hz
GB      0
PC             2.00
```

1H spectrum

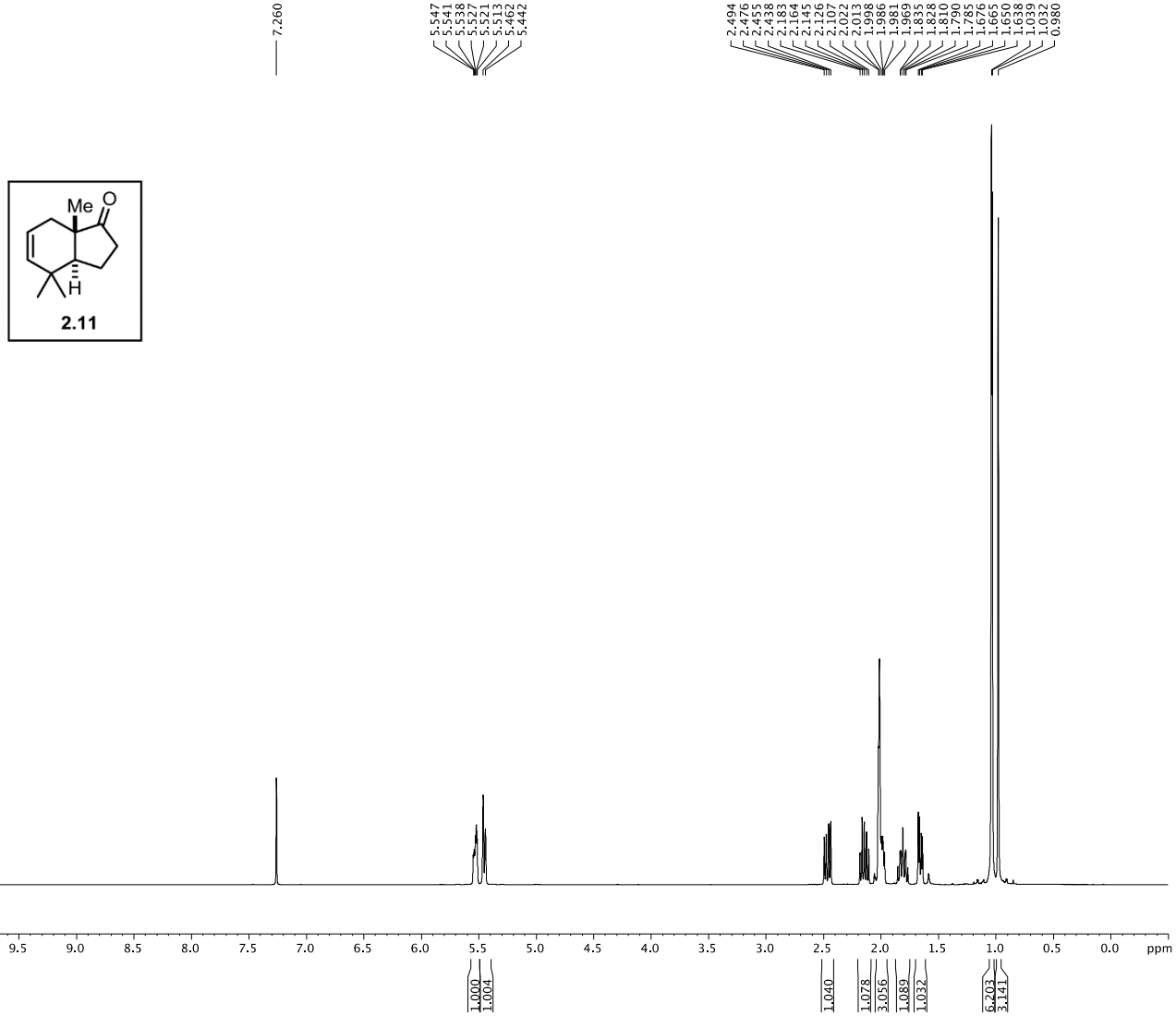

Current Data Parameters
NAME DJT-IV-294
EXPNO 5
PROCNO 1

F2 - Acquisition Parameters
Date_ 20150108
Time 15.03
INSTRUM cryo500
PROBHD 5 mm CPTCI 1H-
PULPROG zg30
TD 32048
SOLVENT CDCl3
NS 30
DS 0
SWH 8012.820 Hz
FIDRES 0.250026 Hz
AQ 1.9997952 sec
RG 8
DW 62.400 usec
DE 6.00 usec
TE 298.0 K
D1 0.10000000 sec
MCREST 0 sec
MCWRK 0.01500000 sec

======== CHANNEL f1 =====
NUC1 1H
P1 7.50 usec
PL1 1.60 dB
SFO1 500.2235015 MHz

F2 - Processing parameters
SI 65536
SF 500.2200317 MHz
WDW EM
SSB 0
LB 0.30 Hz
GB 0
PC 4.00

Z-restored spin-echo 13C spectrum with 1H decoupling

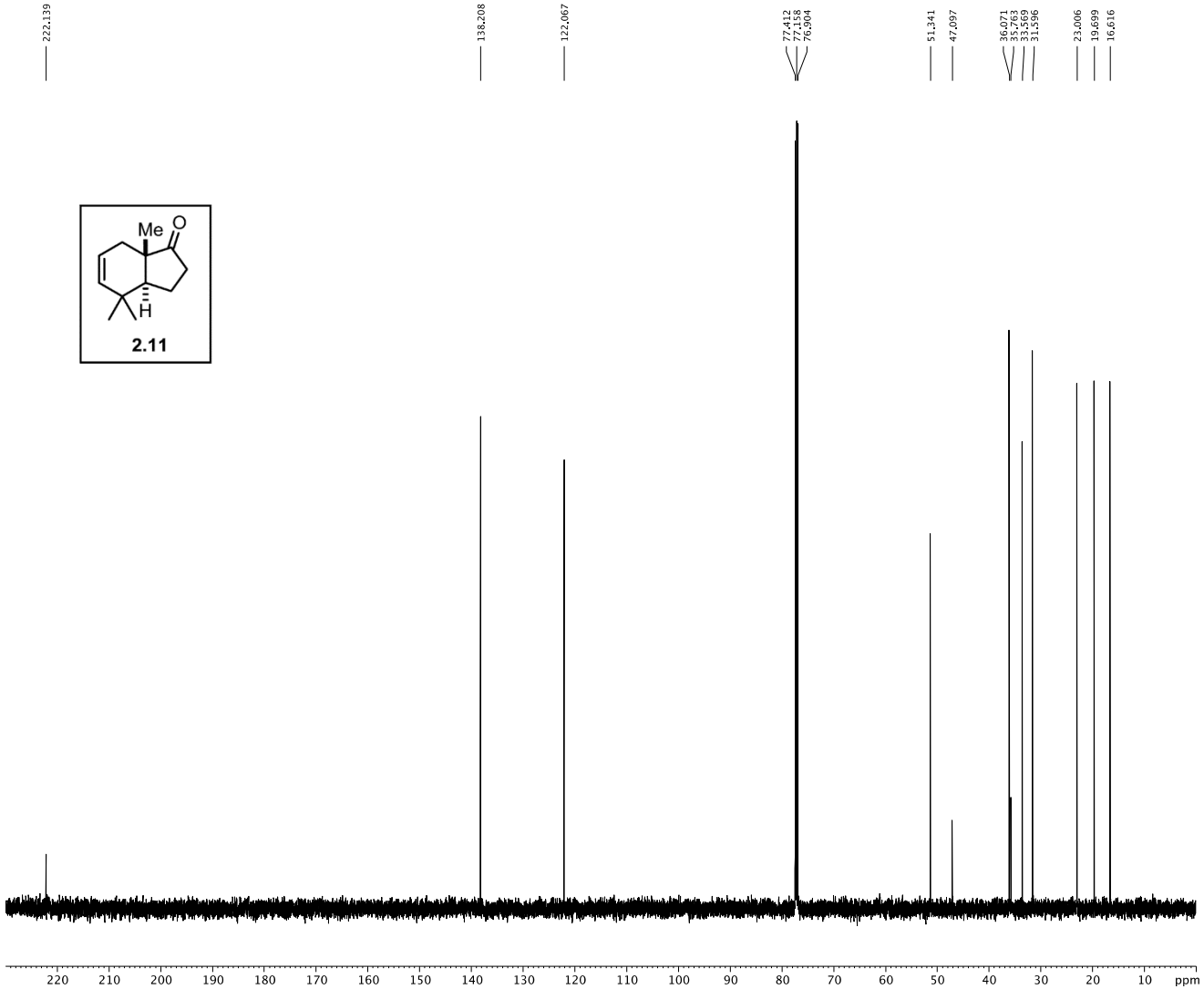


```
Current Data Parameters
NAME        DJT-IV-294
EXPNO            4
PROCNO           1

F2 - Acquisition Parameters
Date_       20150108
Time          15.07
INSTRUM       cryo500
PROBHD   5 mm CPTCI 1H-
PULPROG  SpinEchopg30gp.prd
TD          65536
SOLVENT       CDCl3
NS            309
DS              0
SWH         30303.031 Hz
FIDRES       0.462388 Hz
AQ          1.08134440 sec
RG           7298.2
DW           16.500 usec
DE            6.00 usec
TE           298.0 K
D1         0.25000000 sec
d11        0.03000000 sec
D16        0.00020000 sec
d17        0.00019600 sec
MCREST   0 sec
MCWRK      0.01500000 sec
P2           33.10 usec

======== CHANNEL f1 ========
NUC1           13C
P1           16.55 usec
P11          500.00 usec
P12         2000.00 usec
PL0          120.00 dB
PL1           -1.00 dB
SFO1      125.7942548 MHz
SP1           2.70 dB
SP2           2.70 dB
SPNAM[1] Crp60,0.5,20.1
SPNAM[2]   Crp60comp.4
SPOFF1   0 Hz
SPOFF2   0 Hz

======== CHANNEL f2 ========
CPDPRG[2       waltz16
NUC2           1H
PCPD2        100.00 usec
PL2          1.60 dB
PL12         24.50 dB
SFO2      500.2225011 MHz

====== GRADIENT CHANNEL =====
GPNAM[1]      SINE.100
GPNAM[2]      SINE.100
GPX1     0 %
GPX2     0 %
GPY1     0 %
GPY2     0 %
GPZ1         30.00 %
GPZ2         50.00 %
p15         500.00 usec
p16        1000.00 usec

F2 - Processing parameters
SI          65536
SF       125.7804084 MHz
WDW            EM
SSB     0
LB          1.00 Hz
GB      0
PC          2.00
```

1H spectrum

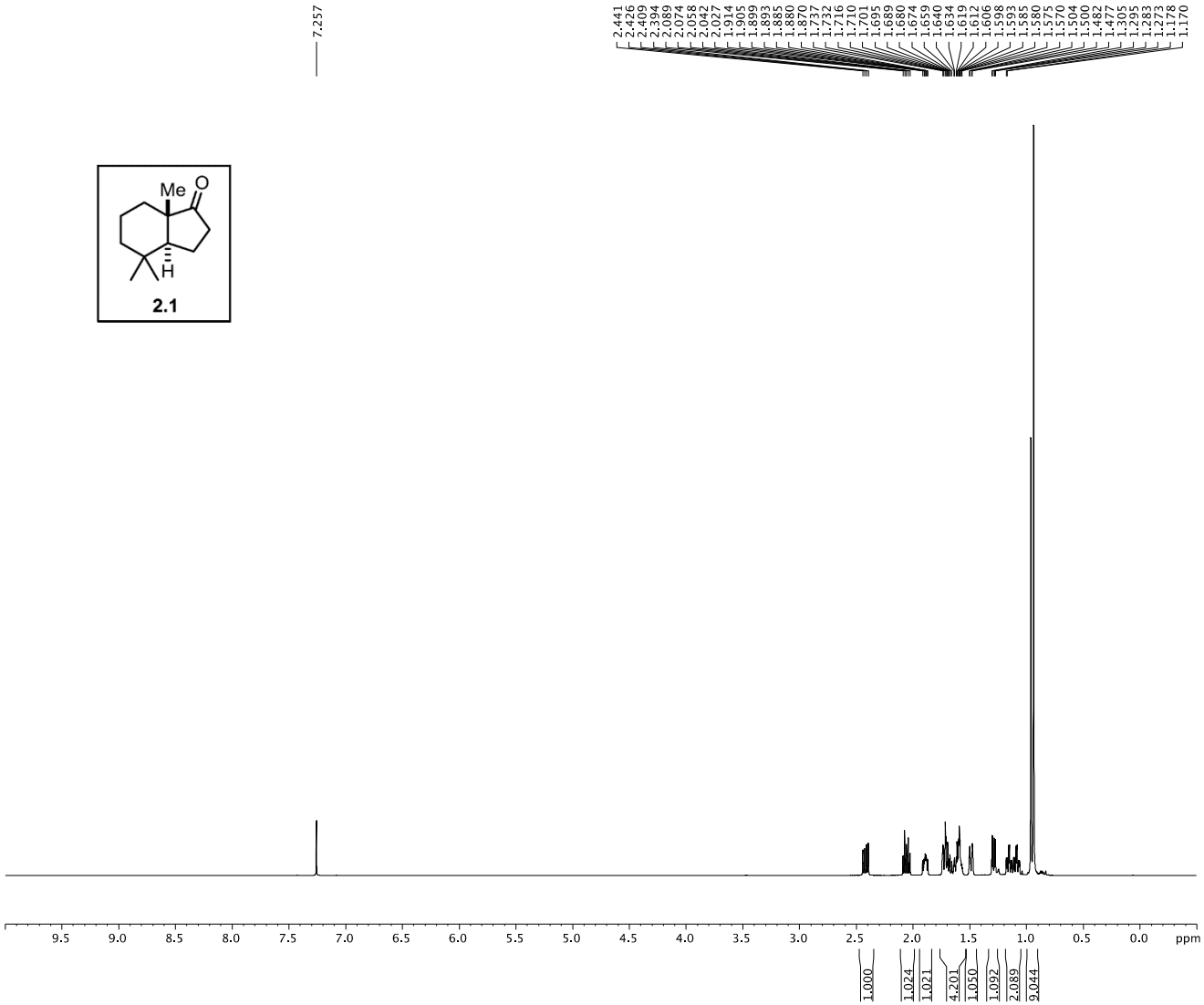

Current Data Parameters
NAME DJT-IV-295
EXPNO 1
PROCNO 1

F2 - Acquisition Parameters
Date_ 20150109
Time 13.56
INSTRUM av600
PROBHD 5 mm TBI 1H/13
PULPROG zg30
TD 38460
SOLVENT CDCl3
NS 20
DS 0
SWH 9615.385 Hz
FIDRES 0.250010 Hz
AQ 1.9999200 sec
RG 512
DW 52.000 usec
DE 14.54 usec
TE 298.2 K
D1 0.10000000 sec
TD0 1

======== CHANNEL f1 =====
SFO1 600.1342009 MHz
NUC1 1H
P1 8.00 usec
PLW1 23.01441956 W

F2 - Processing parameters
SI 65536
SF 600.1300350 MHz
WDW EM
SSB 0
LB 0.30 Hz
GB 0
PC 1.00

Z-restored spin-echo 13C spectrum with 1H decoupling

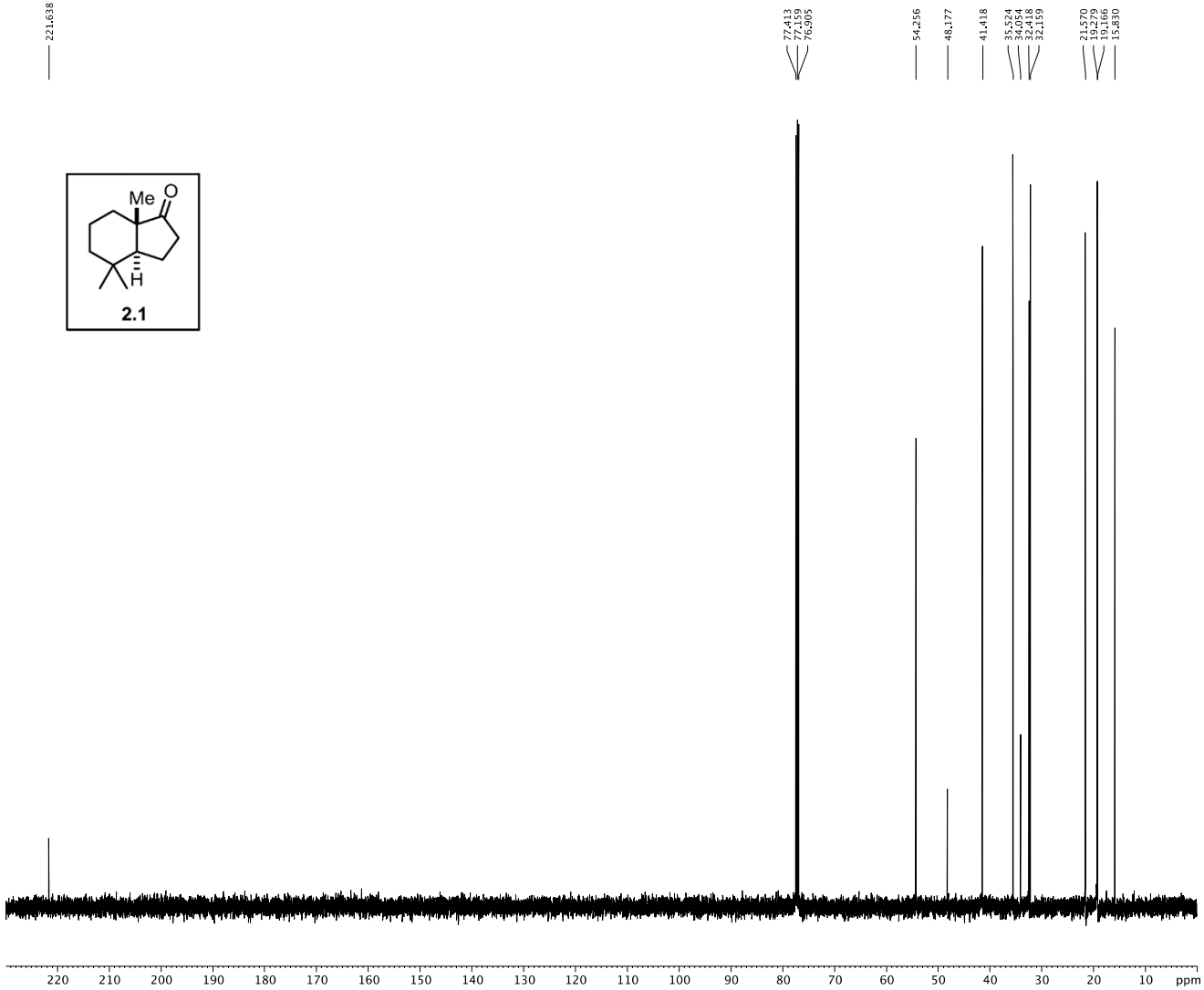


```
Current Data Parameters
NAME        DJT-IV-295
EXPNO            3
PROCNO           1

F2 - Acquisition Parameters
Date_       20150109
Time          17.27
INSTRUM       cryo500
PROBHD   5 mm CPTCI 1H-
PULPROG  SpinEchopg30gp.prd
TD          65536
SOLVENT       CDCl3
NS            271
DS              0
SWH       30303.031 Hz
FIDRES     0.462388 Hz
AQ        1.0813440 sec
RG            13004
DW            16.500 usec
DE             6.00 usec
TE            298.0 K
D1        0.25000000 sec
d11       0.03000000 sec
D16       0.00020000 sec
d17       0.00019600 sec
MCREST   0 sec
MCWRK      0.01500000 sec
P2            33.10 usec

======== CHANNEL f1 ========
NUC1            13C
P1            16.55 usec
P11           500.00 usec
P12          2000.00 usec
PL0           120.00 dB
PL1           -1.00 dB
SFO1       125.7942548 MHz
SP1            2.70 dB
SP2            2.70 dB
SPNAM[1] Crp60.0.5.20.1
SPNAM[2]   Crp60comp.4
SPOFF1   0 Hz
SPOFF2   0 Hz

======== CHANNEL f2 ========
CPDPRG[2        waltz16
NUC2             1H
PCPD2          100.00 usec
PL2            1.60 dB
PL12           24.50 dB
SFO2       500.2225011 MHz

====== GRADIENT CHANNEL =====
GPNAM[1]       SINE.100
GPNAM[2]       SINE.100
GPX1     0 %
GPX2     0 %
GPY1     0 %
GPY2     0 %
GPZ1           30.00 %
GPZ2           50.00 %
p15           500.00 usec
p16          1000.00 usec

F2 - Processing parameters
SI          65536
SF       125.7804090 MHz
WDW            EM
SSB      0
LB             1.00 Hz
GB       0
PC             2.00
```

1H spectrum

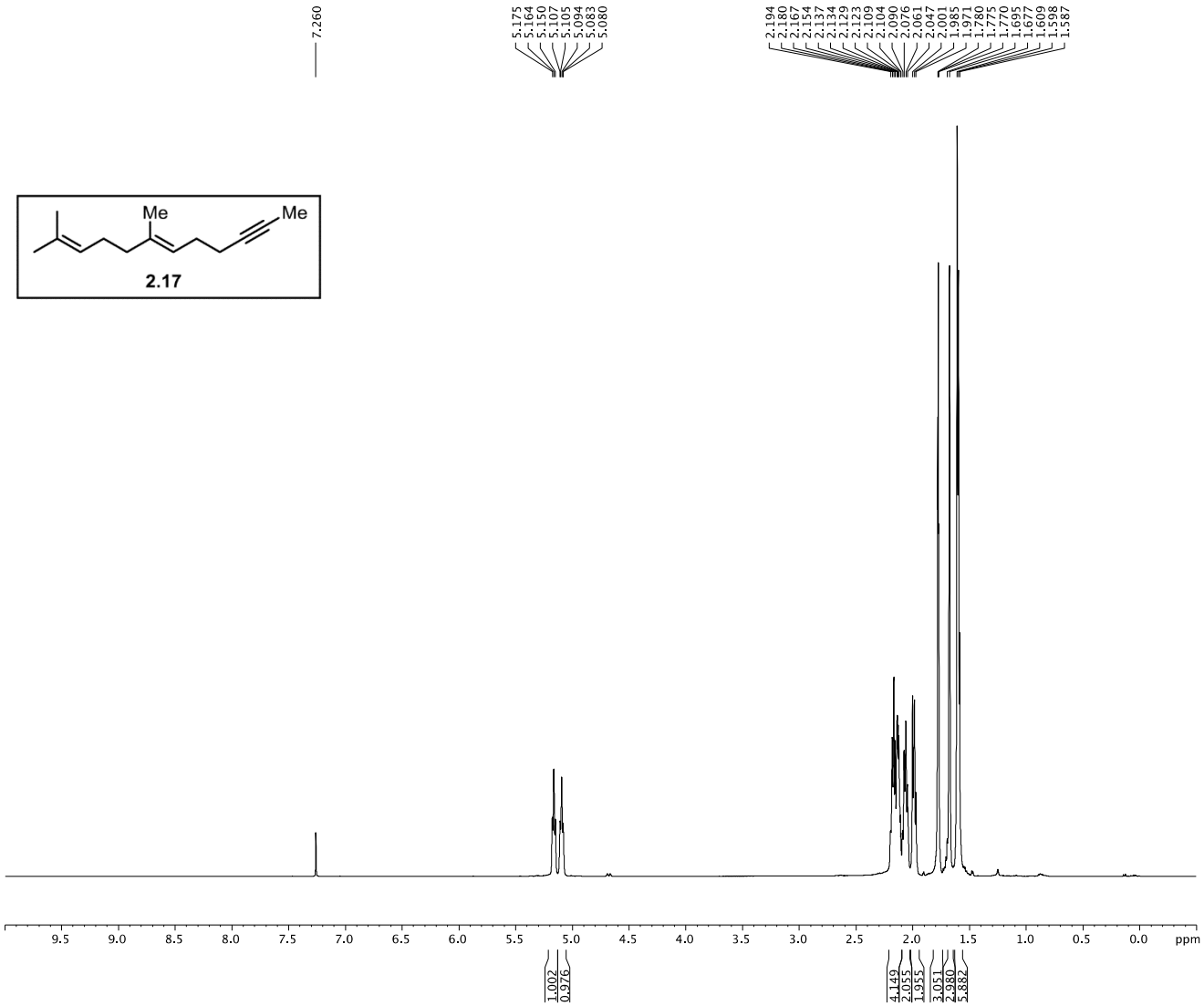

Current Data Parameters
NAME DJT-III-113
EXPNO 5
PROCNO 1

F2 - Acquisition Parameters
Date_ 20140811
Time 15.18
INSTRUM cryo500
PROBHD 5 mm CPTCI 1H-
PULPROG zg30
TD 81728
SOLVENT CDCl3
NS 12
DS 2
SWH 8012.820 Hz
FIDRES 0.098043 Hz
AQ 5.0998273 sec
RG 4
DW 62.400 usec
DE 6.00 usec
TE 298.0 K
D1 0.10000000 sec
MCREST 0 sec
MCWRK 0.01500000 sec

======== CHANNEL f1 =====
NUC1 1H
P1 7.50 usec
PL1 1.60 dB
SFO1 500.2235015 MHz

F2 - Processing parameters
SI 65536
SF 500.2200311 MHz
WDW EM
SSB 0
LB 0.30 Hz
GB 0
PC 4.00

Z-restored spin-echo 13C spectrum with 1H decoupling

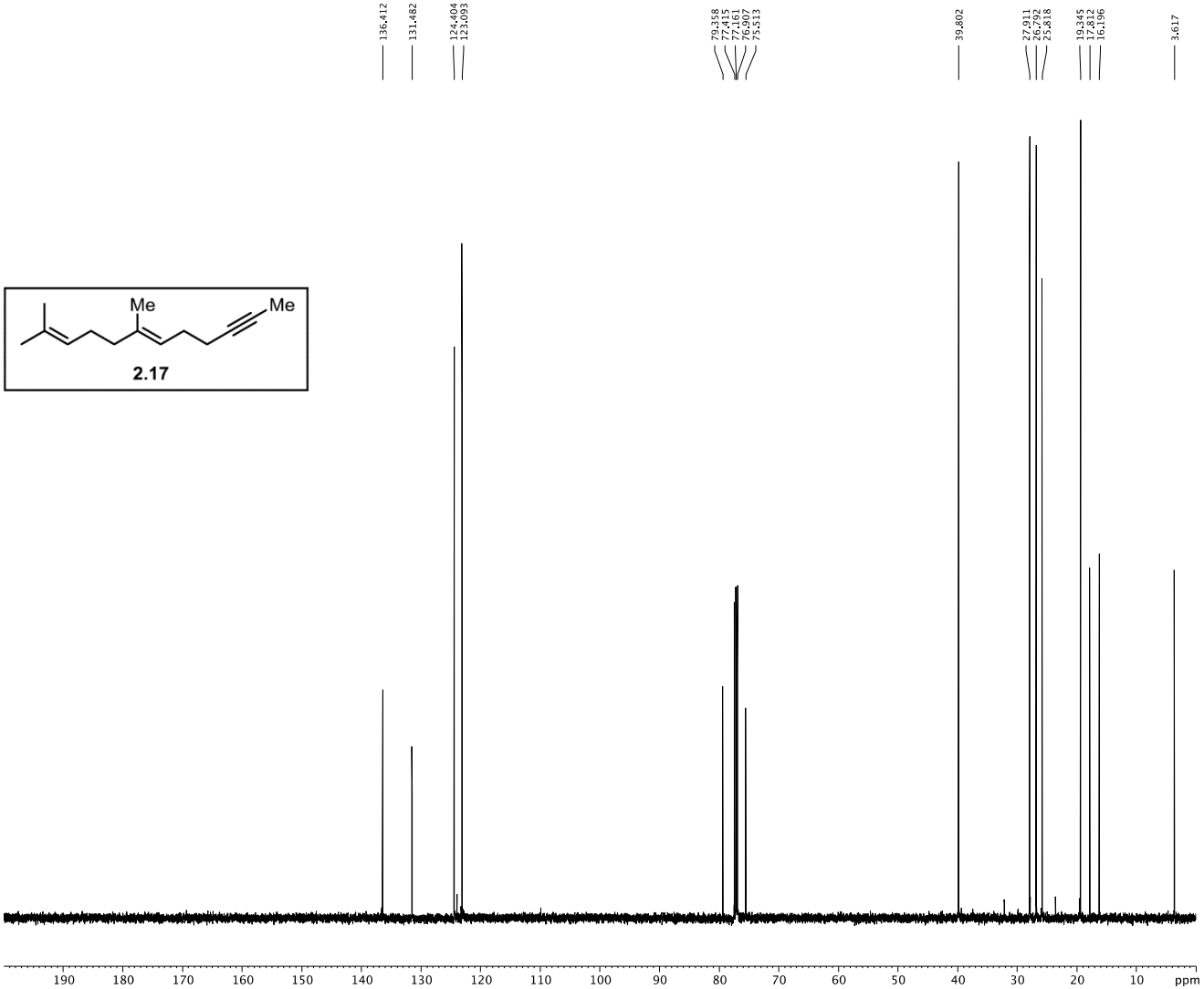

Current Data Parameters
NAME DJT-III-113
EXPNO 6
PROCNO 1

F2 - Acquisition Parameters
Date_ 20140811
Time 15.22
INSTRUM cryo500
PROBHD 5 mm CPTCI 1H-
PULPROG SpinEchopg30gp.prd
TD 65536
SOLVENT CDCl3
NS 143
DS 16
SWH 30303.031 Hz
FIDRES 0.462388 Hz
AQ 1.0813440 sec
RG 5160.6
DW 16.500 usec
DE 6.00 usec
TE 298.0 K
D1 0.25000000 sec
d11 0.03000000 sec
D16 0.00020000 sec
d17 0.00019600 sec
MCREST 0 sec
MCWRK 0.01500000 sec
P2 31.00 usec

======== CHANNEL f1 ========
NUC1 13C
P1 15.50 usec
P11 500.00 usec
P12 2000.00 usec
PL0 120.00 dB
PL1 -1.00 dB
SFO1 125.7942548 MHz
SP1 3.20 dB
SP2 3.20 dB
SPNAM[1] Crp60,0.5,20.1
SPNAM[2] Crp60comp.4
SPOFF1 0 Hz
SPOFF2 0 Hz

======== CHANNEL f2 ========
CPDPRG[2 waltz16
NUC2 1H
PCPD2 100.00 usec
PL2 1.60 dB
PL12 24.60 dB
SFO2 500.2225011 MHz

====== GRADIENT CHANNEL =====
GPNAM[1] SINE.100
GPNAM[2] SINE.100
GPX1 0 %
GPX2 0 %
GPY1 0 %
GPY2 0 %
GPZ1 30.00 %
GPZ2 50.00 %
p15 500.00 usec
p16 1000.00 usec

F2 - Processing parameters
SI 65536
SF 125.7804080 MHz
WDW EM
SSB 0
LB 1.00 Hz
GB 0
PC 2.00

1H spectrum

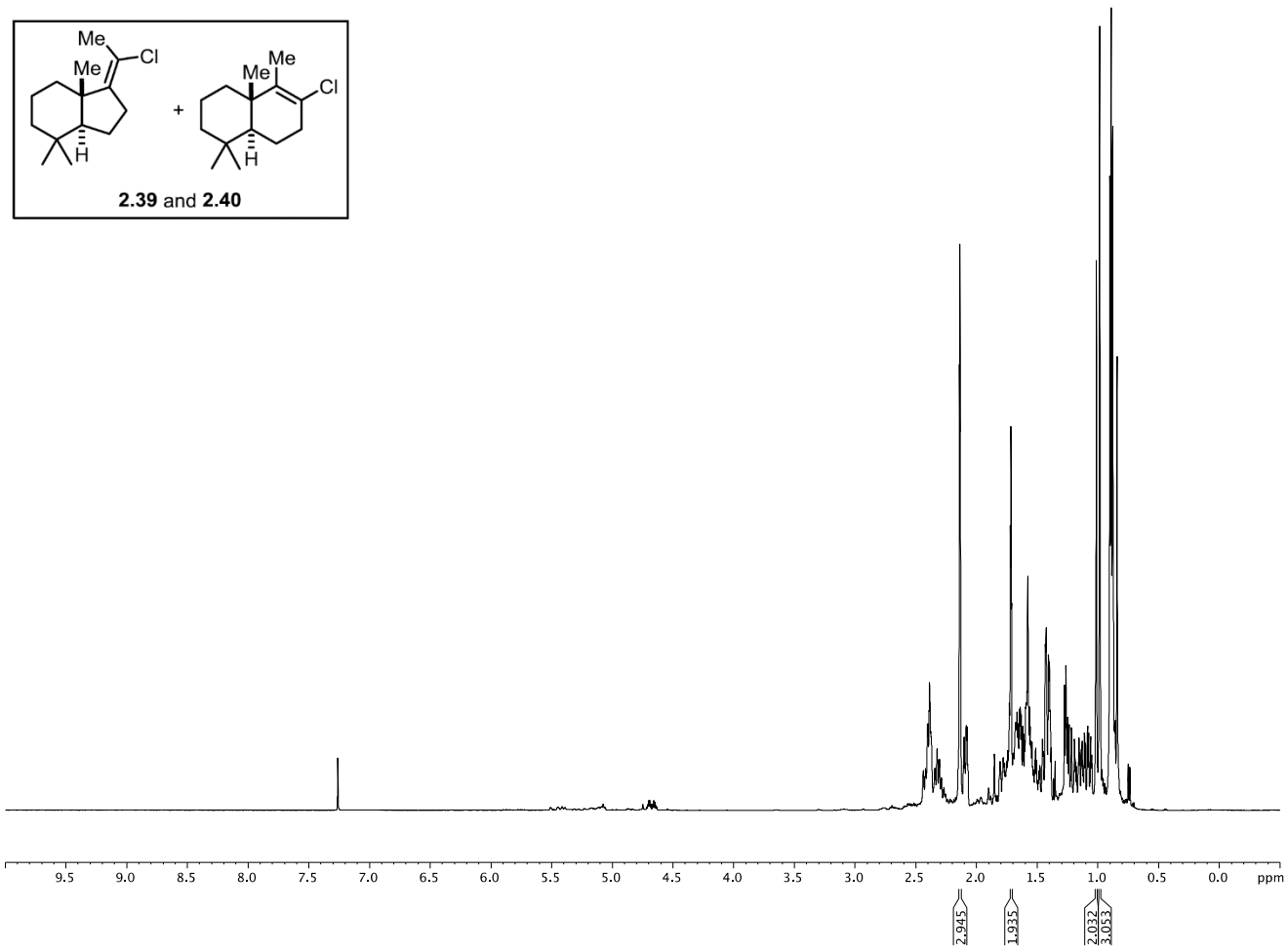

Current Data Parameters
NAME DJT-III-135
EXPNO 5
PROCNO 1

F2 - Acquisition Parameters
Date_ 20140811
Time 15.26
INSTRUM cryo500
PROBHD 5 mm CPTCI 1H-
PULPROG zg30
TD 81728
SOLVENT CDCl3
NS 20
DS 2
SWH 8012.820 Hz
FIDRES 0.098043 Hz
AQ 5.0998273 sec
RG 4
DW 62.400 usec
DE 6.00 usec
TE 298.0 K
D1 0.10000000 sec
MCREST 0 sec
MCWRK 0.01500000 sec

======== CHANNEL f1 =====
NUC1 1H
P1 7.50 usec
PL1 1.60 dB
SFO1 500.2235015 MHz

F2 - Processing parameters
SI 65536
SF 500.2200306 MHz
WDW EM
SSB 0
LB 0.30 Hz
GB 0
PC 4.00

1H spectrum

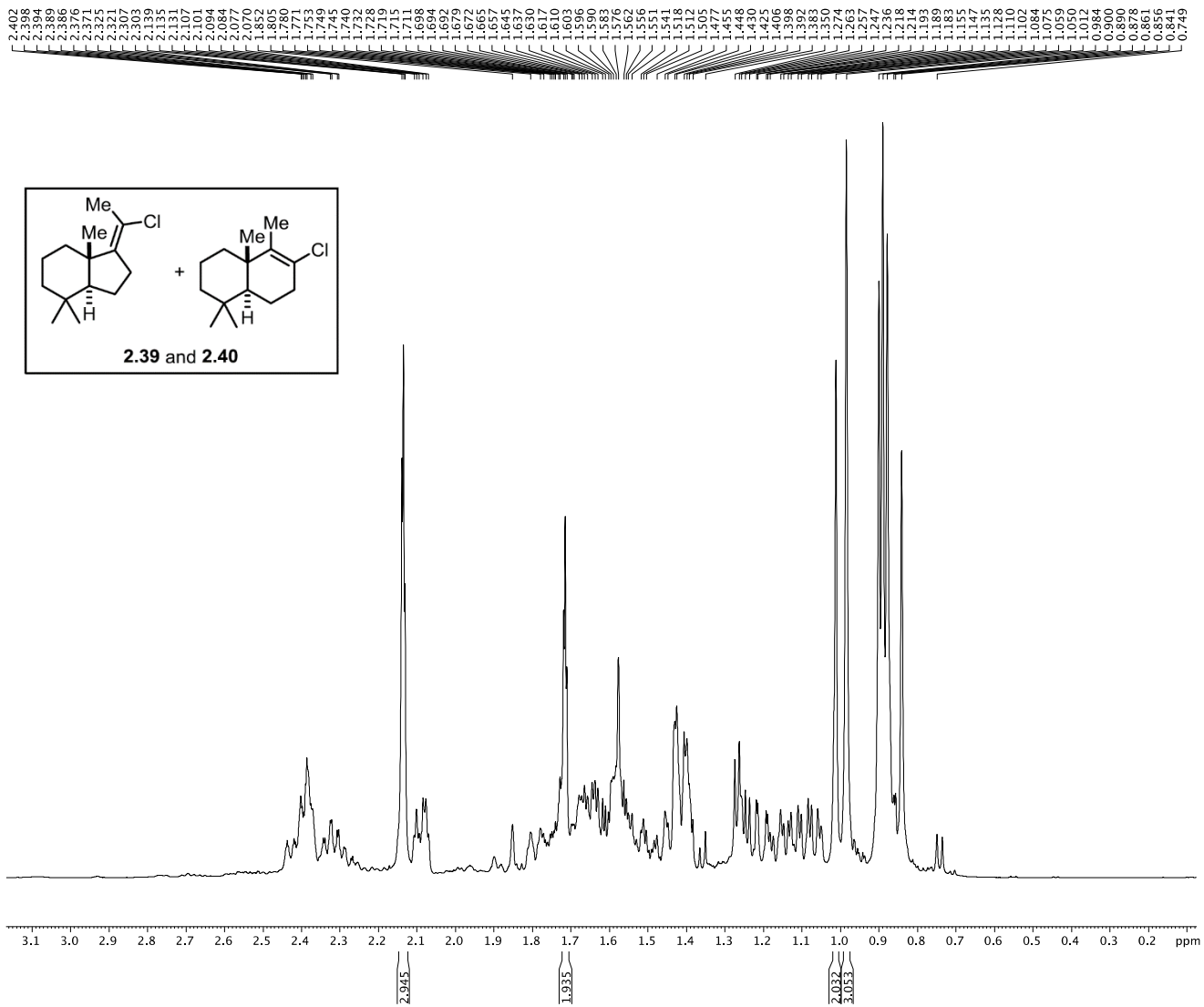

Current Data Parameters
NAME DJT-III-135
EXPNO 5
PROCNO 1

F2 - Acquisition Parameters
Date_ 20140811
Time 15.26
INSTRUM cryo500
PROBHD 5 mm CPTCI 1H-
PULPROG zg30
TD 81728
SOLVENT CDCl3
NS 20
DS 2
SWH 8012.820 Hz
FIDRES 0.098043 Hz
AQ 5.0998273 sec
RG 4
DW 62.400 usec
DE 6.00 usec
TE 298.0 K
D1 0.10000000 sec
MCREST 0 sec
MCWRK 0.01500000 sec

======== CHANNEL f1 =====
NUC1 1H
P1 7.50 usec
PL1 1.60 dB
SFO1 500.2235015 MHz

F2 - Processing parameters
SI 65536
SF 500.2200306 MHz
WDW EM
SSB 0
LB 0.30 Hz
GB 0
PC 4.00

Z-restored spin-echo 13C spectrum with 1H decoupling

2.39 and **2.40**

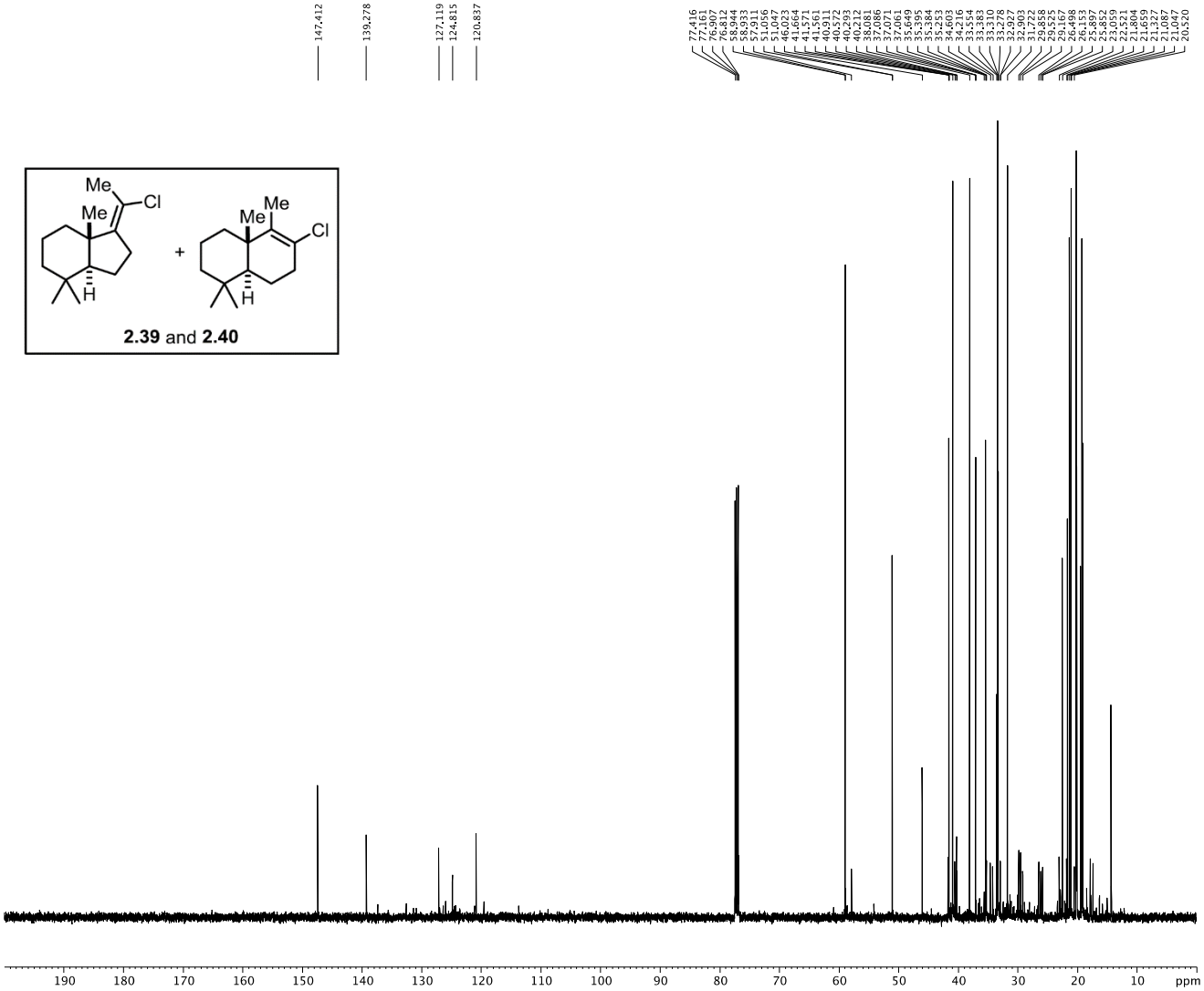

Current Data Parameters
NAME DJT-III-135
EXPNO 6
PROCNO 1

F2 - Acquisition Parameters
Date_ 20140811
Time 15.33
INSTRUM cryo500
PROBHD 5 mm CPTCI 1H-
PULPROG SpinEchopg30gp.prd
TD 65536
SOLVENT CDCl3
NS 317
DS 16
SWH 30303.031 Hz
FIDRES 0.462388 Hz
AQ 1.0813440 sec
RG 7298.2
DW 16.500 usec
DE 6.00 usec
TE 298.0 K
D1 0.25000000 sec
d11 0.03000000 sec
D16 0.00020000 sec
d17 0.00019600 sec
MCREST 0 sec
MCWRK 0.01500000 sec
P2 31.00 usec

======== CHANNEL f1 ========
NUC1 13C
P1 15.50 usec
P11 500.00 usec
P12 2000.00 usec
PL0 120.00 dB
PL1 -1.00 dB
SFO1 125.7942548 MHz
SP1 3.20 dB
SP2 3.20 dB
SPNAM[1] Crp60,0.5,20.1
SPNAM[2] Crp60comp.4
SPOFF1 0 Hz
SPOFF2 0 Hz

======== CHANNEL f2 ========
CPDPRG[2 waltz16
NUC2 1H
PCPD2 100.00 usec
PL2 1.60 dB
PL12 24.60 dB
SFO2 500.2225011 MHz

====== GRADIENT CHANNEL =====
GPNAM[1] SINE.100
GPNAM[2] SINE.100
GPX1 0 %
GPX2 0 %
GPY1 0 %
GPY2 0 %
GPZ1 30.00 %
GPZ2 50.00 %
p15 500.00 usec
p16 1000.00 usec

F2 - Processing parameters
SI 65536
SF 125.7804085 MHz
WDW EM
SSB 0
LB 1.00 Hz
GB 0
PC 2.00

Appendix C: Chapter 3 NMR Spectra

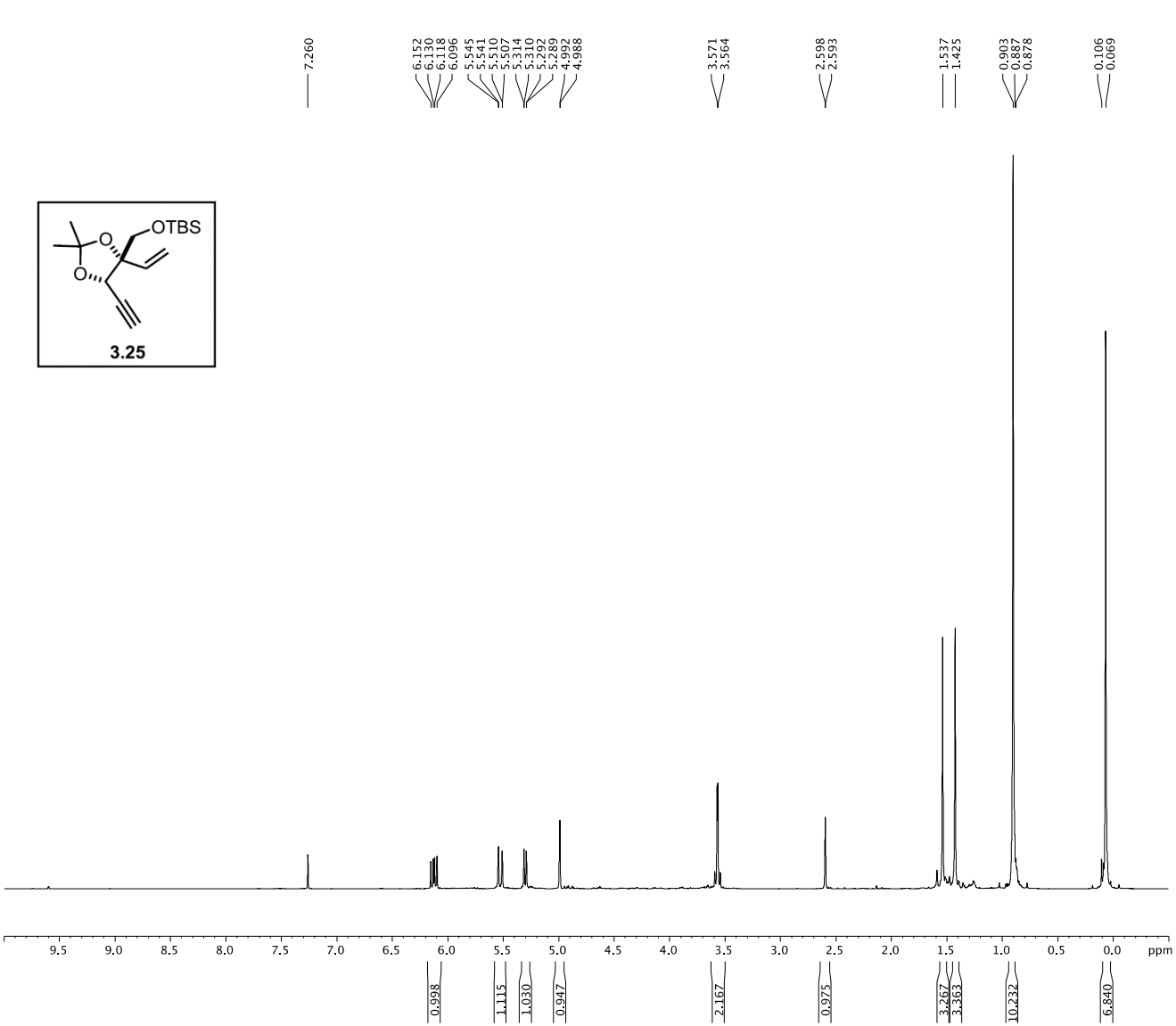

Current Data Parameters
NAME DJT-II-295
EXPNO 3
PROCNO 1

F2 - Acquisition Parameters
Date_ 20131130
Time 15.24
INSTRUM cryo500
PROBHD 5 mm CPTCI 1H-
PULPROG zg30
TD 81728
SOLVENT CDCl3
NS 8
DS 2
SWH 8012.820 Hz
FIDRES 0.098043 Hz
AQ 5.0998273 sec
RG 8
DW 62.400 usec
DE 6.00 usec
TE 298.0 K
D1 0.10000000 sec
MCREST 0 sec
MCWRK 0.01500000 sec

======== CHANNEL f1 ========
NUC1 1H
P1 7.50 usec
PL1 1.60 dB
SFO1 500.2235015 MHz

F2 - Processing parameters
SI 65536
SF 500.2200308 MHz
WDW EM
SSB 0
LB 0.30 Hz
GB 0
PC 4.00

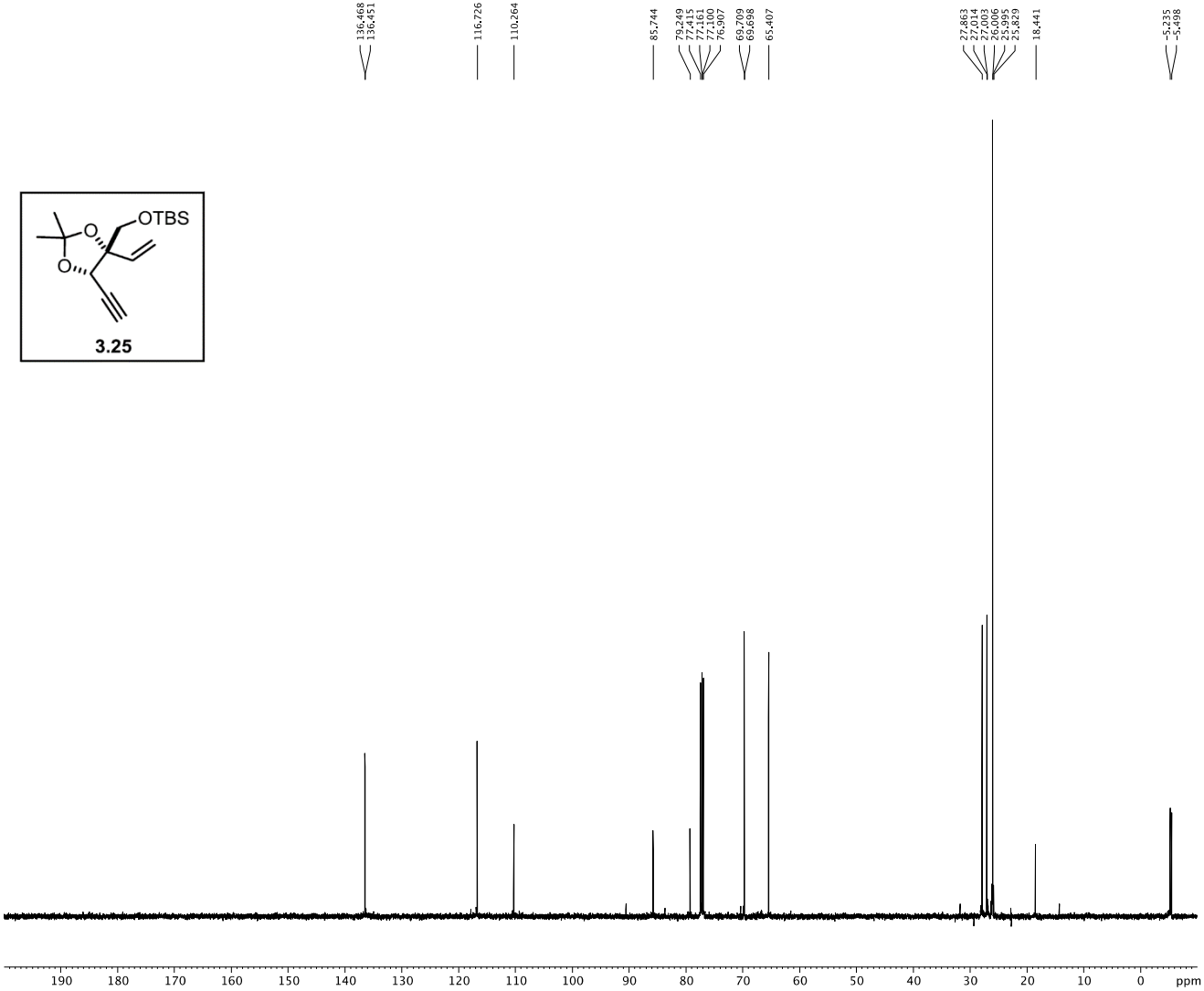

Current Data Parameters
NAME DJT-II-295
EXPNO 4
PROCNO 1

F2 - Acquisition Parameters
Date_ 20131130
Time 15.34
INSTRUM cryo500
PROBHD 5 mm CPTCI 1H-
PULPROG SpinEchopg30gp.prd
TD 65536
SOLVENT CDCl3
NS 385
DS 16
SWH 30303.031 Hz
FIDRES 0.462388 Hz
AQ 1.0813440 sec
RG 14596.5
DW 16.500 usec
DE 6.00 usec
TE 298.0 K
D1 0.25000000 sec
d11 0.03000000 sec
D16 0.00020000 sec
d17 0.00019600 sec
MCREST 0 sec
MCWRK 0.01500000 sec
P2 31.00 usec

======== CHANNEL f1 ========
NUC1 13C
P1 15.50 usec
P11 500.00 usec
P12 2000.00 usec
PL0 120.00 dB
PL1 -1.00 dB
SFO1 125.7942548 MHz
SP1 3.20 dB
SP2 3.20 dB
SPNAM[1] Crp60,0.5,20.1
SPNAM[2] Crp60comp.4
SPOFF1 0 Hz
SPOFF2 0 Hz

======== CHANNEL f2 ========
CPDPRG[2 waltz16
NUC2 1H
PCPD2 100.00 usec
PL2 1.60 dB
PL12 24.60 dB
SFO2 500.2225011 MHz

====== GRADIENT CHANNEL =====
GPNAM[1] SINE.100
GPNAM[2] SINE.100
GPX1 0 %
GPX2 0 %
GPY1 0 %
GPY2 0 %
GPZ1 30.00 %
GPZ2 50.00 %
p15 500.00 usec
p16 1000.00 usec

F2 - Processing parameters
SI 65536
SF 125.7804076 MHz
WDW EM
SSB 0
LB 1.00 Hz
GB 0
PC 2.00

3.26

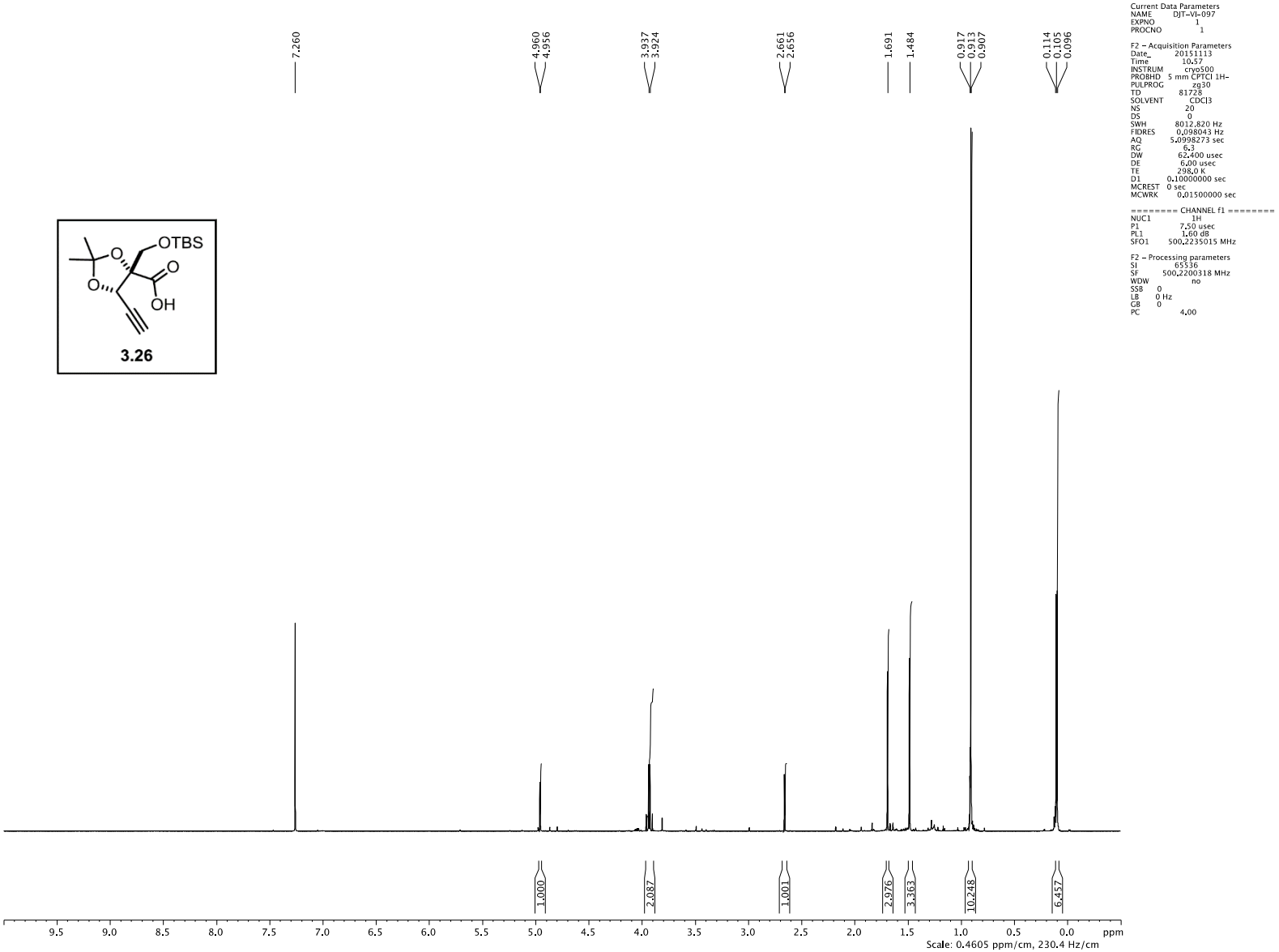

Current Data Parameters
NAME DJT-VI-097
EXPNO 1
PROCNO 1

F2 - Acquisition Parameters
Date_ 20151113
Time 10.57
INSTRUM cryo500
PROBHD 5 mm CPTCI 1H-
PULPROG zg30
TD 81728
SOLVENT CDCl3
NS 20
DS 0
SWH 8012.820 Hz
FIDRES 0.098043 Hz
AQ 5.0998273 sec
RG 6.3
DW 62.400 usec
DE 6.00 usec
TE 298.0 K
D1 0.10000000 sec
MCREST 0 sec
MCWRK 0.01500000 sec

======== CHANNEL f1 ========
NUC1 1H
P1 7.50 usec
PL1 1.60 dB
SFO1 500.2235015 MHz

F2 - Processing parameters
SI 65536
SF 500.2200318 MHz
WDW no
SSB 0
LB 0 Hz
GB 0
PC 4.00

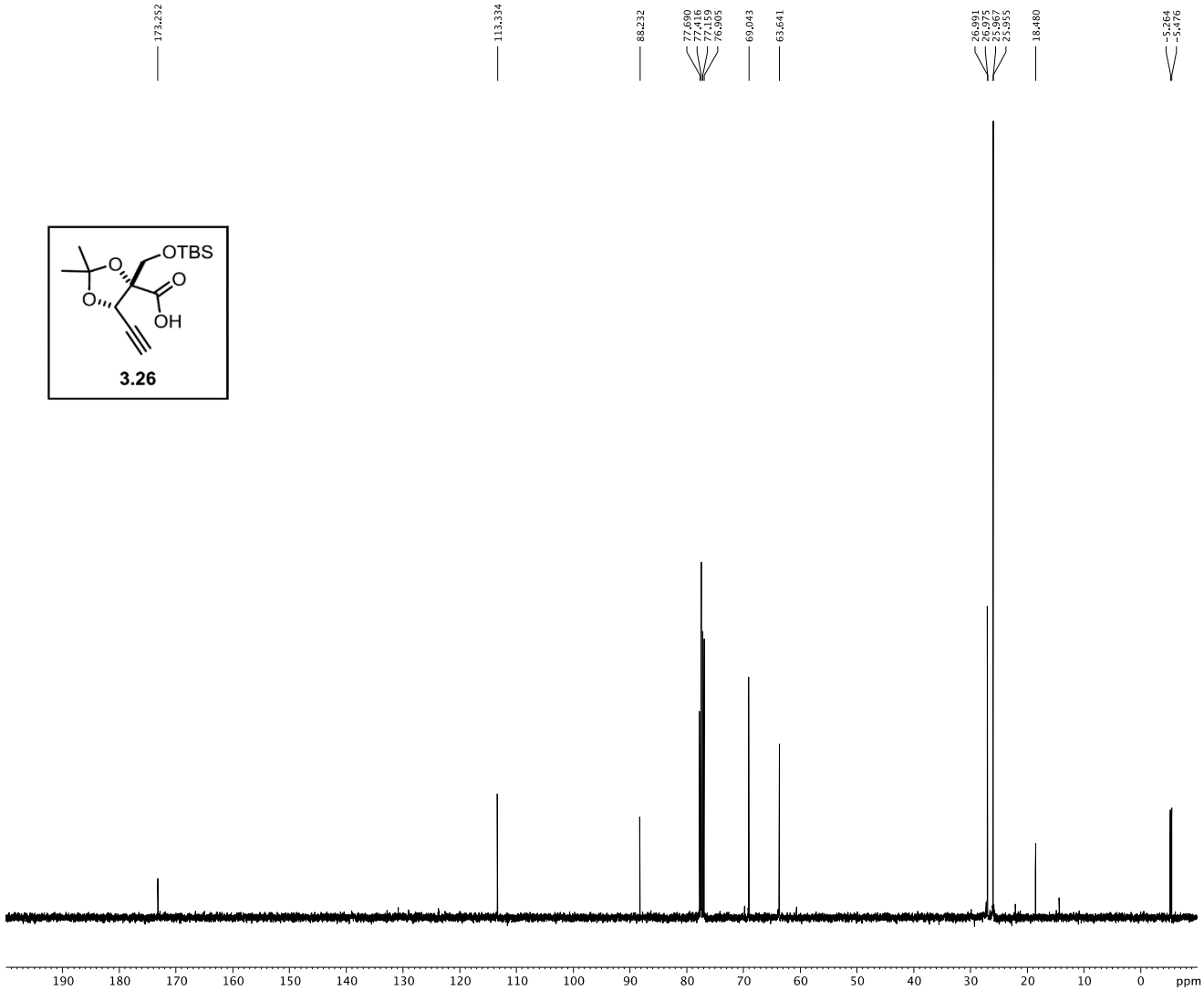

Current Data Parameters
NAME DJT-III-043
EXPNO 4
PROCNO 1

F2 - Acquisition Parameters
Date_ 20131129
Time 13.55
INSTRUM cryo500
PROBHD 5 mm CPTCI 1H-
PULPROG SpinEchopg30gp.prd
TD 65536
SOLVENT CDCl3
NS 175
DS 16
SWH 30303.031 Hz
FIDRES 0.462388 Hz
AQ 1.0813440 sec
RG 13004
DW 16.500 usec
DE 6.00 usec
TE 298.0 K
D1 0.25000000 sec
d11 0.03000000 sec
D16 0.00020000 sec
d17 0.00019600 sec
MCREST 0 sec
MCWRK 0.01500000 sec
P2 31.00 usec

======== CHANNEL f1 ========
NUC1 13C
P1 15.50 usec
P11 500.00 usec
P12 2000.00 usec
PL0 120.00 dB
PL1 -1.00 dB
SFO1 125.7942548 MHz
SP1 3.20 dB
SP2 3.20 dB
SPNAM[1] Crp60,0.5,20.1
SPNAM[2] Crp60comp.4
SPOFF1 0 Hz
SPOFF2 0 Hz

======== CHANNEL f2 ========
CPDPRG[2 waltz16
NUC2 1H
PCPD2 100.00 usec
PL2 1.60 dB
PL12 24.60 dB
SFO2 500.2225011 MHz

====== GRADIENT CHANNEL =====
GPNAM[1] SINE.100
GPNAM[2] SINE.100
GPX1 0 %
GPX2 0 %
GPY1 0 %
GPY2 0 %
GPZ1 30.00 %
GPZ2 50.00 %
p15 500.00 usec
p16 1000.00 usec

F2 - Processing parameters
SI 65536
SF 125.7804085 MHz
WDW EM
SSB 0
LB 1.00 Hz
GB 0
PC 2.00

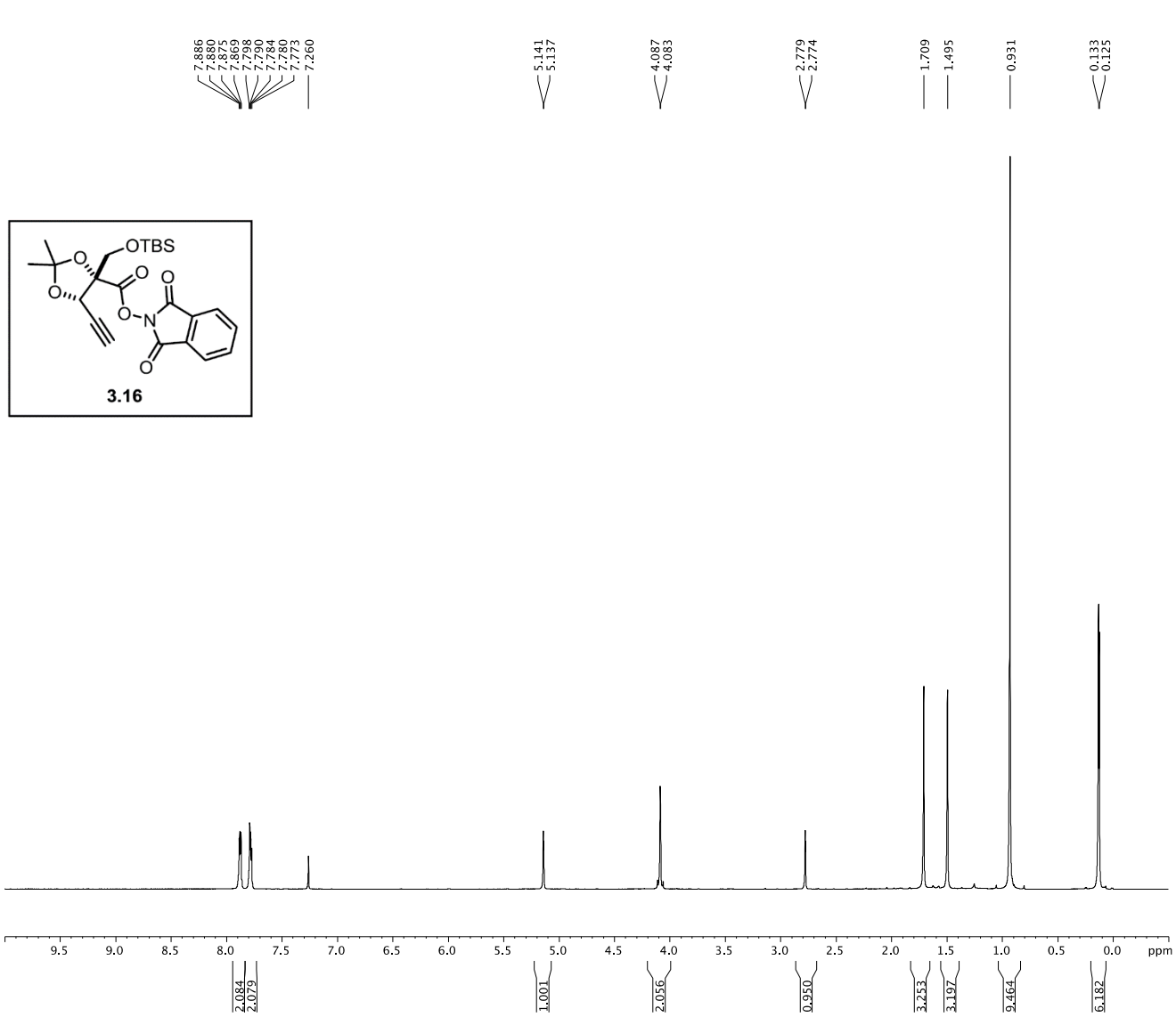

Current Data Parameters
NAME DJT-III-081
EXPNO 2
PROCNO 1

F2 - Acquisition Parameters
Date_ 20131206
Time 13.53
INSTRUM gn500
PROBHD 5 mm broadband
PULPROG zg30
TD 81728
SOLVENT $CDCl_3$
NS 16
DS 0
SWH 8012.820 Hz
FIDRES 0.098043 Hz
AQ 5.0998273 sec
RG 114
DW 62.400 usec
DE 6.00 usec
TE 298.0 K
D1 0.10000000 sec
MCREST 0 sec
MCWRK 0.01500000 sec

======== CHANNEL f1 ========
NUC1 1H
P1 12.20 usec
PL1 -5.00 dB
SFO1 499.2934950 MHz

F2 - Processing parameters
SI 65536
SF 499.2900294 MHz
WDW EM
SSB 0
LB 0.30 Hz
GB 0
PC 1.00

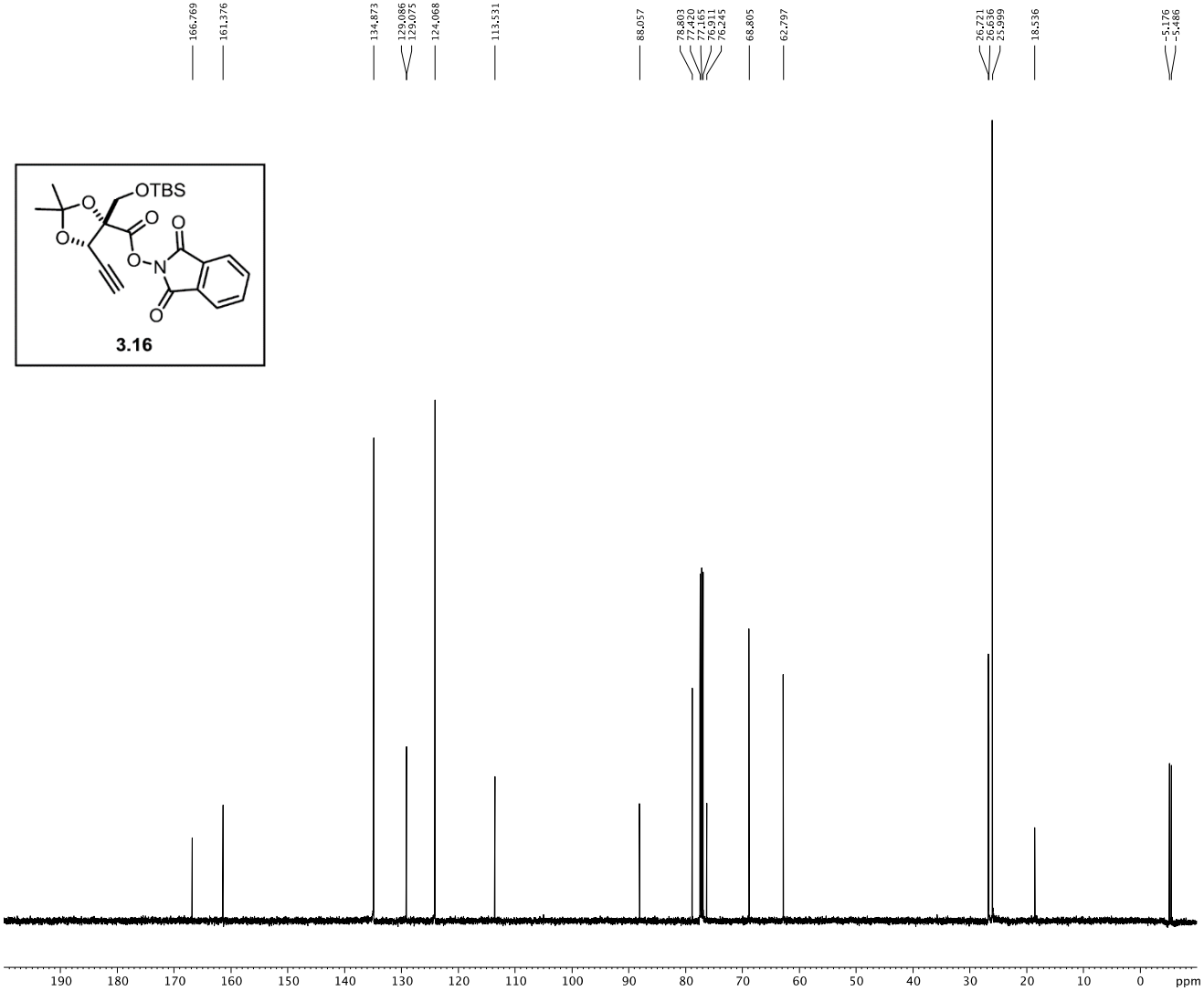

Current Data Parameters
NAME DJT-II-081
EXPNO 3
PROCNO 1

F2 - Acquisition Parameters
Date_ 20131207
Time 11.22
INSTRUM cryo500
PROBHD 5 mm CPTCI 1H-
PULPROG SpinEchopg30gp.prd
TD 65536
SOLVENT CDCl3
NS 338
DS 16
SWH 30303.031 Hz
FIDRES 0.462388 Hz
AQ 1.0813440 sec
RG 7298.2
DW 16.500 usec
DE 6.00 usec
TE 298.0 K
D1 0.25000000 sec
d11 0.03000000 sec
D16 0.00020000 sec
d17 0.00019600 sec
MCREST 0 sec
MCWRK 0.01500000 sec
P2 31.00 usec

======== CHANNEL f1 ========
NUC1 13C
P1 15.50 usec
P11 500.00 usec
P12 2000.00 usec
PL0 120.00 dB
PL1 -1.00 dB
SFO1 125.7942548 MHz
SP1 3.20 dB
SP2 3.20 dB
SPNAM[1] Crp60.0.5.20.1
SPNAM[2] Crp60comp.4
SPOFF1 0 Hz
SPOFF2 0 Hz

======== CHANNEL f2 ========
CPDPRG[2 waltz16
NUC2 1H
PCPD2 100.00 usec
PL2 1.60 dB
PL12 24.60 dB
SFO2 500.2225011 MHz

====== GRADIENT CHANNEL =====
GPNAM[1] SINE.100
GPNAM[2] SINE.100
GPX1 0 %
GPX2 0 %
GPY1 0 %
GPY2 0 %
GPZ1 30.00 %
GPZ2 50.00 %
p15 500.00 usec
p16 1000.00 usec

F2 - Processing parameters
SI 65536
SF 125.7804080 MHz
WDW EM
SSB 0
LB 1.00 Hz
GB 0
PC 2.00

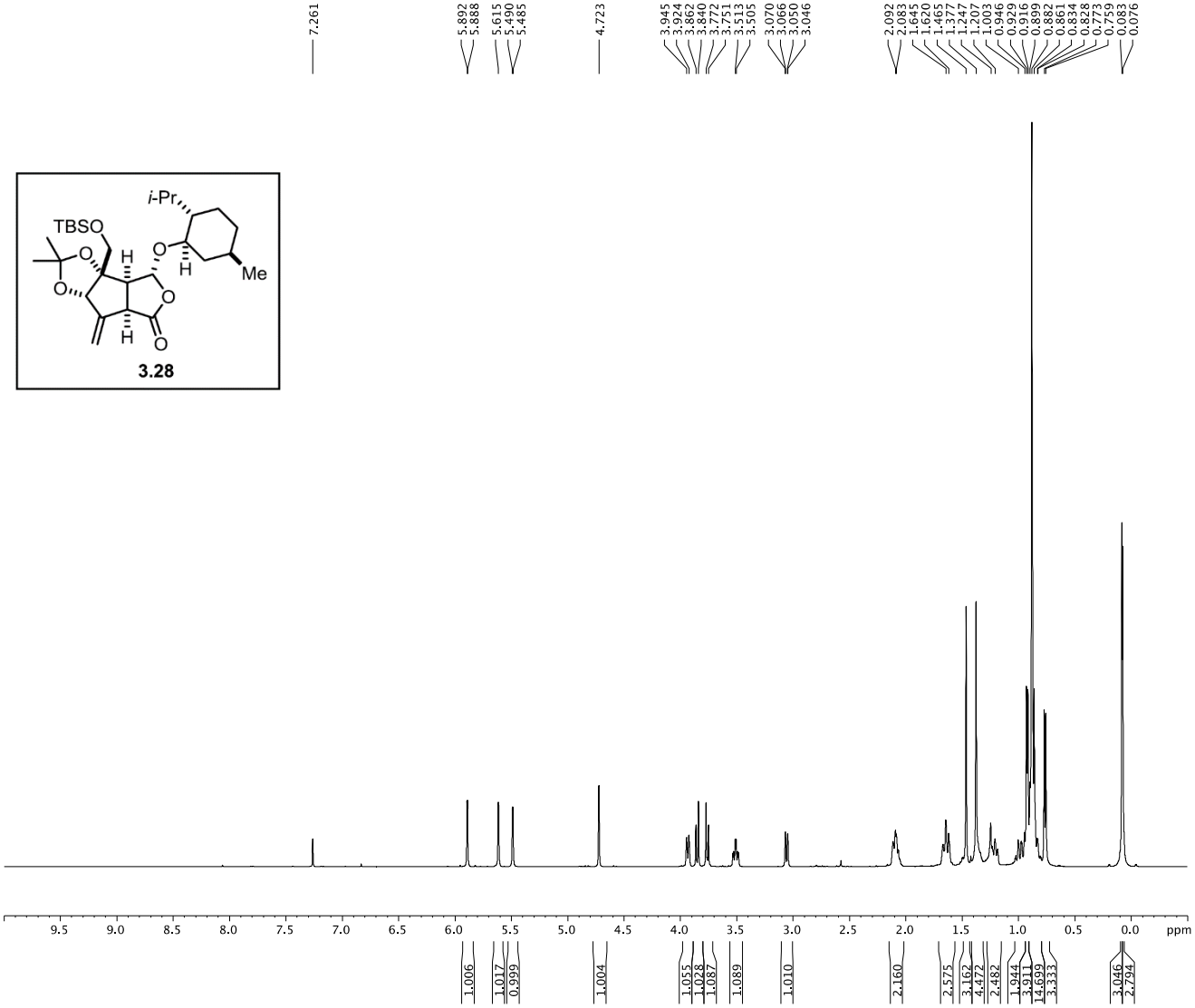

Current Data Parameters
NAME DJT-III-088
EXPNO 1
PROCNO 1

F2 - Acquisition Parameters
Date_ 20131209
Time 14.43
INSTRUM cryo500
PROBHD 5 mm CPTCI 1H-
PULPROG zg30
TD 81728
SOLVENT CDCl3
NS 16
DS 0
SWH 8012.820 Hz
FIDRES 0.098043 Hz
AQ 5.0998273 sec
RG 4
DW 62.400 usec
DE 6.00 usec
TE 298.0 K
D1 0.10000000 sec
MCREST 0 sec
MCWRK 0.01500000 sec

======== CHANNEL f1 ========
NUC1 1H
P1 7.50 usec
PL1 1.60 dB
SFO1 500.2235015 MHz

F2 - Processing parameters
SI 65536
SF 500.2200302 MHz
WDW EM
SSB 0
LB 0.30 Hz
GB 0
PC 4.00

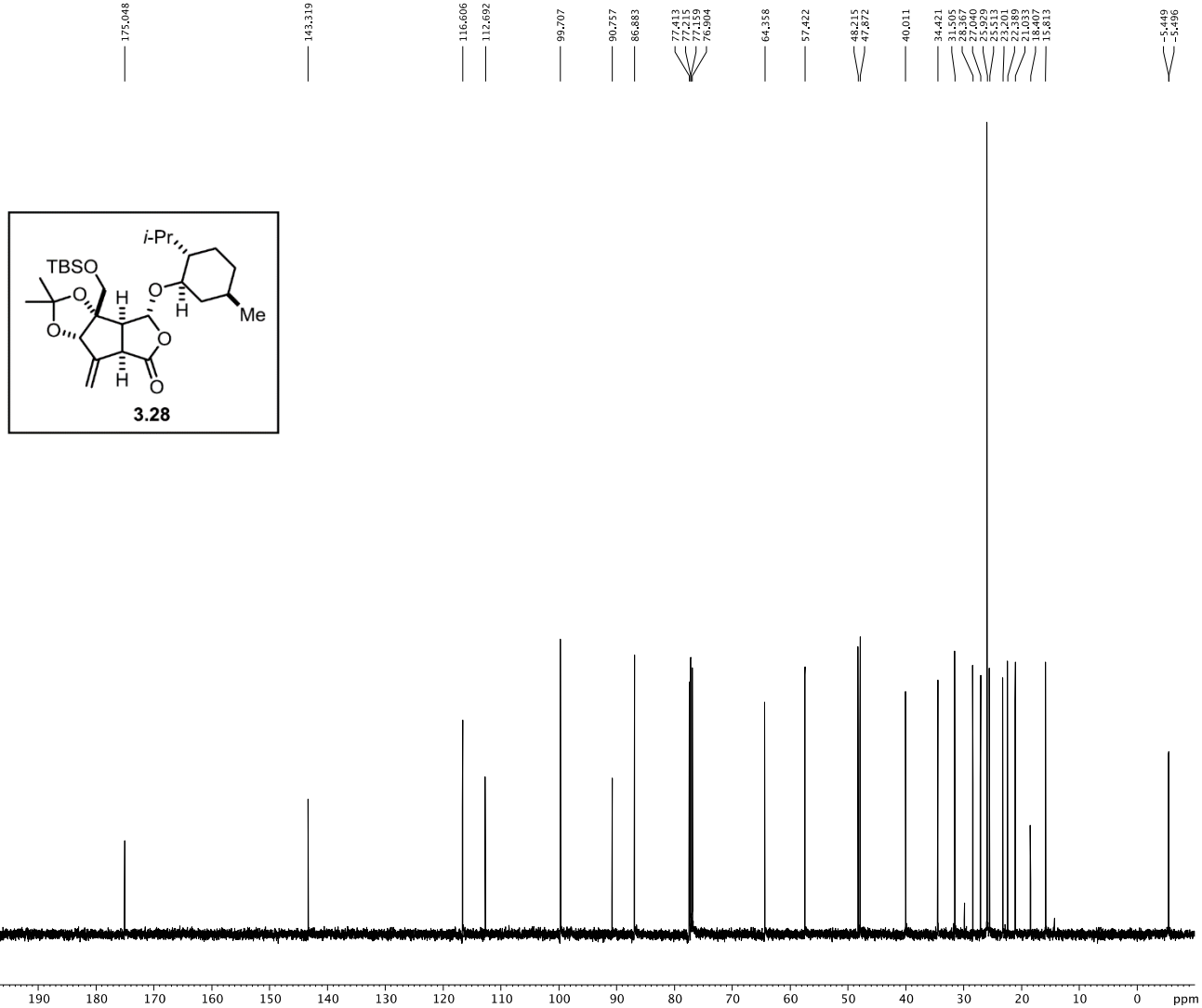

Current Data Parameters
NAME DJT-III-088
EXPNO 2
PROCNO 1

F2 - Acquisition Parameters
Date_ 20131209
Time 14.48
INSTRUM cryo500
PROBHD 5 mm CPTCI 1H-
PULPROG SpinEchopg30gp.prd
TD 65536
SOLVENT CDCl3
NS 143
DS 16
SWH 30303.031 Hz
FIDRES 0.462388 Hz
AQ 1.0813440 sec
RC 8192
DW 16.500 usec
DE 6.00 usec
TE 298.0 K
D1 0.25000000 sec
d11 0.03000000 sec
D16 0.00020000 sec
d17 0.00019600 sec
MCREST 0 sec
MCWRK 0.01500000 sec
P2 31.00 usec

======== CHANNEL f1 ========
NUC1 13C
P1 15.50 usec
P11 500.00 usec
P12 2000.00 usec
PL0 120.00 dB
PL1 -1.00 dB
SFO1 125.7942548 MHz
SP1 3.20 dB
SP2 3.20 dB
SPNAM[1] Crp60,0.5,20.1
SPNAM[2] Crp60comp.4
SPOFF1 0 Hz
SPOFF2 0 Hz

======== CHANNEL f2 ========
CPDPRG[2 waltz16
NUC2 1H
PCPD2 100.00 usec
PL2 1.60 dB
PL12 24.60 dB
SFO2 500.2225011 MHz

====== GRADIENT CHANNEL =====
GPNAM[1] SINE.100
GPNAM[2] SINE.100
GPX1 0 %
GPX2 0 %
GPY1 0 %
GPY2 0 %
GPZ1 30.00 %
GPZ2 50.00 %
p15 500.00 usec
p16 1000.00 usec

F2 - Processing parameters
SI 65536
SF 125.7804090 MHz
WDW EM
SSB 0
LB 1.00 Hz
GB 0
PC 2.00

1H spectrum

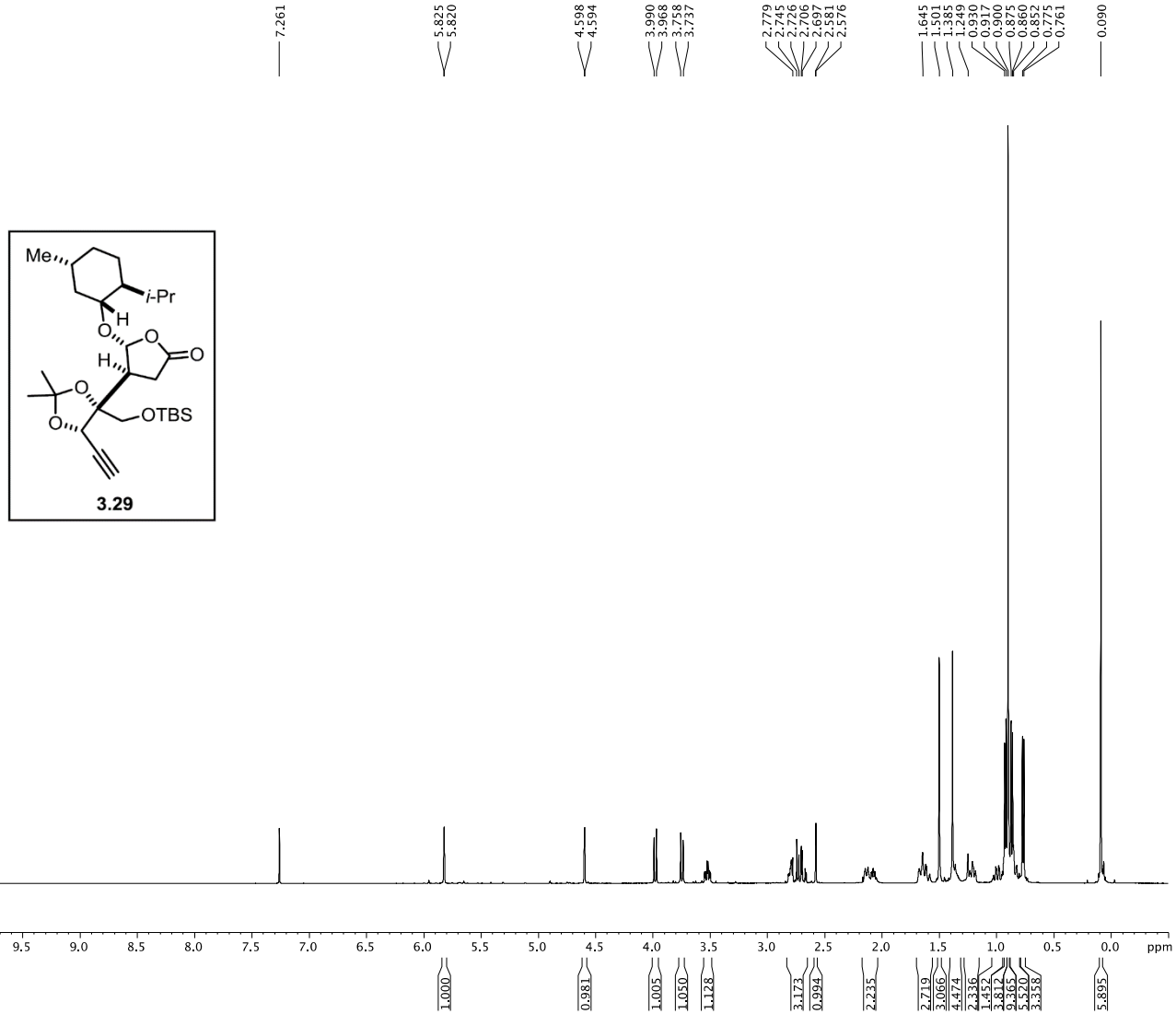


```
Current Data Parameters
NAME        DJT-VI-099
EXPNO            2
PROCNO           1

F2 - Acquisition Parameters
Date_       20151117
Time            8.14
INSTRUM      cryo500
PROBHD   5 mm CPTCI 1H-
PULPROG         zg30
TD             81728
SOLVENT        CDCl3
NS               16
DS                0
SWH          8012.820 Hz
FIDRES       0.098043 Hz
AQ           5.0998273 sec
RG               6.3
DW            62.400 usec
DE             6.00 usec
TE            298.0 K
D1           0.10000000 sec
MCREST   0 sec
MCWRK        0.01500000 sec

======== CHANNEL f1 =====
NUC1             1H
P1             7.50 usec
PL1            1.60 dB
SFO1        500.2235015 MHz

F2 - Processing parameters
SI             65536
SF         500.2200319 MHz
WDW              EM
SSB     0
LB            0.30 Hz
GB      0
PC             4.00
```

Z-restored spin-echo 13C spectrum with 1H decoupling

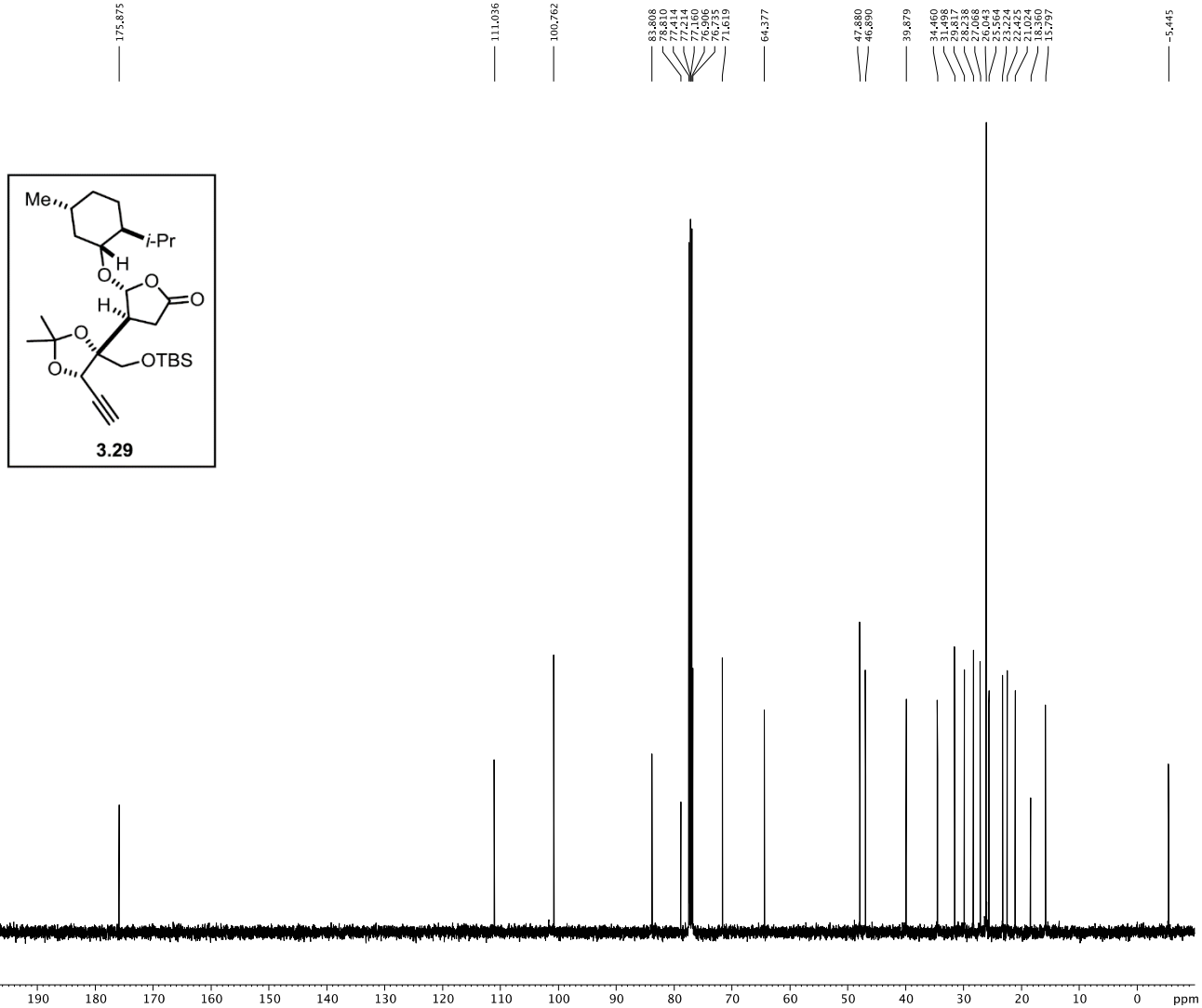

Current Data Parameters
NAME DJT-VI-099
EXPNO 4
PROCNO 1

F2 - Acquisition Parameters
Date_ 20151117
Time 8.29
INSTRUM cryo500
PROBHD 5 mm CPTCI 1H-
PULPROG SpinEchopg30gp.prd
TD 65536
SOLVENT CDCl3
NS 393
DS 0
SWH 30303.031 Hz
FIDRES 0.462388 Hz
AQ 1.0813440 sec
RG 7298.2
DW 16.500 usec
DE 6.00 usec
TE 298.0 K
D1 0.25000000 sec
d11 0.03000000 sec
D16 0.00020000 sec
d17 0.00019600 sec
MCREST 0 sec
MCWRK 0.01500000 sec
P2 33.10 usec

======== CHANNEL f1 ========
NUC1 13C
P1 16.55 usec
P11 500.00 usec
P12 2000.00 usec
PL0 120.00 dB
PL1 -1.00 dB
SFO1 125.7942548 MHz
SP1 2.70 dB
SP2 2.70 dB
SPNAM[1] Crp60,0.5,20.1
SPNAM[2] Crp60comp.4
SPOFF1 0 Hz
SPOFF2 0 Hz

======== CHANNEL f2 ========
CPDPRG[2 waltz16
NUC2 1H
PCPD2 100.00 usec
PL2 1.60 dB
PL12 24.50 dB
SFO2 500.2225011 MHz

====== GRADIENT CHANNEL =====
GPNAM[1] SINE.100
GPNAM[2] SINE.100
GPX1 0 %
GPX2 0 %
GPY1 0 %
GPY2 0 %
GPZ1 30.00 %
GPZ2 50.00 %
p15 500.00 usec
p16 1000.00 usec

F2 - Processing parameters
SI 65536
SF 125.7804085 MHz
WDW EM
SSB 0
LB 1.00 Hz
GB 0
PC 2.00

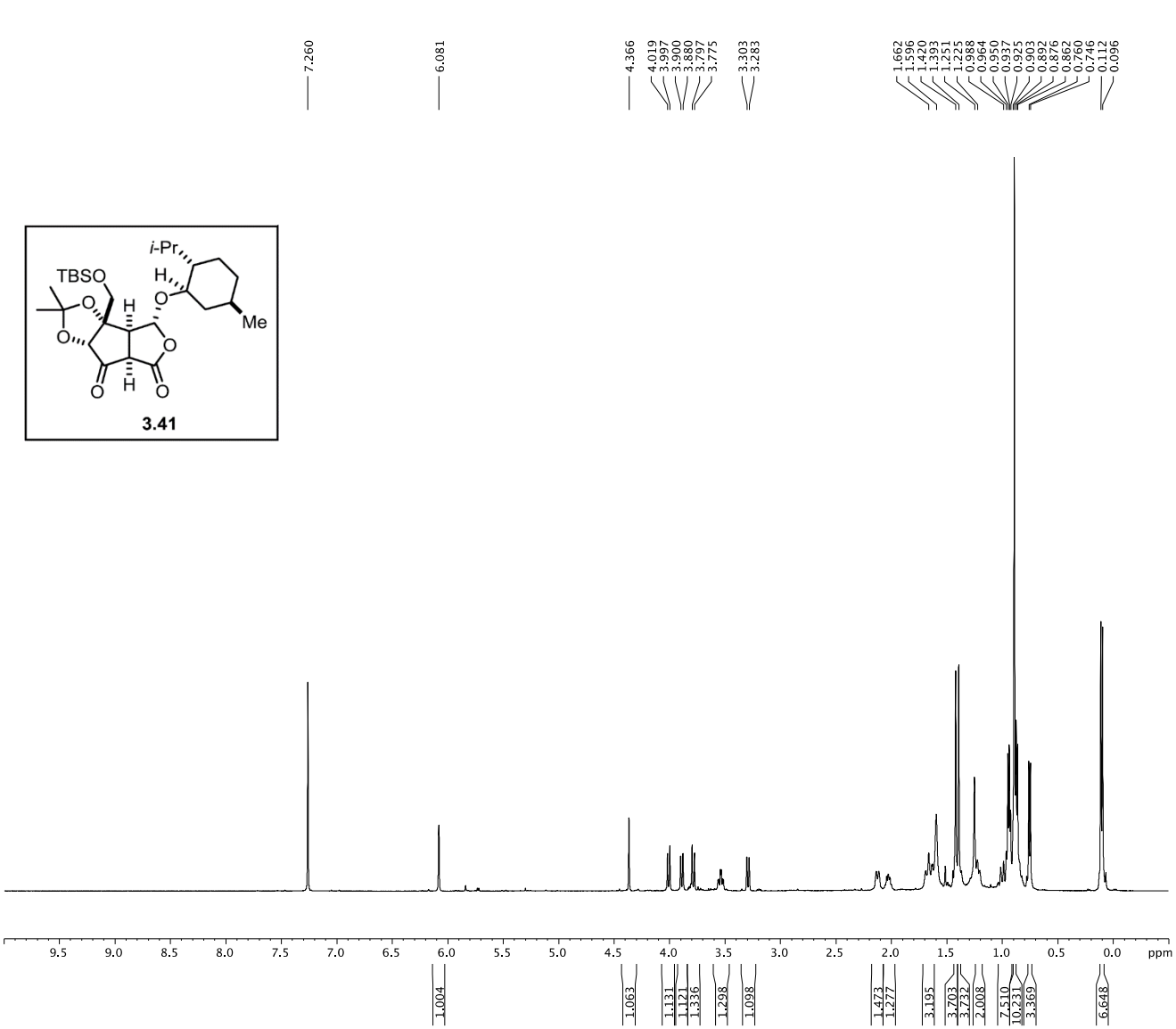

Current Data Parameters
NAME DJT-III-030
EXPNO 5
PROCNO 1

F2 - Acquisition Parameters
Date_ 20131204
Time 16.28
INSTRUM cryo500
PROBHD 5 mm CPTCI 1H-
PULPROG zg30
TD 81728
SOLVENT CDCl3
NS 16
DS 0
SWH 8012.820 Hz
FIDRES 0.098043 Hz
AQ 5.0998273 sec
RG 4.5
DW 62.400 usec
DE 6.00 usec
TE 298.0 K
D1 0.10000000 sec
MCREST 0 sec
MCWRK 0.01500000 sec

======== CHANNEL f1 ========
NUC1 1H
P1 7.50 usec
PL1 1.60 dB
SFO1 500.2235015 MHz

F2 - Processing parameters
SI 65536
SF 500.2200306 MHz
WDW EM
SSB 0
LB 0.30 Hz
GB 0
PC 4.00

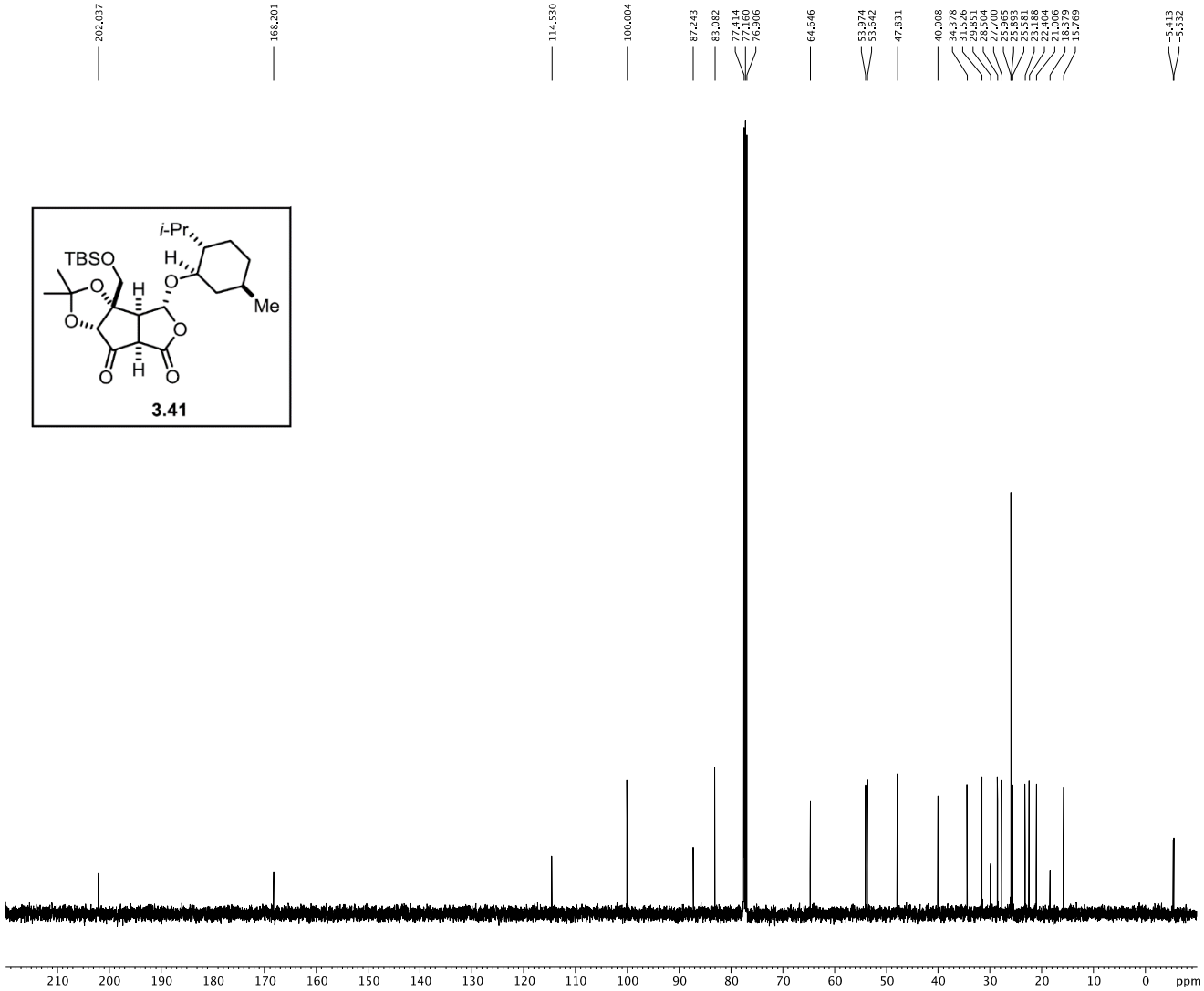

Current Data Parameters
NAME DJT-III-030
EXPNO 6
PROCNO 1

F2 - Acquisition Parameters
Date_ 20131204
Time 16.32
INSTRUM cryo500
PROBHD 5 mm CPTCI 1H-
PULPROG SpinEchopg30gp.prd
TD 65536
SOLVENT CDCl3
NS 494
DS 16
SWH 30303.031 Hz
FIDRES 0.462388 Hz
AQ 1.0813440 sec
RG 7298.2
DW 16.500 usec
DE 6.00 usec
TE 298.0 K
D1 0.25000000 sec
d11 0.03000000 sec
D16 0.00020000 sec
d17 0.00019600 sec
MCREST 0 sec
MCWRK 0.01500000 sec
P2 31.00 usec

======== CHANNEL f1 ========
NUC1 13C
P1 15.50 usec
P11 500.00 usec
P12 2000.00 usec
PL0 120.00 dB
PL1 -1.00 dB
SFO1 125.7942548 MHz
SP1 3.20 dB
SP2 3.20 dB
SPNAM[1] Crp60.0.5.20.1
SPNAM[2] Crp60comp.4
SPOFF1 0 Hz
SPOFF2 0 Hz

======== CHANNEL f2 ========
CPDPRG[2 waltz16
NUC2 1H
PCPD2 100.00 usec
PL2 1.60 dB
PL12 24.60 dB
SFO2 500.2225011 MHz

====== GRADIENT CHANNEL =====
GPNAM[1] SINE.100
GPNAM[2] SINE.100
GPX1 0 %
GPX2 0 %
GPY1 0 %
GPY2 0 %
GPZ1 30.00 %
GPZ2 50.00 %
p15 500.00 usec
p16 1000.00 usec

F2 - Processing parameters
SI 65536
SF 125.7804076 MHz
WDW EM
SSB 0
LB 1.00 Hz
GB 0
PC 2.00

1H spectrum

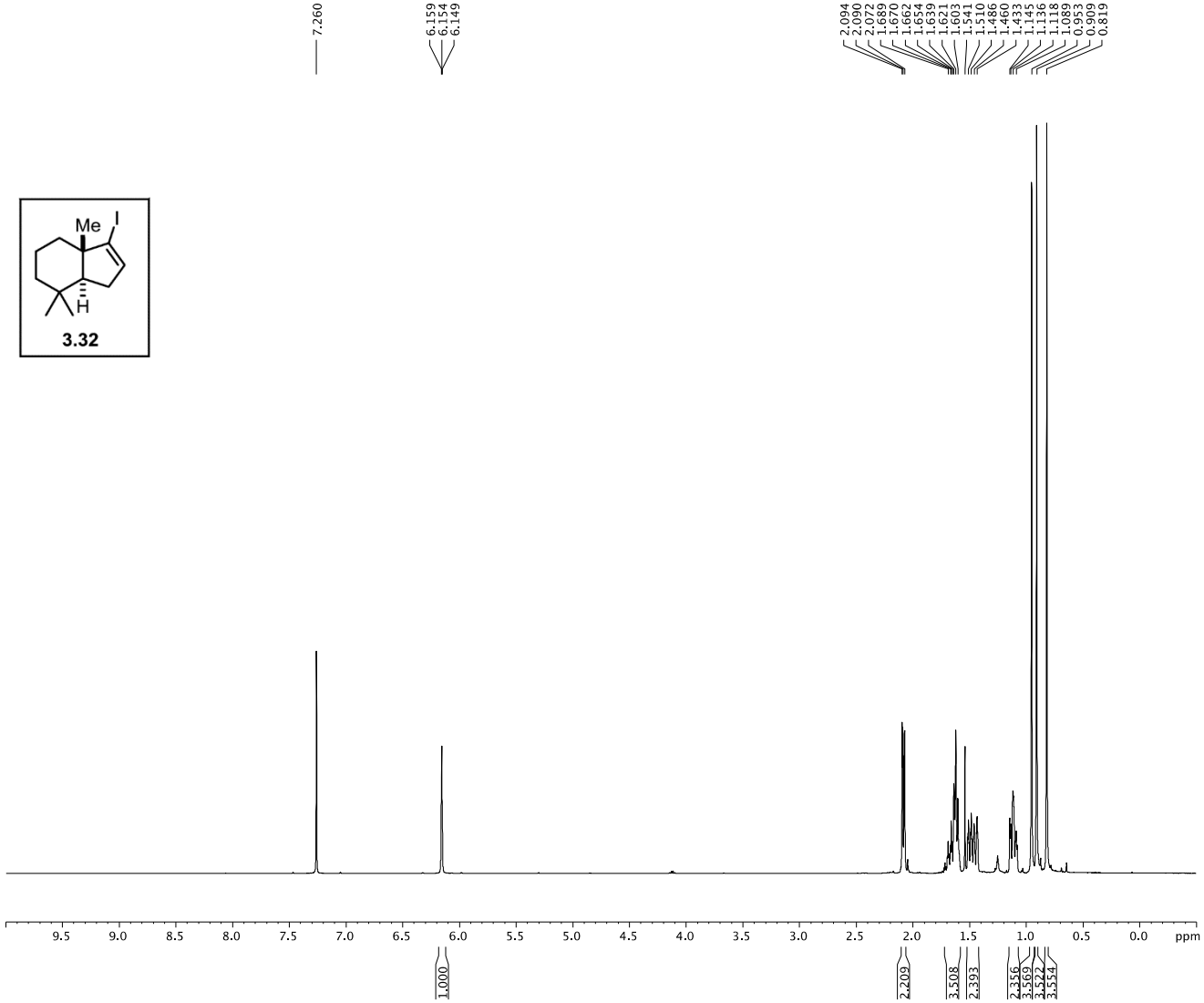

Current Data Parameters
NAME DJT-V-036
EXPNO 1
PROCNO 1

F2 - Acquisition Parameters
Date_ 20150203
Time 18.19
INSTRUM cryo500
PROBHD 5 mm CPTCI 1H-
PULPROG zg30
TD 16022
SOLVENT CDCl3
NS 60
DS 0
SWH 8012.820 Hz
FIDRES 0.500114 Hz
AQ 0.9997728 sec
RG 5.7
DW 62.400 usec
DE 6.00 usec
TE 298.0 K
D1 0.10000000 sec
MCREST 0 sec
MCWRK 0.01500000 sec

======== CHANNEL f1 =====
NUC1 1H
P1 7.50 usec
PL1 1.60 dB
SFO1 500.2235015 MHz

F2 - Processing parameters
SI 65536
SF 500.2200311 MHz
WDW EM
SSB 0
LB 0.30 Hz
GB 0
PC 4.00

Z-restored spin-echo 13C spectrum with 1H decoupling

3.32

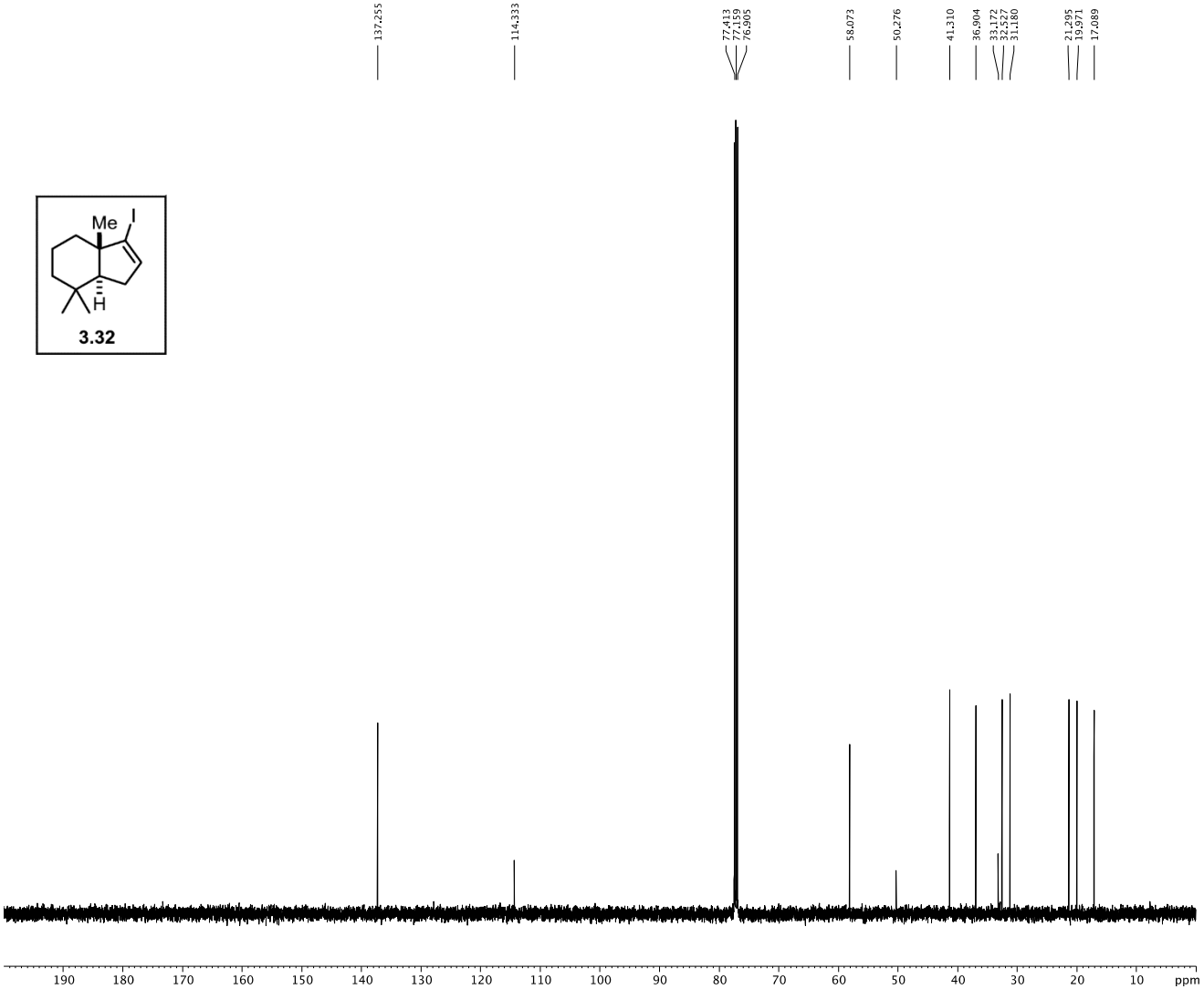


```
Current Data Parameters
NAME        DJT-V-036
EXPNO               2
PROCNO              1

F2 - Acquisition Parameters
Date_        20150203
Time            18.24
INSTRUM        cryo500
PROBHD   5 mm CPTCI 1H-
PULPROG  SpinEchopg30gp.prd
TD              65536
SOLVENT          CDCl3
NS                 391
DS                   0
SWH          30303.031 Hz
FIDRES        0.462388 Hz
AQ           1.0813440 sec
RG               13004
DW               16.500 usec
DE                6.00 usec
TE               298.0 K
D1          0.25000000 sec
d11         0.03000000 sec
D16         0.00020000 sec
d17         0.00019600 sec
MCREST   0 sec
MCWRK       0.01500000 sec
P2               33.10 usec

======== CHANNEL f1 ========
NUC1               13C
P1               16.55 usec
P11             500.00 usec
P12            2000.00 usec
PL0             120.00 dB
PL1              -1.00 dB
SFO1        125.7942548 MHz
SP1               2.70 dB
SP2               2.70 dB
SPNAM[1] Crp60,0.5,20.1
SPNAM[2]    Crp60comp.4
SPOFF1   0 Hz
SPOFF2   0 Hz

======== CHANNEL f2 ========
CPDPRG[2         waltz16
NUC2                1H
PCPD2            100.00 usec
PL2               1.60 dB
PL12             24.50 dB
SFO2        500.2225011 MHz

====== GRADIENT CHANNEL =====
GPNAM[1]         SINE.100
GPNAM[2]         SINE.100
GPX1     0 %
GPX2     0 %
GPY1     0 %
GPY2     0 %
GPZ1            30.00 %
GPZ2            50.00 %
p15            500.00 usec
p16           1000.00 usec

F2 - Processing parameters
SI               65536
SF          125.7804074 MHz
WDW                 EM
SSB     0
LB              1.00 Hz
GB      0
PC               2.00
```

1H spectrum

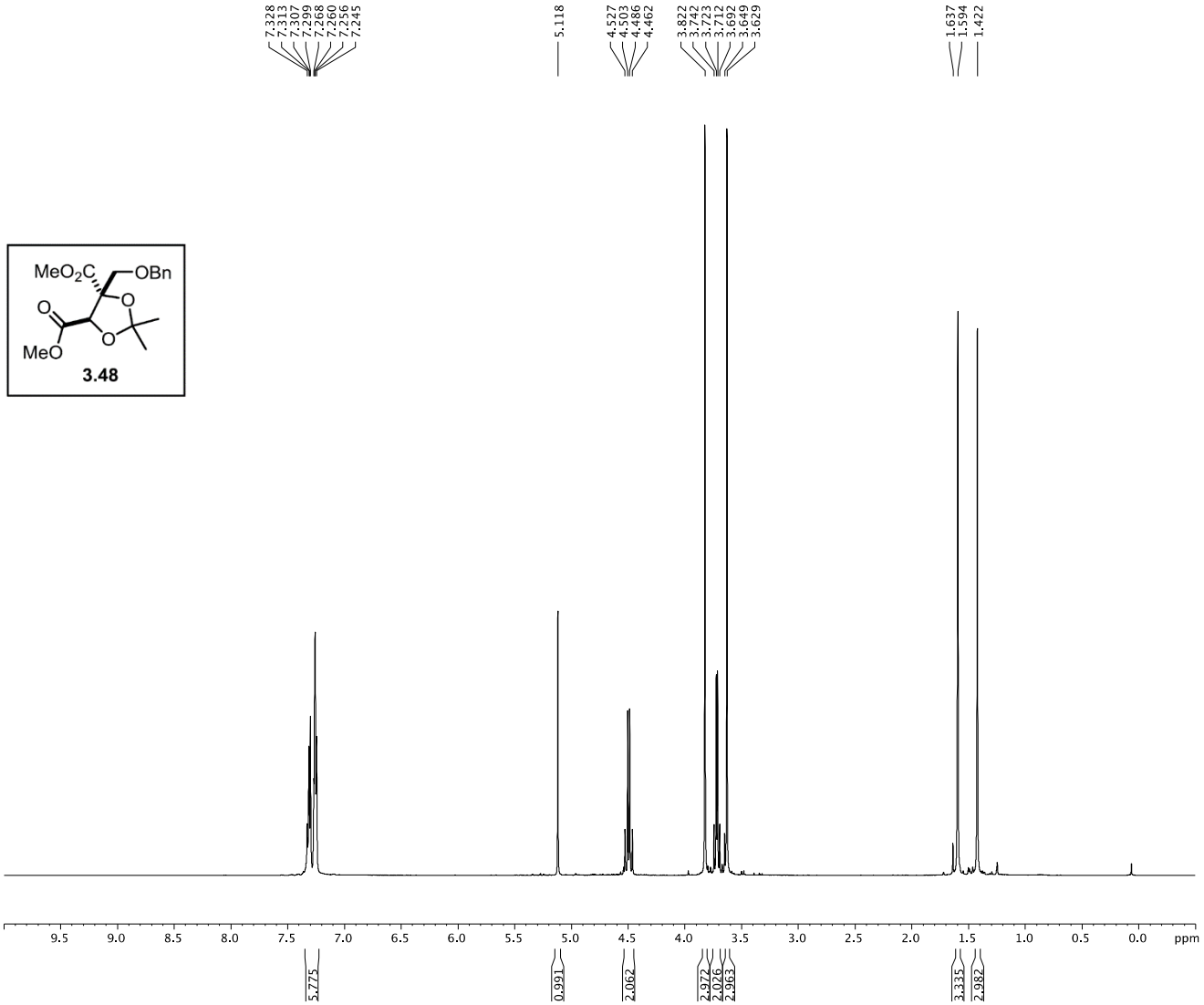

3.48

```
Current Data Parameters
NAME        DJT-VI-104
EXPNO            1
PROCNO           1

F2 - Acquisition Parameters
Date_       20151118
Time            7.36
INSTRUM       cryo500
PROBHD   5 mm CPTCI 1H-
PULPROG         zg30
TD             80126
SOLVENT        CDCl3
NS               30
DS                0
SWH           8012.820 Hz
FIDRES        0.100003 Hz
AQ          4.9998622 sec
RG                8
DW             62.400 usec
DE              6.00 usec
TE            298.0 K
D1          0.10000000 sec
MCREST   0 sec
MCWRK       0.01500000 sec

======== CHANNEL f1 =====
NUC1              1H
P1             7.50 usec
PL1            1.60 dB
SFO1       500.2235015 MHz

F2 - Processing parameters
SI            65536
SF        500.2200335 MHz
WDW              EM
SSB     0
LB             0.30 Hz
GB      0
PC             4.00
```

Z-restored spin-echo 13C spectrum with 1H decoupling

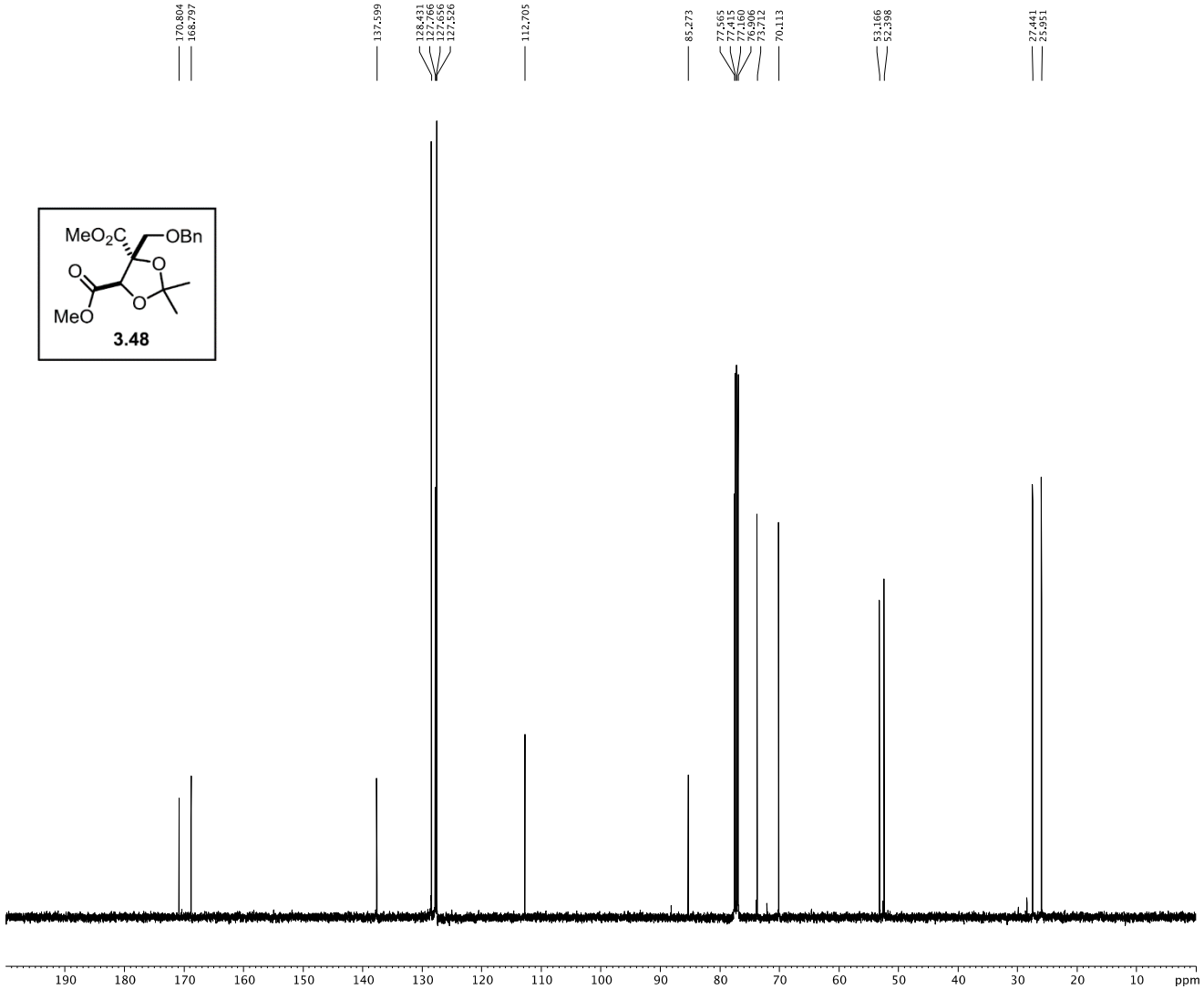


```
Current Data Parameters
NAME        DJT-VI-104
EXPNO              2
PROCNO             1

F2 - Acquisition Parameters
Date_        20151118
Time            7.42
INSTRUM        cryo500
PROBHD   5 mm CPTCI 1H-
PULPROG  SpinEchopg30gp.prd
TD             65536
SOLVENT         CDCl3
NS               374
DS                 0
SWH         30303.031 Hz
FIDRES       0.462388 Hz
AQ          1.0813440 sec
RG             6502
DW            16.500 usec
DE             6.00 usec
TE            298.0 K
D1         0.25000000 sec
d11        0.03000000 sec
D16        0.00020000 sec
d17        0.00019600 sec
MCREST   0 sec
MCWRK      0.01500000 sec
P2            33.10 usec

======== CHANNEL f1 ========
NUC1             13C
P1            16.55 usec
P11          500.00 usec
P12         2000.00 usec
PL0          120.00 dB
PL1           -1.00 dB
SFO1       125.7942548 MHz
SP1            2.70 dB
SP2            2.70 dB
SPNAM[1] Crp60,0.5,20.1
SPNAM[2]   Crp60comp.4
SPOFF1   0 Hz
SPOFF2   0 Hz

======== CHANNEL f2 ========
CPDPRG[2        waltz16
NUC2             1H
PCPD2         100.00 usec
PL2            1.60 dB
PL12          24.50 dB
SFO2       500.2225011 MHz

====== GRADIENT CHANNEL =====
GPNAM[1]        SINE.100
GPNAM[2]        SINE.100
GPX1     0 %
GPX2     0 %
GPY1     0 %
GPY2     0 %
GPZ1          30.00 %
GPZ2          50.00 %
p15          500.00 usec
p16         1000.00 usec

F2 - Processing parameters
SI             65536
SF        125.7804103 MHz
WDW              EM
SSB     0
LB            1.00 Hz
GB      0
PC            2.00
```

1H spectrum

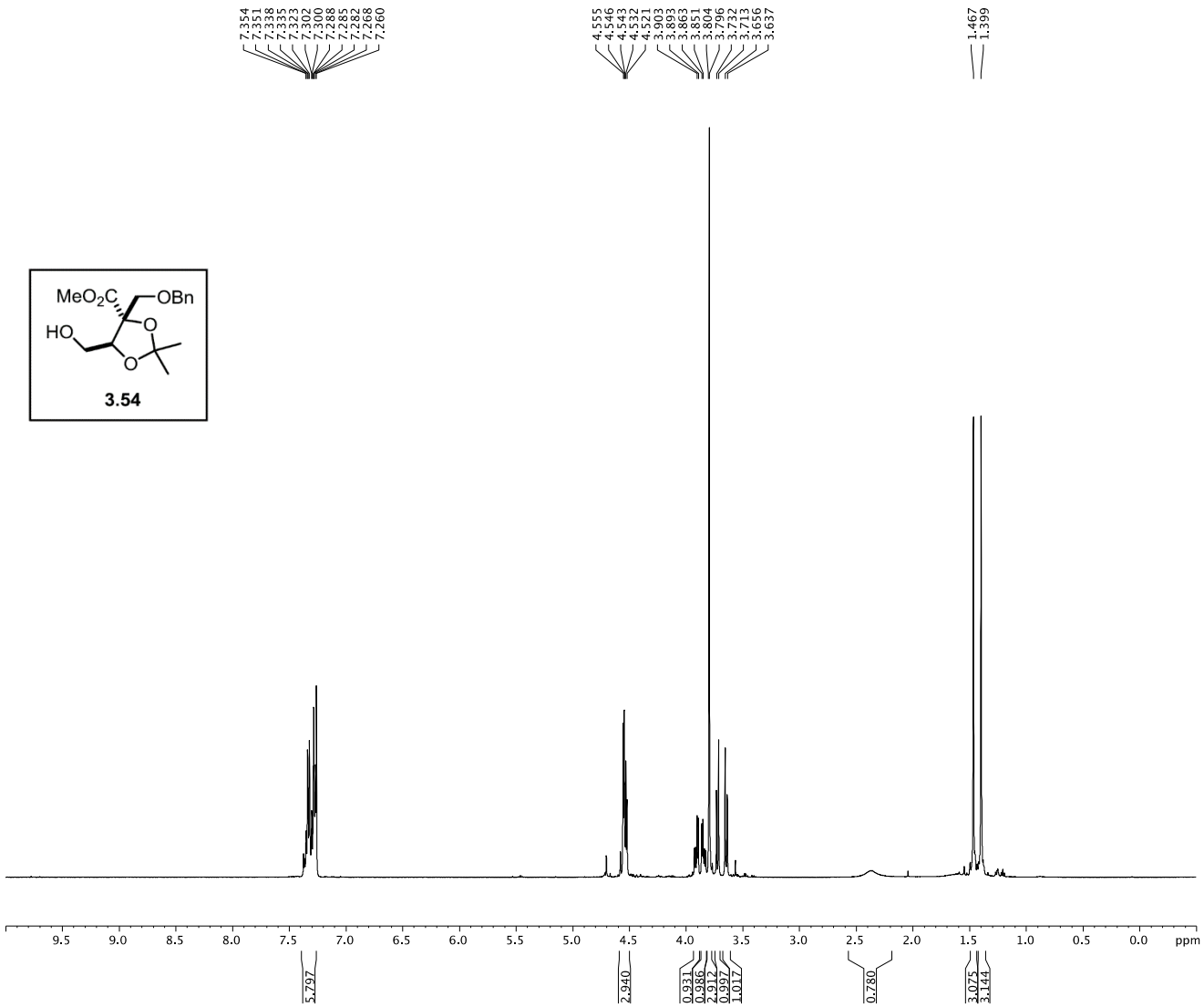

3.54

```
Current Data Parameters
NAME        DJT-IV-110
EXPNO              1
PROCNO             1

F2 - Acquisition Parameters
Date_       20140813
Time          14.46
INSTRUM       cryo500
PROBHD  5 mm CPTCI 1H-
PULPROG         zg30
TD            81728
SOLVENT        CDCl3
NS                 8
DS                 2
SWH         8012.820 Hz
FIDRES      0.098043 Hz
AQ        5.0998273 sec
RG               7.1
DW           62.400 usec
DE            6.00 usec
TE           298.0 K
D1        0.10000000 sec
MCREST  0 sec
MCWRK     0.01500000 sec

======== CHANNEL f1 =====
NUC1              1H
P1             7.50 usec
PL1            1.60 dB
SFO1      500.2235015 MHz

F2 - Processing parameters
SI            65536
SF      500.2200307 MHz
WDW             EM
SSB     0
LB            0.30 Hz
GB      0
PC             4.00
```

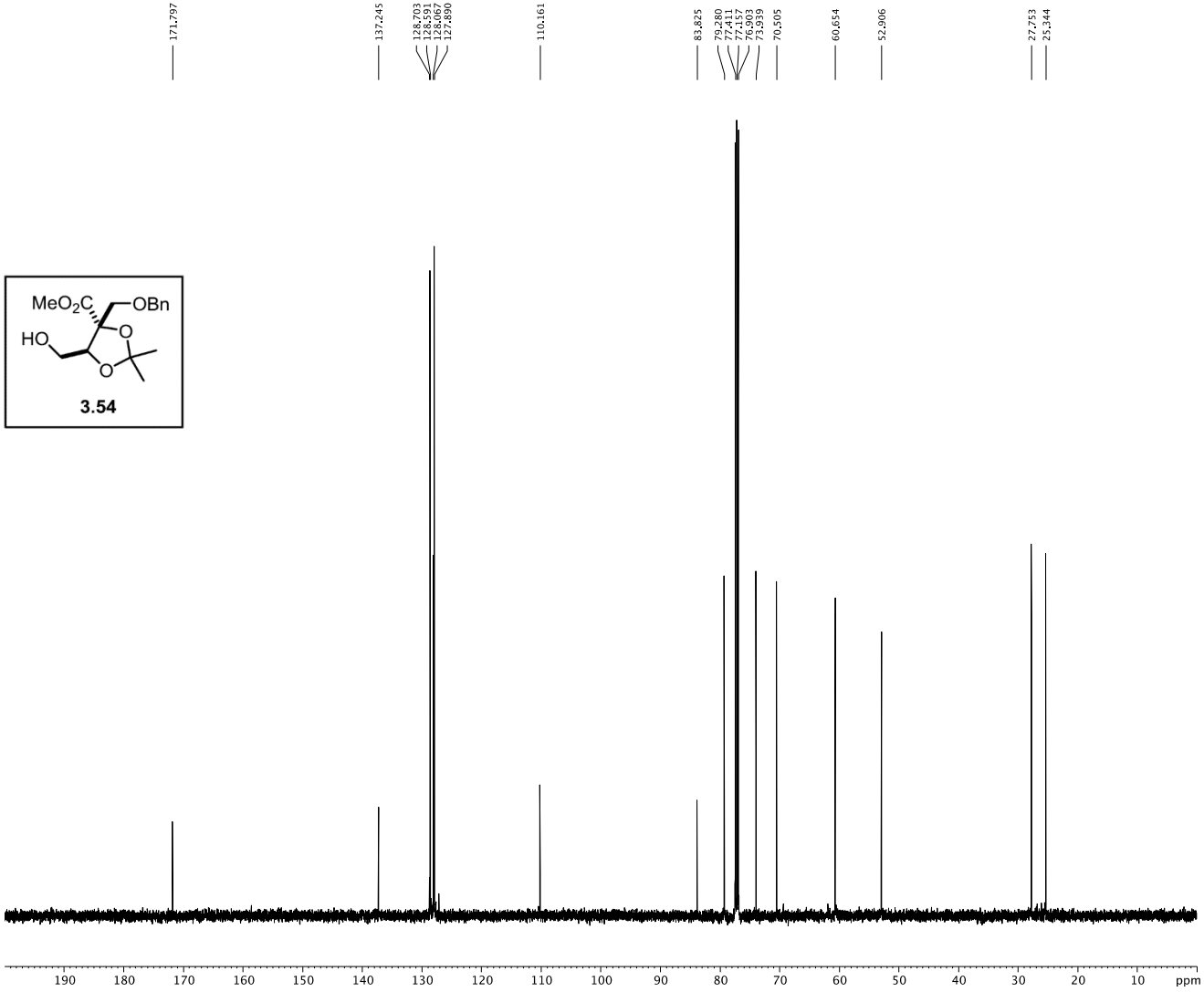

Current Data Parameters
NAME DJT-IV-110
EXPNO 2
PROCNO 1

F2 - Acquisition Parameters
Date_ 20140814
Time 11.08
INSTRUM cryo500
PROBHD 5 mm CPTCI 1H-
PULPROG SpinEchopg30gp.prd
TD 65536
SOLVENT CDCl3
NS 562
DS 16
SWH 30303.031 Hz
FIDRES 0.462388 Hz
AQ 1.0813440 sec
RG 7298.2
DW 16.500 usec
DE 6.00 usec
TE 298.0 K
D1 0.25000000 sec
d11 0.03000000 sec
D16 0.00020000 sec
d17 0.00019600 sec
MCREST 0 sec
MCWRK 0.01500000 sec
P2 31.00 usec

======== CHANNEL f1 ========
NUC1 13C
P1 15.50 usec
P11 500.00 usec
P12 2000.00 usec
PL0 120.00 dB
PL1 -1.00 dB
SFO1 125.7942548 MHz
SP1 3.20 dB
SP2 3.20 dB
SPNAM[1] Crp60.0.5.20.1
SPNAM[2] Crp60comp.4
SPOFF1 0 Hz
SPOFF2 0 Hz

======== CHANNEL f2 ========
CPDPRG[2 waltz16
NUC2 1H
PCPD2 100.00 usec
PL2 1.60 dB
PL12 24.60 dB
SFO2 500.2225011 MHz

====== GRADIENT CHANNEL =====
GPNAM[1] SINE.100
GPNAM[2] SINE.100
GPX1 0 %
GPX2 0 %
GPY1 0 %
GPY2 0 %
GPZ1 30.00 %
GPZ2 50.00 %
p15 500.00 usec
p16 1000.00 usec

F2 - Processing parameters
SI 65536
SF 125.7804089 MHz
WDW EM
SSB 0
LB 1.00 Hz
GB 0
PC 2.00

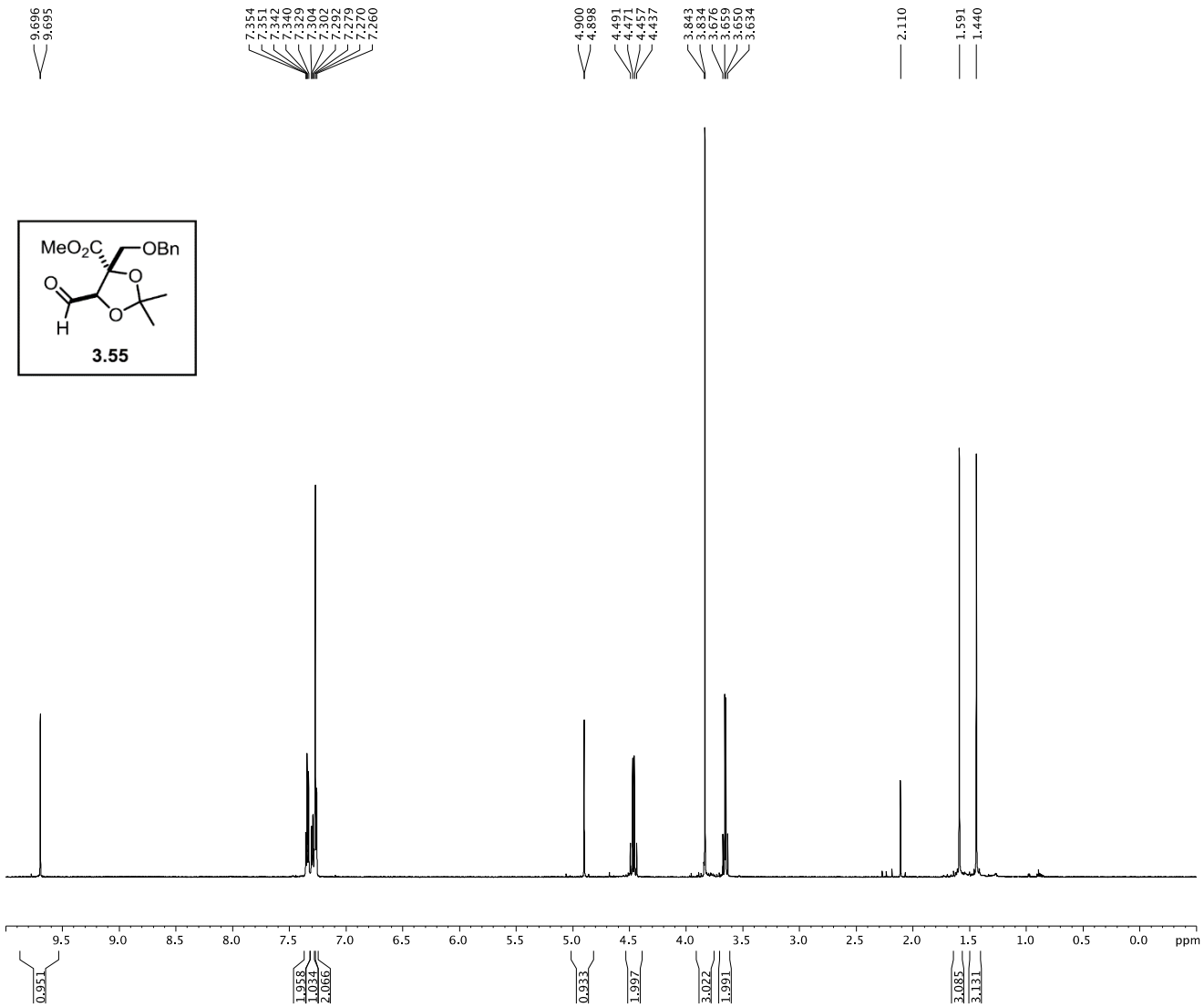

Current Data Parameters
NAME YS-III-303
EXPNO 1
PROCNO 1

F2 - Acquisition Parameters
Date_ 20151128
Time 13.45
INSTRUM av600
PROBHD 5 mm TBI 1H/13
PULPROG zg30
TD 38460
SOLVENT CDCl3
NS 8
DS 2
SWH 9615.385 Hz
FIDRES 0.250010 Hz
AQ 1.9999200 sec
RG 1620
DW 52.000 usec
DE 14.54 usec
TE 298.0 K
D1 0.10000000 sec
TD0 1

======== CHANNEL f1 =====
SFO1 600.1342009 MHz
NUC1 1H
P1 8.00 usec
PLW1 24.00000000 W

F2 - Processing parameters
SI 65536
SF 600.1300297 MHz
WDW EM
SSB 0
LB 0.30 Hz
GB 0
PC 1.00

Z-restored spin-echo 13C spectrum with 1H decoupling

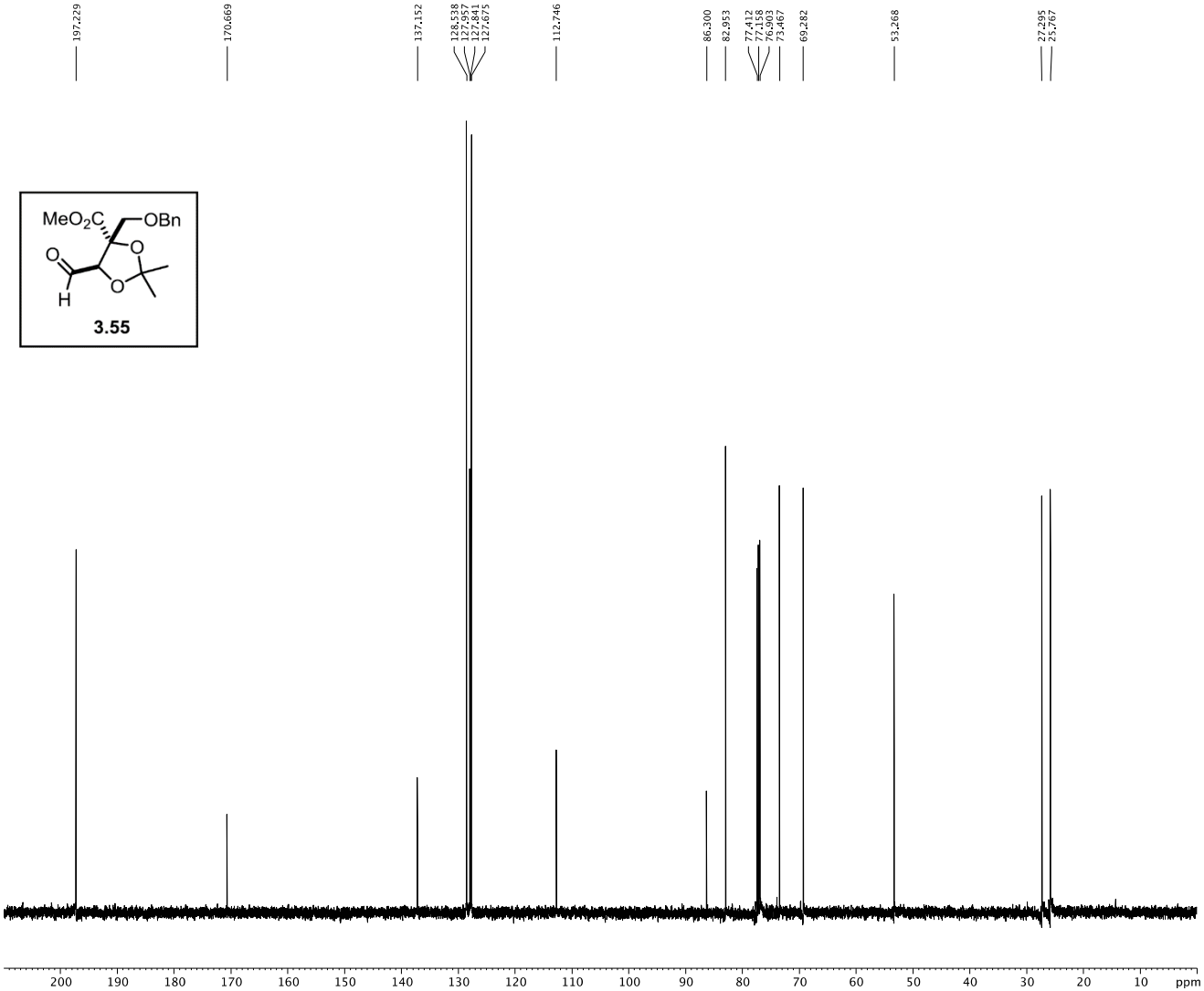


```
Current Data Parameters
NAME        DJT-IV-040
EXPNO             2
PROCNO            1

F2 - Acquisition Parameters
Date_       20140616
Time          16.32
INSTRUM       cryo500
PROBHD   5 mm CPTC1 1H-
PULPROG  SpinEchopg30gp.prd
TD          65536
SOLVENT       CDCl3
NS            101
DS              0
SWH       30303.031 Hz
FIDRES     0.462388 Hz
AQ       1.0813440 sec
RG            6502
DW          16.500 usec
DE           6.00 usec
TE          298.0 K
D1       0.25000000 sec
d11      0.03000000 sec
D16      0.00020000 sec
d17      0.00019600 sec
MCREST   0 sec
MCWRK    0.01500000 sec
P2          31.00 usec

======== CHANNEL f1 ========
NUC1          13C
P1          15.50 usec
P11        500.00 usec
P12       2000.00 usec
PL0        120.00 dB
PL1         -1.00 dB
SFO1    125.7942548 MHz
SP1          3.20 dB
SP2          3.20 dB
SPNAM[1] Crp60,0.5,20.1
SPNAM[2]   Crp60comp.4
SPOFF1   0 Hz
SPOFF2   0 Hz

======== CHANNEL f2 ========
CPDPRG[2       waltz16
NUC2             1H
PCPD2        100.00 usec
PL2           1.60 dB
PL12         24.60 dB
SFO2     500.2225011 MHz

====== GRADIENT CHANNEL =====
GPNAM[1]      SINE.100
GPNAM[2]      SINE.100
GPX1     0 %
GPX2     0 %
GPY1     0 %
GPY2     0 %
GPZ1         30.00 %
GPZ2         50.00 %
p15         500.00 usec
p16        1000.00 usec

F2 - Processing parameters
SI          65536
SF     125.7804122 MHz
WDW            EM
SSB     0
LB          1.00 Hz
GB      0
PC          2.00
```

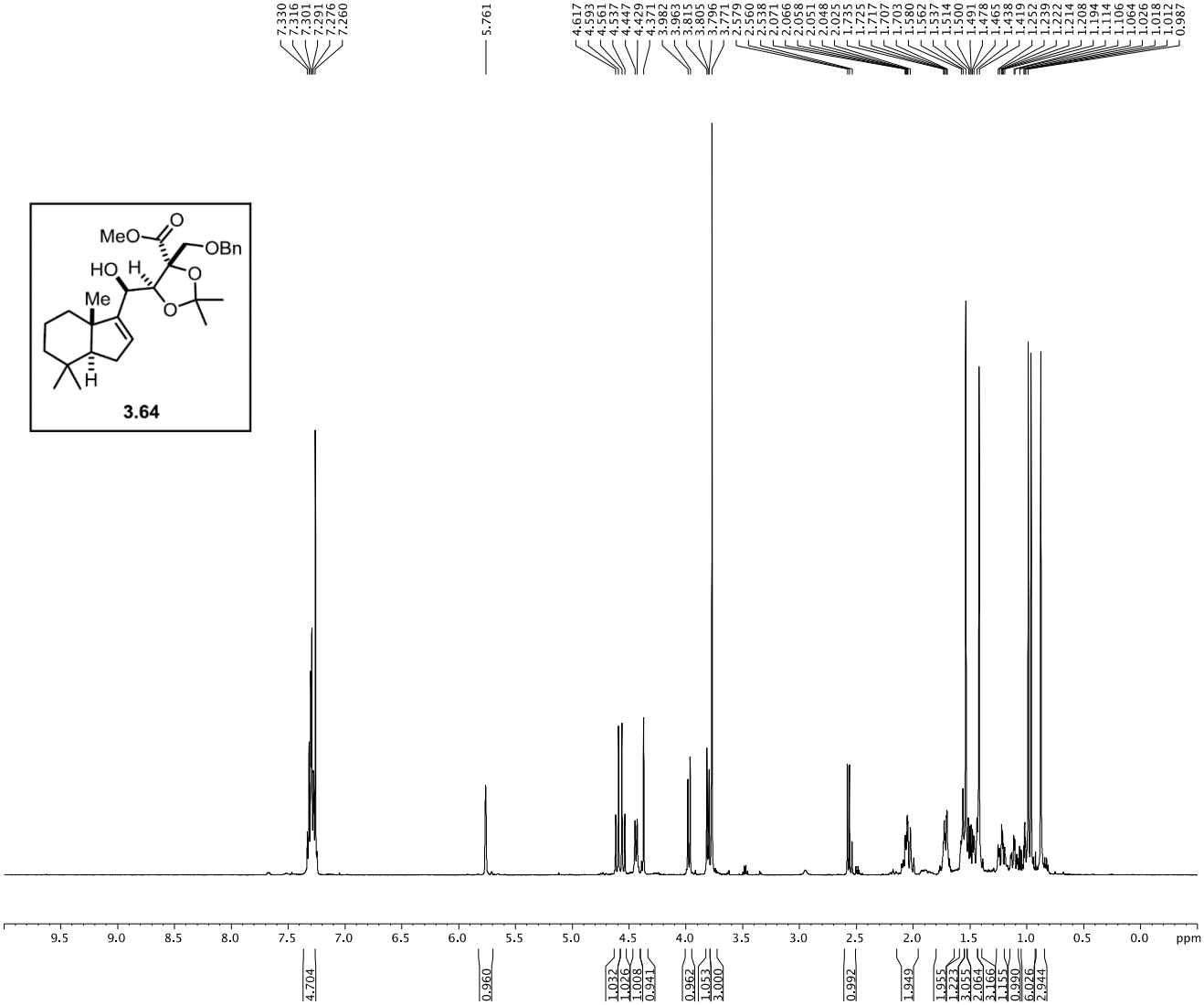

Current Data Parameters
NAME YS-III-303
EXPNO 5
PROCNO 1

F2 - Acquisition Parameters
Date_ 20151202
Time 13.46
INSTRUM cryo500
PROBHD 5 mm CPTCI 1H-
PULPROG zg30
TD 81728
SOLVENT CDCl3
NS 8
DS 2
SWH 8012.820 Hz
FIDRES 0.098043 Hz
AQ 5.0998273 sec
RG 8
DW 62.400 usec
DE 6.00 usec
TE 298.0 K
D1 0.10000000 sec
MCREST 0 sec
MCWRK 0.01500000 sec

======== CHANNEL f1 =====
NUC1 1H
P1 7.50 usec
PL1 1.60 dB
SFO1 500.2235015 MHz

F2 - Processing parameters
SI 65536
SF 500.2200320 MHz
WDW EM
SSB 0
LB 0.30 Hz
GB 0
PC 4.00

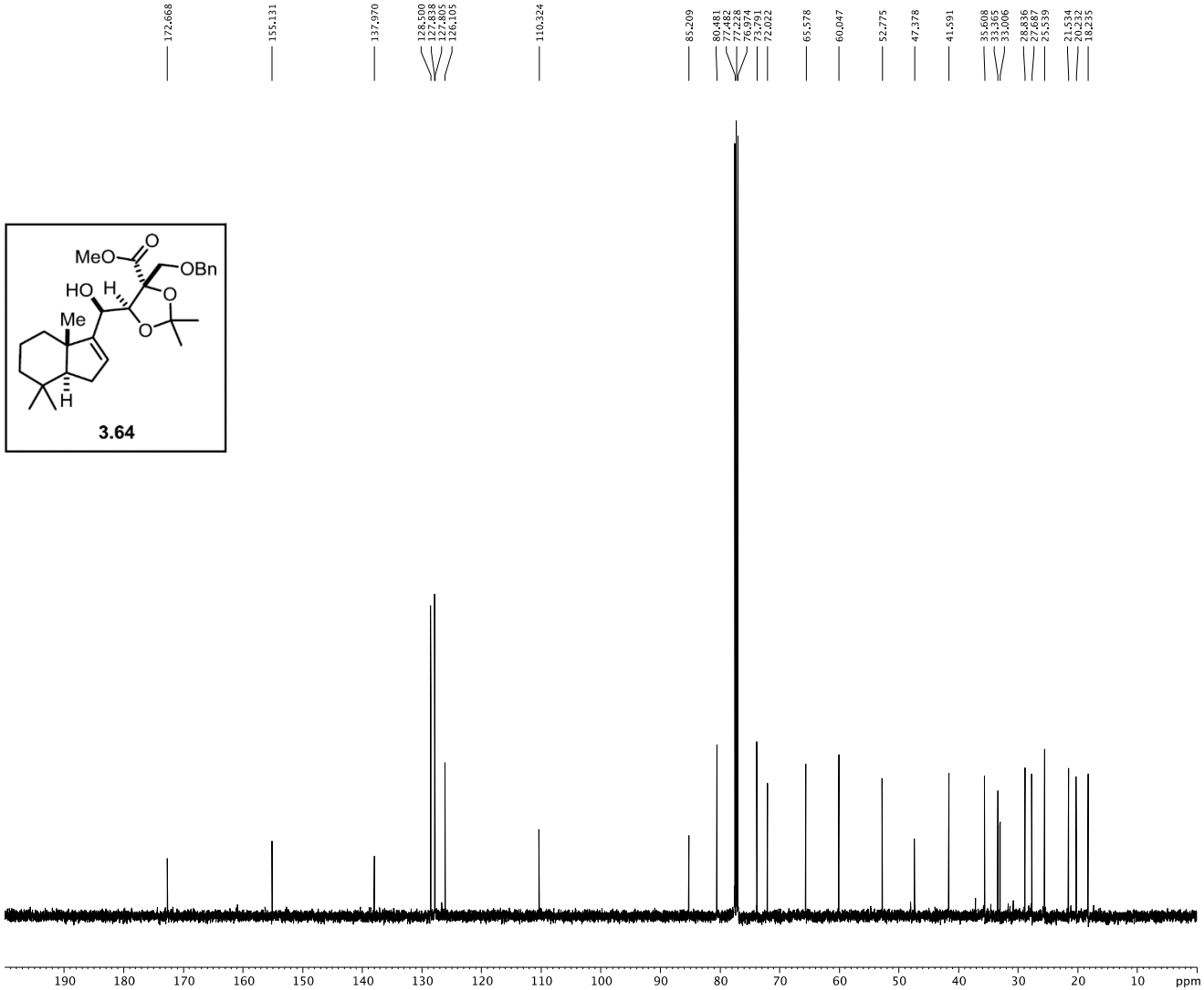

Current Data Parameters
NAME YS-III-303
EXPNO 6
PROCNO 1

F2 - Acquisition Parameters
Date_ 20151202
Time 13.57
INSTRUM cryo500
PROBHD 5 mm CPTCI 1H-
PULPROG SpinEchopg30gp.prd
TD 65536
SOLVENT CDCl3
NS 496
DS 2
SWH 30303.031 Hz
FIDRES 0.462388 Hz
AQ 1.0813440 sec
RG 2580.3
DW 16.500 usec
DE 6.00 usec
TE 298.0 K
D1 0.25000000 sec
d11 0.03000000 sec
D16 0.00020000 sec
d17 0.00019600 sec
MCREST 0 sec
MCWRK 0.01500000 sec
P2 33.10 usec

======== CHANNEL f1 ========
NUC1 13C
P1 16.55 usec
P11 500.00 usec
P12 2000.00 usec
PL0 120.00 dB
PL1 -1.00 dB
SFO1 125.7942548 MHz
SP1 2.70 dB
SP2 2.70 dB
SPNAM[1] Crp60,0.5,20.1
SPNAM[2] Crp60comp.4
SPOFF1 0 Hz
SPOFF2 0 Hz

======== CHANNEL f2 ========
CPDPRG[2 waltz16
NUC2 1H
PCPD2 100.00 usec
PL2 1.60 dB
PL12 24.50 dB
SFO2 500.2225011 MHz

====== GRADIENT CHANNEL =====
GPNAM[1] SINE.100
GPNAM[2] SINE.100
GPX1 0 %
GPX2 0 %
GPY1 0 %
GPY2 0 %
GPZ1 30.00 %
GPZ2 50.00 %
p15 500.00 usec
p16 1000.00 usec

F2 - Processing parameters
SI 65536
SF 125.7803996 MHz
WDW EM
SSB 0
LB 1.00 Hz
GB 0
PC 2.00

1H spectrum

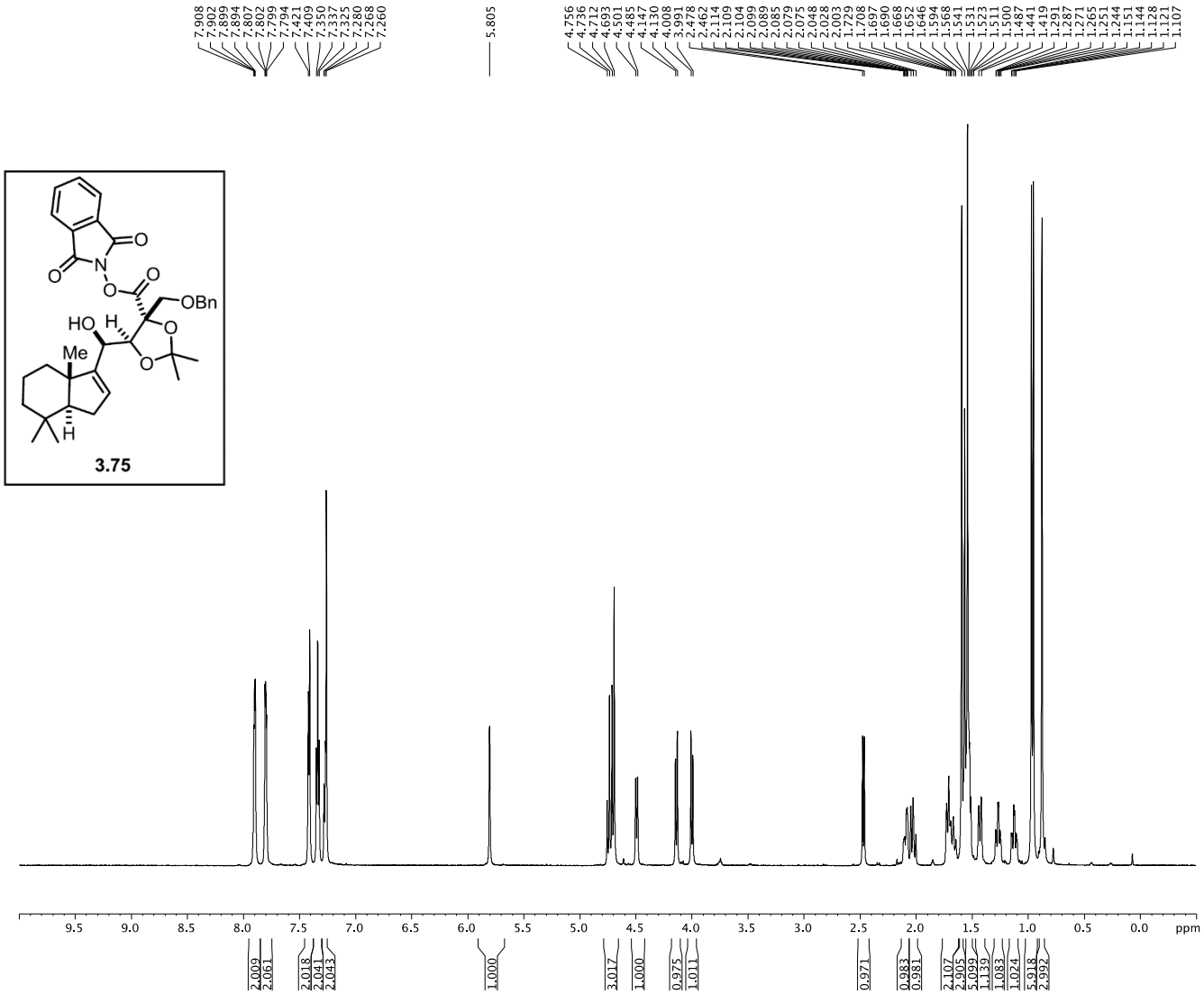

Current Data Parameters
NAME DJT-IV-203
EXPNO 1
PROCNO 1

F2 - Acquisition Parameters
Date_ 20141013
Time 16.31
INSTRUM av600
PROBHD 5 mm TBI 1H/13
PULPROG zg30
TD 98074
SOLVENT CDCl3
NS 12
DS 0
SWH 9615.385 Hz
FIDRES 0.098042 Hz
AQ 5.0998478 sec
RG 322
DW 52.000 usec
DE 14.54 usec
TE 298.0 K
D1 0.10000000 sec
TD0 1

======== CHANNEL f1 =====
SFO1 600.1342009 MHz
NUC1 1H
P1 8.00 usec
PLW1 23.01441956 W

F2 - Processing parameters
SI 65536
SF 600.1300343 MHz
WDW EM
SSB 0
LB 0.30 Hz
GB 0
PC 1.00

Z-restored spin-echo 13C spectrum with 1H decoupling

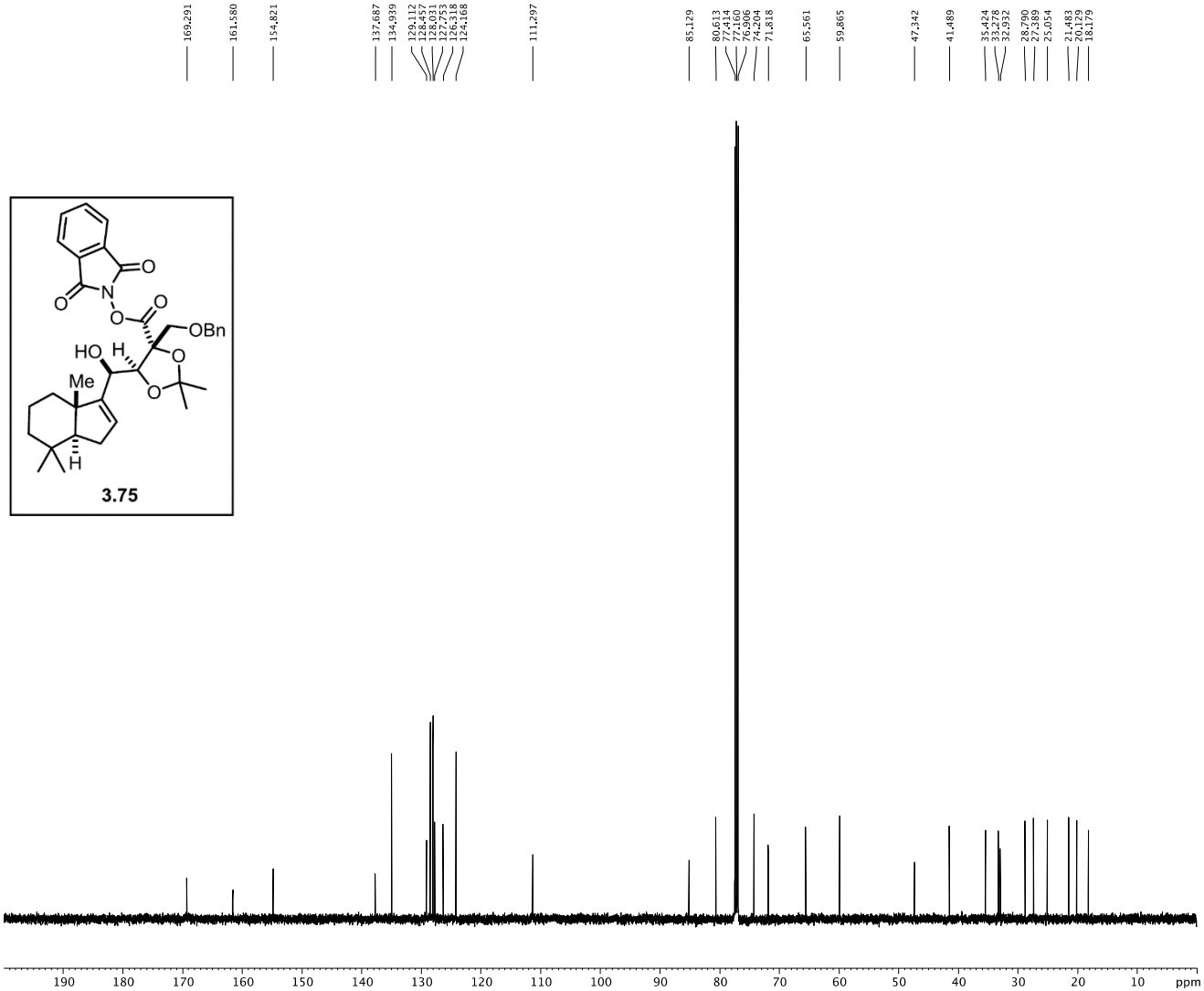


```
Current Data Parameters
NAME        DJT-IV-203
EXPNO             8
PROCNO            1

F2 - Acquisition Parameters
Date_       20150414
Time            8.55
INSTRUM       cryo500
PROBHD   5 mm CPTC1 1H-
PULPROG  SpinEchopg30gp.prd
TD          65536
SOLVENT       CDCl3
NS            857
DS              0
SWH        30303.031 Hz
FIDRES      0.462388 Hz
AQ         1.0813440 sec
RG          7298.2
DW          16.500 usec
DE           6.00 usec
TE          298.0 K
D1         0.25000000 sec
d11        0.03000000 sec
D16        0.00020000 sec
d17        0.00019600 sec
MCREST   0 sec
MCWRK      0.01500000 sec
P2          33.10 usec

======== CHANNEL f1 ========
NUC1            13C
P1            16.55 usec
P11          500.00 usec
P12         2000.00 usec
PL0          120.00 dB
PL1          -1.00 dB
SFO1      125.7942548 MHz
SP1           2.70 dB
SP2           2.70 dB
SPNAM[1] Crp60,0.5,20.1
SPNAM[2]   Crp60comp.4
SPOFF1   0 Hz
SPOFF2   0 Hz

======== CHANNEL f2 ========
CPDPRG[2       waltz16
NUC2             1H
PCPD2         100.00 usec
PL2           1.60 dB
PL12          24.50 dB
SFO2      500.2225011 MHz

====== GRADIENT CHANNEL =====
GPNAM[1]       SINE.100
GPNAM[2]       SINE.100
GPX1     0 %
GPX2     0 %
GPY1     0 %
GPY2     0 %
GPZ1          30.00 %
GPZ2          50.00 %
p15          500.00 usec
p16         1000.00 usec

F2 - Processing parameters
SI          65536
SF      125.7804076 MHz
WDW             EM
SSB     0
LB          1.00 Hz
GB      0
PC          2.00
```

1H spectrum

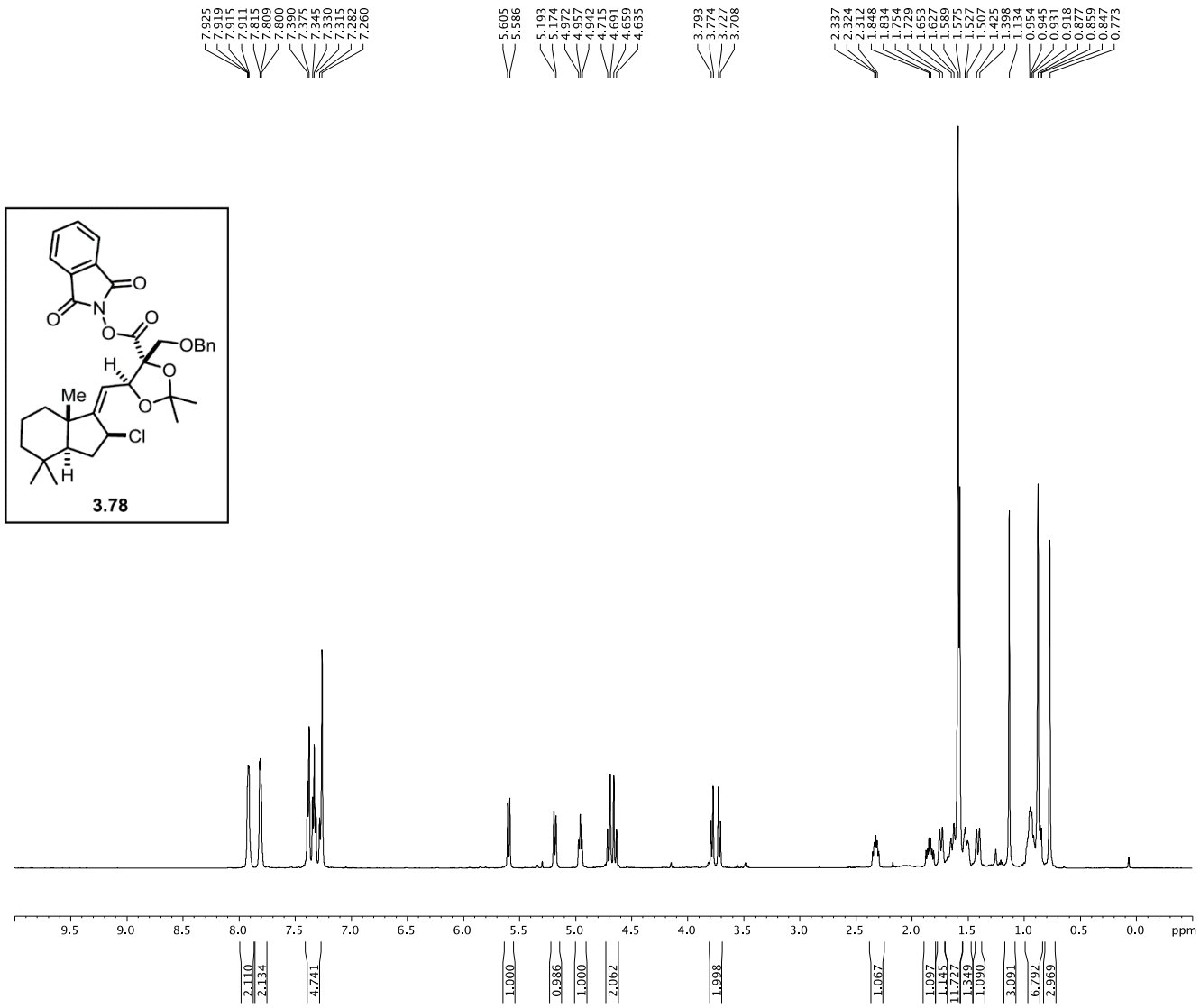

Current Data Parameters
NAME DJT-IV-271
EXPNO 3
PROCNO 1

F2 - Acquisition Parameters
Date_ 20141206
Time 11.39
INSTRUM cryo500
PROBHD 5 mm CPTCI 1H-
PULPROG zg30
TD 81728
SOLVENT CDCl3
NS 48
DS 2
SWH 8012.820 Hz
FIDRES 0.098043 Hz
AQ 5.0998273 sec
RG 5.7
DW 62.400 usec
DE 6.00 usec
TE 298.0 K
D1 0.10000000 sec
MCREST 0 sec
MCWRK 0.01500000 sec

======== CHANNEL f1 =====
NUC1 1H
P1 7.50 usec
PL1 1.60 dB
SFO1 500.2235015 MHz

F2 - Processing parameters
SI 65536
SF 500.2200345 MHz
WDW EM
SSB 0
LB 0.30 Hz
GB 0
PC 4.00

Z-restored spin-echo 13C spectrum with 1H decoupling

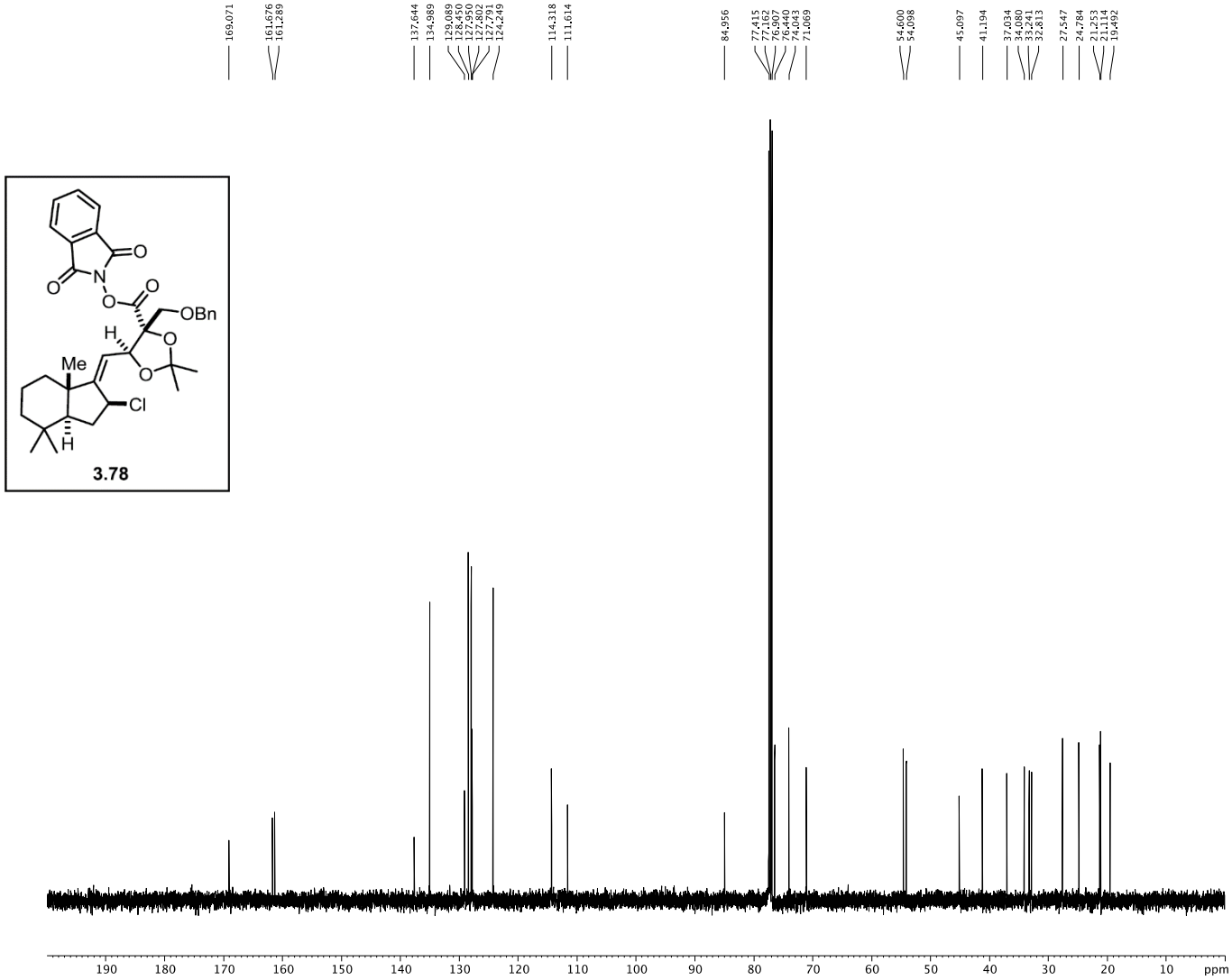

Current Data Parameters
NAME DJT-IV-271
EXPNO 4
PROCNO 1

F2 - Acquisition Parameters
Date_ 20141206
Time 11.49
INSTRUM cryo500
PROBHD 5 mm CPTCI 1H-
PULPROG SpinEchopg30gp.prd
TD 65536
SOLVENT CDCl3
NS 269
DS 16
SWH 30303.031 Hz
FIDRES 0.462388 Hz
AQ 1.0813440 sec
RG 7298.2
DW 16.500 usec
DE 6.00 usec
TE 298.0 K
D1 0.25000000 sec
d11 0.03000000 sec
D16 0.00020000 sec
d17 0.00019600 sec
MCREST 0 sec
MCWRK 0.01500000 sec
P2 33.10 usec

======== CHANNEL f1 ========
NUC1 13C
P1 16.55 usec
P11 500.00 usec
P12 2000.00 usec
PL0 120.00 dB
PL1 -1.00 dB
SFO1 125.7942548 MHz
SP1 2.70 dB
SP2 2.70 dB
SPNAM[1] Crp60,0.5,20.1
SPNAM[2] Crp60comp.4
SPOFF1 0 Hz
SPOFF2 0 Hz

======== CHANNEL f2 ========
CPDPRG[2 waltz16
NUC2 1H
PCPD2 100.00 usec
PL2 1.60 dB
PL12 24.50 dB
SFO2 500.2225011 MHz

====== GRADIENT CHANNEL =====
GPNAM[1] SINE.100
GPNAM[2] SINE.100
GPX1 0 %
GPX2 0 %
GPY1 0 %
GPY2 0 %
GPZ1 30.00 %
GPZ2 50.00 %
p15 500.00 usec
p16 1000.00 usec

F2 - Processing parameters
SI 65536
SF 125.7804099 MHz
WDW EM
SSB 0
LB 1.00 Hz
GB 0
PC 2.00

1H spectrum

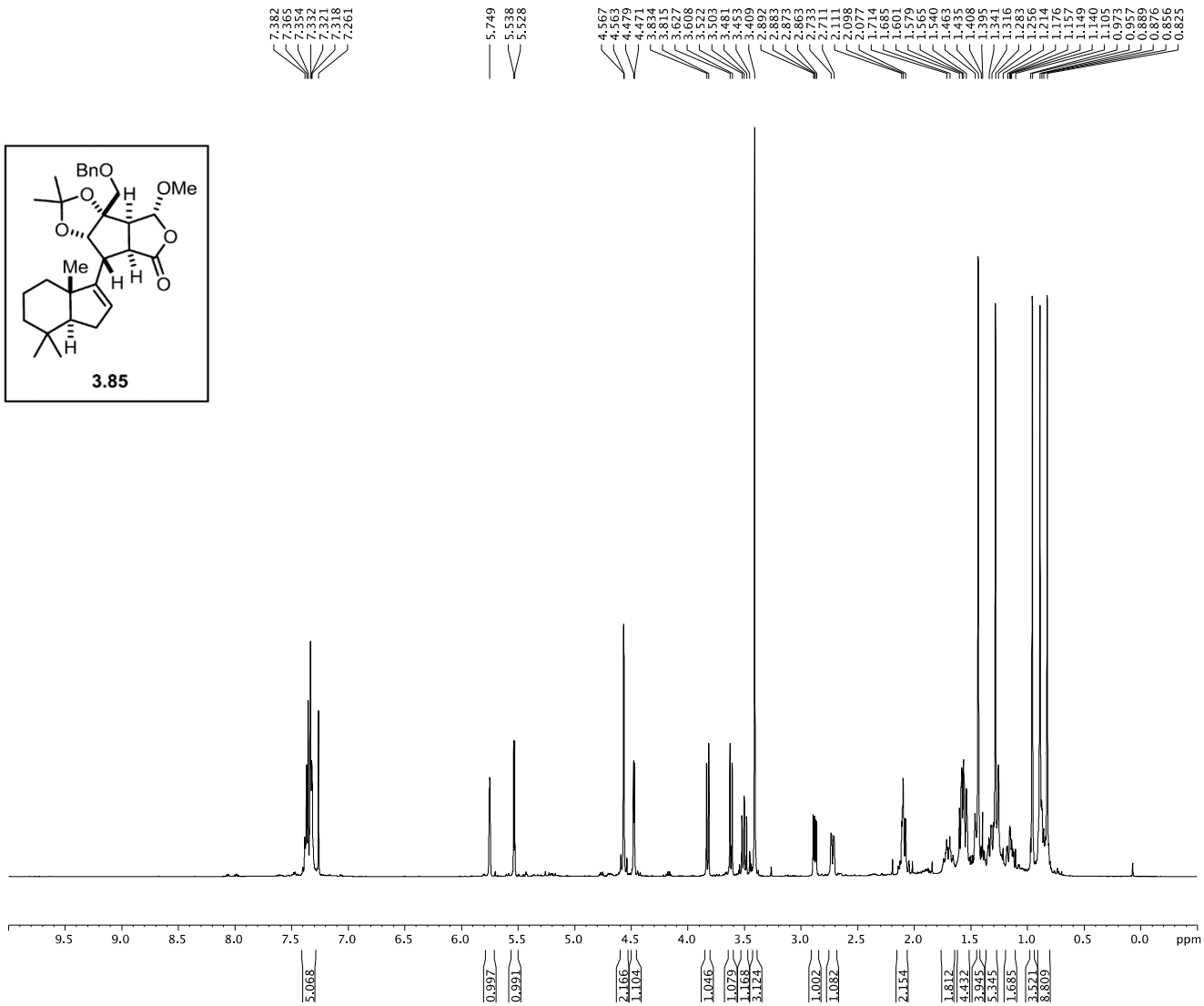

Current Data Parameters
NAME DJT-V-103
EXPNO 2
PROCNO 1

F2 - Acquisition Parameters
Date_ 20150328
Time 14.19
INSTRUM cryo500
PROBHD 5 mm CPTCI 1H-
PULPROG zg30
TD 16022
SOLVENT CDCl3
NS 60
DS 0
SWH 8012.820 Hz
FIDRES 0.500114 Hz
AQ 0.9997728 sec
RG 5
DW 62.400 usec
DE 6.00 usec
TE 298.0 K
D1 0.10000000 sec
MCREST 0 sec
MCWRK 0.01500000 sec

======== CHANNEL f1 =====
NUC1 1H
P1 7.50 usec
PL1 1.60 dB
SFO1 500.2235015 MHz

F2 - Processing parameters
SI 65536
SF 500.2200304 MHz
WDW EM
SSB 0
LB 0.30 Hz
GB 0
PC 4.00

Z-restored spin-echo 13C spectrum with 1H decoupling

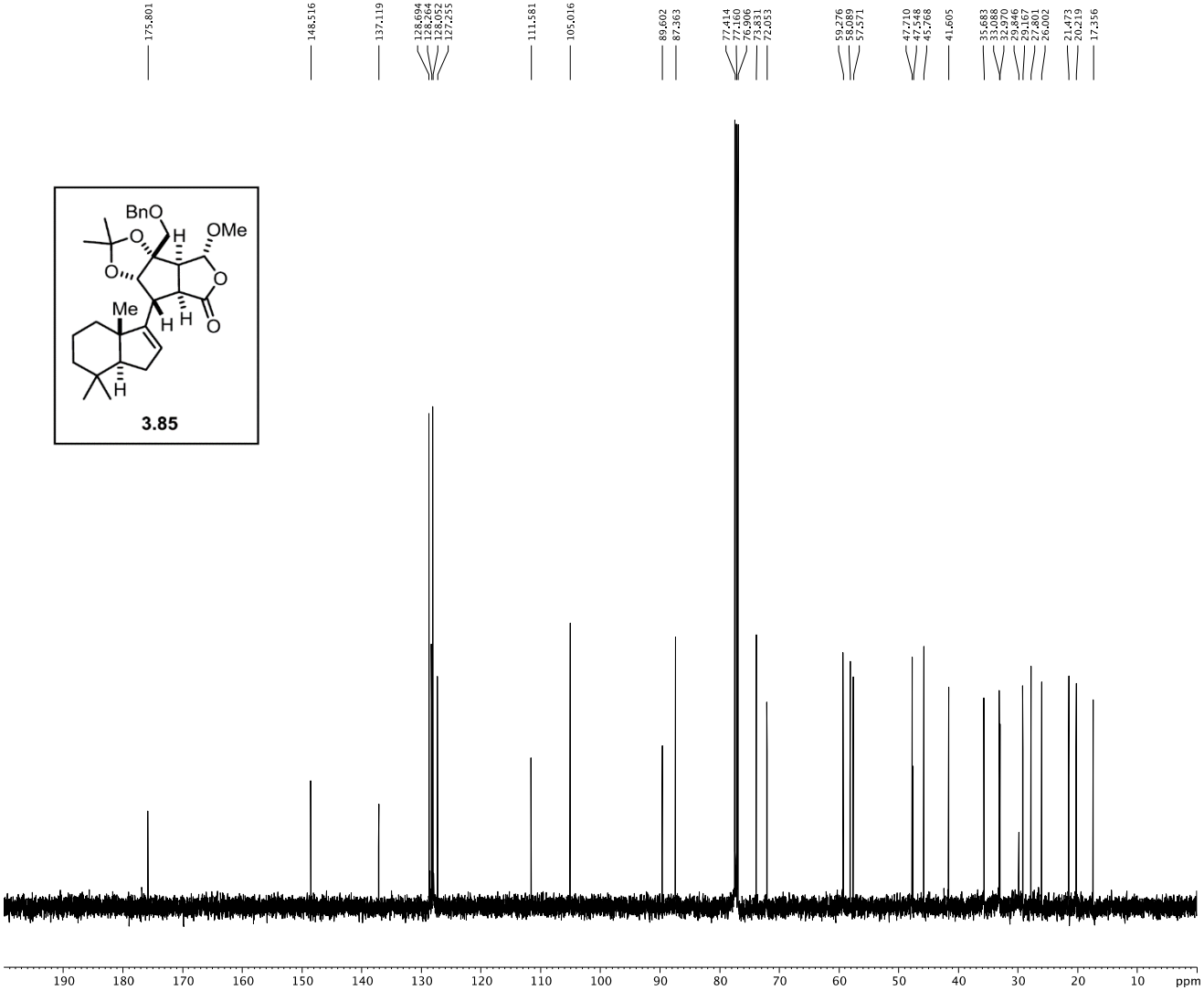

Current Data Parameters
NAME DJT-V-056
EXPNO 6
PROCNO 1

F2 - Acquisition Parameters
Date_ 20150225
Time 16.33
INSTRUM cryo500
PROBHD 5 mm CPTCI 1H-
PULPROG SpinEchopg30gp.prd
TD 65536
SOLVENT CDCl3
NS 135
DS 0
SWH 30303.031 Hz
FIDRES 0.462388 Hz
AQ 1.0813440 sec
RC 3251
DW 16.500 usec
DE 6.00 usec
TE 298.0 K
D1 0.25000000 sec
d11 0.03000000 sec
D16 0.00020000 sec
d17 0.00019600 sec
MCREST 0 sec
MCWRK 0.01500000 sec
P2 33.10 usec

======== CHANNEL f1 ========
NUC1 13C
P1 16.55 usec
P11 500.00 usec
P12 2000.00 usec
PL0 120.00 dB
PL1 -1.00 dB
SFO1 125.7942548 MHz
SP1 2.70 dB
SP2 2.70 dB
SPNAM[1] Crp60,0.5,20.1
SPNAM[2] Crp60comp.4
SPOFF1 0 Hz
SPOFF2 0 Hz

======== CHANNEL f2 ========
CPDPRG[2 waltz16
NUC2 1H
PCPD2 100.00 usec
PL2 1.60 dB
PL12 24.50 dB
SFO2 500.2225011 MHz

====== GRADIENT CHANNEL =====
GPNAM[1] SINE.100
GPNAM[2] SINE.100
GPX1 0 %
GPX2 0 %
GPY1 0 %
GPY2 0 %
GPZ1 30.00 %
GPZ2 50.00 %
p15 500.00 usec
p16 1000.00 usec

F2 - Processing parameters
SI 65536
SF 125.7804085 MHz
WDW EM
SSB 0
LB 1.00 Hz
GB 0
PC 2.00

1H spectrum

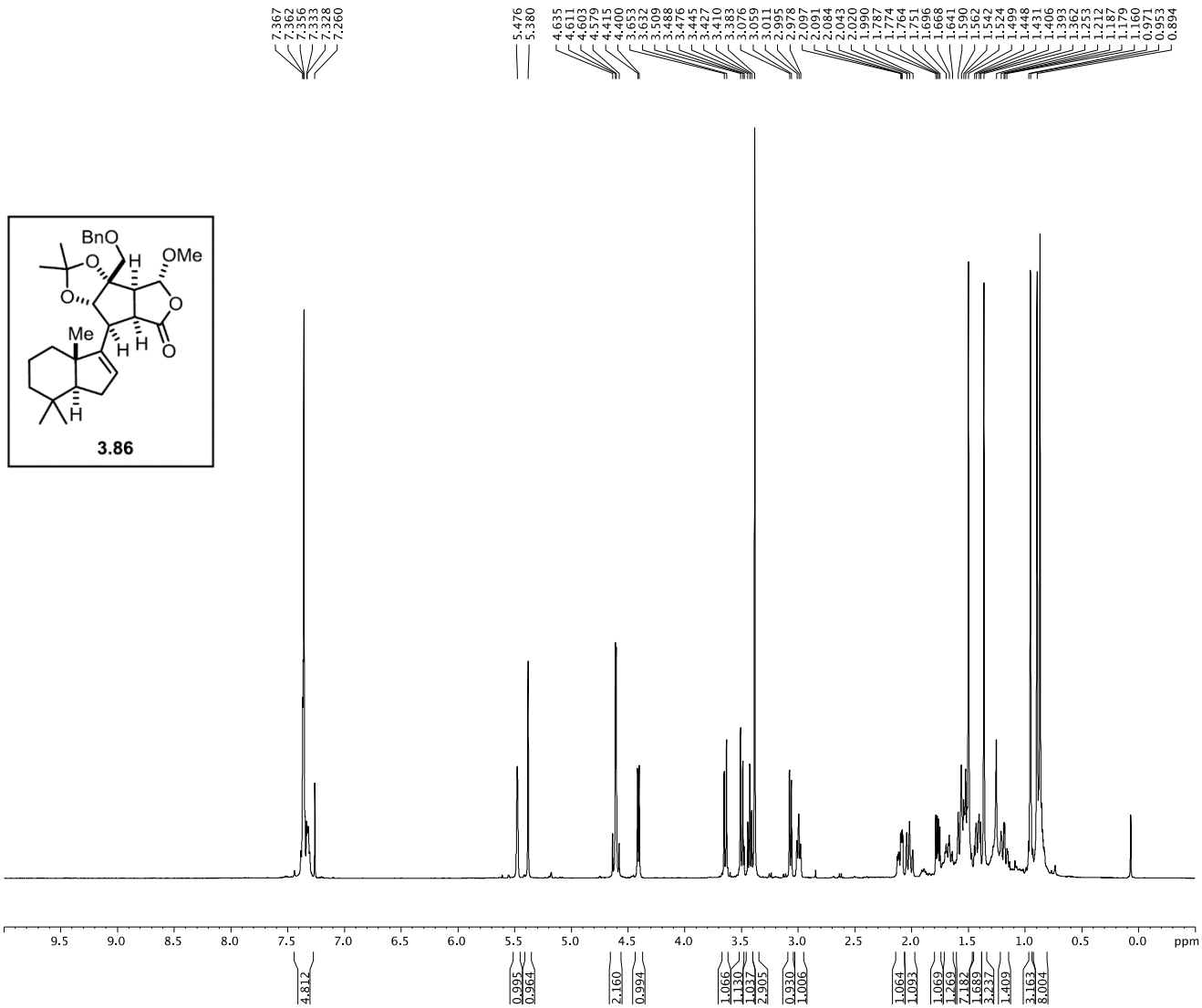

Current Data Parameters
NAME DJT-V-103
EXPNO 1
PROCNO 1

F2 - Acquisition Parameters
Date_ 20150328
Time 14.16
INSTRUM cryo500
PROBHD 5 mm CPTCI 1H-
PULPROG zg30
TD 16022
SOLVENT $CDCl_3$
NS 30
DS 0
SWH 8012.820 Hz
FIDRES 0.500114 Hz
AQ 0.9997728 sec
RG 3.6
DW 62.400 usec
DE 6.00 usec
TE 298.0 K
D1 0.10000000 sec
MCREST 0 sec
MCWRK 0.01500000 sec

======== CHANNEL f1 =====
NUC1 1H
P1 7.50 usec
PL1 1.60 dB
SFO1 500.2235015 MHz

F2 - Processing parameters
SI 65536
SF 500.2200308 MHz
WDW EM
SSB 0
LB 0.30 Hz
GB 0
PC 4.00

Z-restored spin-echo 13C spectrum with 1H decoupling

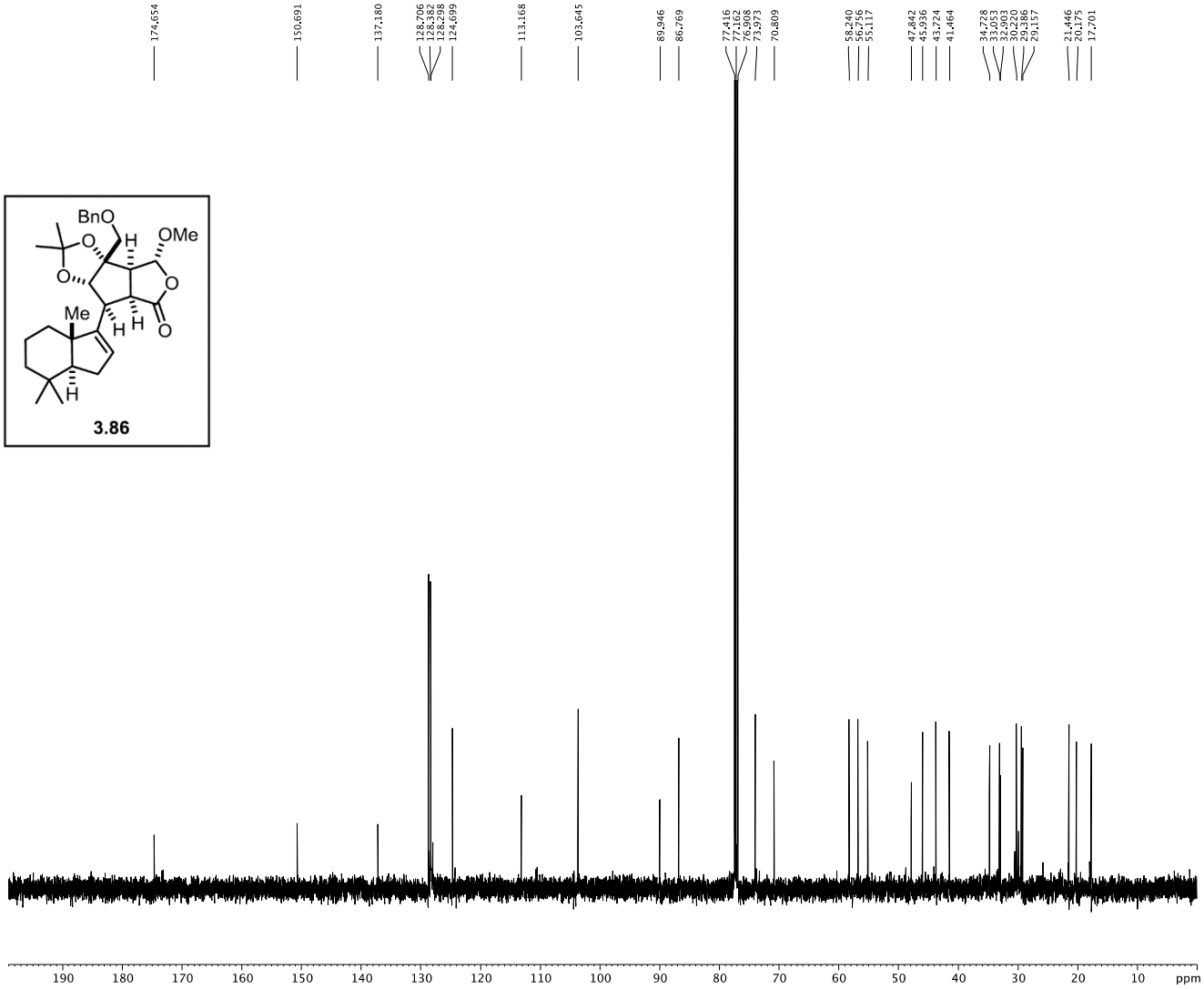

Current Data Parameters
NAME DJT-V-027
EXPNO 6
PROCNO 1

F2 - Acquisition Parameters
Date_ 20150128
Time 8.37
INSTRUM cryo500
PROBHD 5 mm CPTCI 1H-
PULPROG SpinEchopg30gp.prd
TD 65536
SOLVENT CDCl3
NS 260
DS 16
SWH 30303.031 Hz
FIDRES 0.462388 Hz
AQ 1.0813440 sec
RG 6502
DW 16.500 usec
DE 6.00 usec
TE 298.0 K
D1 0.25000000 sec
d11 0.03000000 sec
D16 0.00020000 sec
d17 0.00019600 sec
MCREST 0 sec
MCWRK 0.01500000 sec
P2 33.10 usec

======== CHANNEL f1 ========
NUC1 13C
P1 16.55 usec
P11 500.00 usec
P12 2000.00 usec
PL0 120.00 dB
PL1 -1.00 dB
SFO1 125.7942548 MHz
SP1 2.70 dB
SP2 2.70 dB
SPNAM[1] Crp60,0.5,20.1
SPNAM[2] Crp60comp.4
SPOFF1 0 Hz
SPOFF2 0 Hz

======== CHANNEL f2 ========
CPDPRG[2 waltz16
NUC2 1H
PCPD2 100.00 usec
PL2 1.60 dB
PL12 24.50 dB
SFO2 500.2225011 MHz

====== GRADIENT CHANNEL =====
GPNAM[1] SINE.100
GPNAM[2] SINE.100
GPX1 0 %
GPX2 0 %
GPY1 0 %
GPY2 0 %
GPZ1 30.00 %
GPZ2 50.00 %
p15 500.00 usec
p16 1000.00 usec

F2 - Processing parameters
SI 65536
SF 125.7804076 MHz
WDW EM
SSB 0
LB 1.00 Hz
GB 0
PC 2.00

1H spectrum

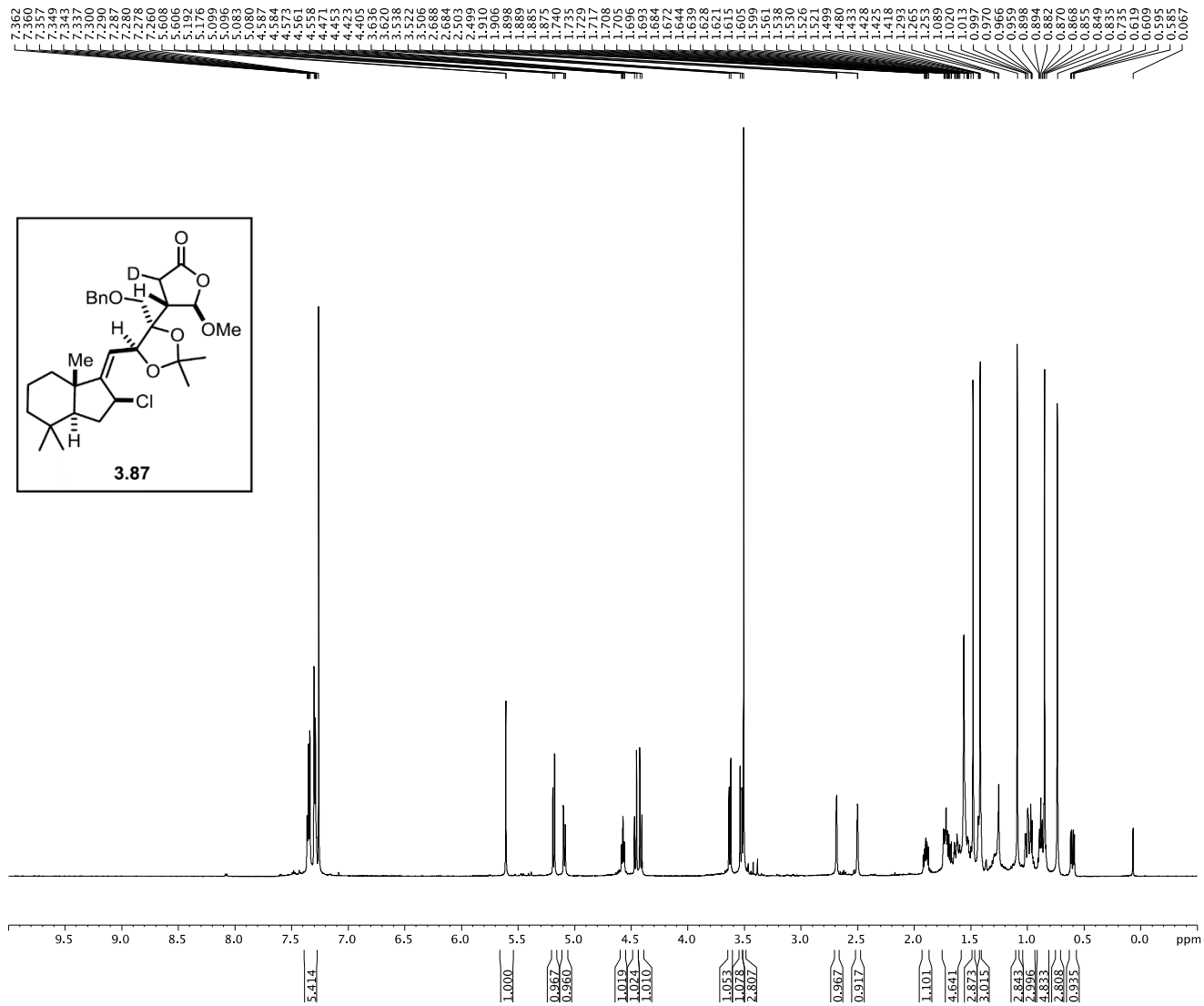

3.87

Current Data Parameters
NAME DJT-V-263
EXPNO 19
PROCNO 1

F2 - Acquisition Parameters
Date_ 20151009
Time 15.47
INSTRUM av600
PROBHD 5 mm TBI 1H/13
PULPROG zg30
TD 98074
SOLVENT CDCl3
NS 89
DS 0
SWH 9615.385 Hz
FIDRES 0.098042 Hz
AQ 5.0998478 sec
RG 1030
DW 52.000 usec
DE 14.54 usec
TE 296.2 K
D1 0.10000000 sec
TD0 1

======== CHANNEL f1 =====
SFO1 600.1342009 MHz
NUC1 1H
P1 8.00 usec
PLW1 24.00000000 W

F2 - Processing parameters
SI 65536
SF 600.1300357 MHz
WDW EM
SSB 0
LB 0.30 Hz
GB 0
PC 1.00

Z-restored spin-echo 13C spectrum with 1H decoupling

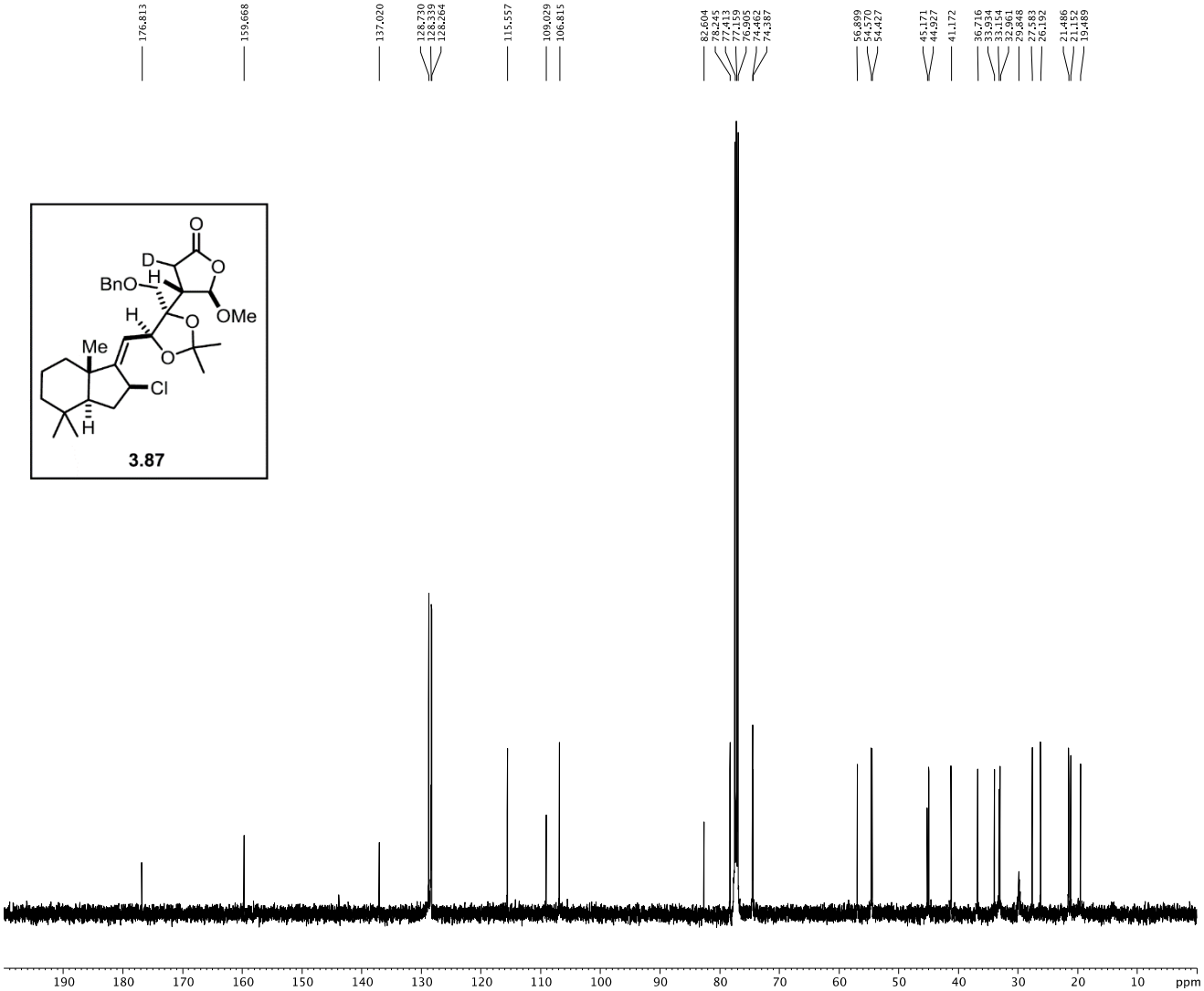


```
Current Data Parameters
NAME          DJT-V-263
EXPNO               21
PROCNO               1

F2 - Acquisition Parameters
Date_         20151010
Time              9.52
INSTRUM         cryo500
PROBHD   5 mm CPTCI 1H-
PULPROG  SpinEchopg30gp.prd
TD              65536
SOLVENT         CDCl3
NS                842
DS                  0
SWH           30303.031 Hz
FIDRES         0.462388 Hz
AQ           1.0813440 sec
RC             5792.6
DW              16.500 usec
DE               6.00 usec
TE              298.0 K
D1           0.25000000 sec
d11          0.03000000 sec
D16          0.00020000 sec
d17          0.00019600 sec
MCREST   0 sec
MCWRK        0.01500000 sec
P2              33.10 usec

======== CHANNEL f1 ========
NUC1              13C
P1              16.55 usec
P11            500.00 usec
P12           2000.00 usec
PL0            120.00 dB
PL1             -1.00 dB
SFO1         125.7942548 MHz
SP1              2.70 dB
SP2              2.70 dB
SPNAM[1] Crp60,0.5,20.1
SPNAM[2]   Crp60comp.4
SPOFF1   0 Hz
SPOFF2   0 Hz

======== CHANNEL f2 ========
CPDPRG[2        waltz16
NUC2               1H
PCPD2           100.00 usec
PL2              1.60 dB
PL12            24.50 dB
SFO2         500.2225011 MHz

====== GRADIENT CHANNEL =====
GPNAM[1]        SINE.100
GPNAM[2]        SINE.100
GPX1     0 %
GPX2     0 %
GPY1     0 %
GPY2     0 %
GPZ1            30.00 %
GPZ2            50.00 %
p15            500.00 usec
p16           1000.00 usec

F2 - Processing parameters
SI              65536
SF         125.7804080 MHz
WDW               EM
SSB     0
LB              1.00 Hz
GB      0
PC              2.00
```

1H spectrum

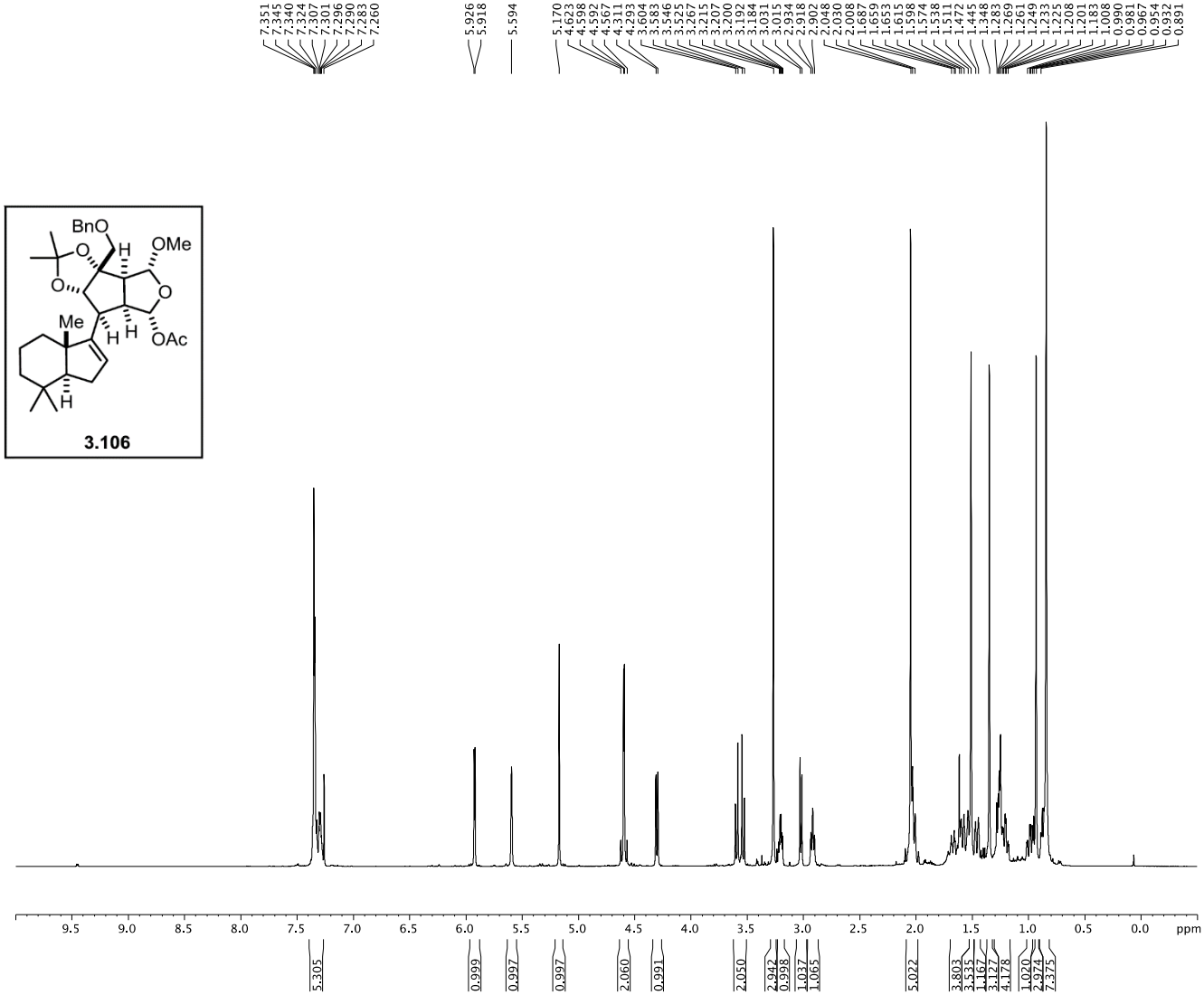

Current Data Parameters
NAME DJT-V-268
EXPNO 1
PROCNO 1

F2 - Acquisition Parameters
Date_ 20150821
Time 11.02
INSTRUM cryo500
PROBHD 5 mm CPTCI 1H-
PULPROG zg30
TD 81728
SOLVENT CDCl3
NS 20
DS 0
SWH 8012.820 Hz
FIDRES 0.098043 Hz
AQ 5.0998273 sec
RG 6.3
DW 62.400 usec
DE 6.00 usec
TE 298.0 K
D1 0.10000000 sec
MCREST 0 sec
MCWRK 0.01500000 sec

======== CHANNEL f1 =====
NUC1 1H
P1 7.50 usec
PL1 1.60 dB
SFO1 500.2235015 MHz

F2 - Processing parameters
SI 65536
SF 500.2200313 MHz
WDW EM
SSB 0
LB 0.30 Hz
GB 0
PC 4.00

Z-restored spin-echo 13C spectrum with 1H decoupling

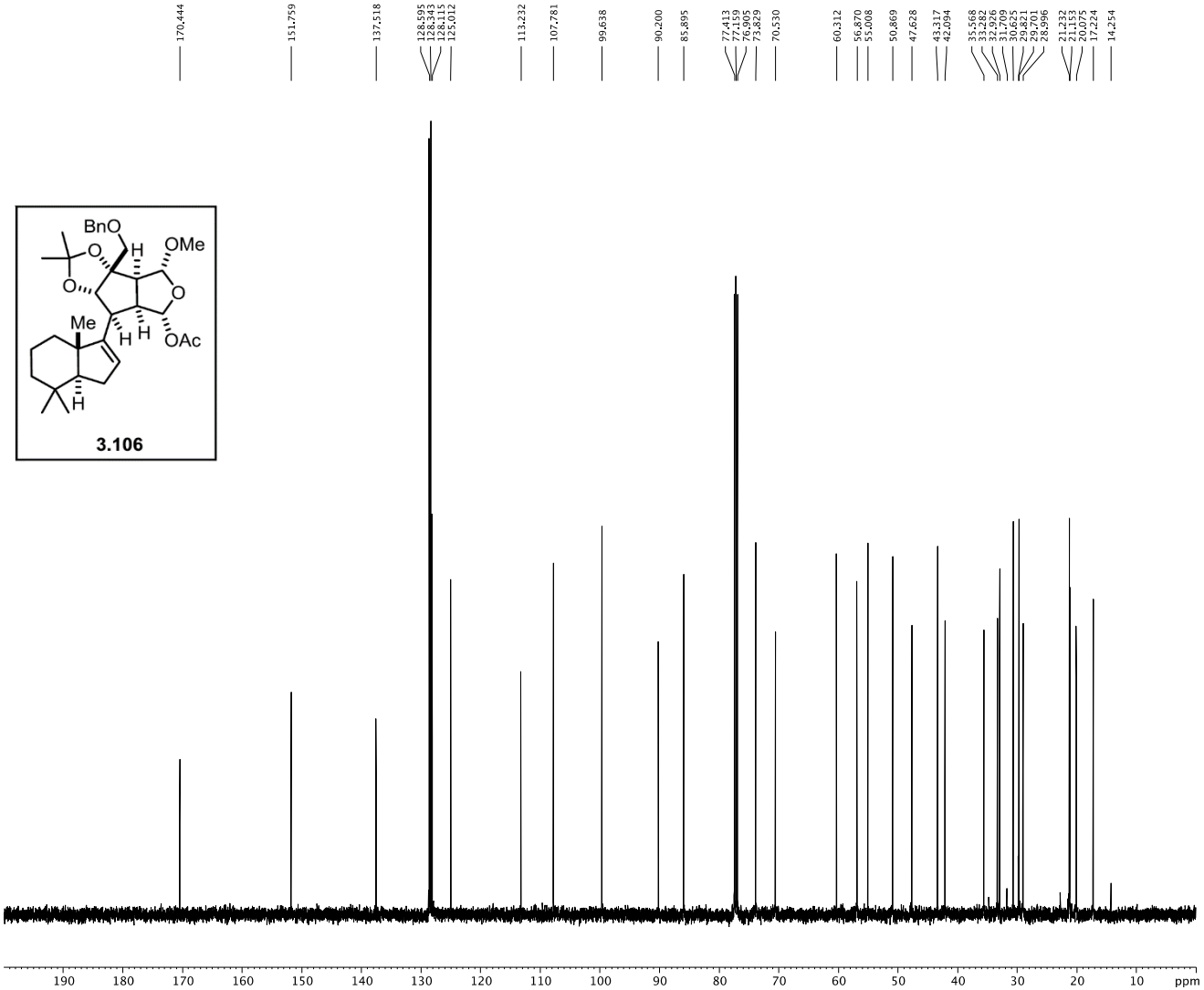

Current Data Parameters
NAME DJT-V-268
EXPNO 2
PROCNO 1

F2 - Acquisition Parameters
Date_ 20150821
Time 11.07
INSTRUM cryo500
PROBHD 5 mm CPTCI 1H-
PULPROG SpinEchopg30gp.prd
TD 65536
SOLVENT CDCl3
NS 171
DS 0
SWH 30303.031 Hz
FIDRES 0.462388 Hz
AQ 1.0813440 sec
RG 5792.6
DW 16.500 usec
DE 6.00 usec
TE 298.0 K
D1 0.25000000 sec
d11 0.03000000 sec
D16 0.00020000 sec
d17 0.00019600 sec
MCREST 0 sec
MCWRK 0.01500000 sec
P2 33.10 usec

======== CHANNEL f1 ========
NUC1 13C
P1 16.55 usec
P11 500.00 usec
P12 2000.00 usec
PL0 120.00 dB
PL1 -1.00 dB
SFO1 125.7942548 MHz
SP1 2.70 dB
SP2 2.70 dB
SPNAM[1] Crp60.0.5.20.1
SPNAM[2] Crp60comp.4
SPOFF1 0 Hz
SPOFF2 0 Hz

======== CHANNEL f2 ========
CPDPRG[2 waltz16
NUC2 1H
PCPD2 100.00 usec
PL2 1.60 dB
PL12 24.50 dB
SFO2 500.2225011 MHz

====== GRADIENT CHANNEL =====
GPNAM[1] SINE.100
GPNAM[2] SINE.100
GPX1 0 %
GPX2 0 %
GPY1 0 %
GPY2 0 %
GPZ1 30.00 %
GPZ2 50.00 %
p15 500.00 usec
p16 1000.00 usec

F2 - Processing parameters
SI 65536
SF 125.7804108 MHz
WDW EM
SSB 0
LB 1.00 Hz
GB 0
PC 2.00

1H spectrum

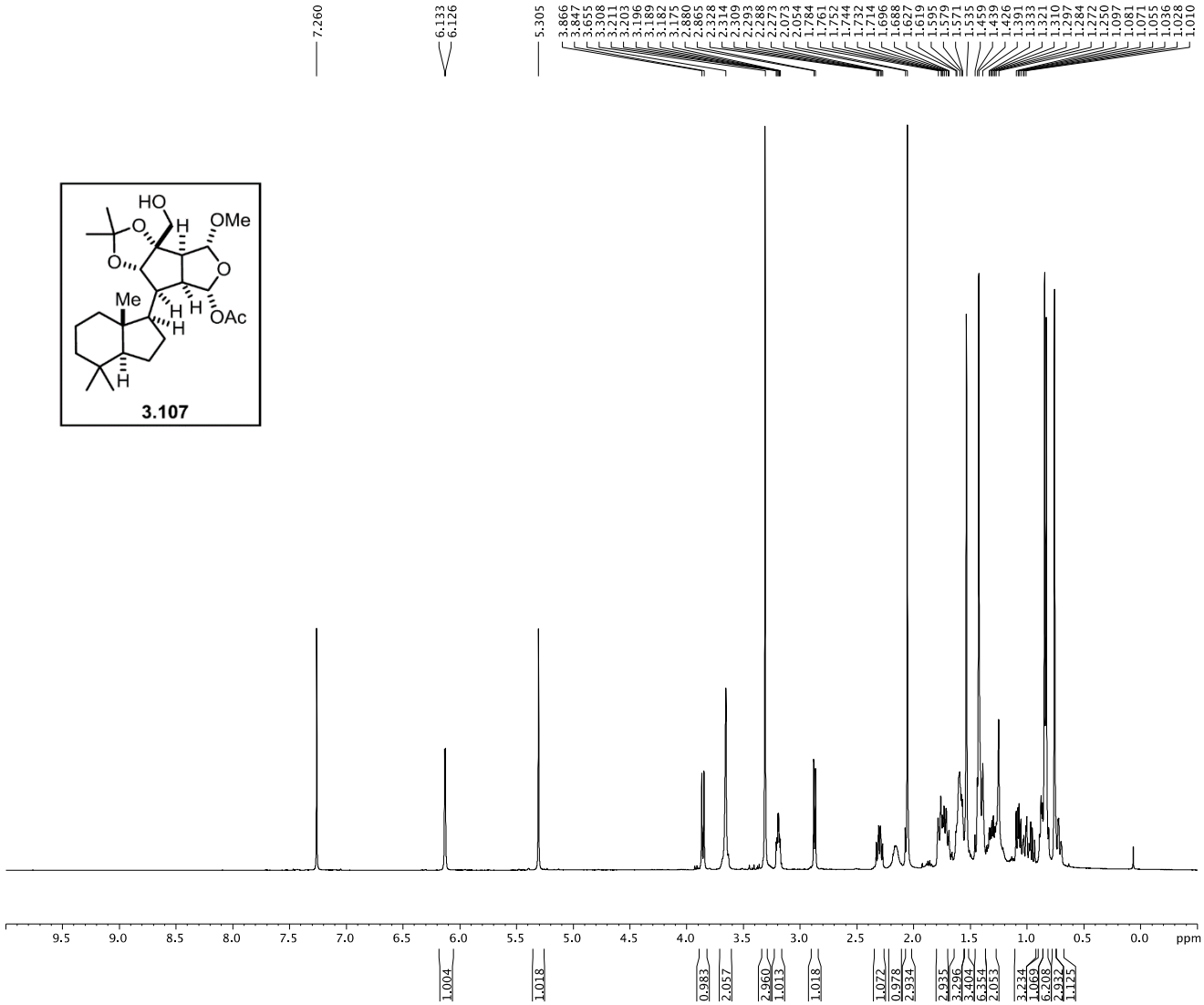


```
Current Data Parameters
NAME        DJT-V-270
EXPNO           5
PROCNO          1

F2 - Acquisition Parameters
Date_       20150824
Time           13.07
INSTRUM       cryo500
PROBHD  5 mm CPTCI 1H-
PULPROG         zg30
TD             81728
SOLVENT        CDCl3
NS               20
DS                0
SWH          8012.820 Hz
FIDRES       0.098043 Hz
AQ          5.0998273 sec
RG                5
DW            62.400 usec
DE             6.00 usec
TE            298.0 K
D1          0.10000000 sec
MCREST  0 sec
MCWRK       0.01500000 sec

======== CHANNEL f1 =====
NUC1             1H
P1            7.50 usec
PL1           1.60 dB
SFO1      500.2235015 MHz

F2 - Processing parameters
SI            65536
SF       500.2200312 MHz
WDW             EM
SSB     0
LB            0.30 Hz
GB      0
PC            4.00
```

Z-restored spin-echo 13C spectrum with 1H decoupling

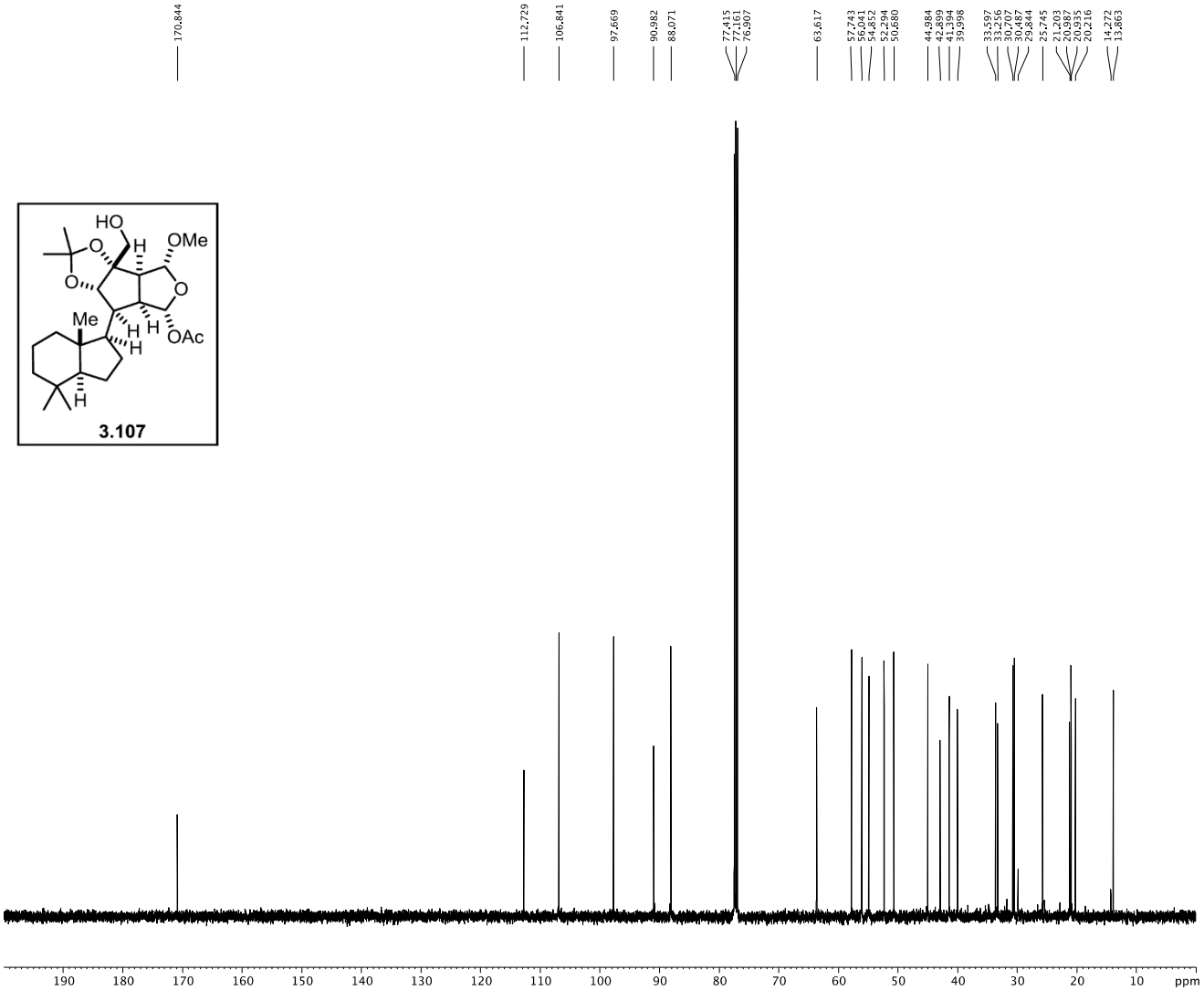


```
Current Data Parameters
NAME        DJT-V-270
EXPNO           6
PROCNO          1

F2 - Acquisition Parameters
Date_       20150824
Time          13.11
INSTRUM       cryo500
PROBHD   5 mm CPTCI 1H-
PULPROG  SpinEchopg30gp.prd
TD          65536
SOLVENT       CDCl3
NS            498
DS              0
SWH         30303.031 Hz
FIDRES       0.462388 Hz
AQ          1.0813440 sec
RG            4096
DW           16.500 usec
DE            6.00 usec
TE           298.0 K
D1         0.25000000 sec
d11        0.03000000 sec
D16        0.00020000 sec
d17        0.00019600 sec
MCREST   0 sec
MCWRK      0.01500000 sec
P2           33.10 usec

======== CHANNEL f1 ========
NUC1           13C
P1           16.55 usec
P11         500.00 usec
P12        2000.00 usec
PL0         120.00 dB
PL1          -1.00 dB
SFO1      125.7942548 MHz
SP1           2.70 dB
SP2           2.70 dB
SPNAM[1] Crp60,0.5,20.1
SPNAM[2]   Crp60comp.4
SPOFF1   0 Hz
SPOFF2   0 Hz

======== CHANNEL f2 ========
CPDPRG[2       waltz16
NUC2            1H
PCPD2        100.00 usec
PL2           1.60 dB
PL12         24.50 dB
SFO2      500.2225011 MHz

====== GRADIENT CHANNEL =====
GPNAM[1]       SINE.100
GPNAM[2]       SINE.100
GPX1     0 %
GPX2     0 %
GPY1     0 %
GPY2     0 %
GPZ1         30.00 %
GPZ2         50.00 %
p15         500.00 usec
p16        1000.00 usec

F2 - Processing parameters
SI          65536
SF      125.7804080 MHz
WDW            EM
SSB     0
LB          1.00 Hz
GB      0
PC          2.00
```

1H spectrum

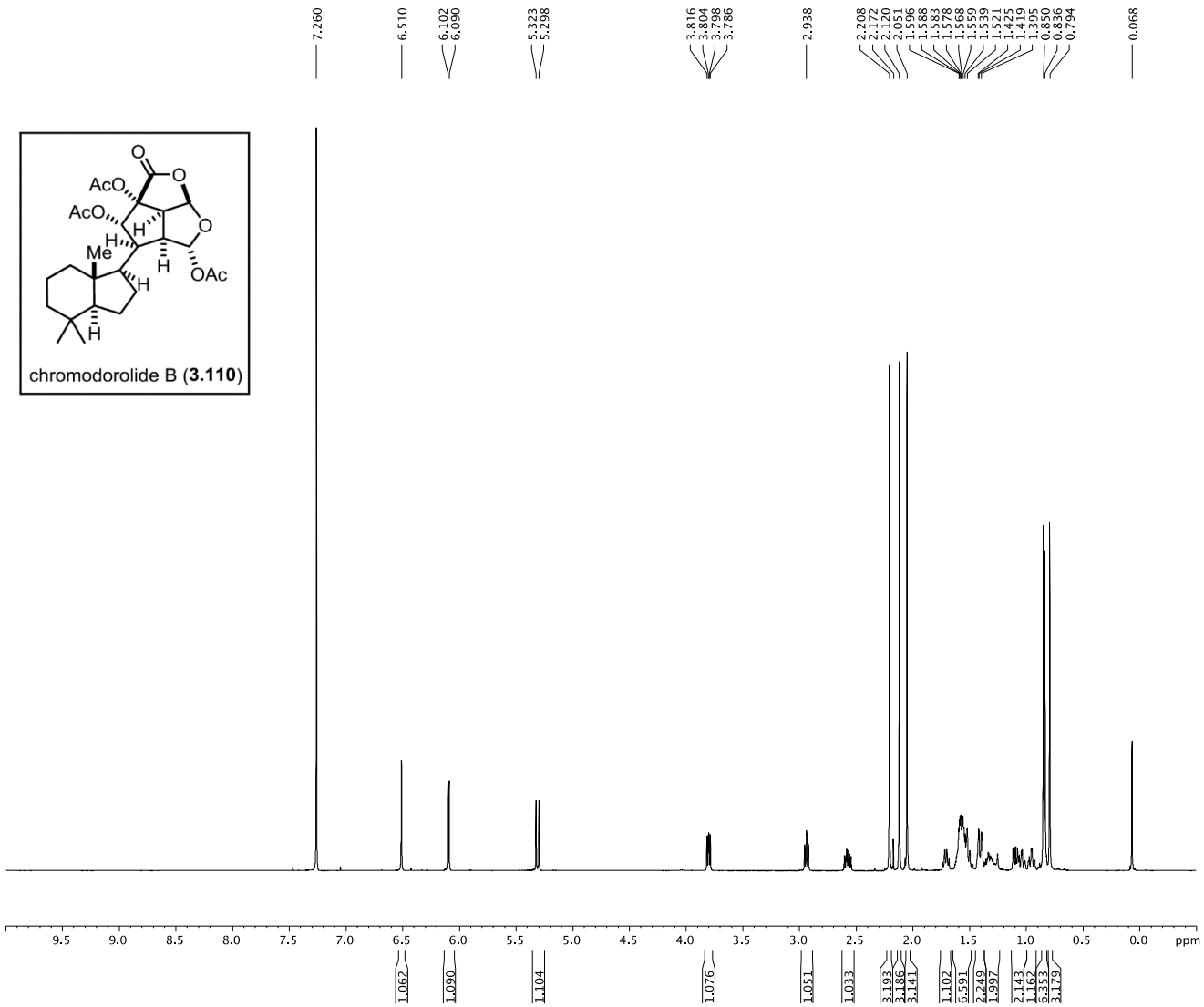

chromodorolide B (**3.110**)

```
Current Data Parameters
NAME        DJT-V-272
EXPNO             5
PROCNO            1

F2 - Acquisition Parameters
Date_       20150907
Time            9.43
INSTRUM       cryo500
PROBHD   5 mm CPTCI 1H-
PULPROG         zg30
TD             81728
SOLVENT        CDCl3
NS               140
DS                 0
SWH          8012.820 Hz
FIDRES       0.098043 Hz
AQ         5.0998273 sec
RG                 8
DW            62.400 usec
DE             6.00 usec
TE            298.0 K
D1         0.10000000 sec
MCREST   0 sec
MCWRK      0.01500000 sec

======== CHANNEL f1 =====
NUC1              1H
P1             7.50 usec
PL1            1.60 dB
SFO1      500.2235015 MHz

F2 - Processing parameters
SI             65536
SF       500.2200312 MHz
WDW              EM
SSB     0
LB            0.30 Hz
GB      0
PC             4.00
```

Z-restored spin-echo 13C spectrum with 1H decoupling

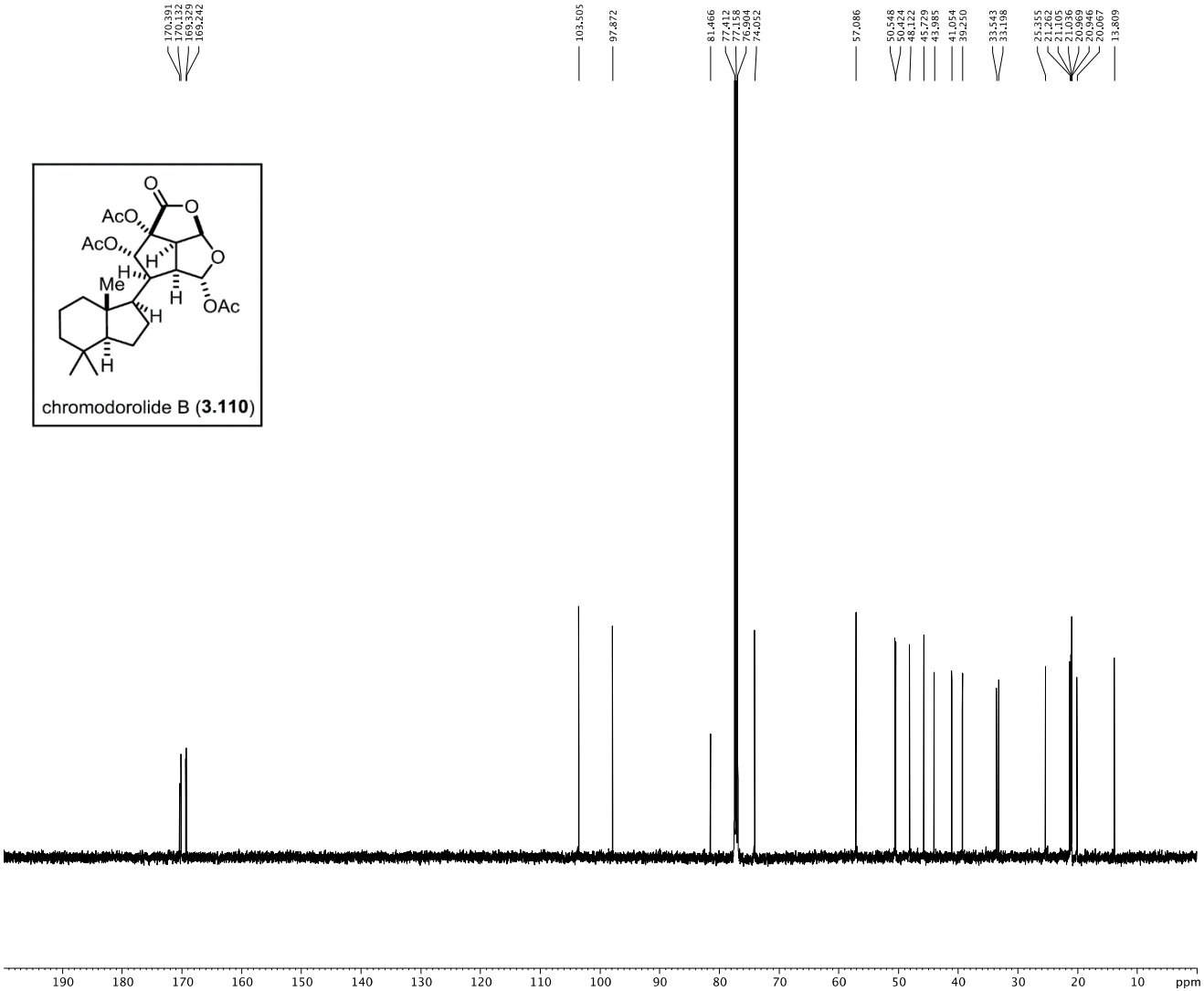


```
Current Data Parameters
NAME          DJT-V-272
EXPNO               10
PROCNO               1

F2 - Acquisition Parameters
Date_         20151012
Time              7.21
INSTRUM          cryo500
PROBHD   5 mm CPTCI 1H-
PULPROG  SpinEchopg30gp.prd
TD              65536
SOLVENT          CDCl3
NS               2116
DS                  0
SWH          30303.031 Hz
FIDRES        0.462388 Hz
AQ          1.0813440 sec
RC             2298.8
DW             16.500 usec
DE              6.00 usec
TE             298.0 K
D1          0.25000000 sec
d11         0.03000000 sec
D16         0.00020000 sec
d17         0.00019600 sec
MCREST   0 sec
MCWRK       0.01500000 sec
P2             33.10 usec

======== CHANNEL f1 ========
NUC1             13C
P1             16.55 usec
P11           500.00 usec
P12          2000.00 usec
PL0           120.00 dB
PL1           -1.00 dB
SFO1        125.7942548 MHz
SP1             2.70 dB
SP2             2.70 dB
SPNAM[1] Crp60,0.5,20.1
SPNAM[2]    Crp60comp.4
SPOFF1   0 Hz
SPOFF2   0 Hz

======== CHANNEL f2 ========
CPDPRG[2        waltz16
NUC2              1H
PCPD2           100.00 usec
PL2             1.60 dB
PL12            24.50 dB
SFO2        500.2225011 MHz

====== GRADIENT CHANNEL =====
GPNAM[1]        SINE.100
GPNAM[2]        SINE.100
GPX1     0 %
GPX2     0 %
GPY1     0 %
GPY2     0 %
GPZ1            30.00 %
GPZ2            50.00 %
p15            500.00 usec
p16           1000.00 usec

F2 - Processing parameters
SI               65536
SF          125.7804080 MHz
WDW                EM
SSB     0
LB            1.00 Hz
GB      0
PC            2.00
```

Appendix D: Chapter 4 NMR Spectra

1H spectrum

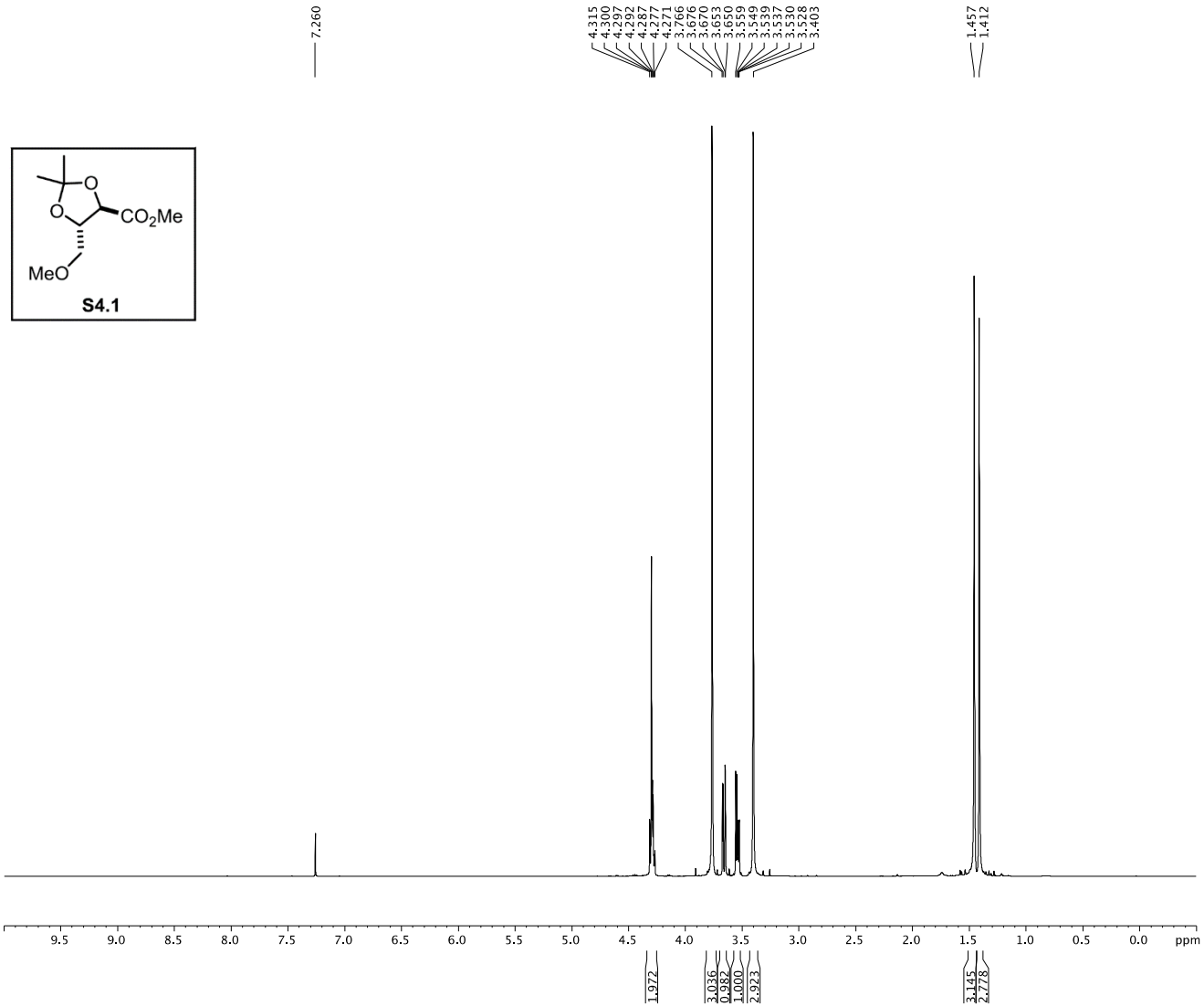

S4.1

```
Current Data Parameters
NAME        DJT-VI-157
EXPNO            5
PROCNO           1

F2 - Acquisition Parameters
Date_       20160114
Time            8.30
INSTRUM       cryo500
PROBHD   5 mm CPTCI 1H-
PULPROG          zg30
TD             81728
SOLVENT        CDCl3
NS               28
DS                0
SWH          8012.820 Hz
FIDRES       0.098043 Hz
AQ         5.0998273 sec
RG                8
DW            62.400 usec
DE             6.00 usec
TE            298.0 K
D1         0.10000000 sec
MCREST   0 sec
MCWRK      0.01500000 sec

======== CHANNEL f1 =====
NUC1             1H
P1            7.50 usec
PL1           1.60 dB
SFO1      500.2235015 MHz

F2 - Processing parameters
SI            65536
SF       500.2200312 MHz
WDW              EM
SSB     0
LB            0.30 Hz
GB      0
PC            4.00
```

Z-restored spin-echo 13C spectrum with 1H decoupling

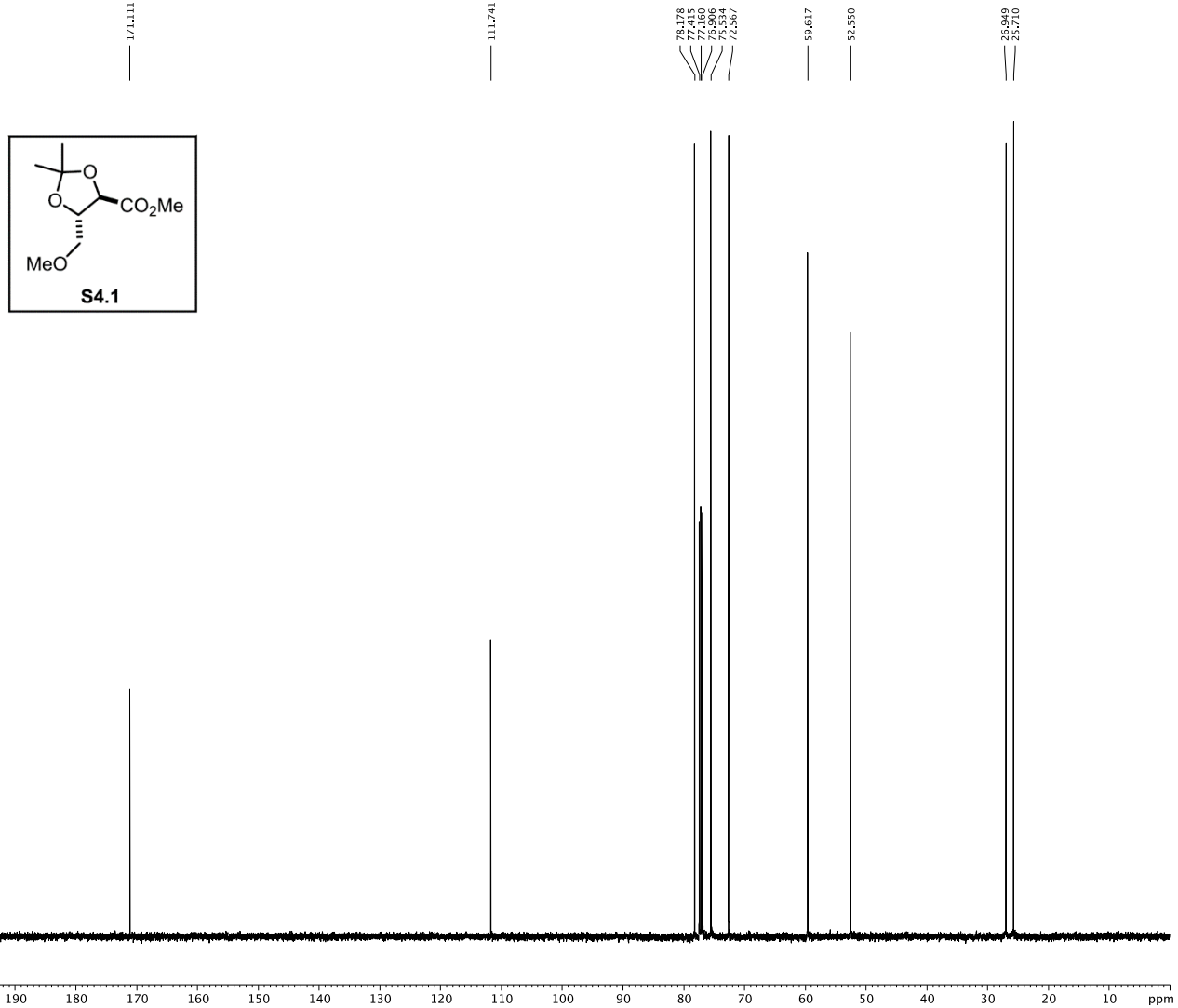

Current Data Parameters
NAME DJT-VI-157
EXPNO 6
PROCNO 1

F2 - Acquisition Parameters
Date_ 20160112
Time 15.12
INSTRUM cryo500
PROBHD 5 mm CPTCI 1H-
PULPROG SpinEchopg30gp.prd
TD 65536
SOLVENT CDCl3
NS 111
DS 0
SWH 30303.031 Hz
FIDRES 0.462388 Hz
AQ 1.0813440 sec
RG 5792.6
DW 16.500 usec
DE 6.00 usec
TE 298.0 K
D1 0.25000000 sec
d11 0.03000000 sec
D16 0.00020000 sec
d17 0.00019600 sec
MCREST 0 sec
MCWRK 0.01500000 sec
P2 33.10 usec

======== CHANNEL f1 ========
NUC1 13C
P1 16.55 usec
P11 500.00 usec
P12 2000.00 usec
PL0 120.00 dB
PL1 -1.00 dB
SFO1 125.7942548 MHz
SP1 2.70 dB
SP2 2.70 dB
SPNAM[1] Crp60,0.5,20.1
SPNAM[2] Crp60comp.4
SPOFF1 0 Hz
SPOFF2 0 Hz

======== CHANNEL f2 ========
CPDPRG[2 waltz16
NUC2 1H
PCPD2 100.00 usec
PL2 1.60 dB
PL12 24.50 dB
SFO2 500.2225011 MHz

====== GRADIENT CHANNEL =====
GPNAM[1] SINE.100
GPNAM[2] SINE.100
GPX1 0 %
GPX2 0 %
GPY1 0 %
GPY2 0 %
GPZ1 30.00 %
GPZ2 50.00 %
p15 500.00 usec
p16 1000.00 usec

F2 - Processing parameters
SI 65536
SF 125.7804140 MHz
WDW EM
SSB 0
LB 1.00 Hz
GB 0
PC 2.00

1H spectrum

4.40a

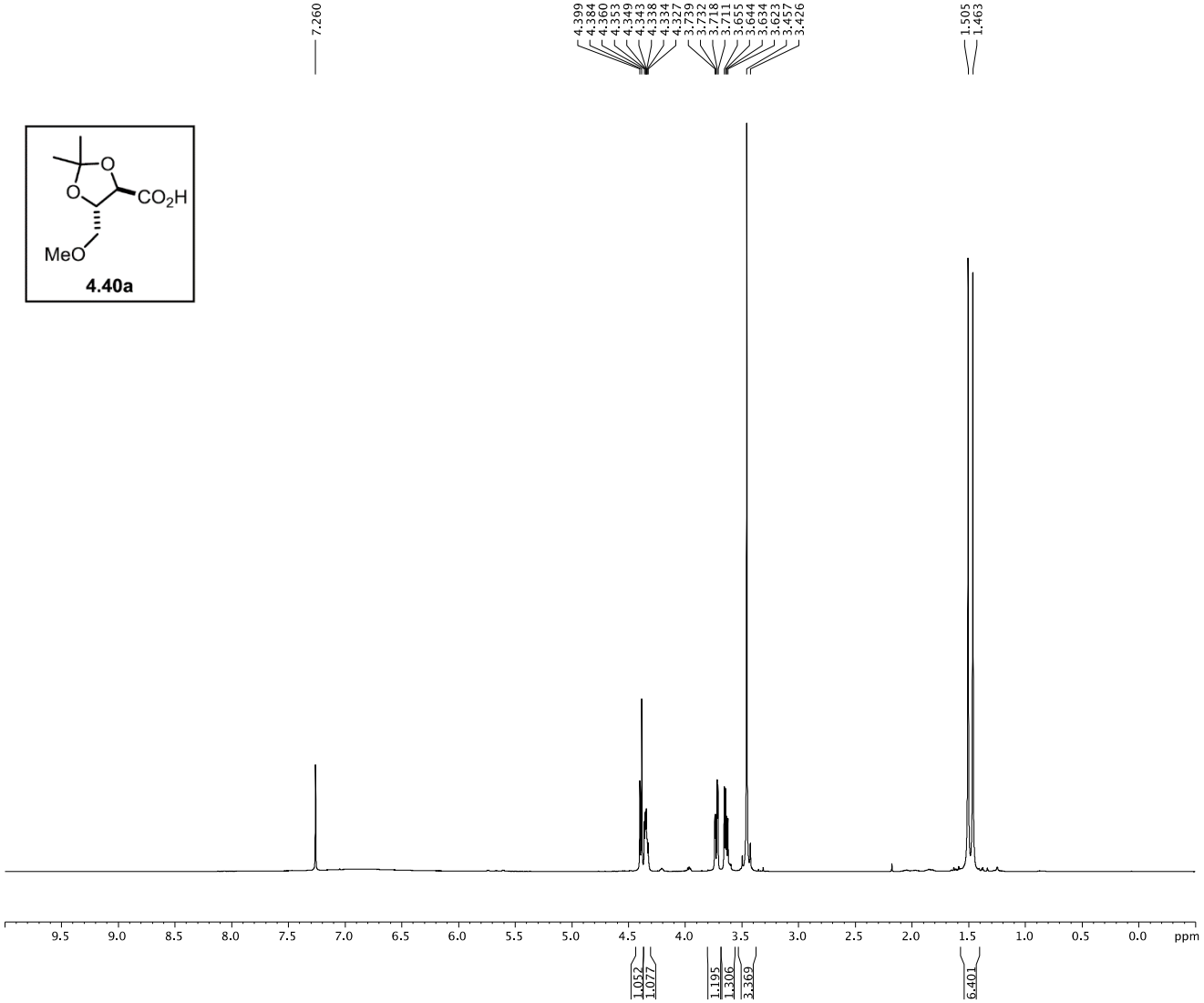

Current Data Parameters
NAME DJT-VI-160
EXPNO 1
PROCNO 1

F2 - Acquisition Parameters
Date_ 20160113
Time 11.31
INSTRUM cryo500
PROBHD 5 mm CPTCI 1H-
PULPROG zg30
TD 32048
SOLVENT CDCl3
NS 20
DS 0
SWH 8012.820 Hz
FIDRES 0.250026 Hz
AQ 1.9997952 sec
RG 8
DW 62.400 usec
DE 6.00 usec
TE 298.0 K
D1 0.10000000 sec
MCREST 0 sec
MCWRK 0.01500000 sec

======== CHANNEL f1 =====
NUC1 1H
P1 7.50 usec
PL1 1.60 dB
SFO1 500.2235015 MHz

F2 - Processing parameters
SI 65536
SF 500.2200301 MHz
WDW EM
SSB 0
LB 0.30 Hz
GB 0
PC 4.00

Z-restored spin-echo 13C spectrum with 1H decoupling

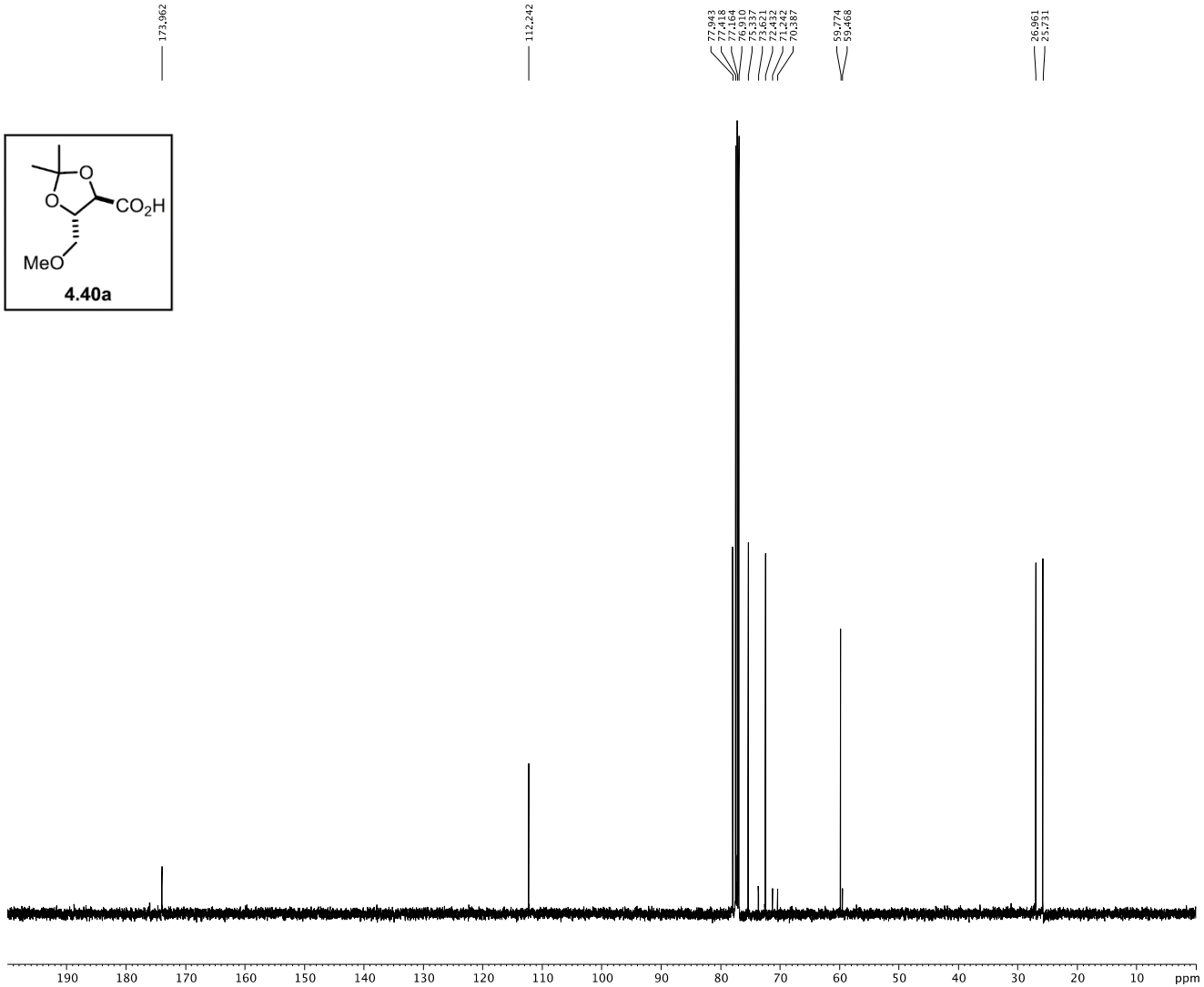

Current Data Parameters
NAME DJT-VI-160
EXPNO 2
PROCNO 1

F2 - Acquisition Parameters
Date_ 20160114
Time 8.20
INSTRUM cryo500
PROBHD 5 mm CPTCI 1H-
PULPROG SpinEchopg30gp.prd
TD 65536
SOLVENT CDCl3
NS 328
DS 0
SWH 30303.031 Hz
FIDRES 0.462388 Hz
AQ 1.0813440 sec
RG 4597.6
DW 16.500 usec
DE 6.00 usec
TE 298.0 K
D1 0.25000000 sec
d11 0.03000000 sec
D16 0.00020000 sec
d17 0.00019600 sec
MCREST 0 sec
MCWRK 0.01500000 sec
P2 33.10 usec

======== CHANNEL f1 ========
NUC1 13C
P1 16.55 usec
P11 500.00 usec
P12 2000.00 usec
PL0 120.00 dB
PL1 -1.00 dB
SFO1 125.7942548 MHz
SP1 2.70 dB
SP2 2.70 dB
SPNAM[1] Crp60,0.5,20.1
SPNAM[2] Crp60comp.4
SPOFF1 0 Hz
SPOFF2 0 Hz

======== CHANNEL f2 ========
CPDPRG[2 waltz16
NUC2 1H
PCPD2 100.00 usec
PL2 1.60 dB
PL12 24.50 dB
SFO2 500.2225011 MHz

====== GRADIENT CHANNEL =====
GPNAM[1] SINE.100
GPNAM[2] SINE.100
GPX1 0 %
GPX2 0 %
GPY1 0 %
GPY2 0 %
GPZ1 30.00 %
GPZ2 50.00 %
p15 500.00 usec
p16 1000.00 usec

F2 - Processing parameters
SI 65536
SF 125.7804076 MHz
WDW EM
SSB 0
LB 1.00 Hz
GB 0
PC 2.00

1H spectrum

4.40a (1.0 equiv) + **4.3** (1.1 equiv) → (37%) **4.41a** + **4.42a** (3.5 : 1)

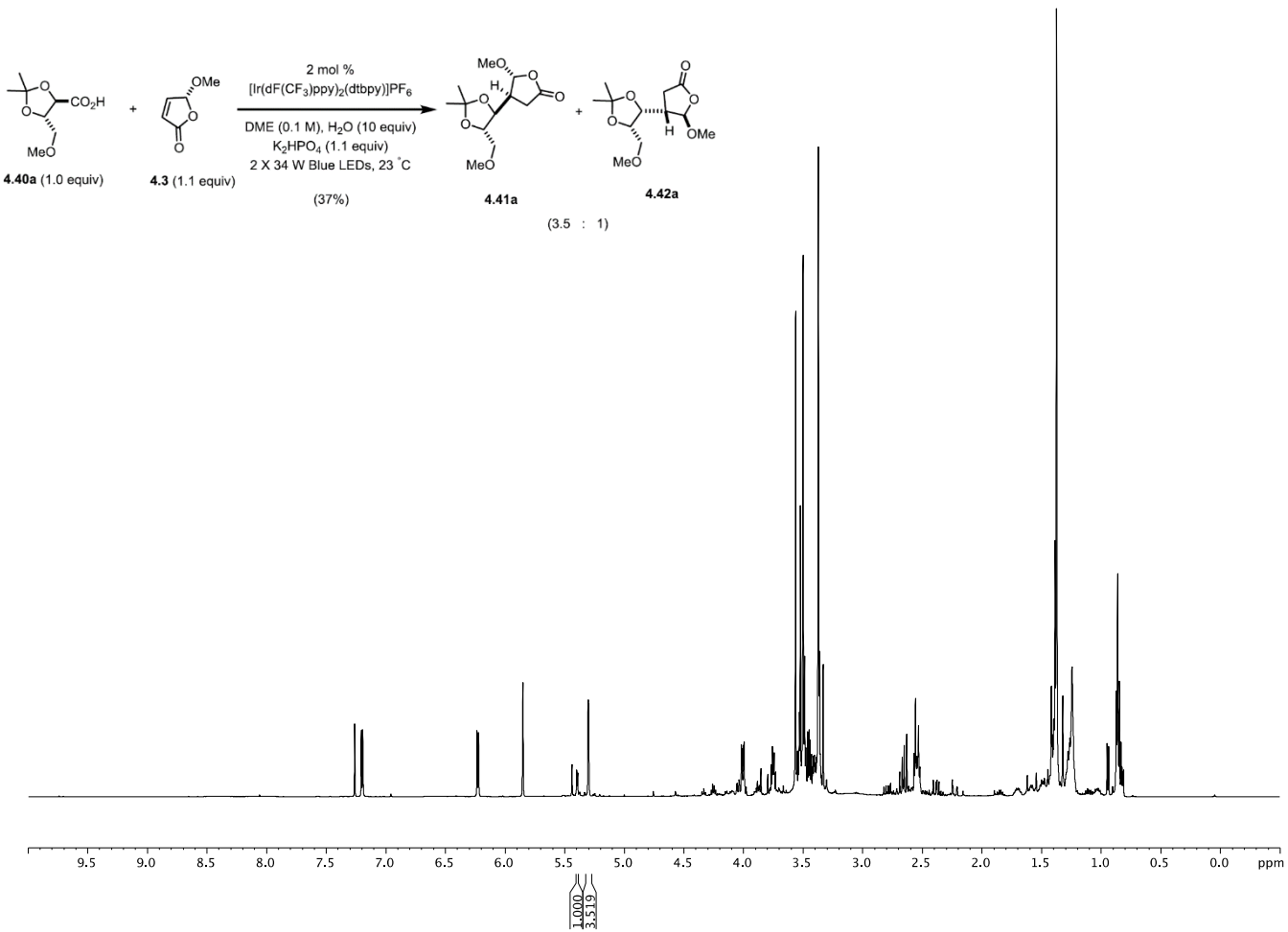

Current Data Parameters
NAME DJT-VI-162
EXPNO 1
PROCNO 1

F2 - Acquisition Parameters
Date_ 20160114
Time 8.07
INSTRUM cryo500
PROBHD 5 mm CPTCI 1H-
PULPROG zg30
TD 81728
SOLVENT CDCl3
NS 20
DS 0
SWH 8012.820 Hz
FIDRES 0.098043 Hz
AQ 5.0998273 sec
RG 5.7
DW 62.400 usec
DE 6.00 usec
TE 298.0 K
D1 0.10000000 sec
MCREST 0 sec
MCWRK 0.01500000 sec

======== CHANNEL f1 =====
NUC1 1H
P1 7.50 usec
PL1 1.60 dB
SFO1 500.2235015 MHz

F2 - Processing parameters
SI 65536
SF 500.2200299 MHz
WDW EM
SSB 0
LB 0.30 Hz
GB 0
PC 4.00

1H spectrum

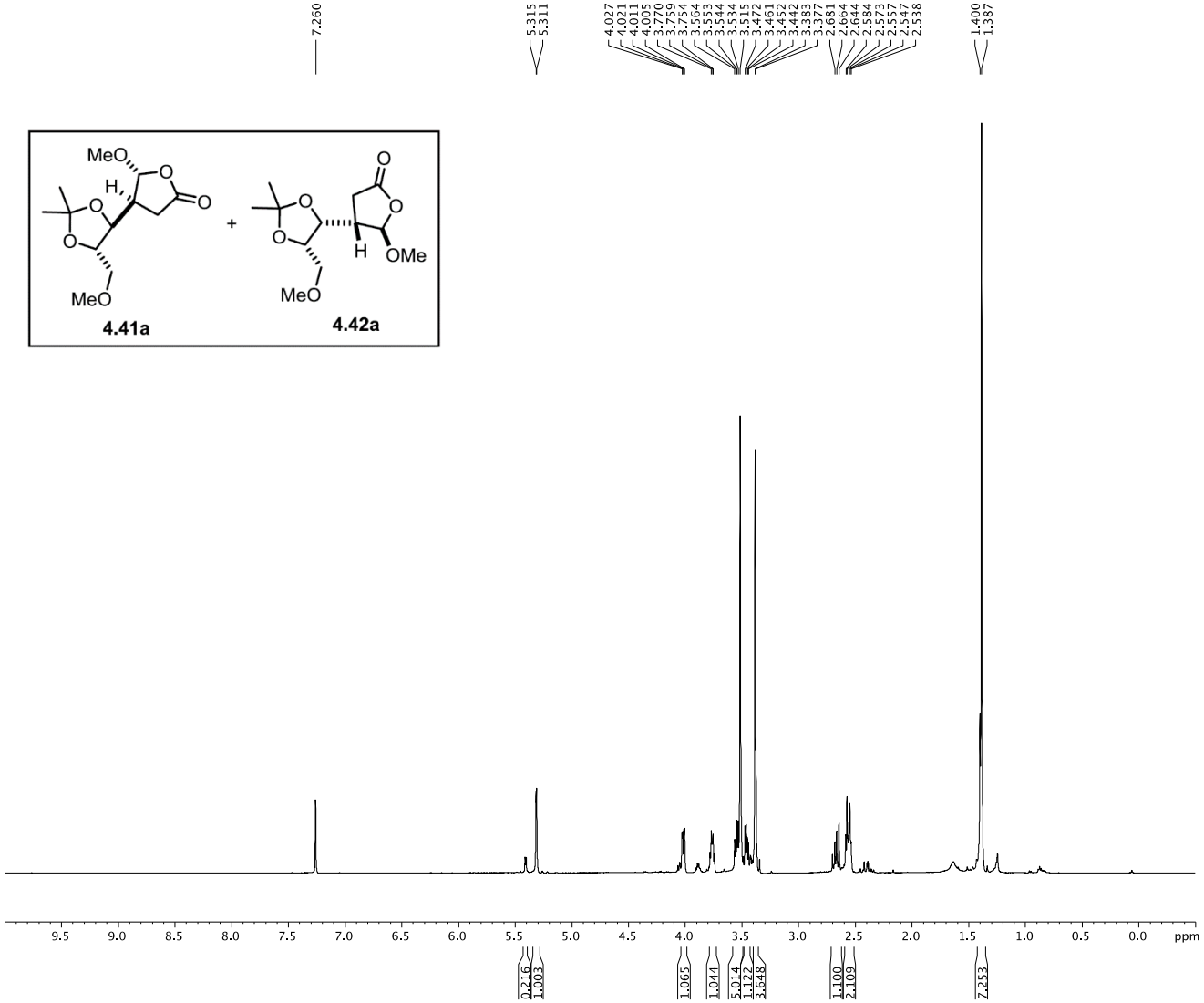

Current Data Parameters
NAME DJT-VI-162
EXPNO 5
PROCNO 1

F2 - Acquisition Parameters
Date_ 20160115
Time 9.03
INSTRUM cryo500
PROBHD 5 mm CPTCI 1H-
PULPROG zg30
TD 81728
SOLVENT CDCl3
NS 20
DS 0
SWH 8012.820 Hz
FIDRES 0.098043 Hz
AQ 5.0998273 sec
RG 6.3
DW 62.400 usec
DE 6.00 usec
TE 298.0 K
D1 0.10000000 sec
MCREST 0 sec
MCWRK 0.01500000 sec

======== CHANNEL f1 =====
NUC1 1H
P1 7.50 usec
PL1 1.60 dB
SFO1 500.2235015 MHz

F2 - Processing parameters
SI 65536
SF 500.2200301 MHz
WDW EM
SSB 0
LB 0.30 Hz
GB 0
PC 4.00

Z-restored spin-echo 13C spectrum with 1H decoupling

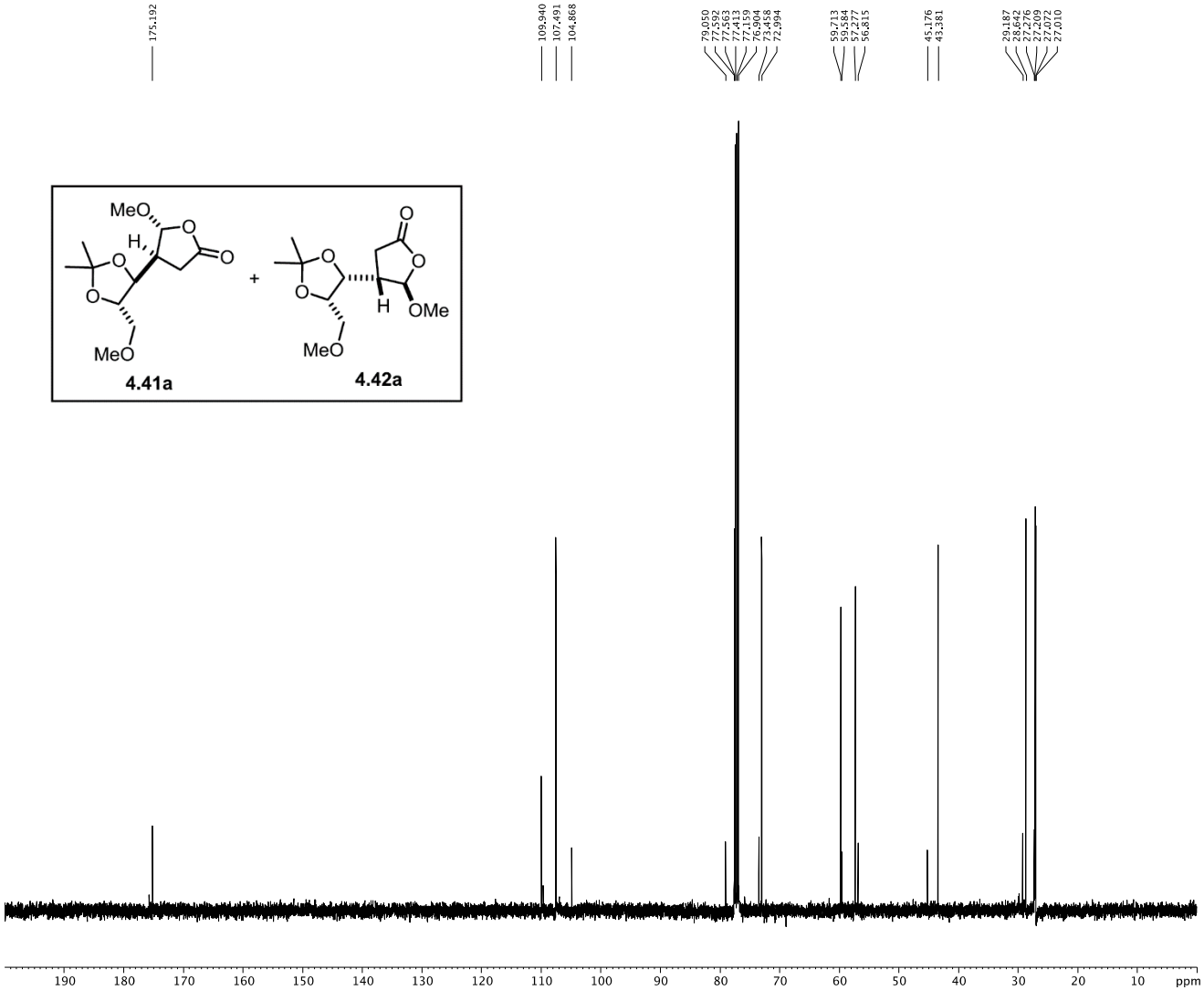

Current Data Parameters
NAME DJT-VI-162
EXPNO 6
PROCNO 1

F2 - Acquisition Parameters
Date_ 20160115
Time 9.08
INSTRUM cryo500
PROBHD 5 mm CPTCI 1H-
PULPROG SpinEchopg30gp.prd
TD 65536
SOLVENT CDCl3
NS 314
DS 0
SWH 30303.031 Hz
FIDRES 0.462388 Hz
AQ 1.0813440 sec
RG 7298.2
DW 16.500 usec
DE 6.00 usec
TE 298.0 K
D1 0.25000000 sec
d11 0.03000000 sec
D16 0.00020000 sec
d17 0.00019600 sec
MCREST 0 sec
MCWRK 0.01500000 sec
P2 33.10 usec

======== CHANNEL f1 ========
NUC1 13C
P1 16.55 usec
P11 500.00 usec
P12 2000.00 usec
PL0 120.00 dB
PL1 -1.00 dB
SFO1 125.7942548 MHz
SP1 2.70 dB
SP2 2.70 dB
SPNAM[1] Crp60,0.5,20.1
SPNAM[2] Crp60comp.4
SPOFF1 0 Hz
SPOFF2 0 Hz

======== CHANNEL f2 ========
CPDPRG[2 waltz16
NUC2 1H
PCPD2 100.00 usec
PL2 1.60 dB
PL12 24.50 dB
SFO2 500.2225011 MHz

====== GRADIENT CHANNEL =====
GPNAM[1] SINE.100
GPNAM[2] SINE.100
GPX1 0 %
GPX2 0 %
GPY1 0 %
GPY2 0 %
GPZ1 30.00 %
GPZ2 50.00 %
p15 500.00 usec
p16 1000.00 usec

F2 - Processing parameters
SI 65536
SF 125.7804085 MHz
WDW EM
SSB 0
LB 1.00 Hz
GB 0
PC 2.00

1H spectrum

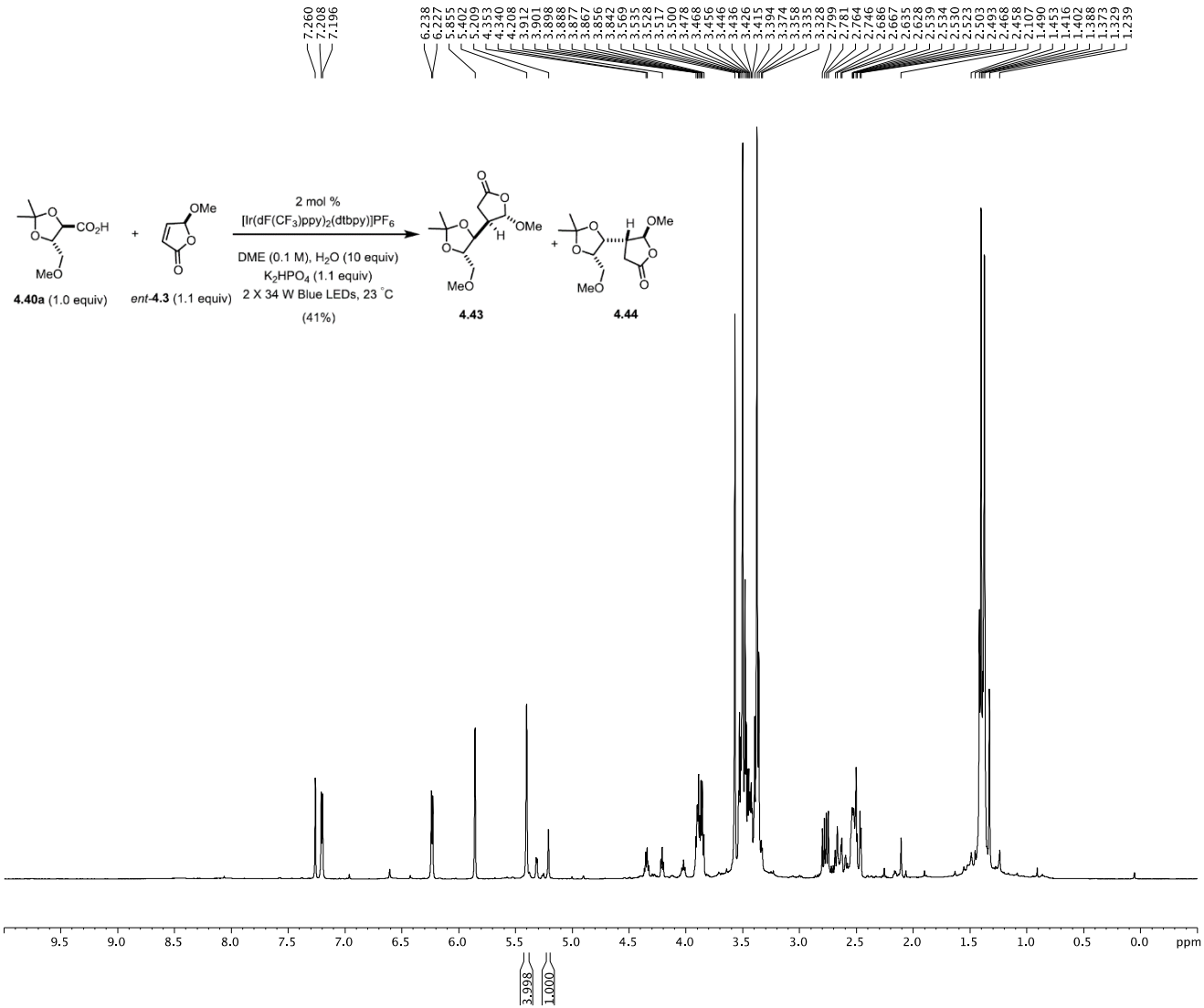

Current Data Parameters
NAME DJT-VI-184
EXPNO 1
PROCNO 1

F2 - Acquisition Parameters
Date_ 20160201
Time 8.08
INSTRUM cryo500
PROBHD 5 mm CPTCI 1H-
PULPROG zg30
TD 81728
SOLVENT CDCl3
NS 20
DS 0
SWH 8012.820 Hz
FIDRES 0.098043 Hz
AQ 5.0998273 sec
RG 7.1
DW 62.400 usec
DE 6.00 usec
TE 298.0 K
D1 0.10000000 sec
MCREST 0 sec
MCWRK 0.01500000 sec

======== CHANNEL f1 =====
NUC1 1H
P1 7.50 usec
PL1 1.60 dB
SFO1 500.2235015 MHz

F2 - Processing parameters
SI 65536
SF 500.2200322 MHz
WDW EM
SSB 0
LB 0.30 Hz
GB 0
PC 4.00

1H spectrum

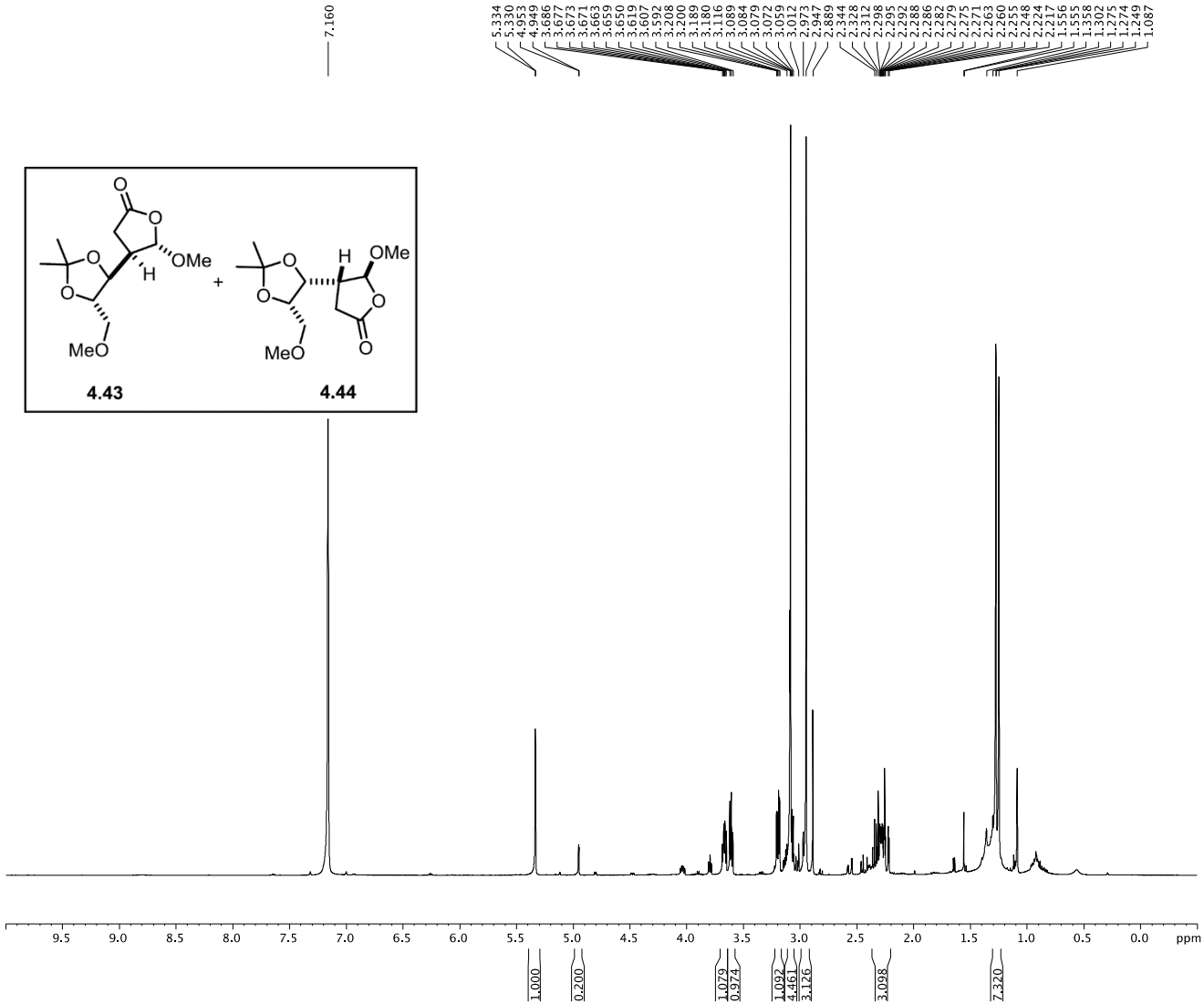

Current Data Parameters
NAME DJT-VI-184
EXPNO 6
PROCNO 1

F2 - Acquisition Parameters
Date_ 20160202
Time 9.16
INSTRUM cryo500
PROBHD 5 mm CPTCI 1H-
PULPROG zg30
TD 81728
SOLVENT CDCl3
NS 20
DS 0
SWH 8012.820 Hz
FIDRES 0.098043 Hz
AQ 5.0998273 sec
RG 4.5
DW 62.400 usec
DE 6.00 usec
TE 298.0 K
D1 0.10000000 sec
MCREST 0 sec
MCWRK 0.01500000 sec

======== CHANNEL f1 =====
NUC1 1H
P1 7.50 usec
PL1 1.60 dB
SFO1 500.2235015 MHz

F2 - Processing parameters
SI 65536
SF 500.2200007 MHz
WDW EM
SSB 0
LB 0.30 Hz
GB 0
PC 4.00

Z-restored spin-echo 13C spectrum with 1H decoupling

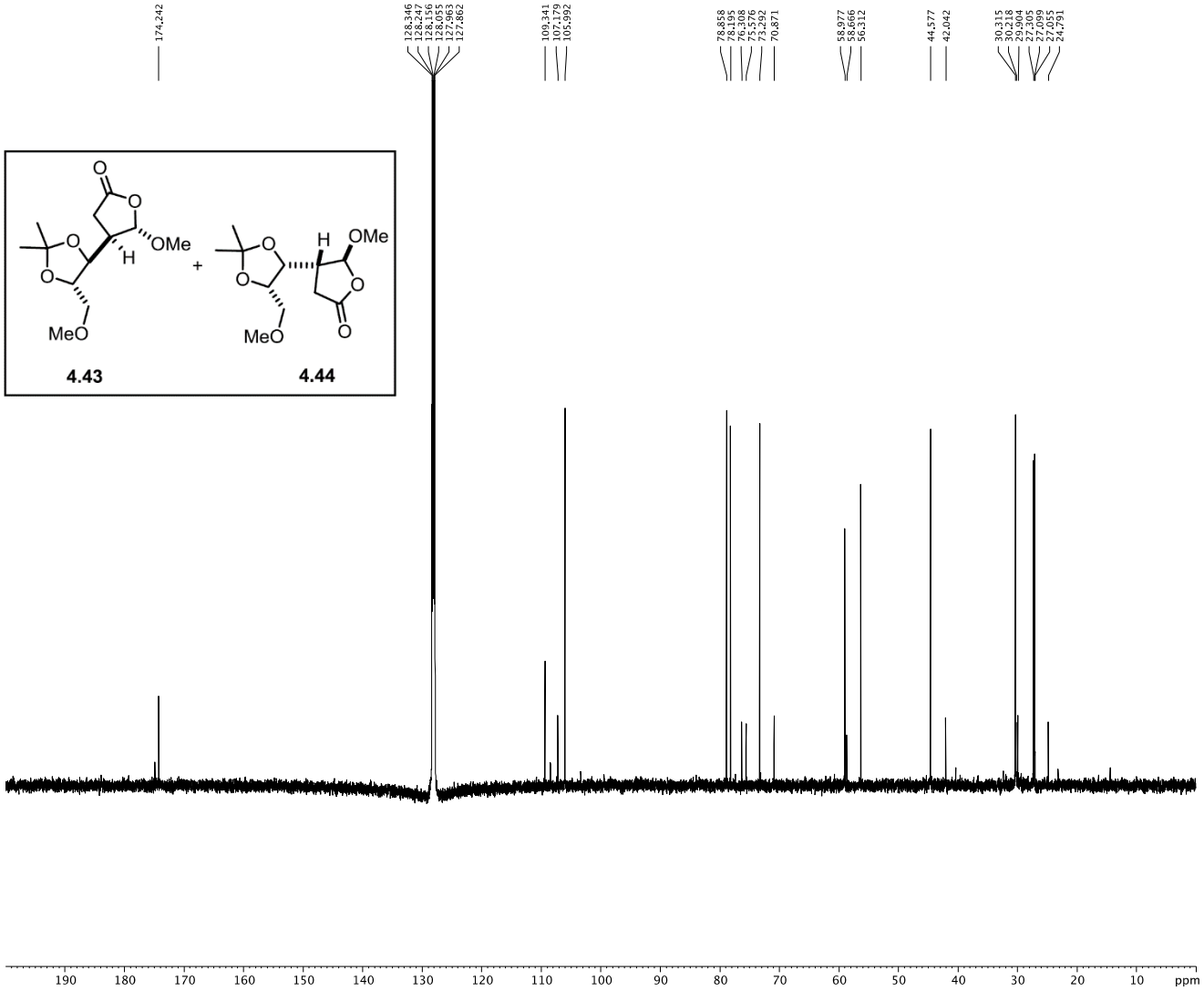


```
Current Data Parameters
NAME        DJT-VI-184
EXPNO              8
PROCNO             1

F2 - Acquisition Parameters
Date_        20160202
Time            9.32
INSTRUM        cryo500
PROBHD   5 mm CPTCI 1H-
PULPROG  SpinEchopg30gp.prd
TD             65536
SOLVENT         CDCl3
NS               401
DS                 0
SWH         30303.031 Hz
FIDRES       0.462388 Hz
AQ          1.0813440 sec
RG               4096
DW            16.500 usec
DE             6.00 usec
TE            298.0 K
D1          0.25000000 sec
d11         0.03000000 sec
D16         0.00020000 sec
d17         0.00019600 sec
MCREST   0 sec
MCWRK       0.01500000 sec
P2            33.10 usec

======== CHANNEL f1 ========
NUC1            13C
P1            16.55 usec
P11          500.00 usec
P12         2000.00 usec
PL0          120.00 dB
PL1           -1.00 dB
SFO1        125.7942548 MHz
SP1            2.70 dB
SP2            2.70 dB
SPNAM[1] Crp60,0.5,20.1
SPNAM[2]   Crp60comp.4
SPOFF1   0 Hz
SPOFF2   0 Hz

======== CHANNEL f2 ========
CPDPRG[2        waltz16
NUC2             1H
PCPD2          100.00 usec
PL2            1.60 dB
PL12          24.50 dB
SFO2        500.2225011 MHz

====== GRADIENT CHANNEL =====
GPNAM[1]        SINE.100
GPNAM[2]        SINE.100
GPX1     0 %
GPX2     0 %
GPY1     0 %
GPY2     0 %
GPZ1           30.00 %
GPZ2           50.00 %
p15           500.00 usec
p16          1000.00 usec

F2 - Processing parameters
SI             65536
SF        125.7803755 MHz
WDW              EM
SSB     0
LB            1.00 Hz
GB      0
PC            2.00
```

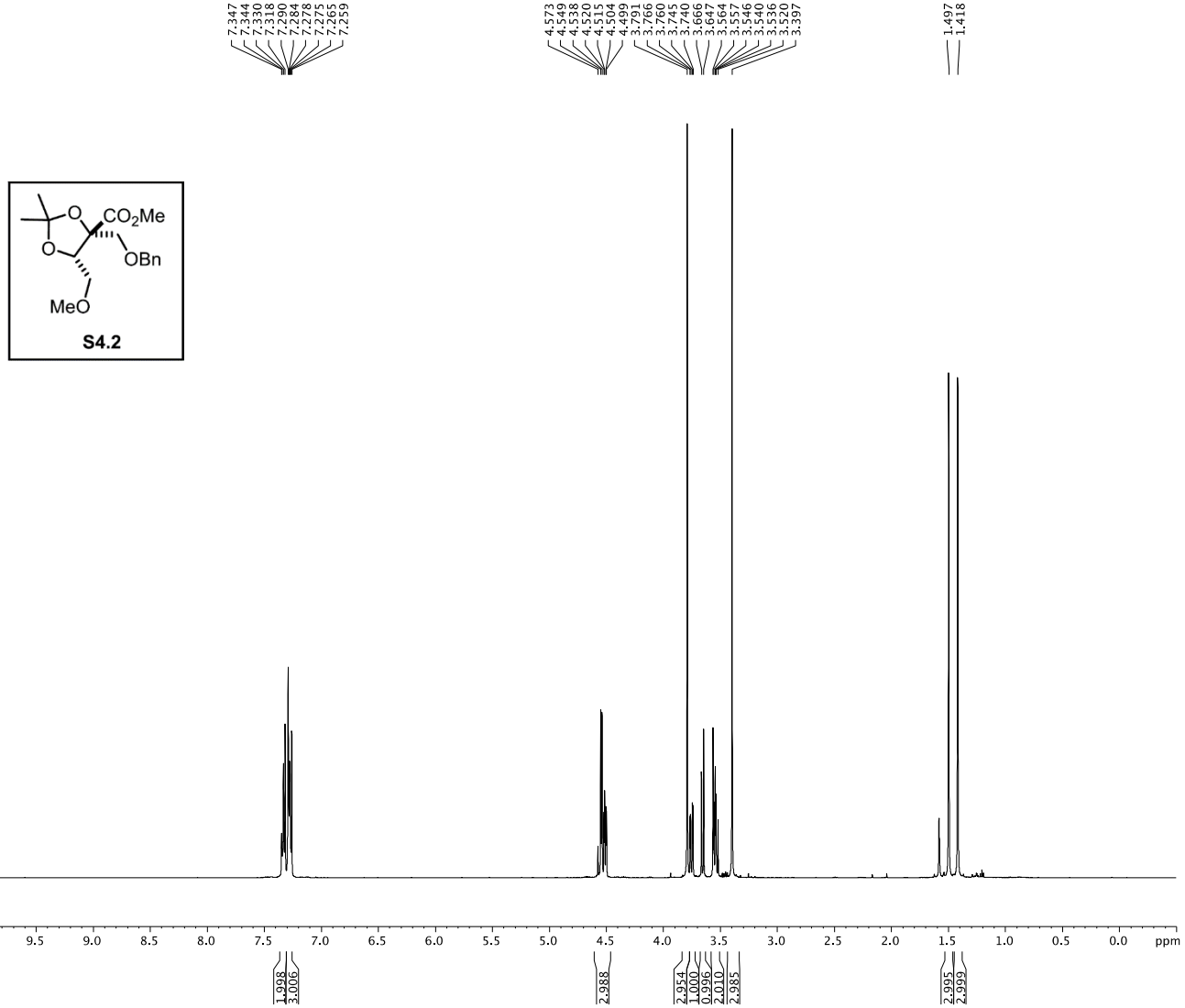


```
Current Data Parameters
NAME          YS-IV-39
EXPNO              2
PROCNO             1

F2 - Acquisition Parameters
Date_        20160114
Time             9.08
INSTRUM        cryo500
PROBHD   5 mm CPTCI 1H-
PULPROG          zg30
TD              81728
SOLVENT         CDCl3
NS                 8
DS                 2
SWH          8012.820 Hz
FIDRES       0.098043 Hz
AQ          5.0998273 sec
RG                 6.3
DW              62.400 usec
DE               6.00 usec
TE              298.0 K
D1          0.10000000 sec
MCREST   0 sec
MCWRK       0.01500000 sec

======== CHANNEL f1 ========
NUC1               1H
P1              7.50 usec
PL1             1.60 dB
SFO1       500.2235015 MHz

F2 - Processing parameters
SI             65536
SF        500.2200309 MHz
WDW              EM
SSB      0
LB              0.30 Hz
GB       0
PC               4.00
```

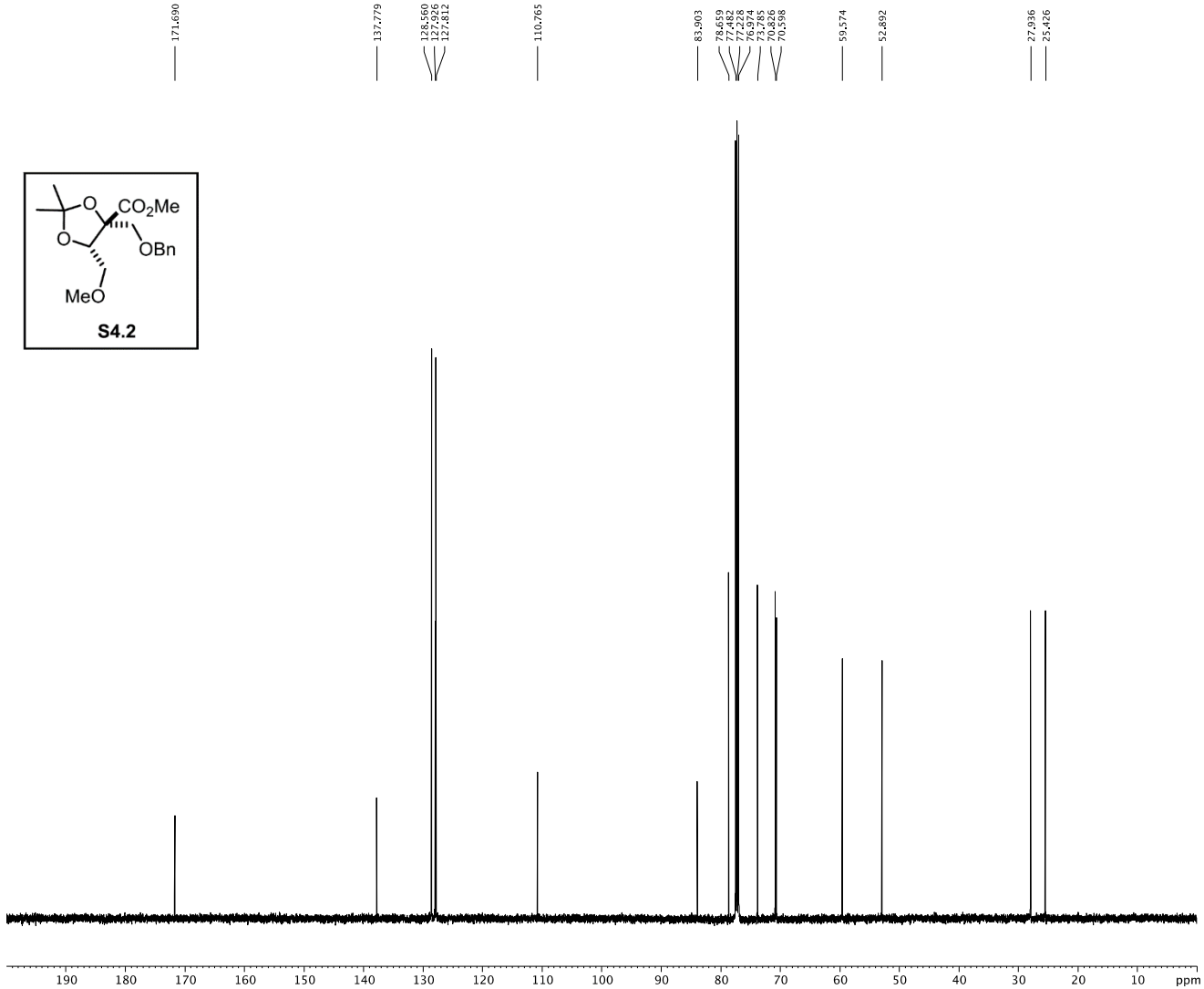


```
Current Data Parameters
NAME          YS-IV-39
EXPNO            3
PROCNO           1

F2 - Acquisition Parameters
Date_       20160114
Time           9.13
INSTRUM      cryo500
PROBHD   5 mm CPTC 1H-
PULPROG  SpinEchopg30gp.prd
TD          65536
SOLVENT       CDCl3
NS             568
DS               2
SWH        30303.031 Hz
FIDRES      0.462388 Hz
AQ         1.0813440 sec
RG          4597.6
DW          16.500 usec
DE           6.00 usec
TE          298.0 K
D1         0.25000000 sec
d11        0.03000000 sec
D16        0.00020000 sec
d17        0.00019600 sec
MCREST   0 sec
MCWRK      0.01500000 sec
P2          33.10 usec

======== CHANNEL f1 ========
NUC1            13C
P1            16.55 usec
P11          500.00 usec
P12         2000.00 usec
PL0          120.00 dB
PL1          -1.00 dB
SFO1      125.7942548 MHz
SP1           2.70 dB
SP2           2.70 dB
SPNAM[1] Crp60,0.5,20.1
SPNAM[2]   Crp60comp.4
SPOFF1   0 Hz
SPOFF2   0 Hz

======== CHANNEL f2 ========
CPDPRG[2       waltz16
NUC2             1H
PCPD2         100.00 usec
PL2           1.60 dB
PL12         24.50 dB
SFO2      500.2225011 MHz

====== GRADIENT CHANNEL =====
GPNAM[1]       SINE.100
GPNAM[2]       SINE.100
GPX1     0 %
GPX2     0 %
GPY1     0 %
GPY2     0 %
GPZ1          30.00 %
GPZ2          50.00 %
p15          500.00 usec
p16         1000.00 usec

F2 - Processing parameters
SI          65536
SF      125.7804000 MHz
WDW            EM
SSB     0
LB          1.00 Hz
GB      0
PC          2.00
```

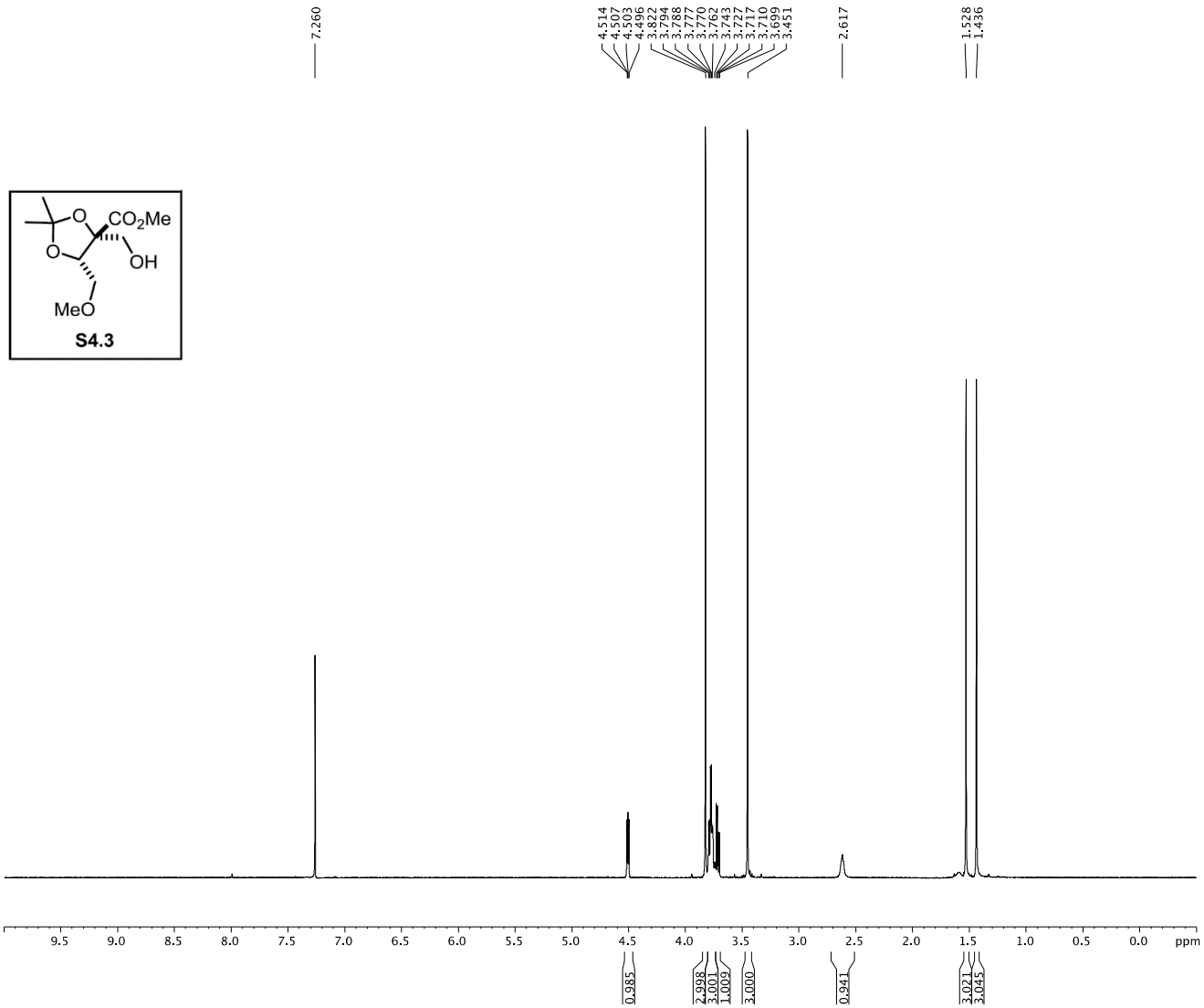

Current Data Parameters
NAME YS-IV-41
EXPNO 1
PROCNO 1

F2 - Acquisition Parameters
Date_ 20160116
Time 10.21
INSTRUM av600
PROBHD 5 mm TBI 1H/13
PULPROG zg30
TD 98074
SOLVENT CDCl3
NS 8
DS 2
SWH 9615.385 Hz
FIDRES 0.098042 Hz
AQ 5.0998478 sec
RG 1440
DW 52.000 usec
DE 14.54 usec
TE 293.1 K
D1 0.10000000 sec
TD0 1

======== CHANNEL f1 ========
SFO1 600.1342009 MHz
NUC1 1H
P1 8.00 usec
PLW1 24.00000000 W

F2 - Processing parameters
SI 65536
SF 600.1300354 MHz
WDW EM
SSB 0
LB 0.30 Hz
GB 0
PC 1.00

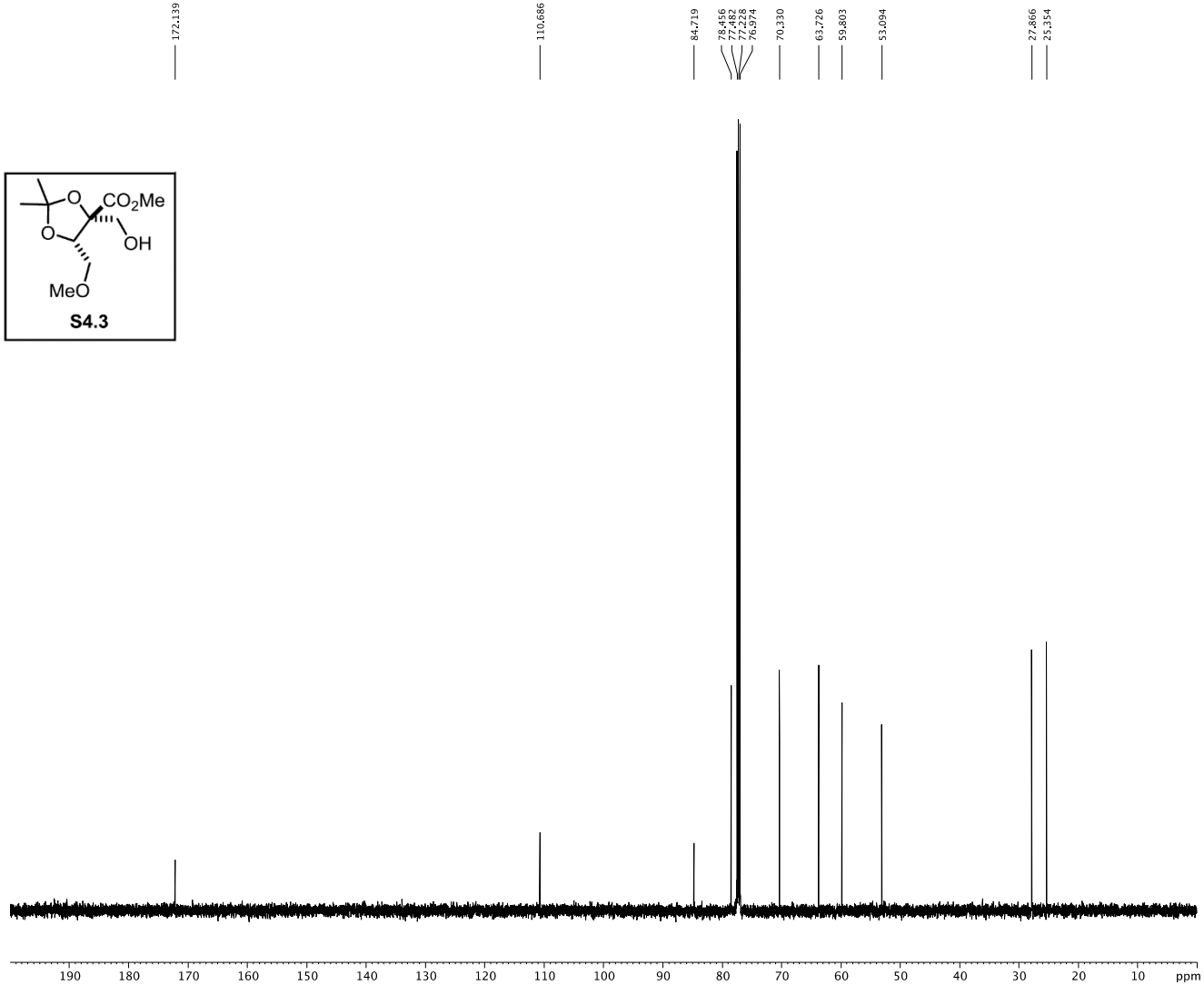


```
Current Data Parameters
NAME          YS-IV-41
EXPNO              2
PROCNO             1

F2 - Acquisition Parameters
Date_        20160116
Time           10.28
INSTRUM        cryo500
PROBHD   5 mm CPTCI 1H-
PULPROG  SpinEchopg30gp.prd
TD             65536
SOLVENT        CDCl3
NS               500
DS                 2
SWH          30303.031 Hz
FIDRES        0.462388 Hz
AQ          1.0813440 sec
RC            7298.2
DW             16.500 usec
DE              6.00 usec
TE             298.0 K
D1          0.25000000 sec
d11         0.03000000 sec
D16         0.00020000 sec
d17         0.00019600 sec
MCREST   0 sec
MCWRK       0.01500000 sec
P2             33.10 usec

======== CHANNEL f1 ========
NUC1             13C
P1             16.55 usec
P11           500.00 usec
P12          2000.00 usec
PL0           120.00 dB
PL1           -1.00 dB
SFO1       125.7942548 MHz
SP1             2.70 dB
SP2             2.70 dB
SPNAM[1] Crp60,0.5,20.1
SPNAM[2]   Crp60comp.4
SPOFF1   0 Hz
SPOFF2   0 Hz

======== CHANNEL f2 ========
CPDPRG[2        waltz16
NUC2              1H
PCPD2           100.00 usec
PL2             1.60 dB
PL12            24.50 dB
SFO2       500.2225011 MHz

====== GRADIENT CHANNEL =====
GPNAM[1]        SINE.100
GPNAM[2]        SINE.100
GPX1     0 %
GPX2     0 %
GPY1     0 %
GPY2     0 %
GPZ1            30.00 %
GPZ2            50.00 %
p15            500.00 usec
p16           1000.00 usec

F2 - Processing parameters
SI              65536
SF         125.7803988 MHz
WDW               EM
SSB      0
LB            1.00 Hz
GB       0
PC            2.00
```

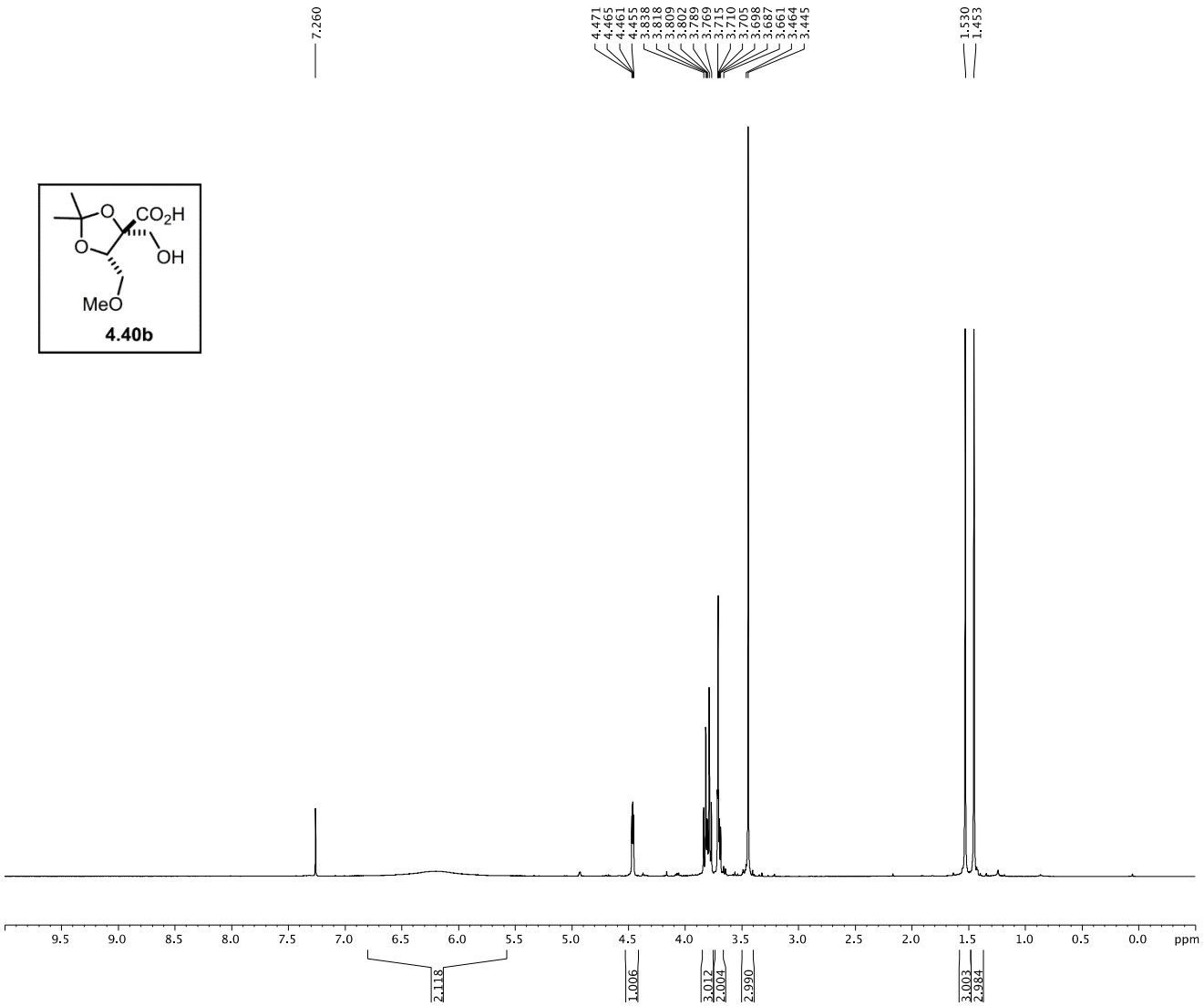

Current Data Parameters
NAME YS-IV-43
EXPNO 1
PROCNO 1

F2 - Acquisition Parameters
Date_ 20160119
Time 15.44
INSTRUM av600
PROBHD 5 mm TBI 1H/13
PULPROG zg30
TD 98074
SOLVENT CDCl3
NS 8
DS 2
SWH 9615.385 Hz
FIDRES 0.098042 Hz
AQ 5.0998478 sec
RG 322
DW 52.000 usec
DE 14.54 usec
TE 298.1 K
D1 0.10000000 sec
TD0 1

======== CHANNEL f1 ========
SFO1 600.1342009 MHz
NUC1 1H
P1 8.00 usec
PLW1 24.00000000 W

F2 - Processing parameters
SI 65536
SF 600.1300352 MHz
WDW EM
SSB 0
LB 0.30 Hz
GB 0
PC 1.00

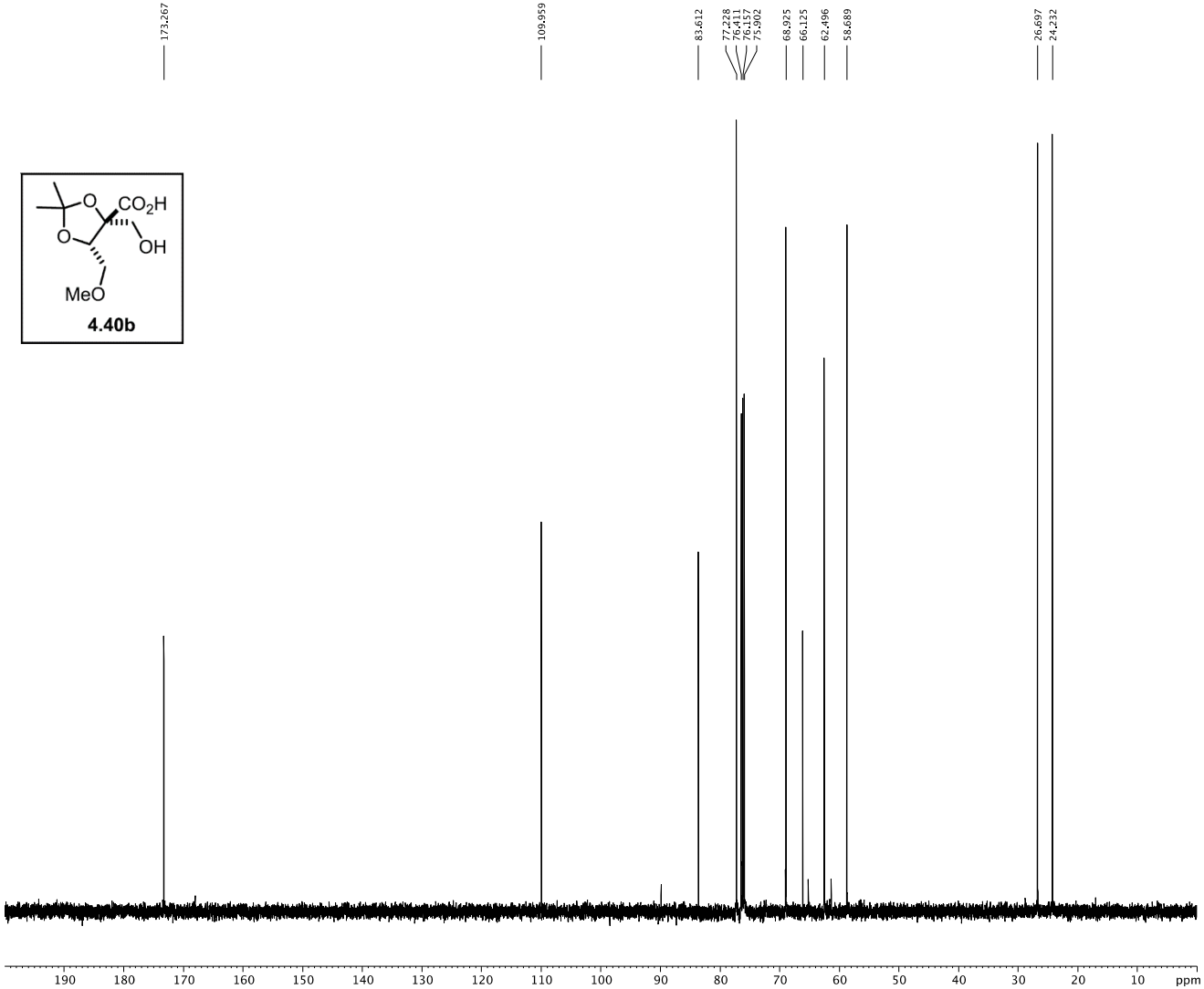

Current Data Parameters
NAME YS-IV-43
EXPNO 3
PROCNO 1

F2 - Acquisition Parameters
Date_ 20160119
Time 16.58
INSTRUM cryo500
PROBHD 5 mm CPTCl 1H-
PULPROG SpinEchopg30gp.prd
TD 65536
SOLVENT CDCl3
NS 168
DS 2
SWH 30303.031 Hz
FIDRES 0.462388 Hz
AQ 1.0813440 sec
RG 3251
DW 16.500 usec
DE 6.00 usec
TE 298.0 K
D1 0.25000000 sec
d11 0.03000000 sec
D16 0.00020000 sec
d17 0.00019600 sec
MCREST 0 sec
MCWRK 0.01500000 sec
P2 33.10 usec

======== CHANNEL f1 ========
NUC1 13C
P1 16.55 usec
P11 500.00 usec
P12 2000.00 usec
PL0 120.00 dB
PL1 -1.00 dB
SFO1 125.7942548 MHz
SP1 2.70 dB
SP2 2.70 dB
SPNAM[1] Crp60,0.5,20.1
SPNAM[2] Crp60comp.4
SPOFF1 0 Hz
SPOFF2 0 Hz

======== CHANNEL f2 ========
CPDPRG[2 waltz16
NUC2 1H
PCPD2 100.00 usec
PL2 1.60 dB
PL12 24.50 dB
SFO2 500.2225011 MHz

====== GRADIENT CHANNEL =====
GPNAM[1] SINE.100
GPNAM[2] SINE.100
GPX1 0 %
GPX2 0 %
GPY1 0 %
GPY2 0 %
GPZ1 30.00 %
GPZ2 50.00 %
p15 500.00 usec
p16 1000.00 usec

F2 - Processing parameters
SI 65536
SF 125.7805370 MHz
WDW EM
SSB 0
LB 1.00 Hz
GB 0
PC 2.00

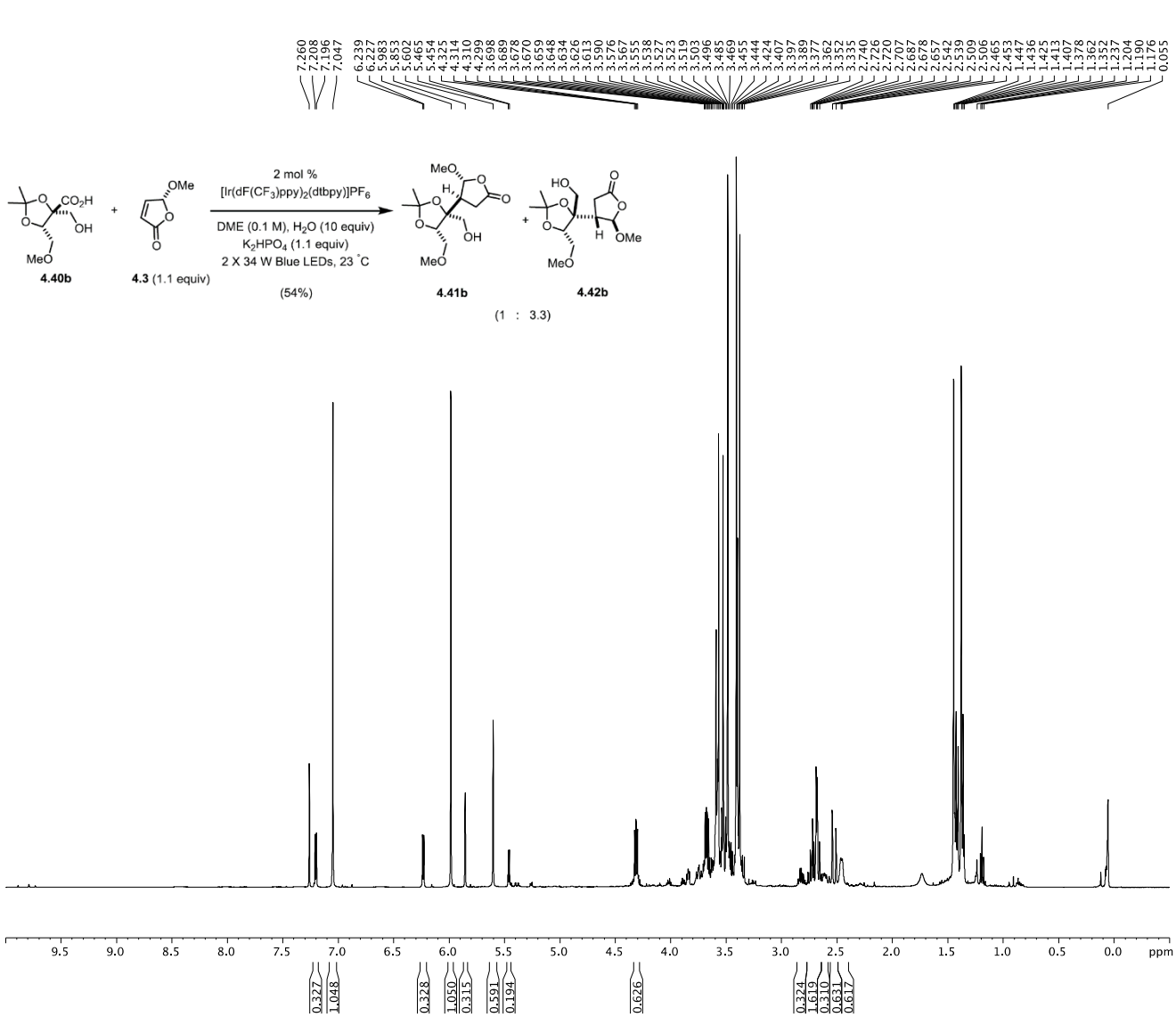

Current Data Parameters
NAME YS-IV-51
EXPNO 1
PROCNO 1

F2 - Acquisition Parameters
Date_ 20160121
Time 10.14
INSTRUM cryo500
PROBHD 5 mm CPTCI 1H-
PULPROG zg30
TD 81728
SOLVENT CDCl3
NS 8
DS 2
SWH 8012.820 Hz
FIDRES 0.098043 Hz
AQ 5.0998273 sec
RG 8
DW 62.400 usec
DE 6.00 usec
TE 298.0 K
D1 0.10000000 sec
MCREST 0 sec
MCWRK 0.01500000 sec

======== CHANNEL f1 ========
NUC1 1H
P1 7.50 usec
PL1 1.60 dB
SFO1 500.2235015 MHz

F2 - Processing parameters
SI 65536
SF 500.2200312 MHz
WDW EM
SSB 0
LB 0.30 Hz
GB 0
PC 4.00

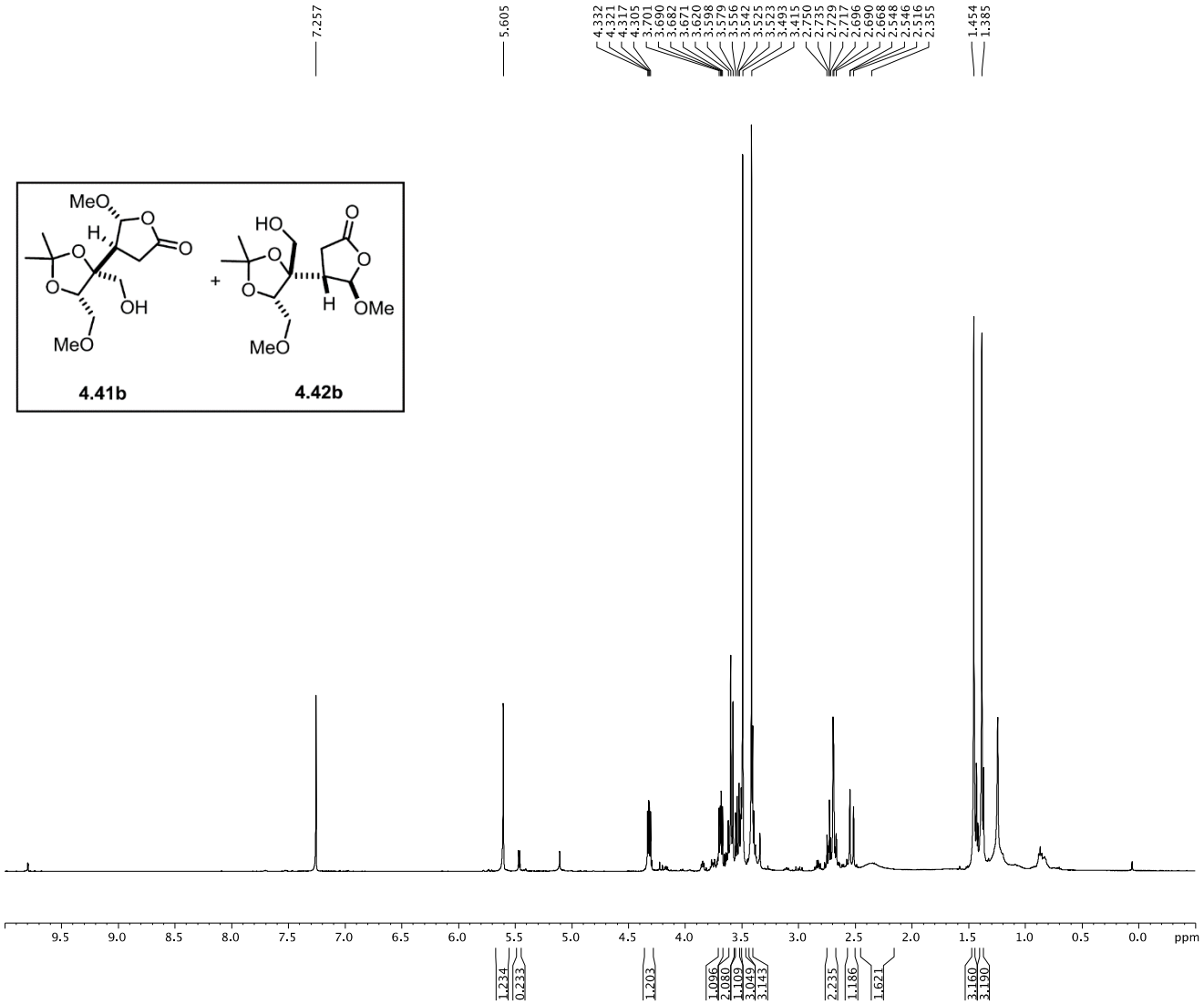

Current Data Parameters
NAME YS-IV-51
EXPNO 11
PROCNO 1

F2 - Acquisition Parameters
Date_ 20160202
Time 8.41
INSTRUM cryo500
PROBHD 5 mm CPTCI 1H-
PULPROG zg30
TD 81728
SOLVENT CDCl3
NS 8
DS 2
SWH 8012.820 Hz
FIDRES 0.098043 Hz
AQ 5.0998273 sec
RG 5.7
DW 62.400 usec
DE 6.00 usec
TE 298.0 K
D1 0.10000000 sec
MCREST 0 sec
MCWRK 0.01500000 sec

======== CHANNEL f1 ========
NUC1 1H
P1 7.50 usec
PL1 1.60 dB
SFO1 500.2235015 MHz

F2 - Processing parameters
SI 65536
SF 500.2200339 MHz
WDW EM
SSB 0
LB 0.30 Hz
GB 0
PC 4.00

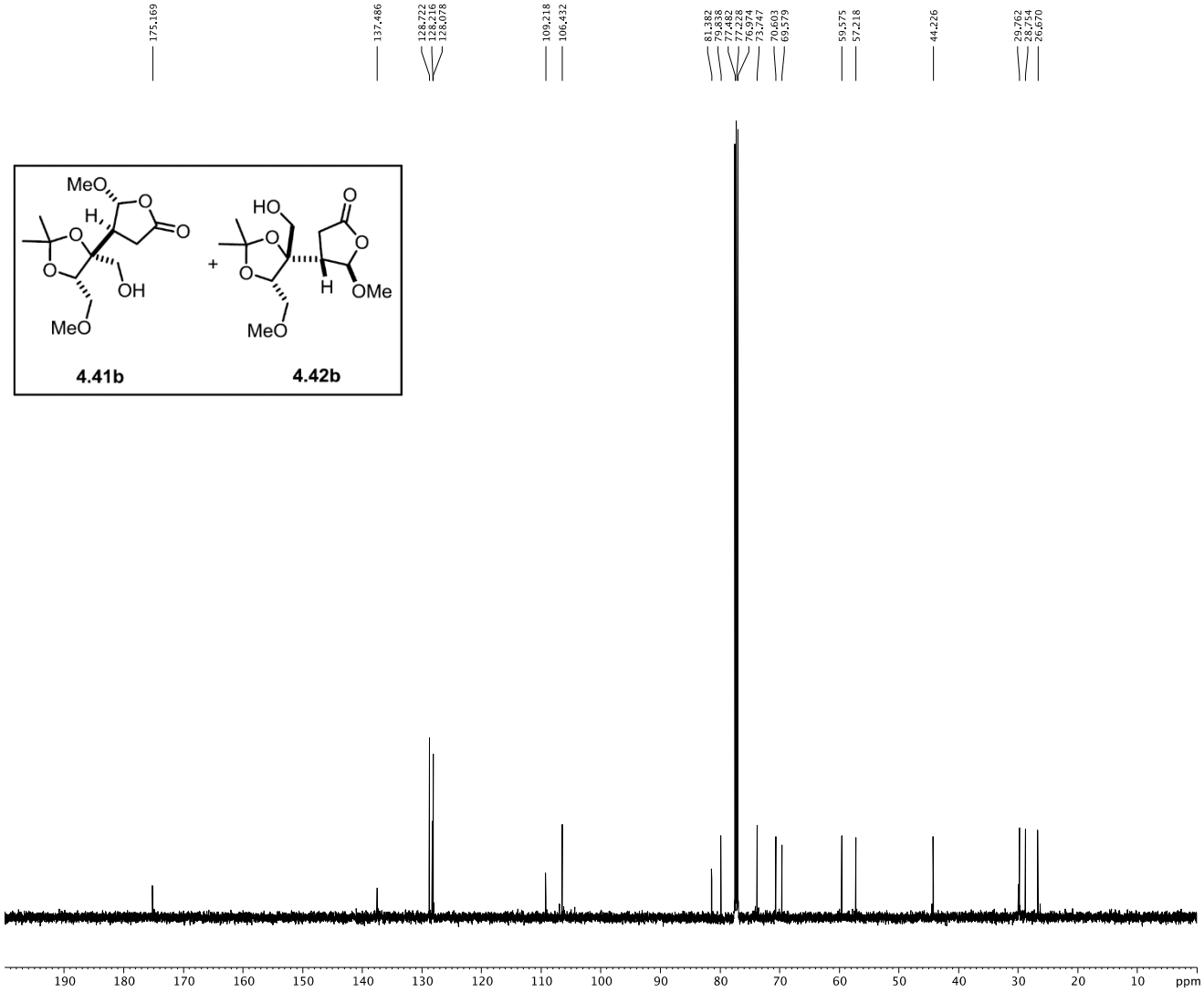

Current Data Parameters
NAME YS-IV-61
EXPNO 8
PROCNO 1

F2 - Acquisition Parameters
Date_ 20160127
Time 17.26
INSTRUM cryo500
PROBHD 5 mm CPTCI 1H-
PULPROG SpinEchopg30gp.prd
TD 65536
SOLVENT CDCl3
NS 584
DS 1
SWH 30303.031 Hz
FIDRES 0.462388 Hz
AQ 1.0813440 sec
RG 5160.6
DW 16.500 usec
DE 6.00 usec
TE 298.0 K
D1 0.25000000 sec
d11 0.03000000 sec
D16 0.00020000 sec
d17 0.00019600 sec
MCREST 0 sec
MCWRK 0.01500000 sec
P2 33.10 usec

======== CHANNEL f1 ========
NUC1 13C
P1 16.55 usec
P11 500.00 usec
P12 2000.00 usec
PL0 120.00 dB
PL1 -1.00 dB
SFO1 125.7942548 MHz
SP1 2.70 dB
SP2 2.70 dB
SPNAM[1] Crp60,0.5,20.1
SPNAM[2] Crp60comp.4
SPOFF1 0 Hz
SPOFF2 0 Hz

======== CHANNEL f2 ========
CPDPRG[2 waltz16
NUC2 1H
PCPD2 100.00 usec
PL2 1.60 dB
PL12 24.50 dB
SFO2 500.2225011 MHz

====== GRADIENT CHANNEL =====
GPNAM[1] SINE.100
GPNAM[2] SINE.100
GPX1 0 %
GPX2 0 %
GPY1 0 %
GPY2 0 %
GPZ1 30.00 %
GPZ2 50.00 %
p15 500.00 usec
p16 1000.00 usec

F2 - Processing parameters
SI 65536
SF 125.7803987 MHz
WDW EM
SSB 0
LB 1.00 Hz
GB 0
PC 2.00

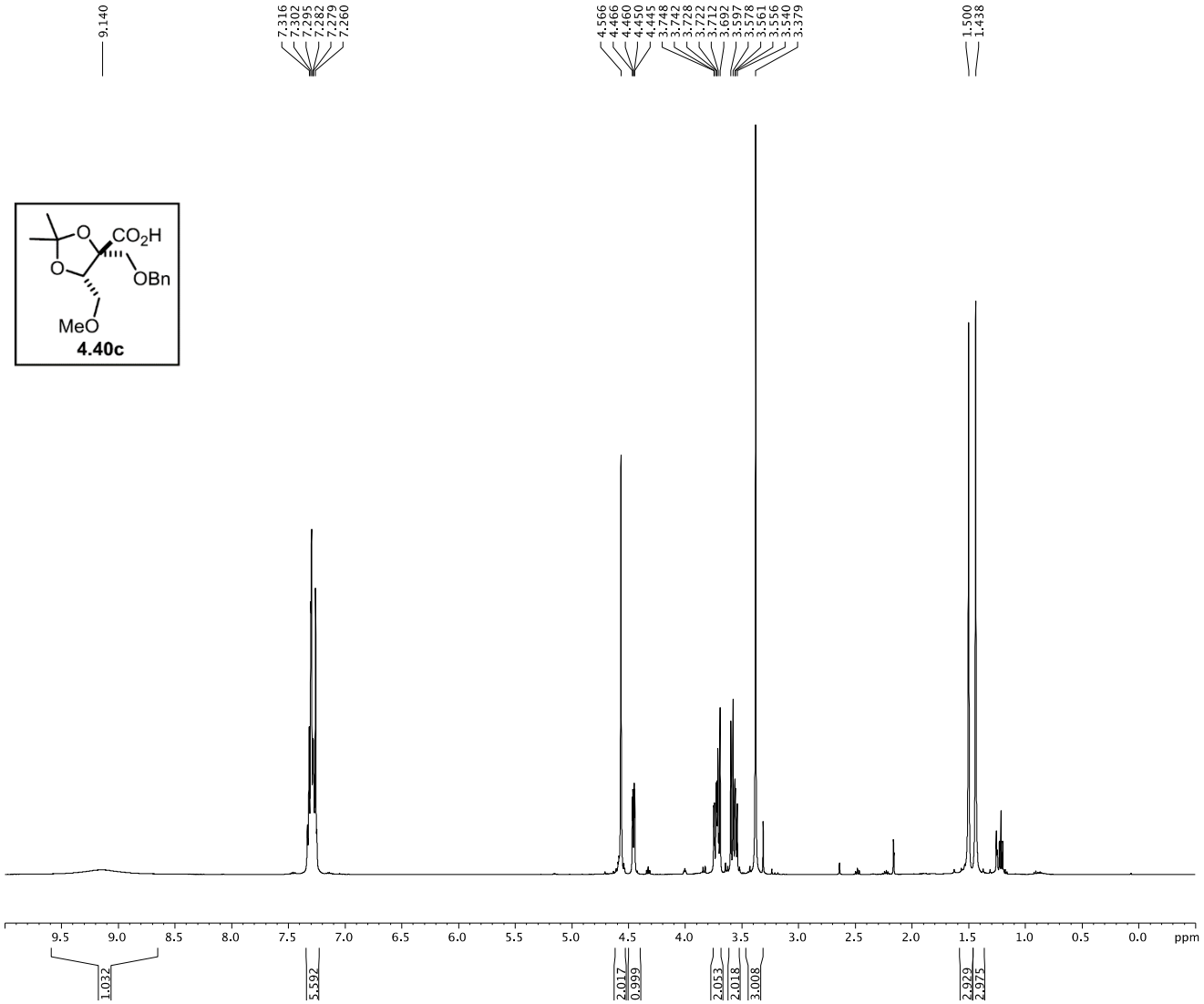

Current Data Parameters
NAME YS-IV-58
EXPNO 2
PROCNO 1

F2 - Acquisition Parameters
Date_ 20160126
Time 17.13
INSTRUM cryo500
PROBHD 5 mm CPTCI 1H-
PULPROG zg30
TD 81728
SOLVENT CDCl3
NS 8
DS 2
SWH 8012.820 Hz
FIDRES 0.098043 Hz
AQ 5.0998273 sec
RG 5.7
DW 62.400 usec
DE 6.00 usec
TE 298.0 K
D1 0.10000000 sec
MCREST 0 sec
MCWRK 0.01500000 sec

======== CHANNEL f1 ========
NUC1 1H
P1 7.50 usec
PL1 1.60 dB
SFO1 500.2235015 MHz

F2 - Processing parameters
SI 65536
SF 500.2200304 MHz
WDW EM
SSB 0
LB 0.30 Hz
GB 0
PC 4.00

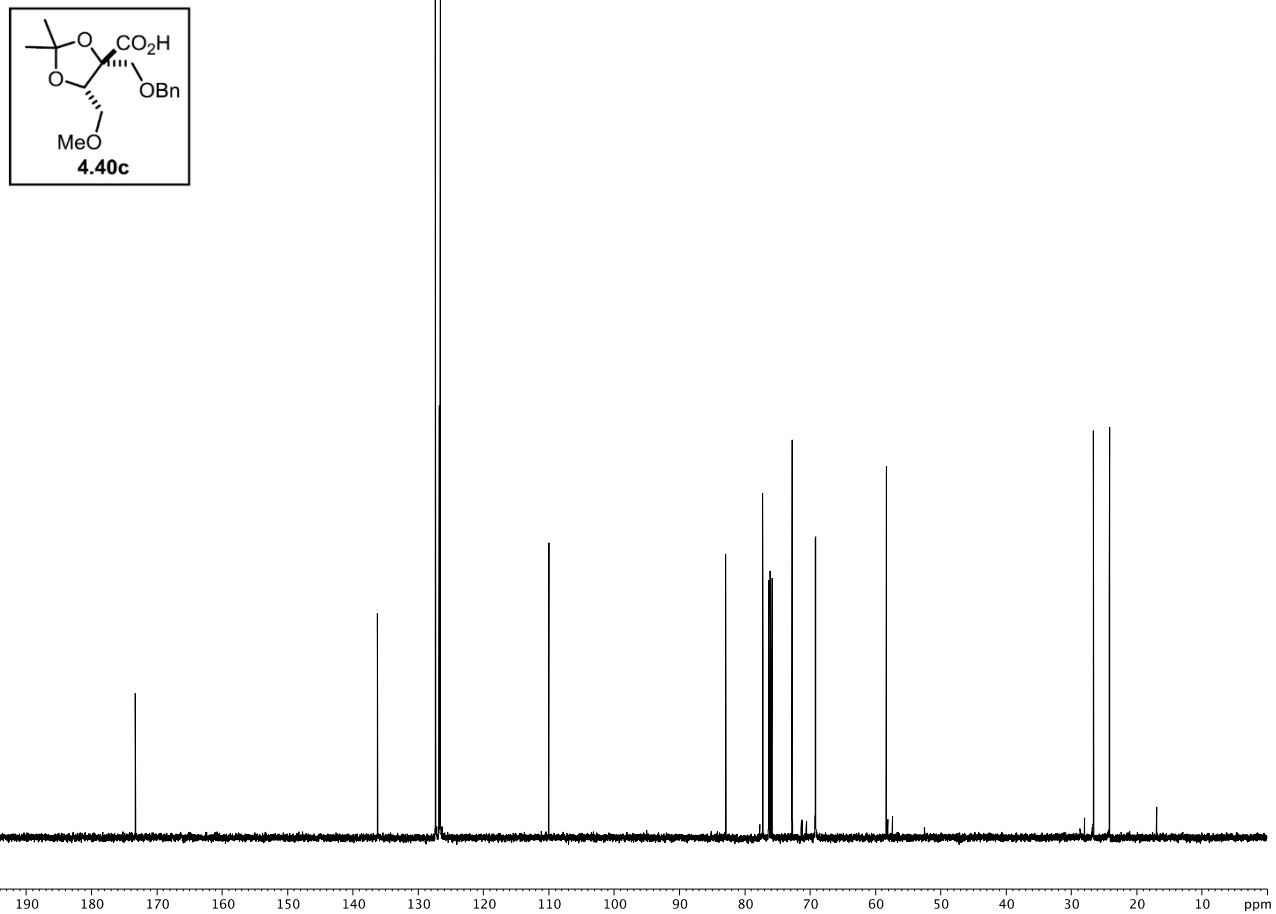


```
Current Data Parameters
NAME          YS-IV-58
EXPNO              3
PROCNO             1

F2 - Acquisition Parameters
Date_         20160126
Time           17.15
INSTRUM        cryo500
PROBHD   5 mm CPTCI 1H-
PULPROG  SpinEchopg30gp.prd
TD             65536
SOLVENT          CDCl3
NS                32
DS                 1
SWH          30303.031 Hz
FIDRES        0.462388 Hz
AQ          1.0813440 sec
RG            2580.3
DW            16.500 usec
DE             6.00 usec
TE            298.0 K
D1         0.50000000 sec
d11        0.03000000 sec
D16        0.00020000 sec
d17        0.00019600 sec
MCREST   0 sec
MCWRK      0.01500000 sec
P2            33.10 usec

======== CHANNEL f1 ========
NUC1             13C
P1            16.55 usec
P11          500.00 usec
P12         2000.00 usec
PL0          120.00 dB
PL1          -1.00 dB
SFO1       125.7942548 MHz
SP1            2.70 dB
SP2            2.70 dB
SPNAM[1] Crp60,0.5,20.1
SPNAM[2]   Crp60comp.4
SPOFF1   0 Hz
SPOFF2   0 Hz

======== CHANNEL f2 ========
CPDPRG[2        waltz16
NUC2             1H
PCPD2          100.00 usec
PL2            1.60 dB
PL12           24.50 dB
SFO2       500.2225011 MHz

====== GRADIENT CHANNEL =====
GPNAM[1]       SINE.100
GPNAM[2]       SINE.100
GPX1     0 %
GPX2     0 %
GPY1     0 %
GPY2     0 %
GPZ1           30.00 %
GPZ2           50.00 %
p15          500.00 usec
p16         1000.00 usec

F2 - Processing parameters
SI             65536
SF        125.7805602 MHz
WDW              EM
SSB     0
LB            1.00 Hz
GB      0
PC            2.00
```

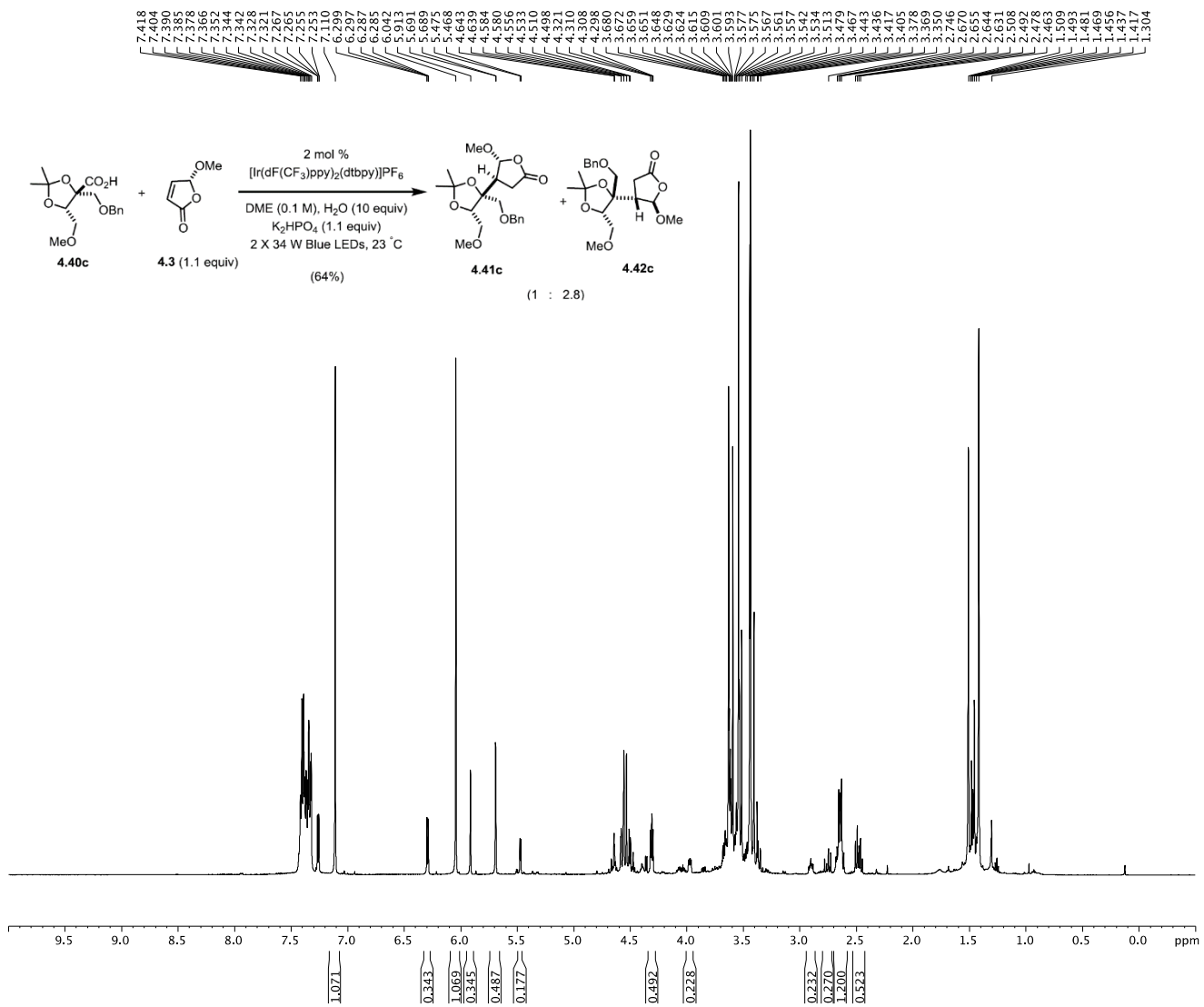

Current Data Parameters
NAME YS-IV-61
EXPNO 1
PROCNO 1

F2 - Acquisition Parameters
Date_ 20160127
Time 12.55
INSTRUM cryo500
PROBHD 5 mm CPTCI 1H-
PULPROG zg30
TD 81728
SOLVENT CDCl3
NS 8
DS 2
SWH 8012.820 Hz
FIDRES 0.098043 Hz
AQ 5.0998273 sec
RG 6.3
DW 62.400 usec
DE 6.00 usec
TE 298.0 K
D1 0.10000000 sec
MCREST 0 sec
MCWRK 0.01500000 sec

======== CHANNEL f1 ========
NUC1 1H
P1 7.50 usec
PL1 1.60 dB
SFO1 500.2235015 MHz

F2 - Processing parameters
SI 65536
SF 500.2200000 MHz
WDW EM
SSB 0
LB 0.30 Hz
GB 0
PC 4.00

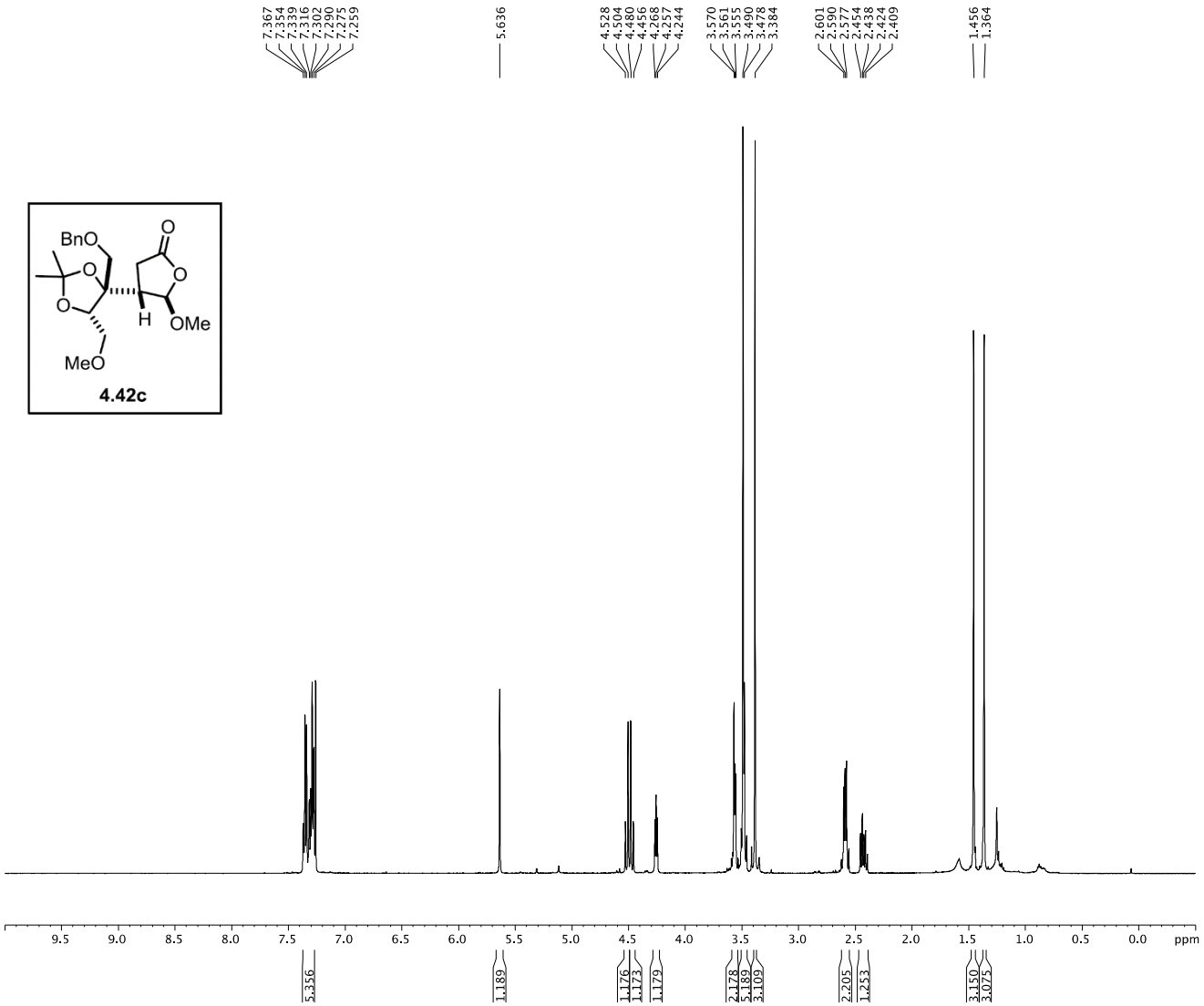

Current Data Parameters
NAME YS-IV-61
EXPNO 2
PROCNO 1

F2 - Acquisition Parameters
Date_ 20160127
Time 17.06
INSTRUM cryo500
PROBHD 5 mm CPTCI 1H-
PULPROG zg30
TD 81728
SOLVENT CDCl3
NS 8
DS 2
SWH 8012.820 Hz
FIDRES 0.098043 Hz
AQ 5.0998273 sec
RG 9
DW 62.400 usec
DE 6.00 usec
TE 298.0 K
D1 0.10000000 sec
MCREST 0 sec
MCWRK 0.01500000 sec

======== CHANNEL f1 ========
NUC1 1H
P1 7.50 usec
PL1 1.60 dB
SFO1 500.2235015 MHz

F2 - Processing parameters
SI 65536
SF 500.2200311 MHz
WDW EM
SSB 0
LB 0.30 Hz
GB 0
PC 4.00

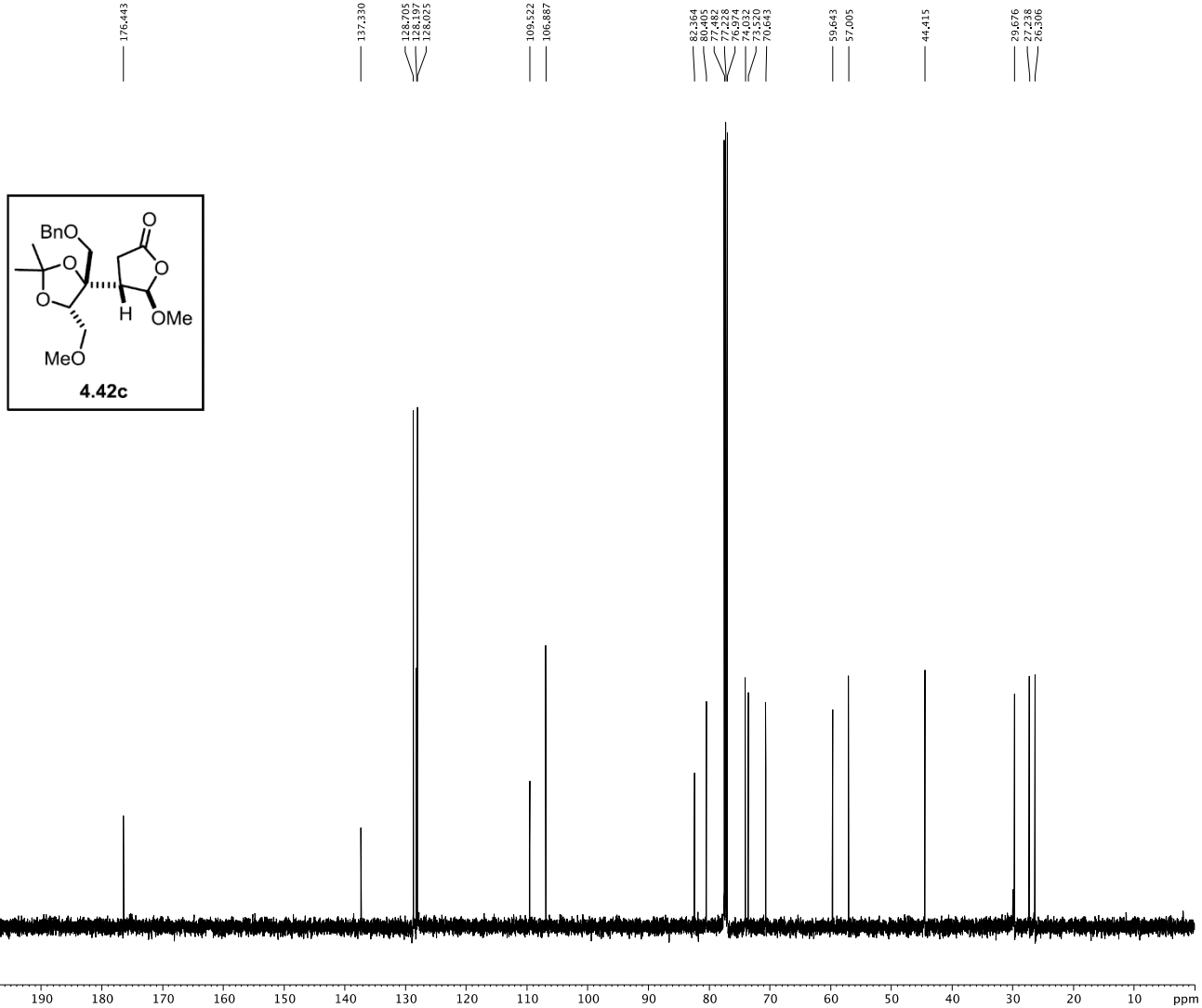

4.42c

Current Data Parameters
NAME YS-IV-61
EXPNO 5
PROCNO 1

F2 - Acquisition Parameters
Date_ 20160127
Time 17.07
INSTRUM cryo500
PROBHD 5 mm CPTCI 1H-
PULPROG SpinEchopg30gp.prd
TD 65536
SOLVENT CDCl3
NS 200
DS 1
SWH 30303.031 Hz
FIDRES 0.462388 Hz
AQ 1.0813440 sec
RG 7298.2
DW 16.500 usec
DE 6.00 usec
TE 298.0 K
D1 0.25000000 sec
d11 0.03000000 sec
D16 0.00020000 sec
d17 0.00019600 sec
MCREST 0 sec
MCWRK 0.01500000 sec
P2 33.10 usec

======== CHANNEL f1 ========
NUC1 13C
P1 16.55 usec
P11 500.00 usec
P12 2000.00 usec
PL0 120.00 dB
PL1 -1.00 dB
SFO1 125.7942548 MHz
SP1 2.70 dB
SP2 2.70 dB
SPNAM[1] Crp60,0.5,20.1
SPNAM[2] Crp60comp.4
SPOFF1 0 Hz
SPOFF2 0 Hz

======== CHANNEL f2 ========
CPDPRG[2 waltz16
NUC2 1H
PCPD2 100.00 usec
PL2 1.60 dB
PL12 24.50 dB
SFO2 500.2225011 MHz

====== GRADIENT CHANNEL =====
GPNAM[1] SINE.100
GPNAM[2] SINE.100
GPX1 0 %
GPX2 0 %
GPY1 0 %
GPY2 0 %
GPZ1 30.00 %
GPZ2 50.00 %
p15 500.00 usec
p16 1000.00 usec

F2 - Processing parameters
SI 65536
SF 125.7803997 MHz
WDW EM
SSB 0
LB 1.00 Hz
GB 0
PC 2.00

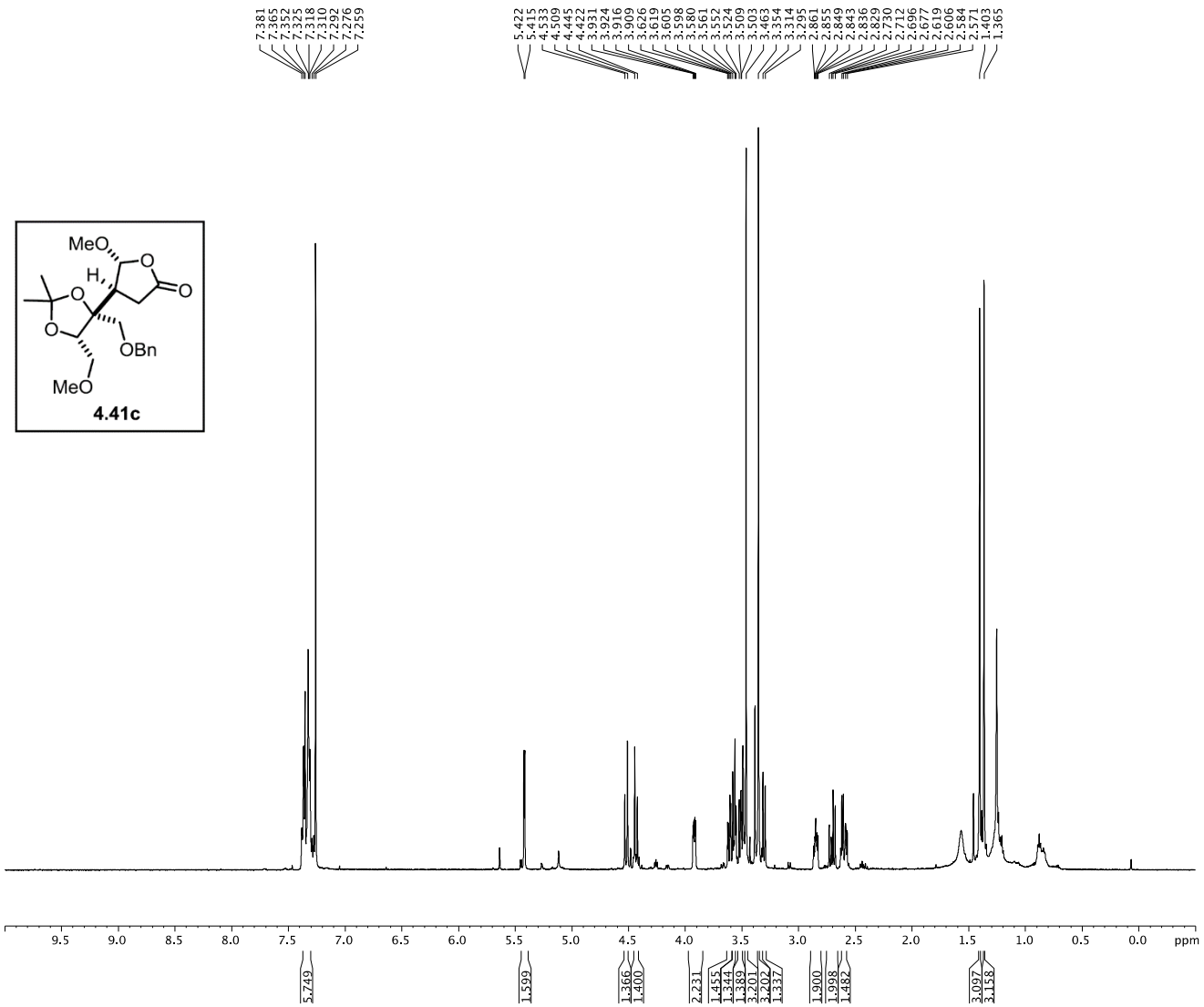

Current Data Parameters
NAME YS-IV-61
EXPNO 3
PROCNO 1

F2 - Acquisition Parameters
Date_ 20160127
Time 17.24
INSTRUM cryo500
PROBHD 5 mm CPTCI 1H-
PULPROG zg30
TD 81728
SOLVENT CDCl3
NS 8
DS 2
SWH 8012.820 Hz
FIDRES 0.098043 Hz
AQ 5.0998273 sec
RG 10.1
DW 62.400 usec
DE 6.00 usec
TE 298.0 K
D1 0.10000000 sec
MCREST 0 sec
MCWRK 0.01500000 sec

======== CHANNEL f1 ========
NUC1 1H
P1 7.50 usec
PL1 1.60 dB
SFO1 500.2235015 MHz

F2 - Processing parameters
SI 65536
SF 500.2200311 MHz
WDW EM
SSB 0
LB 0.30 Hz
GB 0
PC 4.00

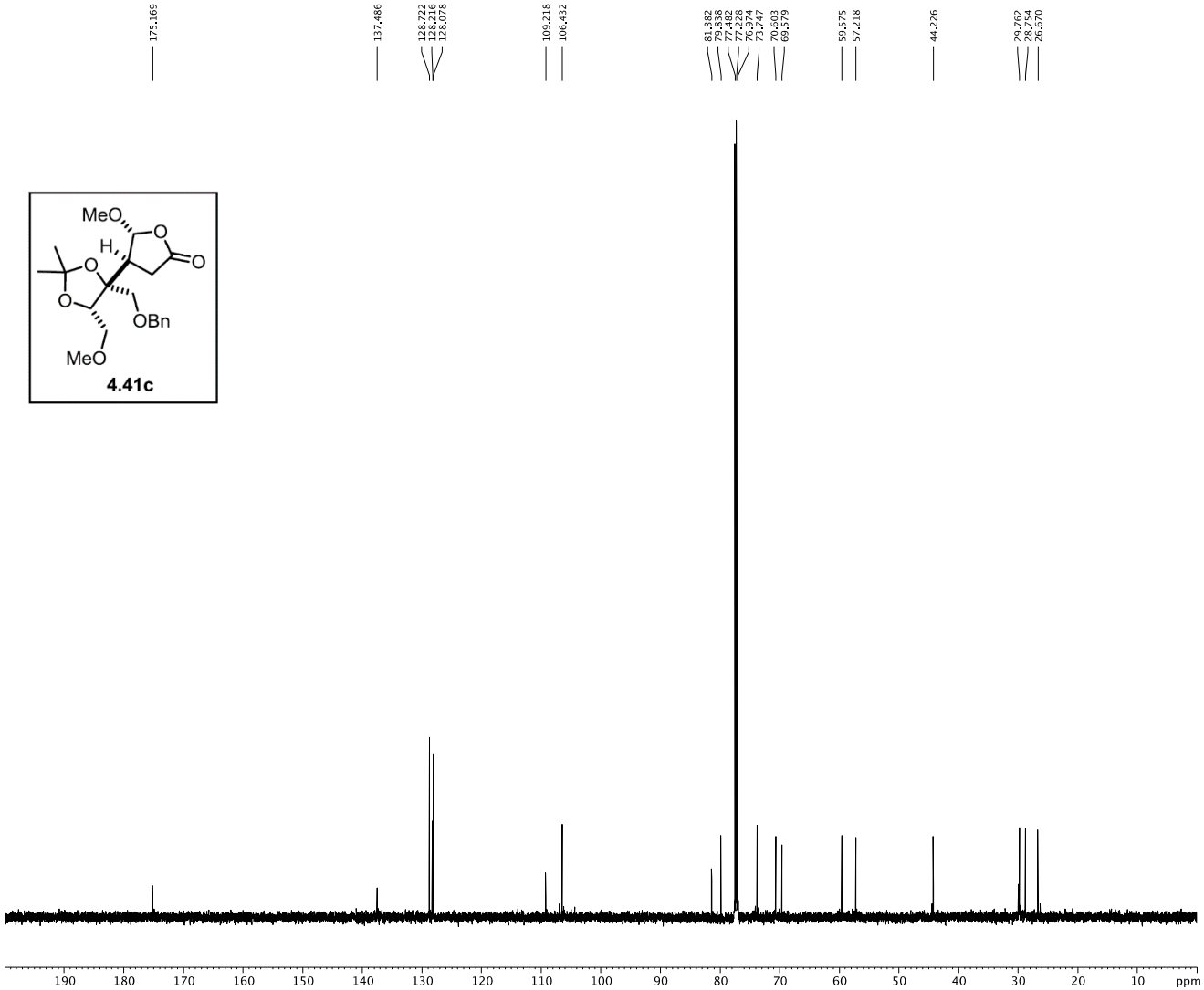

Current Data Parameters
NAME YS-IV-61
EXPNO 8
PROCNO 1

F2 - Acquisition Parameters
Date_ 20160127
Time 17.26
INSTRUM cryo500
PROBHD 5 mm CPTCI 1H-
PULPROG SpinEchopg30gp.prd
TD 65536
SOLVENT CDCl3
NS 584
DS 1
SWH 30303.031 Hz
FIDRES 0.462388 Hz
AQ 1.0813440 sec
RG 5160.6
DW 16.500 usec
DE 6.00 usec
TE 298.0 K
D1 0.25000000 sec
d11 0.03000000 sec
D16 0.00020000 sec
d17 0.00019600 sec
MCREST 0 sec
MCWRK 0.01500000 sec
P2 33.10 usec

======== CHANNEL f1 ========
NUC1 13C
P1 16.55 usec
P11 500.00 usec
P12 2000.00 usec
PL0 120.00 dB
PL1 -1.00 dB
SFO1 125.7942548 MHz
SP1 2.70 dB
SP2 2.70 dB
SPNAM[1] Crp60,0.5,20.1
SPNAM[2] Crp60comp.4
SPOFF1 0 Hz
SPOFF2 0 Hz

======== CHANNEL f2 ========
CPDPRG[2 waltz16
NUC2 1H
PCPD2 100.00 usec
PL2 1.60 dB
PL12 24.50 dB
SFO2 500.2225011 MHz

====== GRADIENT CHANNEL =====
GPNAM[1] SINE.100
GPNAM[2] SINE.100
GPX1 0 %
GPX2 0 %
GPY1 0 %
GPY2 0 %
GPZ1 30.00 %
GPZ2 50.00 %
p15 500.00 usec
p16 1000.00 usec

F2 - Processing parameters
SI 65536
SF 125.7803987 MHz
WDW EM
SSB 0
LB 1.00 Hz
GB 0
PC 2.00

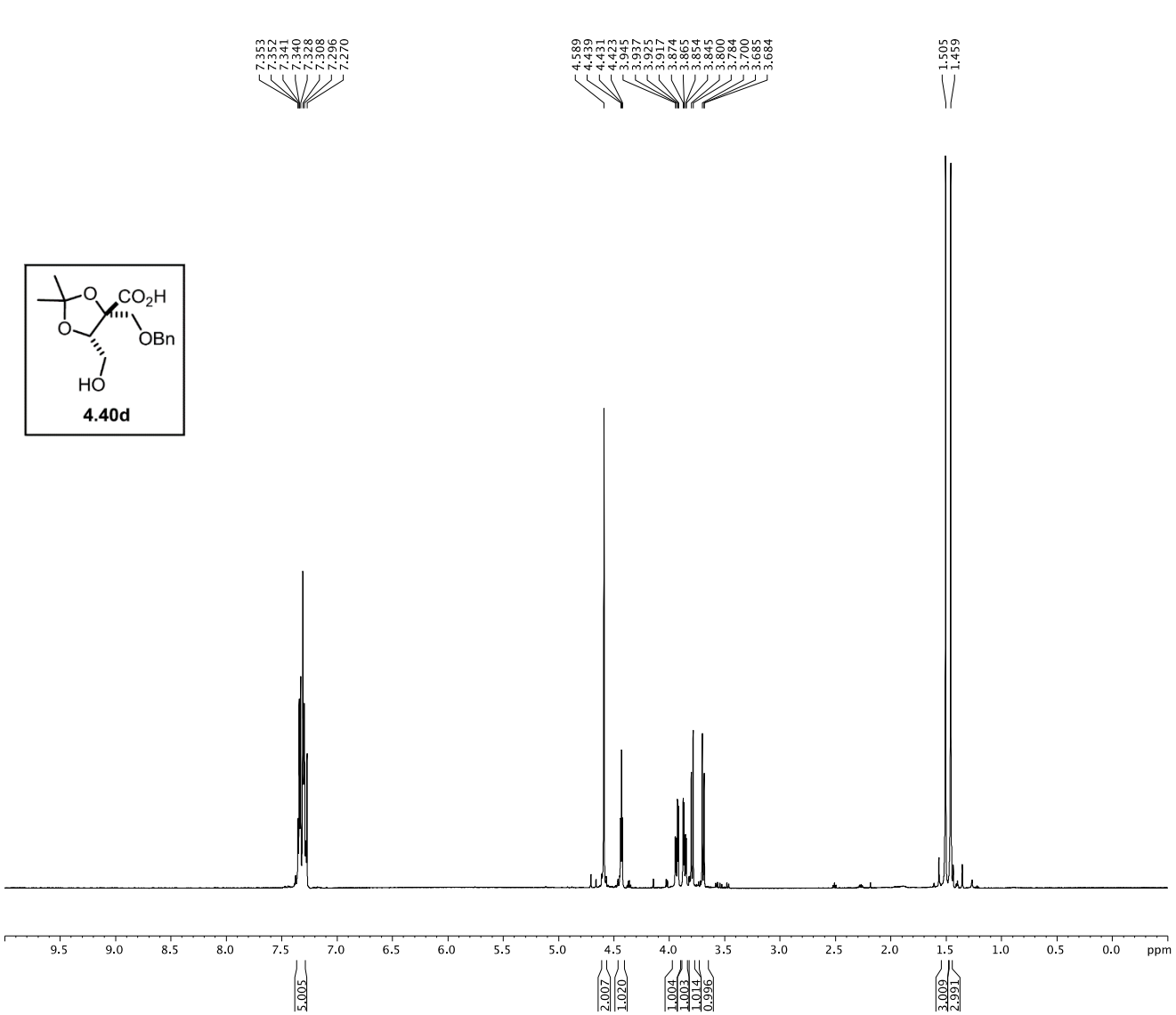


```
Current Data Parameters
NAME        YS-IV-37
EXPNO          2
PROCNO         1

F2 - Acquisition Parameters
Date_      20160118
Time          8.44
INSTRUM      av600
PROBHD  5 mm TBI 1H/13
PULPROG      zg30
TD          98074
SOLVENT     CDCl3
NS             8
DS             2
SWH       9615.385 Hz
FIDRES    0.098042 Hz
AQ        5.0998478 sec
RG           456
DW         52.000 usec
DE         14.54 usec
TE         298.0 K
D1       0.10000000 sec
TD0            1

======== CHANNEL f1 ========
SFO1    600.1342009 MHz
NUC1          1H
P1          8.00 usec
PLW1     24.00000000 W

F2 - Processing parameters
SI          65536
SF      600.1300281 MHz
WDW           EM
SSB     0
LB          0.30 Hz
GB      0
PC          1.00
```

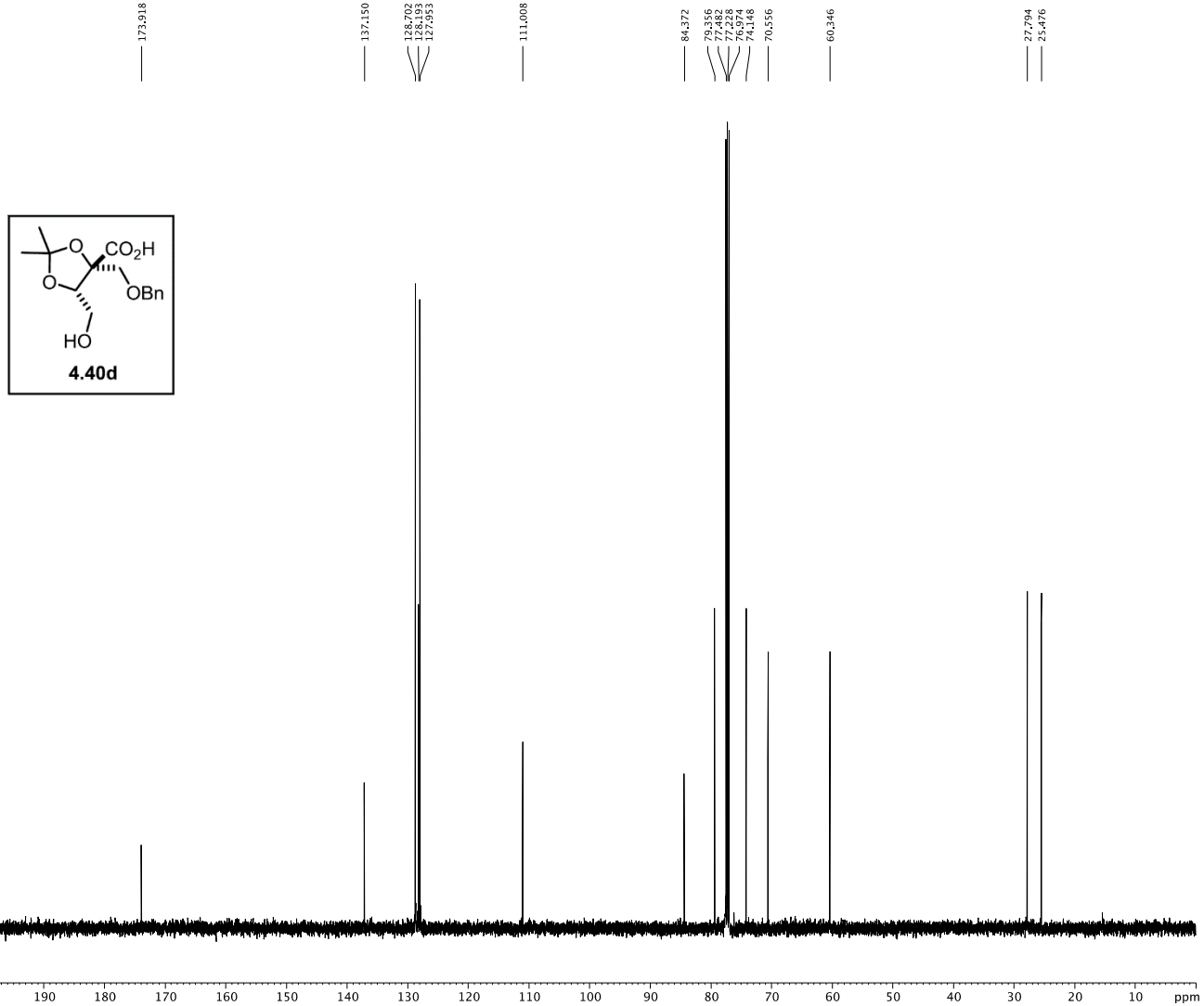

Current Data Parameters
NAME YS-IV-37
EXPNO 3
PROCNO 1

F2 - Acquisition Parameters
Date_ 20160116
Time 14.23
INSTRUM cryo500
PROBHD 5 mm CPTCI 1H-
PULPROG SpinEchopg30gp.prd
TD 65536
SOLVENT CDCl3
NS 304
DS 16
SWH 30303.031 Hz
FIDRES 0.462388 Hz
AQ 1.0813440 sec
RG 7298.2
DW 16.500 usec
DE 6.00 usec
TE 298.0 K
D1 0.25000000 sec
d11 0.03000000 sec
D16 0.00020000 sec
d17 0.00019600 sec
MCREST 0 sec
MCWRK 0.01500000 sec
P2 33.10 usec

======== CHANNEL f1 ========
NUC1 13C
P1 16.55 usec
P11 500.00 usec
P12 2000.00 usec
PL0 120.00 dB
PL1 -1.00 dB
SFO1 125.7942548 MHz
SP1 2.70 dB
SP2 2.70 dB
SPNAM[1] Crp60,0.5,20.1
SPNAM[2] Crp60comp.4
SPOFF1 0 Hz
SPOFF2 0 Hz

======== CHANNEL f2 ========
CPDPRG[2 waltz16
NUC2 1H
PCPD2 100.00 usec
PL2 1.60 dB
PL12 24.50 dB
SFO2 500.2225011 MHz

====== GRADIENT CHANNEL =====
GPNAM[1] SINE.100
GPNAM[2] SINE.100
GPX1 0 %
GPX2 0 %
GPY1 0 %
GPY2 0 %
GPZ1 30.00 %
GPZ2 50.00 %
p15 500.00 usec
p16 1000.00 usec

F2 - Processing parameters
SI 65536
SF 125.7803997 MHz
WDW EM
SSB 0
LB 1.00 Hz
GB 0
PC 2.00

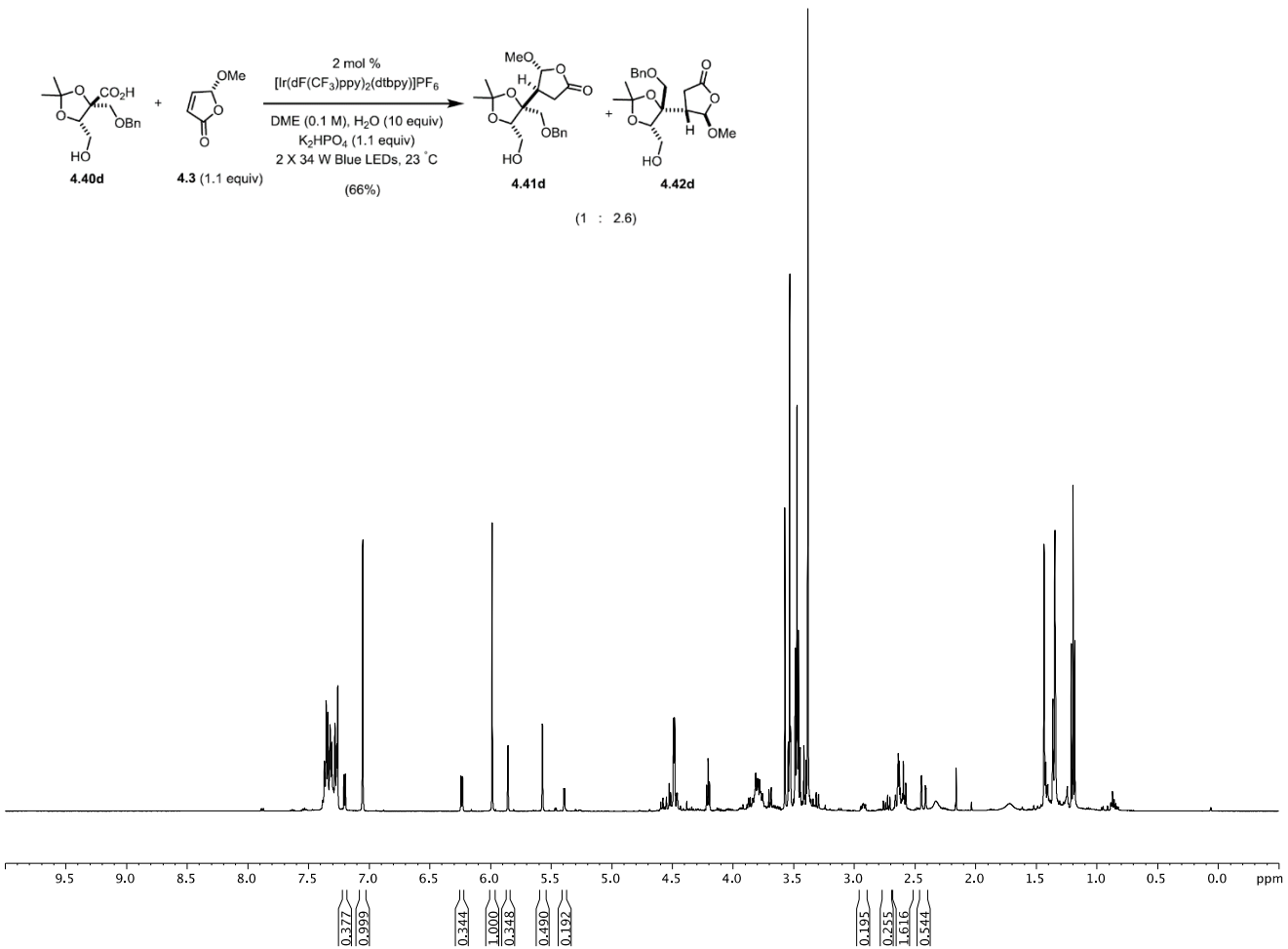

Current Data Parameters
NAME YS-IV-45
EXPNO 1
PROCNO 1

F2 - Acquisition Parameters
Date_ 20160119
Time 9.34
INSTRUM cryo500
PROBHD 5 mm CPTCI 1H-
PULPROG zg30
TD 81728
SOLVENT CDCl3
NS 8
DS 2
SWH 8012.820 Hz
FIDRES 0.098043 Hz
AQ 5.0998273 sec
RG 6.3
DW 62.400 usec
DE 6.00 usec
TE 298.0 K
D1 0.10000000 sec
MCREST 0 sec
MCWRK 0.01500000 sec

======== CHANNEL f1 ========
NUC1 1H
P1 7.50 usec
PL1 1.60 dB
SFO1 500.2235015 MHz

F2 - Processing parameters
SI 65536
SF 500.2200308 MHz
WDW EM
SSB 0
LB 0.30 Hz
GB 0
PC 4.00

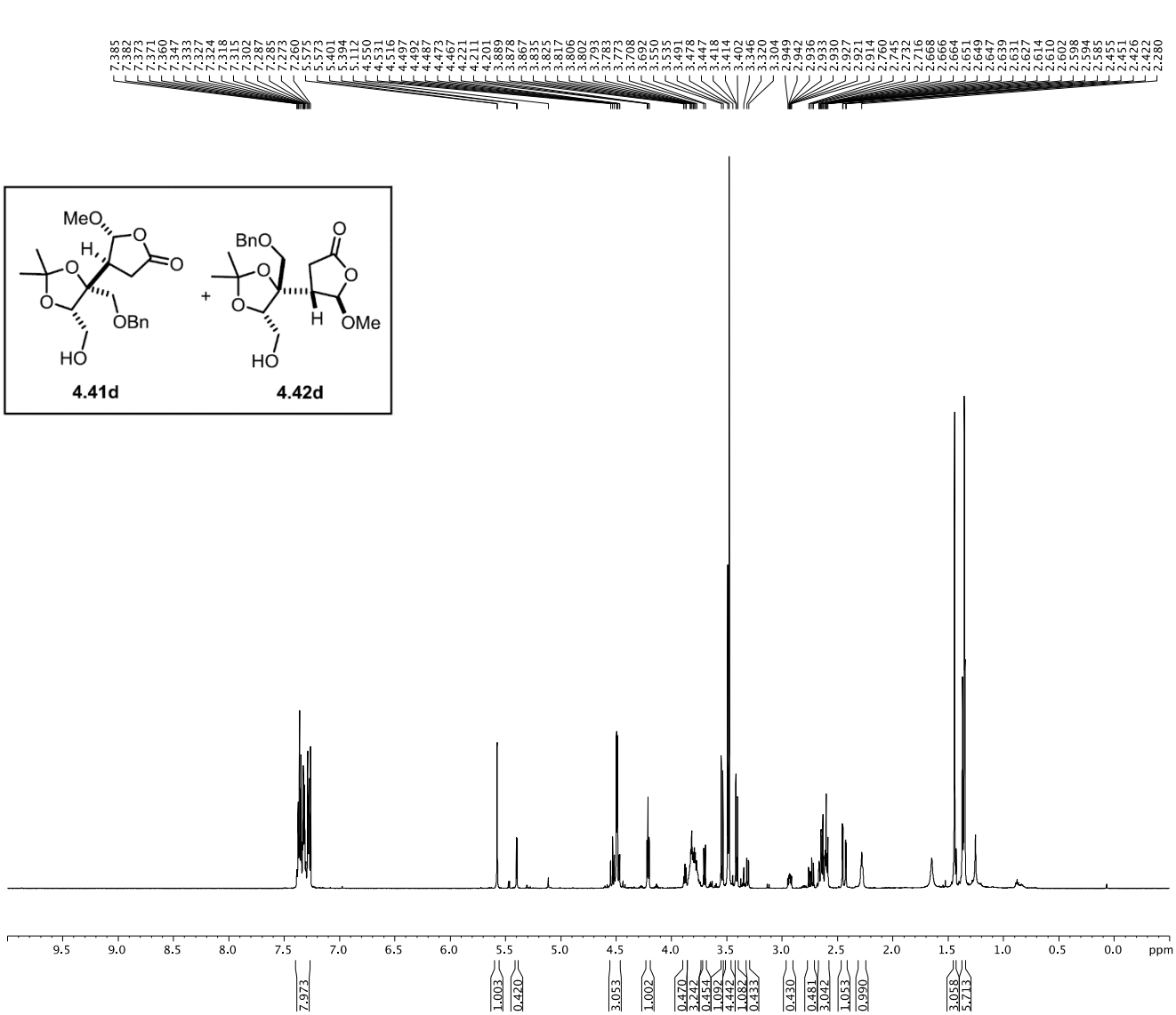


```
Current Data Parameters
NAME          YS-IV-45
EXPNO            2
PROCNO           1

F2 - Acquisition Parameters
Date_       20160119
Time          15.53
INSTRUM       av600
PROBHD  5 mm TBI 1H/13
PULPROG       zg30
TD           98074
SOLVENT       CDCl3
NS               8
DS               2
SWH        9615.385 Hz
FIDRES     0.098042 Hz
AQ        5.0998478 sec
RG             362
DW          52.000 usec
DE          14.54 usec
TE          298.1 K
D1       0.10000000 sec
TD0              1

======== CHANNEL f1 ========
SFO1     600.1342009 MHz
NUC1           1H
P1           8.00 usec
PLW1     24.00000000 W

F2 - Processing parameters
SI           65536
SF      600.1300352 MHz
WDW            EM
SSB     0
LB          0.30 Hz
GB      0
PC           1.00
```

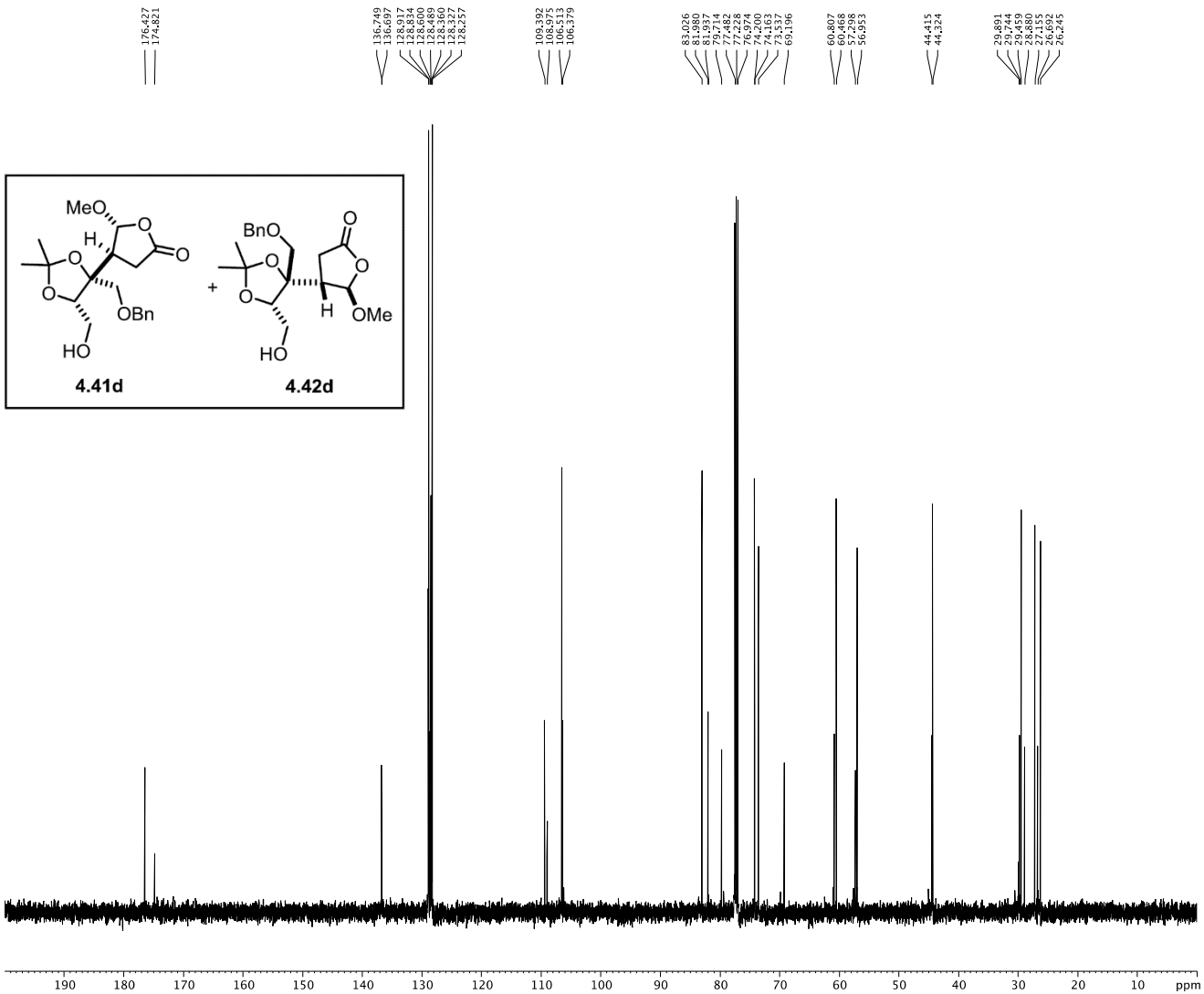

Current Data Parameters
NAME YS-IV-45
EXPNO 3
PROCNO 1

F2 - Acquisition Parameters
Date_ 20160119
Time 16.42
INSTRUM cryo500
PROBHD 5 mm CPTCI 1H-
PULPROG SpinEchopg30gp.prd
TD 65536
SOLVENT CDCl3
NS 200
DS 16
SWH 30303.031 Hz
FIDRES 0.462388 Hz
AQ 1.0813440 sec
RG 9195.2
DW 16.500 usec
DE 6.00 usec
TE 298.0 K
D1 0.25000000 sec
d11 0.03000000 sec
D16 0.00020000 sec
d17 0.00019600 sec
MCREST 0 sec
MCWRK 0.01500000 sec
P2 33.10 usec

======== CHANNEL f1 ========
NUC1 13C
P1 16.55 usec
P11 500.00 usec
P12 2000.00 usec
PL0 120.00 dB
PL1 -1.00 dB
SFO1 125.7942548 MHz
SP1 2.70 dB
SP2 2.70 dB
SPNAM[1] Crp60,0.5,20.1
SPNAM[2] Crp60comp.4
SPOFF1 0 Hz
SPOFF2 0 Hz

======== CHANNEL f2 ========
CPDPRG[2 waltz16
NUC2 1H
PCPD2 100.00 usec
PL2 1.60 dB
PL12 24.50 dB
SFO2 500.2225011 MHz

====== GRADIENT CHANNEL =====
GPNAM[1] SINE.100
GPNAM[2] SINE.100
GPX1 0 %
GPX2 0 %
GPY1 0 %
GPY2 0 %
GPZ1 30.00 %
GPZ2 50.00 %
p15 500.00 usec
p16 1000.00 usec

F2 - Processing parameters
SI 65536
SF 125.7804020 MHz
WDW EM
SSB 0
LB 1.00 Hz
GB 0
PC 2.00

1H spectrum

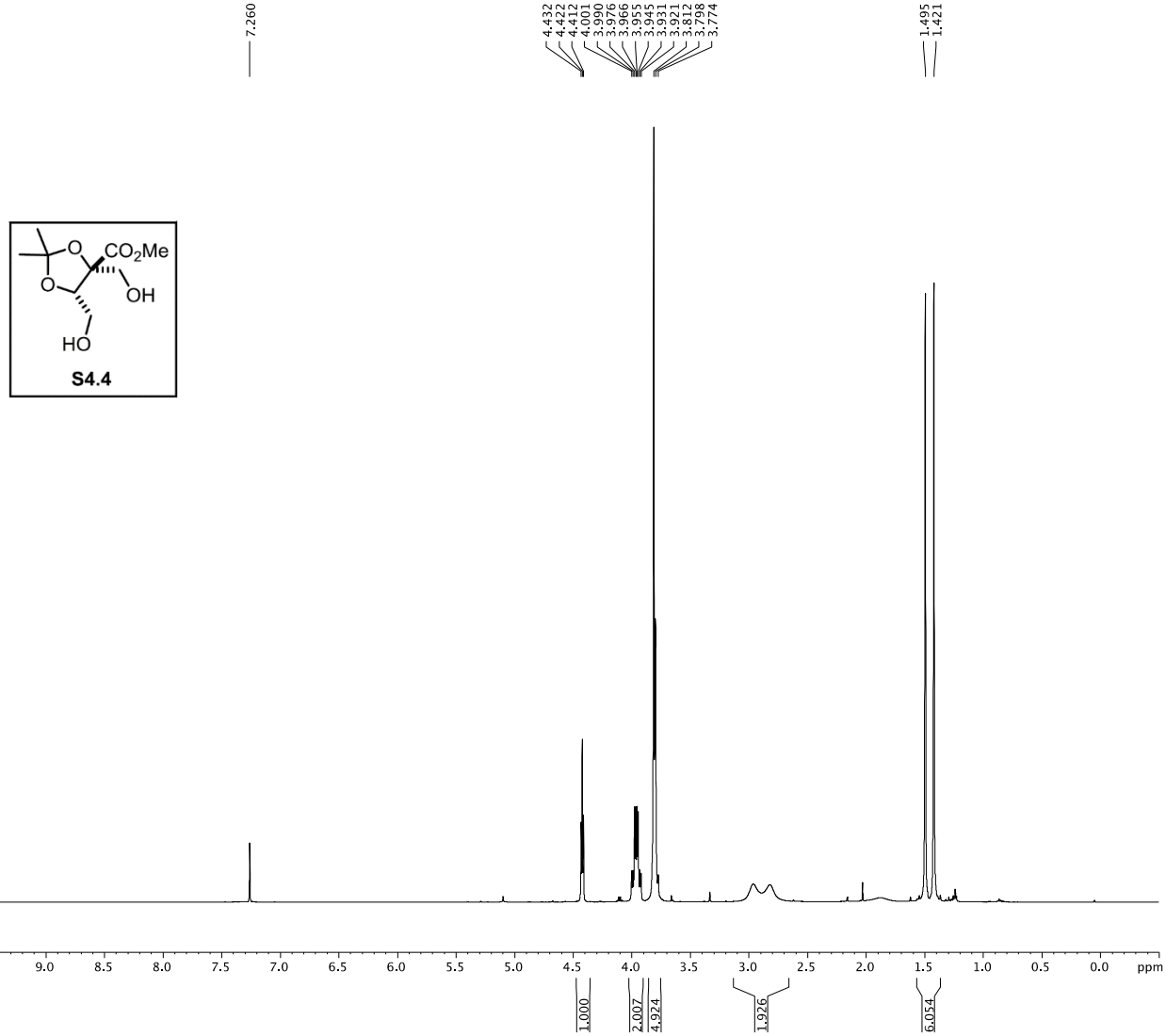

Current Data Parameters
NAME DJT-VI-211
EXPNO 1
PROCNO 1

F2 - Acquisition Parameters
Date_ 20160302
Time 9.32
INSTRUM cryo500
PROBHD 5 mm CPTCI 1H-
PULPROG zg30
TD 81728
SOLVENT CDCl3
NS 8
DS 0
SWH 8012.820 Hz
FIDRES 0.098043 Hz
AQ 5.0998273 sec
RG 4.5
DW 62.400 usec
DE 6.00 usec
TE 298.0 K
D1 0.10000000 sec
MCREST 0 sec
MCWRK 0.01500000 sec

======== CHANNEL f1 =====
NUC1 1H
P1 7.50 usec
PL1 1.60 dB
SFO1 500.2235015 MHz

F2 - Processing parameters
SI 65536
SF 500.2200313 MHz
WDW EM
SSB 0
LB 0.30 Hz
GB 0
PC 4.00

Z-restored spin-echo 13C spectrum with 1H decoupling

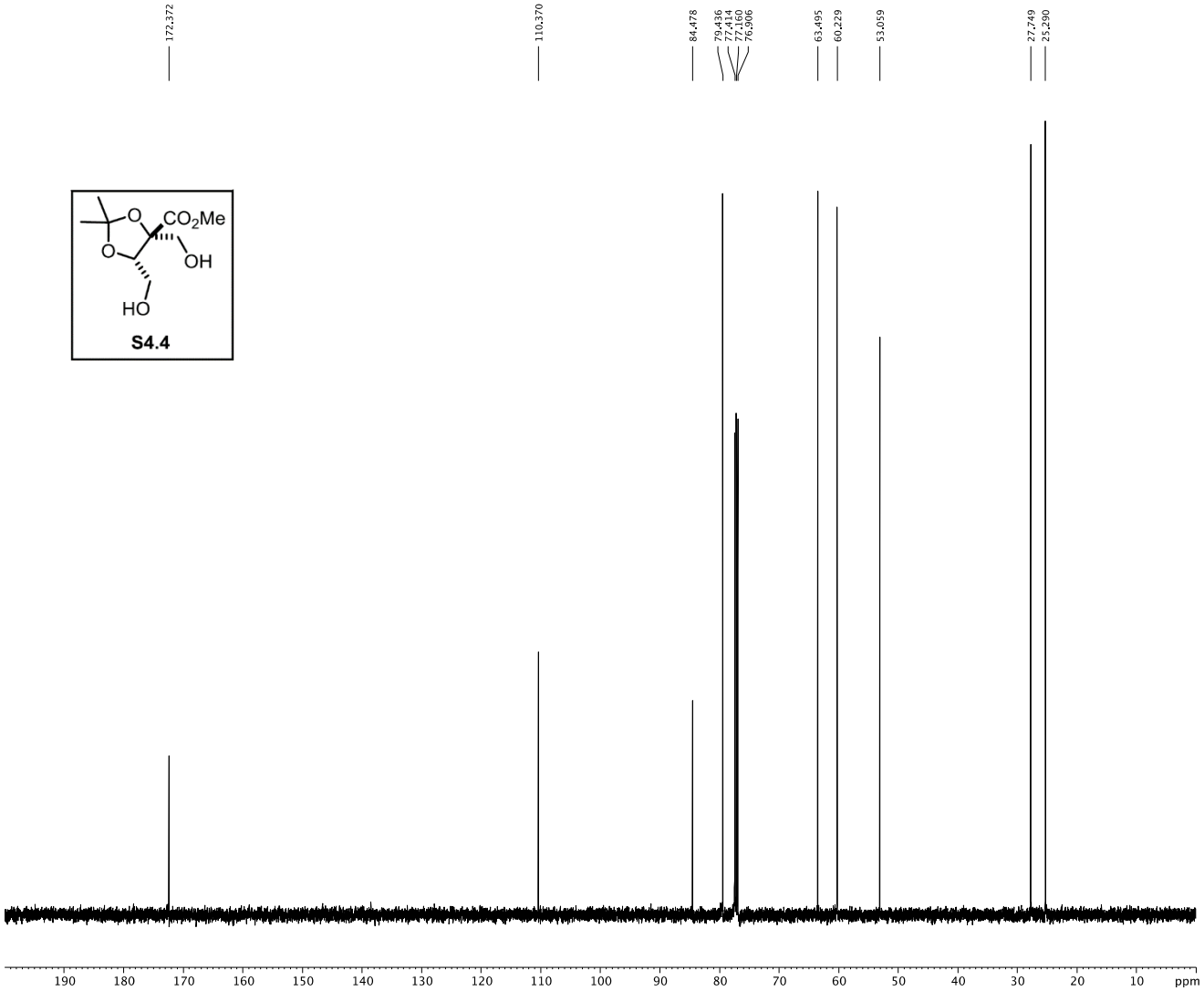

Current Data Parameters
NAME DJT-VI-211
EXPNO 2
PROCNO 1

F2 - Acquisition Parameters
Date_ 20160302
Time 9.34
INSTRUM cryo500
PROBHD 5 mm CPTCI 1H-
PULPROG SpinEchopg30gp.prd
TD 65536
SOLVENT CDCl3
NS 116
DS 0
SWH 30303.031 Hz
FIDRES 0.462388 Hz
AQ 1.0813440 sec
RG 5160.6
DW 16.500 usec
DE 6.00 usec
TE 298.0 K
D1 0.25000000 sec
d11 0.03000000 sec
D16 0.00020000 sec
d17 0.00019600 sec
MCREST 0 sec
MCWRK 0.01500000 sec
P2 33.10 usec

======== CHANNEL f1 ========
NUC1 13C
P1 16.55 usec
P11 500.00 usec
P12 2000.00 usec
PL0 120.00 dB
PL1 -1.00 dB
SFO1 125.7942548 MHz
SP1 2.70 dB
SP2 2.70 dB
SPNAM[1] Crp60.0.5.20.1
SPNAM[2] Crp60comp.4
SPOFF1 0 Hz
SPOFF2 0 Hz

======== CHANNEL f2 ========
CPDPRG[2 waltz16
NUC2 1H
PCPD2 100.00 usec
PL2 1.60 dB
PL12 24.50 dB
SFO2 500.2225011 MHz

====== GRADIENT CHANNEL =====
GPNAM[1] SINE.100
GPNAM[2] SINE.100
GPX1 0 %
GPX2 0 %
GPY1 0 %
GPY2 0 %
GPZ1 30.00 %
GPZ2 50.00 %
p15 500.00 usec
p16 1000.00 usec

F2 - Processing parameters
SI 65536
SF 125.7804113 MHz
WDW EM
SSB 0
LB 1.00 Hz
GB 0
PC 2.00

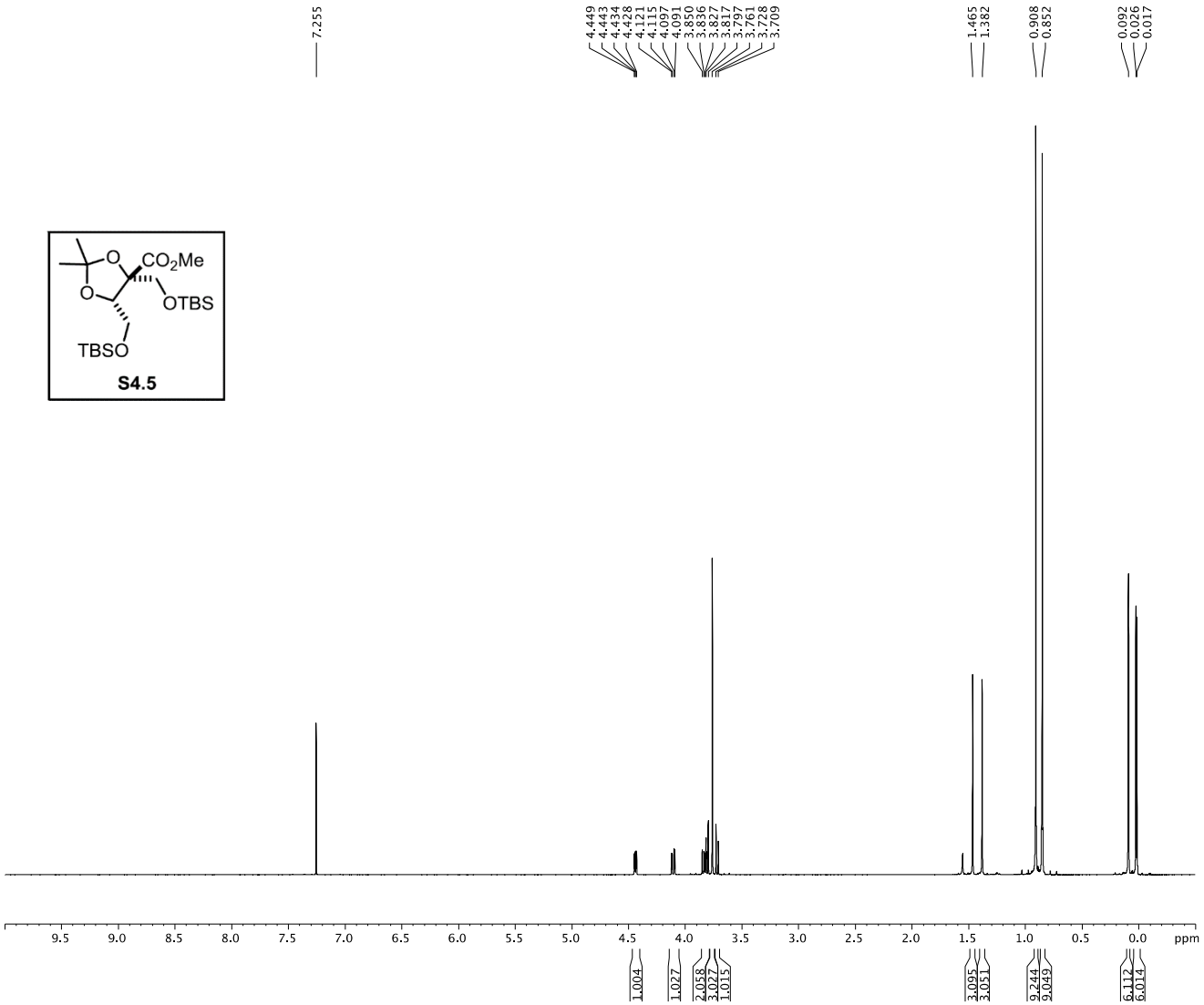

S4.5

```
Current Data Parameters
NAME        DJT-VI-110
EXPNO            1
PROCNO           1

F2 - Acquisition Parameters
Date_       20160202
Time            8.57
INSTRUM       cryo500
PROBHD   5 mm CPTCI 1H-
PULPROG         zg30
TD             81728
SOLVENT        CDCl3
NS               8
DS               2
SWH          8012.820 Hz
FIDRES       0.098043 Hz
AQ          5.0998273 sec
RG               6.3
DW            62.400 usec
DE             6.00 usec
TE            298.0 K
D1          0.10000000 sec
MCREST   0 sec
MCWRK       0.01500000 sec

======== CHANNEL f1 ========
NUC1            1H
P1            7.50 usec
PL1           1.60 dB
SFO1       500.2235015 MHz

F2 - Processing parameters
SI            65536
SF        500.2200346 MHz
WDW             no
SSB      0
LB       0 Hz
GB       0
PC            4.00
```

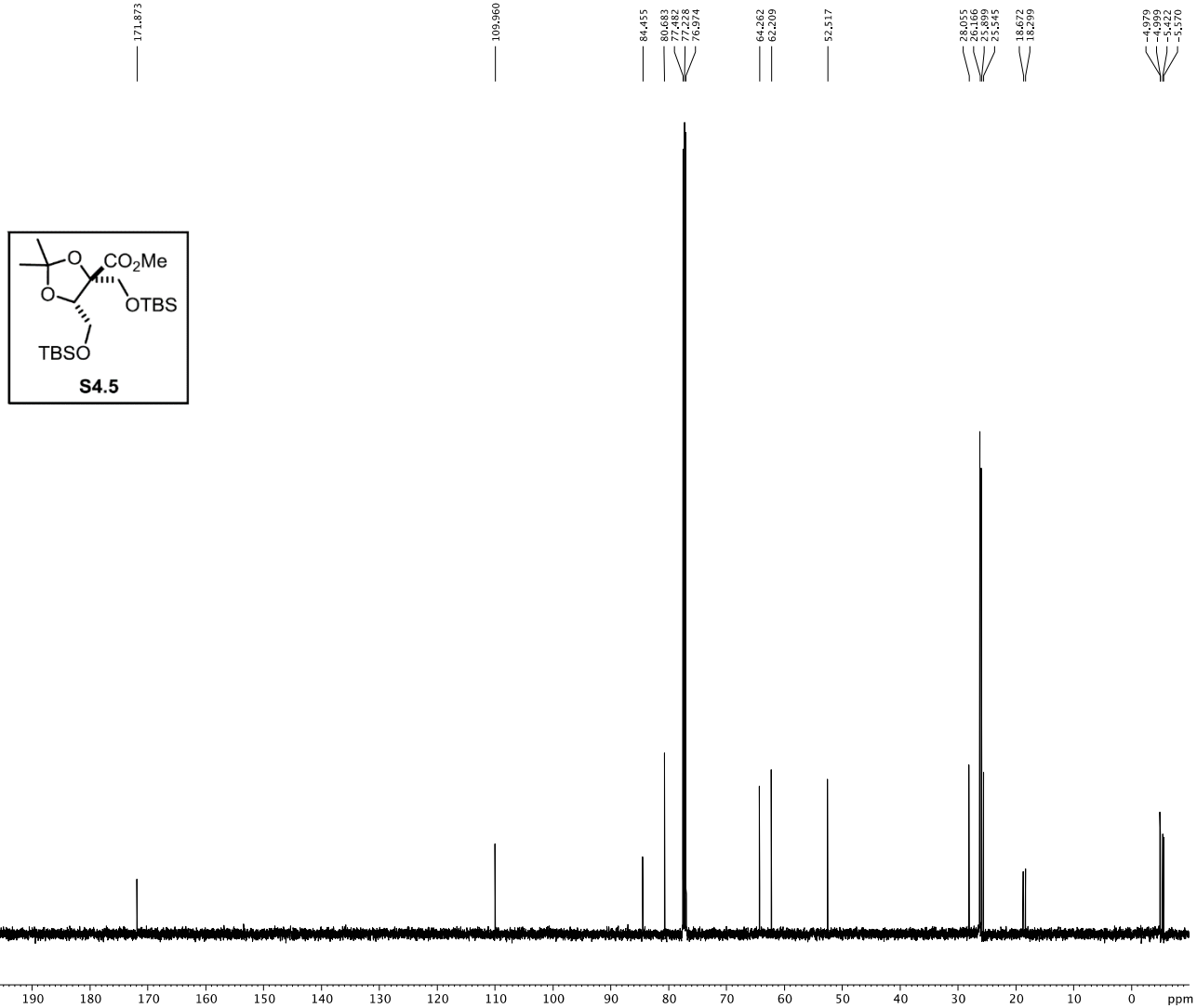

Current Data Parameters
NAME DJT-VI-110
EXPNO 2
PROCNO 1

F2 - Acquisition Parameters
Date_ 20160202
Time 8.59
INSTRUM cryo500
PROBHD 5 mm CPTCI 1H-
PULPROG SpinEchopg30gp.prd
TD 65536
SOLVENT CDCl3
NS 328
DS 1
SWH 30303.031 Hz
FIDRES 0.462388 Hz
AQ 1.0813440 sec
RG 2298.8
DW 16.500 usec
DE 6.00 usec
TE 298.0 K
D1 0.25000000 sec
d11 0.03000000 sec
D16 0.00020000 sec
d17 0.00019600 sec
MCREST 0 sec
MCWRK 0.01500000 sec
P2 33.10 usec

======== CHANNEL f1 ========
NUC1 13C
P1 16.55 usec
P11 500.00 usec
P12 2000.00 usec
PL0 120.00 dB
PL1 -1.00 dB
SFO1 125.7942548 MHz
SP1 2.70 dB
SP2 2.70 dB
SPNAM[1] Crp60,0.5,20.1
SPNAM[2] Crp60comp.4
SPOFF1 0 Hz
SPOFF2 0 Hz

======== CHANNEL f2 ========
CPDPRG[2 waltz16
NUC2 1H
PCPD2 100.00 usec
PL2 1.60 dB
PL12 24.50 dB
SFO2 500.2225011 MHz

====== GRADIENT CHANNEL =====
GPNAM[1] SINE.100
GPNAM[2] SINE.100
GPX1 0 %
GPX2 0 %
GPY1 0 %
GPY2 0 %
GPZ1 30.00 %
GPZ2 50.00 %
p15 500.00 usec
p16 1000.00 usec

F2 - Processing parameters
SI 65536
SF 125.7803989 MHz
WDW EM
SSB 0
LB 1.00 Hz
GB 0
PC 2.00

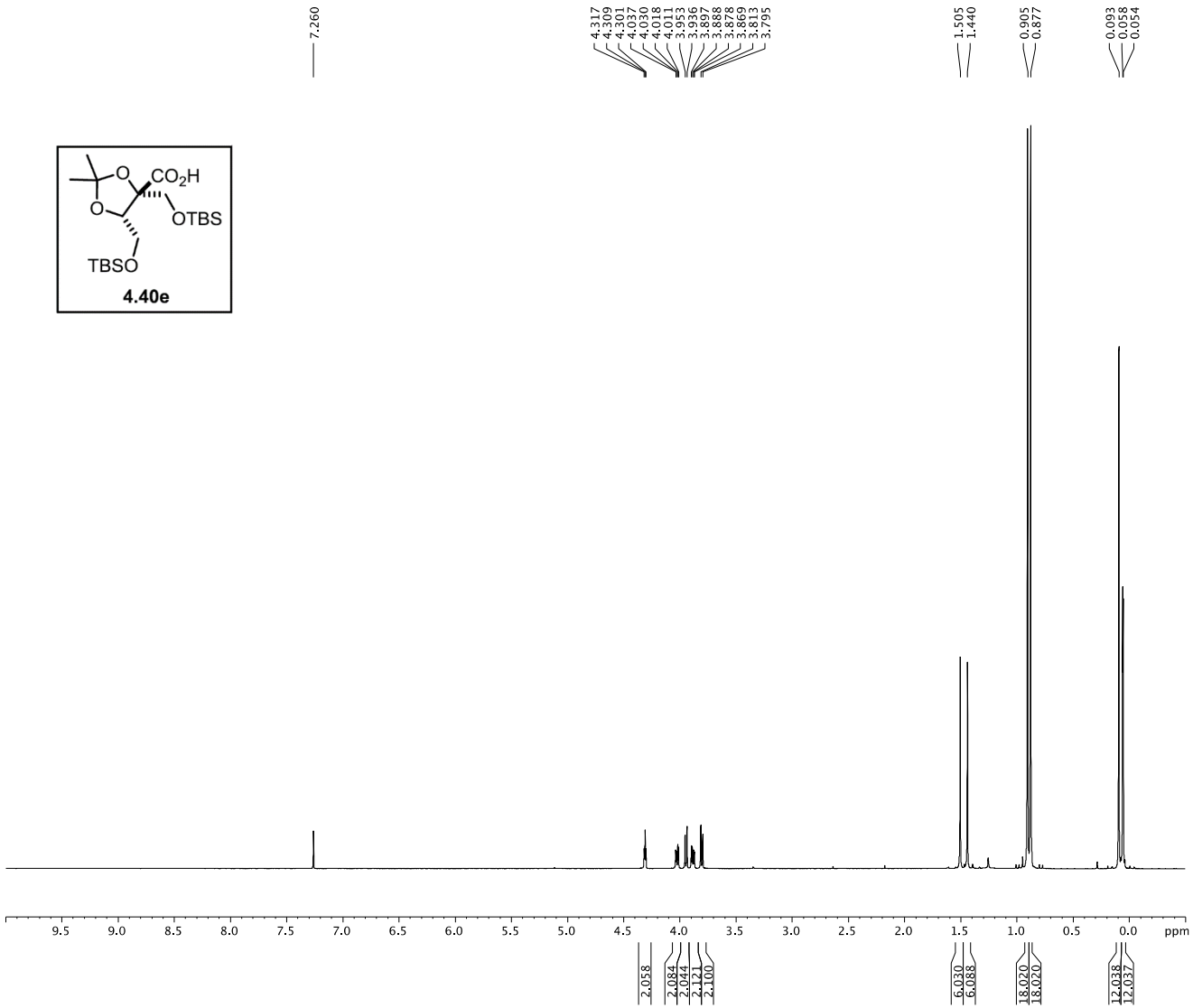

Current Data Parameters
NAME YS-IV-38
EXPNO 3
PROCNO 1

F2 - Acquisition Parameters
Date_ 20160118
Time 8.50
INSTRUM av600
PROBHD 5 mm TBI 1H/13
PULPROG zg30
TD 98074
SOLVENT CDCl3
NS 8
DS 2
SWH 9615.385 Hz
FIDRES 0.098042 Hz
AQ 5.0998478 sec
RG 322
DW 52.000 usec
DE 14.54 usec
TE 298.0 K
D1 0.10000000 sec
TD0 1

======== CHANNEL f1 ========
SFO1 600.1342009 MHz
NUC1 1H
P1 8.00 usec
PLW1 24.00000000 W

F2 - Processing parameters
SI 65536
SF 600.1300343 MHz
WDW EM
SSB 0
LB 0.30 Hz
GB 0
PC 1.00

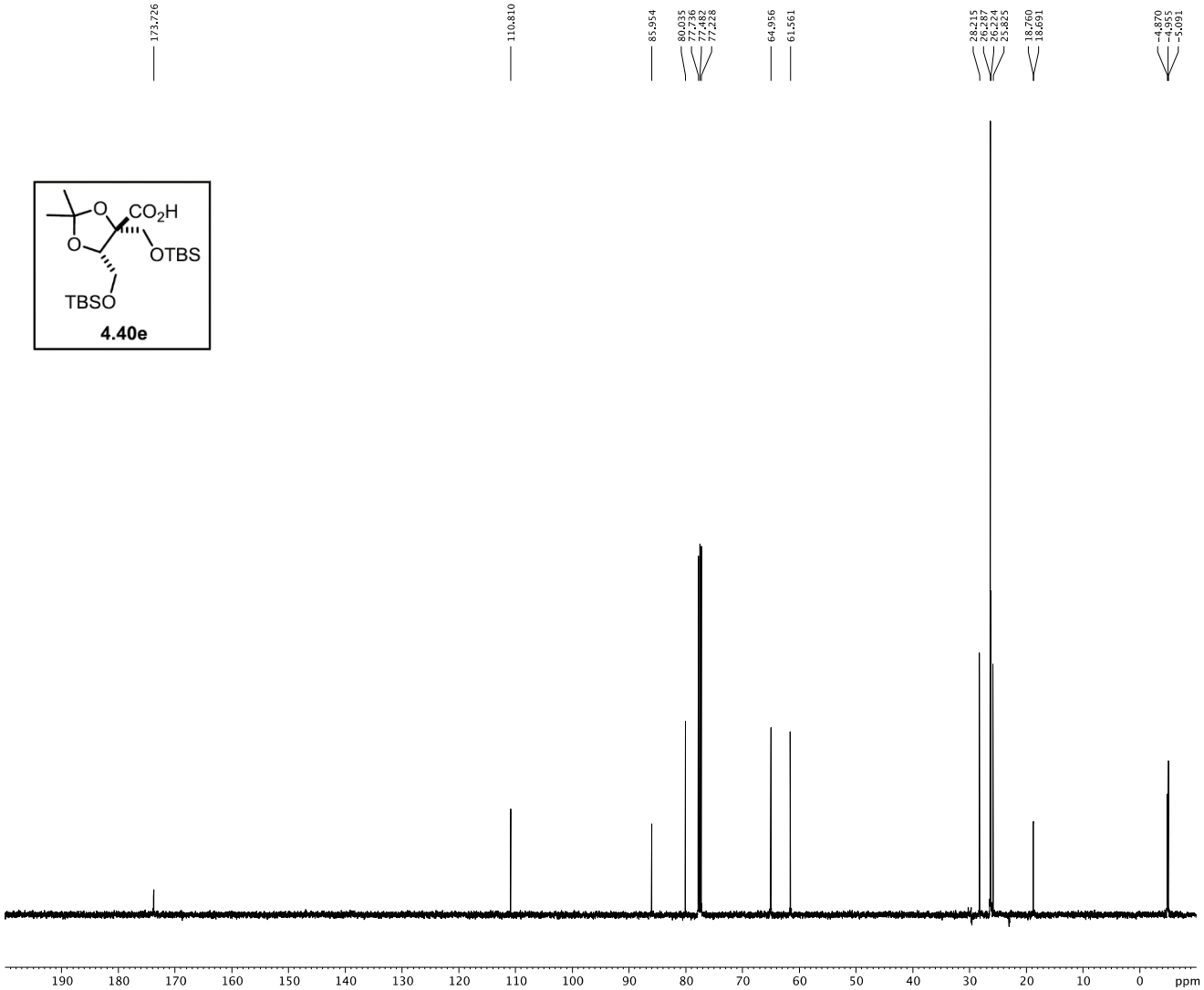


```
Current Data Parameters
NAME          YS-IV-38
EXPNO            4
PROCNO           1

F2 - Acquisition Parameters
Date_       20160118
Time          9.36
INSTRUM       cryo500
PROBHD   5 mm CPTCI 1H-
PULPROG  SpinEchopg30gp.prd
TD          65536
SOLVENT        CDCl3
NS             536
DS               2
SWH         30303.031 Hz
FIDRES       0.462388 Hz
AQ          1.0813440 sec
RG           7298.2
DW           16.500 usec
DE            6.00 usec
TE           298.0 K
D1          0.25000000 sec
d11         0.03000000 sec
D16         0.00020000 sec
d17         0.00019600 sec
MCREST   0 sec
MCWRK       0.01500000 sec
P2           33.10 usec

======== CHANNEL f1 ========
NUC1           13C
P1           16.55 usec
P11          500.00 usec
P12         2000.00 usec
PL0          120.00 dB
PL1          -1.00 dB
SFO1       125.7942548 MHz
SP1           2.70 dB
SP2           2.70 dB
SPNAM[1] Crp60,0.5,20.1
SPNAM[2]   Crp60comp.4
SPOFF1   0 Hz
SPOFF2   0 Hz

======== CHANNEL f2 ========
CPDPRG[2       waltz16
NUC2           1H
PCPD2        100.00 usec
PL2           1.60 dB
PL12         24.50 dB
SFO2       500.2225011 MHz

====== GRADIENT CHANNEL =====
GPNAM[1]      SINE.100
GPNAM[2]      SINE.100
GPX1     0 %
GPX2     0 %
GPY1     0 %
GPY2     0 %
GPZ1          30.00 %
GPZ2          50.00 %
p15          500.00 usec
p16         1000.00 usec

F2 - Processing parameters
SI          65536
SF       125.7803666 MHz
WDW            EM
SSB      0
LB           1.00 Hz
GB       0
PC           2.00
```

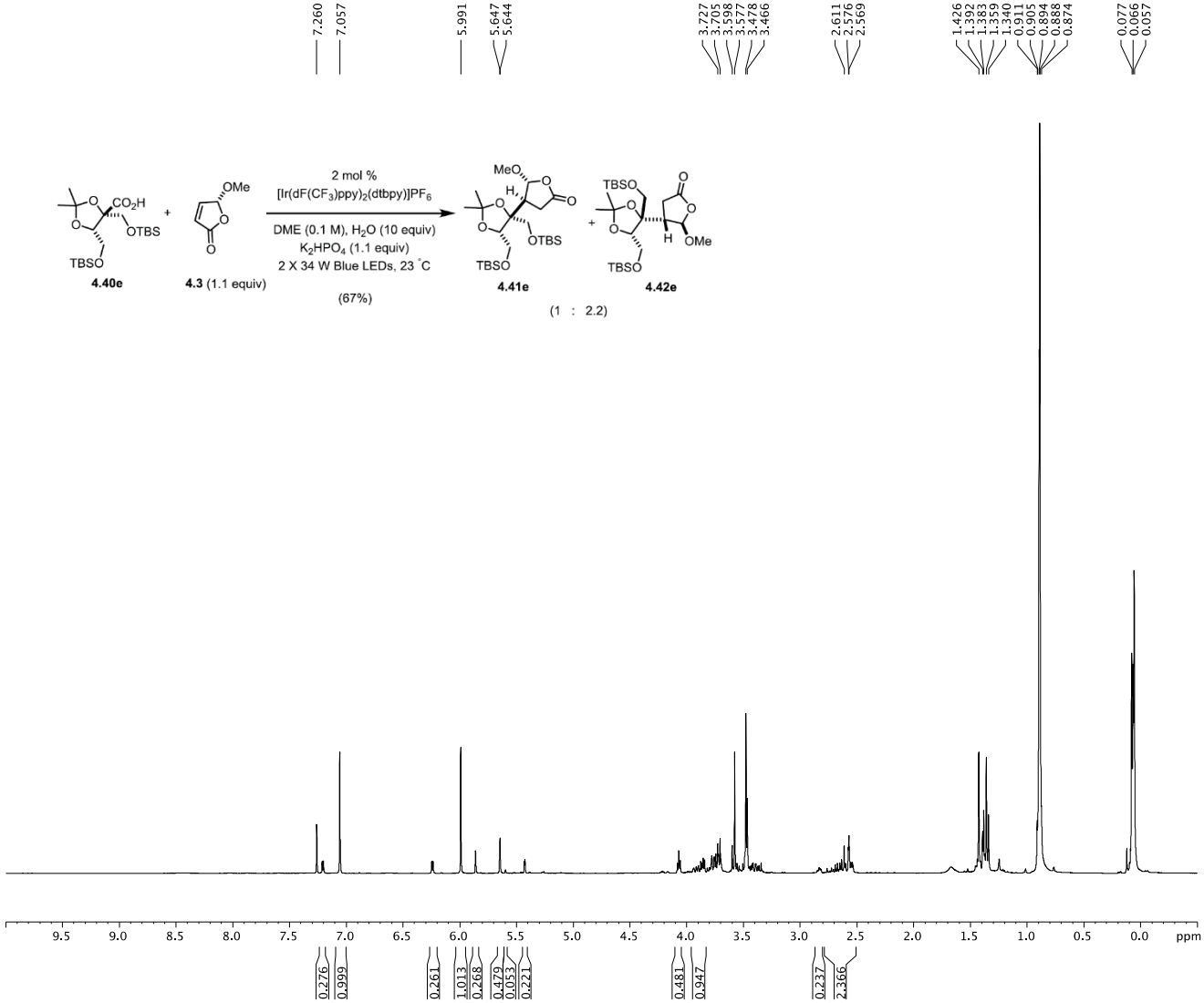

Current Data Parameters
NAME YS-IV-44
EXPNO 1
PROCNO 1

F2 - Acquisition Parameters
Date_ 20160119
Time 9.31
INSTRUM cryo500
PROBHD 5 mm CPTCI 1H-
PULPROG zg30
TD 81728
SOLVENT CDCl3
NS 8
DS 2
SWH 8012.820 Hz
FIDRES 0.098043 Hz
AQ 5.0998273 sec
RG 5.7
DW 62.400 usec
DE 6.00 usec
TE 298.0 K
D1 0.10000000 sec
MCREST 0 sec
MCWRK 0.01500000 sec

======== CHANNEL f1 ========
NUC1 1H
P1 7.50 usec
PL1 1.60 dB
SFO1 500.2235015 MHz

F2 - Processing parameters
SI 65536
SF 500.2200304 MHz
WDW EM
SSB 0
LB 0.30 Hz
GB 0
PC 4.00

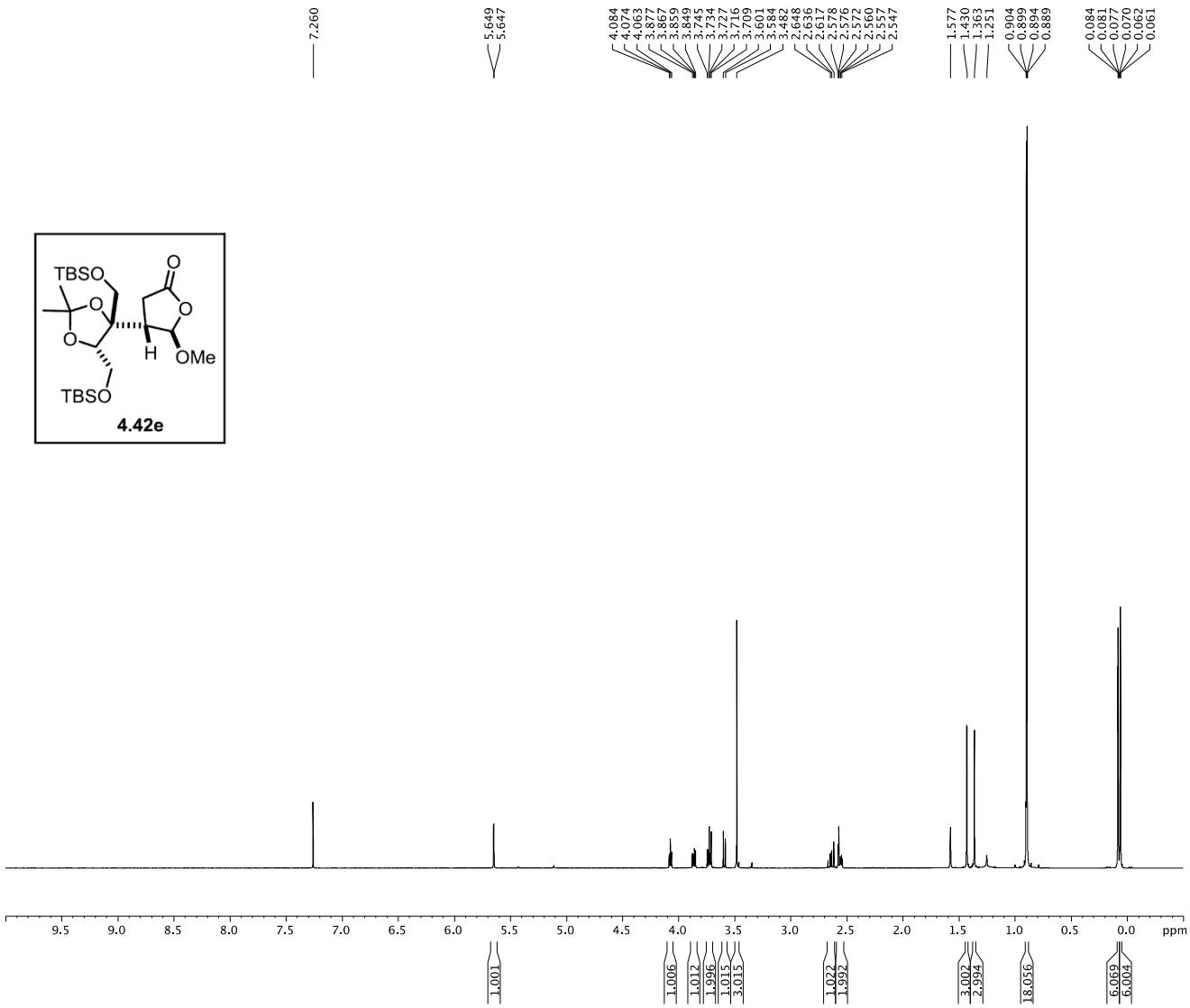

4.42e

```
Current Data Parameters
NAME          YS-IV-44
EXPNO              2
PROCNO             1

F2 - Acquisition Parameters
Date_        20160119
Time            15.47
INSTRUM         av600
PROBHD   5 mm TBI 1H/13
PULPROG          zg30
TD              98074
SOLVENT         CDCl3
NS                 8
DS                 2
SWH          9615.385 Hz
FIDRES       0.098042 Hz
AQ          5.0998478 sec
RG               406
DW            52.000 usec
DE            14.54 usec
TE            298.1 K
D1          0.10000000 sec
TD0                1

======== CHANNEL f1 ========
SFO1       600.1342009 MHz
NUC1             1H
P1             8.00 usec
PLW1        24.00000000 W

F2 - Processing parameters
SI             65536
SF        600.1300357 MHz
WDW              EM
SSB      0
LB            0.30 Hz
GB       0
PC             1.00
```

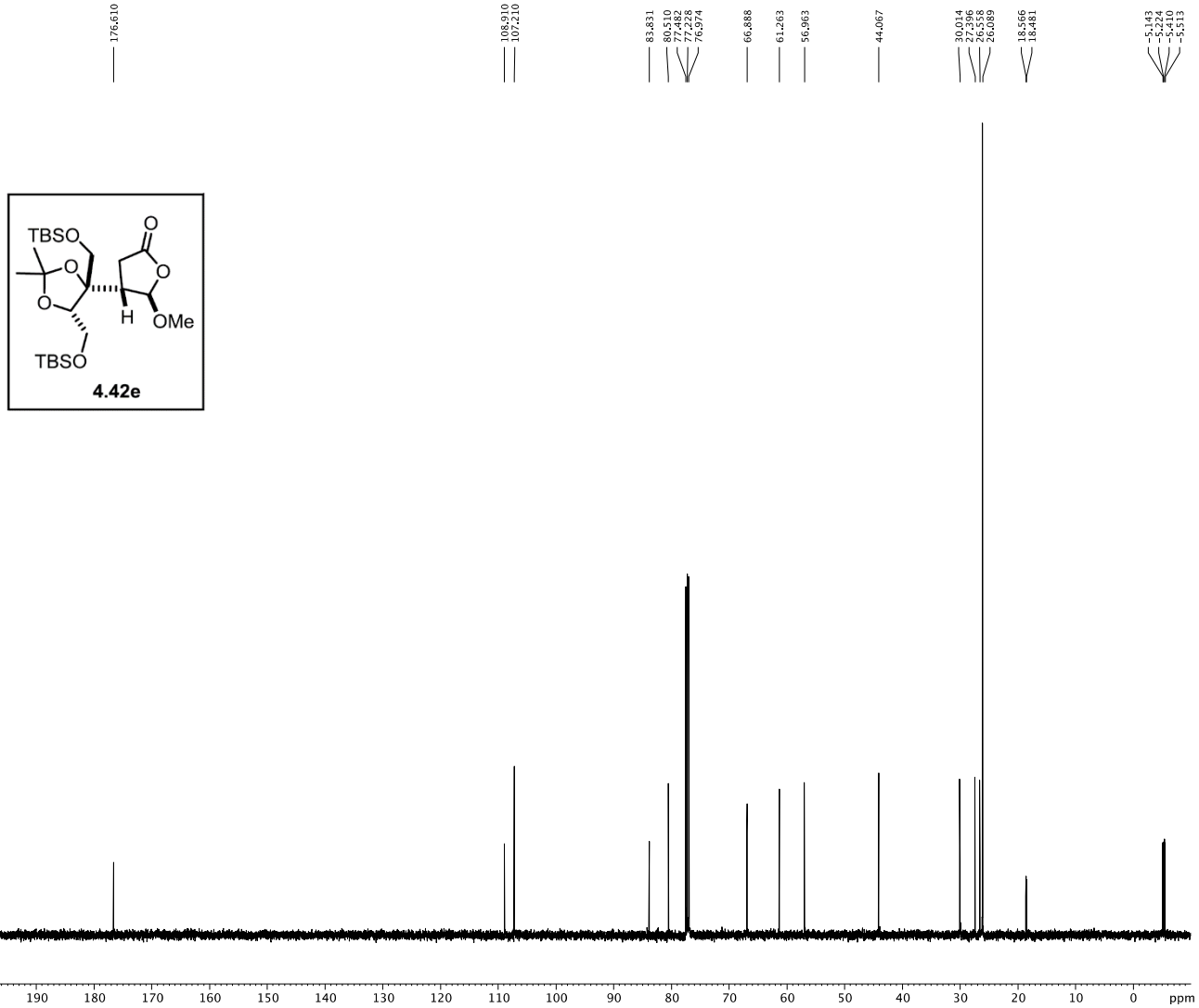

4.42e

```
Current Data Parameters
NAME          YS-IV-44
EXPNO              3
PROCNO             1

F2 - Acquisition Parameters
Date_        20160119
Time           16.13
INSTRUM       cryo500
PROBHD  5 mm CPTCI 1H-
PULPROG  SpinEchopg30gp.prd
TD            65536
SOLVENT         CDCl3
NS              200
DS               16
SWH         30303.031 Hz
FIDRES       0.462388 Hz
AQ          1.0813440 sec
RG            7298.2
DW            16.500 usec
DE             6.00 usec
TE            298.0 K
D1         0.25000000 sec
d11        0.03000000 sec
D16        0.00020000 sec
d17        0.00019600 sec
MCREST   0 sec
MCWRK      0.01500000 sec
P2            33.10 usec

======== CHANNEL f1 ========
NUC1             13C
P1            16.55 usec
P11           500.00 usec
P12          2000.00 usec
PL0           120.00 dB
PL1           -1.00 dB
SFO1       125.7942548 MHz
SP1            2.70 dB
SP2            2.70 dB
SPNAM[1] Crp60,0.5,20.1
SPNAM[2]    Crp60comp.4
SPOFF1   0 Hz
SPOFF2   0 Hz

======== CHANNEL f2 ========
CPDPRG[2        waltz16
NUC2             1H
PCPD2          100.00 usec
PL2            1.60 dB
PL12           24.50 dB
SFO2       500.2225011 MHz

====== GRADIENT CHANNEL =====
GPNAM[1]       SINE.100
GPNAM[2]       SINE.100
GPX1     0 %
GPX2     0 %
GPY1     0 %
GPY2     0 %
GPZ1           30.00 %
GPZ2           50.00 %
p15           500.00 usec
p16          1000.00 usec

F2 - Processing parameters
SI            65536
SF       125.7803991 MHz
WDW              EM
SSB     0
LB            1.00 Hz
GB      0
PC            2.00
```

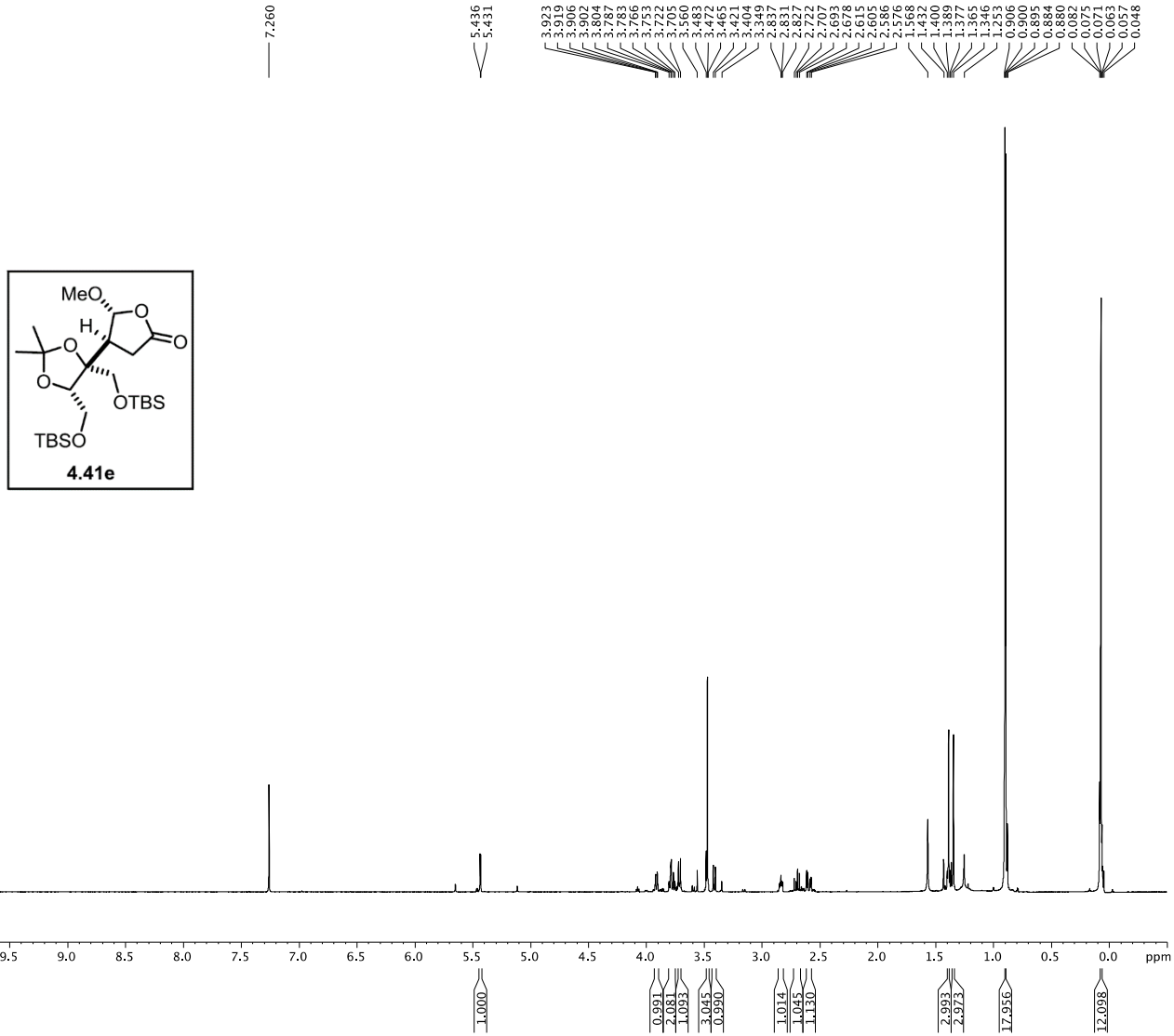

4.41e

Current Data Parameters
NAME YS-IV-44
EXPNO 4
PROCNO 1

F2 - Acquisition Parameters
Date_ 20160119
Time 15.50
INSTRUM av600
PROBHD 5 mm TBI 1H/13
PULPROG zg30
TD 98074
SOLVENT CDCl3
NS 8
DS 2
SWH 9615.385 Hz
FIDRES 0.098042 Hz
AQ 5.0998478 sec
RG 575
DW 52.000 usec
DE 14.54 usec
TE 298.0 K
D1 0.10000000 sec
TD0 1

======== CHANNEL f1 ========
SFO1 600.1342009 MHz
NUC1 1H
P1 8.00 usec
PLW1 24.00000000 W

F2 - Processing parameters
SI 65536
SF 600.1300351 MHz
WDW EM
SSB 0
LB 0.30 Hz
GB 0
PC 1.00

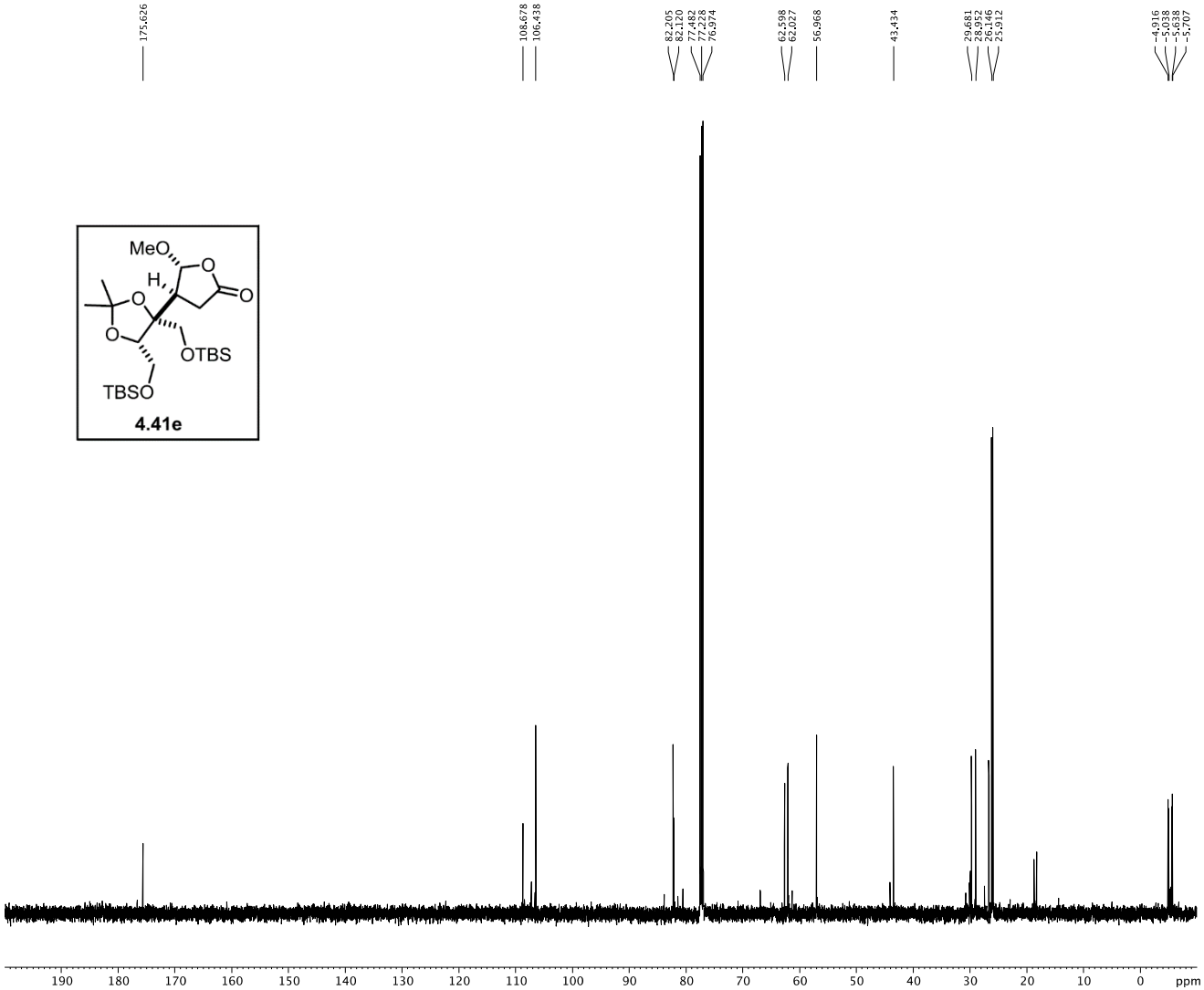

Current Data Parameters
NAME YS-IV-44
EXPNO 5
PROCNO 1

F2 - Acquisition Parameters
Date_ 20160119
Time 16.31
INSTRUM cryo500
PROBHD 5 mm CPTCI 1H-
PULPROG SpinEchopg30gp.prd
TD 65536
SOLVENT CDCl3
NS 320
DS 16
SWH 30303.031 Hz
FIDRES 0.462388 Hz
AQ 1.0813440 sec
RG 7298.2
DW 16.500 usec
DE 6.00 usec
TE 298.0 K
D1 0.25000000 sec
d11 0.03000000 sec
D16 0.00020000 sec
d17 0.00019600 sec
MCREST 0 sec
MCWRK 0.01500000 sec
P2 33.10 usec

======== CHANNEL f1 ========
NUC1 13C
P1 16.55 usec
P11 500.00 usec
P12 2000.00 usec
PL0 120.00 dB
PL1 -1.00 dB
SFO1 125.7942548 MHz
SP1 2.70 dB
SP2 2.70 dB
SPNAM[1] Crp60,0.5,20.1
SPNAM[2] Crp60comp.4
SPOFF1 0 Hz
SPOFF2 0 Hz

======== CHANNEL f2 ========
CPDPRG[2 waltz16
NUC2 1H
PCPD2 100.00 usec
PL2 1.60 dB
PL12 24.50 dB
SFO2 500.2225011 MHz

====== GRADIENT CHANNEL =====
GPNAM[1] SINE.100
GPNAM[2] SINE.100
GPX1 0 %
GPX2 0 %
GPY1 0 %
GPY2 0 %
GPZ1 30.00 %
GPZ2 50.00 %
p15 500.00 usec
p16 1000.00 usec

F2 - Processing parameters
SI 65536
SF 125.7803990 MHz
WDW EM
SSB 0
LB 1.00 Hz
GB 0
PC 2.00

1H spectrum

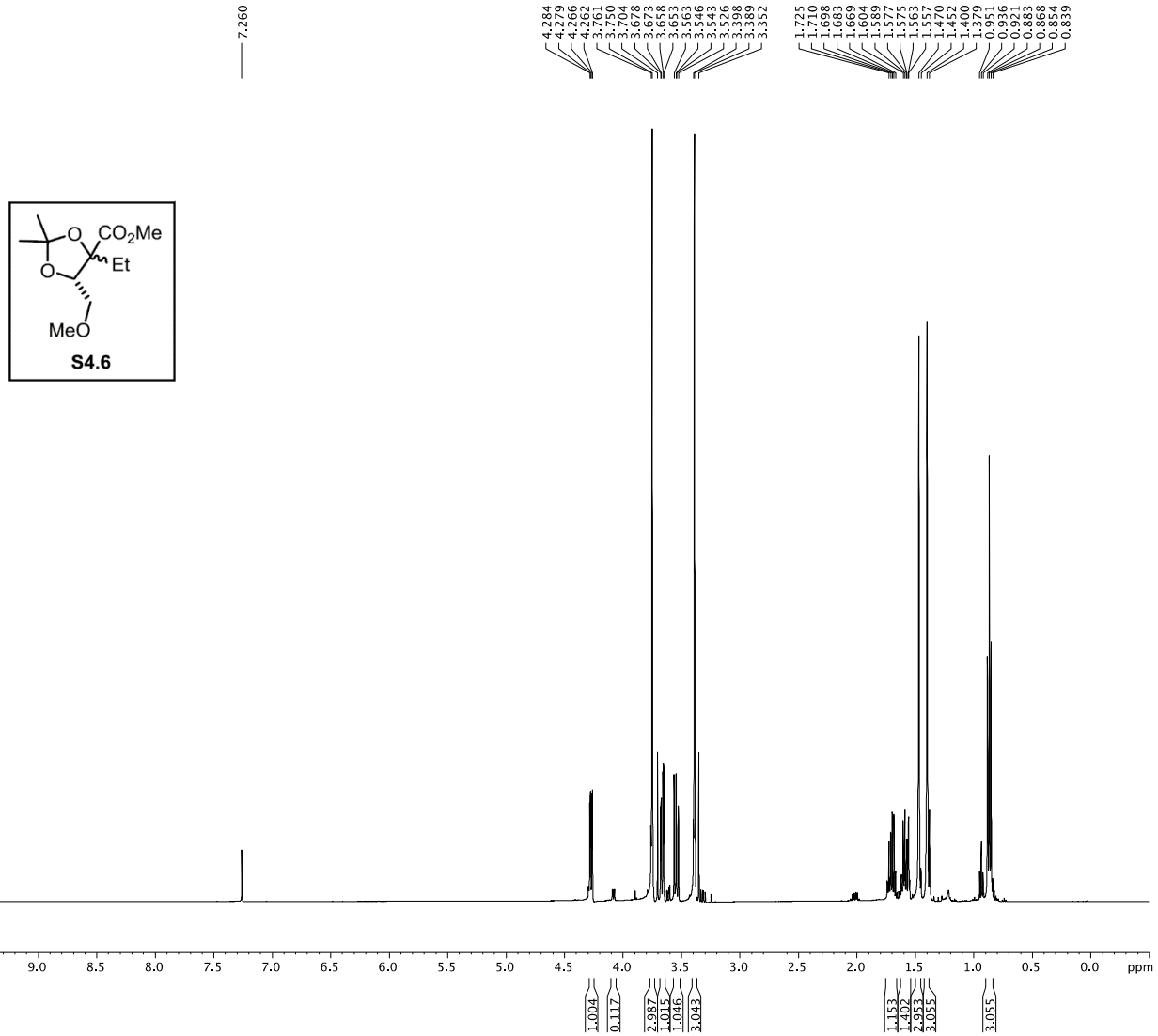

Current Data Parameters
NAME DJT-VI-161
EXPNO 5
PROCNO 1

F2 - Acquisition Parameters
Date_ 20160112
Time 15.17
INSTRUM cryo500
PROBHD 5 mm CPTCI 1H-
PULPROG zg30
TD 81728
SOLVENT CDCl3
NS 10
DS 0
SWH 8012.820 Hz
FIDRES 0.098043 Hz
AQ 5.0998273 sec
RG 5.7
DW 62.400 usec
DE 6.00 usec
TE 298.0 K
D1 0.10000000 sec
MCREST 0 sec
MCWRK 0.01500000 sec

======== CHANNEL f1 =====
NUC1 1H
P1 7.50 usec
PL1 1.60 dB
SFO1 500.2235015 MHz

F2 - Processing parameters
SI 65536
SF 500.2200302 MHz
WDW EM
SSB 0
LB 0.30 Hz
GB 0
PC 4.00

Z-restored spin-echo 13C spectrum with 1H decoupling

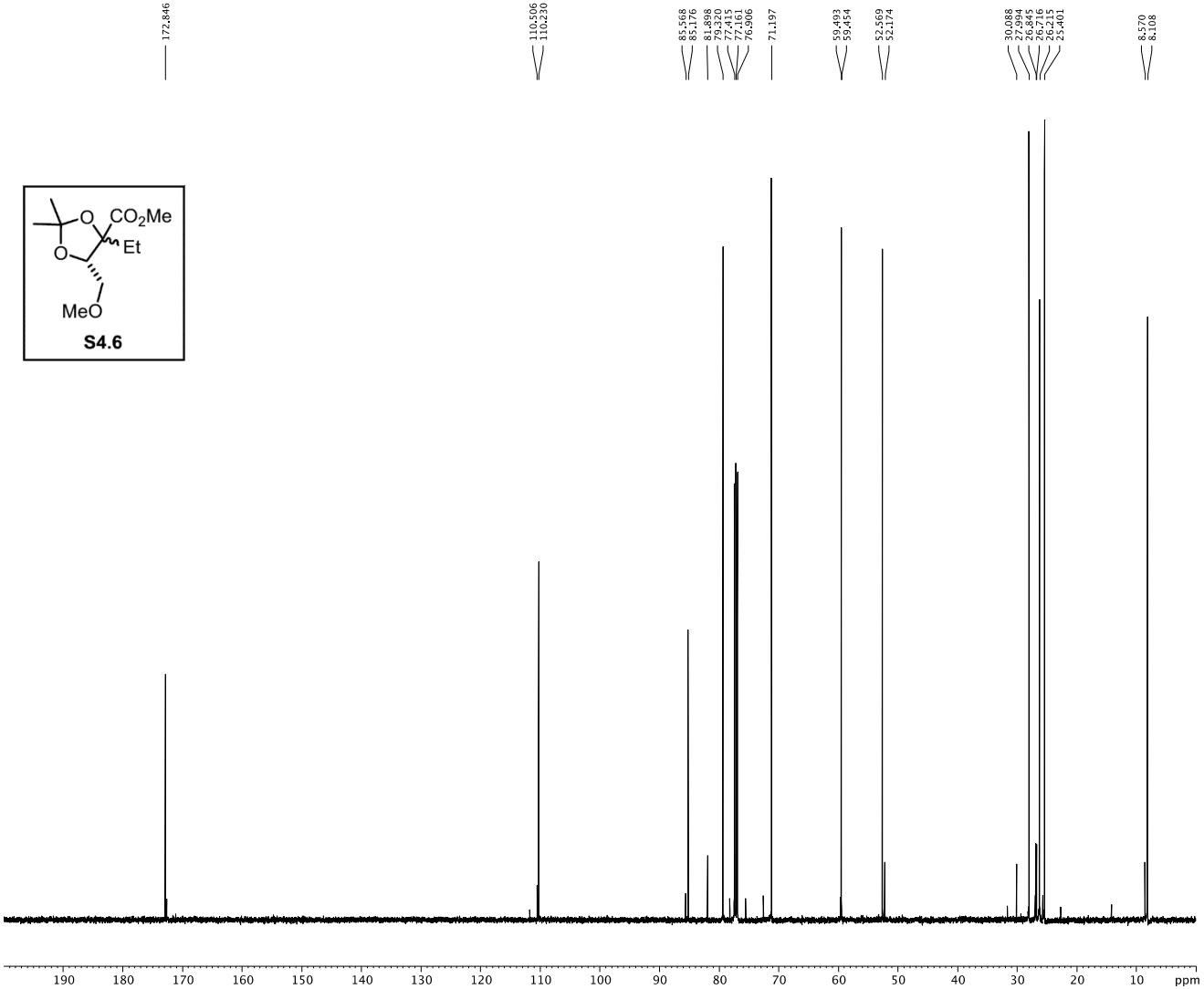

Current Data Parameters
NAME DJT-VI-161
EXPNO 6
PROCNO 1

F2 - Acquisition Parameters
Date_ 20160112
Time 15.21
INSTRUM cryo500
PROBHD 5 mm CPTCI 1H-
PULPROG SpinEchopg30gp.prd
TD 65536
SOLVENT CDCl3
NS 253
DS 0
SWH 30303.031 Hz
FIDRES 0.462388 Hz
AQ 1.0813440 sec
RG 7298.2
DW 16.500 usec
DE 6.00 usec
TE 298.0 K
D1 0.25000000 sec
d11 0.03000000 sec
D16 0.00020000 sec
d17 0.00019600 sec
MCREST 0 sec
MCWRK 0.01500000 sec
P2 33.10 usec

======== CHANNEL f1 ========
NUC1 13C
P1 16.55 usec
P11 500.00 usec
P12 2000.00 usec
PL0 120.00 dB
PL1 -1.00 dB
SFO1 125.7942548 MHz
SP1 2.70 dB
SP2 2.70 dB
SPNAM[1] Crp60,0.5,20.1
SPNAM[2] Crp60comp.4
SPOFF1 0 Hz
SPOFF2 0 Hz

======== CHANNEL f2 ========
CPDPRG[2 waltz16
NUC2 1H
PCPD2 100.00 usec
PL2 1.60 dB
PL12 24.50 dB
SFO2 500.2225011 MHz

====== GRADIENT CHANNEL =====
GPNAM[1] SINE.100
GPNAM[2] SINE.100
GPX1 0 %
GPX2 0 %
GPY1 0 %
GPY2 0 %
GPZ1 30.00 %
GPZ2 50.00 %
p15 500.00 usec
p16 1000.00 usec

F2 - Processing parameters
SI 65536
SF 125.7804145 MHz
WDW EM
SSB 0
LB 1.00 Hz
GB 0
PC 2.00

1H spectrum

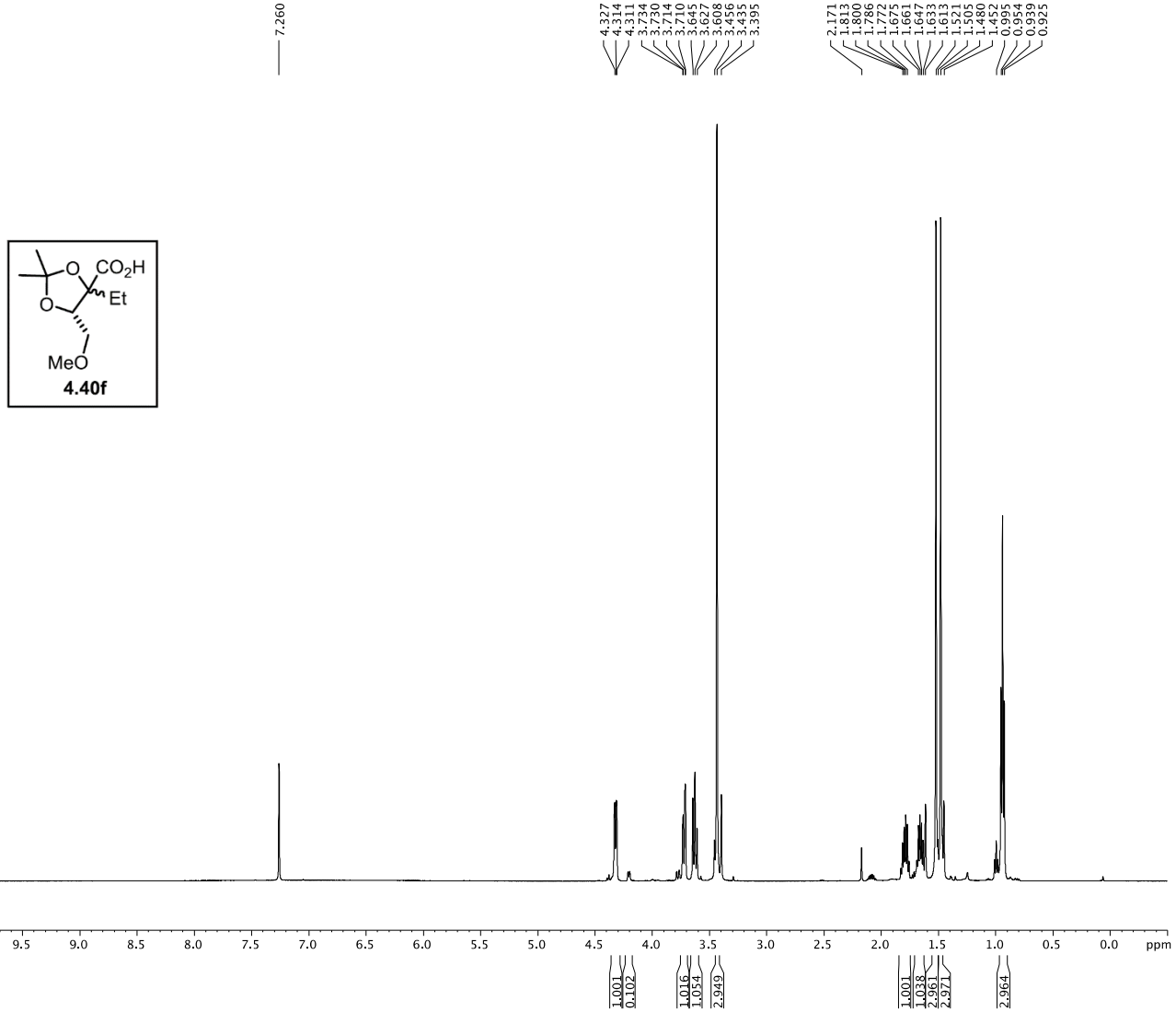

4.40f

```
Current Data Parameters
NAME        DJT-VI-164
EXPNO            2
PROCNO           1

F2 - Acquisition Parameters
Date_       20160115
Time          10.35
INSTRUM       cryo500
PROBHD   5 mm CPTCI 1H-
PULPROG         zg30
TD            81728
SOLVENT       CDCl3
NS              10
DS               0
SWH         8012.820 Hz
FIDRES      0.098043 Hz
AQ          5.0998273 sec
RG               9
DW            62.400 usec
DE             6.00 usec
TE            298.0 K
D1          0.10000000 sec
MCREST   0 sec
MCWRK       0.01500000 sec

======== CHANNEL f1 =====
NUC1             1H
P1            7.50 usec
PL1           1.60 dB
SFO1       500.2235015 MHz

F2 - Processing parameters
SI           65536
SF        500.2200299 MHz
WDW             EM
SSB      0
LB            0.30 Hz
GB       0
PC            4.00
```

Z-restored spin-echo 13C spectrum with 1H decoupling

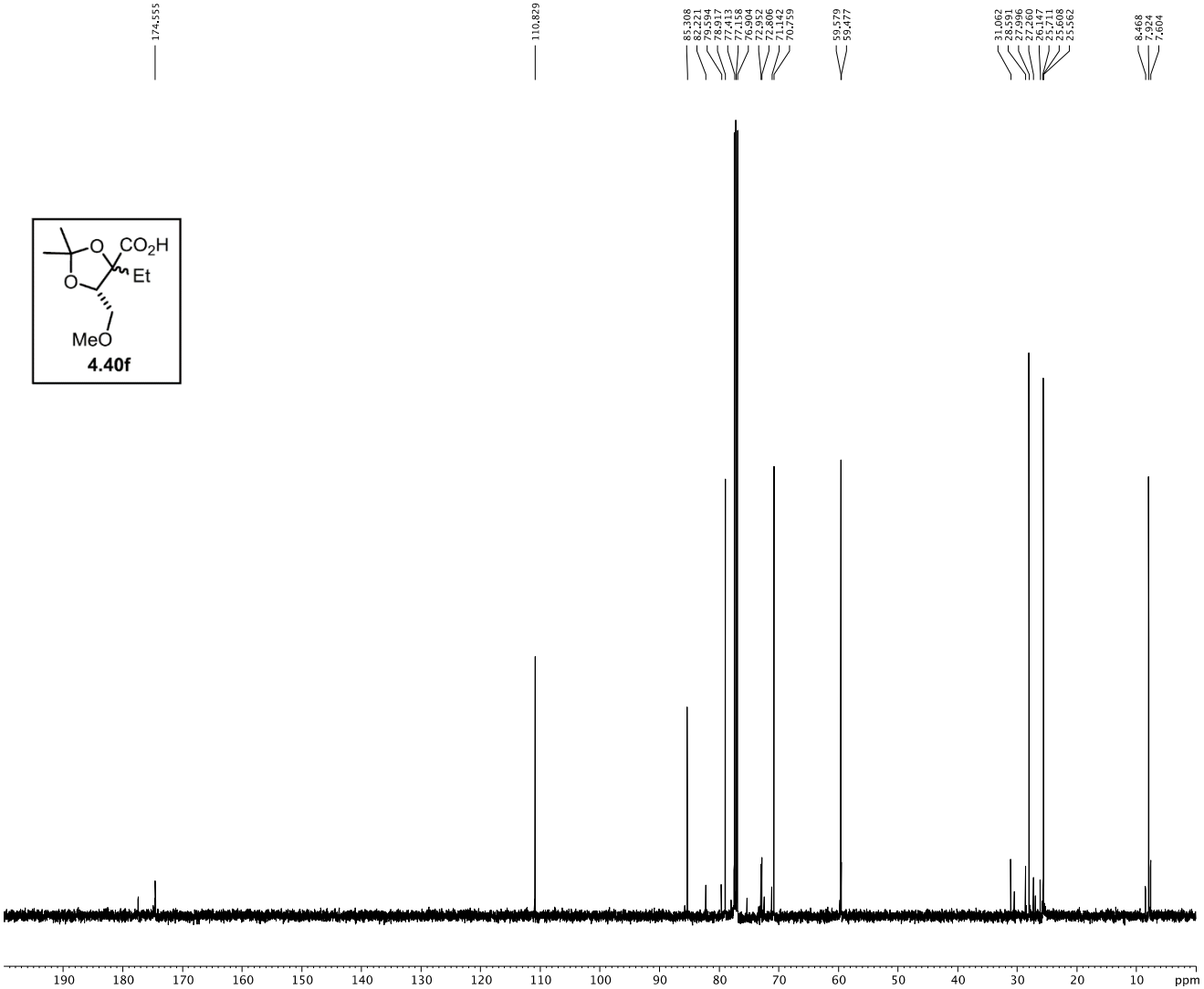

Current Data Parameters
NAME DJT-VI-164
EXPNO 4
PROCNO 1

F2 - Acquisition Parameters
Date_ 20160115
Time 14.44
INSTRUM cryo500
PROBHD 5 mm CPTCI 1H-
PULPROG SpinEchopg30gp.prd
TD 65536
SOLVENT CDCl3
NS 284
DS 0
SWH 30303.031 Hz
FIDRES 0.462388 Hz
AQ 1.0813440 sec
RG 6502
DW 16.500 usec
DE 6.00 usec
TE 298.0 K
D1 0.25000000 sec
d11 0.03000000 sec
D16 0.00020000 sec
d17 0.00019600 sec
MCREST 0 sec
MCWRK 0.01500000 sec
P2 33.10 usec

======== CHANNEL f1 ========
NUC1 13C
P1 16.55 usec
P11 500.00 usec
P12 2000.00 usec
PL0 120.00 dB
PL1 -1.00 dB
SFO1 125.7942548 MHz
SP1 2.70 dB
SP2 2.70 dB
SPNAM[1] Crp60.0.5.20.1
SPNAM[2] Crp60comp.4
SPOFF1 0 Hz
SPOFF2 0 Hz

======== CHANNEL f2 ========
CPDPRG[2 waltz16
NUC2 1H
PCPD2 100.00 usec
PL2 1.60 dB
PL12 24.50 dB
SFO2 500.2225011 MHz

====== GRADIENT CHANNEL =====
GPNAM[1] SINE.100
GPNAM[2] SINE.100
GPX1 0 %
GPX2 0 %
GPY1 0 %
GPY2 0 %
GPZ1 30.00 %
GPZ2 50.00 %
p15 500.00 usec
p16 1000.00 usec

F2 - Processing parameters
SI 65536
SF 125.7804099 MHz
WDW EM
SSB 0
LB 1.00 Hz
GB 0
PC 2.00

1H spectrum

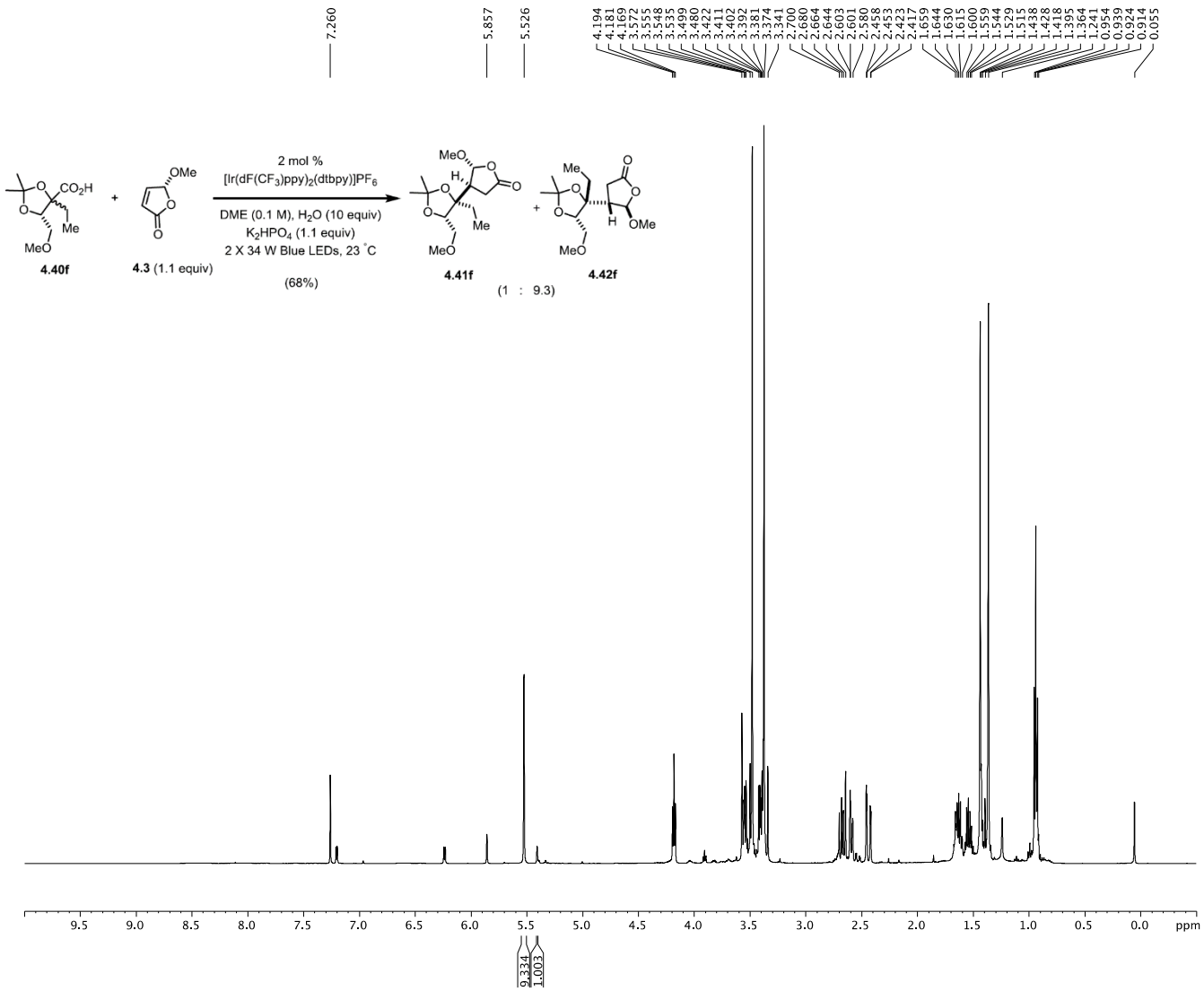

Current Data Parameters
NAME DJT-VI-165
EXPNO 1
PROCNO 1

F2 - Acquisition Parameters
Date_ 20160116
Time 16.28
INSTRUM cryo500
PROBHD 5 mm CPTCI 1H-
PULPROG zg30
TD 81728
SOLVENT CDCl3
NS 20
DS 0
SWH 8012.820 Hz
FIDRES 0.098043 Hz
AQ 5.0998273 sec
RG 6.3
DW 62.400 usec
DE 6.00 usec
TE 298.0 K
D1 0.10000000 sec
MCREST 0 sec
MCWRK 0.01500000 sec

======== CHANNEL f1 =====
NUC1 1H
P1 7.50 usec
PL1 1.60 dB
SFO1 500.2235015 MHz

F2 - Processing parameters
SI 65536
SF 500.2200299 MHz
WDW EM
SSB 0
LB 0.30 Hz
GB 0
PC 4.00

1H spectrum

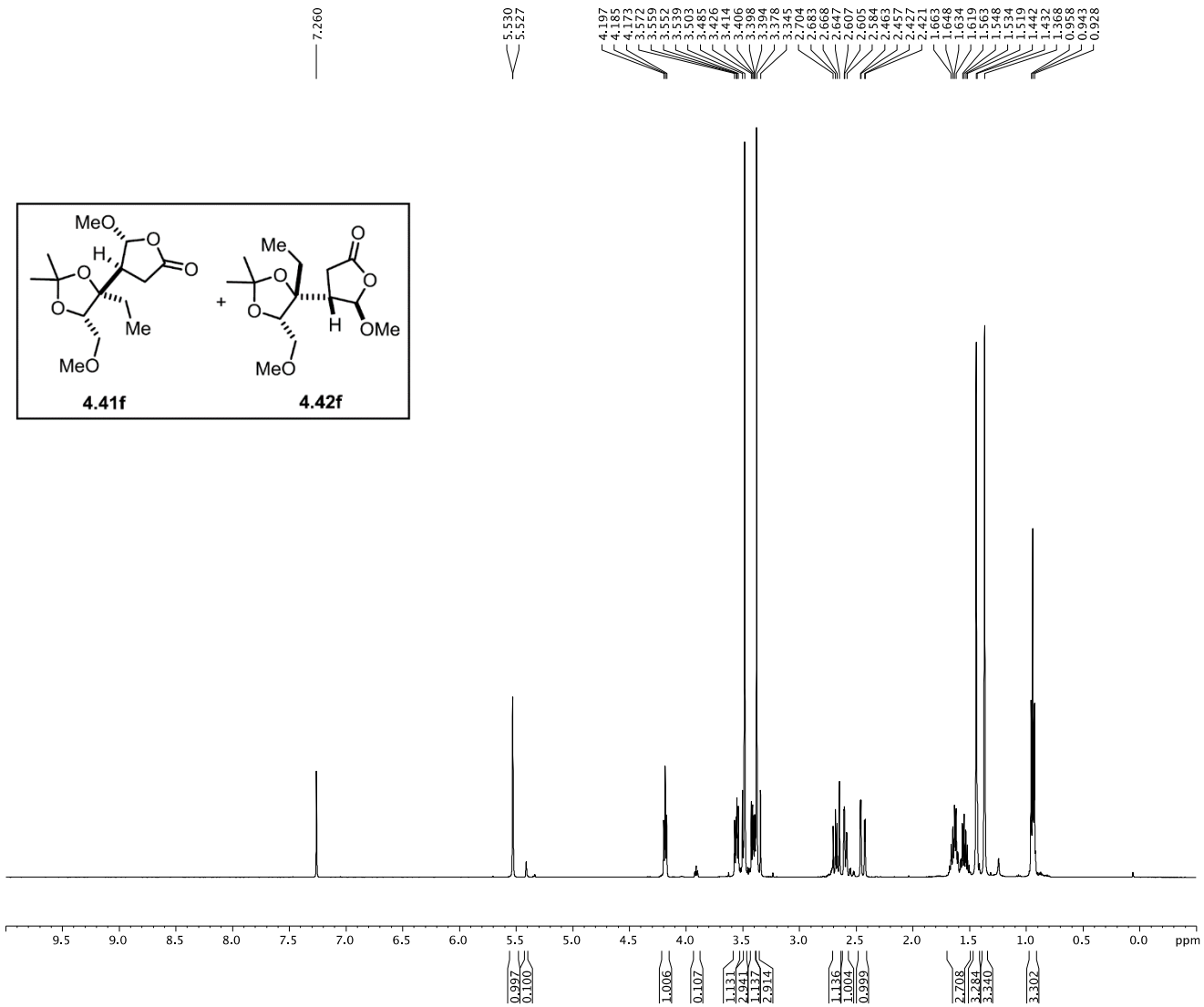

Current Data Parameters
NAME DJT-VI-165
EXPNO 2
PROCNO 1

F2 - Acquisition Parameters
Date_ 20160118
Time 10.01
INSTRUM cryo500
PROBHD 5 mm CPTCI 1H-
PULPROG zg30
TD 81728
SOLVENT CDCl3
NS 20
DS 0
SWH 8012.820 Hz
FIDRES 0.098043 Hz
AQ 5.0998273 sec
RG 6.3
DW 62.400 usec
DE 6.00 usec
TE 298.0 K
D1 0.10000000 sec
MCREST 0 sec
MCWRK 0.01500000 sec

======== CHANNEL f1 =====
NUC1 1H
P1 7.50 usec
PL1 1.60 dB
SFO1 500.2235015 MHz

F2 - Processing parameters
SI 65536
SF 500.2200302 MHz
WDW EM
SSB 0
LB 0.30 Hz
GB 0
PC 4.00

Z-restored spin-echo 13C spectrum with 1H decoupling

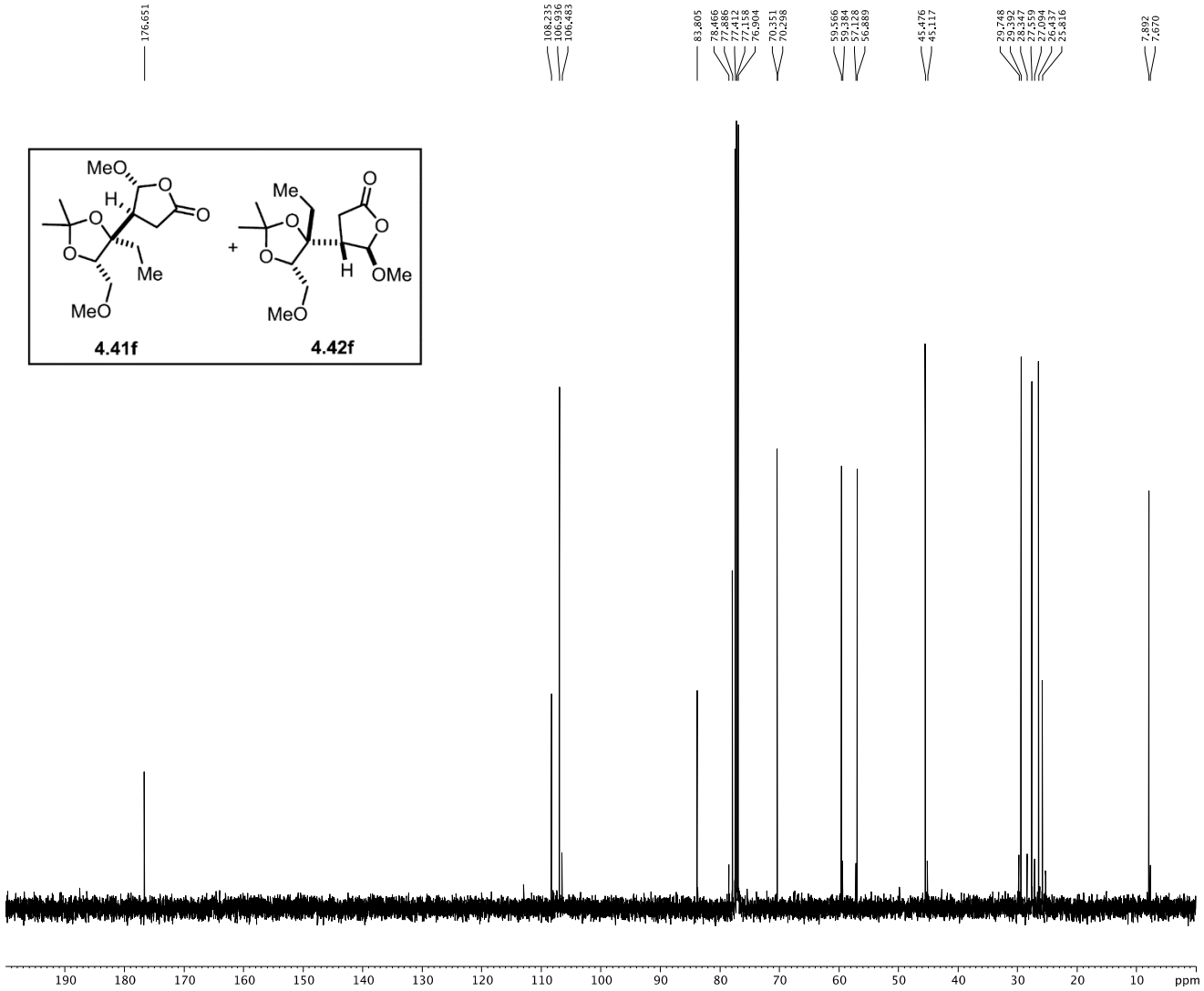

Current Data Parameters
NAME DJT-VI-165
EXPNO 3
PROCNO 1

F2 - Acquisition Parameters
Date_ 20160118
Time 10.05
INSTRUM cryo500
PROBHD 5 mm CPTCI 1H-
PULPROG SpinEchopg30gp.prd
TD 65536
SOLVENT CDCl3
NS 124
DS 0
SWH 30303.031 Hz
FIDRES 0.462388 Hz
AQ 1.0813440 sec
RG 5792.6
DW 16.500 usec
DE 6.00 usec
TE 298.0 K
D1 0.25000000 sec
d11 0.03000000 sec
D16 0.00020000 sec
d17 0.00019600 sec
MCREST 0 sec
MCWRK 0.01500000 sec
P2 33.10 usec

======== CHANNEL f1 ========
NUC1 13C
P1 16.55 usec
P11 500.00 usec
P12 2000.00 usec
PL0 120.00 dB
PL1 -1.00 dB
SFO1 125.7942548 MHz
SP1 2.70 dB
SP2 2.70 dB
SPNAM[1] Crp60,0.5,20.1
SPNAM[2] Crp60comp.4
SPOFF1 0 Hz
SPOFF2 0 Hz

======== CHANNEL f2 ========
CPDPRG[2 waltz16
NUC2 1H
PCPD2 100.00 usec
PL2 1.60 dB
PL12 24.50 dB
SFO2 500.2225011 MHz

====== GRADIENT CHANNEL =====
GPNAM[1] SINE.100
GPNAM[2] SINE.100
GPX1 0 %
GPX2 0 %
GPY1 0 %
GPY2 0 %
GPZ1 30.00 %
GPZ2 50.00 %
p15 500.00 usec
p16 1000.00 usec

F2 - Processing parameters
SI 65536
SF 125.7804089 MHz
WDW EM
SSB 0
LB 1.00 Hz
GB 0
PC 2.00

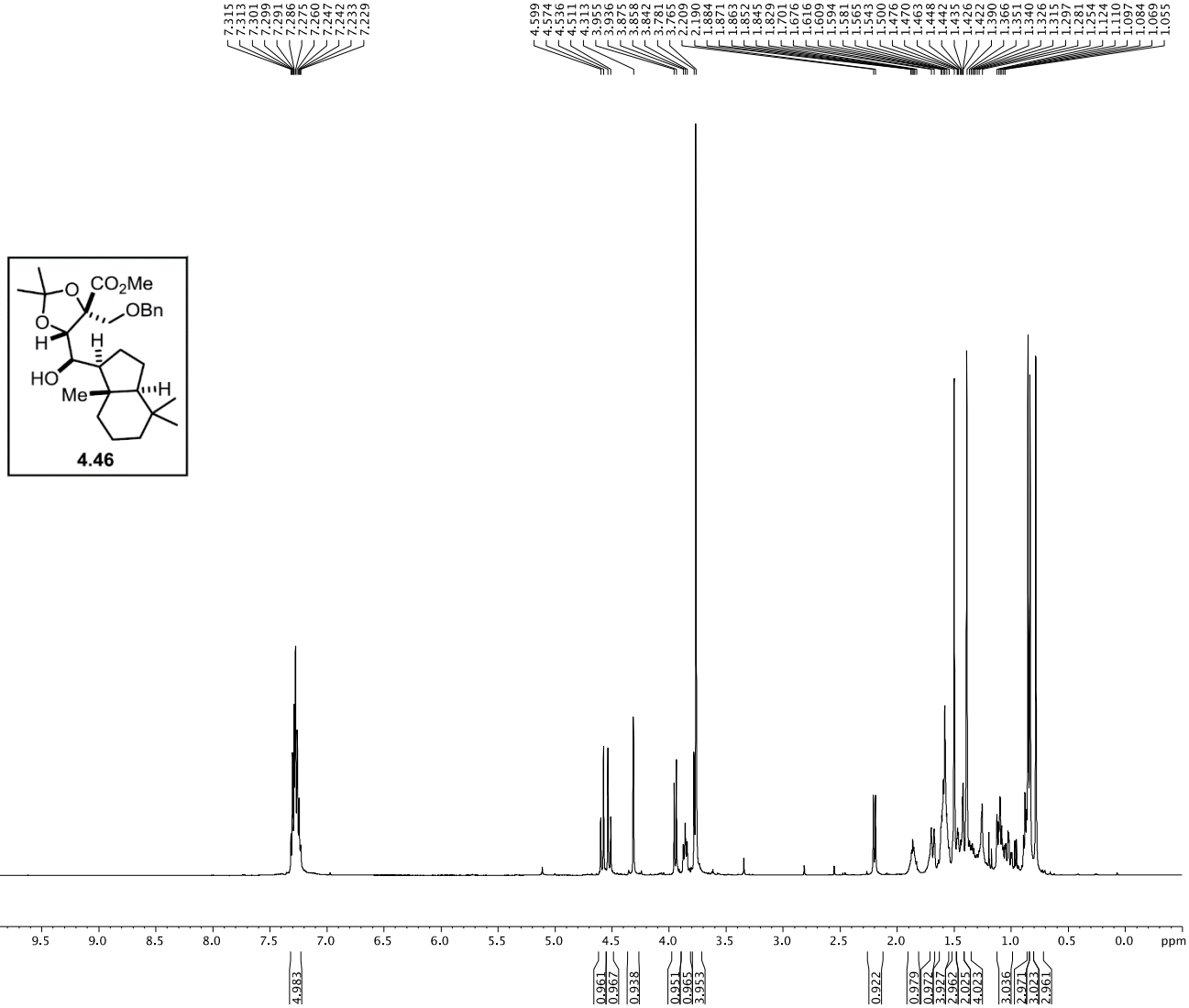

Current Data Parameters
NAME YS-IV-55
EXPNO 1
PROCNO 1

F2 - Acquisition Parameters
Date_ 20160123
Time 13.30
INSTRUM qn500
PROBHD 5 mm broadband
PULPROG zg30
TD 81728
SOLVENT CDCl3T
NS 8
DS 2
SWH 8012.820 Hz
FIDRES 0.098043 Hz
AQ 5.0998273 sec
RG 40.3
DW 62.400 usec
DE 6.00 usec
TE 298.0 K
D1 0.10000000 sec
MCREST 0 sec
MCWRK 0.01500000 sec

======== CHANNEL f1 ========
NUC1 1H
P1 12.00 usec
PL1 -5.80 dB
SFO1 499.1834943 MHz

F2 - Processing parameters
SI 65536
SF 499.1800270 MHz
WDW EM
SSB 0
LB 0.30 Hz
GB 0
PC 1.00

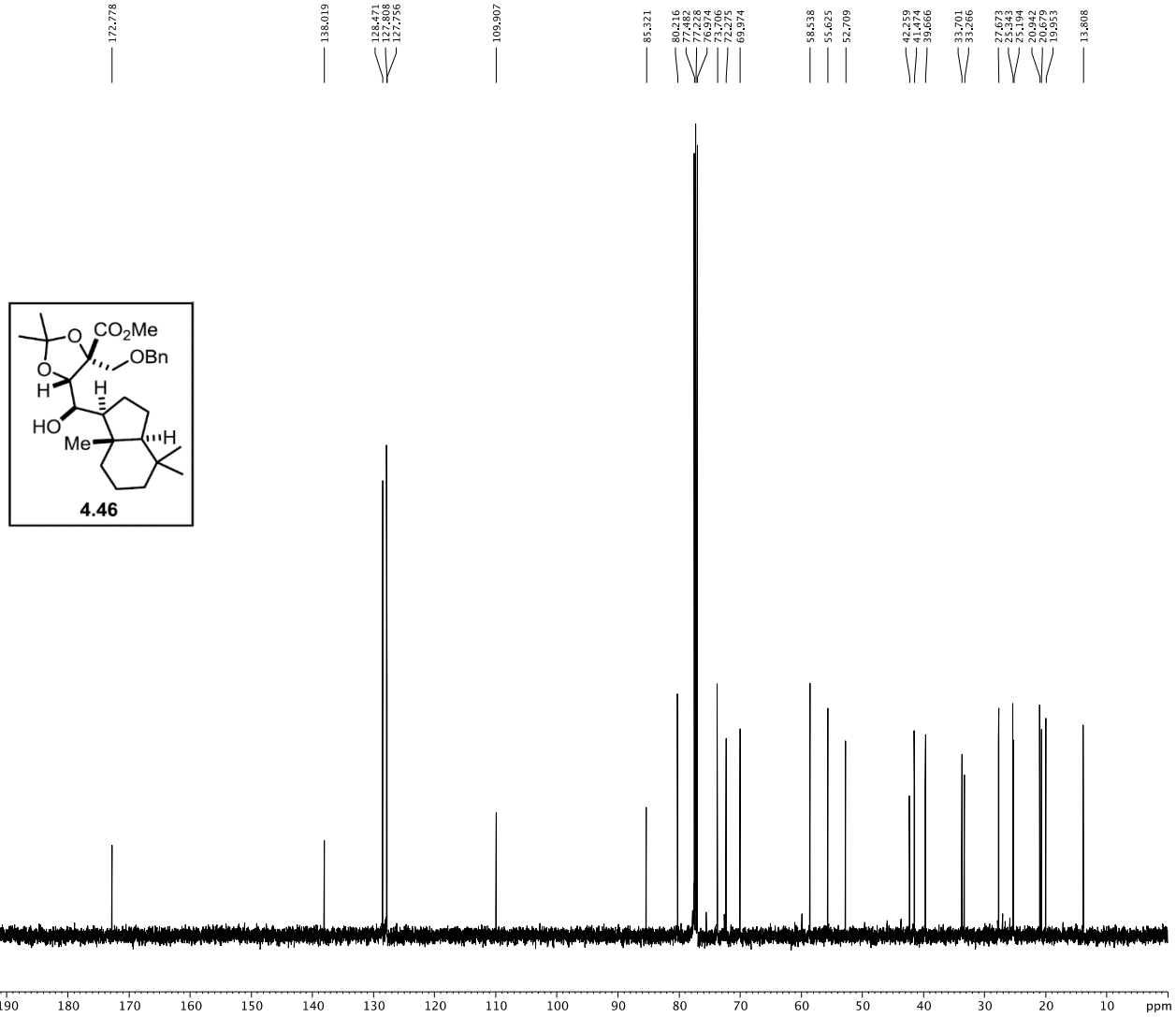

Current Data Parameters
NAME YS-IV-55
EXPNO 4
PROCNO 1

F2 - Acquisition Parameters
Date_ 20160125
Time 16.51
INSTRUM cryo500
PROBHD 5 mm CPTCI 1H-
PULPROG SpinEchopg30gp.prd
TD 65536
SOLVENT CDCl3
NS 256
DS 1
SWH 30303.031 Hz
FIDRES 0.462388 Hz
AQ 1.0813440 sec
RG 7298.2
DW 16.500 usec
DE 6.00 usec
TE 298.0 K
D1 0.50000000 sec
d11 0.03000000 sec
D16 0.00020000 sec
d17 0.00019600 sec
MCREST 0 sec
MCWRK 0.01500000 sec
P2 33.10 usec

======== CHANNEL f1 ========
NUC1 13C
P1 16.55 usec
P11 500.00 usec
P12 2000.00 usec
PL0 120.00 dB
PL1 -1.00 dB
SFO1 125.7942548 MHz
SP1 2.70 dB
SP2 2.70 dB
SPNAM[1] Crp60,0.5,20.1
SPNAM[2] Crp60comp.4
SPOFF1 0 Hz
SPOFF2 0 Hz

======== CHANNEL f2 ========
CPDPRG[2 waltz16
NUC2 1H
PCPD2 100.00 usec
PL2 1.60 dB
PL12 24.50 dB
SFO2 500.2225011 MHz

====== GRADIENT CHANNEL =====
GPNAM[1] SINE.100
GPNAM[2] SINE.100
GPX1 0 %
GPX2 0 %
GPY1 0 %
GPY2 0 %
GPZ1 30.00 %
GPZ2 50.00 %
p15 500.00 usec
p16 1000.00 usec

F2 - Processing parameters
SI 65536
SF 125.7803998 MHz
WDW EM
SSB 0
LB 1.00 Hz
GB 0
PC 2.00

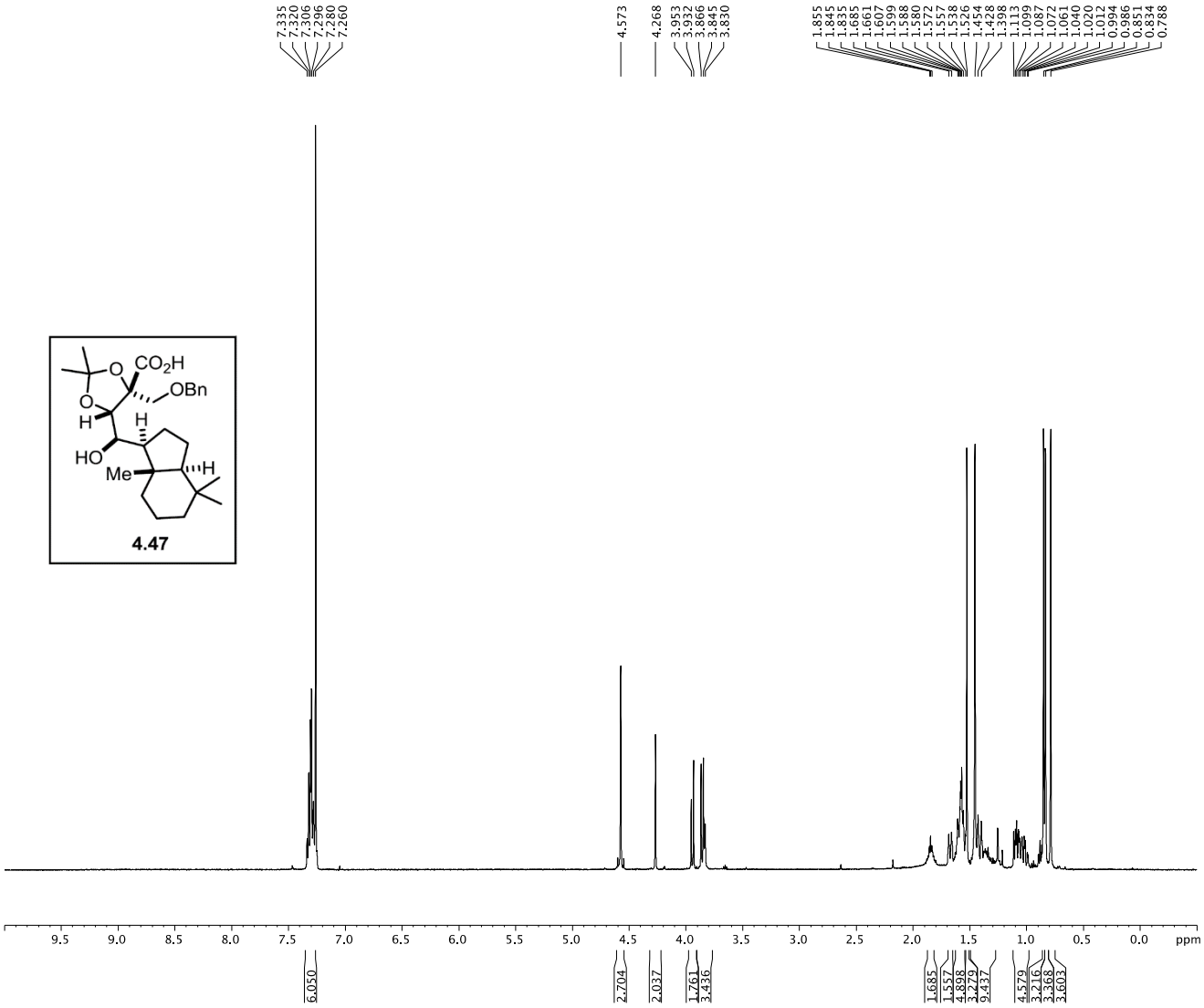

4.47

```
Current Data Parameters
NAME          YS-IV-56
EXPNO            1
PROCNO           1

F2 - Acquisition Parameters
Date_        20160128
Time           12.18
INSTRUM       cryo500
PROBHD   5 mm CPTCI 1H-
PULPROG         zg30
TD            81728
SOLVENT        CDCl3
NS               8
DS               2
SWH          8012.820 Hz
FIDRES       0.098043 Hz
AQ          5.0998273 sec
RG              6.3
DW            62.400 usec
DE             6.00 usec
TE            298.0 K
D1          0.10000000 sec
MCREST   0 sec
MCWRK       0.01500000 sec

======== CHANNEL f1 ========
NUC1             1H
P1            7.50 usec
PL1           1.60 dB
SFO1       500.2235015 MHz

F2 - Processing parameters
SI            65536
SF        500.2200325 MHz
WDW             EM
SSB      0
LB            0.30 Hz
GB       0
PC            4.00
```

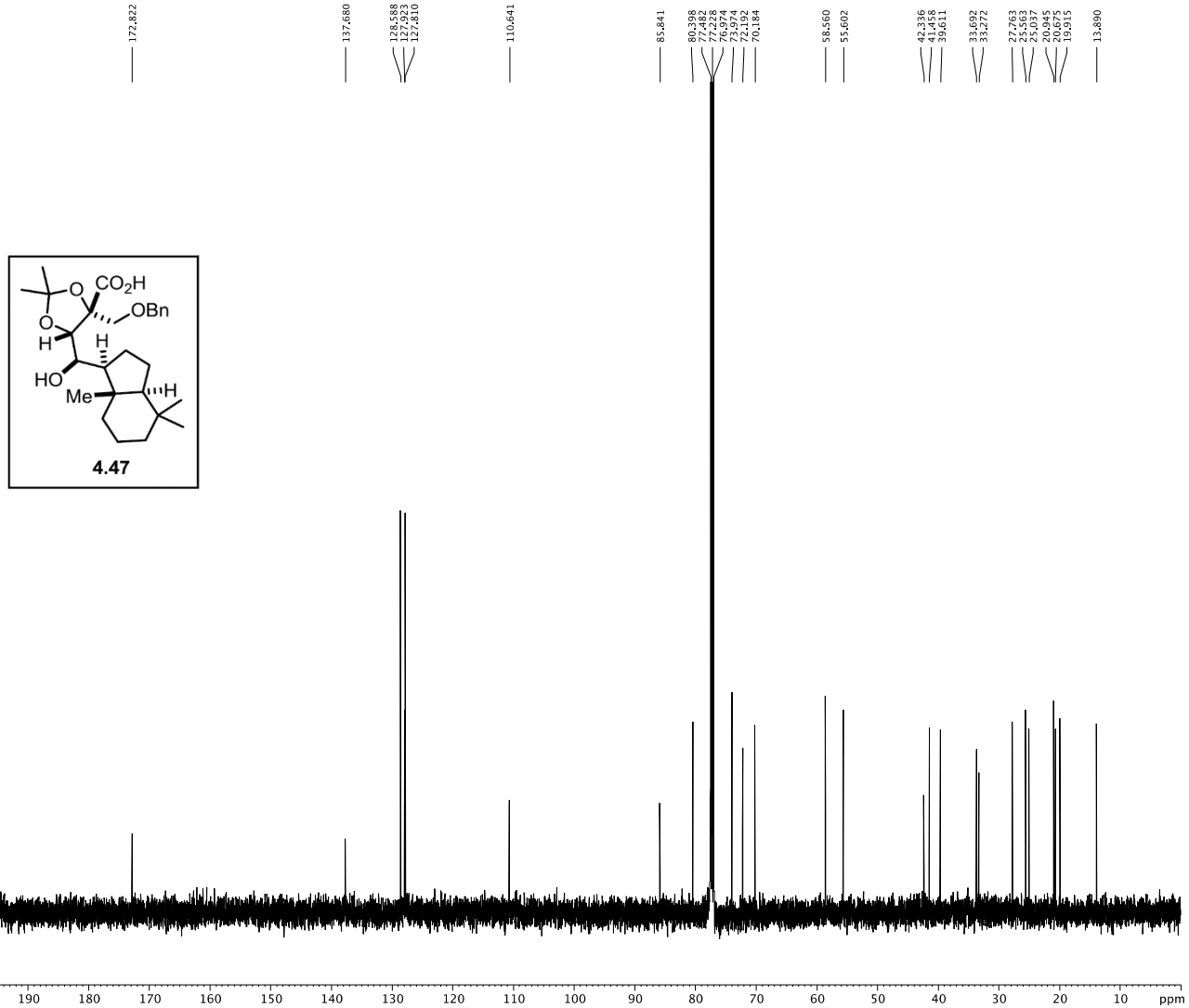


```
Current Data Parameters
NAME          YS-IV-56
EXPNO              2
PROCNO             1

F2 - Acquisition Parameters
Date_        20160128
Time           12.24
INSTRUM        cryo500
PROBHD   5 mm CPTCI 1H-
PULPROG  SpinEchopg30gp.prd
TD           65536
SOLVENT        CDCl3
NS             700
DS               1
SWH          30303.031 Hz
FIDRES        0.462388 Hz
AQ           1.0813440 sec
RG            5792.6
DW             16.500 usec
DE              6.00 usec
TE            298.0 K
D1          0.25000000 sec
d11         0.03000000 sec
D16         0.00020000 sec
d17         0.00019600 sec
MCREST   0 sec
MCWRK       0.01500000 sec
P2             33.10 usec

======== CHANNEL f1 ========
NUC1             13C
P1             16.55 usec
P11            500.00 usec
P12           2000.00 usec
PL0            120.00 dB
PL1             -1.00 dB
SFO1       125.7942548 MHz
SP1              2.70 dB
SP2              2.70 dB
SPNAM[1] Crp60,0.5,20.1
SPNAM[2]   Crp60comp.4
SPOFF1   0 Hz
SPOFF2   0 Hz

======== CHANNEL f2 ========
CPDPRG[2        waltz16
NUC2             1H
PCPD2          100.00 usec
PL2              1.60 dB
PL12            24.50 dB
SFO2       500.2225011 MHz

====== GRADIENT CHANNEL =====
GPNAM[1]       SINE.100
GPNAM[2]       SINE.100
GPX1     0 %
GPX2     0 %
GPY1     0 %
GPY2     0 %
GPZ1            30.00 %
GPZ2            50.00 %
p15            500.00 usec
p16           1000.00 usec

F2 - Processing parameters
SI           65536
SF        125.7803992 MHz
WDW              EM
SSB      0
LB            1.00 Hz
GB       0
PC            2.00
```

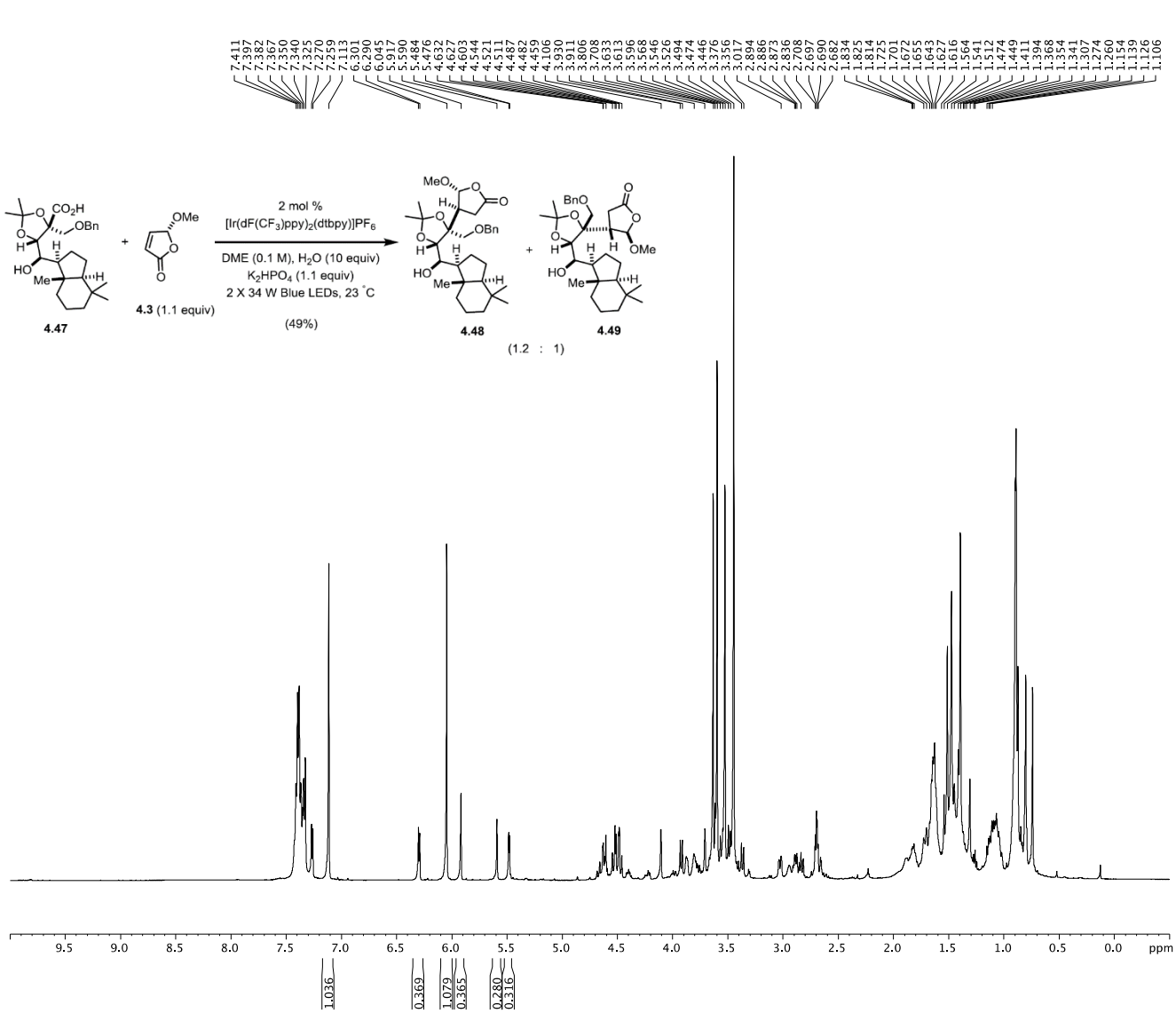

Current Data Parameters
NAME YS-IV-63
EXPNO 1
PROCNO 1

F2 - Acquisition Parameters
Date_ 20160129
Time 14.11
INSTRUM cryo500
PROBHD 5 mm CPTCI 1H-
PULPROG zg30
TD 81728
SOLVENT CDCl3
NS 8
DS 2
SWH 8012.820 Hz
FIDRES 0.098043 Hz
AQ 5.0998273 sec
RG 4.5
DW 62.400 usec
DE 6.00 usec
TE 298.0 K
D1 0.10000000 sec
MCREST 0 sec
MCWRK 0.01500000 sec

======== CHANNEL f1 ========
NUC1 1H
P1 7.50 usec
PL1 1.60 dB
SFO1 500.2235015 MHz

F2 - Processing parameters
SI 65536
SF 500.2199993 MHz
WDW EM
SSB 0
LB 0.30 Hz
GB 0
PC 4.00

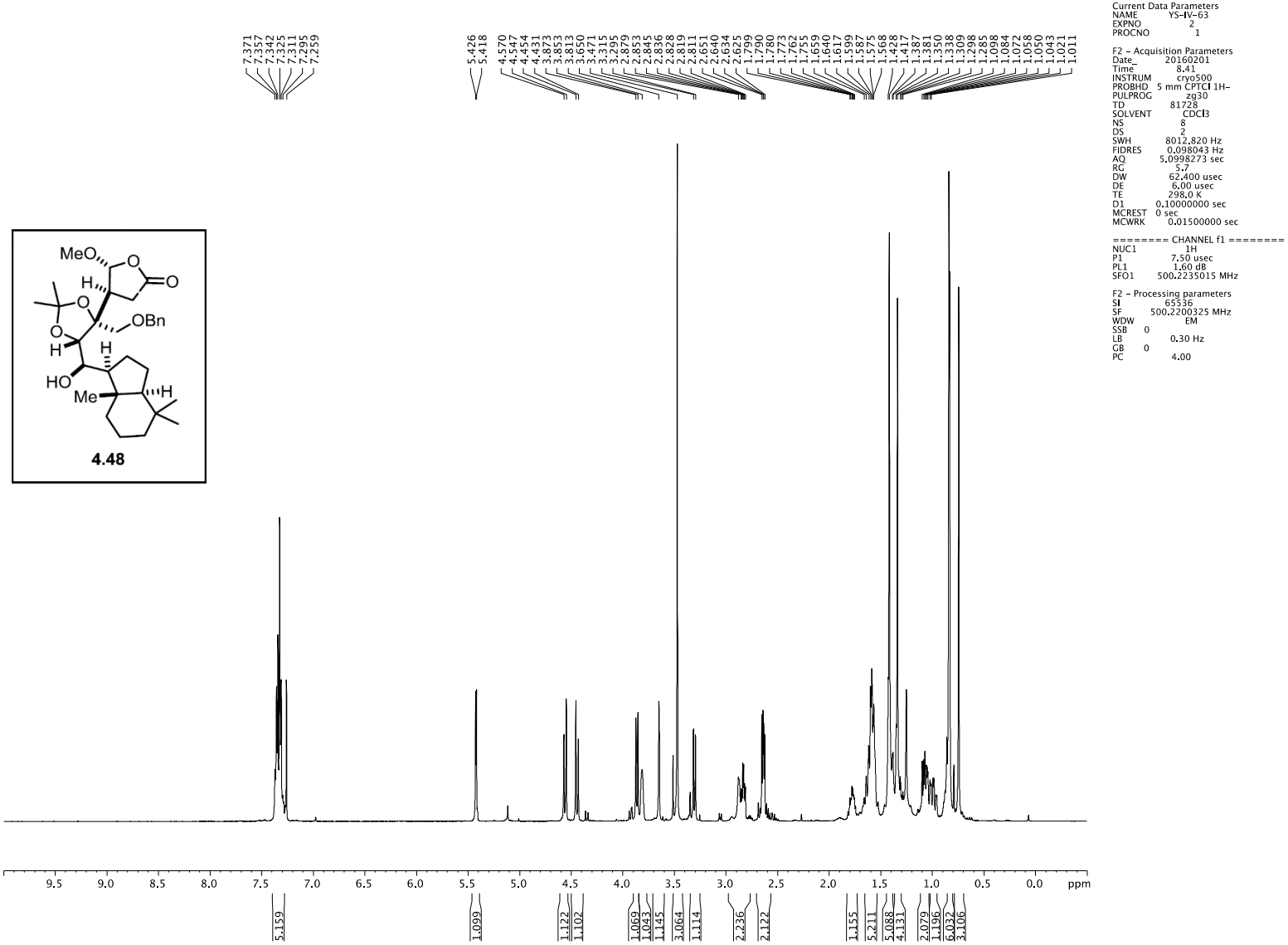

4.48

```
Current Data Parameters
NAME        YS-IV-63
EXPNO              2
PROCNO             1

F2 - Acquisition Parameters
Date_       20160201
Time            8.41
INSTRUM       cryo500
PROBHD   5 mm CPTCI 1H-
PULPROG         zg30
TD             81728
SOLVENT        CDCl3
NS                 8
DS                 2
SWH          8012.820 Hz
FIDRES       0.098043 Hz
AQ           5.0998273 sec
RG               5.7
DW             62.400 usec
DE              6.00 usec
TE             298.0 K
D1          0.10000000 sec
MCREST    0 sec
MCWRK       0.01500000 sec

======== CHANNEL f1 ========
NUC1             1H
P1             7.50 usec
PL1            1.60 dB
SFO1       500.2235015 MHz

F2 - Processing parameters
SI             65536
SF        500.2200325 MHz
WDW              EM
SSB     0
LB            0.30 Hz
GB      0
PC             4.00
```

YS-IV-63

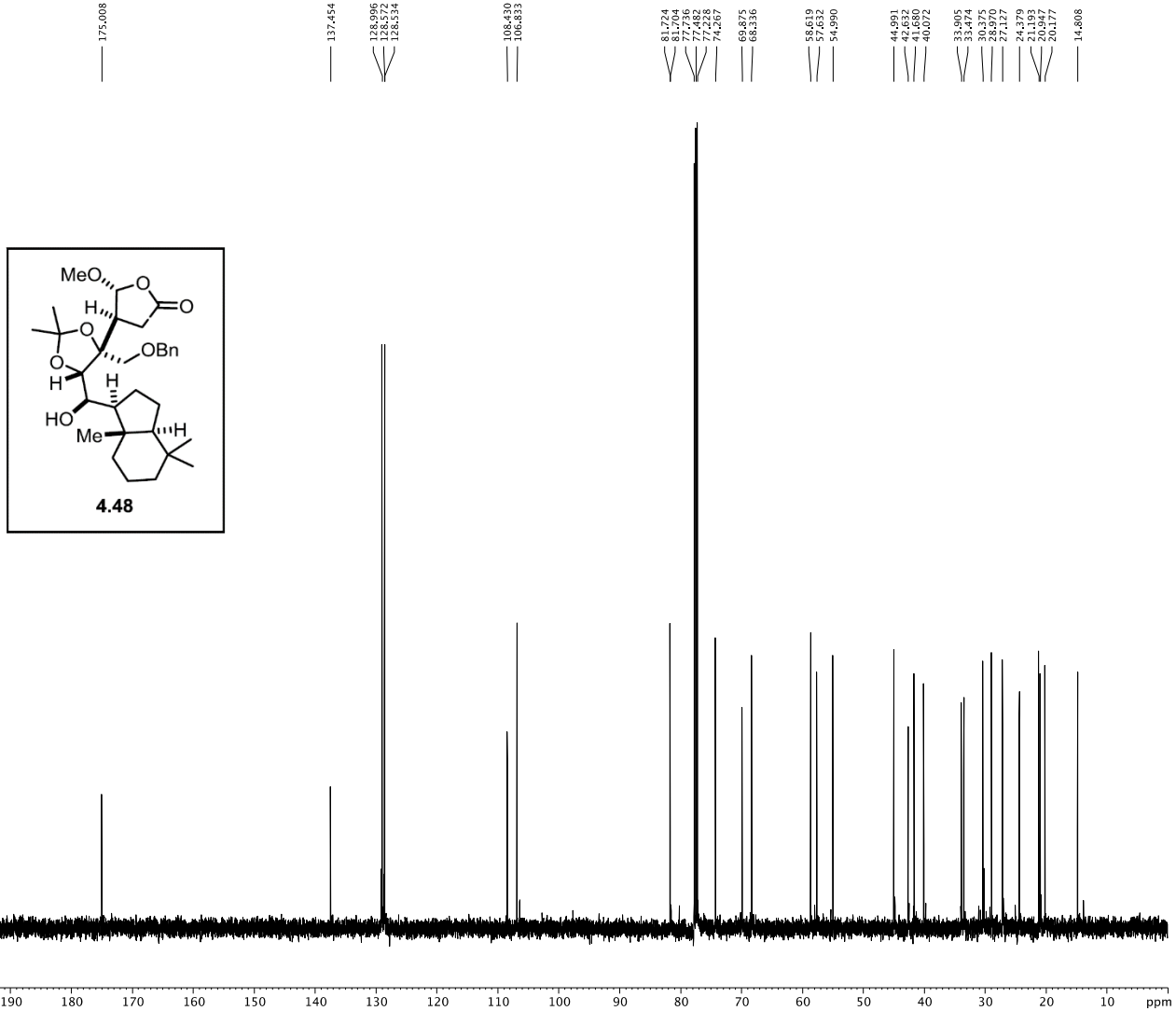

Current Data Parameters
NAME YS-IV-63
EXPNO 3
PROCNO 1

F2 - Acquisition Parameters
Date_ 20160201
Time 8.44
INSTRUM cryo500
PROBHD 5 mm CPTCI 1H-
PULPROG SpinEchopg30gp.prd
TD 65536
SOLVENT CDCl3
NS 96
DS 1
SWH 30303.031 Hz
FIDRES 0.462388 Hz
AQ 1.0813440 sec
RG 7298.2
DW 16.500 usec
DE 6.00 usec
TE 298.0 K
D1 0.25000000 sec
d11 0.03000000 sec
D16 0.00020000 sec
d17 0.00019600 sec
MCREST 0 sec
MCWRK 0.01500000 sec
P2 33.10 usec

======== CHANNEL f1 ========
NUC1 13C
P1 16.55 usec
P11 500.00 usec
P12 2000.00 usec
PL0 120.00 dB
PL1 -1.00 dB
SFO1 125.7942548 MHz
SP1 2.70 dB
SP2 2.70 dB
SPNAM[1] Crp60,0.5,20.1
SPNAM[2] Crp60comp.4
SPOFF1 0 Hz
SPOFF2 0 Hz

======== CHANNEL f2 ========
CPDPRG[2 waltz16
NUC2 1H
PCPD2 100.00 usec
PL2 1.60 dB
PL12 24.50 dB
SFO2 500.2225011 MHz

====== GRADIENT CHANNEL =====
GPNAM[1] SINE.100
GPNAM[2] SINE.100
GPX1 0 %
GPX2 0 %
GPY1 0 %
GPY2 0 %
GPZ1 30.00 %
GPZ2 50.00 %
p15 500.00 usec
p16 1000.00 usec

F2 - Processing parameters
SI 65536
SF 125.7803692 MHz
WDW EM
SSB 0
LB 1.00 Hz
GB 0
PC 2.00

1H spectrum

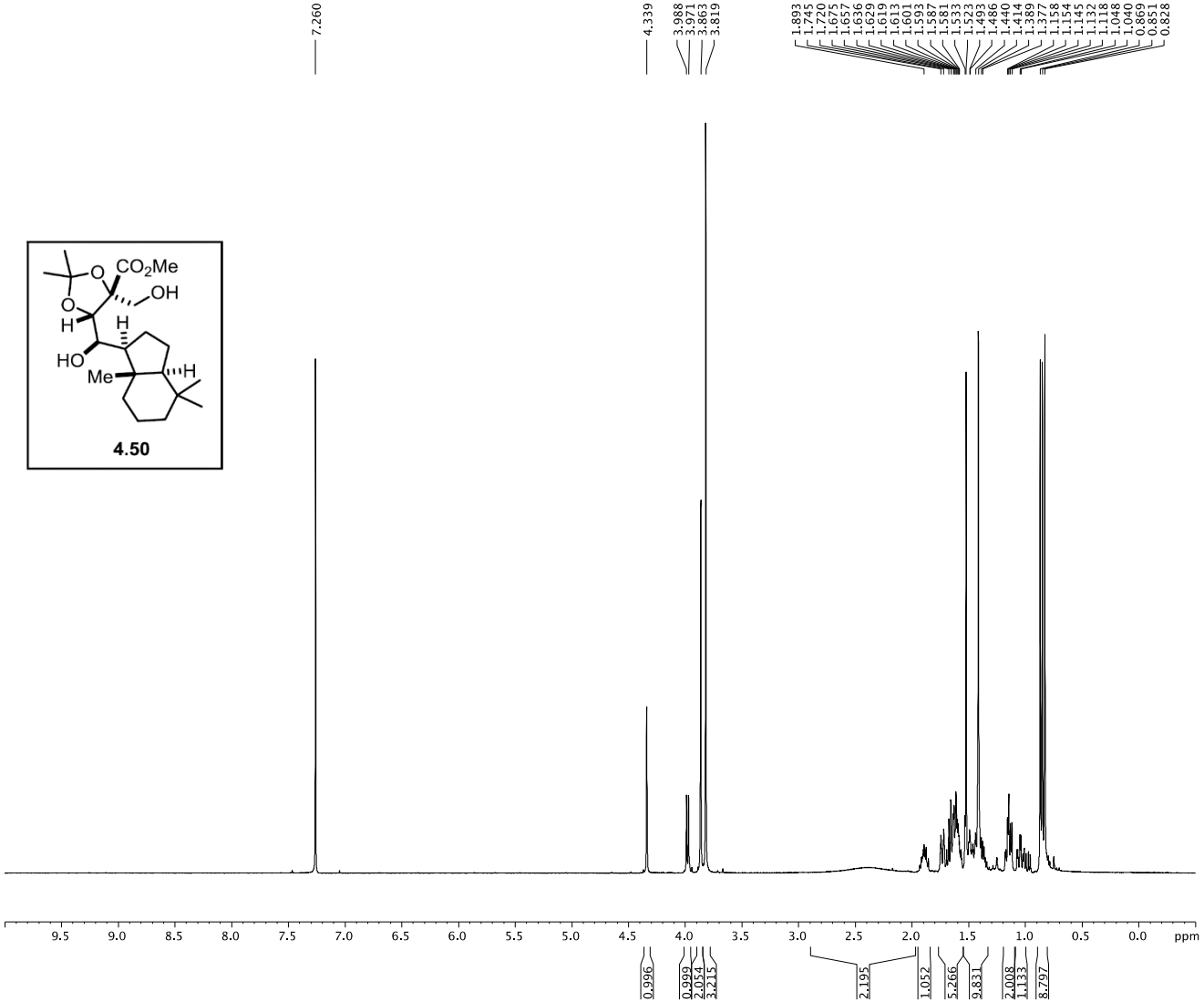

Current Data Parameters
NAME DJT-VI-123
EXPNO 5
PROCNO 1

F2 - Acquisition Parameters
Date_ 20151216
Time 12.47
INSTRUM cryo500
PROBHD 5 mm CPTCI 1H-
PULPROG zg30
TD 81728
SOLVENT CDCl3
NS 20
DS 0
SWH 8012.820 Hz
FIDRES 0.098043 Hz
AQ 5.0998273 sec
RG 7.1
DW 62.400 usec
DE 6.00 usec
TE 298.0 K
D1 0.10000000 sec
MCREST 0 sec
MCWRK 0.01500000 sec

======== CHANNEL f1 =====
NUC1 1H
P1 7.50 usec
PL1 1.60 dB
SFO1 500.2235015 MHz

F2 - Processing parameters
SI 65536
SF 500.2200316 MHz
WDW EM
SSB 0
LB 0.30 Hz
GB 0
PC 4.00

Z-restored spin-echo 13C spectrum with 1H decoupling

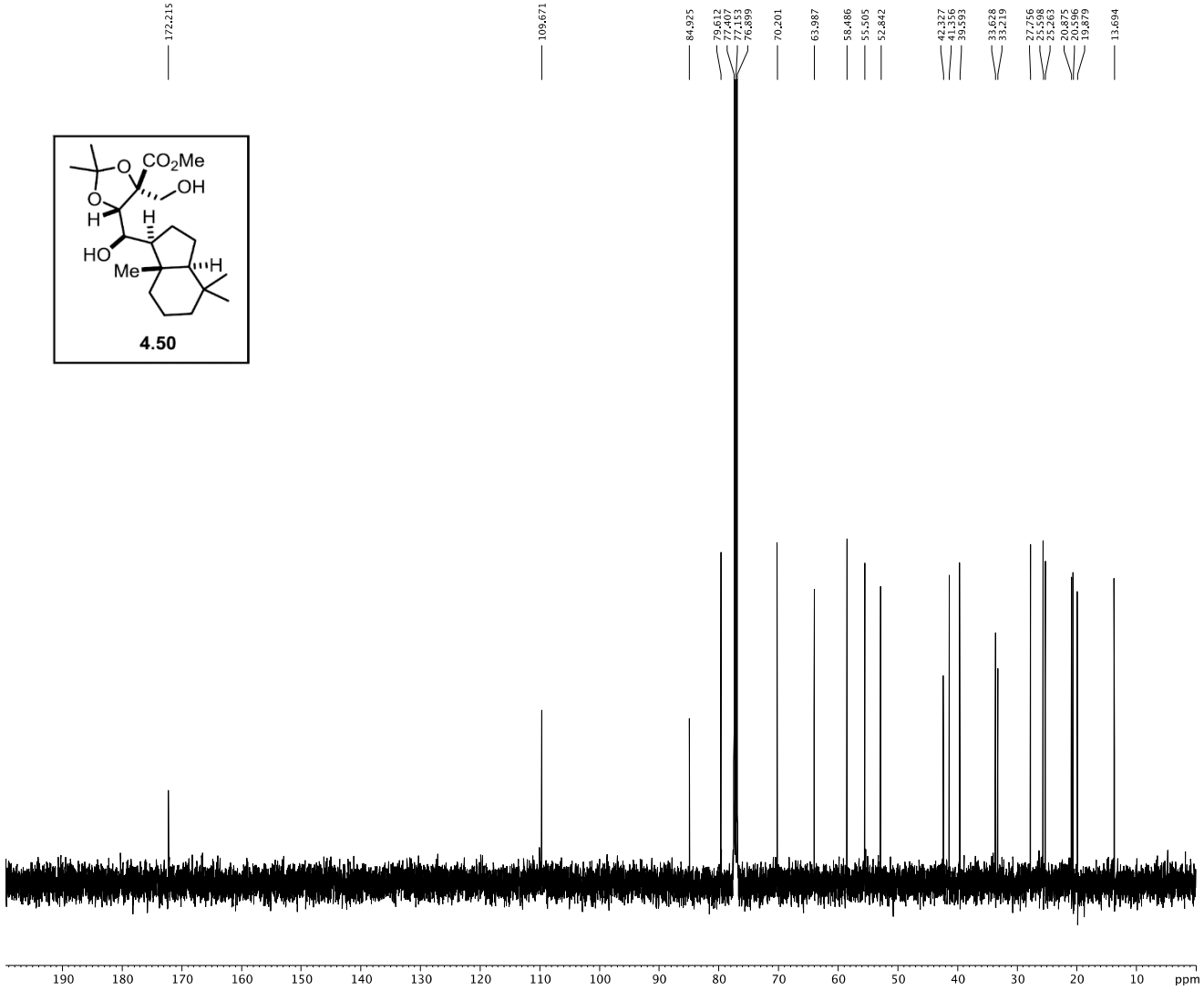

Current Data Parameters
NAME DJT-VI-123
EXPNO 6
PROCNO 1

F2 - Acquisition Parameters
Date_ 20151216
Time 12.53
INSTRUM cryo500
PROBHD 5 mm CPTCI 1H-
PULPROG SpinEchopg30gp.prd
TD 65536
SOLVENT CDCl3
NS 922
DS 0
SWH 30303.031 Hz
FIDRES 0.462388 Hz
AQ 1.0813440 sec
RG 2298.8
DW 16.500 usec
DE 6.00 usec
TE 298.0 K
D1 0.25000000 sec
d11 0.03000000 sec
D16 0.00020000 sec
d17 0.00019600 sec
MCREST 0 sec
MCWRK 0.01500000 sec
P2 33.10 usec

======== CHANNEL f1 ========
NUC1 13C
P1 16.55 usec
P11 500.00 usec
P12 2000.00 usec
PL0 120.00 dB
PL1 -1.00 dB
SFO1 125.7942548 MHz
SP1 2.70 dB
SP2 2.70 dB
SPNAM[1] Crp60,0.5,20.1
SPNAM[2] Crp60comp.4
SPOFF1 0 Hz
SPOFF2 0 Hz

======== CHANNEL f2 ========
CPDPRG[2 waltz16
NUC2 1H
PCPD2 100.00 usec
PL2 1.60 dB
PL12 24.50 dB
SFO2 500.2225011 MHz

====== GRADIENT CHANNEL =====
GPNAM[1] SINE.100
GPNAM[2] SINE.100
GPX1 0 %
GPX2 0 %
GPY1 0 %
GPY2 0 %
GPZ1 30.00 %
GPZ2 50.00 %
p15 500.00 usec
p16 1000.00 usec

F2 - Processing parameters
SI 65536
SF 125.7804084 MHz
WDW EM
SSB 0
LB 1.00 Hz
GB 0
PC 2.00

4.51

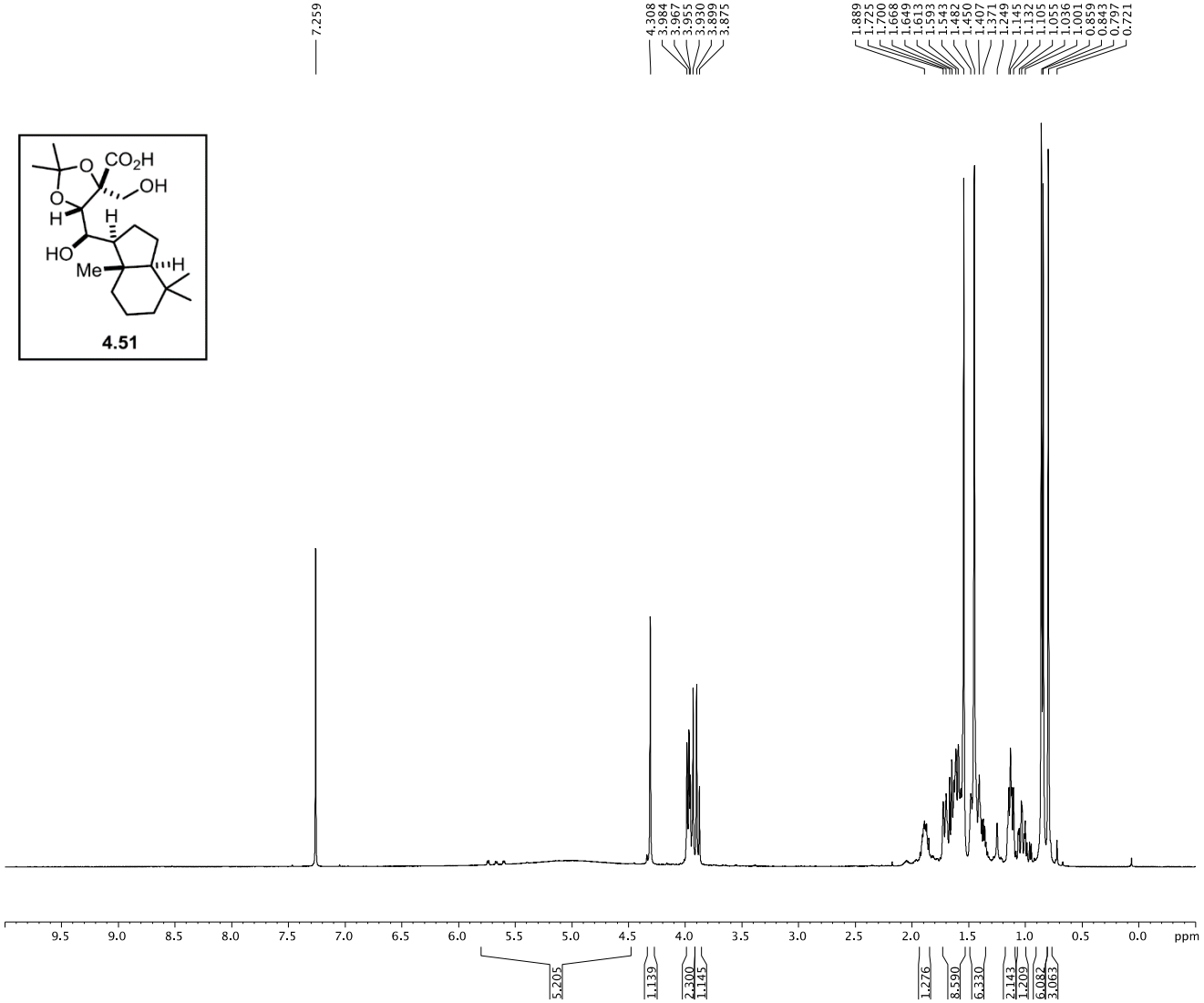

Current Data Parameters
NAME YS-IV-13
EXPNO 2
PROCNO 1

F2 - Acquisition Parameters
Date_ 20151216
Time 8.43
INSTRUM cryo500
PROBHD 5 mm CPTCI 1H-
PULPROG zg30
TD 81728
SOLVENT CDCl3
NS 8
DS 2
SWH 8012.820 Hz
FIDRES 0.098043 Hz
AQ 5.0998273 sec
RG 7.1
DW 62.400 usec
DE 6.00 usec
TE 298.0 K
D1 0.10000000 sec
MCREST 0 sec
MCWRK 0.01500000 sec

======== CHANNEL f1 ========
NUC1 1H
P1 7.50 usec
PL1 1.60 dB
SFO1 500.2235015 MHz

F2 - Processing parameters
SI 65536
SF 500.2200321 MHz
WDW EM
SSB 0
LB 0.30 Hz
GB 0
PC 4.00

YS-IV-13

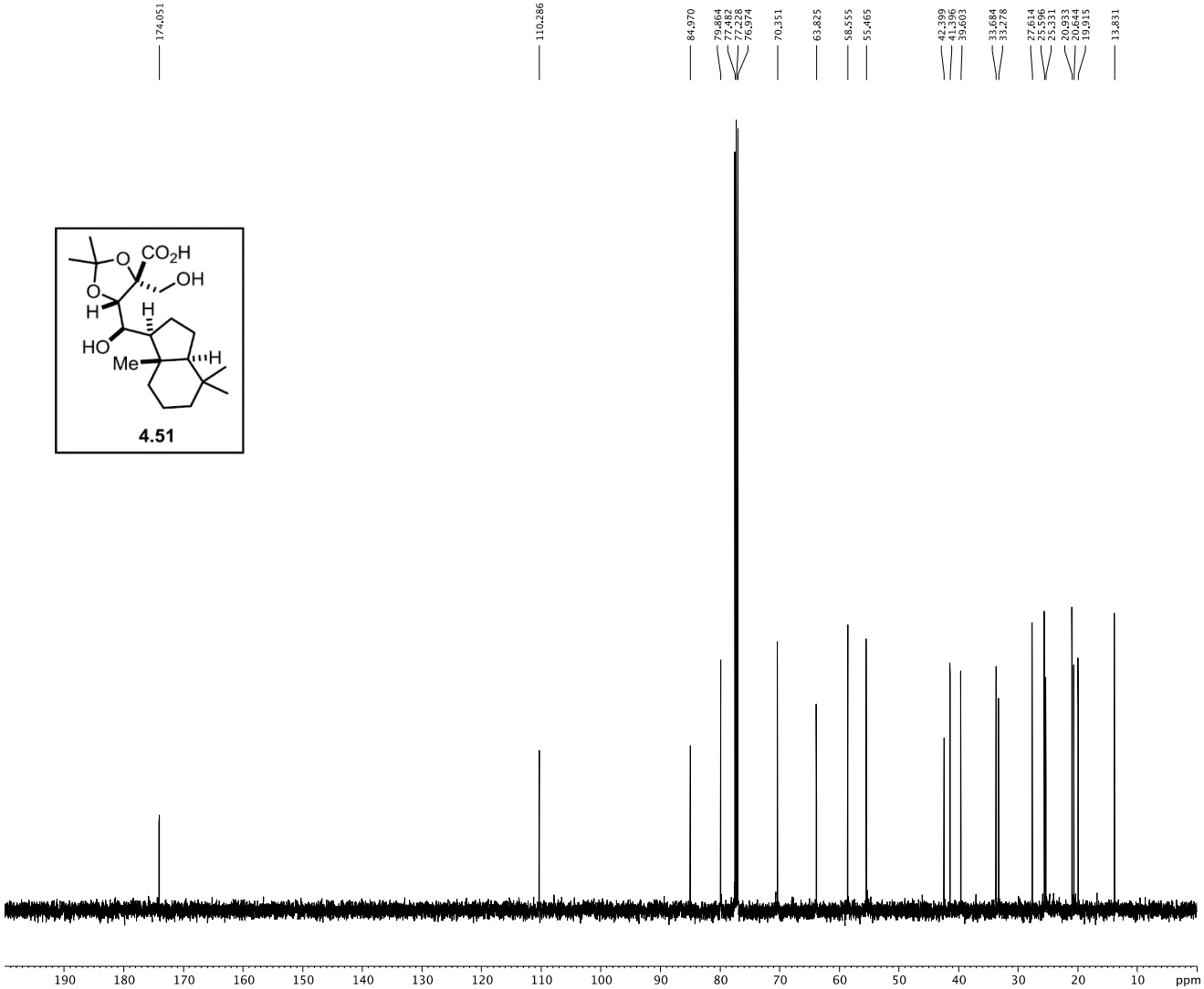

4.51

```
Current Data Parameters
NAME          YS-IV-13
EXPNO              3
PROCNO             1

F2 - Acquisition Parameters
Date_        20151216
Time            8.47
INSTRUM        cryo500
PROBHD   5 mm CPTCI 1H-
PULPROG  SpinEchopg30gp.prd
TD            65536
SOLVENT         CDCl3
NS              320
DS               16
SWH         30303.031 Hz
FIDRES       0.462388 Hz
AQ          1.0813440 sec
RG           10321.3
DW             16.500 usec
DE              6.00 usec
TE            298.0 K
D1          0.25000000 sec
d11         0.03000000 sec
D16         0.00020000 sec
d17         0.00019600 sec
MCREST   0 sec
MCWRK       0.01500000 sec
P2             33.10 usec

======== CHANNEL f1 ========
NUC1            13C
P1             16.55 usec
P11           500.00 usec
P12          2000.00 usec
PL0           120.00 dB
PL1            -1.00 dB
SFO1        125.7942548 MHz
SP1             2.70 dB
SP2             2.70 dB
SPNAM[1] Crp60,0.5,20.1
SPNAM[2]    Crp60comp.4
SPOFF1   0 Hz
SPOFF2   0 Hz

======== CHANNEL f2 ========
CPDPRG[2        waltz16
NUC2             1H
PCPD2          100.00 usec
PL2             1.60 dB
PL12           24.50 dB
SFO2        500.2225011 MHz

====== GRADIENT CHANNEL =====
GPNAM[1]        SINE.100
GPNAM[2]        SINE.100
GPX1     0 %
GPX2     0 %
GPY1     0 %
GPY2     0 %
GPZ1            30.00 %
GPZ2            50.00 %
p15           500.00 usec
p16          1000.00 usec

F2 - Processing parameters
SI            65536
SF        125.7803996 MHz
WDW              EM
SSB      0
LB            1.00 Hz
GB       0
PC             2.00
```

1H spectrum

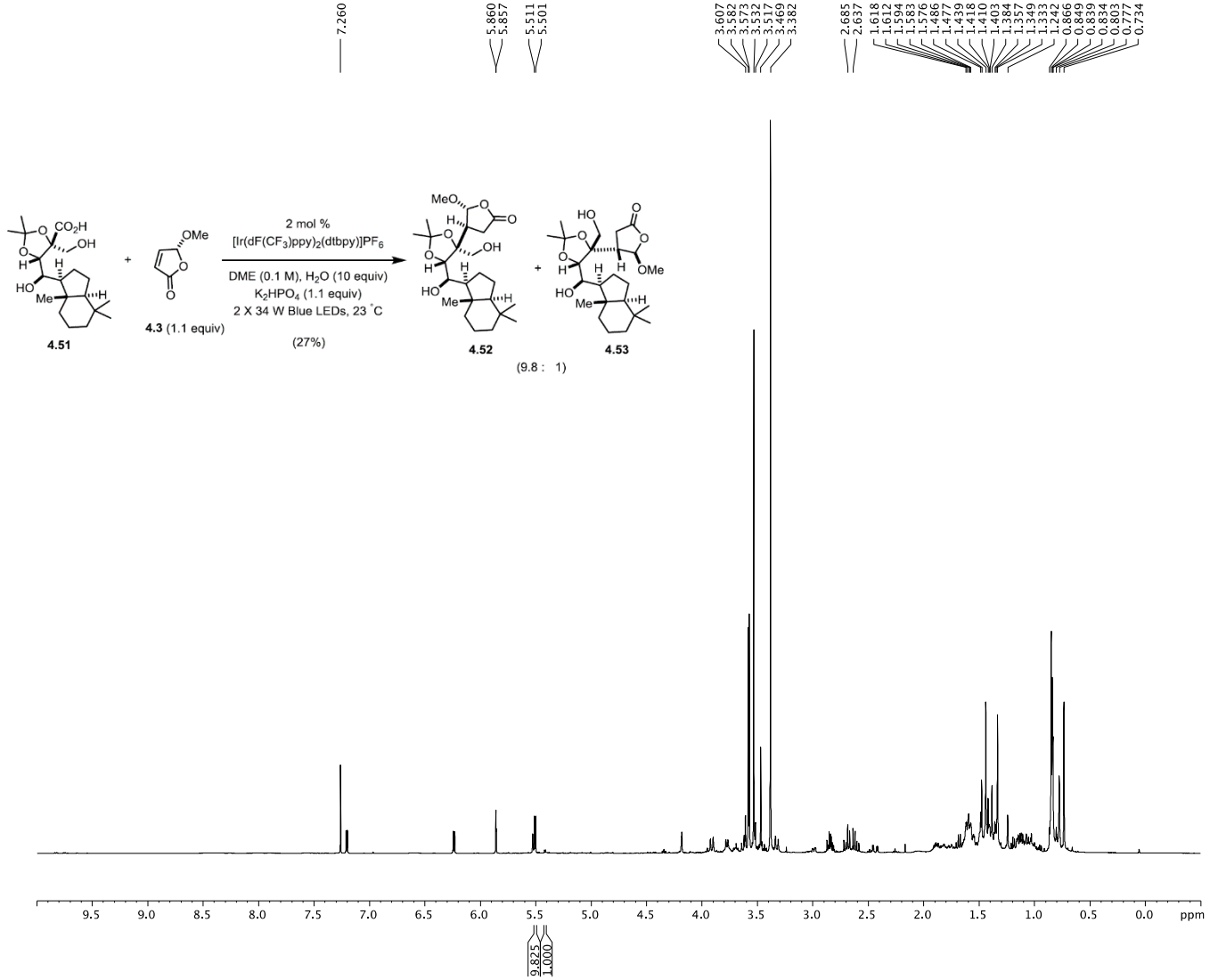

Current Data Parameters
NAME DJT-VI-173
EXPNO 1
PROCNO 1

F2 - Acquisition Parameters
Date_ 20160121
Time 8.05
INSTRUM cryo500
PROBHD 5 mm CPTCI 1H-
PULPROG zg30
TD 81728
SOLVENT CDCl3
NS 20
DS 0
SWH 8012.820 Hz
FIDRES 0.098043 Hz
AQ 5.0998273 sec
RG 6.3
DW 62.400 usec
DE 6.00 usec
TE 298.0 K
D1 0.10000000 sec
MCREST 0 sec
MCWRK 0.01500000 sec

======== CHANNEL f1 =====
NUC1 1H
P1 7.50 usec
PL1 1.60 dB
SFO1 500.2235015 MHz

F2 - Processing parameters
SI 65536
SF 500.2200312 MHz
WDW EM
SSB 0
LB 0.30 Hz
GB 0
PC 4.00

1H spectrum

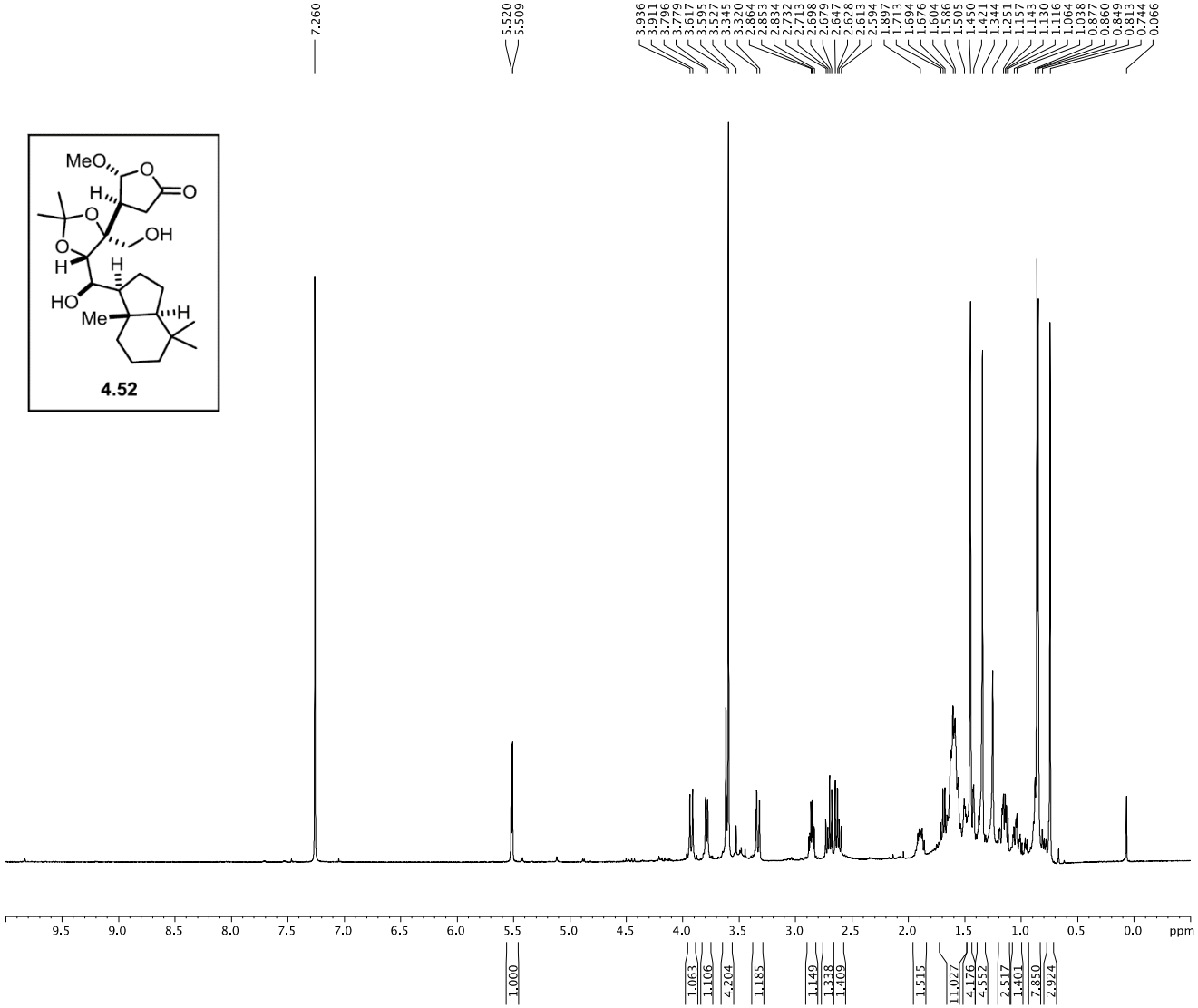

Current Data Parameters
NAME DJT-VI-173
EXPNO 2
PROCNO 1

F2 - Acquisition Parameters
Date_ 20160121
Time 9.54
INSTRUM cryo500
PROBHD 5 mm CPTCI 1H-
PULPROG zg30
TD 81728
SOLVENT CDCl3
NS 20
DS 0
SWH 8012.820 Hz
FIDRES 0.098043 Hz
AQ 5.0998273 sec
RG 5.7
DW 62.400 usec
DE 6.00 usec
TE 298.0 K
D1 0.10000000 sec
MCREST 0 sec
MCWRK 0.01500000 sec

======== CHANNEL f1 =====
NUC1 1H
P1 7.50 usec
PL1 1.60 dB
SFO1 500.2235015 MHz

F2 - Processing parameters
SI 65536
SF 500.2200313 MHz
WDW EM
SSB 0
LB 0.30 Hz
GB 0
PC 4.00

Z-restored spin-echo 13C spectrum with 1H decoupling

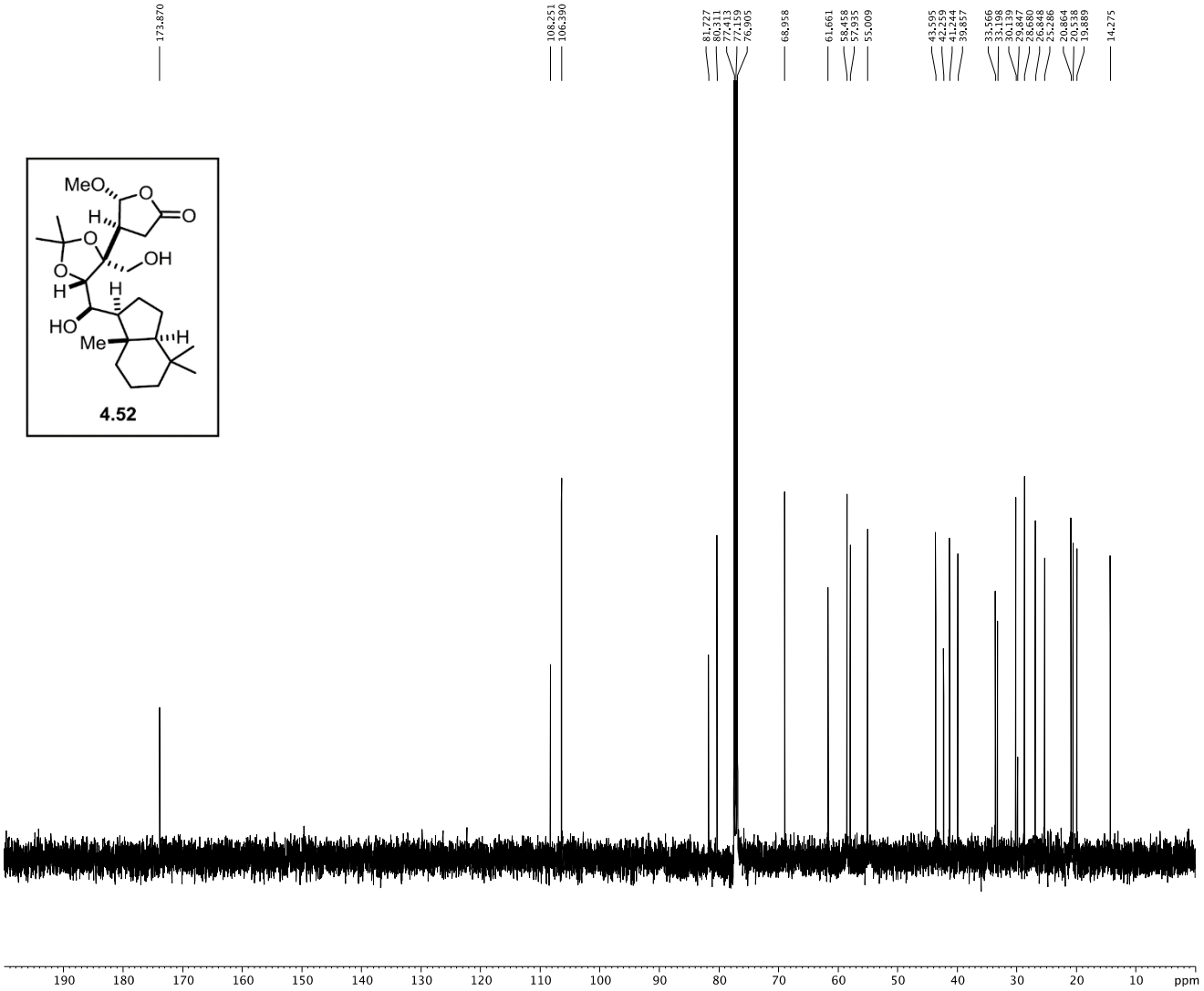

Current Data Parameters
NAME DJT-VI-173
EXPNO 3
PROCNO 1

F2 - Acquisition Parameters
Date_ 20160121
Time 9.59
INSTRUM cryo500
PROBHD 5 mm CPTCI 1H-
PULPROG SpinEchopg30gp.prd
TD 65536
SOLVENT CDCl3
NS 632
DS 0
SWH 30303.031 Hz
FIDRES 0.462388 Hz
AQ 1.0813440 sec
RG 2298.8
DW 16.500 usec
DE 6.00 usec
TE 298.0 K
D1 0.25000000 sec
d11 0.03000000 sec
D16 0.00020000 sec
d17 0.00019600 sec
MCREST 0 sec
MCWRK 0.01500000 sec
P2 33.10 usec

======== CHANNEL f1 ========
NUC1 13C
P1 16.55 usec
P11 500.00 usec
P12 2000.00 usec
PL0 120.00 dB
PL1 -1.00 dB
SFO1 125.7942548 MHz
SP1 2.70 dB
SP2 2.70 dB
SPNAM[1] Crp60,0.5,20.1
SPNAM[2] Crp60comp.4
SPOFF1 0 Hz
SPOFF2 0 Hz

======== CHANNEL f2 ========
CPDPRG[2 waltz16
NUC2 1H
PCPD2 100.00 usec
PL2 1.60 dB
PL12 24.50 dB
SFO2 500.2225011 MHz

===== GRADIENT CHANNEL =====
GPNAM[1] SINE.100
GPNAM[2] SINE.100
GPX1 0 %
GPX2 0 %
GPY1 0 %
GPY2 0 %
GPZ1 30.00 %
GPZ2 50.00 %
p15 500.00 usec
p16 1000.00 usec

F2 - Processing parameters
SI 65536
SF 125.7804080 MHz
WDW EM
SSB 0
LB 1.00 Hz
GB 0
PC 2.00

1H spectrum

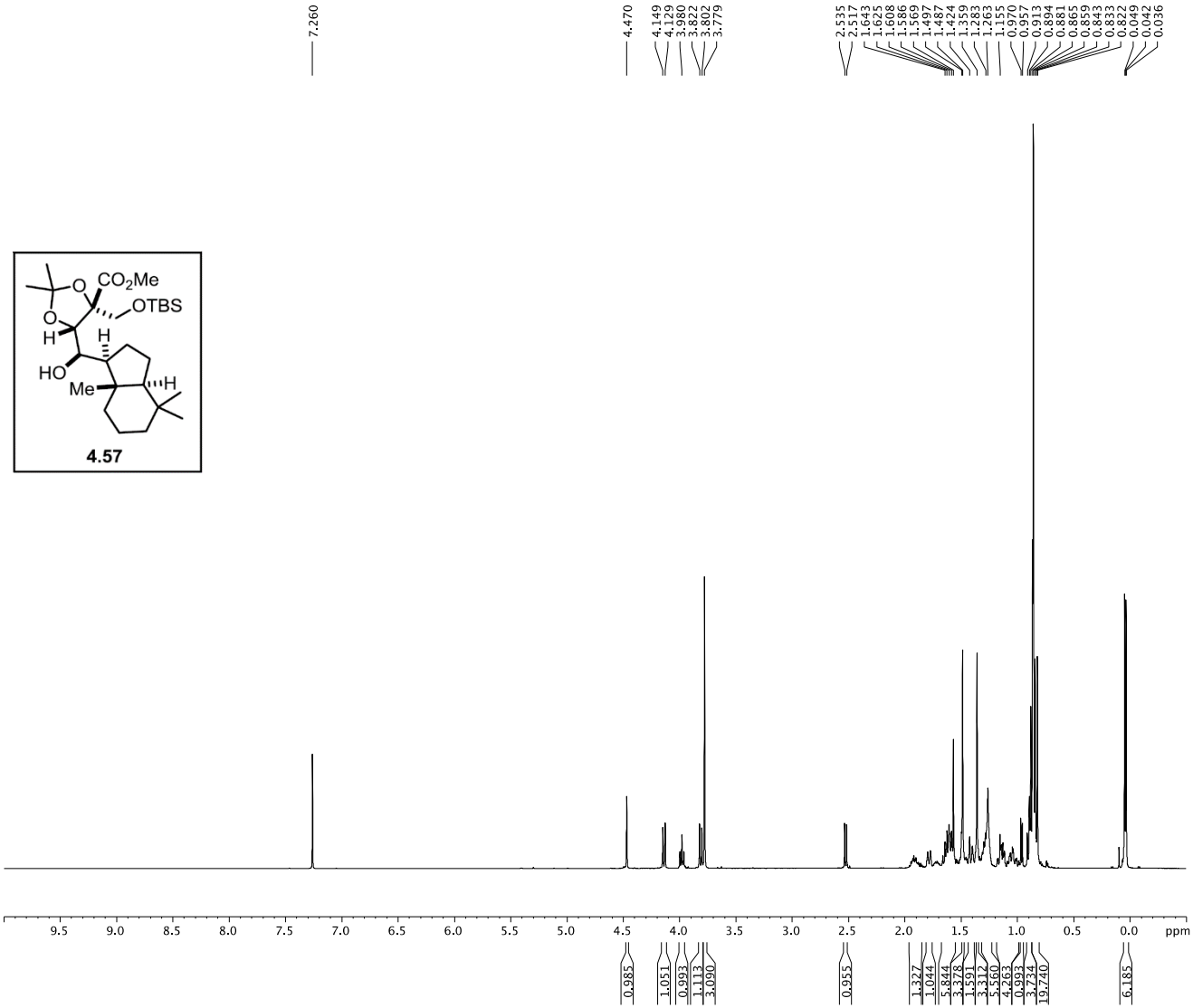

4.57

Current Data Parameters
NAME DJT-VI-131
EXPNO 1
PROCNO 1

F2 - Acquisition Parameters
Date_ 20151204
Time 18.18
INSTRUM cryo500
PROBHD 5 mm CPTCI 1H-
PULPROG zg30
TD 32048
SOLVENT CDCl3
NS 20
DS 0
SWH 8012.820 Hz
FIDRES 0.250026 Hz
AQ 1.9997952 sec
RG 6.3
DW 62.400 usec
DE 6.00 usec
TE 298.0 K
D1 0.10000000 sec
MCREST 0 sec
MCWRK 0.01500000 sec

======== CHANNEL f1 =====
NUC1 1H
P1 7.50 usec
PL1 1.60 dB
SFO1 500.2235015 MHz

F2 - Processing parameters
SI 65536
SF 500.2200318 MHz
WDW EM
SSB 0
LB 0.30 Hz
GB 0
PC 4.00

13C spectrum with 1H decoupling

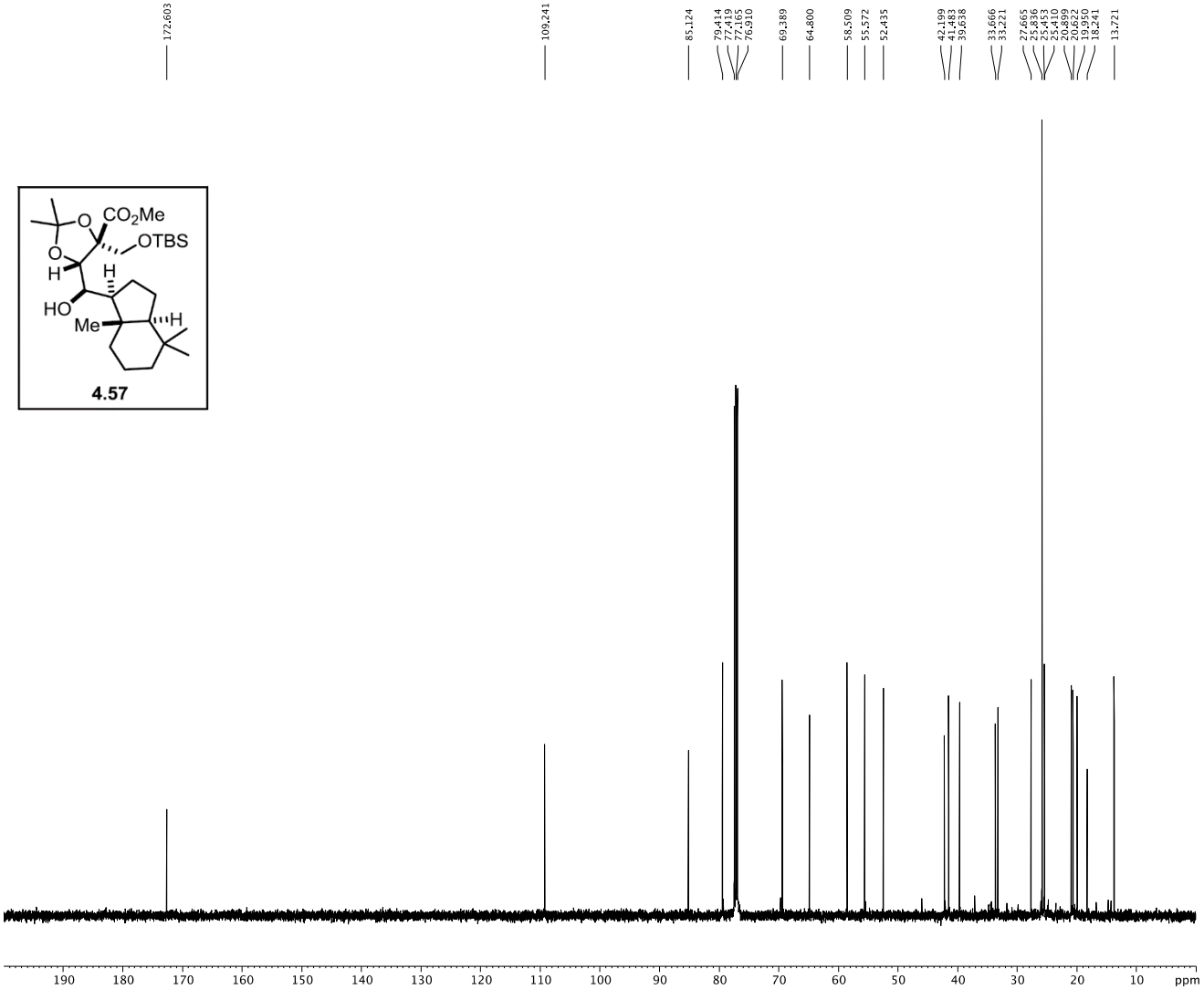

Current Data Parameters
NAME DJT-VI-131
EXPNO 4
PROCNO 1

F2 - Acquisition Parameters
Date_ 20151218
Time 8.27
INSTRUM qn500
PROBHD 5 mm broadband
PULPROG zgdc30
TD 65536
SOLVENT CDCl3
NS 622
DS 0
SWH 30303.031 Hz
FIDRES 0.462388 Hz
AQ 1.0813440 sec
RG 4597.6
DW 16.500 usec
DE 4.50 usec
TE 298.0 K
D1 0.25000000 sec
d11 0.03000000 sec
MCREST 0 sec
MCWRK 0.01500000 sec

======== CHANNEL f1 ========
NUC1 13C
P1 9.00 usec
PL1 -0.60 dB
SFO1 125.5327181 MHz

======== CHANNEL f2 ========
CPDPRG[2 waltz16
NUC2 1H
PCPD2 80.00 usec
PL2 -3.00 dB
PL12 12.80 dB
SFO2 499.1824959 MHz

F2 - Processing parameters
SI 65536
SF 125.5188974 MHz
WDW EM
SSB 0
LB 1.00 Hz
GB 0
PC 2.00

4.58

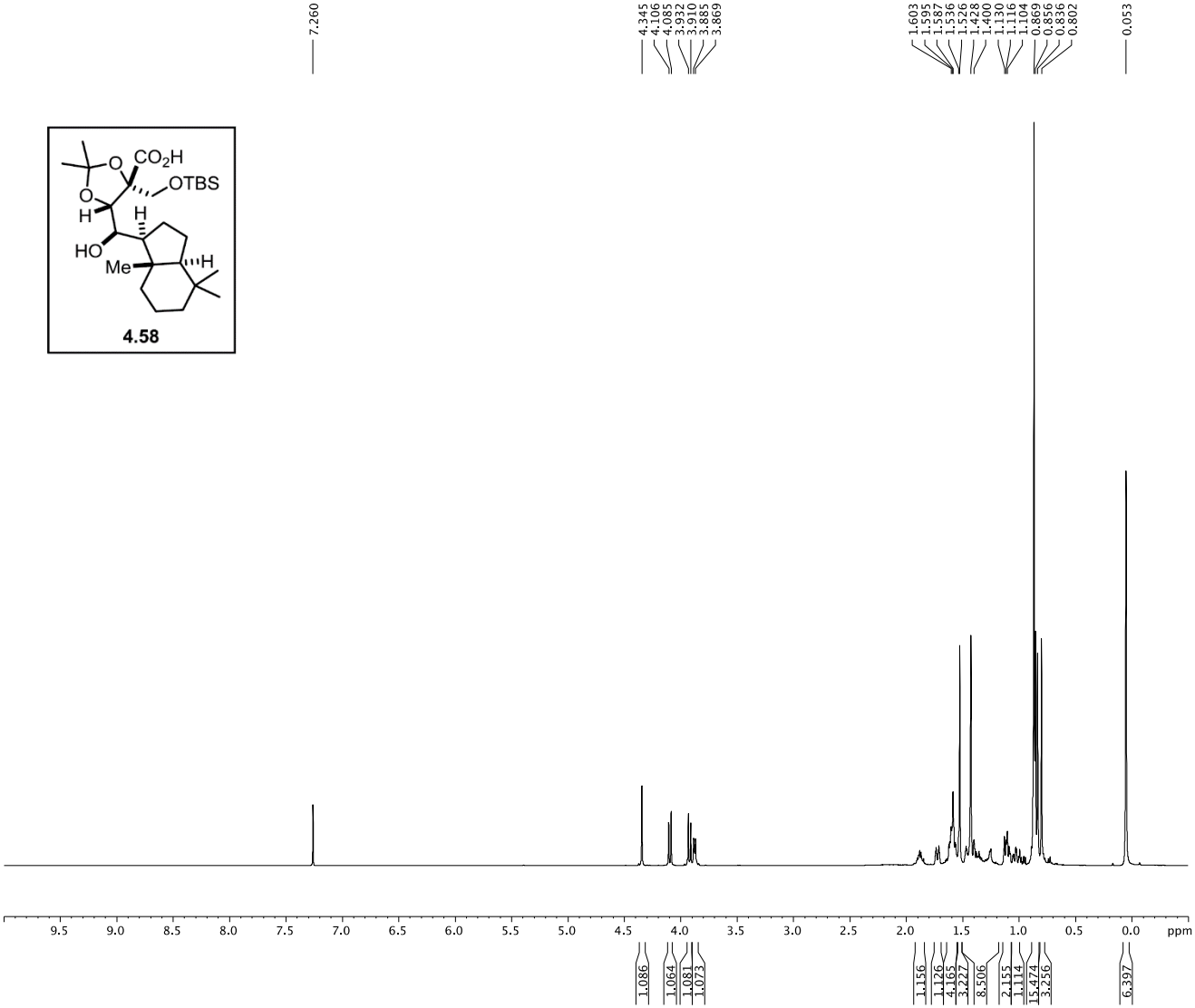


```
Current Data Parameters
NAME          YS-IV-17
EXPNO              2
PROCNO             1

F2 - Acquisition Parameters
Date_        20151215
Time            15.45
INSTRUM        cryo500
PROBHD   5 mm CPTCI 1H-
PULPROG          zg30
TD              81728
SOLVENT         CDCl3
NS                 8
DS                 2
SWH          8012.820 Hz
FIDRES       0.098043 Hz
AQ          5.0998273 sec
RG                 6.3
DW              62.400 usec
DE               6.00 usec
TE              298.0 K
D1          0.10000000 sec
MCREST   0 sec
MCWRK       0.01500000 sec

======== CHANNEL f1 ========
NUC1               1H
P1              7.50 usec
PL1             1.60 dB
SFO1       500.2235015 MHz

F2 - Processing parameters
SI             65536
SF        500.2200316 MHz
WDW               EM
SSB     0
LB              0.30 Hz
GB      0
PC               4.00
```

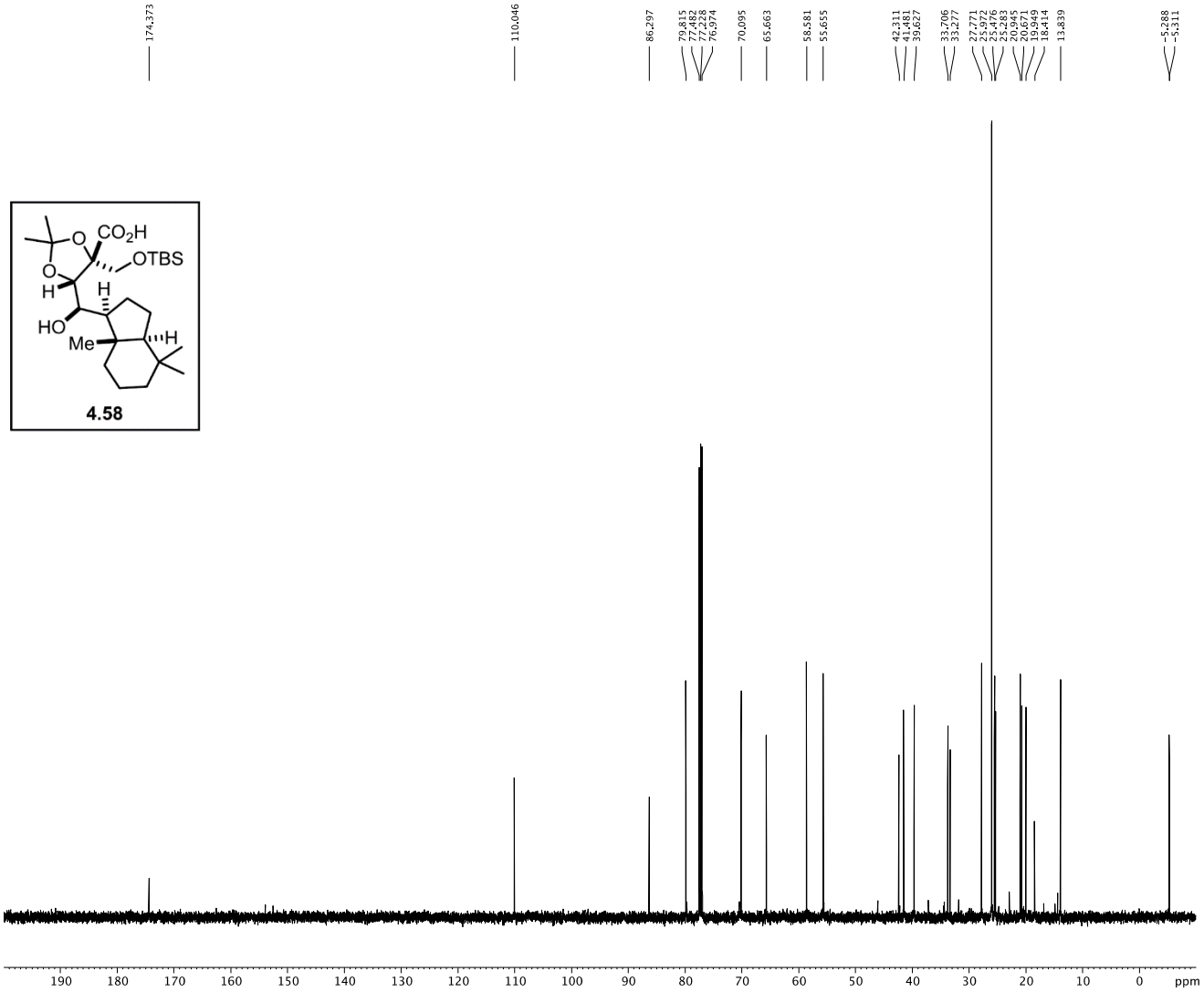

Current Data Parameters
NAME YS-IV-17
EXPNO 3
PROCNO 1

F2 - Acquisition Parameters
Date_ 20151215
Time 15.48
INSTRUM cryo500
PROBHD 5 mm CPTCI 1H-
PULPROG SpinEchopg30gp.prd
TD 65536
SOLVENT CDCl3
NS 216
DS 2
SWH 30303.031 Hz
FIDRES 0.462388 Hz
AQ 1.0813440 sec
RG 3649.1
DW 16.500 usec
DE 6.00 usec
TE 298.0 K
D1 0.25000000 sec
d11 0.03000000 sec
D16 0.00020000 sec
d17 0.00019600 sec
MCREST 0 sec
MCWRK 0.01500000 sec
P2 33.10 usec

======== CHANNEL f1 ========
NUC1 13C
P1 16.55 usec
P11 500.00 usec
P12 2000.00 usec
PL0 120.00 dB
PL1 -1.00 dB
SFO1 125.7942548 MHz
SP1 2.70 dB
SP2 2.70 dB
SPNAM[1] Crp60,0.5,20.1
SPNAM[2] Crp60comp.4
SPOFF1 0 Hz
SPOFF2 0 Hz

======== CHANNEL f2 ========
CPDPRG[2 waltz16
NUC2 1H
PCPD2 100.00 usec
PL2 1.60 dB
PL12 24.50 dB
SFO2 500.2225011 MHz

====== GRADIENT CHANNEL =====
GPNAM[1] SINE.100
GPNAM[2] SINE.100
GPX1 0 %
GPX2 0 %
GPY1 0 %
GPY2 0 %
GPZ1 30.00 %
GPZ2 50.00 %
p15 500.00 usec
p16 1000.00 usec

F2 - Processing parameters
SI 65536
SF 125.7803994 MHz
WDW EM
SSB 0
LB 1.00 Hz
GB 0
PC 2.00

1H spectrum

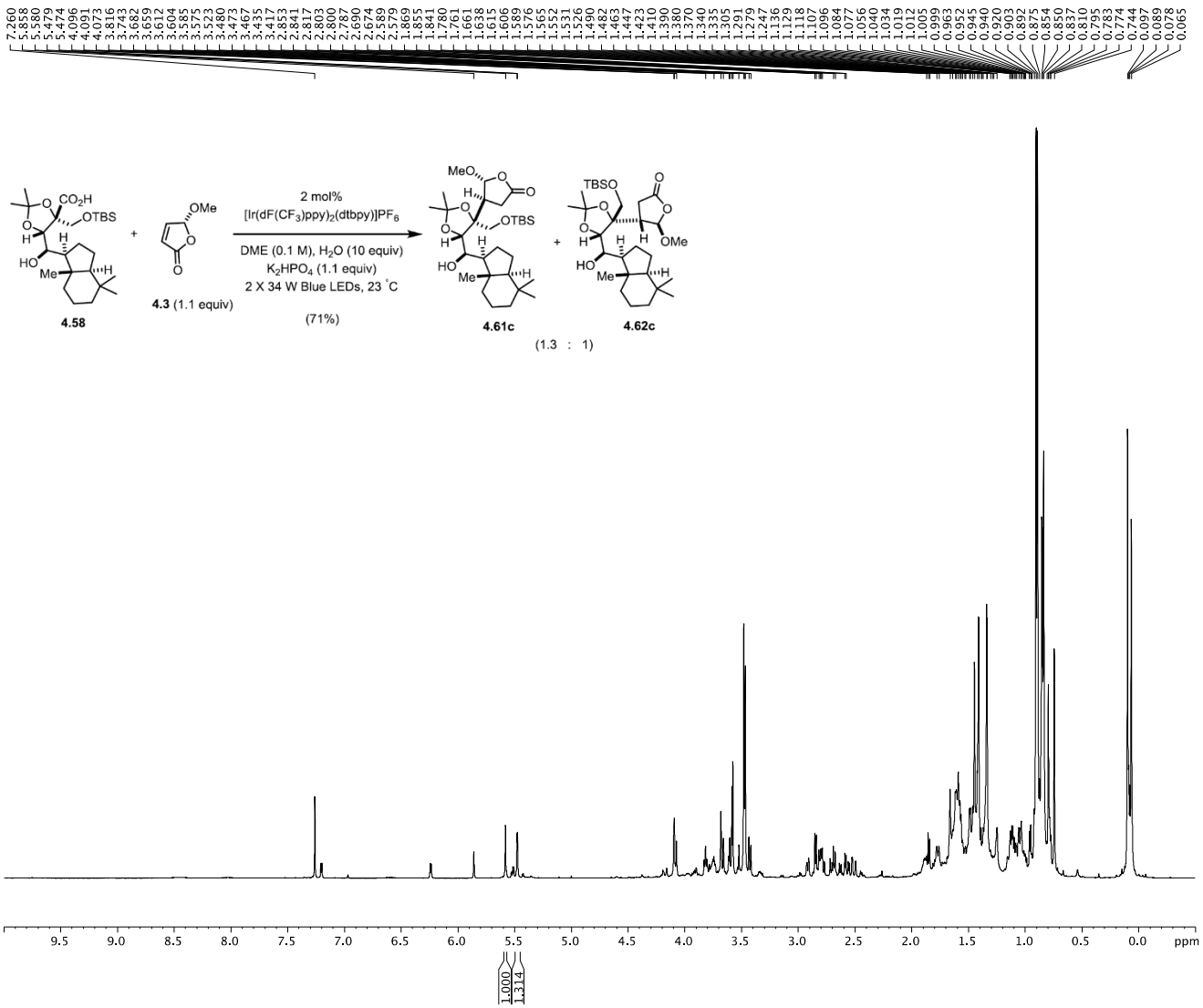

Current Data Parameters
NAME DJT-VI-144
EXPNO 1
PROCNO 1

F2 - Acquisition Parameters
Date_ 20151211
Time 8.59
INSTRUM av600
PROBHD 5 mm TBI 1H/13
PULPROG zg30
TD 98074
SOLVENT CDCl3
NS 20
DS 0
SWH 9615.385 Hz
FIDRES 0.098042 Hz
AQ 5.0998478 sec
RG 71.8
DW 52.000 usec
DE 14.54 usec
TE 298.1 K
D1 0.10000000 sec
TD0 1

======== CHANNEL f1 =====
SFO1 600.1342009 MHz
NUC1 1H
P1 8.00 usec
PLW1 24.00000000 W

F2 - Processing parameters
SI 65536
SF 600.1300358 MHz
WDW EM
SSB 0
LB 0.30 Hz
GB 0
PC 1.00

1H spectrum

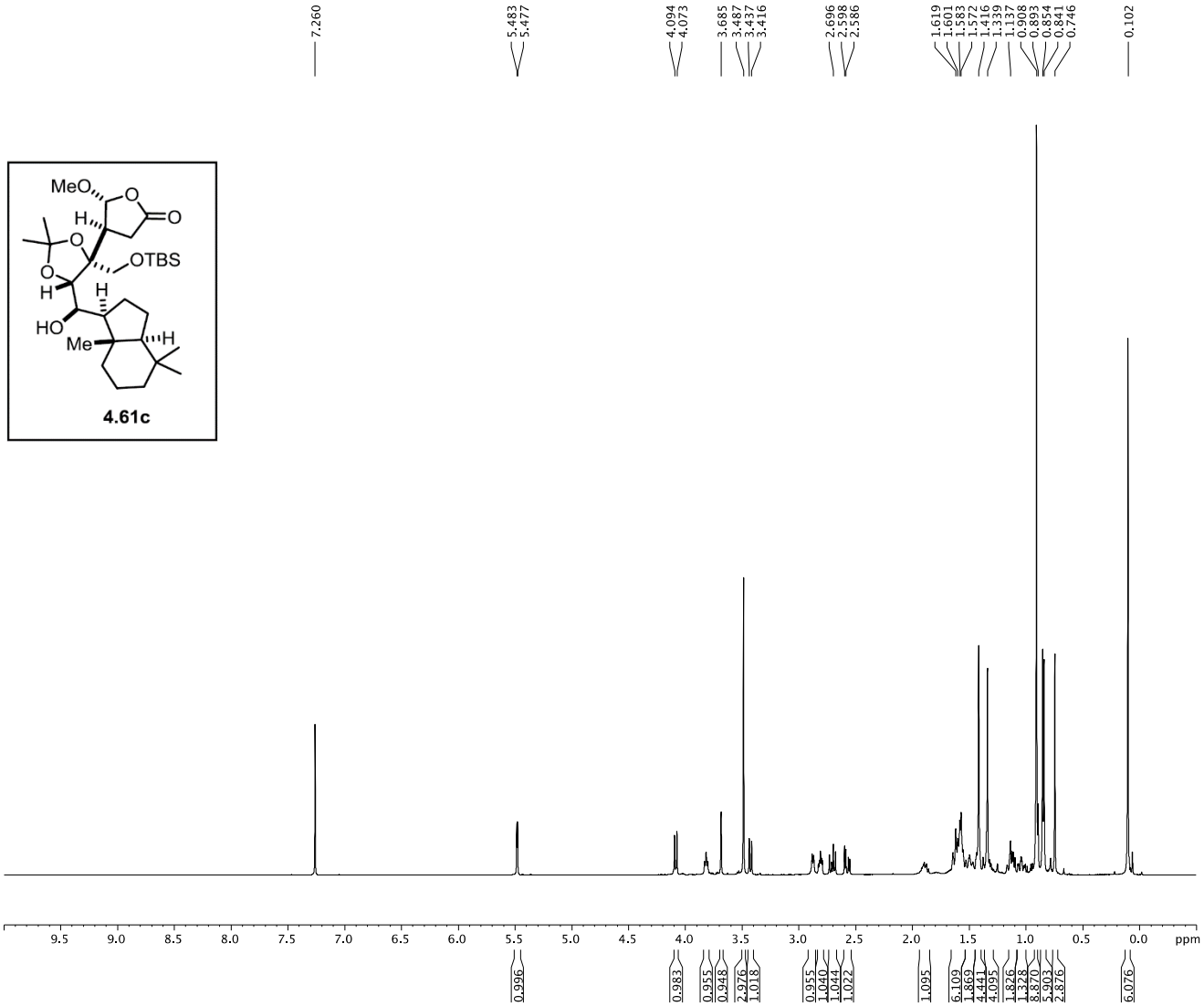

4.61c

```
Current Data Parameters
NAME        DJT-VI-144
EXPNO              8
PROCNO             1

F2 - Acquisition Parameters
Date_       20151214
Time            8.06
INSTRUM       cryo500
PROBHD  5 mm CPTCI 1H-
PULPROG         zg30
TD             81728
SOLVENT        CDCl3
NS               20
DS                0
SWH          8012.820 Hz
FIDRES       0.098043 Hz
AQ         5.0998273 sec
RG               7.1
DW            62.400 usec
DE             6.00 usec
TE            298.0 K
D1         0.10000000 sec
MCREST   0 sec
MCWRK      0.01500000 sec

======== CHANNEL f1 =====
NUC1             1H
P1            7.50 usec
PL1           1.60 dB
SFO1      500.2235015 MHz

F2 - Processing parameters
SI            65536
SF       500.2200316 MHz
WDW             EM
SSB    0
LB            0.30 Hz
GB     0
PC            4.00
```

Z-restored spin-echo 13C spectrum with 1H decoupling

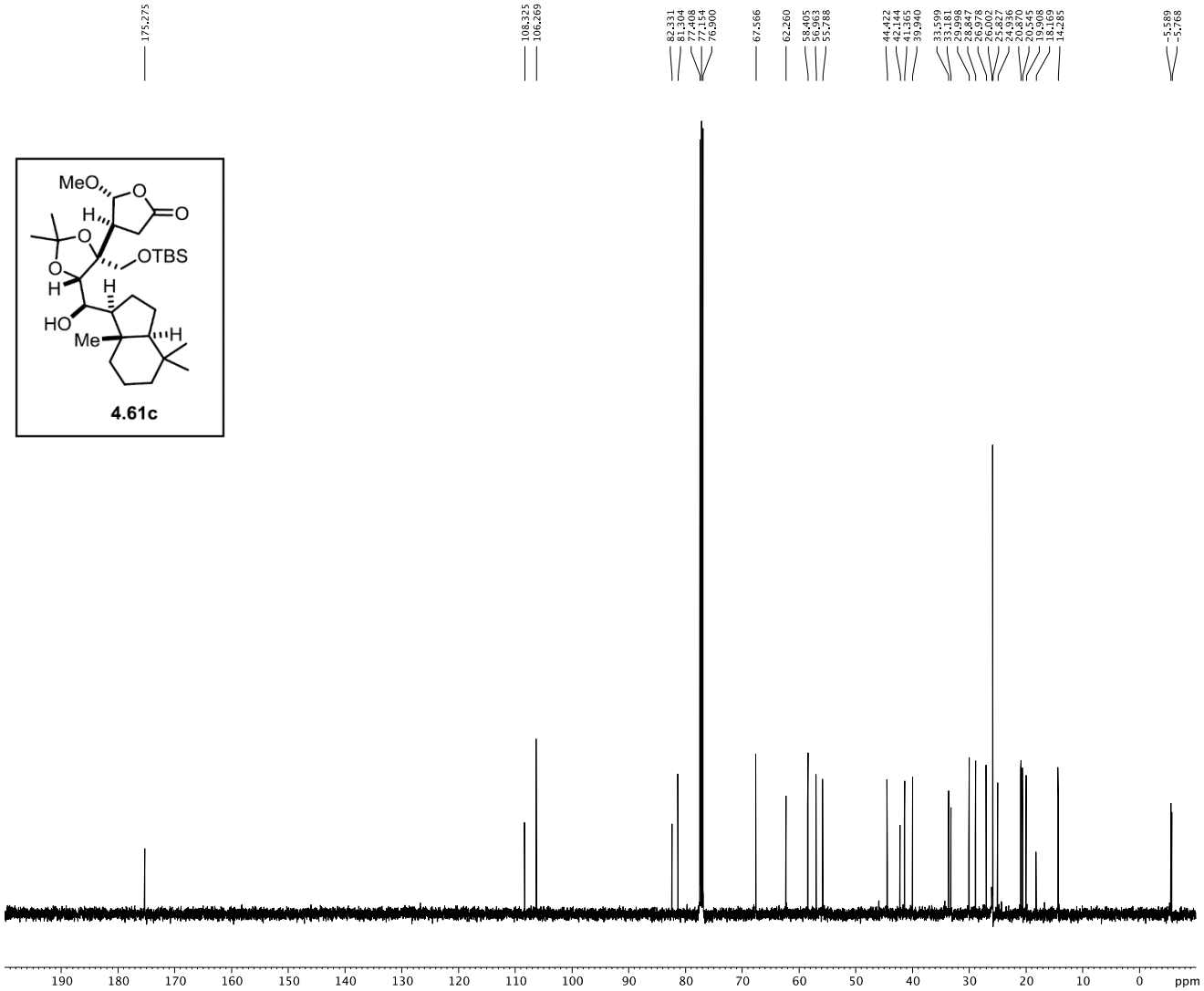

4.61c

Current Data Parameters
NAME DJT-VI-144
EXPNO 9
PROCNO 1

F2 - Acquisition Parameters
Date_ 2015214
Time 8.13
INSTRUM cryo500
PROBHD 5 mm CPTCI 1H-
PULPROG SpinEchopg30gp.prd
TD 65536
SOLVENT CDCl3
NS 518
DS 0
SWH 30303.031 Hz
FIDRES 0.462388 Hz
AQ 1.0813440 sec
RG 10321.3
DW 16.500 usec
DE 6.00 usec
TE 298.0 K
D1 0.25000000 sec
d11 0.03000000 sec
D16 0.00020000 sec
d17 0.00019600 sec
MCREST 0 sec
MCWRK 0.01500000 sec
P2 33.10 usec

======== CHANNEL f1 ========
NUC1 13C
P1 16.55 usec
P11 500.00 usec
P12 2000.00 usec
PL0 120.00 dB
PL1 -1.00 dB
SFO1 125.7942548 MHz
SP1 2.70 dB
SP2 2.70 dB
SPNAM[1] Crp60.0.5.20.1
SPNAM[2] Crp60comp.4
SPOFF1 0 Hz
SPOFF2 0 Hz

======== CHANNEL f2 ========
CPDPRG[2 waltz16
NUC2 1H
PCPD2 100.00 usec
PL2 1.60 dB
PL12 24.50 dB
SFO2 500.2225011 MHz

====== GRADIENT CHANNEL =====
GPNAM[1] SINE.100
GPNAM[2] SINE.100
GPX1 0 %
GPX2 0 %
GPY1 0 %
GPY2 0 %
GPZ1 30.00 %
GPZ2 50.00 %
p15 500.00 usec
p16 1000.00 usec

F2 - Processing parameters
SI 65536
SF 125.7804085 MHz
WDW EM
SSB 0
LB 1.00 Hz
GB 0
PC 2.00

1H spectrum

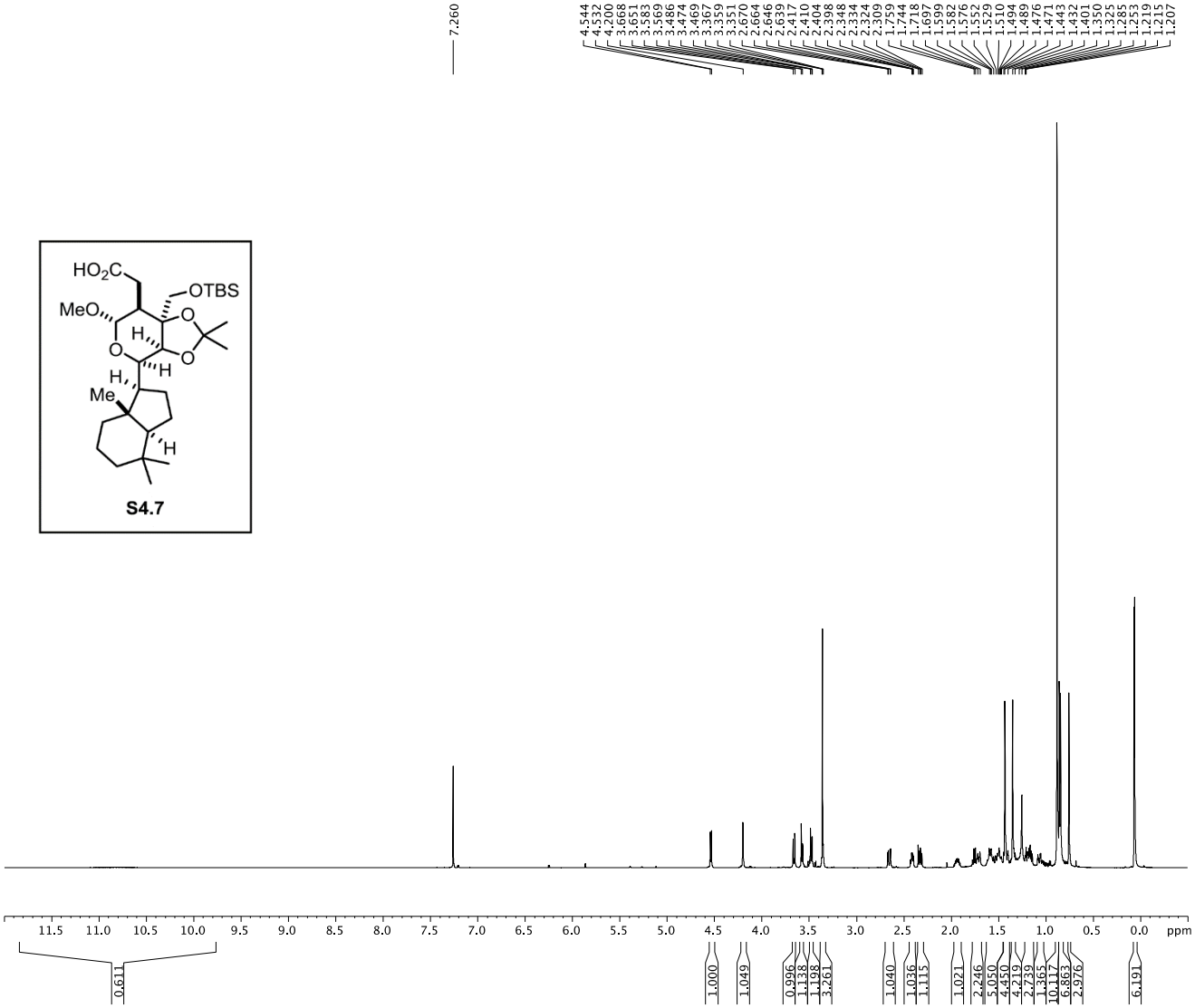

S4.7

Current Data Parameters
NAME DJT-VI-152
EXPNO 1
PROCNO 1

F2 - Acquisition Parameters
Date_ 20160107
Time 12.56
INSTRUM av600
PROBHD 5 mm TBI 1H/13
PULPROG zg30
TD 38460
SOLVENT CDCl3
NS 20
DS 0
SWH 9615.385 Hz
FIDRES 0.250010 Hz
AQ 1.9999200 sec
RG 456
DW 52.000 usec
DE 14.54 usec
TE 298.0 K
D1 0.10000000 sec
TD0 1

======== CHANNEL f1 ======
SFO1 600.1342009 MHz
NUC1 1H
P1 8.00 usec
PLW1 24.00000000 W

F2 - Processing parameters
SI 65536
SF 600.1300357 MHz
WDW EM
SSB 0
LB 0.30 Hz
GB 0
PC 1.00

Z-restored spin-echo 13C spectrum with 1H decoupling

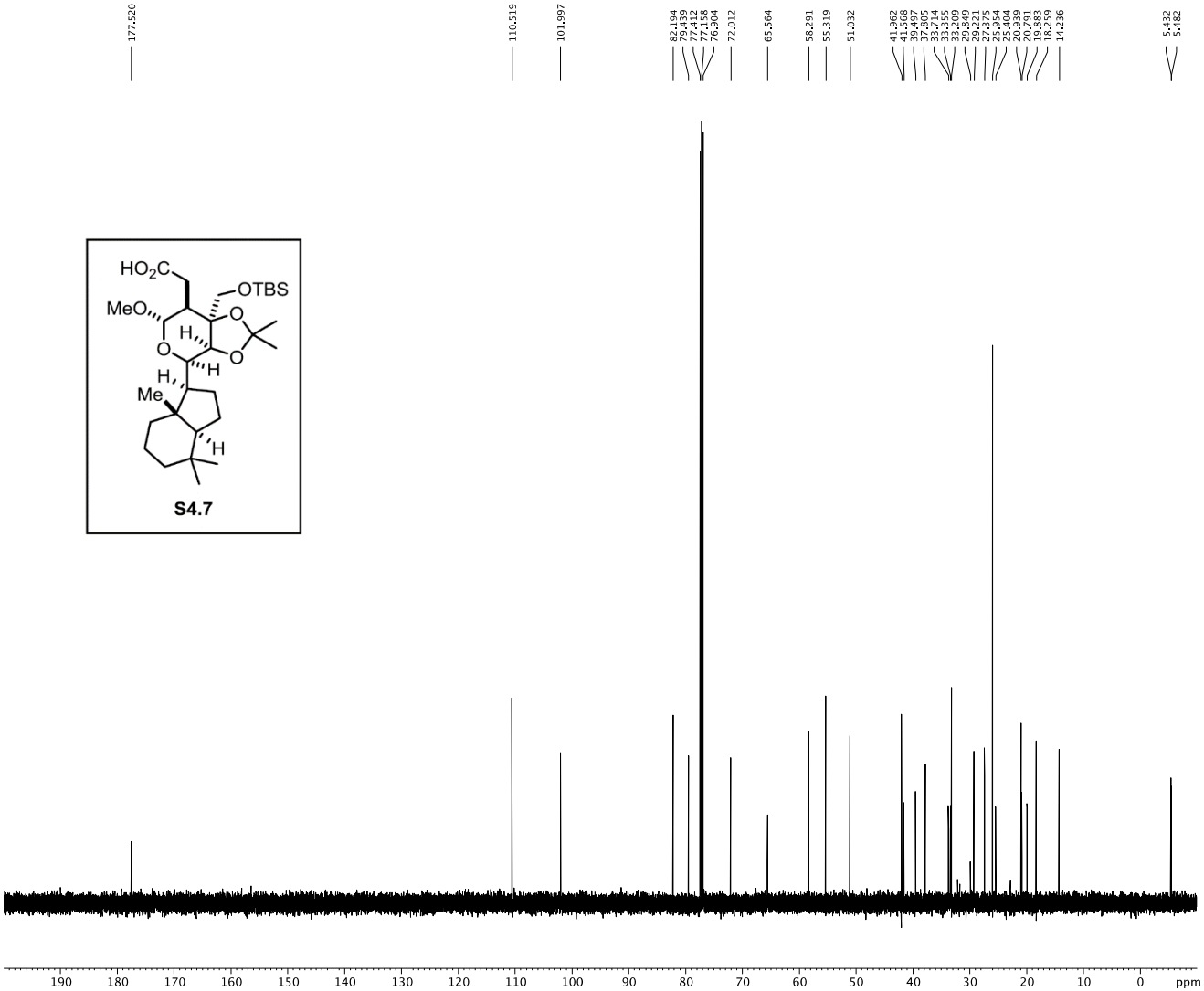

Current Data Parameters
NAME DJT-VI-152
EXPNO 3
PROCNO 1

F2 - Acquisition Parameters
Date_ 20160107
Time 14.14
INSTRUM cryo500
PROBHD 5 mm CPTC 1H-
PULPROG SpinEchopg30gp.prd
TD 65536
SOLVENT CDCl3
NS 253
DS 0
SWH 30303.031 Hz
FIDRES 0.462388 Hz
AQ 1.0813440 sec
RG 4096
DW 16.500 usec
DE 6.00 usec
TE 298.0 K
D1 0.25000000 sec
d11 0.03000000 sec
D16 0.00020000 sec
d17 0.00019600 sec
MCREST 0 sec
MCWRK 0.01500000 sec
P2 33.10 usec

======== CHANNEL f1 ========
NUC1 13C
P1 16.55 usec
P11 500.00 usec
P12 2000.00 usec
PL0 120.00 dB
PL1 -1.00 dB
SFO1 125.7942548 MHz
SP1 2.70 dB
SP2 2.70 dB
SPNAM[1] Crp60,0.5,20.1
SPNAM[2] Crp60comp.4
SPOFF1 0 Hz
SPOFF2 0 Hz

======== CHANNEL f2 ========
CPDPRG[2 waltz16
NUC2 1H
PCPD2 100.00 usec
PL2 1.60 dB
PL12 24.50 dB
SFO2 500.2225011 MHz

====== GRADIENT CHANNEL =====
GPNAM[1] SINE.100
GPNAM[2] SINE.100
GPX1 0 %
GPX2 0 %
GPY1 0 %
GPY2 0 %
GPZ1 30.00 %
GPZ2 50.00 %
p15 500.00 usec
p16 1000.00 usec

F2 - Processing parameters
SI 65536
SF 125.7804071 MHz
WDW no
SSB 0
LB 0 Hz
GB 0
PC 2.00

1H spectrum

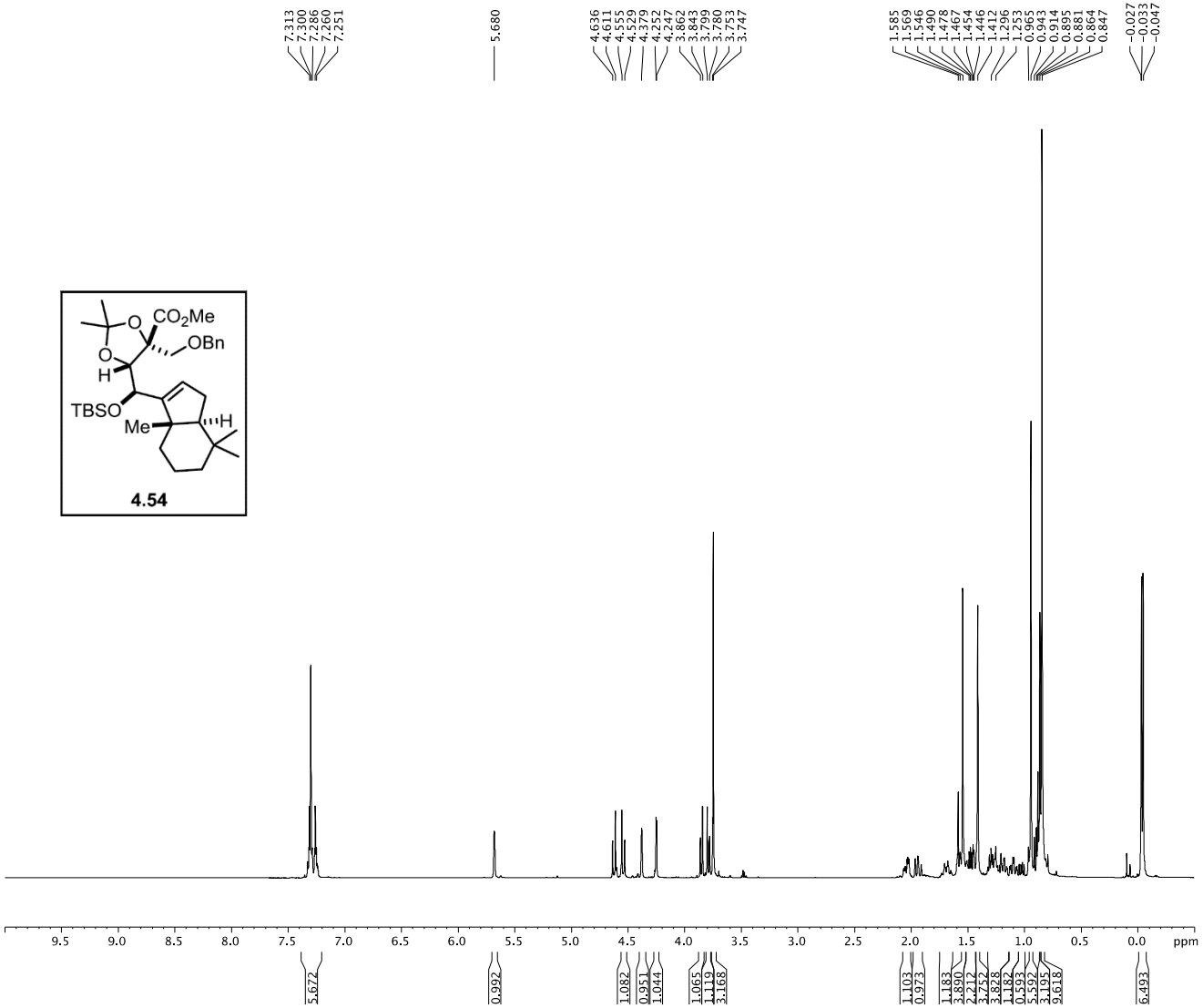

Current Data Parameters
NAME DJT-VI-135
EXPNO 1
PROCNO 1

F2 - Acquisition Parameters
Date_ 20151208
Time 13.53
INSTRUM cryo500
PROBHD 5 mm CPTCI 1H-
PULPROG zg30
TD 32048
SOLVENT CDCl3
NS 30
DS 0
SWH 8012.820 Hz
FIDRES 0.250026 Hz
AQ 1.9997952 sec
RG 5.7
DW 62.400 usec
DE 6.00 usec
TE 298.0 K
D1 0.10000000 sec
MCREST 0 sec
MCWRK 0.01500000 sec

======== CHANNEL f1 =====
NUC1 1H
P1 7.50 usec
PL1 1.60 dB
SFO1 500.2235015 MHz

F2 - Processing parameters
SI 65536
SF 500.2200318 MHz
WDW EM
SSB 0
LB 0.30 Hz
GB 0
PC 4.00

Z-restored spin-echo 13C spectrum with 1H decoupling

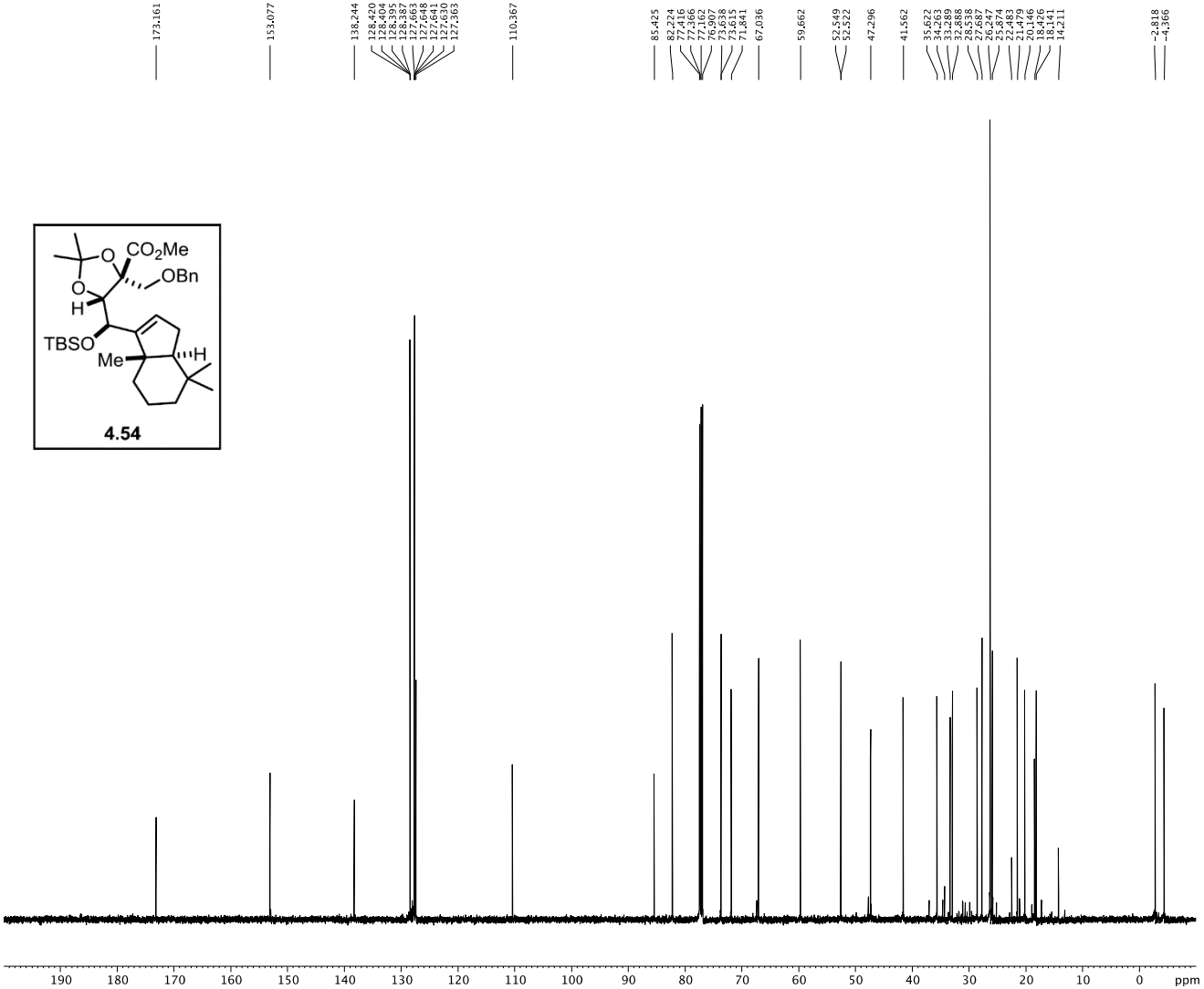

Current Data Parameters
NAME DJT-VI-135
EXPNO 2
PROCNO 1

F2 - Acquisition Parameters
Date_ 20151208
Time 13.57
INSTRUM cryo500
PROBHD 5 mm CPTCI 1H-
PULPROG SpinEchopg30gp.prd
TD 65536
SOLVENT CDCl3
NS 581
DS 0
SWH 30303.031 Hz
FIDRES 0.462388 Hz
AQ 1.0813440 sec
RG 5160.6
DW 16.500 usec
DE 6.00 usec
TE 298.0 K
D1 0.25000000 sec
d11 0.03000000 sec
D16 0.00020000 sec
d17 0.00019600 sec
MCREST 0 sec
MCWRK 0.01500000 sec
P2 33.10 usec

======== CHANNEL f1 ========
NUC1 13C
P1 16.55 usec
P11 500.00 usec
P12 2000.00 usec
PL0 120.00 dB
PL1 -1.00 dB
SFO1 125.7942548 MHz
SP1 2.70 dB
SP2 2.70 dB
SPNAM[1] Crp60,0.5,20.1
SPNAM[2] Crp60comp.4
SPOFF1 0 Hz
SPOFF2 0 Hz

======== CHANNEL f2 ========
CPDPRG[2 waltz16
NUC2 1H
PCPD2 100.00 usec
PL2 1.60 dB
PL12 24.50 dB
SFO2 500.2225011 MHz

====== GRADIENT CHANNEL =====
GPNAM[1] SINE.100
GPNAM[2] SINE.100
GPX1 0 %
GPX2 0 %
GPY1 0 %
GPY2 0 %
GPZ1 30.00 %
GPZ2 50.00 %
p15 500.00 usec
p16 1000.00 usec

F2 - Processing parameters
SI 65536
SF 125.7804090 MHz
WDW EM
SSB 0
LB 1.00 Hz
GB 0
PC 2.00

1H spectrum

4.55

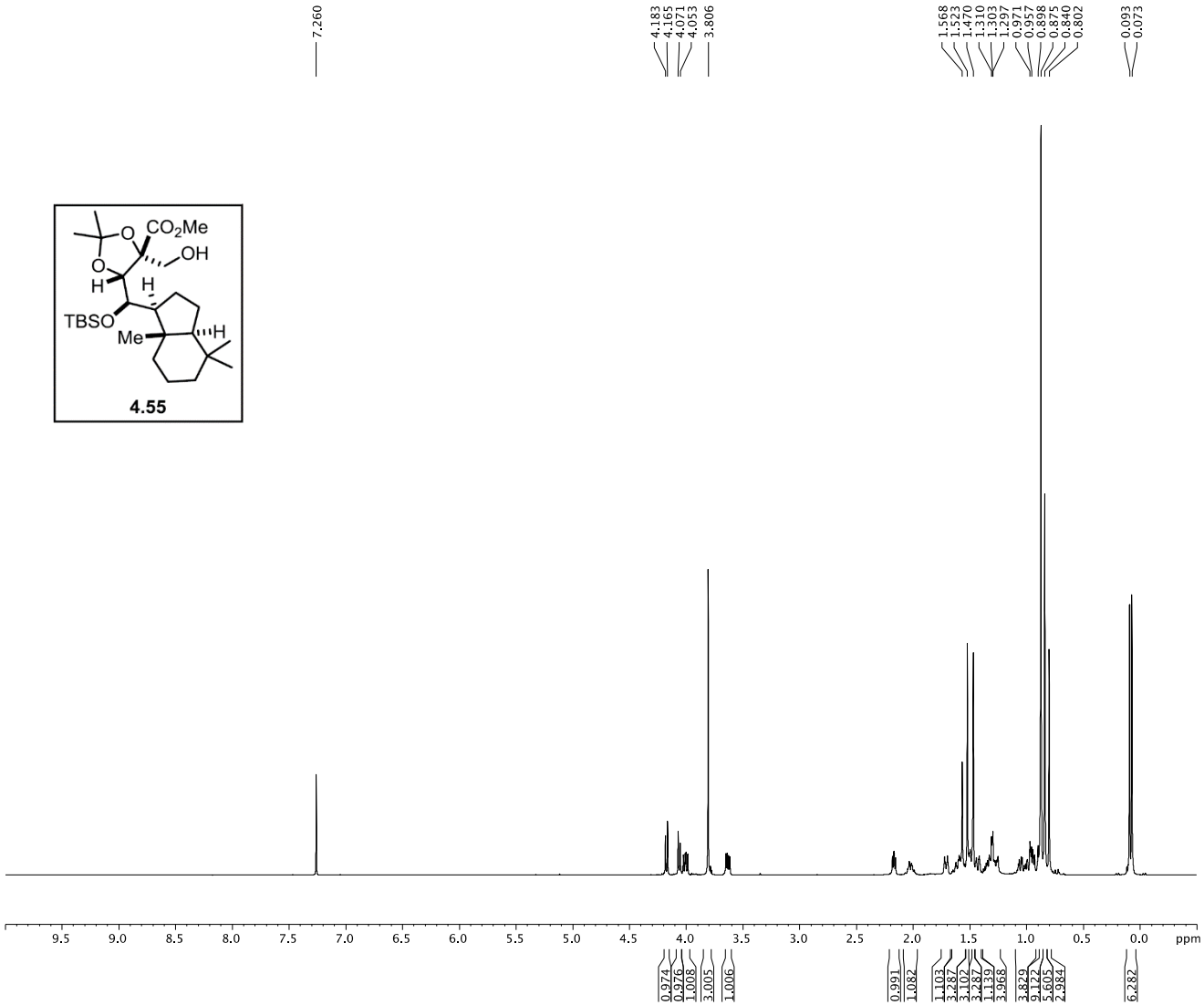

Current Data Parameters
NAME DJT-VI-133
EXPNO 2
PROCNO 1

F2 - Acquisition Parameters
Date_ 20151207
Time 13.32
INSTRUM cryo500
PROBHD 5 mm CPTCI 1H-
PULPROG zg30
TD 40062
SOLVENT CDCl3
NS 30
DS 0
SWH 8012.820 Hz
FIDRES 0.200010 Hz
AQ 2.4998689 sec
RG 8
DW 62.400 usec
DE 6.00 usec
TE 298.0 K
D1 0.10000000 sec
MCREST 0 sec
MCWRK 0.01500000 sec

======== CHANNEL f1 =====
NUC1 1H
P1 7.50 usec
PL1 1.60 dB
SFO1 500.2235015 MHz

F2 - Processing parameters
SI 65536
SF 500.2200317 MHz
WDW EM
SSB 0
LB 0.30 Hz
GB 0
PC 4.00

Z-restored spin-echo 13C spectrum with 1H decoupling

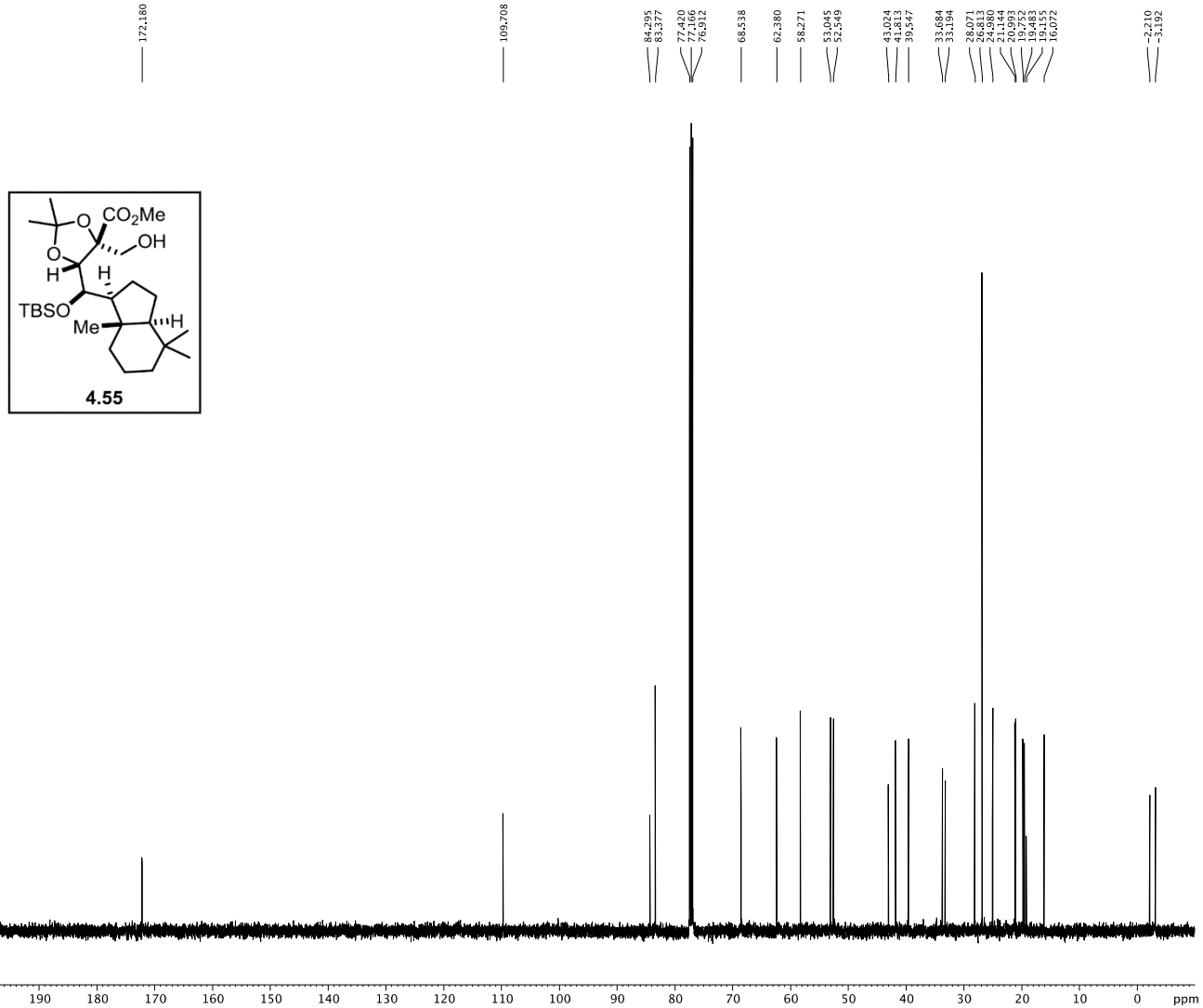

Current Data Parameters
NAME DJT-VI-133
EXPNO 3
PROCNO 1

F2 - Acquisition Parameters
Date_ 20151207
Time 13.36
INSTRUM cryo500
PROBHD 5 mm CPTCI 1H-
PULPROG SpinEchopg30gp.prd
TD 65536
SOLVENT CDCl3
NS 333
DS 0
SWH 30303.031 Hz
FIDRES 0.462388 Hz
AQ 1.0813440 sec
RG 3649.1
DW 16.500 usec
DE 6.00 usec
TE 298.0 K
D1 0.25000000 sec
d11 0.03000000 sec
D16 0.00020000 sec
d17 0.00019600 sec
MCREST 0 sec
MCWRK 0.01500000 sec
P2 33.10 usec

======== CHANNEL f1 ========
NUC1 13C
P1 16.55 usec
P11 500.00 usec
P12 2000.00 usec
PL0 120.00 dB
PL1 -1.00 dB
SFO1 125.7942548 MHz
SP1 2.70 dB
SP2 2.70 dB
SPNAM[1] Crp60,0.5,20.1
SPNAM[2] Crp60comp.4
SPOFF1 0 Hz
SPOFF2 0 Hz

======== CHANNEL f2 ========
CPDPRG[2 waltz16
NUC2 1H
PCPD2 100.00 usec
PL2 1.60 dB
PL12 24.50 dB
SFO2 500.2225011 MHz

====== GRADIENT CHANNEL =====
GPNAM[1] SINE.100
GPNAM[2] SINE.100
GPX1 0 %
GPX2 0 %
GPY1 0 %
GPY2 0 %
GPZ1 30.00 %
GPZ2 50.00 %
p15 500.00 usec
p16 1000.00 usec

F2 - Processing parameters
SI 65536
SF 125.7804071 MHz
WDW EM
SSB 0
LB 1.00 Hz
GB 0
PC 2.00

1H spectrum

4.56

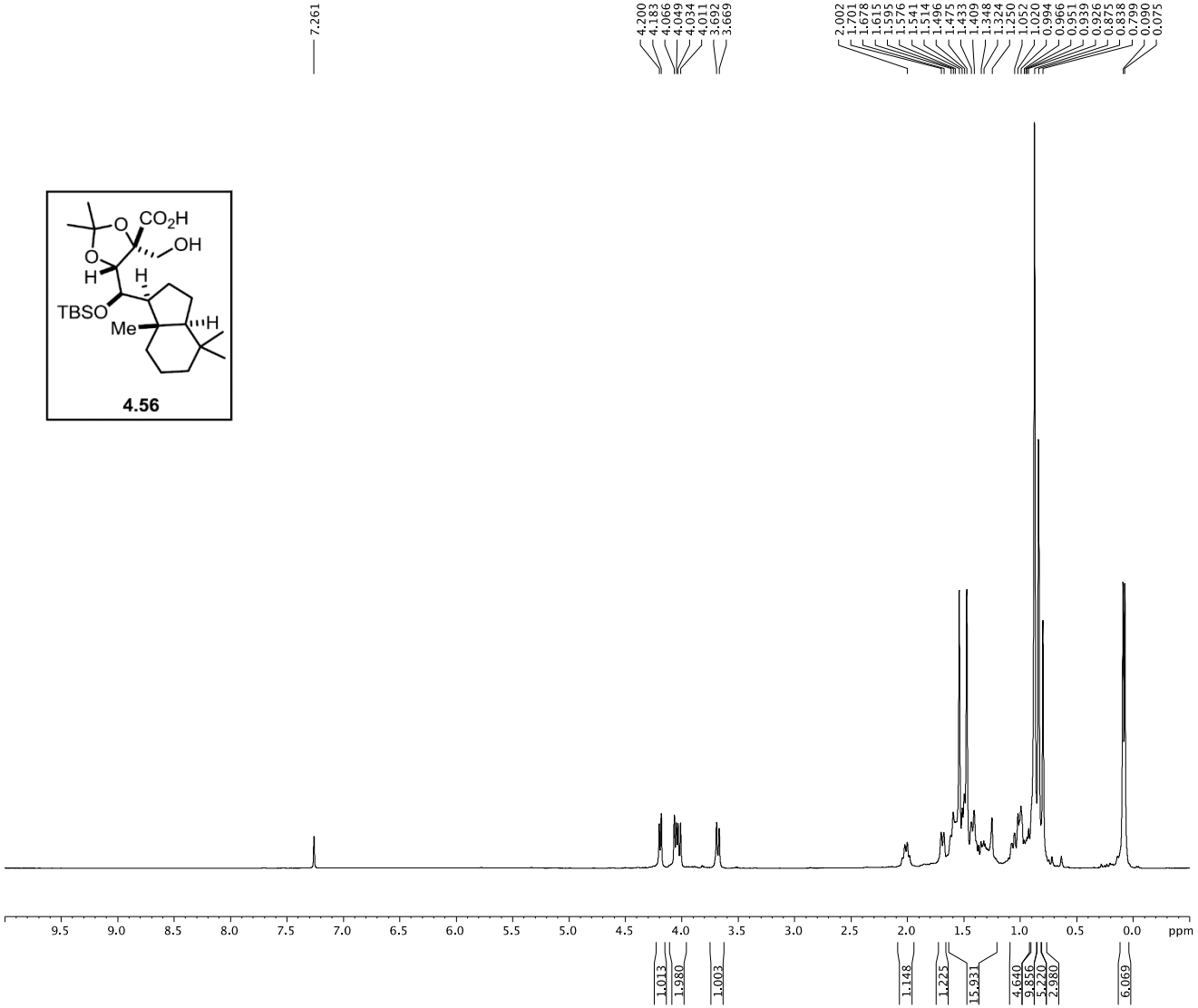

Current Data Parameters
NAME DJT-VI-142
EXPNO 3
PROCNO 1

F2 - Acquisition Parameters
Date_ 20151214
Time 13.08
INSTRUM cryo500
PROBHD 5 mm CPTCI 1H-
PULPROG zg30
TD 81728
SOLVENT CDCl3
NS 20
DS 0
SWH 8012.820 Hz
FIDRES 0.098043 Hz
AQ 5.0998273 sec
RG 4.5
DW 62.400 usec
DE 6.00 usec
TE 298.0 K
D1 0.10000000 sec
MCREST 0 sec
MCWRK 0.01500000 sec

======== CHANNEL f1 =====
NUC1 1H
P1 7.50 usec
PL1 1.60 dB
SFO1 500.2235015 MHz

F2 - Processing parameters
SI 65536
SF 500.2200318 MHz
WDW EM
SSB 0
LB 0.30 Hz
GB 0
PC 4.00

Z-restored spin-echo 13C spectrum with 1H decoupling

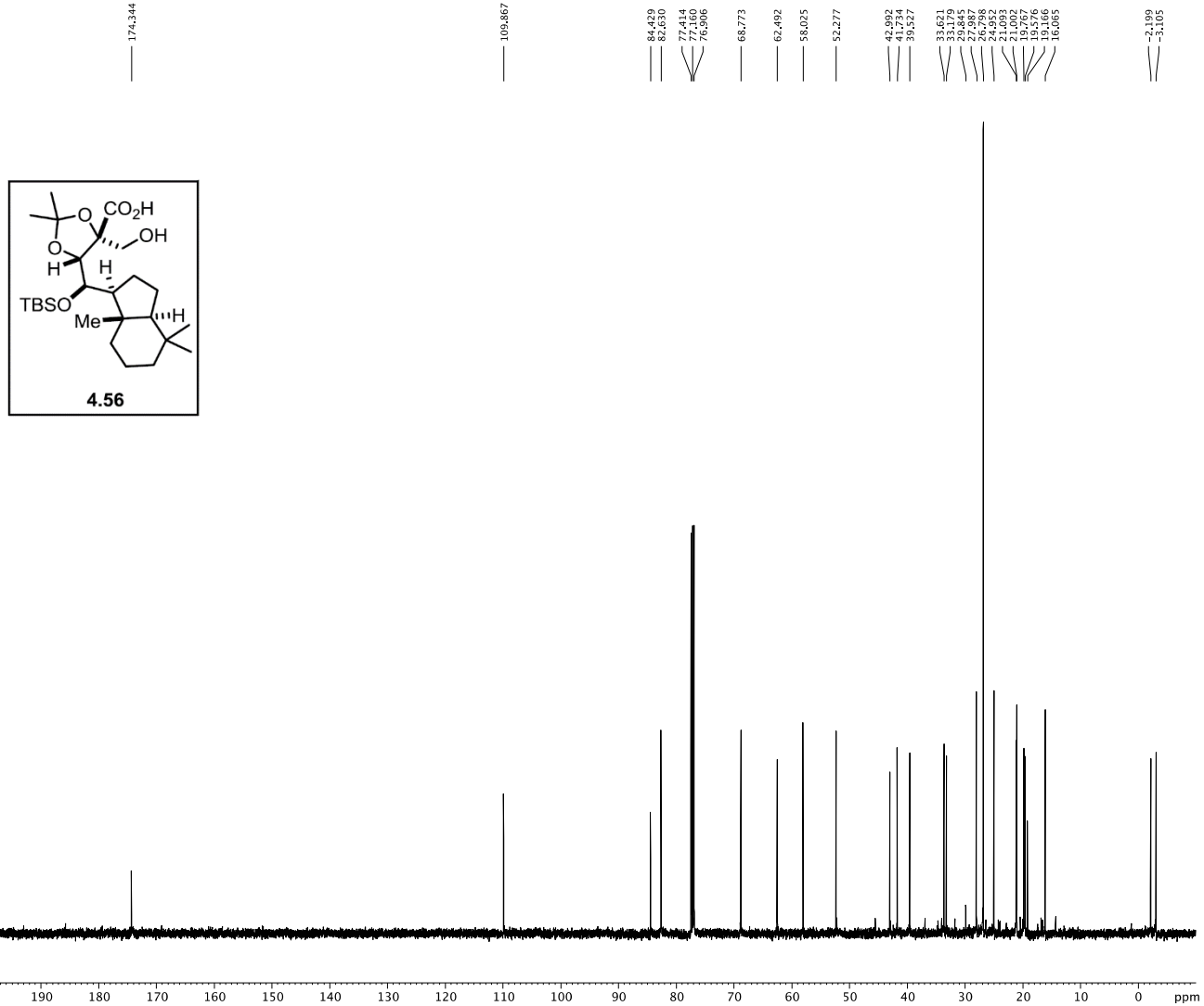

Current Data Parameters
NAME DJT-VI-142
EXPNO 4
PROCNO 1

F2 - Acquisition Parameters
Date_ 20151214
Time 13.11
INSTRUM cryo500
PROBHD 5 mm CPTCI 1H-
PULPROG SpinEchopg30gp.prd
TD 65536
SOLVENT CDCl3
NS 239
DS 16
SWH 30303.031 Hz
FIDRES 0.462388 Hz
AQ 1.0813440 sec
RG 6502
DW 16.500 usec
DE 6.00 usec
TE 298.0 K
D1 0.25000000 sec
d11 0.03000000 sec
D16 0.00020000 sec
d17 0.00019600 sec
MCREST 0 sec
MCWRK 0.01500000 sec
P2 33.10 usec

======== CHANNEL f1 ========
NUC1 13C
P1 16.55 usec
P11 500.00 usec
P12 2000.00 usec
PL0 120.00 dB
PL1 -1.00 dB
SFO1 125.7942548 MHz
SP1 2.70 dB
SP2 2.70 dB
SPNAM[1] Crp60,0.5,20.1
SPNAM[2] Crp60comp.4
SPOFF1 0 Hz
SPOFF2 0 Hz

======== CHANNEL f2 ========
CPDPRG[2 waltz16
NUC2 1H
PCPD2 100.00 usec
PL2 1.60 dB
PL12 24.50 dB
SFO2 500.2225011 MHz

====== GRADIENT CHANNEL =====
GPNAM[1] SINE.100
GPNAM[2] SINE.100
GPX1 0 %
GPX2 0 %
GPY1 0 %
GPY2 0 %
GPZ1 30.00 %
GPZ2 50.00 %
p15 500.00 usec
p16 1000.00 usec

F2 - Processing parameters
SI 65536
SF 125.7804085 MHz
WDW EM
SSB 0
LB 1.00 Hz
GB 0
PC 2.00

1H spectrum

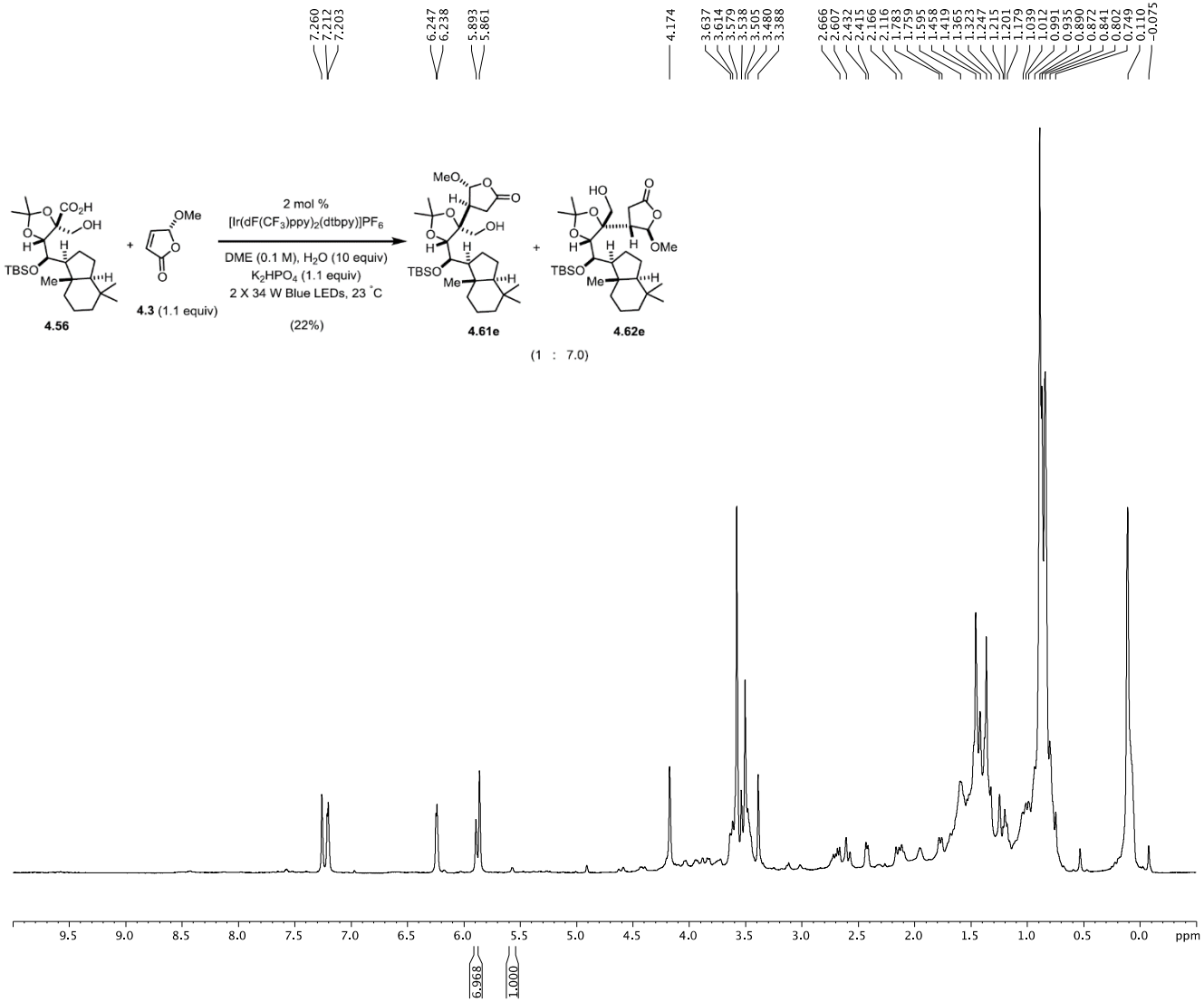

Current Data Parameters
NAME DJT-VI-148
EXPNO 1
PROCNO 1

F2 - Acquisition Parameters
Date_ 20151215
Time 9.33
INSTRUM cryo500
PROBHD 5 mm CPTCI 1H-
PULPROG zg30
TD 81728
SOLVENT CDCl3
NS 20
DS 0
SWH 8012.820 Hz
FIDRES 0.098043 Hz
AQ 5.0998273 sec
RG 5
DW 62.400 usec
DE 6.00 usec
TE 298.0 K
D1 0.10000000 sec
MCREST 0 sec
MCWRK 0.01500000 sec

======== CHANNEL f1 =====
NUC1 1H
P1 7.50 usec
PL1 1.60 dB
SFO1 500.2235015 MHz

F2 - Processing parameters
SI 65536
SF 500.2200324 MHz
WDW EM
SSB 0
LB 0.30 Hz
GB 0
PC 4.00

1H spectrum

4.62e

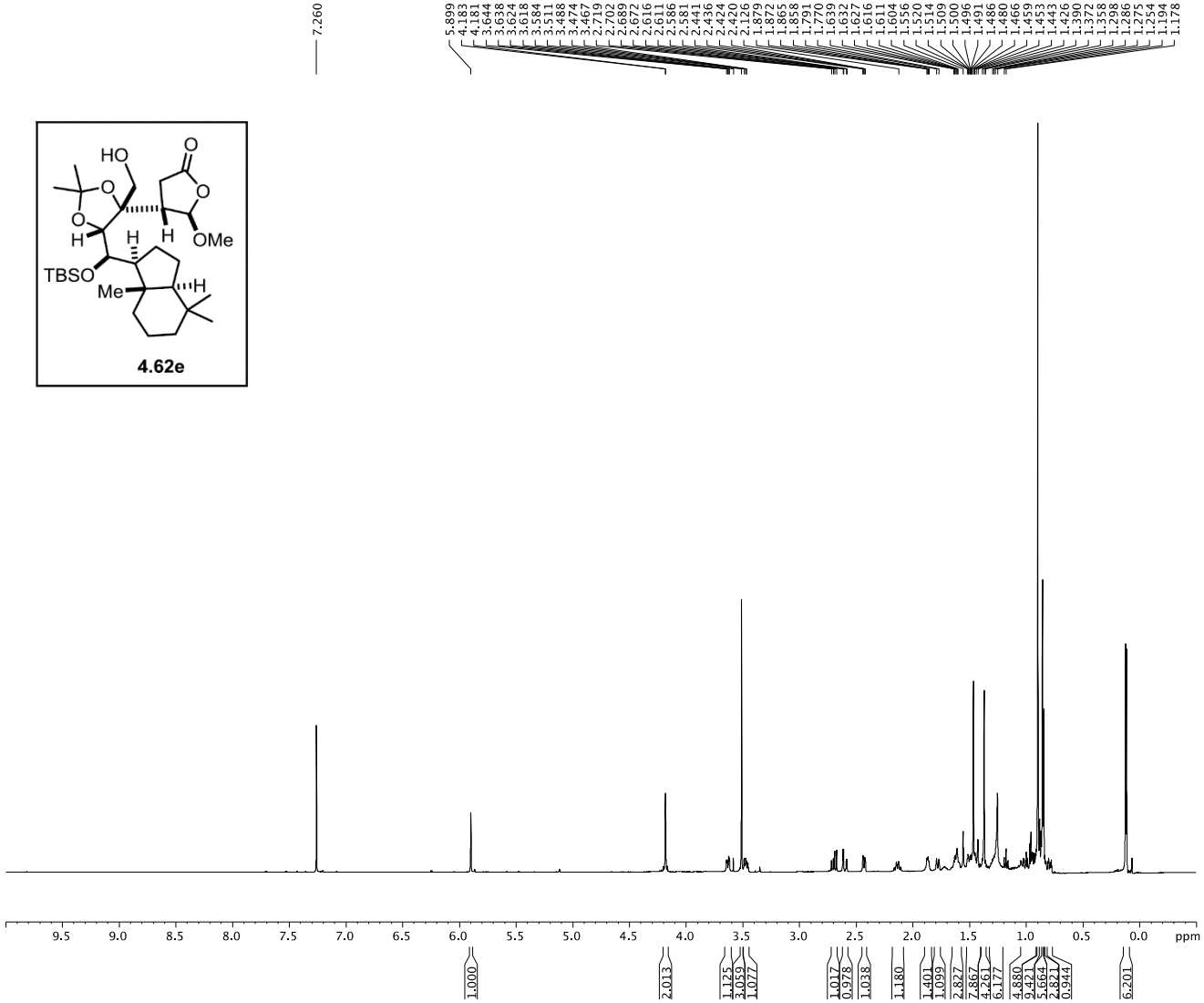

Current Data Parameters
NAME DJT-VI-148
EXPNO 2
PROCNO 1

F2 - Acquisition Parameters
Date_ 20151215
Time 15.04
INSTRUM av600
PROBHD 5 mm TBI 1H/13
PULPROG zg30
TD 98074
SOLVENT CDCl3
NS 20
DS 0
SWH 9615.385 Hz
FIDRES 0.098042 Hz
AQ 5.0998478 sec
RG 181
DW 52.000 usec
DE 14.54 usec
TE 298.0 K
D1 0.10000000 sec
TD0 1

======== CHANNEL f1 =====
SFO1 600.1342009 MHz
NUC1 1H
P1 8.00 usec
PLW1 24.00000000 W

F2 - Processing parameters
SI 65536
SF 600.1300357 MHz
WDW EM
SSB 0
LB 0.30 Hz
GB 0
PC 1.00

Z-restored spin-echo 13C spectrum with 1H decoupling

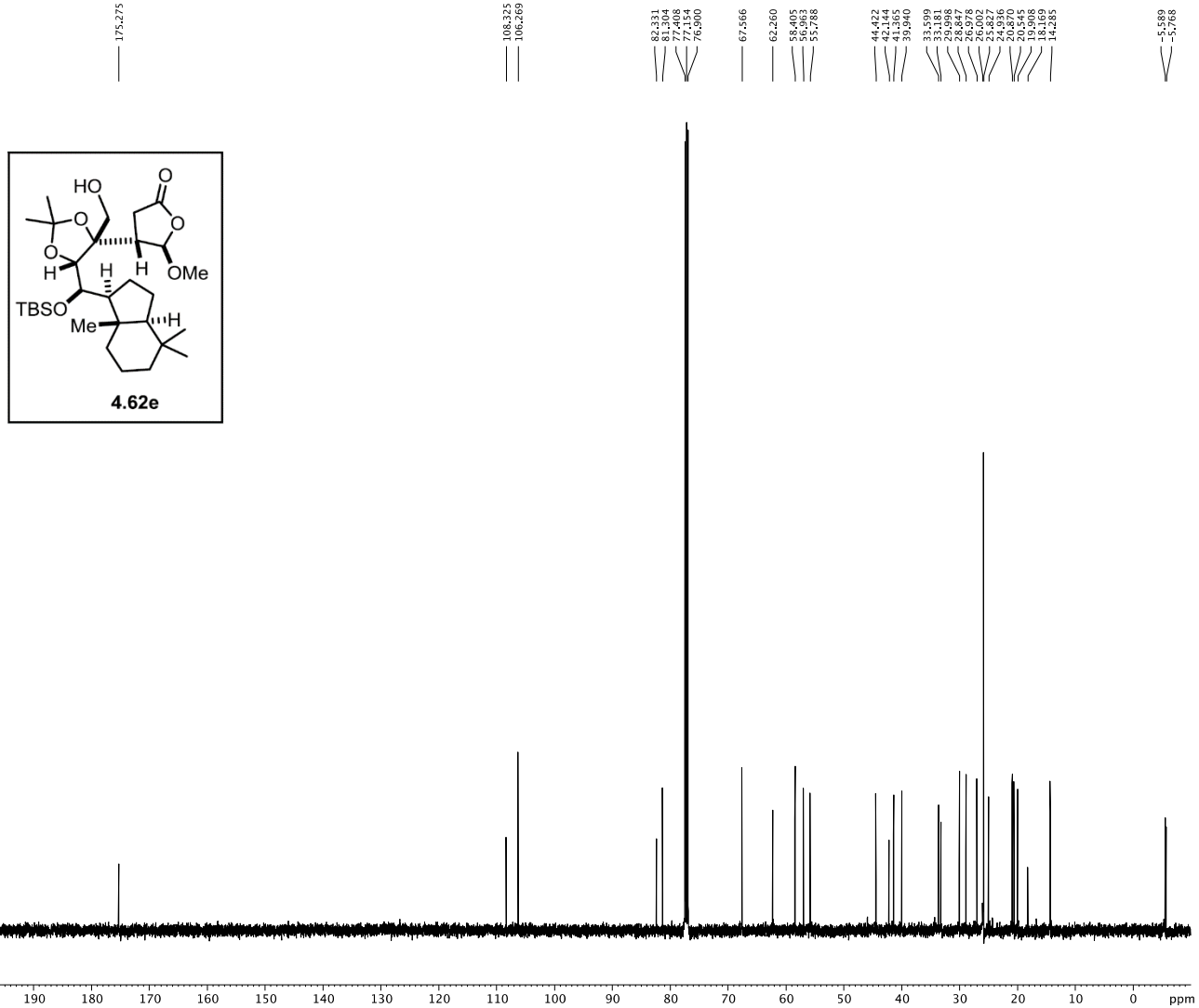

Current Data Parameters
NAME DJT-VI-144
EXPNO 9
PROCNO 1

F2 - Acquisition Parameters
Date_ 20151214
Time 8.13
INSTRUM cryo500
PROBHD 5 mm CPTCI 1H-
PULPROG SpinEchopg30gp.prd
TD 65536
SOLVENT CDCl3
NS 518
DS 0
SWH 30303.031 Hz
FIDRES 0.462388 Hz
AQ 1.0813440 sec
RG 10321.3
DW 16.500 usec
DE 6.00 usec
TE 298.0 K
D1 0.25000000 sec
d11 0.03000000 sec
D16 0.00020000 sec
d17 0.00019600 sec
MCREST 0 sec
MCWRK 0.01500000 sec
P2 33.10 usec

======== CHANNEL f1 ========
NUC1 13C
P1 16.55 usec
P11 500.00 usec
P12 2000.00 usec
PL0 120.00 dB
PL1 -1.00 dB
SFO1 125.7942548 MHz
SP1 2.70 dB
SP2 2.70 dB
SPNAM[1] Crp60,0.5,20.1
SPNAM[2] Crp60comp.4
SPOFF1 0 Hz
SPOFF2 0 Hz

======== CHANNEL f2 ========
CPDPRG[2 waltz16
NUC2 1H
PCPD2 100.00 usec
PL2 1.60 dB
PL12 24.50 dB
SFO2 500.2225011 MHz

====== GRADIENT CHANNEL =====
GPNAM[1] SINE.100
GPNAM[2] SINE.100
GPX1 0 %
GPX2 0 %
GPY1 0 %
GPY2 0 %
GPZ1 30.00 %
GPZ2 50.00 %
p15 500.00 usec
p16 1000.00 usec

F2 - Processing parameters
SI 65536
SF 125.7804085 MHz
WDW EM
SSB 0
LB 1.00 Hz
GB 0
PC 2.00

1H spectrum

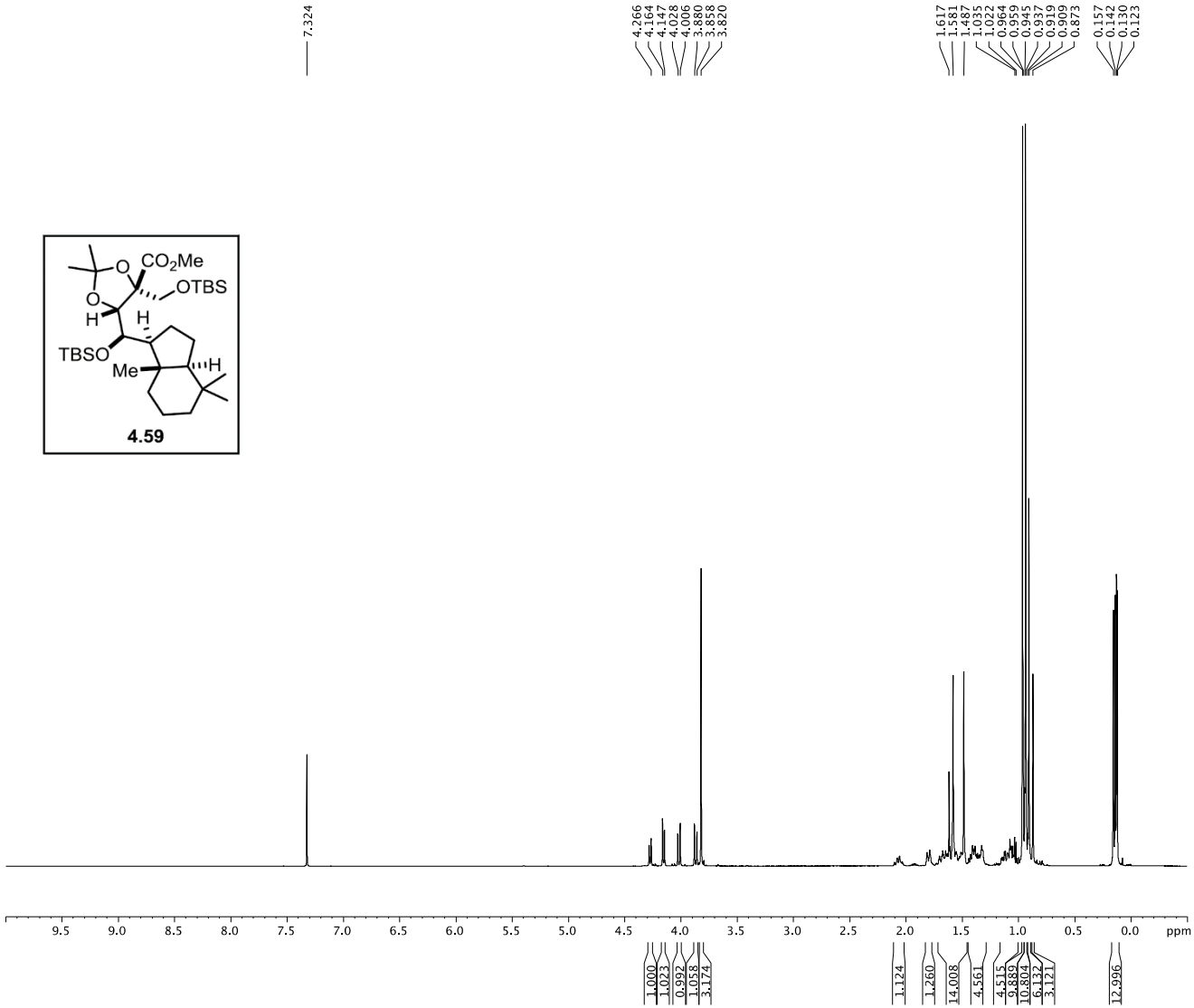

Current Data Parameters
NAME DJT-VI-132
EXPNO 1
PROCNO 1

F2 - Acquisition Parameters
Date_ 20151207
Time 13.48
INSTRUM cryo500
PROBHD 5 mm CPTCI 1H-
PULPROG zg30
TD 40062
SOLVENT CDCl3
NS 20
DS 0
SWH 8012.820 Hz
FIDRES 0.200010 Hz
AQ 2.4998689 sec
RG 10.1
DW 62.400 usec
DE 6.00 usec
TE 298.0 K
D1 0.10000000 sec
MCREST 0 sec
MCWRK 0.01500000 sec

======== CHANNEL f1 =====
NUC1 1H
P1 7.50 usec
PL1 1.60 dB
SFO1 500.2235015 MHz

F2 - Processing parameters
SI 65536
SF 500.2200000 MHz
WDW EM
SSB 0
LB 0.30 Hz
GB 0
PC 4.00

Z-restored spin-echo 13C spectrum with 1H decoupling

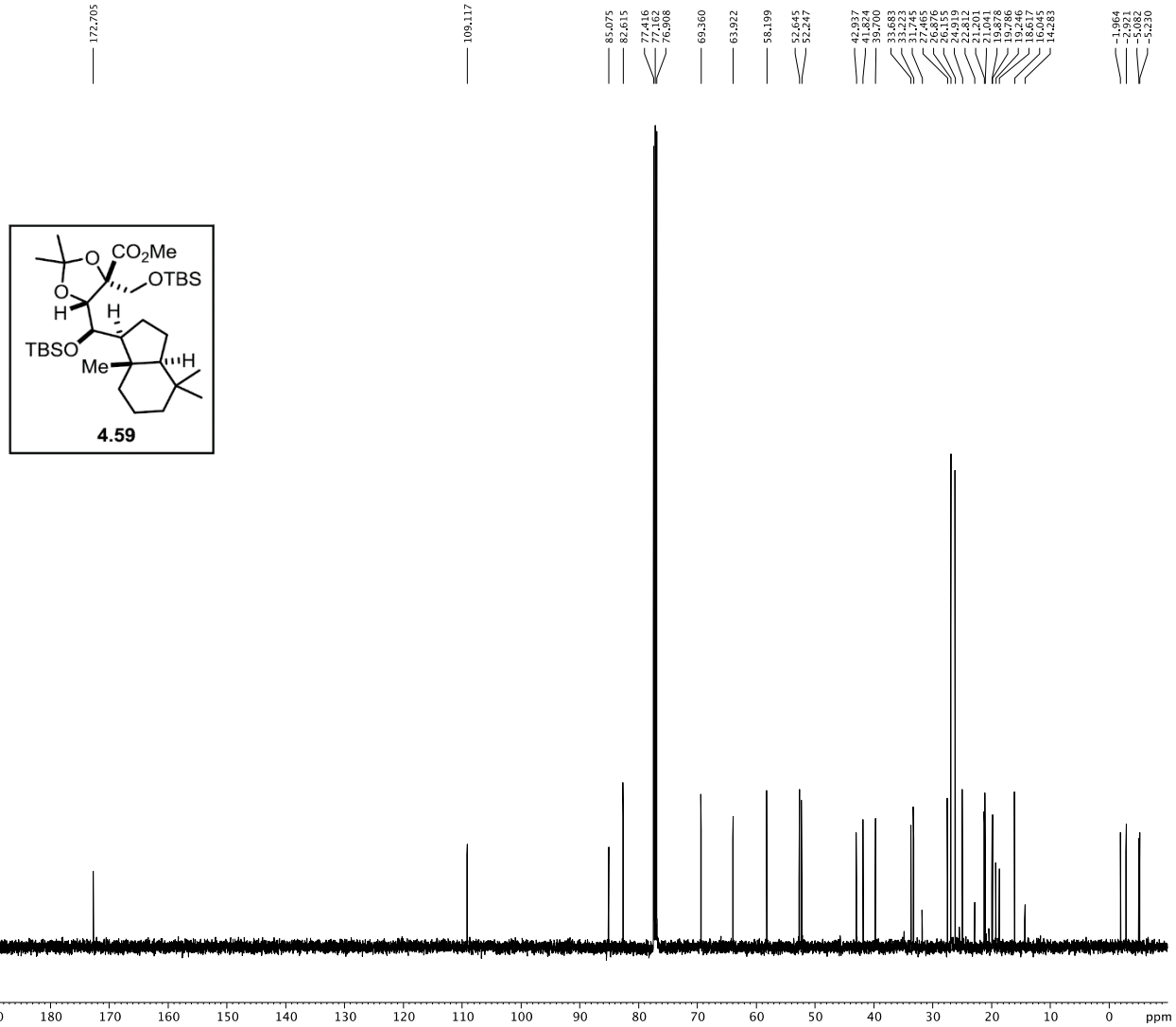

Current Data Parameters
NAME DJT-VI-132
EXPNO 2
PROCNO 1

F2 - Acquisition Parameters
Date_ 20151207
Time 13.51
INSTRUM cryo500
PROBHD 5 mm CPTCI 1H-
PULPROG SpinEchopg30gp.prd
TD 65536
SOLVENT CDCl3
NS 574
DS 0
SWH 30303.031 Hz
FIDRES 0.462388 Hz
AQ 1.0813440 sec
RG 4597.6
DW 16.500 usec
DE 6.00 usec
TE 298.0 K
D1 0.25000000 sec
d11 0.03000000 sec
D16 0.00020000 sec
d17 0.00019600 sec
MCREST 0 sec
MCWRK 0.01500000 sec
P2 33.10 usec

======== CHANNEL f1 ========
NUC1 13C
P1 16.55 usec
P11 500.00 usec
P12 2000.00 usec
PL0 120.00 dB
PL1 -1.00 dB
SFO1 125.7942548 MHz
SP1 2.70 dB
SP2 2.70 dB
SPNAM[1] Crp60.0.5.20.1
SPNAM[2] Crp60comp.4
SPOFF1 0 Hz
SPOFF2 0 Hz

======== CHANNEL f2 ========
CPDPRG[2 waltz16
NUC2 1H
PCPD2 100.00 usec
PL2 1.60 dB
PL12 24.50 dB
SFO2 500.2225011 MHz

====== GRADIENT CHANNEL =====
GPNAM[1] SINE.100
GPNAM[2] SINE.100
GPX1 0 %
GPX2 0 %
GPY1 0 %
GPY2 0 %
GPZ1 30.00 %
GPZ2 50.00 %
p15 500.00 usec
p16 1000.00 usec

F2 - Processing parameters
SI 65536
SF 125.7804071 MHz
WDW EM
SSB 0
LB 1.00 Hz
GB 0
PC 2.00

1H spectrum

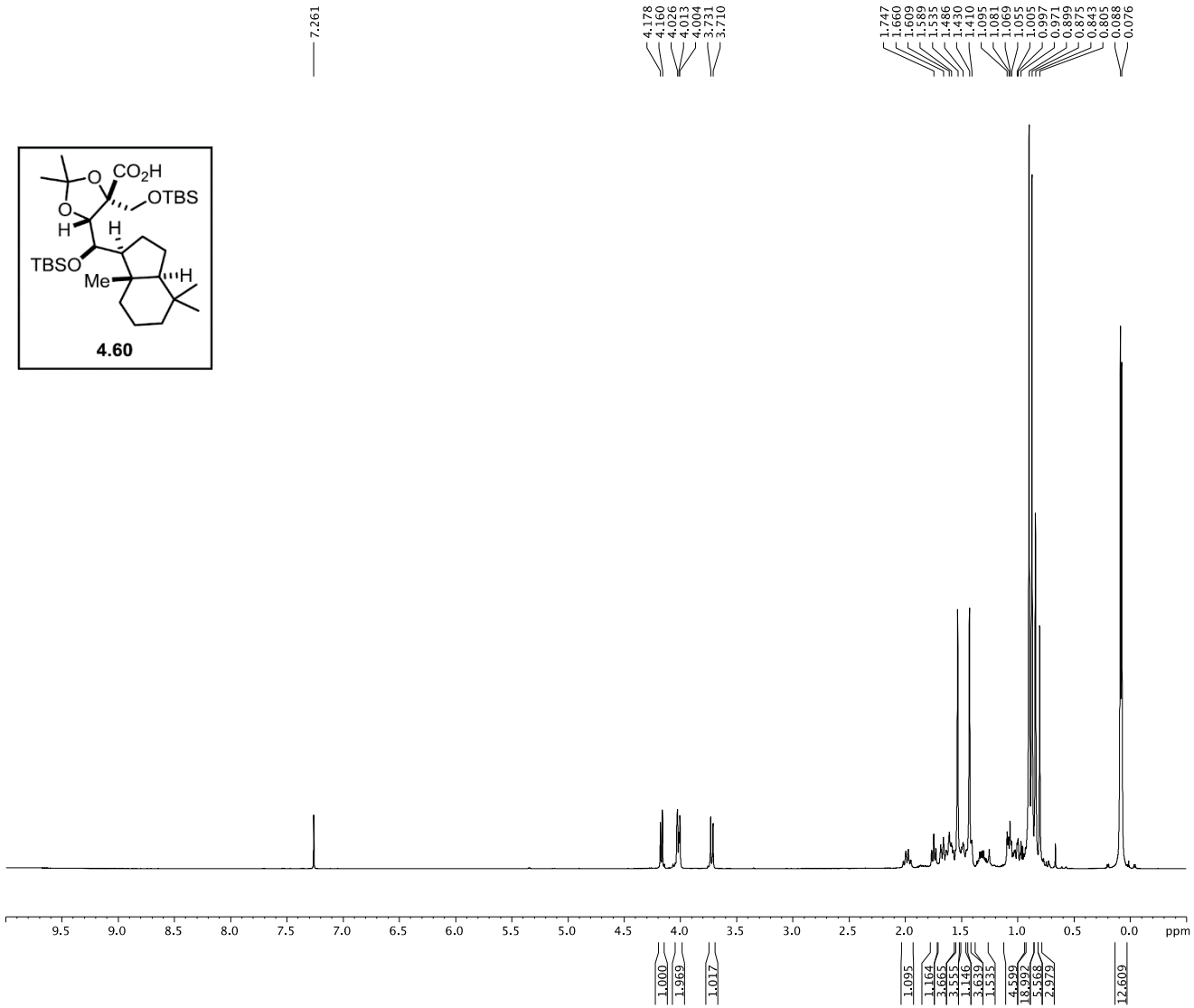

4.60

```
Current Data Parameters
NAME        DJT-VI-143
EXPNO             1
PROCNO            1

F2 - Acquisition Parameters
Date_       20151212
Time          10.10
INSTRUM       cryo500
PROBHD   5 mm CPTCI 1H-
PULPROG          zg30
TD             80126
SOLVENT        CDCl3
NS               20
DS                0
SWH         8012.820 Hz
FIDRES      0.100003 Hz
AQ          4.9998622 sec
RG               4.5
DW            62.400 usec
DE             6.00 usec
TE            298.0 K
D1          0.10000000 sec
MCREST   0 sec
MCWRK       0.01500000 sec

======== CHANNEL f1 =====
NUC1             1H
P1            7.50 usec
PL1           1.60 dB
SFO1       500.2235015 MHz

F2 - Processing parameters
SI            65536
SF        500.2200313 MHz
WDW              no
SSB     0
LB      0 Hz
GB      0
PC            4.00
```

Z-restored spin-echo 13C spectrum with 1H decoupling

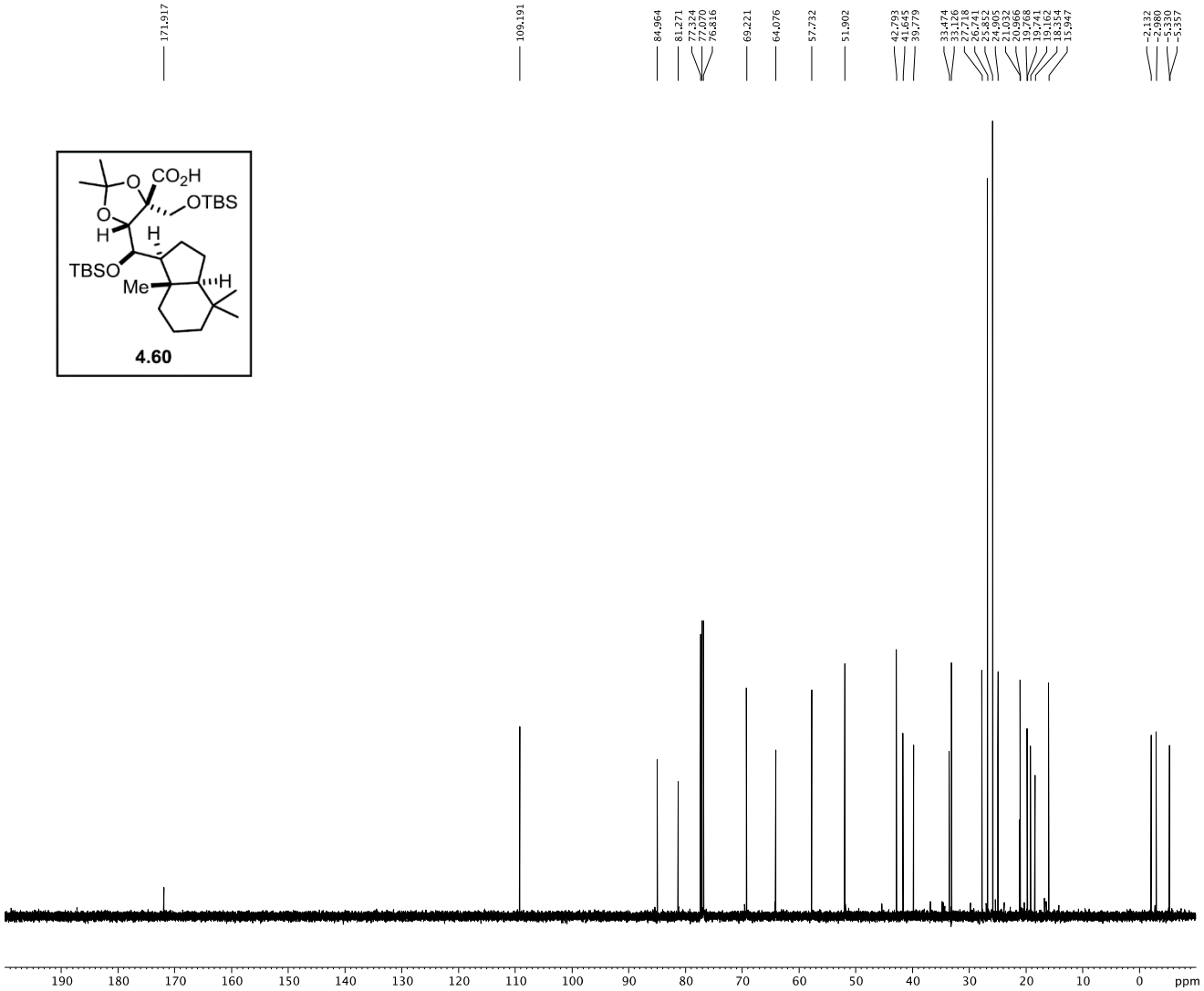


```
Current Data Parameters
NAME        DJT-VI-143
EXPNO            2
PROCNO           1

F2 - Acquisition Parameters
Date_       20151212
Time          10.15
INSTRUM      cryo500
PROBHD  5 mm CPTCI 1H-
PULPROG  SpinEchopg30gp.prd
TD          65536
SOLVENT       CDCl3
NS            377
DS              0
SWH        30303.031 Hz
FIDRES      0.462388 Hz
AQ         1.0813440 sec
RG          11585.2
DW           16.500 usec
DE            6.00 usec
TE          298.0 K
D1        0.25000000 sec
d11       0.03000000 sec
D16       0.00020000 sec
d17       0.00019600 sec
MCREST   0 sec
MCWRK     0.01500000 sec
P2           33.10 usec

======== CHANNEL f1 ========
NUC1           13C
P1           16.55 usec
P11         500.00 usec
P12        2000.00 usec
PL0         120.00 dB
PL1          -1.00 dB
SFO1      125.7942548 MHz
SP1           2.70 dB
SP2           2.70 dB
SPNAM[1] Crp60.0.5.20.1
SPNAM[2]   Crp60comp.4
SPOFF1   0 Hz
SPOFF2   0 Hz

======== CHANNEL f2 ========
CPDPRG[2       waltz16
NUC2            1H
PCPD2         100.00 usec
PL2           1.60 dB
PL12          24.50 dB
SFO2      500.2225011 MHz

====== GRADIENT CHANNEL =====
GPNAM[1]      SINE.100
GPNAM[2]      SINE.100
GPX1     0 %
GPX2     0 %
GPY1     0 %
GPY2     0 %
GPZ1          30.00 %
GPZ2          50.00 %
p15          500.00 usec
p16         1000.00 usec

F2 - Processing parameters
SI          65536
SF      125.7804190 MHz
WDW            no
SSB     0
LB      0 Hz
GB      0
PC           2.00
```

1H spectrum

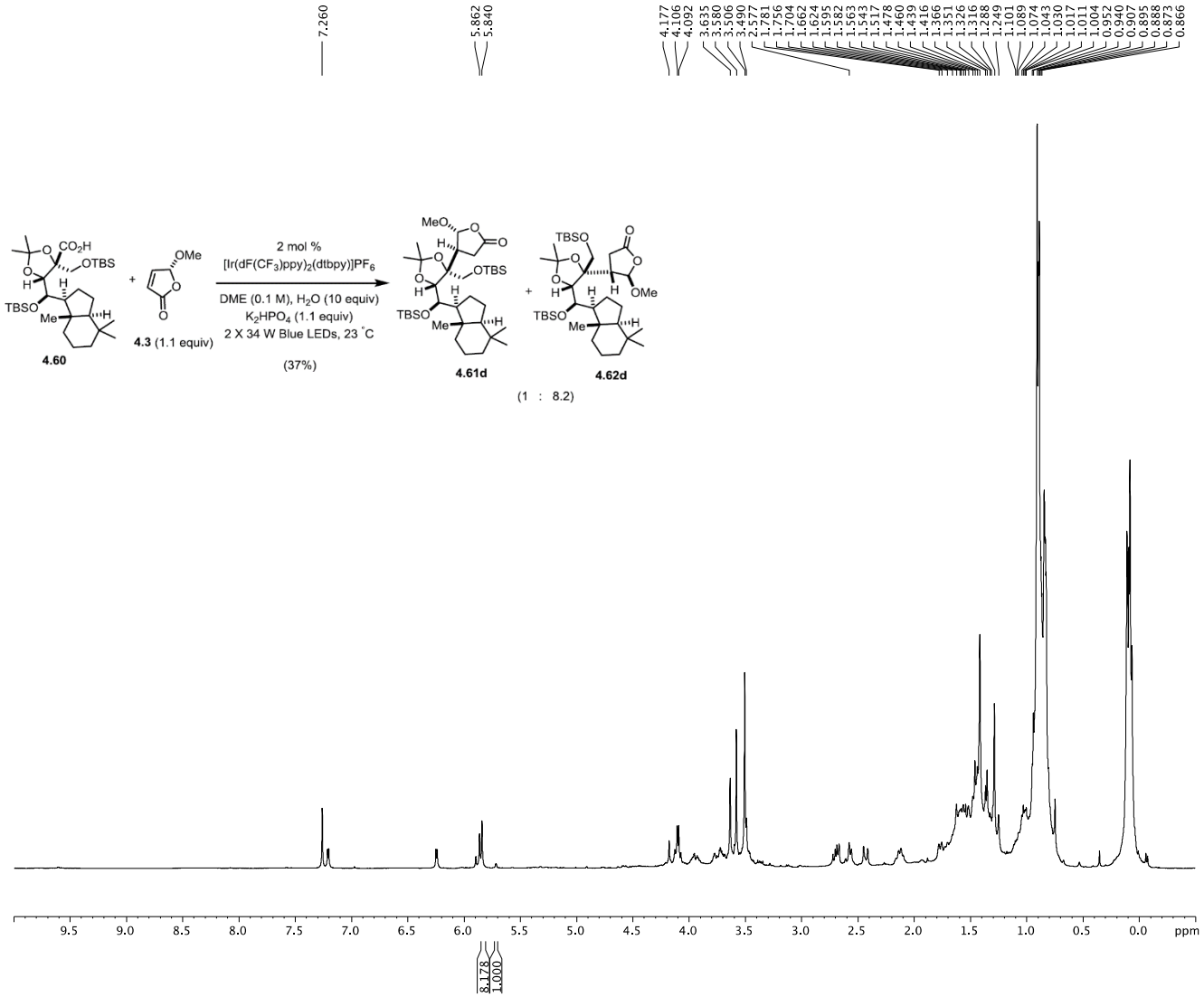

Current Data Parameters
NAME DJT-VI-146
EXPNO 1
PROCNO 1

F2 - Acquisition Parameters
Date_ 20151214
Time 7.50
INSTRUM cryo500
PROBHD 5 mm CPTCI 1H-
PULPROG zg30
TD 80126
SOLVENT CDCl3
NS 20
DS 0
SWH 8012.820 Hz
FIDRES 0.100003 Hz
AQ 4.9998622 sec
RG 4.5
DW 62.400 usec
DE 6.00 usec
TE 298.0 K
D1 0.10000000 sec
MCREST 0 sec
MCWRK 0.01500000 sec

======== CHANNEL f1 =====
NUC1 1H
P1 7.50 usec
PL1 1.60 dB
SFO1 500.2235015 MHz

F2 - Processing parameters
SI 65536
SF 500.2200318 MHz
WDW EM
SSB 0
LB 0.30 Hz
GB 0
PC 4.00

1H spectrum

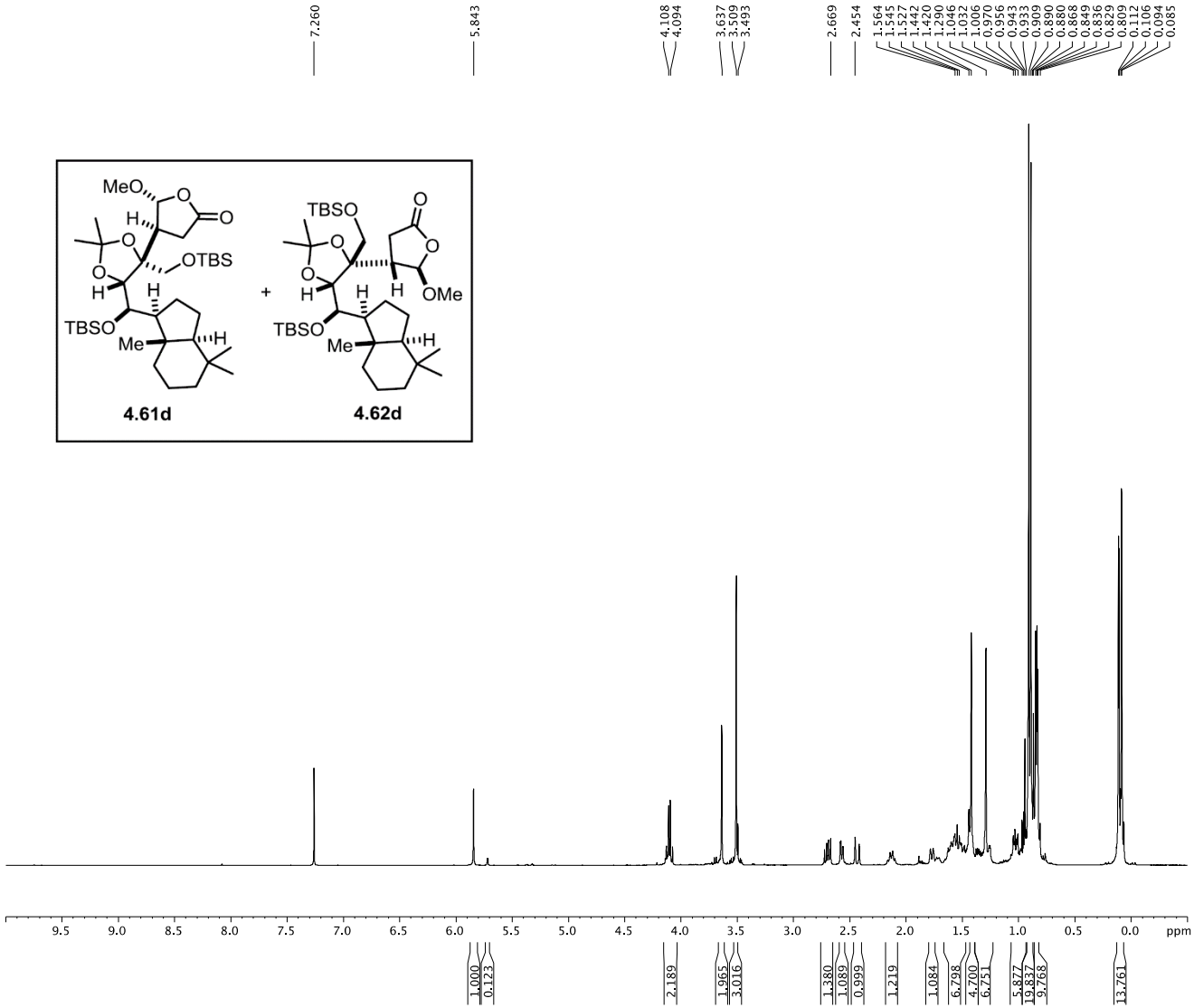

Current Data Parameters
NAME DJT-VI-146
EXPNO 3
PROCNO 1

F2 - Acquisition Parameters
Date_ 20151215
Time 7.40
INSTRUM cryo500
PROBHD 5 mm CPTCI 1H-
PULPROG zg30
TD 81728
SOLVENT CDCl3
NS 20
DS 0
SWH 8012.820 Hz
FIDRES 0.098043 Hz
AQ 5.0998273 sec
RG 5
DW 62.400 usec
DE 6.00 usec
TE 298.0 K
D1 0.10000000 sec
MCREST 0 sec
MCWRK 0.01500000 sec

======== CHANNEL f1 =====
NUC1 1H
P1 7.50 usec
PL1 1.60 dB
SFO1 500.2235015 MHz

F2 - Processing parameters
SI 65536
SF 500.2200316 MHz
WDW EM
SSB 0
LB 0.30 Hz
GB 0
PC 4.00

Z-restored spin-echo 13C spectrum with 1H decoupling

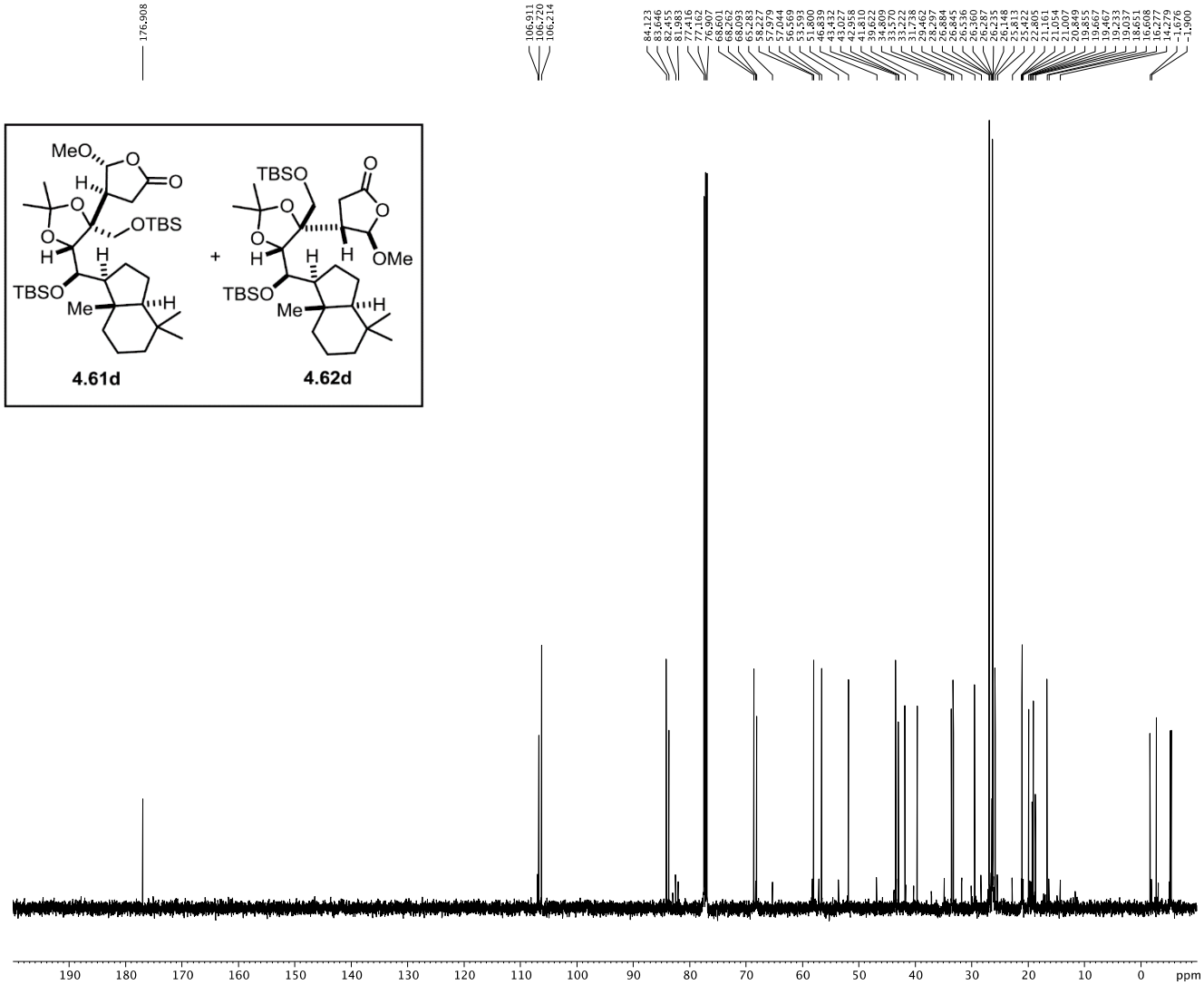

Current Data Parameters
NAME DJT-VI-146
EXPNO 4
PROCNO 1

F2 - Acquisition Parameters
Date_ 20151215
Time 7.46
INSTRUM cryo500
PROBHD 5 mm CPTCI 1H-
PULPROG SpinEchopg30gp.prd
TD 65536
SOLVENT CDCl3
NS 299
DS 0
SWH 30303.031 Hz
FIDRES 0.462388 Hz
AQ 1.0813440 sec
RG 7298.2
DW 16.500 usec
DE 6.00 usec
TE 298.0 K
D1 0.25000000 sec
d11 0.03000000 sec
D16 0.00020000 sec
d17 0.00019600 sec
MCREST 0 sec
MCWRK 0.01500000 sec
P2 33.10 usec

======== CHANNEL f1 ========
NUC1 13C
P1 16.55 usec
P11 500.00 usec
P12 2000.00 usec
PL0 120.00 dB
PL1 -1.00 dB
SFO1 125.7942548 MHz
SP1 2.70 dB
SP2 2.70 dB
SPNAM[1] Crp60.0.5.20.1
SPNAM[2] Crp60comp.4
SPOFF1 0 Hz
SPOFF2 0 Hz

======== CHANNEL f2 ========
CPDPRG[2 waltz16
NUC2 1H
PCPD2 100.00 usec
PL2 1.60 dB
PL12 24.50 dB
SFO2 500.2225011 MHz

====== GRADIENT CHANNEL =====
GPNAM[1] SINE.100
GPNAM[2] SINE.100
GPX1 0 %
GPX2 0 %
GPY1 0 %
GPY2 0 %
GPZ1 30.00 %
GPZ2 50.00 %
p15 500.00 usec
p16 1000.00 usec

F2 - Processing parameters
SI 65536
SF 125.7804076 MHz
WDW EM
SSB 0
LB 1.00 Hz
GB 0
PC 2.00

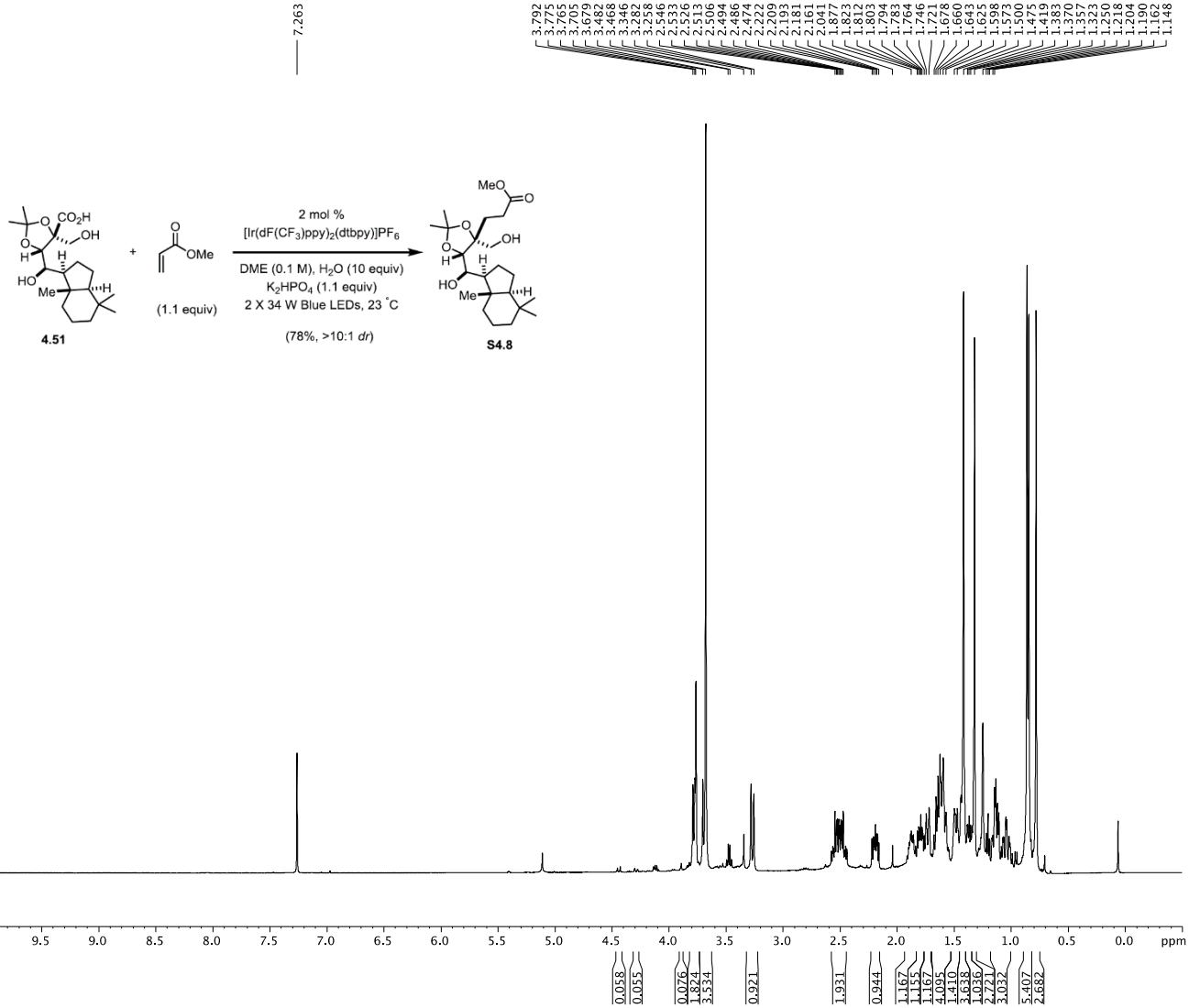

Current Data Parameters
NAME YS-IV-15
EXPNO 2
PROCNO 1

F2 - Acquisition Parameters
Date_ 20151204
Time 17.39
INSTRUM cryo500
PROBHD 5 mm CPTCI 1H-
PULPROG zg30
TD 81728
SOLVENT CDCl3
NS 8
DS 2
SWH 8012.820 Hz
FIDRES 0.098043 Hz
AQ 5.0998273 sec
RG 6.3
DW 62.400 usec
DE 6.00 usec
TE 298.0 K
D1 0.10000000 sec
MCREST 0 sec
MCWRK 0.01500000 sec

======== CHANNEL f1 ========
NUC1 1H
P1 7.50 usec
PL1 1.60 dB
SFO1 500.2235015 MHz

F2 - Processing parameters
SI 65536
SF 500.2200312 MHz
WDW EM
SSB 0
LB 0.30 Hz
GB 0
PC 4.00

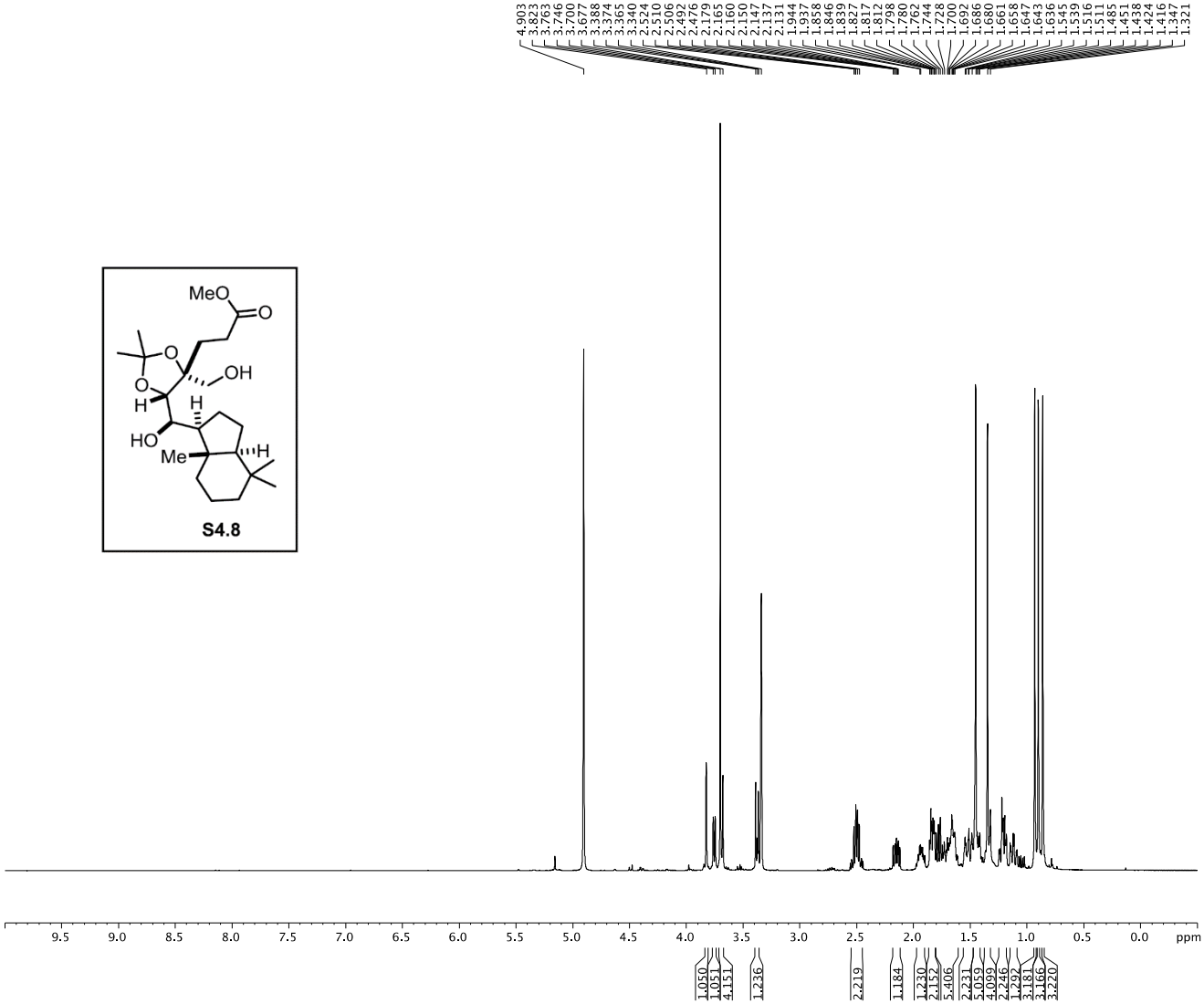

S4.8

Current Data Parameters
NAME YS-IV-15
EXPNO 15
PROCNO 1

F2 - Acquisition Parameters
Date_ 20151216
Time 8.56
INSTRUM cryo500
PROBHD 5 mm CPTCI 1H-
PULPROG zg30
TD 81728
SOLVENT CD3OD
NS 8
DS 2
SWH 8012.820 Hz
FIDRES 0.098043 Hz
AQ 5.0998273 sec
RG 9
DW 62.400 usec
DE 6.00 usec
TE 298.0 K
D1 0.10000000 sec
MCREST 0 sec
MCWRK 0.01500000 sec

======== CHANNEL f1 ========
NUC1 1H
P1 7.50 usec
PL1 1.60 dB
SFO1 500.2235015 MHz

F2 - Processing parameters
SI 65536
SF 500.2200042 MHz
WDW EM
SSB 0
LB 0.30 Hz
GB 0
PC 4.00

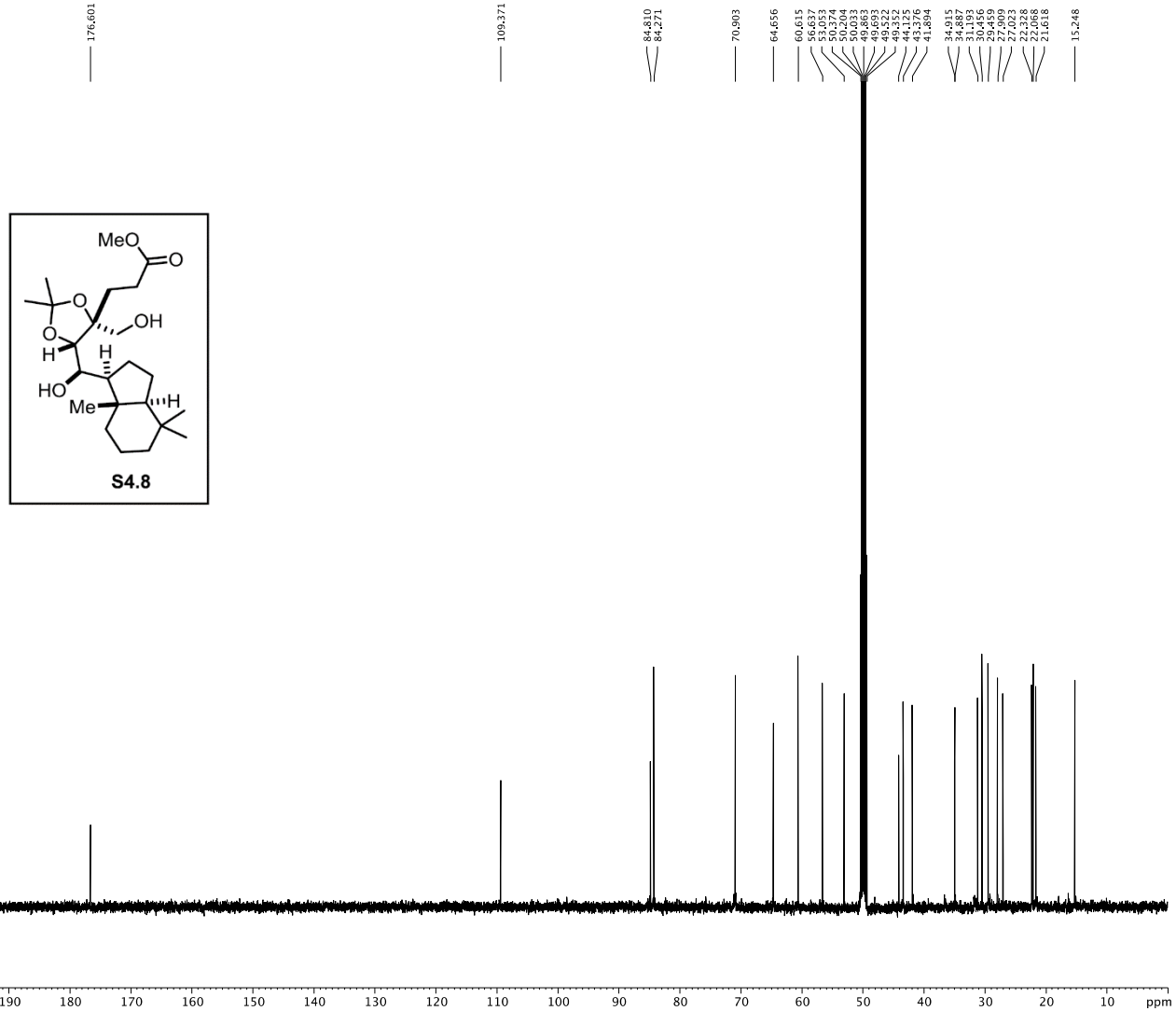

Current Data Parameters
NAME YS-IV-15
EXPNO 16
PROCNO 1

F2 - Acquisition Parameters
Date_ 20151216
Time 8.57
INSTRUM cryo500
PROBHD 5 mm CPTCI 1H-
PULPROG SpinEchopg30gp.prd
TD 65536
SOLVENT CDCl3
NS 320
DS 2
SWH 30303.031 Hz
FIDRES 0.462388 Hz
AQ 1.0813440 sec
RG 4597.6
DW 16.500 usec
DE 6.00 usec
TE 298.0 K
D1 0.25000000 sec
d11 0.03000000 sec
D16 0.00020000 sec
d17 0.00019600 sec
MCREST 0 sec
MCWRK 0.01500000 sec
P2 33.10 usec

======== CHANNEL f1 ========
NUC1 13C
P1 16.55 usec
P11 500.00 usec
P12 2000.00 usec
PL0 120.00 dB
PL1 -1.00 dB
SFO1 125.7942548 MHz
SP1 2.70 dB
SP2 2.70 dB
SPNAM[1] Crp60,0.5,20.1
SPNAM[2] Crp60comp.4
SPOFF1 0 Hz
SPOFF2 0 Hz

======== CHANNEL f2 ========
CPDPRG[2 waltz16
NUC2 1H
PCPD2 100.00 usec
PL2 1.60 dB
PL12 24.50 dB
SFO2 500.2225011 MHz

====== GRADIENT CHANNEL =====
GPNAM[1] SINE.100
GPNAM[2] SINE.100
GPX1 0 %
GPX2 0 %
GPY1 0 %
GPY2 0 %
GPZ1 30.00 %
GPZ2 50.00 %
p15 500.00 usec
p16 1000.00 usec

F2 - Processing parameters
SI 65536
SF 125.7801371 MHz
WDW EM
SSB 0
LB 1.00 Hz
GB 0
PC 2.00

1H spectrum

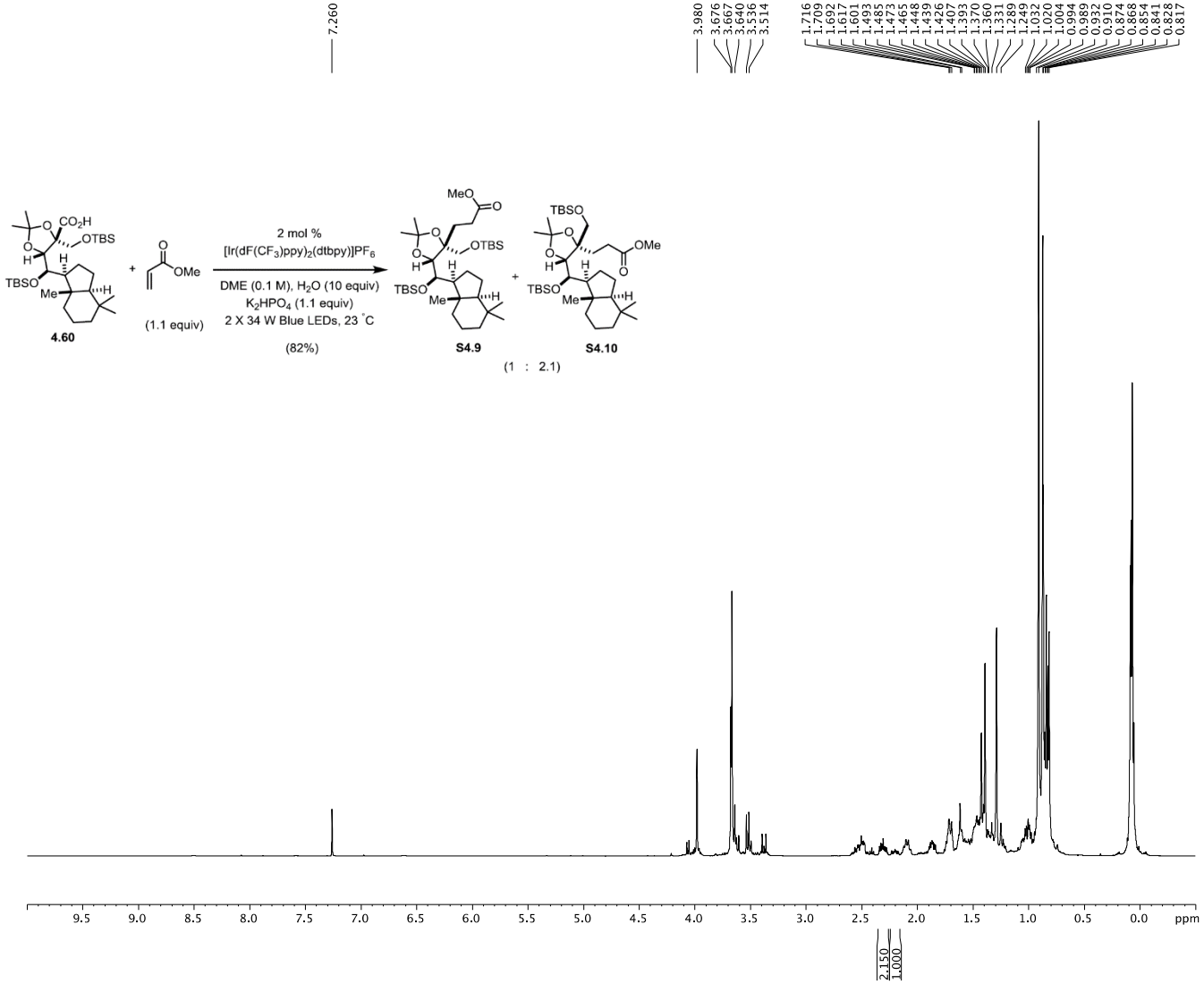

Current Data Parameters
NAME DJT-VI-147
EXPNO 1
PROCNO 1

F2 - Acquisition Parameters
Date_ 20151214
Time 7.55
INSTRUM cryo500
PROBHD 5 mm CPTCI 1H-
PULPROG zg30
TD 81728
SOLVENT CDCl3
NS 20
DS 0
SWH 8012.820 Hz
FIDRES 0.098043 Hz
AQ 5.0998273 sec
RG 4
DW 62.400 usec
DE 6.00 usec
TE 298.0 K
D1 0.10000000 sec
MCREST 0 sec
MCWRK 0.01500000 sec

======== CHANNEL f1 =====
NUC1 1H
P1 7.50 usec
PL1 1.60 dB
SFO1 500.2235015 MHz

F2 - Processing parameters
SI 65536
SF 500.2200314 MHz
WDW EM
SSB 0
LB 0.30 Hz
GB 0
PC 4.00

1H spectrum

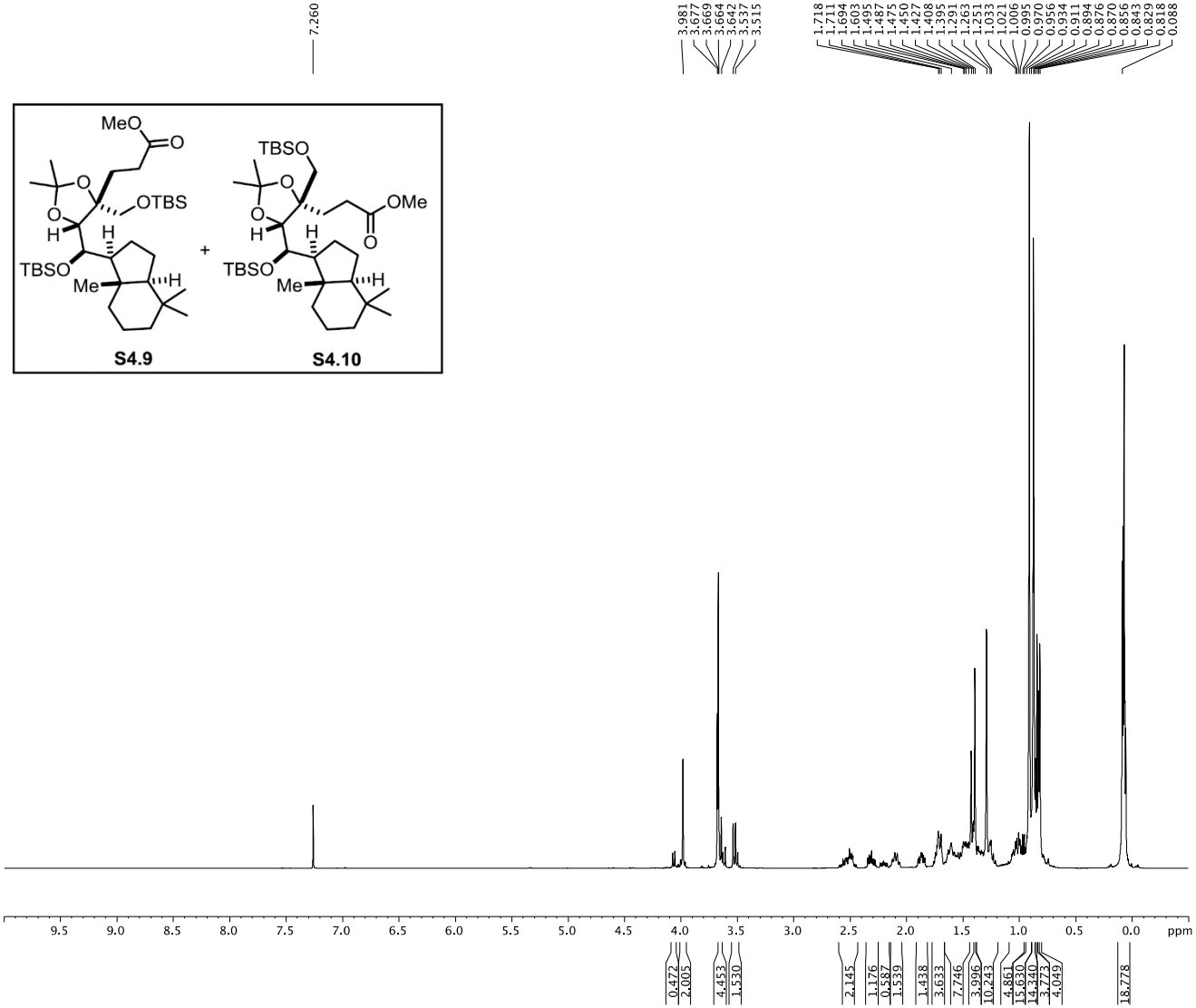

Current Data Parameters
NAME DJT-VI-147
EXPNO 2
PROCNO 1

F2 - Acquisition Parameters
Date_ 20151214
Time 13.17
INSTRUM cryo500
PROBHD 5 mm CPTCI 1H-
PULPROG zg30
TD 81728
SOLVENT CDCl3
NS 20
DS 0
SWH 8012.820 Hz
FIDRES 0.098043 Hz
AQ 5.0998273 sec
RG 5.7
DW 62.400 usec
DE 6.00 usec
TE 298.0 K
D1 0.10000000 sec
MCREST 0 sec
MCWRK 0.01500000 sec

======== CHANNEL f1 =====
NUC1 1H
P1 7.50 usec
PL1 1.60 dB
SFO1 500.2235015 MHz

F2 - Processing parameters
SI 65536
SF 500.2200317 MHz
WDW EM
SSB 0
LB 0.30 Hz
GB 0
PC 4.00

Z-restored spin-echo 13C spectrum with 1H decoupling

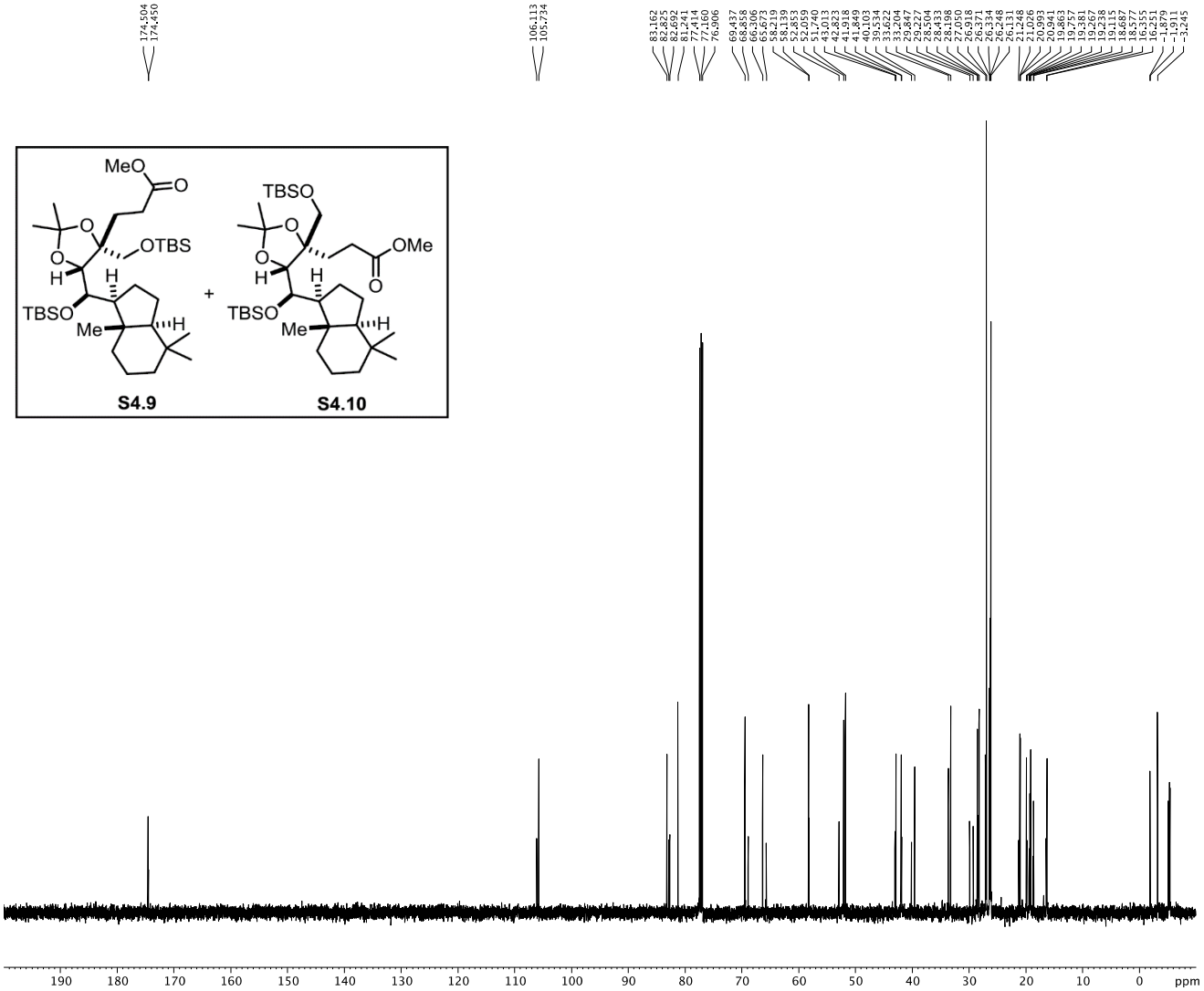

Current Data Parameters
NAME DJT-VI-147
EXPNO 20
PROCNO 1

F2 - Acquisition Parameters
Date_ 20160127
Time 13.06
INSTRUM cryo500
PROBHD 5 mm CPTCI 1H-
PULPROG SpinEchopg30gp.prd
TD 65536
SOLVENT CDCl3
NS 151
DS 0
SWH 30303.031 Hz
FIDRES 0.462388 Hz
AQ 1.0813440 sec
RG 7298.2
DW 16.500 usec
DE 6.00 usec
TE 298.0 K
D1 0.25000000 sec
d11 0.03000000 sec
D16 0.00020000 sec
d17 0.00019600 sec
MCREST 0 sec
MCWRK 0.01500000 sec
P2 33.10 usec

======== CHANNEL f1 ========
NUC1 13C
P1 16.55 usec
P11 500.00 usec
P12 2000.00 usec
PL0 120.00 dB
PL1 -1.00 dB
SFO1 125.7942548 MHz
SP1 2.70 dB
SP2 2.70 dB
SPNAM[1] Crp60.0.5.20.1
SPNAM[2] Crp60comp.4
SPOFF1 0 Hz
SPOFF2 0 Hz

======== CHANNEL f2 ========
CPDPRG[2 waltz16
NUC2 1H
PCPD2 100.00 usec
PL2 1.60 dB
PL12 24.50 dB
SFO2 500.2225011 MHz

====== GRADIENT CHANNEL =====
GPNAM[1] SINE.100
GPNAM[2] SINE.100
GPX1 0 %
GPX2 0 %
GPY1 0 %
GPY2 0 %
GPZ1 30.00 %
GPZ2 50.00 %
p15 500.00 usec
p16 1000.00 usec

F2 - Processing parameters
SI 65536
SF 125.7804071 MHz
WDW EM
SSB 0
LB 1.00 Hz
GB 0
PC 2.00

Appendix E: X-Rau Crystal Structures of 3.28, 3.75, 3.78, 3.110, and 4.42f

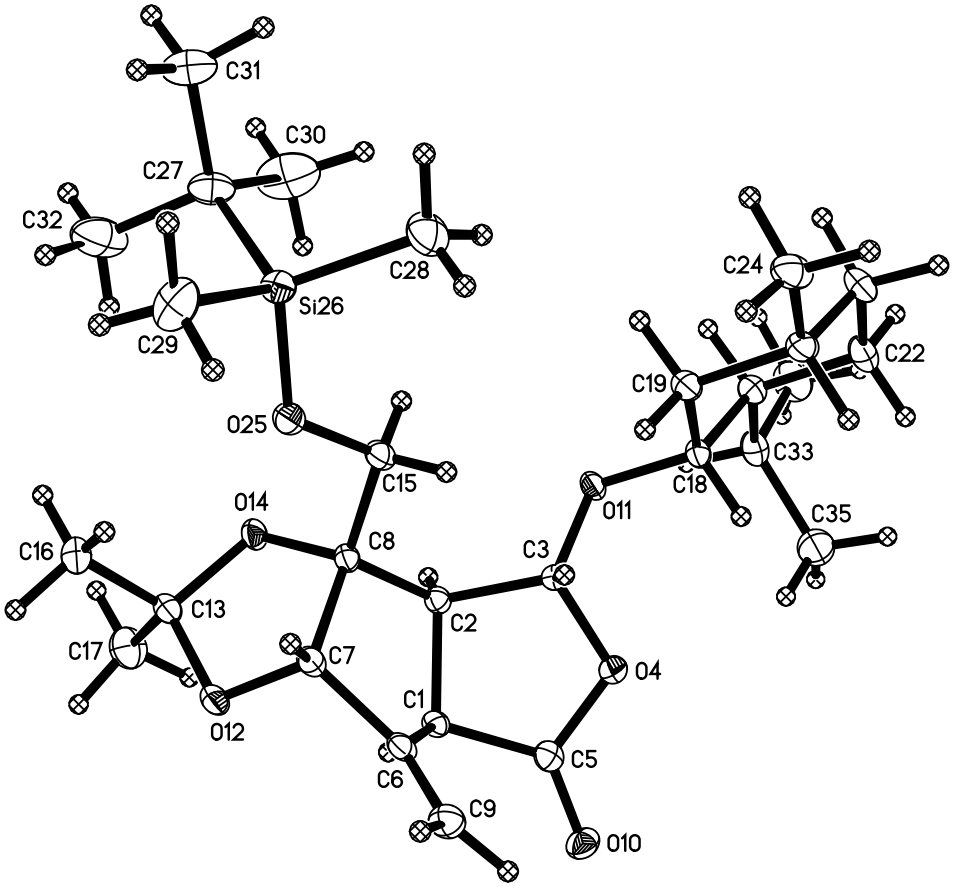

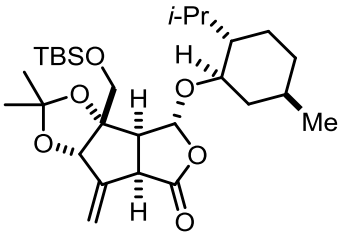

3.28

Table 1. Crystal data and structure refinement for leo275 (**3.28**).

Identification code	leo275 (Daniel Tao)	
Empirical formula	$C_{28}H_{48}O_6Si$	
Formula weight	508.75	
Temperature	88(2) K	
Wavelength	0.71073 Å	
Crystal system	Orthorhombic	
Space group	$P2_12_12_1$	
Unit cell dimensions	a = 7.3379(4) Å	α= 90°.

	b = 15.9392(9) Å	β= 90°.
	c = 24.9121(14) Å	γ = 90°.
Volume	2913.7(3) $Å^3$	
Z	4	
Density (calculated)	1.160 Mg/m^3	
Absorption coefficient	0.118 mm^{-1}	
F(000)	1112	
Crystal color	colorless	
Crystal size	0.370 x 0.322 x 0.204 mm^3	
Theta range for data collection	2.075 to 29.064°	
Index ranges	$-9 \leq h \leq 10$, $-21 \leq k \leq 21$, $-33 \leq l \leq 33$	
Reflections collected	31275	
Independent reflections	7346 [R(int) = 0.0239]	
Completeness to theta = 25.242°	99.9 %	
Absorption correction	Semi-empirical from equivalents	
Max. and min. transmission	0.8621 and 0.7592	
Refinement method	Full-matrix least-squares on F^2	
Data / restraints / parameters	7346 / 0 / 504	
Goodness-of-fit on F^2	1.041	
Final R indices [I>2sigma(I) = 7039 data]	R1 = 0.0278, wR2 = 0.0705	
R indices (all data, 0.73 Å)	R1 = 0.0297, wR2 = 0.0719	
Absolute structure parameter	-0.02(2)	
Largest diff. peak and hole	0.296 and -0.145 $e.Å^{-3}$	

Table 2. Atomic coordinates (x 10^4) and equivalent isotropic displacement parameters ($Å^2$x 10^3) for leo275. U(eq) is defined as one third of the trace of the orthogonalized U^{ij} tensor.

	x	y	z	U(eq)
Si(26)	8718(1)	1958(1)	7899(1)	15(1)
O(4)	10182(1)	1766(1)	5134(1)	15(1)
O(10)	10979(2)	2839(1)	4606(1)	18(1)
O(11)	10129(1)	774(1)	5816(1)	13(1)
O(12)	12403(2)	3881(1)	6513(1)	18(1)
O(14)	12985(1)	2551(1)	6802(1)	15(1)
O(25)	9683(2)	2404(1)	7370(1)	18(1)
C(1)	11641(2)	2876(1)	5570(1)	13(1)
C(2)	11587(2)	2124(1)	5961(1)	12(1)
C(3)	10015(2)	1622(1)	5719(1)	12(1)
C(5)	10947(2)	2525(1)	5047(1)	14(1)
C(6)	10334(2)	3487(1)	5832(1)	14(1)
C(7)	10738(2)	3434(1)	6425(1)	14(1)
C(8)	11275(2)	2504(1)	6528(1)	12(1)
C(9)	9008(2)	3925(1)	5604(1)	19(1)
C(13)	13499(2)	3409(1)	6876(1)	16(1)
C(15)	9923(2)	2009(1)	6865(1)	16(1)
C(16)	13145(3)	3690(1)	7449(1)	23(1)
C(17)	15473(2)	3508(1)	6708(1)	27(1)
C(18)	8449(2)	334(1)	5676(1)	14(1)
C(19)	7077(2)	411(1)	6134(1)	16(1)
C(20)	5288(2)	-38(1)	6006(1)	18(1)
C(21)	5690(2)	-955(1)	5866(1)	22(1)
C(22)	7107(2)	-1034(1)	5419(1)	22(1)
C(23)	8903(2)	-581(1)	5555(1)	16(1)
C(24)	3936(2)	46(1)	6469(1)	22(1)
C(27)	10469(2)	1355(1)	8300(1)	22(1)
C(28)	6820(3)	1266(1)	7676(1)	28(1)
C(29)	7832(3)	2853(1)	8299(1)	27(1)
C(30)	11206(3)	604(1)	7984(1)	40(1)
C(31)	9585(3)	1029(1)	8819(1)	31(1)

C(32)	12063(3)	1938(2)	8449(1)	39(1)
C(33)	10404(2)	-684(1)	5126(1)	19(1)
C(34)	10986(3)	-1603(1)	5068(1)	29(1)
C(35)	9888(3)	-325(1)	4576(1)	25(1)

Table 3. Bond lengths [Å] and angles [°] for leo275.

Si(26)-O(25)	1.6587(11)
Si(26)-C(29)	1.8568(17)
Si(26)-C(28)	1.8614(18)
Si(26)-C(27)	1.8888(16)
O(4)-C(5)	1.3510(17)
O(4)-C(3)	1.4809(16)
O(10)-C(5)	1.2069(17)
O(11)-C(3)	1.3744(16)
O(11)-C(18)	1.4609(16)
O(12)-C(13)	1.4245(18)
O(12)-C(7)	1.4317(17)
O(14)-C(8)	1.4307(16)
O(14)-C(13)	1.4307(17)
O(25)-C(15)	1.4170(16)
C(1)-C(5)	1.5071(19)
C(1)-C(6)	1.5150(19)
C(1)-C(2)	1.5434(18)
C(2)-C(3)	1.5284(19)
C(2)-C(8)	1.5553(18)
C(6)-C(9)	1.326(2)
C(6)-C(7)	1.5091(19)
C(7)-C(8)	1.5544(19)
C(8)-C(15)	1.5198(19)
C(13)-C(17)	1.516(2)
C(13)-C(16)	1.519(2)
C(18)-C(23)	1.5265(19)
C(18)-C(19)	1.528(2)
C(19)-C(20)	1.530(2)
C(20)-C(24)	1.528(2)
C(20)-C(21)	1.530(2)
C(21)-C(22)	1.530(2)
C(22)-C(23)	1.541(2)
C(23)-C(33)	1.545(2)
C(27)-C(30)	1.532(2)

C(27)-C(31)	1.537(2)
C(27)-C(32)	1.538(3)
C(33)-C(34)	1.532(2)
C(33)-C(35)	1.532(2)

O(25)-Si(26)-C(29)	104.25(7)
O(25)-Si(26)-C(28)	109.60(7)
C(29)-Si(26)-C(28)	110.68(9)
O(25)-Si(26)-C(27)	110.37(7)
C(29)-Si(26)-C(27)	110.22(8)
C(28)-Si(26)-C(27)	111.48(8)
C(5)-O(4)-C(3)	109.31(10)
C(3)-O(11)-C(18)	112.20(11)
C(13)-O(12)-C(7)	108.40(10)
C(8)-O(14)-C(13)	110.04(10)
C(15)-O(25)-Si(26)	124.67(9)
C(5)-C(1)-C(6)	113.37(11)
C(5)-C(1)-C(2)	104.38(11)
C(6)-C(1)-C(2)	102.23(11)
C(3)-C(2)-C(1)	100.25(10)
C(3)-C(2)-C(8)	116.82(11)
C(1)-C(2)-C(8)	105.89(11)
O(11)-C(3)-O(4)	108.76(10)
O(11)-C(3)-C(2)	113.52(11)
O(4)-C(3)-C(2)	104.13(10)
O(10)-C(5)-O(4)	121.61(13)
O(10)-C(5)-C(1)	128.82(13)
O(4)-C(5)-C(1)	109.55(11)
C(9)-C(6)-C(7)	126.40(14)
C(9)-C(6)-C(1)	128.23(14)
C(7)-C(6)-C(1)	105.14(11)
O(12)-C(7)-C(6)	106.79(11)
O(12)-C(7)-C(8)	103.50(11)
C(6)-C(7)-C(8)	105.35(11)
O(14)-C(8)-C(15)	109.64(11)
O(14)-C(8)-C(7)	104.53(10)

C(15)-C(8)-C(7)	114.86(11)
O(14)-C(8)-C(2)	108.98(11)
C(15)-C(8)-C(2)	113.32(11)
C(7)-C(8)-C(2)	105.01(10)
O(12)-C(13)-O(14)	105.94(11)
O(12)-C(13)-C(17)	108.07(13)
O(14)-C(13)-C(17)	108.39(13)
O(12)-C(13)-C(16)	110.14(13)
O(14)-C(13)-C(16)	110.92(12)
C(17)-C(13)-C(16)	113.09(13)
O(25)-C(15)-C(8)	109.90(11)
O(11)-C(18)-C(23)	108.77(11)
O(11)-C(18)-C(19)	109.80(11)
C(23)-C(18)-C(19)	111.53(12)
C(18)-C(19)-C(20)	111.80(12)
C(24)-C(20)-C(19)	110.96(12)
C(24)-C(20)-C(21)	112.41(12)
C(19)-C(20)-C(21)	109.20(13)
C(22)-C(21)-C(20)	112.07(13)
C(21)-C(22)-C(23)	112.44(13)
C(18)-C(23)-C(22)	107.75(12)
C(18)-C(23)-C(33)	113.16(12)
C(22)-C(23)-C(33)	114.03(12)
C(30)-C(27)-C(31)	108.45(15)
C(30)-C(27)-C(32)	109.11(18)
C(31)-C(27)-C(32)	108.79(16)
C(30)-C(27)-Si(26)	111.48(13)
C(31)-C(27)-Si(26)	109.20(12)
C(32)-C(27)-Si(26)	109.76(11)
C(34)-C(33)-C(35)	110.01(14)
C(34)-C(33)-C(23)	111.42(13)
C(35)-C(33)-C(23)	113.80(13)

Table 4. Anisotropic displacement parameters ($Å^2 x 10^3$) for leo275. The anisotropic displacement factor exponent takes the form: $-2\pi^2[h^2 a^{*2} U^{11} + ... + 2 h k a^* b^* U^{12}]$

U^{11}	U^{22}	U^{33}	U^{23}	U^{13}	U^{12}
Si(26)16(1)	15(1)	15(1)	-1(1)	4(1)	1(1)
O(4) 16(1)	16(1)	12(1)	1(1)	-1(1)	-3(1)
O(10)17(1)	25(1)	14(1)	4(1)	0(1)	-3(1)
O(11)13(1)	10(1)	18(1)	0(1)	-3(1)	-2(1)
O(12)20(1)	13(1)	22(1)	3(1)	-7(1)	-6(1)
O(14)15(1)	13(1)	19(1)	1(1)	-6(1)	-2(1)
O(25)26(1)	16(1)	13(1)	-2(1)	3(1)	-4(1)
C(1) 11(1)	13(1)	14(1)	2(1)	0(1)	-2(1)
C(2) 11(1)	11(1)	13(1)	0(1)	-1(1)	-1(1)
C(3) 12(1)	11(1)	11(1)	1(1)	-1(1)	-1(1)
C(5) 10(1)	15(1)	17(1)	0(1)	1(1)	0(1)
C(6) 13(1)	10(1)	17(1)	1(1)	0(1)	-3(1)
C(7) 13(1)	11(1)	18(1)	0(1)	-2(1)	-1(1)
C(8) 12(1)	11(1)	13(1)	0(1)	-1(1)	-2(1)
C(9) 19(1)	16(1)	23(1)	2(1)	-3(1)	1(1)
C(13)18(1)	12(1)	18(1)	1(1)	-4(1)	-4(1)
C(15)20(1)	14(1)	14(1)	0(1)	2(1)	-6(1)
C(16)30(1)	18(1)	20(1)	-1(1)	-7(1)	-5(1)
C(17)18(1)	31(1)	33(1)	2(1)	-3(1)	-8(1)
C(18)13(1)	13(1)	16(1)	1(1)	-3(1)	-3(1)
C(19)15(1)	14(1)	18(1)	2(1)	-2(1)	-2(1)
C(20)15(1)	19(1)	20(1)	6(1)	-4(1)	-4(1)
C(21)22(1)	17(1)	26(1)	2(1)	-2(1)	-9(1)
C(22)25(1)	17(1)	24(1)	-3(1)	-2(1)	-8(1)
C(23)20(1)	12(1)	17(1)	0(1)	-3(1)	-2(1)
C(24)14(1)	23(1)	28(1)	8(1)	0(1)	-1(1)
C(27)22(1)	19(1)	25(1)	7(1)	3(1)	4(1)
C(28)25(1)	31(1)	27(1)	-1(1)	5(1)	-10(1)
C(29)31(1)	29(1)	22(1)	-8(1)	1(1)	13(1)
C(30)46(1)	33(1)	40(1)	7(1)	10(1)	24(1)
C(31)35(1)	30(1)	28(1)	11(1)	5(1)	4(1)

C(32)25(1)	40(1)	52(1)	24(1)	-14(1)	-7(1)
C(33)20(1)	16(1)	22(1)	-4(1)	-2(1)	-2(1)
C(34)35(1)	19(1)	32(1)	-6(1)	1(1)	4(1)
C(35)28(1)	27(1)	21(1)	-1(1)	3(1)	-3(1)

Table 5. Hydrogen coordinates (x 10^4) and isotropic displacement parameters ($Å^2$x 10^{-3}) for leo275.

	x	y	z	U(eq)
H(3A)	8824	1844	5852	17
H(1A)	12760(30)	3104(12)	5543(7)	15(4)
H(2A)	12660(30)	1794(11)	5938(7)	11(4)
H(7A)	9810(30)	3642(11)	6677(7)	11(4)
H(9A)	8230(30)	4282(13)	5804(8)	25(5)
H(9B)	8800(30)	3905(11)	5222(7)	14(4)
H(15A)	8830(30)	1973(13)	6670(8)	26(5)
H(15B)	10350(30)	1451(12)	6896(7)	14(4)
H(16A)	11880(30)	3639(13)	7531(8)	24(5)
H(16B)	13470(30)	4282(15)	7488(8)	34(6)
H(16C)	13910(30)	3386(14)	7703(9)	34(6)
H(17A)	15620(30)	3296(15)	6328(10)	40(6)
H(17B)	16230(30)	3207(15)	6959(9)	34(6)
H(17C)	15770(30)	4089(15)	6705(8)	32(6)
H(18A)	7940(30)	581(11)	5360(7)	13(4)
H(19A)	6860(30)	1007(12)	6215(7)	14(4)
H(19B)	7620(30)	170(11)	6463(7)	15(4)
H(20A)	4690(30)	274(11)	5681(7)	15(4)
H(21A)	6100(30)	-1234(12)	6185(8)	20(5)
H(21B)	4570(30)	-1240(13)	5747(8)	25(5)
H(22A)	6640(30)	-787(13)	5098(8)	24(5)
H(22B)	7370(30)	-1617(15)	5349(8)	32(6)
H(23A)	9430(30)	-816(12)	5885(8)	19(5)
H(24A)	3760(30)	626(14)	6572(9)	32(6)
H(24B)	4390(30)	-256(13)	6795(8)	25(5)
H(24C)	2780(30)	-189(12)	6374(8)	20(5)
H(28A)	5900(40)	1589(17)	7484(10)	51(7)
H(28B)	6260(40)	1001(16)	7977(9)	41(6)
H(28C)	7200(40)	827(17)	7425(10)	52(8)
H(29A)	7030(40)	3186(17)	8054(10)	51(7)

H(29B)	8760(40)	3173(15)	8433(10)	41(6)
H(29C)	7080(40)	2651(17)	8619(11)	51(7)
H(30A)	12070(40)	291(16)	8197(10)	49(7)
H(30B)	11830(40)	766(15)	7645(10)	40(6)
H(30C)	10250(40)	224(18)	7844(12)	59(8)
H(31A)	10500(40)	716(16)	9057(10)	46(7)
H(31B)	8570(40)	618(15)	8745(9)	39(6)
H(31C)	9090(40)	1486(17)	9028(10)	45(7)
H(32A)	12970(40)	1654(17)	8643(11)	54(8)
H(32B)	11630(40)	2460(20)	8622(12)	62(9)
H(32C)	12640(40)	2149(16)	8148(10)	43(6)
H(33A)	11450(30)	-398(13)	5256(8)	24(5)
H(34A)	12100(30)	-1640(14)	4834(9)	33(6)
H(34B)	10090(40)	-1911(16)	4907(11)	48(7)
H(34C)	11250(30)	-1850(14)	5423(9)	33(5)
H(35A)	10840(30)	-395(14)	4310(9)	33(6)
H(35B)	9660(30)	276(15)	4608(9)	34(6)
H(35C)	8840(40)	-603(14)	4427(9)	34(6)

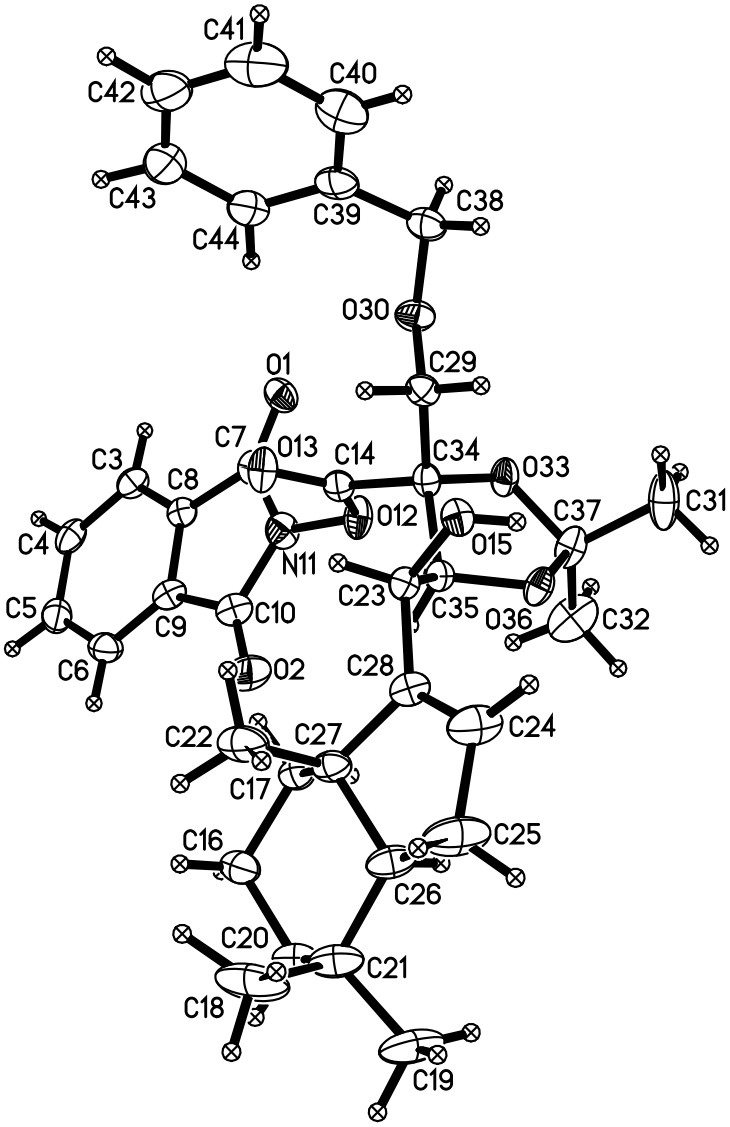

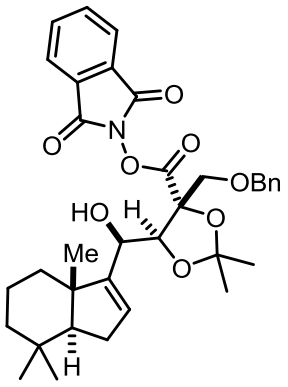

3.75

Table 1. Crystal data and structure refinement for leo283 (**3.75**).

Identification code	leo283 (David Tao)	
Empirical formula	$C_{35}\ H_{41}\ N\ O_8$	
Formula weight	603.69	
Temperature	88(2) K	
Wavelength	0.71073 Å	
Crystal system	Monoclinic	
Space group	$P2_1$	
Unit cell dimensions	a = 10.1766(4) Å	α= 90°.

	b = 12.5435(5) Å	β= 97.7659(5)°.
	c = 12.7623(5) Å	γ = 90°.
Volume	1614.17(11) $Å^3$	
Z	2	
Density (calculated)	1.242 Mg/m^3	
Absorption coefficient	0.088 mm^{-1}	
F(000)	644	
Crystal color	colorless	
Crystal size	0.417 x 0.264 x 0.112 mm^3	
Theta range for data collection	1.610 to 27.484°	
Index ranges	$-13 \leq h \leq 13$, $-16 \leq k \leq 16$, $-16 \leq l \leq 16$	
Reflections collected	19408	
Independent reflections	7390 [R(int) = 0.0219]	
Completeness to theta = 25.500°	100.0 %	
Absorption correction	Semi-empirical from equivalents	
Max. and min. transmission	0.8622 and 0.8148	
Refinement method	Full-matrix least-squares on F^2	
Data / restraints / parameters	7390 / 1 / 561	
Goodness-of-fit on F^2	1.034	
Final R indices [I>2sigma(I) = 6804 data]	R1 = 0.0330, wR2 = 0.0750	
R indices (all data, 0.77Å)	R1 = 0.0371, wR2 = 0.0776	
Absolute structure parameter	0.1(3)	
Largest diff. peak and hole	0.202 and -0.159 $e.Å^{-3}$	

Table 2. Atomic coordinates (x 10^4) and equivalent isotropic displacement parameters ($Å^2$x 10^3) for leo283. U(eq) is defined as one third of the trace of the orthogonalized U^{ij} tensor.

	x	y	z	U(eq)
O(1)	14562(1)	9418(1)	5002(1)	27(1)
O(2)	11048(2)	9622(1)	2348(1)	37(1)
C(3)	14810(2)	11656(2)	3919(2)	24(1)
C(4)	14580(2)	12575(2)	3305(2)	27(1)
C(5)	13488(2)	12657(2)	2528(2)	29(1)
C(6)	12589(2)	11820(2)	2320(2)	28(1)
C(7)	13876(2)	9793(2)	4252(2)	21(1)
C(8)	13916(2)	10833(2)	3708(2)	20(1)
C(9)	12830(2)	10909(2)	2916(2)	22(1)
C(10)	12051(2)	9902(2)	2890(2)	25(1)
N(11)	12774(2)	9287(1)	3683(1)	27(1)
O(12)	12451(1)	8234(1)	3875(1)	27(1)
O(13)	11043(1)	8901(1)	4946(1)	28(1)
C(14)	11507(2)	8155(2)	4553(2)	20(1)
O(15)	8309(1)	6115(1)	4939(1)	21(1)
C(16)	7293(3)	9131(2)	1128(2)	34(1)
C(17)	7967(2)	8429(2)	2036(2)	26(1)
C(18)	4233(3)	8361(4)	899(2)	60(1)
C(19)	4943(3)	6960(3)	-275(2)	50(1)
C(20)	6473(2)	8486(2)	246(2)	33(1)
C(21)	5438(2)	7736(2)	623(2)	37(1)
C(22)	6063(3)	8413(3)	3109(2)	42(1)
C(23)	8470(2)	6881(2)	4152(1)	18(1)
C(24)	6577(2)	5969(2)	3010(2)	38(1)
C(25)	5557(3)	6165(3)	2055(2)	50(1)
C(26)	6201(2)	7092(2)	1532(2)	31(1)
C(27)	6943(2)	7727(2)	2476(2)	24(1)
C(28)	7398(2)	6794(2)	3212(2)	23(1)
C(29)	10876(2)	6805(2)	5809(2)	22(1)
O(30)	12122(1)	7008(1)	6423(1)	27(1)
C(31)	11758(2)	4430(2)	4014(3)	39(1)

C(32)	11914(3)	5753(3)	2539(2)	43(1)
O(33)	12053(1)	6293(1)	4365(1)	24(1)
C(34)	11079(2)	7002(2)	4660(2)	19(1)
C(35)	9852(2)	6790(2)	3811(2)	19(1)
O(36)	10053(1)	5714(1)	3539(1)	22(1)
C(37)	11445(2)	5540(2)	3593(2)	25(1)
C(38)	12144(2)	6685(2)	7495(2)	30(1)
C(39)	11557(2)	7490(2)	8184(2)	30(1)
C(40)	11036(2)	7156(2)	9078(2)	41(1)
C(41)	10597(3)	7893(3)	9764(2)	51(1)
C(42)	10682(3)	8976(3)	9566(2)	50(1)
C(43)	11177(3)	9313(2)	8671(2)	48(1)
C(44)	11616(3)	8579(2)	7980(2)	38(1)

Table 3. Bond lengths [Å] and angles [°] for leo283.

O(1)-C(7)	1.201(2)
O(2)-C(10)	1.205(3)
C(3)-C(8)	1.379(3)
C(3)-C(4)	1.396(3)
C(4)-C(5)	1.389(3)
C(5)-C(6)	1.394(3)
C(6)-C(9)	1.377(3)
C(7)-N(11)	1.403(3)
C(7)-C(8)	1.481(3)
C(8)-C(9)	1.396(3)
C(9)-C(10)	1.489(3)
C(10)-N(11)	1.399(3)
N(11)-O(12)	1.390(2)
O(12)-C(14)	1.381(2)
O(13)-C(14)	1.189(2)
C(14)-C(34)	1.523(3)
O(15)-C(23)	1.416(2)
C(16)-C(20)	1.538(3)
C(16)-C(17)	1.540(3)
C(17)-C(27)	1.528(3)
C(18)-C(21)	1.536(4)
C(19)-C(21)	1.536(4)
C(20)-C(21)	1.538(3)
C(21)-C(26)	1.535(3)
C(22)-C(27)	1.546(3)
C(23)-C(28)	1.512(3)
C(23)-C(35)	1.531(2)
C(24)-C(28)	1.333(3)
C(24)-C(25)	1.510(3)
C(25)-C(26)	1.532(3)
C(26)-C(27)	1.553(3)
C(27)-C(28)	1.533(3)
C(29)-O(30)	1.420(2)
C(29)-C(34)	1.528(3)

O(30)-C(38)	1.424(3)
C(31)-C(37)	1.512(3)
C(32)-C(37)	1.510(3)
O(33)-C(34)	1.419(2)
O(33)-C(37)	1.443(2)
C(34)-C(35)	1.562(3)
C(35)-O(36)	1.417(2)
O(36)-C(37)	1.425(2)
C(38)-C(39)	1.514(3)
C(39)-C(40)	1.386(3)
C(39)-C(44)	1.393(4)
C(40)-C(41)	1.388(4)
C(41)-C(42)	1.386(5)
C(42)-C(43)	1.375(4)
C(43)-C(44)	1.390(4)

C(8)-C(3)-C(4)	116.94(19)
C(5)-C(4)-C(3)	121.26(19)
C(4)-C(5)-C(6)	121.4(2)
C(9)-C(6)-C(5)	117.19(19)
O(1)-C(7)-N(11)	125.01(18)
O(1)-C(7)-C(8)	131.93(19)
N(11)-C(7)-C(8)	103.06(16)
C(3)-C(8)-C(9)	121.79(18)
C(3)-C(8)-C(7)	128.86(18)
C(9)-C(8)-C(7)	109.32(16)
C(6)-C(9)-C(8)	121.40(18)
C(6)-C(9)-C(10)	129.63(19)
C(8)-C(9)-C(10)	108.95(17)
O(2)-C(10)-N(11)	125.2(2)
O(2)-C(10)-C(9)	131.8(2)
N(11)-C(10)-C(9)	103.03(16)
O(12)-N(11)-C(10)	122.53(16)
O(12)-N(11)-C(7)	121.95(16)
C(10)-N(11)-C(7)	115.49(16)
C(14)-O(12)-N(11)	112.32(14)

O(13)-C(14)-O(12)	123.86(17)
O(13)-C(14)-C(34)	125.13(17)
O(12)-C(14)-C(34)	110.87(15)
C(20)-C(16)-C(17)	113.13(19)
C(27)-C(17)-C(16)	110.46(18)
C(21)-C(20)-C(16)	114.77(19)
C(26)-C(21)-C(19)	108.2(2)
C(26)-C(21)-C(18)	115.7(2)
C(19)-C(21)-C(18)	107.7(2)
C(26)-C(21)-C(20)	105.11(17)
C(19)-C(21)-C(20)	108.84(19)
C(18)-C(21)-C(20)	111.2(3)
O(15)-C(23)-C(28)	111.93(15)
O(15)-C(23)-C(35)	110.48(15)
C(28)-C(23)-C(35)	111.13(15)
C(28)-C(24)-C(25)	112.0(2)
C(24)-C(25)-C(26)	100.80(18)
C(25)-C(26)-C(21)	121.76(19)
C(25)-C(26)-C(27)	104.09(18)
C(21)-C(26)-C(27)	117.4(2)
C(17)-C(27)-C(28)	120.06(16)
C(17)-C(27)-C(22)	110.1(2)
C(28)-C(27)-C(22)	104.64(17)
C(17)-C(27)-C(26)	107.16(16)
C(28)-C(27)-C(26)	99.14(17)
C(22)-C(27)-C(26)	115.81(18)
C(24)-C(28)-C(23)	125.1(2)
C(24)-C(28)-C(27)	110.17(18)
C(23)-C(28)-C(27)	123.83(17)
O(30)-C(29)-C(34)	105.92(15)
C(29)-O(30)-C(38)	112.08(16)
C(34)-O(33)-C(37)	109.93(14)
O(33)-C(34)-C(14)	110.66(15)
O(33)-C(34)-C(29)	110.08(15)
C(14)-C(34)-C(29)	108.47(15)
O(33)-C(34)-C(35)	103.36(14)

C(14)-C(34)-C(35)	108.10(15)
C(29)-C(34)-C(35)	116.07(15)
O(36)-C(35)-C(23)	108.02(14)
O(36)-C(35)-C(34)	101.76(14)
C(23)-C(35)-C(34)	117.98(15)
C(35)-O(36)-C(37)	108.00(14)
O(36)-C(37)-O(33)	105.36(15)
O(36)-C(37)-C(32)	111.21(19)
O(33)-C(37)-C(32)	109.56(18)
O(36)-C(37)-C(31)	108.54(16)
O(33)-C(37)-C(31)	108.05(19)
C(32)-C(37)-C(31)	113.7(2)
O(30)-C(38)-C(39)	114.33(18)
C(40)-C(39)-C(44)	118.7(2)
C(40)-C(39)-C(38)	120.1(2)
C(44)-C(39)-C(38)	121.0(2)
C(39)-C(40)-C(41)	120.6(3)
C(42)-C(41)-C(40)	120.3(3)
C(43)-C(42)-C(41)	119.4(3)
C(42)-C(43)-C(44)	120.6(3)
C(43)-C(44)-C(39)	120.4(3)

Table 4. Anisotropic displacement parameters ($Å^2 x 10^3$) for leo283. The anisotropic displacement factor exponent takes the form: $-2\pi^2[h^2 a^{*2} U^{11} + ... + 2 h k a^* b^* U^{12}]$

	U^{11}	U^{22}	U^{33}	U^{23}	U^{13}	U^{12}
O(1)	24(1)	29(1)	30(1)	4(1)	5(1)	5(1)
O(2)	28(1)	46(1)	34(1)	-3(1)	-4(1)	-14(1)
C(3)	22(1)	25(1)	24(1)	-3(1)	4(1)	-5(1)
C(4)	36(1)	22(1)	26(1)	-6(1)	10(1)	-9(1)
C(5)	43(1)	22(1)	24(1)	2(1)	11(1)	2(1)
C(6)	29(1)	32(1)	22(1)	2(1)	2(1)	3(1)
C(7)	17(1)	23(1)	26(1)	-2(1)	9(1)	1(1)
C(8)	17(1)	23(1)	20(1)	0(1)	7(1)	0(1)
C(9)	19(1)	28(1)	20(1)	-3(1)	6(1)	-4(1)
C(10)	22(1)	32(1)	23(1)	-1(1)	5(1)	-4(1)
N(11)	25(1)	22(1)	33(1)	3(1)	4(1)	-7(1)
O(12)	28(1)	17(1)	39(1)	-2(1)	14(1)	-4(1)
O(13)	26(1)	19(1)	42(1)	-5(1)	12(1)	-1(1)
C(14)	13(1)	20(1)	24(1)	-1(1)	0(1)	-1(1)
O(15)	21(1)	20(1)	24(1)	2(1)	8(1)	0(1)
C(16)	39(1)	31(1)	29(1)	4(1)	-7(1)	1(1)
C(17)	25(1)	25(1)	25(1)	-1(1)	-5(1)	-2(1)
C(18)	25(1)	112(3)	39(2)	9(2)	-8(1)	15(2)
C(19)	44(2)	74(2)	29(1)	-1(1)	-9(1)	-26(2)
C(20)	31(1)	43(1)	23(1)	1(1)	-5(1)	-1(1)
C(21)	24(1)	58(2)	26(1)	-1(1)	-4(1)	-6(1)
C(22)	31(1)	68(2)	26(1)	-7(1)	-1(1)	24(1)
C(23)	18(1)	18(1)	20(1)	0(1)	4(1)	-2(1)
C(24)	35(1)	49(2)	30(1)	4(1)	1(1)	-21(1)
C(25)	40(2)	72(2)	34(1)	7(1)	-6(1)	-33(1)
C(26)	22(1)	45(1)	23(1)	-2(1)	-1(1)	-11(1)
C(27)	16(1)	34(1)	21(1)	-3(1)	0(1)	3(1)
C(28)	18(1)	31(1)	20(1)	-2(1)	6(1)	-4(1)
C(29)	17(1)	24(1)	24(1)	2(1)	0(1)	-1(1)
O(30)	20(1)	33(1)	25(1)	1(1)	-4(1)	-2(1)
C(31)	24(1)	21(1)	76(2)	-7(1)	20(1)	-1(1)

C(32)32(1)	59(2)	41(1)	-12(1)	19(1)	-12(1)
O(33)19(1)	19(1)	34(1)	-5(1)	4(1)	2(1)
C(34)15(1)	17(1)	26(1)	0(1)	3(1)	0(1)
C(35)18(1)	18(1)	20(1)	1(1)	3(1)	-3(1)
O(36)20(1)	20(1)	28(1)	-7(1)	8(1)	-4(1)
C(37)20(1)	23(1)	35(1)	-8(1)	11(1)	-5(1)
C(38)28(1)	33(1)	28(1)	3(1)	-6(1)	4(1)
C(39)21(1)	40(1)	26(1)	2(1)	-6(1)	3(1)
C(40)28(1)	53(2)	42(1)	9(1)	4(1)	2(1)
C(41)33(1)	86(2)	37(1)	5(1)	9(1)	13(1)
C(42)41(1)	70(2)	35(1)	-8(1)	-4(1)	26(1)
C(43)54(2)	48(2)	38(1)	-6(1)	-6(1)	18(1)
C(44)44(1)	40(1)	28(1)	1(1)	-2(1)	9(1)

Table 5. Hydrogen coordinates (x 10^4) and isotropic displacement parameters ($Å^2$x 10^{-3}) for leo283.

	x	y	z	U(eq)
H(3A)	15530(20)	11558(18)	4439(19)	25(6)
H(4A)	15160(30)	13140(20)	3430(20)	35(7)
H(5A)	13370(20)	13320(20)	2140(20)	37(7)
H(6A)	11830(30)	11890(20)	1810(20)	39(7)
H(15)	8590(20)	5540(20)	4758(19)	28(6)
H(16A)	6730(30)	9650(20)	1420(20)	43(8)
H(16B)	8010(30)	9580(20)	820(20)	48(8)
H(17A)	8640(20)	7989(18)	1755(18)	22(6)
H(17B)	8450(20)	8880(20)	2557(19)	28(6)
H(18A)	4520(40)	9100(30)	1410(30)	77(11)
H(18B)	3620(40)	7890(30)	1270(30)	76(11)
H(18C)	3720(30)	8610(30)	270(30)	66(10)
H(19A)	5670(30)	6460(30)	-440(20)	55(9)
H(19B)	4580(30)	7400(20)	-940(20)	50(8)
H(19C)	4230(30)	6510(20)	-70(20)	41(7)
H(20A)	6050(30)	8980(20)	-330(20)	43(7)
H(20B)	7090(20)	8030(20)	-98(18)	26(6)
H(22A)	5180(30)	8000(30)	3200(30)	59(9)
H(22B)	5780(30)	9130(30)	2770(20)	52(8)
H(22C)	6560(30)	8550(20)	3830(20)	50(8)
H(23A)	8400(20)	7563(18)	4472(16)	15(5)
H(24A)	6590(30)	5310(20)	3450(20)	44(7)
H(25A)	4660(30)	6380(30)	2280(30)	67(10)
H(25B)	5410(30)	5580(30)	1580(30)	58(9)
H(26A)	6920(20)	6720(20)	1215(18)	30(6)
H(29A)	10190(20)	7308(17)	6024(16)	15(5)
H(29B)	10600(20)	6080(20)	5875(17)	21(5)
H(31A)	12690(30)	4350(20)	4100(20)	39(7)
H(31B)	11390(30)	3930(30)	3510(30)	62(9)
H(31C)	11350(30)	4320(20)	4690(20)	51(8)

H(32A)	12850(30)	5650(20)	2650(20)	48(8)
H(32B)	11730(30)	6480(30)	2330(20)	42(8)
H(32C)	11510(30)	5240(30)	1980(30)	64(9)
H(35A)	9933(19)	7259(17)	3192(16)	12(5)
H(38A)	13080(30)	6600(20)	7760(20)	39(7)
H(38B)	11690(30)	5980(20)	7500(20)	43(7)
H(40A)	10970(30)	6440(20)	9210(20)	39(7)
H(41A)	10280(40)	7670(30)	10350(30)	73(11)
H(42A)	10370(30)	9480(30)	10070(30)	51(8)
H(43A)	11240(30)	10110(30)	8550(20)	56(9)
H(44A)	11970(30)	8760(20)	7290(20)	44(7)

Table 6. Torsion angles [°] for leo283.

C(8)-C(3)-C(4)-C(5)	0.9(3)
C(3)-C(4)-C(5)-C(6)	-1.0(3)
C(4)-C(5)-C(6)-C(9)	-0.1(3)
C(4)-C(3)-C(8)-C(9)	0.2(3)
C(4)-C(3)-C(8)-C(7)	-177.36(18)
O(1)-C(7)-C(8)-C(3)	2.0(3)
N(11)-C(7)-C(8)-C(3)	-178.86(19)
O(1)-C(7)-C(8)-C(9)	-175.8(2)
N(11)-C(7)-C(8)-C(9)	3.3(2)
C(5)-C(6)-C(9)-C(8)	1.2(3)
C(5)-C(6)-C(9)-C(10)	179.0(2)
C(3)-C(8)-C(9)-C(6)	-1.3(3)
C(7)-C(8)-C(9)-C(6)	176.73(18)
C(3)-C(8)-C(9)-C(10)	-179.51(17)
C(7)-C(8)-C(9)-C(10)	-1.5(2)
C(6)-C(9)-C(10)-O(2)	1.2(4)
C(8)-C(9)-C(10)-O(2)	179.3(2)
C(6)-C(9)-C(10)-N(11)	-179.0(2)
C(8)-C(9)-C(10)-N(11)	-0.9(2)
O(2)-C(10)-N(11)-O(12)	5.1(3)
C(9)-C(10)-N(11)-O(12)	-174.73(16)
O(2)-C(10)-N(11)-C(7)	-176.9(2)
C(9)-C(10)-N(11)-C(7)	3.3(2)
O(1)-C(7)-N(11)-O(12)	-6.9(3)
C(8)-C(7)-N(11)-O(12)	173.87(16)
O(1)-C(7)-N(11)-C(10)	174.99(19)
C(8)-C(7)-N(11)-C(10)	-4.2(2)
C(10)-N(11)-O(12)-C(14)	-86.0(2)
C(7)-N(11)-O(12)-C(14)	96.0(2)
N(11)-O(12)-C(14)-O(13)	-1.5(3)
N(11)-O(12)-C(14)-C(34)	174.40(15)
C(20)-C(16)-C(17)-C(27)	-54.5(3)
C(17)-C(16)-C(20)-C(21)	53.6(3)
C(16)-C(20)-C(21)-C(26)	-50.7(3)

C(16)-C(20)-C(21)-C(19)	-166.4(2)
C(16)-C(20)-C(21)-C(18)	75.1(3)
C(28)-C(24)-C(25)-C(26)	17.4(3)
C(24)-C(25)-C(26)-C(21)	-168.6(2)
C(24)-C(25)-C(26)-C(27)	-33.1(3)
C(19)-C(21)-C(26)-C(25)	-57.3(3)
C(18)-C(21)-C(26)-C(25)	63.5(4)
C(20)-C(21)-C(26)-C(25)	-173.4(2)
C(19)-C(21)-C(26)-C(27)	172.70(19)
C(18)-C(21)-C(26)-C(27)	-66.5(3)
C(20)-C(21)-C(26)-C(27)	56.5(2)
C(16)-C(17)-C(27)-C(28)	166.70(18)
C(16)-C(17)-C(27)-C(22)	-71.8(2)
C(16)-C(17)-C(27)-C(26)	54.9(2)
C(25)-C(26)-C(27)-C(17)	161.6(2)
C(21)-C(26)-C(27)-C(17)	-60.6(2)
C(25)-C(26)-C(27)-C(28)	36.1(2)
C(21)-C(26)-C(27)-C(28)	173.88(18)
C(25)-C(26)-C(27)-C(22)	-75.2(3)
C(21)-C(26)-C(27)-C(22)	62.6(3)
C(25)-C(24)-C(28)-C(23)	175.8(2)
C(25)-C(24)-C(28)-C(27)	6.2(3)
O(15)-C(23)-C(28)-C(24)	-14.5(3)
C(35)-C(23)-C(28)-C(24)	109.6(2)
O(15)-C(23)-C(28)-C(27)	153.74(16)
C(35)-C(23)-C(28)-C(27)	-82.2(2)
C(17)-C(27)-C(28)-C(24)	-142.5(2)
C(22)-C(27)-C(28)-C(24)	93.3(2)
C(26)-C(27)-C(28)-C(24)	-26.5(2)
C(17)-C(27)-C(28)-C(23)	47.8(3)
C(22)-C(27)-C(28)-C(23)	-76.4(2)
C(26)-C(27)-C(28)-C(23)	163.76(17)
C(34)-C(29)-O(30)-C(38)	-170.15(16)
C(37)-O(33)-C(34)-C(14)	-128.02(16)
C(37)-O(33)-C(34)-C(29)	112.09(17)
C(37)-O(33)-C(34)-C(35)	-12.50(19)

O(13)-C(14)-C(34)-O(33)	-163.29(18)
O(12)-C(14)-C(34)-O(33)	20.9(2)
O(13)-C(14)-C(34)-C(29)	-42.4(2)
O(12)-C(14)-C(34)-C(29)	141.72(15)
O(13)-C(14)-C(34)-C(35)	84.2(2)
O(12)-C(14)-C(34)-C(35)	-91.65(17)
O(30)-C(29)-C(34)-O(33)	60.93(19)
O(30)-C(29)-C(34)-C(14)	-60.28(19)
O(30)-C(29)-C(34)-C(35)	177.85(15)
O(15)-C(23)-C(35)-O(36)	52.11(19)
C(28)-C(23)-C(35)-O(36)	-72.76(19)
O(15)-C(23)-C(35)-C(34)	-62.4(2)
C(28)-C(23)-C(35)-C(34)	172.69(16)
O(33)-C(34)-C(35)-O(36)	28.31(17)
C(14)-C(34)-C(35)-O(36)	145.65(14)
C(29)-C(34)-C(35)-O(36)	-92.29(17)
O(33)-C(34)-C(35)-C(23)	146.25(16)
C(14)-C(34)-C(35)-C(23)	-96.42(18)
C(29)-C(34)-C(35)-C(23)	25.6(2)
C(23)-C(35)-O(36)-C(37)	-159.41(15)
C(34)-C(35)-O(36)-C(37)	-34.54(18)
C(35)-O(36)-C(37)-O(33)	27.84(19)
C(35)-O(36)-C(37)-C(32)	-90.8(2)
C(35)-O(36)-C(37)-C(31)	143.37(19)
C(34)-O(33)-C(37)-O(36)	-8.0(2)
C(34)-O(33)-C(37)-C(32)	111.7(2)
C(34)-O(33)-C(37)-C(31)	-123.87(17)
C(29)-O(30)-C(38)-C(39)	-82.7(2)
O(30)-C(38)-C(39)-C(40)	154.6(2)
O(30)-C(38)-C(39)-C(44)	-30.2(3)
C(44)-C(39)-C(40)-C(41)	-0.9(4)
C(38)-C(39)-C(40)-C(41)	174.5(2)
C(39)-C(40)-C(41)-C(42)	-0.3(4)
C(40)-C(41)-C(42)-C(43)	1.4(4)
C(41)-C(42)-C(43)-C(44)	-1.3(4)
C(42)-C(43)-C(44)-C(39)	0.1(4)

C(40)-C(39)-C(44)-C(43)	1.0(4)
C(38)-C(39)-C(44)-C(43)	-174.4(2)

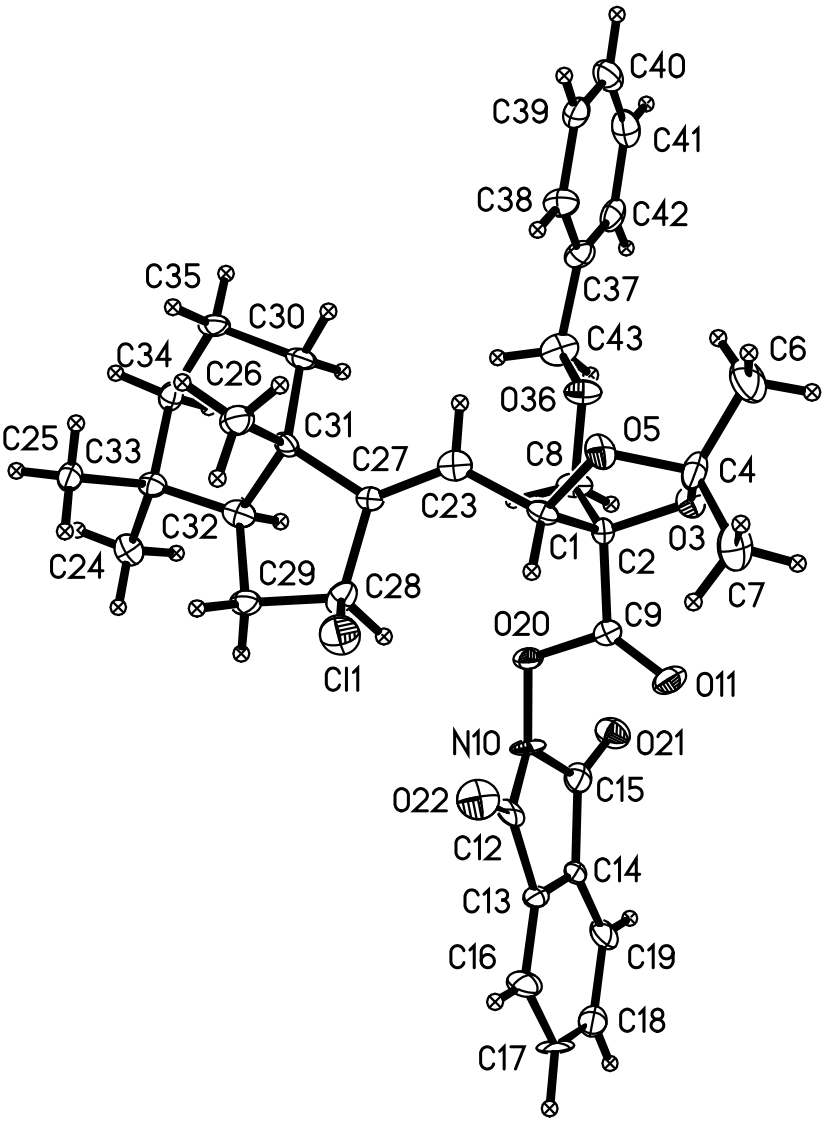

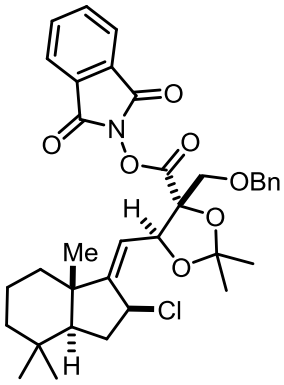

3.78

Table 1. Crystal data and structure refinement for leo282 (**3.78**).

Identification code	leo282 (Daniel Tao)	
Empirical formula	$C_{35}H_{40}ClNO_7$	
Formula weight	622.13	
Temperature	133(2) K	
Wavelength	0.71073 Å	
Crystal system	Monoclinic	
Space group	$P2_1$	
Unit cell dimensions	a = 6.6266(14) Å	α= 90°.
	b = 37.219(8) Å	β= 90.126(3)°.
	c = 12.785(3) Å	γ = 90°.

Volume	3153.1(11) $Å^3$
Z	4
Density (calculated)	1.311 Mg/m^3
Absorption coefficient	0.172 mm^{-1}
F(000)	1320
Crystal color	colorless
Crystal size	0.314 x 0.163 x 0.102 mm^3
Theta range for data collection	1.593 to 25.350°
Index ranges	$-7 \leq h \leq 7$, $-44 \leq k \leq 44$, $-15 \leq l \leq 15$
Reflections collected	28152
Independent reflections	11455 [R(int) = 0.0540]
Completeness to theta = 25.500°	98.4 %
Absorption correction	Semi-empirical from equivalents
Max. and min. transmission	0.8621 and 0.7805
Refinement method	Full-matrix least-squares on F^2
Data / restraints / parameters	11455 / 1 / 799
Goodness-of-fit on F^2	1.087
Final R indices [I>2sigma(I) = 10194 data]	R1 = 0.0504, wR2 = 0.0870
R indices (all data, 0.83 Å)	R1 = 0.0600, wR2 = 0.0902
Absolute structure parameter	0.02(3)
Largest diff. peak and hole	0.486 and -0.420 $e.Å^{-3}$

Table 2. Atomic coordinates (x 10^4) and equivalent isotropic displacement parameters ($Å^2$x 10^3) for leo282. U(eq) is defined as one third of the trace of the orthogonalized U^{ij} tensor.

	x	y	z	U(eq)
Cl(1)	9589(3)	3517(1)	-5872(1)	33(1)
O(3)	5179(6)	4531(1)	-3044(3)	19(1)
O(5)	7977(6)	4180(1)	-2945(3)	20(1)
O(11)	4210(7)	4680(1)	-5060(3)	26(1)
O(20)	3464(7)	4096(1)	-5383(3)	19(1)
O(21)	-140(7)	4472(1)	-5878(4)	27(1)
O(22)	6061(7)	4154(1)	-7112(4)	31(1)
O(36)	3489(6)	3935(1)	-2169(3)	20(1)
N(10)	2881(9)	4208(1)	-6378(4)	21(1)
C(1)	6834(9)	4024(2)	-3776(5)	16(1)
C(2)	4758(10)	4233(2)	-3690(5)	16(1)
C(4)	7327(10)	4537(2)	-2773(5)	23(2)
C(6)	7499(13)	4616(2)	-1622(5)	38(2)
C(7)	8417(11)	4797(2)	-3461(6)	32(2)
C(8)	3008(9)	4022(2)	-3236(5)	17(1)
C(9)	4143(9)	4378(2)	-4783(5)	13(1)
C(12)	4338(11)	4260(2)	-7160(5)	19(2)
C(13)	3204(10)	4454(2)	-8010(5)	18(2)
C(14)	1317(11)	4545(2)	-7622(5)	20(2)
C(15)	1106(10)	4417(2)	-6536(5)	21(2)
C(16)	3782(12)	4539(2)	-8998(5)	30(2)
C(17)	2412(13)	4726(2)	-9625(5)	36(2)
C(18)	508(14)	4814(2)	-9268(5)	33(2)
C(19)	-66(12)	4728(2)	-8246(5)	30(2)
C(23)	6739(9)	3630(2)	-3600(5)	17(1)
C(24)	3314(10)	2360(2)	-5791(5)	23(2)
C(25)	6762(11)	2179(2)	-5223(5)	23(2)
C(26)	9022(10)	2833(2)	-4005(5)	23(2)
C(27)	6907(9)	3362(2)	-4290(4)	12(1)
C(28)	7010(10)	3392(2)	-5469(5)	20(2)
C(29)	6440(10)	3017(2)	-5902(5)	20(2)

C(39)	4496(12)	3541(2)	899(5)	26(2)
C(30)	5785(10)	2865(2)	-2992(4)	19(1)
C(31)	6798(10)	2967(2)	-4022(5)	16(1)
C(32)	5504(10)	2833(2)	-4948(4)	18(1)
C(33)	4965(9)	2430(2)	-4966(5)	16(1)
C(34)	4098(9)	2338(2)	-3880(5)	17(2)
C(35)	5396(10)	2463(2)	-2946(5)	20(2)
C(37)	2279(10)	3697(2)	-537(5)	20(2)
C(38)	4202(11)	3601(2)	-154(5)	23(2)
C(43)	1876(11)	3743(2)	-1696(5)	28(2)
C(40)	2896(12)	3568(2)	1588(5)	29(2)
C(41)	1002(11)	3666(2)	1217(5)	27(2)
C(42)	720(11)	3733(2)	165(5)	22(2)
Cl(1A)	-5544(3)	1568(1)	381(1)	26(1)
O(3A)	-243(7)	654(1)	3040(3)	21(1)
O(5A)	-2912(6)	1034(1)	3146(3)	16(1)
O(11A)	524(8)	439(1)	1037(4)	30(1)
O(20A)	1118(6)	1015(1)	542(3)	17(1)
O(22A)	-1423(7)	933(1)	-1241(3)	26(1)
O(21A)	4793(7)	647(1)	138(3)	28(1)
O(36A)	1610(7)	1294(1)	3699(3)	27(1)
N(10A)	1685(8)	874(1)	-415(4)	19(1)
C(1A)	-1922(9)	1145(2)	2211(5)	14(1)
C(2A)	127(9)	927(2)	2303(5)	16(1)
C(4A)	-2353(10)	673(2)	3343(5)	19(2)
C(6A)	-2402(11)	603(2)	4507(5)	26(2)
C(7A)	-3578(11)	406(2)	2710(6)	31(2)
C(8A)	1969(9)	1151(2)	2682(5)	20(2)
C(9A)	578(10)	748(2)	1262(5)	20(2)
C(12A)	276(11)	832(2)	-1234(5)	21(2)
C(13A)	1486(10)	632(2)	-2030(5)	16(1)
C(14A)	3401(10)	550(2)	-1630(5)	17(1)
C(15A)	3522(10)	685(2)	-529(5)	21(2)
C(16A)	944(12)	535(2)	-3049(5)	25(2)
C(17A)	2349(13)	350(2)	-3631(5)	33(2)
C(18A)	4265(14)	272(2)	-3226(6)	35(2)

C(19A)	4794(12)	371(2)	-2219(5)	26(2)
C(23A)	-1630(9)	1541(2)	2181(5)	15(1)
C(24A)	706(11)	2518(2)	-1327(5)	25(2)
C(25A)	-1882(11)	2839(2)	-282(5)	23(2)
C(26A)	-3379(10)	2360(2)	1613(5)	22(2)
C(27A)	-1973(9)	1755(2)	1363(4)	14(1)
C(28A)	-2834(9)	1653(2)	295(5)	15(1)
C(29A)	-2435(10)	1971(2)	-430(5)	20(2)
C(30A)	330(11)	2281(2)	2011(4)	18(1)
C(31A)	-1459(9)	2156(2)	1315(5)	14(1)
C(32A)	-840(9)	2186(2)	158(4)	14(1)
C(33A)	-170(9)	2562(2)	-220(5)	18(1)
C(34A)	1501(10)	2688(2)	523(5)	21(2)
C(35A)	973(11)	2660(2)	1693(5)	23(2)
C(37A)	2496(10)	1318(2)	5521(5)	22(2)
C(38A)	647(10)	1462(2)	5776(5)	21(2)
C(39A)	313(11)	1582(2)	6798(5)	27(2)
C(40A)	1794(12)	1557(2)	7556(5)	29(2)
C(41A)	3661(11)	1415(2)	7300(5)	24(2)
C(42A)	4006(10)	1299(2)	6299(5)	22(2)
C(43A)	2932(11)	1165(2)	4455(5)	31(2)

Table 3. Bond lengths [Å] and angles [°] for leo282.

Cl(1)-C(28)	1.845(6)
O(3)-C(2)	1.411(7)
O(3)-C(4)	1.465(8)
O(5)-C(4)	1.415(7)
O(5)-C(1)	1.426(7)
O(11)-C(9)	1.179(7)
O(20)-C(9)	1.374(7)
O(20)-N(10)	1.392(6)
O(21)-C(15)	1.198(8)
O(22)-C(12)	1.209(8)
O(36)-C(43)	1.423(8)
O(36)-C(8)	1.437(7)
N(10)-C(12)	1.405(9)
N(10)-C(15)	1.424(8)
C(1)-C(23)	1.487(9)
C(1)-C(2)	1.584(9)
C(2)-C(8)	1.517(8)
C(2)-C(9)	1.551(8)
C(4)-C(7)	1.494(9)
C(4)-C(6)	1.503(9)
C(12)-C(13)	1.505(9)
C(13)-C(16)	1.358(9)
C(13)-C(14)	1.388(9)
C(14)-C(19)	1.392(9)
C(14)-C(15)	1.474(9)
C(16)-C(17)	1.395(10)
C(17)-C(18)	1.382(11)
C(18)-C(19)	1.399(10)
C(23)-C(27)	1.335(8)
C(24)-C(33)	1.540(8)
C(25)-C(33)	1.550(9)
C(26)-C(31)	1.555(9)
C(27)-C(28)	1.512(9)
C(27)-C(31)	1.513(8)

C(28)-C(29)	1.548(9)
C(29)-C(32)	1.533(8)
C(39)-C(38)	1.379(9)
C(39)-C(40)	1.384(10)
C(30)-C(35)	1.519(8)
C(30)-C(31)	1.528(8)
C(31)-C(32)	1.543(8)
C(32)-C(33)	1.540(8)
C(33)-C(34)	1.543(8)
C(34)-C(35)	1.541(8)
C(37)-C(42)	1.376(9)
C(37)-C(38)	1.409(9)
C(37)-C(43)	1.515(9)
C(40)-C(41)	1.388(10)
C(41)-C(42)	1.382(9)
Cl(1A)-C(28A)	1.827(6)
O(3A)-C(2A)	1.408(7)
O(3A)-C(4A)	1.454(7)
O(5A)-C(4A)	1.416(7)
O(5A)-C(1A)	1.426(7)
O(11A)-C(9A)	1.185(7)
O(20A)-N(10A)	1.384(6)
O(20A)-C(9A)	1.402(7)
O(22A)-C(12A)	1.187(8)
O(21A)-C(15A)	1.205(8)
O(36A)-C(43A)	1.388(8)
O(36A)-C(8A)	1.425(7)
N(10A)-C(12A)	1.410(8)
N(10A)-C(15A)	1.414(8)
C(1A)-C(23A)	1.487(8)
C(1A)-C(2A)	1.586(8)
C(2A)-C(9A)	1.520(9)
C(2A)-C(8A)	1.553(8)
C(4A)-C(6A)	1.511(9)
C(4A)-C(7A)	1.516(9)
C(12A)-C(13A)	1.495(9)

C(13A)-C(16A)	1.399(9)
C(13A)-C(14A)	1.401(9)
C(14A)-C(19A)	1.366(9)
C(14A)-C(15A)	1.497(9)
C(16A)-C(17A)	1.377(10)
C(17A)-C(18A)	1.400(11)
C(18A)-C(19A)	1.384(10)
C(23A)-C(27A)	1.334(8)
C(24A)-C(33A)	1.540(8)
C(25A)-C(33A)	1.536(9)
C(26A)-C(31A)	1.532(9)
C(27A)-C(28A)	1.528(8)
C(27A)-C(31A)	1.530(8)
C(28A)-C(29A)	1.527(8)
C(29A)-C(32A)	1.523(8)
C(30A)-C(35A)	1.529(8)
C(30A)-C(31A)	1.553(8)
C(31A)-C(32A)	1.540(8)
C(32A)-C(33A)	1.544(8)
C(33A)-C(34A)	1.532(9)
C(34A)-C(35A)	1.540(9)
C(37A)-C(38A)	1.376(9)
C(37A)-C(42A)	1.411(9)
C(37A)-C(43A)	1.505(9)
C(38A)-C(39A)	1.399(9)
C(39A)-C(40A)	1.381(10)
C(40A)-C(41A)	1.385(10)
C(41A)-C(42A)	1.370(9)

C(2)-O(3)-C(4)	110.0(5)
C(4)-O(5)-C(1)	109.7(5)
C(9)-O(20)-N(10)	111.9(4)
C(43)-O(36)-C(8)	110.6(5)
O(20)-N(10)-C(12)	120.1(5)
O(20)-N(10)-C(15)	121.4(5)
C(12)-N(10)-C(15)	113.1(5)

O(5)-C(1)-C(23)	108.1(5)
O(5)-C(1)-C(2)	102.1(5)
C(23)-C(1)-C(2)	115.9(5)
O(3)-C(2)-C(8)	109.5(5)
O(3)-C(2)-C(9)	107.8(5)
C(8)-C(2)-C(9)	109.0(5)
O(3)-C(2)-C(1)	104.8(5)
C(8)-C(2)-C(1)	116.0(5)
C(9)-C(2)-C(1)	109.5(5)
O(5)-C(4)-O(3)	104.1(5)
O(5)-C(4)-C(7)	111.6(6)
O(3)-C(4)-C(7)	110.0(5)
O(5)-C(4)-C(6)	108.2(5)
O(3)-C(4)-C(6)	107.9(6)
C(7)-C(4)-C(6)	114.5(6)
O(36)-C(8)-C(2)	108.1(5)
O(11)-C(9)-O(20)	124.8(5)
O(11)-C(9)-C(2)	126.3(5)
O(20)-C(9)-C(2)	108.9(5)
O(22)-C(12)-N(10)	124.7(6)
O(22)-C(12)-C(13)	131.5(7)
N(10)-C(12)-C(13)	103.7(6)
C(16)-C(13)-C(14)	122.2(6)
C(16)-C(13)-C(12)	129.9(7)
C(14)-C(13)-C(12)	107.9(5)
C(13)-C(14)-C(19)	120.4(6)
C(13)-C(14)-C(15)	110.3(6)
C(19)-C(14)-C(15)	129.3(7)
O(21)-C(15)-N(10)	124.3(6)
O(21)-C(15)-C(14)	132.4(6)
N(10)-C(15)-C(14)	103.3(6)
C(13)-C(16)-C(17)	117.7(7)
C(18)-C(17)-C(16)	121.4(6)
C(17)-C(18)-C(19)	120.3(7)
C(14)-C(19)-C(18)	117.8(7)
C(27)-C(23)-C(1)	129.3(6)

C(23)-C(27)-C(28)	127.3(5)
C(23)-C(27)-C(31)	124.9(5)
C(28)-C(27)-C(31)	107.5(5)
C(27)-C(28)-C(29)	106.1(5)
C(27)-C(28)-Cl(1)	109.9(5)
C(29)-C(28)-Cl(1)	110.6(4)
C(32)-C(29)-C(28)	102.6(5)
C(38)-C(39)-C(40)	120.2(7)
C(35)-C(30)-C(31)	110.6(5)
C(27)-C(31)-C(30)	117.3(5)
C(27)-C(31)-C(32)	99.7(5)
C(30)-C(31)-C(32)	109.7(5)
C(27)-C(31)-C(26)	105.5(5)
C(30)-C(31)-C(26)	109.1(5)
C(32)-C(31)-C(26)	115.7(5)
C(29)-C(32)-C(33)	121.2(5)
C(29)-C(32)-C(31)	103.9(5)
C(33)-C(32)-C(31)	117.0(5)
C(24)-C(33)-C(32)	109.8(5)
C(24)-C(33)-C(34)	108.3(5)
C(32)-C(33)-C(34)	106.9(5)
C(24)-C(33)-C(25)	107.3(5)
C(32)-C(33)-C(25)	114.3(5)
C(34)-C(33)-C(25)	110.1(5)
C(35)-C(34)-C(33)	114.9(5)
C(30)-C(35)-C(34)	111.3(5)
C(42)-C(37)-C(38)	118.6(6)
C(42)-C(37)-C(43)	119.7(6)
C(38)-C(37)-C(43)	121.7(6)
C(39)-C(38)-C(37)	120.4(7)
O(36)-C(43)-C(37)	110.1(5)
C(39)-C(40)-C(41)	119.7(6)
C(42)-C(41)-C(40)	120.0(7)
C(37)-C(42)-C(41)	121.1(7)
C(2A)-O(3A)-C(4A)	108.2(4)
C(4A)-O(5A)-C(1A)	107.7(4)

N(10A)-O(20A)-C(9A)	112.4(4)
C(43A)-O(36A)-C(8A)	113.6(5)
O(20A)-N(10A)-C(12A)	121.2(5)
O(20A)-N(10A)-C(15A)	121.0(5)
C(12A)-N(10A)-C(15A)	116.0(5)
O(5A)-C(1A)-C(23A)	111.7(5)
O(5A)-C(1A)-C(2A)	100.7(4)
C(23A)-C(1A)-C(2A)	113.4(5)
O(3A)-C(2A)-C(9A)	107.6(5)
O(3A)-C(2A)-C(8A)	108.4(5)
C(9A)-C(2A)-C(8A)	110.7(5)
O(3A)-C(2A)-C(1A)	105.6(5)
C(9A)-C(2A)-C(1A)	109.2(5)
C(8A)-C(2A)-C(1A)	114.9(5)
O(5A)-C(4A)-O(3A)	104.5(5)
O(5A)-C(4A)-C(6A)	109.4(5)
O(3A)-C(4A)-C(6A)	106.1(5)
O(5A)-C(4A)-C(7A)	112.8(5)
O(3A)-C(4A)-C(7A)	109.8(5)
C(6A)-C(4A)-C(7A)	113.7(6)
O(36A)-C(8A)-C(2A)	110.6(5)
O(11A)-C(9A)-O(20A)	122.4(6)
O(11A)-C(9A)-C(2A)	129.2(6)
O(20A)-C(9A)-C(2A)	108.4(5)
O(22A)-C(12A)-N(10A)	126.7(6)
O(22A)-C(12A)-C(13A)	131.5(6)
N(10A)-C(12A)-C(13A)	101.8(6)
C(16A)-C(13A)-C(14A)	120.9(6)
C(16A)-C(13A)-C(12A)	128.8(6)
C(14A)-C(13A)-C(12A)	110.3(6)
C(19A)-C(14A)-C(13A)	121.3(6)
C(19A)-C(14A)-C(15A)	130.3(6)
C(13A)-C(14A)-C(15A)	108.4(6)
O(21A)-C(15A)-N(10A)	125.9(6)
O(21A)-C(15A)-C(14A)	131.4(6)
N(10A)-C(15A)-C(14A)	102.7(6)

C(17A)-C(16A)-C(13A) 117.4(7)
C(16A)-C(17A)-C(18A) 121.2(7)
C(19A)-C(18A)-C(17A) 121.1(7)
C(14A)-C(19A)-C(18A) 118.2(7)
C(27A)-C(23A)-C(1A) 126.2(6)
C(23A)-C(27A)-C(28A) 127.9(6)
C(23A)-C(27A)-C(31A) 125.2(6)
C(28A)-C(27A)-C(31A) 106.9(5)
C(29A)-C(28A)-C(27A) 106.5(5)
C(29A)-C(28A)-Cl(1A) 110.0(4)
C(27A)-C(28A)-Cl(1A) 110.7(4)
C(32A)-C(29A)-C(28A) 103.3(5)
C(35A)-C(30A)-C(31A) 109.7(5)
C(27A)-C(31A)-C(26A) 106.8(5)
C(27A)-C(31A)-C(32A) 99.8(5)
C(26A)-C(31A)-C(32A) 115.2(5)
C(27A)-C(31A)-C(30A) 116.1(5)
C(26A)-C(31A)-C(30A) 110.0(5)
C(32A)-C(31A)-C(30A) 108.9(5)
C(29A)-C(32A)-C(31A) 104.4(5)
C(29A)-C(32A)-C(33A) 121.4(5)
C(31A)-C(32A)-C(33A) 116.4(5)
C(34A)-C(33A)-C(25A) 111.0(5)
C(34A)-C(33A)-C(24A) 109.2(5)
C(25A)-C(33A)-C(24A) 107.6(5)
C(34A)-C(33A)-C(32A) 107.0(5)
C(25A)-C(33A)-C(32A) 114.4(5)
C(24A)-C(33A)-C(32A) 107.6(5)
C(33A)-C(34A)-C(35A) 114.6(5)
C(30A)-C(35A)-C(34A) 112.6(5)
C(38A)-C(37A)-C(42A) 118.9(6)
C(38A)-C(37A)-C(43A) 122.3(6)
C(42A)-C(37A)-C(43A) 118.8(6)
C(37A)-C(38A)-C(39A) 119.2(6)
C(40A)-C(39A)-C(38A) 121.4(7)
C(39A)-C(40A)-C(41A) 119.6(6)

C(42A)-C(41A)-C(40A) 119.5(6)

C(41A)-C(42A)-C(37A) 121.5(6)

O(36A)-C(43A)-C(37A) 112.3(5)

Table 4. Anisotropic displacement parameters ($Å^2 x 10^3$) for leo282. The anisotropic displacement factor exponent takes the form: $-2\pi^2[h^2 a^{*2} U^{11} + ... + 2 h k a^* b^* U^{12}]$

U^{11}	U^{22}	U^{33}	U^{23}	U^{13}	U^{12}
Cl(1)36(1)	32(1)	32(1)	2(1)	15(1)	-9(1)
O(3) 15(2)	21(2)	20(2)	-3(2)	-1(2)	1(2)
O(5) 13(2)	23(2)	24(3)	-6(2)	-9(2)	0(2)
O(11)33(3)	19(2)	24(2)	8(2)	-9(2)	-7(2)
O(20)25(3)	19(2)	13(2)	4(2)	-5(2)	-2(2)
O(21)24(3)	35(3)	22(2)	-2(2)	0(2)	5(2)
O(22)19(3)	39(3)	36(3)	0(2)	-7(2)	-5(2)
O(36)12(2)	31(3)	16(2)	6(2)	2(2)	-3(2)
N(10)25(3)	26(3)	11(3)	10(2)	-7(2)	2(3)
C(1) 13(3)	24(3)	11(3)	-1(3)	-1(3)	-1(3)
C(2) 19(4)	13(3)	15(3)	-2(3)	0(3)	1(3)
C(4) 23(4)	12(3)	34(4)	-1(3)	-9(3)	2(3)
C(6) 41(5)	36(5)	36(4)	-13(4)	-13(4)	-3(4)
C(7) 25(4)	28(4)	44(5)	-8(4)	5(4)	-10(3)
C(8) 6(3)	30(4)	15(3)	5(3)	2(3)	0(3)
C(9) 6(3)	17(3)	16(3)	3(3)	4(3)	2(3)
C(12)23(4)	21(3)	12(3)	-6(3)	-7(3)	-9(3)
C(13)28(4)	14(3)	11(3)	1(3)	-9(3)	-8(3)
C(14)38(5)	13(3)	10(3)	-2(3)	-11(3)	0(3)
C(15)22(4)	19(3)	22(4)	-2(3)	-7(3)	0(3)
C(16)47(5)	28(4)	13(3)	0(3)	-8(3)	-9(4)
C(17)75(6)	27(4)	6(3)	9(3)	-13(4)	-14(4)
C(18)58(6)	21(4)	21(4)	-2(3)	-21(4)	6(4)
C(19)46(5)	26(4)	17(3)	-7(3)	-11(3)	9(4)
C(23)5(3)	26(4)	21(3)	2(3)	3(3)	2(3)
C(24)21(4)	24(4)	23(4)	-3(3)	1(3)	-1(3)
C(25)34(4)	15(3)	20(4)	2(3)	7(3)	4(3)
C(26)25(4)	24(4)	20(4)	4(3)	2(3)	1(3)
C(27)5(3)	19(3)	12(3)	1(3)	2(3)	5(3)
C(28)16(4)	18(3)	27(4)	6(3)	6(3)	1(3)
C(29)21(4)	23(3)	15(3)	4(3)	4(3)	4(3)

C(39)37(4)	14(3)	27(4)	1(3)	-7(4)	-1(3)
C(30)21(4)	28(4)	9(3)	0(3)	0(3)	8(3)
C(31)18(4)	18(3)	11(3)	-3(3)	0(3)	6(3)
C(32)10(3)	29(4)	17(3)	0(3)	0(3)	3(3)
C(33)12(3)	20(3)	14(3)	1(3)	-1(3)	1(3)
C(34)17(4)	15(3)	21(3)	0(3)	3(3)	2(3)
C(35)22(4)	26(3)	12(3)	5(3)	5(3)	8(3)
C(37)21(4)	19(3)	21(4)	5(3)	4(3)	-1(3)
C(38)21(4)	29(4)	20(4)	4(3)	1(3)	2(3)
C(43)19(4)	33(4)	30(4)	7(3)	-3(3)	-4(3)
C(40)47(5)	23(4)	18(4)	-2(3)	5(4)	-11(4)
C(41)30(5)	23(4)	28(4)	-5(3)	13(3)	-6(3)
C(42)21(4)	13(3)	33(4)	0(3)	-7(3)	-4(3)
Cl(1A)19(1)	38(1)	23(1)	4(1)	-2(1)	-10(1)
O(3A)17(2)	27(2)	20(2)	11(2)	7(2)	7(2)
O(5A)17(3)	16(2)	15(2)	7(2)	7(2)	4(2)
O(11A)39(3)	21(3)	30(3)	-2(2)	11(3)	4(2)
O(20A)16(2)	21(2)	15(2)	-4(2)	4(2)	-1(2)
O(22A)16(3)	34(3)	27(3)	0(2)	-2(2)	0(2)
O(21A)22(3)	42(3)	21(3)	1(2)	0(2)	5(2)
O(36A)17(3)	53(3)	10(2)	-3(2)	2(2)	12(2)
N(10A)20(3)	31(3)	5(2)	-3(2)	1(2)	3(3)
C(2A)12(4)	25(3)	11(3)	3(3)	1(3)	4(3)
C(4A)14(3)	21(3)	22(4)	7(3)	2(3)	5(3)
C(6A)25(4)	23(4)	32(4)	3(3)	9(3)	4(3)
C(7A)25(4)	28(4)	40(5)	9(4)	-3(4)	-2(3)
C(8A)8(3)	38(4)	14(3)	1(3)	-2(3)	1(3)
C(9A)14(4)	22(4)	23(3)	4(3)	7(3)	1(3)
C(12A)23(4)	19(3)	22(4)	5(3)	3(3)	-2(3)
C(13A)23(4)	13(3)	13(3)	6(3)	4(3)	1(3)
C(14A)27(4)	13(3)	11(3)	1(3)	2(3)	-3(3)
C(15A)22(4)	25(4)	17(4)	1(3)	4(3)	-1(3)
C(16A)41(5)	22(4)	14(3)	1(3)	-6(3)	-9(3)
C(17A)60(6)	24(4)	14(4)	-5(3)	1(4)	-4(4)
C(18A)58(6)	17(4)	29(4)	-2(3)	15(4)	0(4)
C(19A)38(5)	15(3)	27(4)	1(3)	4(4)	3(3)

C(23A)14(3)	18(3)	13(3)	2(3)	2(3)	1(3)
C(24A)32(4)	21(4)	21(4)	7(3)	0(3)	-4(3)
C(25A)31(4)	19(3)	19(4)	6(3)	-2(3)	-1(3)
C(26A)23(4)	23(4)	20(4)	3(3)	5(3)	5(3)
C(27A)9(3)	22(3)	10(3)	-1(3)	5(3)	1(3)
C(28A)8(3)	19(3)	18(3)	-1(3)	-1(3)	1(3)
C(29A)16(4)	21(3)	23(3)	0(3)	1(3)	-1(3)
C(30A)28(4)	20(3)	7(3)	3(3)	-7(3)	-3(3)
C(31A)12(3)	18(3)	13(3)	0(3)	-6(3)	6(3)
C(32A)9(3)	18(3)	15(3)	-2(3)	-2(3)	3(3)
C(33A)20(4)	15(3)	18(3)	5(3)	-5(3)	0(3)
C(34A)23(4)	13(3)	27(4)	5(3)	-4(3)	-5(3)
C(35A)28(4)	19(3)	23(4)	0(3)	-11(3)	-3(3)
C(37A)23(4)	21(4)	21(4)	-2(3)	-2(3)	2(3)
C(38A)20(4)	20(3)	22(3)	1(3)	2(3)	3(3)
C(39A)32(4)	25(4)	22(4)	-1(3)	5(3)	-1(4)
C(40A)55(5)	15(3)	18(4)	-3(3)	4(4)	-2(4)
C(41A)35(4)	17(3)	18(4)	-1(3)	-6(3)	-5(3)
C(42A)13(4)	26(4)	27(4)	-1(3)	-8(3)	2(3)
C(43A)23(4)	45(5)	25(4)	-6(3)	-2(3)	10(3)

Table 5. Hydrogen coordinates (x 10^4) and isotropic displacement parameters ($Å^2$x 10^{-3}) for leo282.

	x	y	z	U(eq)
H(1A)	7489	4077	-4463	19
H(6A)	6970	4857	-1480	56
H(6B)	8920	4604	-1410	56
H(6C)	6721	4438	-1227	56
H(7A)	7815	5036	-3387	48
H(7B)	8310	4719	-4190	48
H(7C)	9842	4807	-3256	48
H(8A)	1758	4168	-3266	21
H(8B)	2788	3800	-3644	21
H(16A)	5075	4473	-9254	35
H(17A)	2797	4794	-10312	43
H(18A)	-416	4933	-9719	40
H(19A)	-1358	4793	-7986	35
H(23A)	6529	3558	-2896	21
H(24A)	2940	2105	-5781	34
H(24B)	3825	2424	-6486	34
H(24C)	2126	2507	-5632	34
H(25A)	7691	2171	-4626	34
H(25B)	7475	2270	-5840	34
H(25C)	6257	1936	-5367	34
H(26A)	9615	2863	-4701	34
H(26B)	9057	2579	-3807	34
H(26C)	9796	2974	-3495	34
H(28A)	6024	3576	-5722	24
H(29A)	5455	3037	-6483	24
H(29B)	7648	2886	-6150	24
H(39A)	5801	3480	1153	31
H(30A)	6664	2936	-2400	23
H(30B)	4491	2996	-2925	23
H(32A)	4177	2956	-4854	22

H(34A)	2744	2448	-3819	21
H(34B)	3926	2074	-3833	21
H(35A)	4696	2404	-2285	24
H(35B)	6700	2333	-2952	24
H(38A)	5302	3578	-625	28
H(43A)	1739	3504	-2030	33
H(43B)	596	3876	-1799	33
H(40A)	3092	3521	2312	35
H(41A)	-100	3685	1688	32
H(42A)	-572	3806	-79	27
H(1AA)	-2703	1064	1584	17
H(6AA)	-1874	362	4651	40
H(6AB)	-3796	620	4757	40
H(6AC)	-1569	782	4868	40
H(7AA)	-3139	162	2877	47
H(7AB)	-3377	452	1962	47
H(7AC)	-5012	433	2880	47
H(8AA)	3184	996	2700	24
H(8AB)	2222	1350	2186	24
H(16B)	-343	594	-3329	30
H(17B)	2012	273	-4318	39
H(18B)	5217	149	-3650	42
H(19B)	6091	315	-1944	32
H(23B)	-1153	1652	2803	18
H(24D)	1364	2743	-1538	37
H(24E)	-385	2462	-1819	37
H(24F)	1698	2323	-1329	37
H(25D)	-1452	3043	-714	34
H(25E)	-2206	2924	424	34
H(25F)	-3080	2728	-594	34
H(26D)	-3857	2277	2296	33
H(26E)	-4425	2317	1084	33
H(26F)	-3085	2618	1650	33
H(28B)	-2130	1434	24	18
H(29C)	-1923	1889	-1117	24
H(29D)	-3675	2115	-539	24

H(30C)	-82	2280	2755	22
H(30D)	1480	2114	1930	22
H(32B)	408	2036	105	17
H(34C)	1826	2941	360	25
H(34D)	2728	2544	389	25
H(35C)	2163	2732	2113	28
H(35D)	-134	2830	1852	28
H(38B)	-389	1479	5264	25
H(39B)	-959	1682	6974	32
H(40B)	1533	1636	8249	35
H(41B)	4696	1400	7813	28
H(42B)	5290	1202	6126	26
H(43C)	4331	1228	4255	37
H(43D)	2833	900	4485	37

Table 6. Torsion angles [°] for leo282.

C(9)-O(20)-N(10)-C(12)	81.5(6)
C(9)-O(20)-N(10)-C(15)	-70.8(7)
C(4)-O(5)-C(1)-C(23)	-151.5(5)
C(4)-O(5)-C(1)-C(2)	-28.8(6)
C(4)-O(3)-C(2)-C(8)	128.1(5)
C(4)-O(3)-C(2)-C(9)	-113.5(5)
C(4)-O(3)-C(2)-C(1)	3.1(6)
O(5)-C(1)-C(2)-O(3)	15.0(6)
C(23)-C(1)-C(2)-O(3)	132.3(5)
O(5)-C(1)-C(2)-C(8)	-105.8(5)
C(23)-C(1)-C(2)-C(8)	11.5(8)
O(5)-C(1)-C(2)-C(9)	130.4(5)
C(23)-C(1)-C(2)-C(9)	-112.3(6)
C(1)-O(5)-C(4)-O(3)	31.4(6)
C(1)-O(5)-C(4)-C(7)	-87.2(6)
C(1)-O(5)-C(4)-C(6)	146.0(6)
C(2)-O(3)-C(4)-O(5)	-20.4(6)
C(2)-O(3)-C(4)-C(7)	99.3(6)
C(2)-O(3)-C(4)-C(6)	-135.3(5)
C(43)-O(36)-C(8)-C(2)	178.8(5)
O(3)-C(2)-C(8)-O(36)	-54.1(6)
C(9)-C(2)-C(8)-O(36)	-171.7(5)
C(1)-C(2)-C(8)-O(36)	64.2(7)
N(10)-O(20)-C(9)-O(11)	0.9(8)
N(10)-O(20)-C(9)-C(2)	179.9(5)
O(3)-C(2)-C(9)-O(11)	7.0(9)
C(8)-C(2)-C(9)-O(11)	125.7(7)
C(1)-C(2)-C(9)-O(11)	-106.4(7)
O(3)-C(2)-C(9)-O(20)	-171.9(5)
C(8)-C(2)-C(9)-O(20)	-53.2(6)
C(1)-C(2)-C(9)-O(20)	74.6(6)
O(20)-N(10)-C(12)-O(22)	14.2(9)
C(15)-N(10)-C(12)-O(22)	168.6(6)
O(20)-N(10)-C(12)-C(13)	-167.8(5)

C(15)-N(10)-C(12)-C(13)	-13.4(7)
O(22)-C(12)-C(13)-C(16)	6.0(12)
N(10)-C(12)-C(13)-C(16)	-171.9(6)
O(22)-C(12)-C(13)-C(14)	-174.1(7)
N(10)-C(12)-C(13)-C(14)	8.0(6)
C(16)-C(13)-C(14)-C(19)	0.0(10)
C(12)-C(13)-C(14)-C(19)	-179.9(5)
C(16)-C(13)-C(14)-C(15)	179.6(6)
C(12)-C(13)-C(14)-C(15)	-0.4(7)
O(20)-N(10)-C(15)-O(21)	-10.3(10)
C(12)-N(10)-C(15)-O(21)	-164.3(6)
O(20)-N(10)-C(15)-C(14)	167.2(5)
C(12)-N(10)-C(15)-C(14)	13.1(7)
C(13)-C(14)-C(15)-O(21)	169.9(7)
C(19)-C(14)-C(15)-O(21)	-10.6(12)
C(13)-C(14)-C(15)-N(10)	-7.3(7)
C(19)-C(14)-C(15)-N(10)	172.2(6)
C(14)-C(13)-C(16)-C(17)	0.6(10)
C(12)-C(13)-C(16)-C(17)	-179.5(6)
C(13)-C(16)-C(17)-C(18)	-1.8(10)
C(16)-C(17)-C(18)-C(19)	2.4(11)
C(13)-C(14)-C(19)-C(18)	0.5(9)
C(15)-C(14)-C(19)-C(18)	-178.9(6)
C(17)-C(18)-C(19)-C(14)	-1.7(10)
O(5)-C(1)-C(23)-C(27)	-138.7(7)
C(2)-C(1)-C(23)-C(27)	107.4(8)
C(1)-C(23)-C(27)-C(28)	-7.5(11)
C(1)-C(23)-C(27)-C(31)	179.6(6)
C(23)-C(27)-C(28)-C(29)	-160.4(6)
C(31)-C(27)-C(28)-C(29)	13.4(7)
C(23)-C(27)-C(28)-Cl(1)	80.0(7)
C(31)-C(27)-C(28)-Cl(1)	-106.2(5)
C(27)-C(28)-C(29)-C(32)	14.8(7)
Cl(1)-C(28)-C(29)-C(32)	134.0(5)
C(23)-C(27)-C(31)-C(30)	20.3(9)
C(28)-C(27)-C(31)-C(30)	-153.8(6)

C(23)-C(27)-C(31)-C(32)	138.4(6)
C(28)-C(27)-C(31)-C(32)	-35.6(6)
C(23)-C(27)-C(31)-C(26)	-101.4(7)
C(28)-C(27)-C(31)-C(26)	84.6(6)
C(35)-C(30)-C(31)-C(27)	167.9(6)
C(35)-C(30)-C(31)-C(32)	55.3(7)
C(35)-C(30)-C(31)-C(26)	-72.3(7)
C(28)-C(29)-C(32)-C(33)	-171.6(5)
C(28)-C(29)-C(32)-C(31)	-37.3(6)
C(27)-C(31)-C(32)-C(29)	45.0(6)
C(30)-C(31)-C(32)-C(29)	168.7(5)
C(26)-C(31)-C(32)-C(29)	-67.5(6)
C(27)-C(31)-C(32)-C(33)	-178.5(5)
C(30)-C(31)-C(32)-C(33)	-54.8(7)
C(26)-C(31)-C(32)-C(33)	69.0(7)
C(29)-C(32)-C(33)-C(24)	-63.7(7)
C(31)-C(32)-C(33)-C(24)	167.7(5)
C(29)-C(32)-C(33)-C(34)	179.1(5)
C(31)-C(32)-C(33)-C(34)	50.5(7)
C(29)-C(32)-C(33)-C(25)	57.0(8)
C(31)-C(32)-C(33)-C(25)	-71.6(7)
C(24)-C(33)-C(34)-C(35)	-168.3(5)
C(32)-C(33)-C(34)-C(35)	-50.1(7)
C(25)-C(33)-C(34)-C(35)	74.6(7)
C(31)-C(30)-C(35)-C(34)	-57.0(7)
C(33)-C(34)-C(35)-C(30)	56.2(7)
C(40)-C(39)-C(38)-C(37)	0.9(10)
C(42)-C(37)-C(38)-C(39)	1.0(10)
C(43)-C(37)-C(38)-C(39)	-176.2(6)
C(8)-O(36)-C(43)-C(37)	-172.4(5)
C(42)-C(37)-C(43)-O(36)	139.8(6)
C(38)-C(37)-C(43)-O(36)	-43.0(8)
C(38)-C(39)-C(40)-C(41)	-1.5(10)
C(39)-C(40)-C(41)-C(42)	0.2(10)
C(38)-C(37)-C(42)-C(41)	-2.3(10)
C(43)-C(37)-C(42)-C(41)	174.9(6)

C(40)-C(41)-C(42)-C(37)	1.8(10)
C(9A)-O(20A)-N(10A)-C(12A)	93.2(6)
C(9A)-O(20A)-N(10A)-C(15A)	-70.8(7)
C(4A)-O(5A)-C(1A)-C(23A)	-154.5(5)
C(4A)-O(5A)-C(1A)-C(2A)	-33.8(6)
C(4A)-O(3A)-C(2A)-C(9A)	-112.9(5)
C(4A)-O(3A)-C(2A)-C(8A)	127.4(5)
C(4A)-O(3A)-C(2A)-C(1A)	3.7(6)
O(5A)-C(1A)-C(2A)-O(3A)	17.9(6)
C(23A)-C(1A)-C(2A)-O(3A)	137.3(5)
O(5A)-C(1A)-C(2A)-C(9A)	133.4(5)
C(23A)-C(1A)-C(2A)-C(9A)	-107.2(6)
O(5A)-C(1A)-C(2A)-C(8A)	-101.5(5)
C(23A)-C(1A)-C(2A)-C(8A)	17.9(7)
C(1A)-O(5A)-C(4A)-O(3A)	37.7(6)
C(1A)-O(5A)-C(4A)-C(6A)	150.9(5)
C(1A)-O(5A)-C(4A)-C(7A)	-81.6(6)
C(2A)-O(3A)-C(4A)-O(5A)	-24.5(6)
C(2A)-O(3A)-C(4A)-C(6A)	-140.1(5)
C(2A)-O(3A)-C(4A)-C(7A)	96.7(6)
C(43A)-O(36A)-C(8A)-C(2A)	116.8(6)
O(3A)-C(2A)-C(8A)-O(36A)	-57.3(6)
C(9A)-C(2A)-C(8A)-O(36A)	-175.1(5)
C(1A)-C(2A)-C(8A)-O(36A)	60.6(7)
N(10A)-O(20A)-C(9A)-O(11A)	-3.7(9)
N(10A)-O(20A)-C(9A)-C(2A)	176.0(5)
O(3A)-C(2A)-C(9A)-O(11A)	4.7(10)
C(8A)-C(2A)-C(9A)-O(11A)	123.0(8)
C(1A)-C(2A)-C(9A)-O(11A)	-109.5(8)
O(3A)-C(2A)-C(9A)-O(20A)	-175.1(5)
C(8A)-C(2A)-C(9A)-O(20A)	-56.7(7)
C(1A)-C(2A)-C(9A)-O(20A)	70.8(6)
O(20A)-N(10A)-C(12A)-O(22A)	6.3(10)
C(15A)-N(10A)-C(12A)-O(22A)	171.0(6)
O(20A)-N(10A)-C(12A)-C(13A)	-173.1(5)
C(15A)-N(10A)-C(12A)-C(13A)	-8.3(7)

O(22A)-C(12A)-C(13A)-C(16A)	5.6(12)
N(10A)-C(12A)-C(13A)-C(16A)	-175.1(6)
O(22A)-C(12A)-C(13A)-C(14A)	-175.6(7)
N(10A)-C(12A)-C(13A)-C(14A)	3.7(7)
C(16A)-C(13A)-C(14A)-C(19A)	-0.3(9)
C(12A)-C(13A)-C(14A)-C(19A)	-179.2(6)
C(16A)-C(13A)-C(14A)-C(15A)	-179.6(6)
C(12A)-C(13A)-C(14A)-C(15A)	1.5(7)
O(20A)-N(10A)-C(15A)-O(21A)	-4.9(10)
C(12A)-N(10A)-C(15A)-O(21A)	-169.6(6)
O(20A)-N(10A)-C(15A)-C(14A)	174.0(5)
C(12A)-N(10A)-C(15A)-C(14A)	9.3(7)
C(19A)-C(14A)-C(15A)-O(21A)	-6.5(12)
C(13A)-C(14A)-C(15A)-O(21A)	172.7(7)
C(19A)-C(14A)-C(15A)-N(10A)	174.7(6)
C(13A)-C(14A)-C(15A)-N(10A)	-6.1(7)
C(14A)-C(13A)-C(16A)-C(17A)	1.2(9)
C(12A)-C(13A)-C(16A)-C(17A)	179.9(6)
C(13A)-C(16A)-C(17A)-C(18A)	-1.8(10)
C(16A)-C(17A)-C(18A)-C(19A)	1.6(11)
C(13A)-C(14A)-C(19A)-C(18A)	0.0(9)
C(15A)-C(14A)-C(19A)-C(18A)	179.1(6)
C(17A)-C(18A)-C(19A)-C(14A)	-0.6(10)
O(5A)-C(1A)-C(23A)-C(27A)	-135.4(6)
C(2A)-C(1A)-C(23A)-C(27A)	111.7(7)
C(1A)-C(23A)-C(27A)-C(28A)	3.3(10)
C(1A)-C(23A)-C(27A)-C(31A)	-173.4(6)
C(23A)-C(27A)-C(28A)-C(29A)	-166.3(6)
C(31A)-C(27A)-C(28A)-C(29A)	10.9(6)
C(23A)-C(27A)-C(28A)-Cl(1A)	74.1(7)
C(31A)-C(27A)-C(28A)-Cl(1A)	-108.7(5)
C(27A)-C(28A)-C(29A)-C(32A)	16.5(6)
Cl(1A)-C(28A)-C(29A)-C(32A)	136.5(4)
C(23A)-C(27A)-C(31A)-C(26A)	-95.6(7)
C(28A)-C(27A)-C(31A)-C(26A)	87.1(6)
C(23A)-C(27A)-C(31A)-C(32A)	144.2(6)

C(28A)-C(27A)-C(31A)-C(32A)	-33.1(6)
C(23A)-C(27A)-C(31A)-C(30A)	27.4(9)
C(28A)-C(27A)-C(31A)-C(30A)	-149.8(5)
C(35A)-C(30A)-C(31A)-C(27A)	166.8(5)
C(35A)-C(30A)-C(31A)-C(26A)	-71.9(6)
C(35A)-C(30A)-C(31A)-C(32A)	55.2(7)
C(28A)-C(29A)-C(32A)-C(31A)	-37.9(6)
C(28A)-C(29A)-C(32A)-C(33A)	-171.9(5)
C(27A)-C(31A)-C(32A)-C(29A)	43.8(6)
C(26A)-C(31A)-C(32A)-C(29A)	-70.1(6)
C(30A)-C(31A)-C(32A)-C(29A)	165.8(5)
C(27A)-C(31A)-C(32A)-C(33A)	-179.5(5)
C(26A)-C(31A)-C(32A)-C(33A)	66.6(7)
C(30A)-C(31A)-C(32A)-C(33A)	-57.5(7)
C(29A)-C(32A)-C(33A)-C(34A)	-177.5(5)
C(31A)-C(32A)-C(33A)-C(34A)	53.6(7)
C(29A)-C(32A)-C(33A)-C(25A)	59.2(7)
C(31A)-C(32A)-C(33A)-C(25A)	-69.7(7)
C(29A)-C(32A)-C(33A)-C(24A)	-60.3(7)
C(31A)-C(32A)-C(33A)-C(24A)	170.8(5)
C(25A)-C(33A)-C(34A)-C(35A)	74.8(7)
C(24A)-C(33A)-C(34A)-C(35A)	-166.8(5)
C(32A)-C(33A)-C(34A)-C(35A)	-50.6(7)
C(31A)-C(30A)-C(35A)-C(34A)	-55.5(7)
C(33A)-C(34A)-C(35A)-C(30A)	55.1(7)
C(42A)-C(37A)-C(38A)-C(39A)	-0.5(9)
C(43A)-C(37A)-C(38A)-C(39A)	176.7(6)
C(37A)-C(38A)-C(39A)-C(40A)	-0.4(10)
C(38A)-C(39A)-C(40A)-C(41A)	1.0(11)
C(39A)-C(40A)-C(41A)-C(42A)	-0.7(10)
C(40A)-C(41A)-C(42A)-C(37A)	-0.2(10)
C(38A)-C(37A)-C(42A)-C(41A)	0.8(10)
C(43A)-C(37A)-C(42A)-C(41A)	-176.5(6)
C(8A)-O(36A)-C(43A)-C(37A)	-179.2(6)
C(38A)-C(37A)-C(43A)-O(36A)	20.8(10)
C(42A)-C(37A)-C(43A)-O(36A)	-162.0(6)

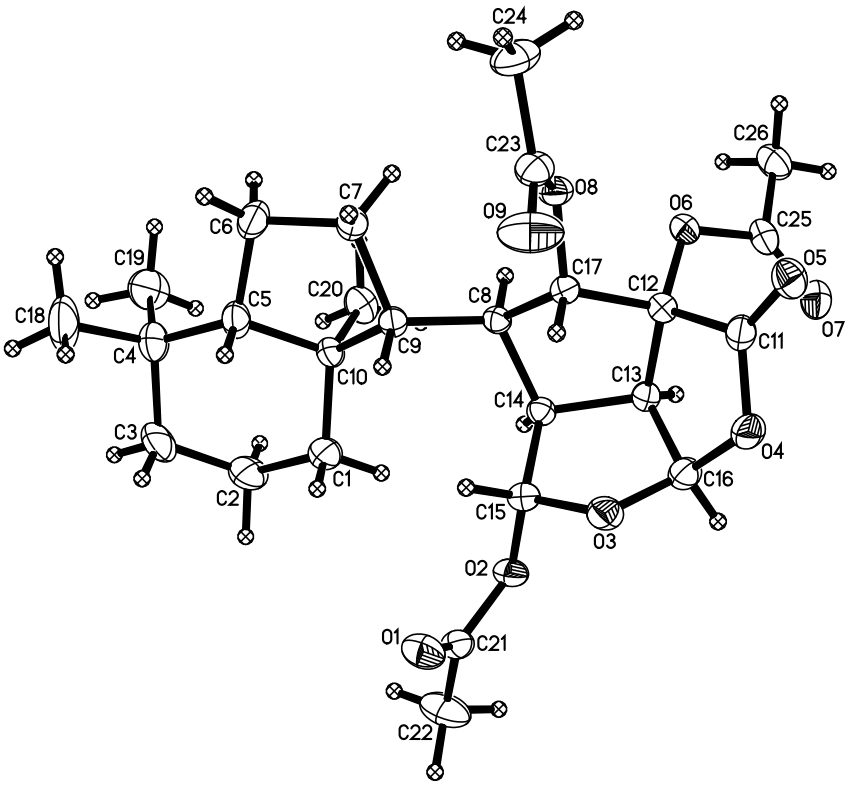

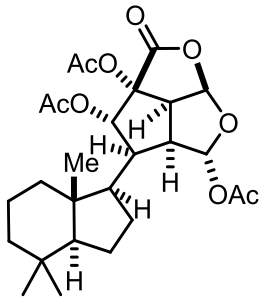

chromodorolide B (**3.110**)

Table 1. Crystal data and structure refinement for leo287 (**3.110**).

Identification code	leo287 (Daniel Tao)
Empirical formula	$C_{26}H_{36}O_9$
Formula weight	492.55
Temperature	133(2) K
Wavelength	0.71073 Å
Crystal system	Orthorhombic
Space group	$P2_12_12_1$

Unit cell dimensions	a = 11.1531(6) Å	α= 90°.
	b = 13.0647(7) Å	β= 90°.
	c = 17.2921(10) Å	γ = 90°.
Volume	2519.7(2) $Å^3$	
Z	4	
Density (calculated)	1.298 Mg/m^3	
Absorption coefficient	0.097 mm^{-1}	
F(000)	1056	
Crystal color	colorless	
Crystal size	0.506 x 0.310 x 0.196 mm^3	
Theta range for data collection	1.954 to 28.784°	
Index ranges	$-14 \leq h \leq 15$, $-17 \leq k \leq 17$, $-23 \leq l \leq 23$	
Reflections collected	30398	
Independent reflections	6192 [R(int) = 0.0257]	
Completeness to theta = 25.500°	100.0 %	
Absorption correction	Semi-empirical from equivalents	
Max. and min. transmission	0.8621 and 0.8201	
Refinement method	Full-matrix least-squares on F^2	
Data / restraints / parameters	6192 / 0 / 322	
Goodness-of-fit on F^2	1.044	
Final R indices [I>2sigma(I) = 5663 data]	R1 = 0.0337, wR2 = 0.0808	
R indices (all data, 0.74Å)	R1 = 0.0387, wR2 = 0.0843	
Absolute structure parameter	0.0(2)	
Largest diff. peak and hole	0.285 and -0.150 $e.Å^{-3}$	

Table 2. Atomic coordinates (x 10^4) and equivalent isotropic displacement parameters ($Å^2$x 10^3) for leo287. U(eq) is defined as one third of the trace of the orthogonalized U^{ij} tensor.

	x	y	z	U(eq)
O(1)	4746(1)	6774(1)	6848(1)	32(1)
O(2)	4147(1)	5212(1)	6443(1)	23(1)
O(3)	6125(1)	4668(1)	6527(1)	26(1)
O(4)	7342(1)	3247(1)	6501(1)	27(1)
O(5)	8745(1)	2661(1)	5684(1)	29(1)
O(6)	6706(1)	2429(1)	4605(1)	22(1)
O(7)	6506(1)	1257(1)	5544(1)	31(1)
O(8)	7755(1)	4150(1)	4156(1)	22(1)
O(9)	9070(1)	5239(1)	4704(1)	44(1)
C(1)	3516(2)	6389(2)	4786(1)	32(1)
C(2)	2412(2)	6996(2)	4514(1)	42(1)
C(3)	2772(2)	7928(2)	4039(1)	42(1)
C(4)	3552(2)	7692(2)	3327(1)	34(1)
C(5)	4589(2)	7007(1)	3608(1)	26(1)
C(6)	5518(2)	6616(2)	3033(1)	31(1)
C(7)	6276(2)	5862(1)	3520(1)	24(1)
C(8)	5699(2)	4586(1)	4601(1)	18(1)
C(9)	5578(2)	5681(1)	4290(1)	19(1)
C(10)	4281(2)	6049(1)	4094(1)	21(1)
C(11)	7753(2)	2969(1)	5790(1)	23(1)
C(12)	6779(2)	3188(1)	5195(1)	20(1)
C(13)	5627(2)	3339(1)	5663(1)	20(1)
C(14)	5037(2)	4334(1)	5366(1)	18(1)
C(15)	5255(2)	5091(1)	6031(1)	21(1)
C(16)	6118(2)	3584(2)	6466(1)	24(1)
C(17)	6976(2)	4239(1)	4806(1)	19(1)
C(18)	4088(3)	8709(2)	3037(2)	55(1)
C(19)	2783(2)	7247(2)	2673(1)	46(1)
C(20)	3631(2)	5206(2)	3642(1)	28(1)
C(21)	4000(2)	6124(2)	6819(1)	24(1)
C(22)	2779(2)	6185(2)	7167(2)	44(1)

C(23)	8772(2)	4727(2)	4163(1)	26(1)
C(24)	9413(2)	4630(2)	3410(1)	37(1)
C(25)	6504(2)	1461(1)	4865(1)	25(1)
C(26)	6291(2)	734(2)	4215(1)	31(1)

Table 3. Bond lengths [Å] and angles [°] for leo287.

O(1)-C(21)	1.191(2)
O(2)-C(21)	1.366(2)
O(2)-C(15)	1.435(2)
O(3)-C(15)	1.409(2)
O(3)-C(16)	1.421(2)
O(4)-C(11)	1.362(2)
O(4)-C(16)	1.436(2)
O(5)-C(11)	1.191(2)
O(6)-C(25)	1.361(2)
O(6)-C(12)	1.426(2)
O(7)-C(25)	1.205(2)
O(8)-C(23)	1.362(2)
O(8)-C(17)	1.426(2)
O(9)-C(23)	1.198(3)
C(1)-C(10)	1.535(3)
C(1)-C(2)	1.538(3)
C(2)-C(3)	1.522(4)
C(3)-C(4)	1.539(3)
C(4)-C(19)	1.534(3)
C(4)-C(18)	1.539(3)
C(4)-C(5)	1.541(3)
C(5)-C(6)	1.524(3)
C(5)-C(10)	1.546(3)
C(6)-C(7)	1.548(3)
C(7)-C(9)	1.560(2)
C(8)-C(9)	1.534(2)
C(8)-C(17)	1.536(2)
C(8)-C(14)	1.550(2)
C(9)-C(10)	1.562(2)
C(10)-C(20)	1.533(3)
C(11)-C(12)	1.523(3)
C(12)-C(13)	1.531(2)
C(12)-C(17)	1.545(2)
C(13)-C(16)	1.528(2)

C(13)-C(14)	1.545(2)
C(14)-C(15)	1.536(2)
C(21)-C(22)	1.491(3)
C(23)-C(24)	1.492(3)
C(25)-C(26)	1.490(3)

C(21)-O(2)-C(15)	115.87(14)
C(15)-O(3)-C(16)	109.97(14)
C(11)-O(4)-C(16)	111.34(14)
C(25)-O(6)-C(12)	114.74(14)
C(23)-O(8)-C(17)	117.04(14)
C(10)-C(1)-C(2)	110.82(17)
C(3)-C(2)-C(1)	111.5(2)
C(2)-C(3)-C(4)	114.90(18)
C(19)-C(4)-C(3)	110.4(2)
C(19)-C(4)-C(18)	107.7(2)
C(3)-C(4)-C(18)	107.9(2)
C(19)-C(4)-C(5)	115.61(18)
C(3)-C(4)-C(5)	106.71(17)
C(18)-C(4)-C(5)	108.23(19)
C(6)-C(5)-C(4)	119.90(17)
C(6)-C(5)-C(10)	103.56(15)
C(4)-C(5)-C(10)	118.39(17)
C(5)-C(6)-C(7)	103.32(15)
C(6)-C(7)-C(9)	106.69(15)
C(9)-C(8)-C(17)	115.99(14)
C(9)-C(8)-C(14)	117.12(14)
C(17)-C(8)-C(14)	100.51(13)
C(8)-C(9)-C(7)	113.38(14)
C(8)-C(9)-C(10)	116.44(14)
C(7)-C(9)-C(10)	103.37(13)
C(20)-C(10)-C(1)	110.06(17)
C(20)-C(10)-C(5)	114.13(15)
C(1)-C(10)-C(5)	108.26(15)
C(20)-C(10)-C(9)	109.07(14)
C(1)-C(10)-C(9)	115.80(15)

C(5)-C(10)-C(9)	99.29(14)
O(5)-C(11)-O(4)	122.80(17)
O(5)-C(11)-C(12)	128.44(17)
O(4)-C(11)-C(12)	108.65(15)
O(6)-C(12)-C(11)	113.21(14)
O(6)-C(12)-C(13)	114.82(14)
C(11)-C(12)-C(13)	105.43(14)
O(6)-C(12)-C(17)	108.31(14)
C(11)-C(12)-C(17)	111.10(14)
C(13)-C(12)-C(17)	103.58(13)
C(16)-C(13)-C(12)	101.91(14)
C(16)-C(13)-C(14)	106.18(14)
C(12)-C(13)-C(14)	106.89(14)
C(15)-C(14)-C(13)	103.04(14)
C(15)-C(14)-C(8)	115.23(14)
C(13)-C(14)-C(8)	105.03(13)
O(3)-C(15)-O(2)	109.52(14)
O(3)-C(15)-C(14)	108.26(14)
O(2)-C(15)-C(14)	107.88(14)
O(3)-C(16)-O(4)	107.25(15)
O(3)-C(16)-C(13)	106.14(15)
O(4)-C(16)-C(13)	108.37(15)
O(8)-C(17)-C(8)	114.02(14)
O(8)-C(17)-C(12)	110.96(14)
C(8)-C(17)-C(12)	103.37(13)
O(1)-C(21)-O(2)	123.89(17)
O(1)-C(21)-C(22)	125.68(19)
O(2)-C(21)-C(22)	110.42(17)
O(9)-C(23)-O(8)	123.21(17)
O(9)-C(23)-C(24)	126.65(19)
O(8)-C(23)-C(24)	110.13(17)
O(7)-C(25)-O(6)	121.89(18)
O(7)-C(25)-C(26)	126.47(18)
O(6)-C(25)-C(26)	111.64(17)

Table 4. Anisotropic displacement parameters ($Å^2 x 10^3$) for leo287. The anisotropic displacement factor exponent takes the form: $-2\pi^2[h^2 a^{*2} U^{11} + ... + 2 h k a^* b^* U^{12}]$

	U^{11}	U^{22}	U^{33}	U^{23}	U^{13}	U^{12}
O(1)	34(1)	29(1)	33(1)	-10(1)	3(1)	-2(1)
O(2)	23(1)	24(1)	22(1)	-4(1)	5(1)	-1(1)
O(3)	27(1)	30(1)	22(1)	-5(1)	-5(1)	4(1)
O(4)	26(1)	35(1)	21(1)	3(1)	-3(1)	7(1)
O(5)	22(1)	32(1)	32(1)	2(1)	-2(1)	6(1)
O(6)	26(1)	18(1)	22(1)	-2(1)	1(1)	3(1)
O(7)	36(1)	24(1)	31(1)	5(1)	-1(1)	3(1)
O(8)	21(1)	26(1)	19(1)	-1(1)	4(1)	1(1)
O(9)	28(1)	63(1)	41(1)	-17(1)	9(1)	-15(1)
C(1)	34(1)	36(1)	26(1)	3(1)	4(1)	13(1)
C(2)	40(1)	49(1)	36(1)	1(1)	8(1)	24(1)
C(3)	51(1)	34(1)	40(1)	-3(1)	-5(1)	24(1)
C(4)	39(1)	29(1)	33(1)	6(1)	-4(1)	11(1)
C(5)	30(1)	21(1)	27(1)	4(1)	-4(1)	4(1)
C(6)	31(1)	33(1)	29(1)	12(1)	3(1)	4(1)
C(7)	23(1)	23(1)	25(1)	4(1)	2(1)	2(1)
C(8)	19(1)	17(1)	17(1)	-2(1)	0(1)	1(1)
C(9)	20(1)	18(1)	19(1)	-1(1)	-2(1)	0(1)
C(10)	22(1)	20(1)	21(1)	0(1)	-1(1)	5(1)
C(11)	25(1)	22(1)	23(1)	4(1)	-1(1)	2(1)
C(12)	21(1)	19(1)	20(1)	0(1)	1(1)	2(1)
C(13)	21(1)	19(1)	20(1)	2(1)	1(1)	1(1)
C(14)	19(1)	18(1)	18(1)	-1(1)	0(1)	0(1)
C(15)	21(1)	22(1)	18(1)	-2(1)	2(1)	-1(1)
C(16)	24(1)	30(1)	20(1)	2(1)	0(1)	3(1)
C(17)	19(1)	20(1)	17(1)	1(1)	1(1)	1(1)
C(18)	65(2)	34(1)	65(2)	21(1)	-3(1)	15(1)
C(19)	49(1)	56(2)	33(1)	1(1)	-12(1)	24(1)
C(20)	23(1)	27(1)	35(1)	-2(1)	-6(1)	2(1)
C(21)	28(1)	27(1)	18(1)	-2(1)	-1(1)	4(1)
C(22)	37(1)	47(1)	49(1)	-15(1)	18(1)	2(1)

C(23)19(1)	34(1)	26(1)	2(1)	3(1)	2(1)
C(24)26(1)	57(1)	26(1)	5(1)	7(1)	2(1)
C(25)22(1)	20(1)	32(1)	1(1)	0(1)	4(1)
C(26)34(1)	22(1)	36(1)	-5(1)	2(1)	3(1)

Table 5. Hydrogen coordinates (x 10^4) and isotropic displacement parameters ($Å^2$x 10^{3}) for leo287.

	x	y	z	U(eq)
H(1A)	4005	6821	5135	39
H(1B)	3251	5779	5080	39
H(2A)	1893	6547	4198	50
H(2B)	1945	7222	4970	50
H(3A)	3215	8408	4378	50
H(3B)	2035	8280	3864	50
H(5A)	5055	7453	3969	31
H(6A)	6017	7184	2833	37
H(6B)	5129	6262	2593	37
H(7A)	7077	6156	3628	29
H(7B)	6384	5208	3239	29
H(8A)	5387	4111	4195	21
H(9A)	5914	6156	4687	23
H(13A)	5080	2733	5652	24
H(14A)	4159	4233	5274	22
H(15A)	5534	5764	5824	25
H(16A)	5621	3263	6883	29
H(17A)	7332	4725	5189	22
H(18A)	3441	9203	2949	82
H(18B)	4521	8590	2552	82
H(18C)	4642	8980	3426	82
H(19A)	2243	7778	2475	69
H(19B)	2309	6673	2872	69
H(19C)	3304	7006	2255	69
H(20A)	2829	5445	3496	42
H(20B)	3560	4593	3965	42
H(20C)	4088	5041	3174	42
H(22A)	2801	6630	7623	66
H(22B)	2515	5499	7320	66
H(22C)	2217	6467	6787	66

H(24A)	10168	5012	3433	55
H(24B)	8910	4908	2995	55
H(24C)	9582	3907	3306	55
H(26A)	6123	52	4423	46
H(26B)	7006	705	3886	46
H(26C)	5605	968	3909	46

Table 6. Torsion angles [°] for leo287.

C(10)-C(1)-C(2)-C(3)	-57.6(3)
C(1)-C(2)-C(3)-C(4)	56.5(3)
C(2)-C(3)-C(4)-C(19)	76.4(3)
C(2)-C(3)-C(4)-C(18)	-166.1(2)
C(2)-C(3)-C(4)-C(5)	-50.0(3)
C(19)-C(4)-C(5)-C(6)	55.5(3)
C(3)-C(4)-C(5)-C(6)	178.72(19)
C(18)-C(4)-C(5)-C(6)	-65.4(3)
C(19)-C(4)-C(5)-C(10)	-72.7(3)
C(3)-C(4)-C(5)-C(10)	50.5(2)
C(18)-C(4)-C(5)-C(10)	166.43(19)
C(4)-C(5)-C(6)-C(7)	-172.85(17)
C(10)-C(5)-C(6)-C(7)	-38.20(19)
C(5)-C(6)-C(7)-C(9)	12.1(2)
C(17)-C(8)-C(9)-C(7)	61.36(19)
C(14)-C(8)-C(9)-C(7)	179.89(14)
C(17)-C(8)-C(9)-C(10)	-178.88(14)
C(14)-C(8)-C(9)-C(10)	-60.4(2)
C(6)-C(7)-C(9)-C(8)	144.84(15)
C(6)-C(7)-C(9)-C(10)	17.87(19)
C(2)-C(1)-C(10)-C(20)	-71.0(2)
C(2)-C(1)-C(10)-C(5)	54.3(2)
C(2)-C(1)-C(10)-C(9)	164.72(18)
C(6)-C(5)-C(10)-C(20)	-66.9(2)
C(4)-C(5)-C(10)-C(20)	68.6(2)
C(6)-C(5)-C(10)-C(1)	170.20(16)
C(4)-C(5)-C(10)-C(1)	-54.3(2)
C(6)-C(5)-C(10)-C(9)	48.98(17)
C(4)-C(5)-C(10)-C(9)	-175.53(16)
C(8)-C(9)-C(10)-C(20)	-45.4(2)
C(7)-C(9)-C(10)-C(20)	79.58(17)
C(8)-C(9)-C(10)-C(1)	79.3(2)
C(7)-C(9)-C(10)-C(1)	-155.65(16)
C(8)-C(9)-C(10)-C(5)	-165.09(14)

C(7)-C(9)-C(10)-C(5)	-40.08(17)
C(16)-O(4)-C(11)-O(5)	-179.69(18)
C(16)-O(4)-C(11)-C(12)	4.0(2)
C(25)-O(6)-C(12)-C(11)	57.77(19)
C(25)-O(6)-C(12)-C(13)	-63.39(19)
C(25)-O(6)-C(12)-C(17)	-178.57(14)
O(5)-C(11)-C(12)-O(6)	41.8(3)
O(4)-C(11)-C(12)-O(6)	-142.13(15)
O(5)-C(11)-C(12)-C(13)	168.11(19)
O(4)-C(11)-C(12)-C(13)	-15.82(19)
O(5)-C(11)-C(12)-C(17)	-80.3(2)
O(4)-C(11)-C(12)-C(17)	95.75(17)
O(6)-C(12)-C(13)-C(16)	145.42(15)
C(11)-C(12)-C(13)-C(16)	20.11(17)
C(17)-C(12)-C(13)-C(16)	-96.69(15)
O(6)-C(12)-C(13)-C(14)	-103.37(16)
C(11)-C(12)-C(13)-C(14)	131.31(14)
C(17)-C(12)-C(13)-C(14)	14.51(17)
C(16)-C(13)-C(14)-C(15)	0.75(17)
C(12)-C(13)-C(14)-C(15)	-107.47(15)
C(16)-C(13)-C(14)-C(8)	121.77(14)
C(12)-C(13)-C(14)-C(8)	13.55(18)
C(9)-C(8)-C(14)-C(15)	-50.0(2)
C(17)-C(8)-C(14)-C(15)	76.55(17)
C(9)-C(8)-C(14)-C(13)	-162.65(14)
C(17)-C(8)-C(14)-C(13)	-36.08(16)
C(16)-O(3)-C(15)-O(2)	91.82(17)
C(16)-O(3)-C(15)-C(14)	-25.57(19)
C(21)-O(2)-C(15)-O(3)	89.18(18)
C(21)-O(2)-C(15)-C(14)	-153.20(14)
C(13)-C(14)-C(15)-O(3)	14.34(17)
C(8)-C(14)-C(15)-O(3)	-99.45(16)
C(13)-C(14)-C(15)-O(2)	-104.09(15)
C(8)-C(14)-C(15)-O(2)	142.12(14)
C(15)-O(3)-C(16)-O(4)	141.23(14)
C(15)-O(3)-C(16)-C(13)	25.55(19)

C(11)-O(4)-C(16)-O(3)	-104.54(17)
C(11)-O(4)-C(16)-C(13)	9.7(2)
C(12)-C(13)-C(16)-O(3)	96.43(16)
C(14)-C(13)-C(16)-O(3)	-15.32(18)
C(12)-C(13)-C(16)-O(4)	-18.49(18)
C(14)-C(13)-C(16)-O(4)	-130.24(15)
C(23)-O(8)-C(17)-C(8)	121.55(16)
C(23)-O(8)-C(17)-C(12)	-122.23(16)
C(9)-C(8)-C(17)-O(8)	-66.63(19)
C(14)-C(8)-C(17)-O(8)	166.05(14)
C(9)-C(8)-C(17)-C(12)	172.80(14)
C(14)-C(8)-C(17)-C(12)	45.49(16)
O(6)-C(12)-C(17)-O(8)	-37.93(18)
C(11)-C(12)-C(17)-O(8)	87.00(17)
C(13)-C(12)-C(17)-O(8)	-160.25(14)
O(6)-C(12)-C(17)-C(8)	84.70(16)
C(11)-C(12)-C(17)-C(8)	-150.38(14)
C(13)-C(12)-C(17)-C(8)	-37.63(17)
C(15)-O(2)-C(21)-O(1)	-3.5(3)
C(15)-O(2)-C(21)-C(22)	175.32(17)
C(17)-O(8)-C(23)-O(9)	5.2(3)
C(17)-O(8)-C(23)-C(24)	-173.91(16)
C(12)-O(6)-C(25)-O(7)	-6.8(2)
C(12)-O(6)-C(25)-C(26)	173.07(15)

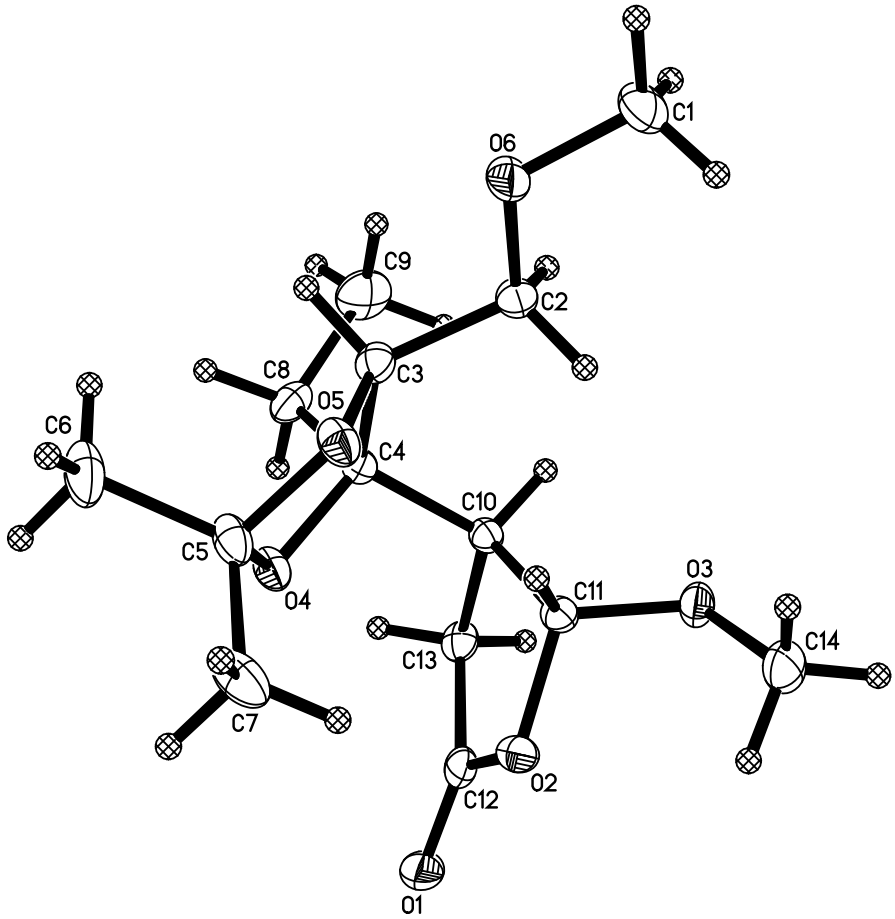

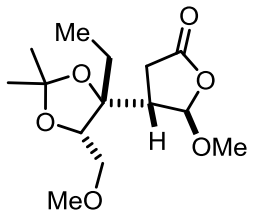

4.42f

Table 1. Crystal data and structure refinement for leo288 (**4.42f**).

Identification code	leo288 (Daniel Tao)	
Empirical formula	$C_{14}H_{24}O_6$	
Formula weight	288.33	
Temperature	133(2) K	
Wavelength	0.71073 Å	
Crystal system	Orthorhombic	
Space group	$P2_12_12_1$	
Unit cell dimensions	a = 7.8890(5) Å	α= 90°.

	b = 8.7473(5) Å	β= 90°.
	c = 21.8246(12) Å	γ = 90°.
Volume	1506.06(15) $Å^3$	
Z	4	
Density (calculated)	1.272 Mg/m^3	
Absorption coefficient	0.099 mm^{-1}	
F(000)	624	
Crystal color	colorless	
Crystal size	0.294 x 0.162 x 0.120 mm^3	
Theta range for data collection	1.866 to 28.767°	
Index ranges	$-10 \leq h \leq 10$, $-11 \leq k \leq 11$, $-29 \leq l \leq 27$	
Reflections collected	16761	
Independent reflections	3671 [R(int) = 0.0295]	
Completeness to theta = 25.500°	100.0 %	
Absorption correction	Semi-empirical from equivalents	
Max. and min. transmission	0.8621 and 0.8225	
Refinement method	Full-matrix least-squares on F^2	
Data / restraints / parameters	3671 / 0 / 277	
Goodness-of-fit on F^2	1.036	
Final R indices [I>2sigma(I) = 3323 data]	R1 = 0.0323, wR2 = 0.0720	
R indices (all data, 0.74Å)	R1 = 0.0387, wR2 = 0.0748	
Absolute structure parameter	-0.3(3)	
Largest diff. peak and hole	0.240 and -0.203 $e.Å^{-3}$	

Table 2. Atomic coordinates (x 10^4) and equivalent isotropic displacement parameters ($Å^2$x 10^3) for leo288. U(eq) is defined as one third of the trace of the orthogonalized U^{ij} tensor.

	x	y	z	U(eq)
O(1)	6661(2)	7242(2)	8202(1)	26(1)
O(2)	7866(2)	6115(1)	7397(1)	18(1)
O(3)	7574(2)	3721(1)	6954(1)	18(1)
O(4)	5964(2)	8225(1)	6522(1)	17(1)
O(5)	7446(2)	7445(1)	5686(1)	18(1)
O(6)	6596(2)	4998(1)	4830(1)	22(1)
C(1)	6902(3)	3496(2)	4612(1)	26(1)
C(2)	6197(2)	4997(2)	5463(1)	17(1)
C(3)	5872(2)	6633(2)	5658(1)	17(1)
C(4)	5082(2)	6884(2)	6304(1)	15(1)
C(5)	7167(2)	8736(2)	6072(1)	20(1)
C(6)	6426(3)	10082(2)	5716(1)	32(1)
C(7)	8813(3)	9130(2)	6386(1)	28(1)
C(8)	3190(2)	7259(2)	6252(1)	20(1)
C(9)	2115(3)	5982(3)	5983(1)	31(1)
C(10)	5439(2)	5598(2)	6768(1)	14(1)
C(11)	7340(2)	5281(2)	6856(1)	14(1)
C(12)	6495(2)	6543(2)	7731(1)	18(1)
C(13)	4901(2)	6009(2)	7425(1)	17(1)
C(14)	9328(3)	3298(3)	6971(1)	27(1)

Table 3. Bond lengths [Å] and angles [°] for leo288.

O(1)-C(12)	1.203(2)
O(2)-C(12)	1.357(2)
O(2)-C(11)	1.4493(19)
O(3)-C(11)	1.393(2)
O(3)-C(14)	1.433(2)
O(4)-C(5)	1.437(2)
O(4)-C(4)	1.445(2)
O(5)-C(5)	1.427(2)
O(5)-C(3)	1.432(2)
O(6)-C(2)	1.4159(19)
O(6)-C(1)	1.418(2)
C(2)-C(3)	1.514(2)
C(3)-C(4)	1.556(2)
C(4)-C(8)	1.532(2)
C(4)-C(10)	1.540(2)
C(5)-C(7)	1.508(3)
C(5)-C(6)	1.526(3)
C(8)-C(9)	1.520(3)
C(10)-C(13)	1.536(2)
C(10)-C(11)	1.537(2)
C(12)-C(13)	1.499(3)
C(12)-O(2)-C(11)	110.43(13)
C(11)-O(3)-C(14)	112.64(14)
C(5)-O(4)-C(4)	110.17(12)
C(5)-O(5)-C(3)	106.46(13)
C(2)-O(6)-C(1)	111.40(13)
O(6)-C(2)-C(3)	108.14(14)
O(5)-C(3)-C(2)	109.50(14)
O(5)-C(3)-C(4)	103.85(13)
C(2)-C(3)-C(4)	117.11(14)
O(4)-C(4)-C(8)	108.63(14)
O(4)-C(4)-C(10)	106.71(13)
C(8)-C(4)-C(10)	112.53(14)

O(4)-C(4)-C(3)	102.75(13)
C(8)-C(4)-C(3)	110.69(14)
C(10)-C(4)-C(3)	114.81(14)
O(5)-C(5)-O(4)	105.05(12)
O(5)-C(5)-C(7)	108.40(16)
O(4)-C(5)-C(7)	109.25(15)
O(5)-C(5)-C(6)	111.69(15)
O(4)-C(5)-C(6)	109.56(16)
C(7)-C(5)-C(6)	112.60(17)
C(9)-C(8)-C(4)	114.51(16)
C(13)-C(10)-C(11)	101.30(13)
C(13)-C(10)-C(4)	113.11(14)
C(11)-C(10)-C(4)	113.09(13)
O(3)-C(11)-O(2)	109.27(13)
O(3)-C(11)-C(10)	108.98(14)
O(2)-C(11)-C(10)	106.84(13)
O(1)-C(12)-O(2)	120.85(17)
O(1)-C(12)-C(13)	129.12(17)
O(2)-C(12)-C(13)	110.03(14)
C(12)-C(13)-C(10)	104.91(14)

Table 4. Anisotropic displacement parameters ($Å^2 x 10^3$) for leo288. The anisotropic displacement factor exponent takes the form: $-2\pi^2[h^2 a^{*2} U^{11} + ... + 2 h k a^* b^* U^{12}]$

	U^{11}	U^{22}	U^{33}	U^{23}	U^{13}	U^{12}
O(1)	36(1)	25(1)	16(1)	-6(1)	-6(1)	7(1)
O(2)	19(1)	19(1)	17(1)	-4(1)	-3(1)	0(1)
O(3)	16(1)	14(1)	23(1)	1(1)	-1(1)	2(1)
O(4)	24(1)	13(1)	15(1)	-1(1)	5(1)	-1(1)
O(5)	24(1)	14(1)	17(1)	-1(1)	6(1)	-2(1)
O(6)	36(1)	18(1)	13(1)	-1(1)	4(1)	5(1)
C(1)	36(1)	22(1)	19(1)	-5(1)	5(1)	4(1)
C(2)	22(1)	17(1)	12(1)	1(1)	2(1)	0(1)
C(3)	20(1)	16(1)	14(1)	2(1)	1(1)	2(1)
C(4)	18(1)	14(1)	13(1)	0(1)	-1(1)	2(1)
C(5)	32(1)	13(1)	16(1)	0(1)	7(1)	-1(1)
C(6)	56(1)	16(1)	24(1)	4(1)	12(1)	5(1)
C(7)	34(1)	23(1)	28(1)	-6(1)	8(1)	-11(1)
C(8)	20(1)	25(1)	16(1)	3(1)	0(1)	8(1)
C(9)	18(1)	40(1)	34(1)	-1(1)	-5(1)	3(1)
C(10)	15(1)	11(1)	14(1)	-1(1)	0(1)	-1(1)
C(11)	16(1)	14(1)	13(1)	0(1)	1(1)	-2(1)
C(12)	25(1)	13(1)	16(1)	3(1)	-2(1)	3(1)
C(13)	21(1)	17(1)	13(1)	3(1)	3(1)	1(1)
C(14)	20(1)	23(1)	38(1)	-4(1)	-7(1)	6(1)

Table 5. Hydrogen coordinates (x 10^4) and isotropic displacement parameters ($Å^2$x 10^{3}) for leo288.

	x	y	z	U(eq)
H(1A)	7120(30)	3540(30)	4184(12)	35(6)
H(1B)	5880(30)	2850(30)	4657(10)	32(6)
H(1C)	7890(30)	3060(30)	4842(12)	41(7)
H(2A)	7100(30)	4540(20)	5694(9)	14(5)
H(2B)	5200(30)	4360(20)	5535(9)	19(5)
H(3A)	5160(30)	7080(20)	5338(9)	18(5)
H(6A)	5420(30)	9750(30)	5479(11)	32(6)
H(6B)	7330(30)	10480(30)	5420(12)	48(7)
H(6C)	6090(30)	10910(30)	5996(11)	35(6)
H(7A)	9230(30)	8250(30)	6642(10)	29(6)
H(7B)	8640(30)	9990(30)	6648(10)	34(6)
H(7C)	9690(30)	9370(30)	6078(11)	34(6)
H(8A)	2780(30)	7550(20)	6656(10)	18(5)
H(8B)	3080(30)	8080(30)	5995(10)	24(5)
H(9A)	930(30)	6340(30)	5947(11)	36(6)
H(9B)	2240(30)	5070(30)	6237(12)	50(7)
H(9C)	2510(30)	5730(30)	5548(13)	43(7)
H(10A)	4990(20)	4690(20)	6643(8)	9(4)
H(11A)	8050(20)	5680(20)	6529(9)	12(5)
H(13A)	4100(30)	6830(30)	7458(10)	24(5)
H(13B)	4490(30)	5120(30)	7661(10)	29(6)
H(14A)	9380(30)	2280(30)	7156(10)	34(6)
H(14B)	9900(30)	3940(30)	7249(10)	29(6)
H(14C)	9770(30)	3360(30)	6557(12)	43(7)

Table 6. Torsion angles [°] for leo288.

C(1)-O(6)-C(2)-C(3)	-179.47(16)
C(5)-O(5)-C(3)-C(2)	-159.32(14)
C(5)-O(5)-C(3)-C(4)	-33.51(16)
O(6)-C(2)-C(3)-O(5)	-73.40(17)
O(6)-C(2)-C(3)-C(4)	168.79(14)
C(5)-O(4)-C(4)-C(8)	-117.87(15)
C(5)-O(4)-C(4)-C(10)	120.56(15)
C(5)-O(4)-C(4)-C(3)	-0.58(16)
O(5)-C(3)-C(4)-O(4)	20.53(15)
C(2)-C(3)-C(4)-O(4)	141.35(15)
O(5)-C(3)-C(4)-C(8)	136.36(14)
C(2)-C(3)-C(4)-C(8)	-102.82(18)
O(5)-C(3)-C(4)-C(10)	-94.89(16)
C(2)-C(3)-C(4)-C(10)	25.9(2)
C(3)-O(5)-C(5)-O(4)	33.55(17)
C(3)-O(5)-C(5)-C(7)	150.25(14)
C(3)-O(5)-C(5)-C(6)	-85.14(18)
C(4)-O(4)-C(5)-O(5)	-19.76(18)
C(4)-O(4)-C(5)-C(7)	-135.88(15)
C(4)-O(4)-C(5)-C(6)	100.34(16)
O(4)-C(4)-C(8)-C(9)	175.88(15)
C(10)-C(4)-C(8)-C(9)	-66.2(2)
C(3)-C(4)-C(8)-C(9)	63.8(2)
O(4)-C(4)-C(10)-C(13)	57.18(17)
C(8)-C(4)-C(10)-C(13)	-61.88(19)
C(3)-C(4)-C(10)-C(13)	170.29(14)
O(4)-C(4)-C(10)-C(11)	-57.24(17)
C(8)-C(4)-C(10)-C(11)	-176.30(14)
C(3)-C(4)-C(10)-C(11)	55.88(19)
C(14)-O(3)-C(11)-O(2)	-70.23(18)
C(14)-O(3)-C(11)-C(10)	173.36(15)
C(12)-O(2)-C(11)-O(3)	-101.62(15)
C(12)-O(2)-C(11)-C(10)	16.14(17)
C(13)-C(10)-C(11)-O(3)	93.64(15)

C(4)-C(10)-C(11)-O(3)	-145.01(13)
C(13)-C(10)-C(11)-O(2)	-24.31(16)
C(4)-C(10)-C(11)-O(2)	97.03(15)
C(11)-O(2)-C(12)-O(1)	179.53(15)
C(11)-O(2)-C(12)-C(13)	-0.15(18)
O(1)-C(12)-C(13)-C(10)	164.61(17)
O(2)-C(12)-C(13)-C(10)	-15.75(18)
C(11)-C(10)-C(13)-C(12)	23.65(17)
C(4)-C(10)-C(13)-C(12)	-97.68(16)